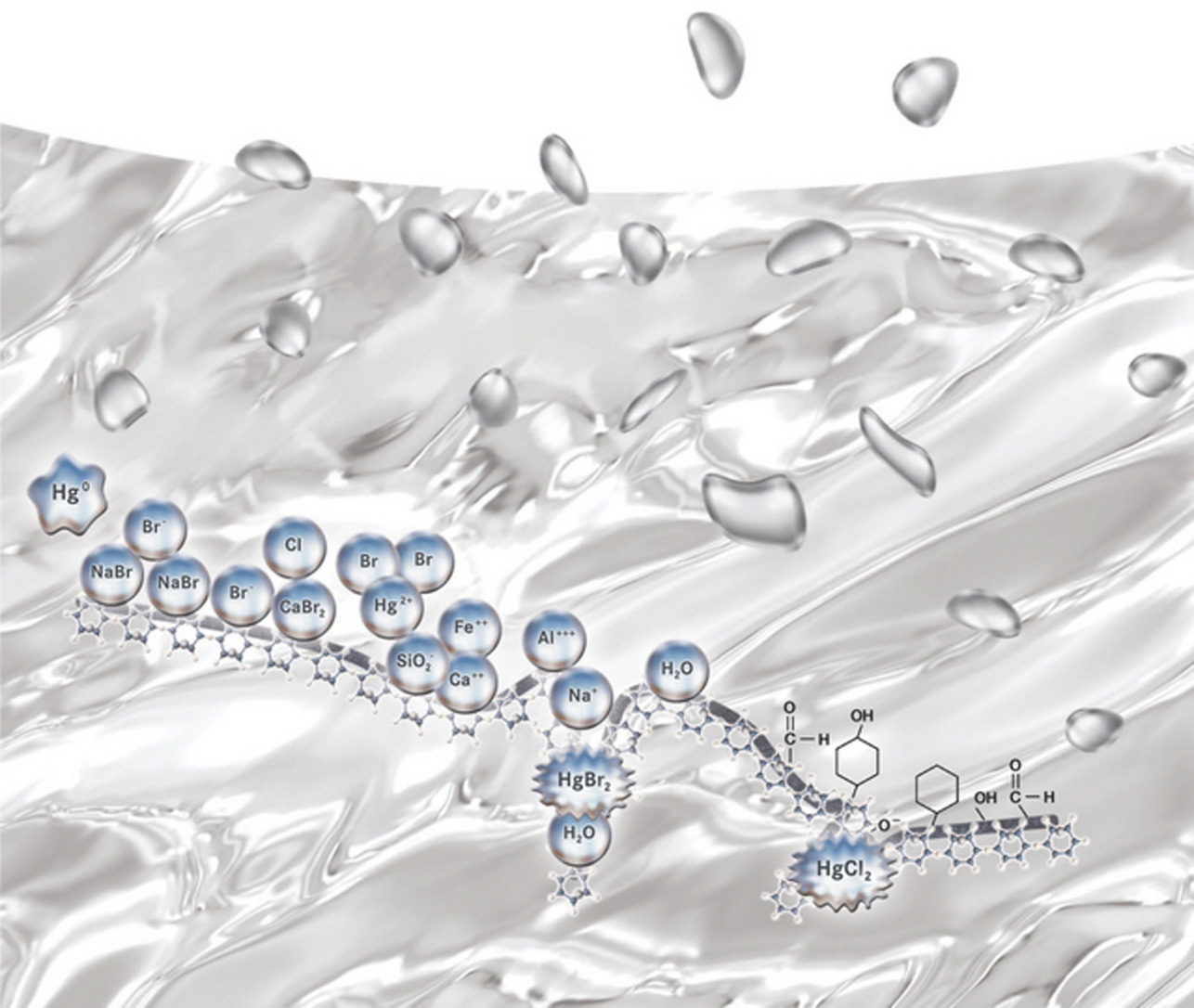


Edited by Evan J. Granite, Henry W. Pennline,
and Constance Senior

Mercury Control

for Coal-Derived Gas Streams



*Edited by
Evan J. Granite,
Henry W. Pennline, and
Constance Senior*

Mercury Control

Related Titles

Cai, Y., Liu, G., O'Driscoll, N. (eds.)

Environmental Chemistry and Toxicology of Mercury

2012

ISBN: 978-0-470-57872-8 (Also available in a variety of electronic formats)

Colbeck, I., Lazaridis, M. (eds.)

Aerosol Science - Technology and Applications

2014

ISBN: 978-1-119-97792-6 (Also available in a variety of electronic formats)

Garland, J.J. (ed.)

Mercury Cadmium Telluride - Growth, Properties and Applications

2011

ISBN: 978-0-470-69706-1 (Also available in a variety of electronic formats)

Agranovski, I. (ed.)

Aerosols - Science and Technology

2010

ISBN: 978-3-527-32660-0

*Edited by Evan J. Granite,
Henry W. Pennline, and
Constance Senior*

Mercury Control

for Coal-Derived Gas Streams

WILEY-VCH
Verlag GmbH & Co. KGaA

The Editors

Dr. Evan J. Granite

US Department of Energy
National Energy Technology Laboratory
PO Box 10940
Pittsburgh, PA 15236
USA

Henry W. Pennline

US Department of Energy
National Energy Technology Laboratory
PO Box 10940
Pittsburgh, PA 15236
USA

Constance Senior

ADA Environmental Solutions
9135 S. Ridgeline Blvd, Suite 200
Highlands Ranch, CO 80129
USA

All books published by **Wiley-VCH** are carefully produced. Nevertheless, authors, editors, and publisher do not warrant the information contained in these books, including this book, to be free of errors. Readers are advised to keep in mind that statements, data, illustrations, procedural details or other items may inadvertently be inaccurate.

Library of Congress Card No.: applied for

British Library Cataloguing-in-Publication Data

A catalogue record for this book is available from the British Library.

Bibliographic information published by the Deutsche Nationalbibliothek

The Deutsche Nationalbibliothek lists this publication in the Deutsche Nationalbibliografie; detailed bibliographic data are available on the Internet at <<http://dnb.d-nb.de>>.

© 2015 Wiley-VCH Verlag GmbH & Co. KGaA, Boschstr. 12, 69469 Weinheim, Germany

All rights reserved (including those of translation into other languages). No part of this book may be reproduced in any form – by photoprinting, microfilm, or any other means – nor transmitted or translated into a machine language without written permission from the publishers. Registered names, trademarks, etc. used in this book, even when not specifically marked as such, are not to be considered unprotected by law.

Print ISBN: 978-3-527-32949-6

ePDF ISBN: 978-3-527-65881-7

ePub ISBN: 978-3-527-65880-0

Mobi ISBN: 978-3-527-65879-4

oBook ISBN: 978-3-527-65878-7

Cover-Design Adam-Design, Weinheim, Germany

Typesetting Laserwords Private Limited, Chennai, India

Printing and Binding Markono Print Media Pte Ltd, Singapore

Printed on acid-free paper

Contents

List of Contributors	<i>XVII</i>
Mercury R&D Book Foreword	<i>XXI</i>
Preface	<i>XXIII</i>
List of Abbreviations	<i>XXVII</i>

Part I: Mercury in the Environment: Origin, Fate, and Regulation 1

1	Mercury in the Environment	3
	<i>Leonard Levin</i>	
1.1	Introduction	3
1.2	Mercury as a Chemical Element	4
1.2.1	Physical and Chemical Properties of the Forms of Mercury	6
1.2.2	Associations with Minerals and Fuels	6
1.3	Direct Uses of Mercury	6
1.4	Atmospheric Transport and Deposition	7
1.5	Atmospheric Reactions and Lifetime	8
1.6	Mercury Biogeochemical Cycling	8
	References	10
2	Mercury and Halogens in Coal	13
	<i>Allan Kolker and Jeffrey C. Quick</i>	
2.1	Introduction	13
2.1.1	Mode of Occurrence of Mercury (Hg) in Coal	13
2.1.2	Effectiveness of Pre-Combustion Mercury Removal	14
2.1.3	Methods for Mercury Determination	15
2.2	Mercury in U.S. Coals	16
2.2.1	U.S. Coal Databases	16
2.2.1.1	USGS COALQUAL Database	16
2.2.1.2	1999 EPA ICR	19
2.2.1.3	2010 EPA ICR	19
2.2.2	Comparison of U.S. Coal Databases	20
2.3	Mercury in International Coals	22
2.3.1	Review of Mercury in Coal in the Largest Coal Producers	22

2.3.1.1	China	23
2.3.1.2	India	24
2.3.1.3	Australia	26
2.3.1.4	South Africa	26
2.3.1.5	Russian Federation	27
2.3.1.6	Indonesia	29
2.4	Halogens in Coal	29
2.4.1	Introduction	29
2.4.1.1	Chlorine (Cl)	30
2.4.1.2	Bromine (Br)	32
2.4.1.3	Iodine (I)	35
2.4.1.4	Fluorine (F)	35
2.5	Summary	36
	Acknowledgments	37
	References	37
3	Regulations	45
	<i>Nick Hutson</i>	
3.1	U.S. Regulations	45
3.1.1	Background	45
3.1.2	Electric Generating Units (EGUs)	46
3.1.3	Mercury and Air Toxics Standards (“MATS”) – Existing Sources	47
3.1.4	Mercury and Air Toxics Standards (“MATS”) – New Sources	49
	References	50
4	International Legislation and Trends	51
	<i>Lesley L. Sloss</i>	
4.1	Introduction	51
4.2	International Legislation	52
4.2.1	UNEP International Legally Binding Instrument on Mercury (“Minamata Convention”)	53
4.2.2	European Union (EU)	53
4.3	Regional and National Legislation	59
4.3.1	Europe	59
4.3.1.1	Germany	59
4.3.1.2	Netherlands	59
4.3.2	Asia	60
4.3.2.1	China	60
4.3.2.2	Japan	62
4.3.2.3	Other Asian Countries	63
4.3.3	Other Countries	64
4.3.3.1	Australia	64
4.3.3.2	Canada	65
4.3.3.3	Russia	65
4.3.3.4	South Africa	65

- 4.4 Summary 65
- References 66

Part II: Mercury Measurement in Coal Gas 69

5 Continuous Mercury Monitors for Fossil Fuel-Fired Utilities 71

Dennis L. Laudal

- 5.1 Introduction 71
- 5.2 Components of a CMM 73
 - 5.2.1 Mercury Analyzer 73
 - 5.2.1.1 Cold-Vapor Atomic Absorption Spectrometry 73
 - 5.2.1.2 Cold-Vapor Atomic Fluorescence Spectrometry 74
 - 5.2.1.3 Other Analytical Methods 75
 - 5.2.2 Pretreatment/Conversion Systems and Probe 75
 - 5.2.2.1 Sampling Probe 76
 - 5.2.2.2 Pretreatment and Mercury Conversion 77
 - 5.2.3 CMM Calibration System 79
- 5.3 Installation and Verification Requirements 82
 - 5.3.1 Installation 82
 - 5.3.2 CMM Verification 82
 - 5.3.2.1 Measurement Error 83
 - 5.3.2.2 Seven-Day Calibration Drift 83
 - 5.3.2.3 Relative Accuracy Test Audit 83
- 5.4 Major CMM Tests 84
- 5.5 CMM Vendors 87
- References 88

6 Batch Methods for Mercury Monitoring 91

Constance Senior

- 6.1 Introduction 91
- 6.2 Wet Chemistry Batch Methods 91
 - 6.2.1 Early EPA Total Hg Methods 91
 - 6.2.2 Development of Wet Chemistry Methods to Speciate Hg 93
 - 6.2.3 Method Application and Data Quality Considerations 94
- 6.3 Dry Batch Methods 95
 - 6.3.1 Sorbent Trap Method History 95
 - 6.3.2 Method Overview 97
 - 6.3.3 Total Hg Measurements 97
 - 6.3.3.1 PS-12B 97
 - 6.3.3.2 Method 30B 98
 - 6.3.4 Speciation Measurements 98
 - 6.3.5 Sampling Protocol 99
 - 6.3.5.1 Procedure and Apparatus 99
 - 6.3.6 Trap Analysis 100
 - 6.3.7 Relative Accuracy and Quality Assurance/Quality Control 100

- 6.4 Recommendations 105
- 6.4.1 Particulate Matter 105
- 6.4.2 Total Versus Speciated Mercury 105
- 6.4.3 Expected Mercury Concentration in the Flue Gas 105
- 6.4.4 Need for Real-Time Data 106
- 6.4.5 Complexity of Installation and Operation 106
- References 106

Part III: Mercury Chemistry in Coal Utilization Systems and Air Pollution Control Devices 109

- 7 Mercury Behavior in Coal Combustion Systems 111**
Constance Senior
 - 7.1 Introduction 111
 - 7.2 Coal Combustion Boilers 112
 - 7.3 Mercury Chemistry in Combustion Systems 113
 - 7.4 Air Pollution Control Devices on Utility and Industrial Boilers 117
 - 7.4.1 PM Control 118
 - 7.4.2 NO_x Control 119
 - 7.4.3 SO₂ Control 119
 - 7.4.4 Boiler Populations in the United States 120
 - 7.5 Mercury Behavior in Coal-Fired Boilers 121
 - 7.5.1 Data Sources 121
 - 7.5.2 Mercury Behavior in APCDs 123
 - 7.6 Summary 129
 - References 130

- 8 Gasification Systems 133**
Nicholas Lentz
 - 8.1 Principles of Coal Gasification 133
 - 8.2 Gasification Technologies Overview and Gasifier Descriptions 134
 - 8.3 Gasification Applications and Downstream Gas Cleanup and Processing 135
 - 8.4 Mercury Transformations and Fate 135
 - 8.5 Hg Measurement in a Reducing Environment 137
 - 8.6 Hg Control Technologies for Gasification 138
 - 8.7 Hg and the MATS Rule for Gasifiers 139
 - References 140

- 9 Mercury Emissions Control for the Cement Manufacturing Industry 141**
Robert Schreiber Jr., Shameem Hasan, Carrie Yonley, and Charles D. Kellett
 - 9.1 Introduction 141
 - 9.2 Cement Manufacturing Process Description 141
 - 9.2.1 Wet Process Kiln 144

9.2.2	Dry Process Kiln	145
9.3	State of Knowledge on the Source and Behavior of Mercury in the Cement Kiln System	147
9.4	Mercury Emissions Control Solutions in the Cement Industry	153
9.4.1	Activated Carbon Injection (ACI)	156
9.4.2	Wet Scrubbing	157
9.4.3	Selective Catalytic Reduction (SCR) and Wet Scrubbing	158
9.5	Conclusions	159
	References	160

Part IV: Mercury Research Programs in the United States 163

10	DOE's Mercury Control Technology Research, Development, and Demonstration Program	165
	<i>Thomas J. Feeley III, Andrew P. Jones, James T. Murphy, Ronald K. Munson, and Jared P. Ciferno</i>	
10.1	Introduction	165
10.2	Background	165
10.2.1	NETL's Hg Control Technology R& D	166
10.2.2	Mercury Speciation	167
10.2.3	Mercury Control Technologies	168
10.2.4	Results from Field Testing Program	169
10.2.5	Oxidation Enhancements	169
10.2.6	Chemical Additives	170
10.2.7	Catalysts	170
10.2.8	Activated Carbon Injection	171
10.2.8.1	Untreated PAC	171
10.2.8.2	Chemically Treated PAC	173
10.2.8.3	Conventional PAC with Chemical Additives	175
10.2.8.4	ACI Upstream of a Hot-Side ESP	176
10.2.9	Remaining Technical Issues	176
10.2.9.1	Impacts on Fly Ash	176
10.2.9.2	Sulfur Trioxide Interference	178
10.2.10	NETL In-House Development of Novel Control Technologies	179
10.2.11	Hg Control Technology Commercial Demonstrations	180
10.2.12	Mercury Control Cost Estimates	180
10.2.12.1	Economic Analyses for ACI	181
10.2.12.2	Economic Analyses for Wet FGD Enhancement	181
10.2.13	Coal Utilization Byproducts (CUB) R& D Program	182
10.2.14	Determining the Fate of Hg in FGD Byproducts	183
10.2.15	Determining the Fate of Hg in Fly Ash	184
10.3	Summary	185
	Disclaimer	186
	References	186

11	U.S. EPA Research Program 191 <i>Nick Hutson</i>
11.1	Introduction 191
11.2	Congressionally Mandated Studies 191
11.3	Control Technology from Work on Municipal Waste Combustors (MWCs) 193
11.4	Mercury Chemistry, Adsorption, and Sorbent Development 194
11.4.1	Halogenated Activated Carbon Sorbents 196
11.4.2	Non-Carbonaceous Sorbents 197
11.4.3	Mercury Control in a Wet-FGD Scrubber 198
11.4.4	Effect of SCR on Mercury Oxidation/Capture 200
11.5	Coal Combustion Residues and By-Products 201
11.6	EPA SBIR Program 202
	References 202
12	The Electric Power Research Institute's Program to Control Mercury Emissions from Coal-Fired Power Plants 205 <i>Ramsay Chang</i>
12.1	Introduction 205
12.2	Co-Benefits of Installed Controls 205
12.2.1	Selective Catalytic Reduction/Flue Gas Desulfurization 205
12.2.2	Unburned Carbon 206
12.3	Sorbent Injection 207
12.3.1	Units Equipped with Electrostatic Precipitators 208
12.3.1.1	Western Coals 208
12.3.1.2	Eastern Bituminous Coals and High-Sulfur Flue Gases 208
12.3.2	Units Equipped with Fabric Filters or TOXECON® 209
12.3.3	Challenges and Responses 211
12.3.3.1	Preserving Fly Ash Sales 211
12.3.3.2	Optimizing Electrostatic Precipitator Performance 211
12.3.3.3	Optimizing Fabric Filter and TOXECON Performance 212
12.4	Boiler Chemical Addition 213
12.4.1	Combined Technologies 214
12.4.2	Challenges and Responses 215
12.4.2.1	Wet Flue Gas Desulfurization Chemistry and Mercury Partitioning 216
12.4.2.2	Corrosion along Flue Gas Path and in the wFGD 216
12.4.2.3	Preserving Fly Ash Sales 217
12.4.2.4	Selenium Partitioning in Wet Flue Gas Desulfurization Systems 217
12.4.2.5	Bromide Leaching from Fly Ash 217
12.5	Novel Concepts for Mercury Control 218
12.5.1	TOXECON II® 218
12.5.2	Gore® Carbon Polymer Composite Modules 218
12.5.3	Sorbent Activation Process 220

- 12.6 Integration of Controls for Mercury with Controls for Other Air Pollutants 221
- 12.7 Summary 222
- References 222

Part V: Mercury Control Processes 225

- 13 Mercury Control Using Combustion Modification 227**
Thomas K. Gale
- 13.1 Mercury Speciation in Coal-Fired Power Plants without Added Catalysts 227
 - 13.1.1 Mercury is all Liberated and Isolated in the Furnace 227
 - 13.1.2 Chlorine Speciation in Coal-Fired Power Plants 227
 - 13.1.3 Mechanisms Governing Mercury Speciation 228
- 13.2 Role of Unburned Carbon in Mercury Oxidation and Adsorption 229
 - 13.2.1 UBC is the Only Catalyst with Enough Activity in Coal-Fired Power Plants 229
 - 13.2.2 UBC can Remove Hg or Oxidize Hg, Depending on the UBC Concentration 230
 - 13.2.3 Nature of Carbon Type Depends on Parent Coal and Combustion Efficiency 231
 - 13.2.4 Concentration of UBC Needed to Oxidize or Remove Mercury from Flue Gas 232
- 13.3 Synergistic Relationship between UBC and Calcium in Flyash 233
 - 13.3.1 Calcium Enhances the Retention of Mercury on Carbon 233
 - 13.3.2 Calcium/Carbon Synergism is Limited to a Range of Conditions 234
- 13.4 Potential Combustion Modification Strategies to Mitigate Mercury Emissions 236
- 13.5 Effects of Combustion Modifications on Mercury Oxidation across SCR Catalysts 238
 - 13.5.1 Inhibition of Mercury Oxidation can Occur in Low-Chlorine Flue Gas 238
 - References 238
- 14 Fuel and Flue-Gas Additives 241**
John Meier, Bruce Keiser, and Brian S. Higgins
- 14.1 Background 241
 - 14.1.1 Bromine-Salt Mercury Oxidation 242
 - 14.1.2 Fuel Additive Injection Equipment 242
 - 14.1.3 Case Study Results 243
 - 14.1.3.1 Case Studies where Halogen-containing Fuel Additives are Advantageous 244

14.1.4	Case Studies where Conditions are Disadvantageous to Fuel Additive	248
14.1.4.1	Units Burning High Chlorine Fuel with an SCR	249
14.1.4.2	Subbituminous Fired Units with Flue Gas Conditioning (SO ₃ Injection)	249
14.1.4.3	Units without Acid Gas Scrubbing and a Fabric Filter (FF)	250
14.2	Summary	250
	References	250
15	Catalysts for the Oxidation of Mercury	253
	<i>April Freeman Sibley</i>	
15.1	Introduction	253
15.1.1	Process Overview	253
15.2	Hg ⁰ Oxidation and Affecting Parameters	254
15.2.1	Hg ⁰ Oxidation Reaction Mechanism	255
15.2.2	Homogeneous Oxidation of Mercury	255
15.2.3	Heterogeneous Oxidation of Mercury over SCR Catalysts	255
15.2.4	SCR Operation-Hg ⁰ Reaction Effects	257
15.2.5	Hg ⁰ Oxidation and SO ₂ /SO ₃ Conversion	258
15.3	Conclusions and Future Research	259
	References	260
16	Mercury Capture in Wet Flue Gas Desulfurization Systems	261
	<i>Gary Blythe</i>	
16.1	Introduction	261
16.2	Fate of Net Mercury Removed by Wet FGD Systems	263
16.2.1	Phase Partitioning	263
16.2.2	Mercury in FGD By-product Streams	264
16.3	Mercury Reemissions	267
16.3.1	Definition and Reporting Conventions	267
16.3.2	Reemission Chemistry	269
16.3.3	Reemission Additives	271
16.4	Effects of Flue Gas Mercury Oxidation Technologies on FGD Capture of Mercury	272
	References	274
17	Introduction to Carbon Sorbents for Pollution Control	277
	<i>Joe Wong</i>	
17.1	Carbon Materials	277
17.2	Carbon Activation	277
17.3	Carbon Particle Shapes and Forms	280
17.3.1	Powdered Activated Carbon (PAC)	280
17.3.2	Granular Activated Carbon (GAC)	281
17.3.3	Shaped Activated Carbon	282
17.3.4	Other Activated Carbon Forms	282

17.4	Activated Carbon Applications	282
17.5	Activated Carbon Properties in Emission Systems	283
17.5.1	Activated Carbon Surface	285
17.5.2	Activated Carbon Pores	286
17.5.3	Activated Carbon Particles	289
17.6	Summary	291
	References	291
18	Activated Carbon Injection	293
	<i>Sharon M. Sjostrom</i>	
18.1	Introduction	293
18.2	The Activated Carbon Injection System	294
18.2.1	Powdered Activated Carbon Storage	294
18.2.2	Process Equipment	295
18.2.2.1	Metering	295
18.2.2.2	Conveying	295
18.2.3	PAC Distribution	296
18.3	Factors Influencing the Effectiveness of Activated Carbon	296
18.3.1	Site-Specific Factors	296
18.3.1.1	Flue Gas Characteristics: Halogens and SO ₃	297
18.3.1.2	TOXECON™	303
18.3.2	PAC-Specific Factors	303
18.3.3	ACI System Design-Specific Factors	304
18.3.3.1	Injection Location	304
18.3.3.2	Distribution	304
18.4	Balance-of-Plant Impacts	305
18.4.1	Coal Combustion By-Products	305
18.4.1.1	Autoignition of PAC in Ash Hoppers	306
18.4.1.2	Impacts on Particulate Emissions	306
18.4.1.3	Corrosion Issues	307
18.5	Future Considerations	307
	References	307
19	Halogenated Carbon Sorbents	311
	<i>Robert Nebergall</i>	
19.1	Introduction	311
19.2	Application of Activated Carbon for Mercury Control	311
19.3	Development of Halogenated Activated Carbon	313
19.3.1	Motivation	313
19.3.2	Manufacture	315
19.3.3	Performance	316
19.3.4	Balance-of-Plant Impacts	319
	References	320

20	Concrete-Compatible Activated Carbon	323
	<i>S. Behrooz Ghorishi</i>	
20.1	Introduction	323
20.2	Concrete-Compatibility Metrics	324
20.2.1	The New and Innovative Concrete-Friendly™ Metrics; the Acid Blue Index	326
20.3	Production of Concrete-Compatible Products Including C-PAC™	329
20.4	C-PAC™ Specification	331
20.4.1	Commercial Application of C-PAC™	331
20.4.2	Full-Scale C-PAC™ Trials at Midwest Generation's Crawford Station	332
20.4.3	Full-Scale C-PAC™ Trials the PPL Montana Corette Station	333
20.4.4	Cement Kiln Mercury Emission Control Using C-PAC™	334
20.5	Concrete Compatibility Test – Field Fly Ash/C-PAC™ Mixture	335
20.5.1	Air Content of Fresh Concrete	336
20.5.2	Unconfined Compressive Strength (UCS)	336
20.5.3	Stability of Mercury in Fly Ash and Concrete	337
	References	337
21	Novel Capture Technologies: Non-carbon Sorbents and Photochemical Oxidations	339
	<i>Karen J. Uffalussy and Evan J. Granite</i>	
21.1	Introduction	339
21.2	Non-carbon Sorbents	340
21.2.1	Amended Silicates, Novinda	340
21.2.1.1	Background and Motivations	340
21.2.1.2	How Does the Amended Silicates Sorbent Work?	341
21.2.1.3	Demonstrations	342
21.2.1.4	Conclusions	344
21.2.2	MinPlus CDEM Group BV	345
21.2.2.1	Background and Motivations	345
21.2.2.2	How Does the MinPlus Sorbent Work?	345
21.2.2.3	Demonstrations of Sorbent	347
21.2.2.4	Conclusions	348
21.2.3	Pahlman Process – Enviroscrub	348
21.2.3.1	Background and Motivations	348
21.2.3.2	How Does the Process and Sorbent Work?	349
21.2.3.3	Demonstrations	349
21.2.3.4	Conclusions	350
21.3	Photochemical Removal of Mercury from Flue Gas	350
21.3.1	Sensitized Oxidation of Mercury: GP-254 Process	350

21.3.2	Photocatalytic Oxidation of Mercury	352
	Disclaimer	352
	References	353
22	Sorbents for Gasification Processes	357
	<i>Henry W. Pennline and Evan J. Granite</i>	
22.1	Introduction	357
22.2	Background	358
22.3	Warm/Humid Gas Temperature Mercury Sorbent Capture Techniques	360
22.4	Cold Gas Cleanup of Mercury	366
22.4.1	Carbon-Based Materials	367
22.4.2	Other Materials	368
22.4.3	Wet Scrubbing Technique	369
22.5	Summary	370
	Disclaimer	370
	References	371
	Part VI: Modeling of Mercury Chemistry in Air Pollution Control Devices	375
23	Mercury-Carbon Surface Chemistry	377
	<i>Edwin S. Olson</i>	
23.1	Nature of the Bonding of Mercury to the Carbon Surface	377
23.2	Effects of Acid Gases on Mercury Capacities on Carbon	378
23.3	Kinetic HCl Effect	382
23.4	Summary	385
	References	386
24	Atomistic-Level Models	389
	<i>Jennifer Wilcox</i>	
24.1	Introduction	389
24.2	Homogeneous Mercury Oxidation Kinetics	390
24.2.1	Mercury – Chlorine Chemistry	390
24.2.2	Mercury – Bromine Chemistry	397
24.3	Heterogeneous Chemistry	400
24.3.1	Mercury Adsorption on Activated Carbon	400
24.3.2	Mercury Adsorption on Precious Metals	404
24.4	Conclusions and Future Work	407
	References	407
25	Predicting Hg Emissions Rates with Device-Level Models and Reaction Mechanisms	413
	<i>Stephen Niksa and Balaji Krishnakumar</i>	
25.1	Introduction and Scope	413

25.2	The Reaction System	414
25.3	Hg Transformations	416
25.3.1	In-Furnace Transformations	416
25.3.2	In-Flight Transformations	419
25.3.3	Hg ⁰ Oxidation across SCR Catalysts	427
25.3.4	Hg Transformations within WFGDs	430
25.4	Summary	433
	References	435

Index	437
--------------	-----

List of Contributors

Gary Blythe

URS Corporation
Process Technology Office
9400 Amberglen Blvd.
Austin, TX 78729
USA

Ramsay Chang

Electric Power Research Institute
3420 Hillview Ave
Palo Alto, CA 94304-1338
USA

Jared P. Ciferno

U.S. Department of Energy
National Energy Technology
Laboratory
Pittsburgh, PA 15236-0940
USA

Thomas J. Feeley III

U.S. Department of Energy
National Energy Technology
Laboratory
Pittsburgh, PA 15236-0940
USA

Thomas K. Gale

Novinda Corp.
999 18th Street
Suite 1755
North Tower
Denver, CO 80202
USA

S. Behrooz Ghorishi

CoaLogix – SCR Tech
11707 Steele Creek Road
Charlotte, NC 28273
USA

Evan J. Granite

US Department of Energy
National Energy Technology
Laboratory
PO Box 10940
Pittsburgh, PA 15236
USA

Shameem Hasan

Schreiber
Yonley & Associates
16252 Westwoods Business
Park Drive
Ellisville, MO 63021
USA

Brian S. Higgins

EnviroCare International
507 Green Island Road
American Canyon, CA 94503
USA

Nick Hutson

U.S. Environmental Protection
Agency
Energy Strategies Group
Office of Air Quality Planning
and Standards
109 T. W. Alexander Drive
(D243-01)
Research Triangle Park
NC 27711
USA

Andrew P. Jones

U.S. Department of Energy
National Energy Technology
Laboratory
Pittsburgh, PA 15236-0940
USA

Bruce Keiser

Nalco, An Ecolab Company
1601 West Diehl Road
Naperville, IL 60563-1198
USA

Charles D. Kellett

Schreiber
Yonley & Associates
16252 Westwoods Business
Park Drive
Ellisville, MO 63021
USA

Allan Kolker

U.S. Geological Survey
12201 Sunrise Valley Drive
Mail Stop 956
Reston, Virginia 20192-0002
USA

Balaji Krishnakumar

Niksa Energy Associates LLC
1745 Terrace Drive
Belmont, CA 94002
USA

Dennis L. Laudal

University of North Dakota
Energy & Environmental
Research Center (EERC)
15 North 23rd Street
Stop 9018
Grand Forks, ND 58202-9018
USA

Nicholas Lentz

University of North Dakota
Institute for Energy Studies
243 Centennial Drive Stop 8153
Upson II Room 366L
Grand Forks, ND 58202-8153
USA

Leonard Levin

Electric Power Research Institute
3420 Hillview Ave.
Palo Alto, CA 94304
USA

John Meier

Nalco, An Ecolab Company
1601 West Diehl Road
Naperville, IL 60563-1198
USA

Larry S. Monroe

Southern Company
Birmingham, AL
USA

Ronald K. Munson

Leonardo Technologies, Inc.
Bannock, OH 43972
USA

James T. Murphy

Leonardo Technologies, Inc.
Bannock, OH 43972
USA

Robert Nebergall

Cabot Norit Activated Carbon
3200 University Avenue
Marshall, TX 75670
USA

Stephen Niksa

Niksa Energy Associates LLC
1745 Terrace Drive
Belmont, CA 94002
USA

Edwin S. Olson

University of North Dakota
Energy & Environmental
Research Center (EERC)
15 North 23rd Street
Stop 9018
Grand Forks, ND 58202-9018
USA

Henry W. Pennline

US Department of Energy
National Energy Technology
Laboratory
P.O. Box 10940
Pittsburgh, PA 15236
USA

Jeffrey C. Quick

Utah Geological Survey
1594 West North Temple
Suite 3110
Salt Lake City, UT 84114-6100
USA

Robert Schreiber Jr.

Schreiber Yonley & Associates
16252 Westwoods Business
Park Drive
Ellisville, MO 63021
USA

Constance Senior

ADA Environmental Solutions
9135 S. Ridgeline Boulevard
Suite 200
Highlands Ranch, CO 80129
USA

April Freeman Sibley

Southern Company Services
Birmingham, AL 35242
USA

Sharon M. Sjostrom

ADA Environment Solutions
9135 S. Ridgeline Boulevard
Suite 200
Highlands Ranch, CO 80129
USA

Lesley L. Sloss

IEA Clean Coal Centre
Park House
14 Northfields
London SW18 6DD
UK

Karen J. Uffalussy

US Department of Energy
National Energy Technology Lab
626 Cochrans Mill Road
Pittsburgh, PA 15236-0940
USA

Jennifer Wilcox

Stanford University
Department of Energy Resources
Engineering
367 Panama Street
Green Earth Sciences 092A
Stanford, CA 94305-2220
USA

Joe Wong

ADA Carbon Solutions LLC
1460 W. Canal Court
Littleton, CO 80120-5632
USA

Carrie Yonley

Schreiber
Yonley & Associates
16252 Westwoods Business
Park Drive
Ellisville, MO 63021
USA

Mercury R&D Book Foreword

This book is very timely and important, because as I write this foreword, the U.S. Environmental Protection Agency (EPA) is finalizing the first mercury emission limitations on coal-fired power plants, known as the *Mercury and Air Toxics Standards (MATS)* rule. This regulation will require significant reductions of the amount of mercury (and other chemicals) contained in the coal fuel before the flue gas is released into the atmosphere.

The information in this volume has mostly been developed over the past decade, where I was engaged as a front line research manager for one of the largest power companies in the United States, Southern Company, which has many coal-fired power plants in its fleet. I have testified before the U.S. Senate on mercury chemistry and behavior in coal-fired boilers (http://epw.senate.gov/108th/Monroe_060503.htm), and have been in a leadership position for the utility industry in several organizations, namely, the Electric Power Research Institute (EPRI), the Coal Utilization Research Council (CURC), and the Utility Air Regulatory Group (UARG). I was the project manager for one of the first full-scale power plant tests of dedicated mercury control, at Alabama Power's Plant Gaston – which won an *R&D Magazine* "R&D 100" award in 2003. The Gaston project involved many of the authors included in this volume, especially Tom Feeley, Ramsay Chang, and Sharon Sjostrom. This is a subject that I know well.

In addition, several authors and I have collaborated on other related mercury studies. One of the most intriguing was the innovative research of the fate of mercury in coal power plant plumes, using first a fixed wing airplane and then an airship for plume sampling. This effort was led by Leonard Levin of EPRI, and included Dennis Laudal (University of North Dakota) and Jeff Ryan (U.S. EPA). Another cooperative effort through EPRI has been the computer modeling of mercury in power plants in two different efforts, led by Constance Senior and Steve Niksa.

The utility industry was taken by surprise with the announcement by the outgoing Clinton administration that it would be subject to a Maximum Achievable Control Technology (MACT) rule for mercury on 14 December 2000. That action kicked the industry into a frantic search for any data or information that could help us develop reliable control technology choices. Notably, EPRI, through the efforts of Ramsay Chang, and the U.S. Department of Energy (DOE)'s National

Energy Technology Laboratory (NETL), had already started working on mercury chemistry and control for coal-fired power plants. The subsequent efforts have largely been successful as an example of a public – private R&D partnership; where the utility industry and the suppliers of technology and materials to the industry worked with the DOE NETL to quickly advance the state of knowledge.

As the R&D progressed, an informal steering group of utility researchers, vendors of hardware and materials, and the U.S. DOE NETL was able to leverage the NETL funding to explore different options for controlling mercury from almost all power plant and coal-type combinations. In the early years of R&D, we found that we knew less and less about mercury chemistry with every new test and discovery, as contradictory results were more the rule.

The editors have assembled an experienced group of authors to make this volume, a “Who’s Who’s” of mercury research from the United States over the past decade. I feel lucky to have worked with virtually every one of the assembled group, and call most of them close friends. There is no better group of technical professionals to guide you in understanding the issues of mercury in coal-derived gas streams.

The volume is arranged in a logical sequence, beginning with the fate of mercury in the environment, written by Leonard Levin of EPRI. The applicable regulations, both for the United States and the international context, follow along with descriptions of trace elements in coal and the means to measure mercury in gas streams. The heart of the work is presented in the following sections on mercury chemistry, research programs, and the different technology systems that can be used and adapted for mercury control. The important topic of the stability of mercury in the solid coal combustion residues is also addressed next. Finally, the state-of-the-art in mercury modeling, both at the fundamental and process levels, is presented.

This is the manuscript that I – and the whole industry – needed back in 2000, as we contemplated what we would have do to reduce mercury emissions to meet upcoming regulations. It will serve as both a reference for those already engaged in the research and control efforts, and as an invaluable introduction for those just now becoming interested in the subject. I highly recommend it to the technical reader.

October 2014

*Larry S. Monroe
Georgia Power Company
Atlanta, GA, USA*

Preface

This book has its genesis in a Department of Energy (DOE) Topical Report on “Sorbents for Mercury Removal from Flue Gas” that Henry Pennline asked me to write in 1996. As a new post-doc hired to study sorbents for the capture of mercury, Henry suggested that a thorough literature review and survey would be an excellent way to start. As the topical report progressed and was nearly complete in 1997, I suggested to Henry that we write a book about mercury in flue gas. Henry shot this idea down at the time, correctly stating that we had much more to learn. Henry Pennline has turned out to be the best supervisor, researcher, colleague, and friend I could ever have. He was a little skeptical of my abilities at first, having observed my unusual photographic memory for foods; my suit and tie attire in the laboratory (unusual at DOE); and my dropping a large \$25 quartz tube for the micro-balance on my first day on the job. I hope I end up doing something good in my research career to justify Henry’s faith in me.

Mercury is a semi-noble metal, with both a fascinating chemistry and numerous applications throughout human history. Coal-derived flue gas and coal-derived syngas are both complex stews containing numerous species and exist over a wide temperature range at pulverized combustion and integrated gasification combined cycle (IGCC) plants, respectively. Having completed a MS thesis on coal gasification, I already knew going into the DOE that one could happily study coal flue gas and syngas for many lifetimes. Being introduced to mercury at DOE, I quickly found a terrific subject, with many wonderful colleagues.

In 1998 I met Dr Constance Senior at DOE in Pittsburgh. Constance was leading a large DOE-funded study on the behavior of the trace elements in coal-fired power plants. She impressed me immediately as a tenacious leader and terrific researcher. Constance exhibited extraordinary leadership – her efforts in corralling a large and diverse group of researchers from industry, academia, and the government resulted in a nearly 800-page report for DOE; a special issue of *Fuel Processing Technology* on the trace elements in coal-fired power plants in 2000; and a great expansion of our understanding of mercury in flue gas. I had the pleasure of meeting Constance again at the Workshop on Source Emission and Ambient Air Monitoring in Minneapolis in 1999. Despite the fact that I was an unknown post-doc at DOE, she introduced me to many of the researchers at dinner (a large pot of minestrone soup and a gigantic pizza that covered the

entire table) in the Mall of America. I learned a lesson that day from Constance; always be nice to your colleagues. Hopefully I have done this. Dr Senior made Herculean efforts to help this book get completed; she is one-in-a-million.

Our work at DOE has allowed us to meet many wonderful colleagues at venues such as the Annual Mercury Control Technology Meetings that were held in Pittsburgh; the AIChE and ACS National Meetings; the Air Quality Conferences, and the Mega Symposiums. At the joint ACS-AIChE National Meeting held in the spring of 2008 in New Orleans, I recruited Tom Feeley, Ramsay Chang, and Constance Senior to be my keynote speakers on mercury. They did an outstanding job, highlighting a program that had 29 speakers on the various aspects of mercury in coal-derived gases. The idea for the book on mercury, having never left my mind, was revived. In 2009 I came up with a draft outline for this book, and happily in 2010, Dr Julia Stuthe from John Wiley recruited me to organize a book on mercury in coal-derived gases. Having already planned a book, I bent her ears with a 40-page PowerPoint presentation, abstract, and outline over a burrito and spicy chicken tortilla soup dinner in San Antonio during the 2010 AIChE National Meeting. Julia – forgive me. Dr Stuthe has recently left John Wiley, and I wish her great success. Lesley Belfit from John Wiley has done an outstanding job in helping us complete this book.

Coal contains a trace level of mercury of approximately 0.1 ppm. Mercury is a neurotoxin, and can travel long distances once emitted through the stacks of coal-burning power plants. Approximately 30–40% of the electricity in the United States is generated through the combustion of coal. Coal is an abundant resource in the United States – the country has a supply for at least 200 years. The challenge is to utilize the abundant domestic coal for energy independence in environmentally friendly ways.

With the US EPA issuing a national regulation on 21 December, 2011, requiring 91% removal of mercury, and many states already with their own regulations, the need exists for low-cost mercury removal techniques that can be applied to coal-burning power plants. The injection of powdered activated carbon into the ductwork upstream of the particulate control device is the most developed technology for mercury capture. Alternative techniques for mercury capture will also play a role in the near future because of the numerous configurations of air pollution control devices present within the power plants, as well as the many different coals being burned. These methods employ sorbents, catalysts, scrubber liquors, flue gas or coal additives, combustion modification, flue gas cooling, barrier discharges, and ultraviolet radiation for the removal of mercury from flue gas streams. The DOE Mercury Program has been a huge success, spurring development, demonstration, and commercialization of many technologies for the capture of mercury.

The future research needs for mercury control include improved sorbent-flue gas contact, development of poison-resistant sorbents and catalysts, new scrubber additives for retention of mercury within wet flue gas desulfurization

(WFGD) systems, concrete-friendly activated carbons, new continuous measurement methods, by-products research, and development of an ASTM standard laboratory test for sorbent activity for mercury capture.

This book aims to cover the technologies for mercury capture and measurement from coal-derived flue gas. The fate of mercury in the environment, a great motivation for the regulations, research, development, and commercialization of capture and measurement methods, is covered in Chapter 1. The trace elements in coal are detailed in Chapter 2. In addition, the regulatory issues, both in the United States and internationally, are discussed in Chapters 3 and 4. Methods for the detection of mercury in flue gas are covered in Chapters 5 and 6. Later chapters discuss the many methods for mercury control, the various research programs, activated carbon technologies, the cement industry, gasification, mercury carbon surface chemistry, and modeling.

I thank Constance and Henry for their outstanding efforts in making this book become a reality. Constance and Henry took my crude initial outline for the book and greatly improved it. Tom Feeley deserves many thanks for the great success of the DOE Mercury Program, and for supporting our in-house research on flue gas. Gary Stiegel and Jenny Tennant from DOE have been terrific in supporting our efforts in understanding the trace elements in gasification systems. Our authors and colleagues Constance Senior, Henry Pennline, Larry Monroe, Leonard Levin, Allan Kolker, Jeff Quick, Leslie Sloss, Nick Hutson, Denny Laudal, Carrie Yonley, Tom Feeley, Ramsay Chang, Tom Gale, Brian Higgins, April Sibley, Gary Blythe, Joe Wong, Nick Lentz, Sharon Sjostrom, Rob Nebergall, Behrooz Ghorshi, Ed Olson, Karen Uffalussy, Jennifer Wilcox, and Steve Niksa did an outstanding job. They are the leading figures in the mercury capture research, development, demonstration-commercialization communities; and are also terrific colleagues and friends. Some of our authors have been working on the mercury issue for over 20 years.

Finally, I thank Phil and Rita Granite, for interest in mercury, suggestions over the years for techniques for mercury control, and for being terrific parents. The same thanks also go to my brother Larry Granite at Environmental Protection Agency (EPA). Linda Granite has humored me, feigning interest in mercury while we were dating (I bent her ears with papers on sorbents and photochemical removal of mercury on our first date – a steak dinner; despite this she went out with me again!), and has been an angel through the years as my mind is sometimes elsewhere on the topic of mercury. Linda and our daughters Ana and Marissa Granite always provide inspiration.

October 2014

*Evan Granite
Pittsburgh, PA*

List of Abbreviations

ACI	Activated carbon injection
APCD	Air pollution control device
APH	Air preheater
BAT	Best available technique or technology
BEP	Best environmental practice
CAMR	Clean air mercury rule
CEMS	Continuous emission monitoring system
CFBC	Circulating fluidized bed combustor
CSAPR	Cross-states air pollution rule
CS-ESP	Cold-side ESP
DOE	Department of Energy
DSI	Dry sorbent injection
EC	European Commission
ECN	Economizer
EGU	Electricity generating unit
ELV	Emission limit value
EPA	Environmental Protection Agency
EPRI	Electric Power Research Institute
ESP	Electrostatic precipitator
ESPC	Cold-side electrostatic precipitator
ESPh	Hot-side electrostatic precipitator
EU	European Union
FBC	Fluidized bed combustor
FF	Fabric (or baghouse) filter
FGD	Flue gas desulfurization
GHSV	Gas hourly space velocity
HAP	Hazardous air pollutant
HELCOM	Helsinki Commission
ICI	Industrial, commercial, and institutional
ICR	Information collection request
IED	Industrial Emissions Directive
IPPC	Integrated pollution prevention and control
L/G	Ratio of volumetric flowrates of liquid to gas in WFGD

LCPD	Large Combustion Plant Directive
LNB	Low NO _x burner
LOI	Loss on ignition
LRTAP	Long-range transboundary air pollution
MATS	Mercury and air toxics standards
MEPOP	Mercury and persistent organic pollutants
MW	Megawatt
NARAP	North American regional action plan
NEPM	National Environmental Protection Measures (Australia)
NERP	National Emission Reduction Plan
NETL	National Energy Technology Laboratory
NHMRC	National Health and Medical Research Council (Australia)
NPI	National Pollutants Inventory
OFA	Overfire air
OSPAR	Oslo and Paris Commission
PAC	Powdered activated carbon
PCD	Particulate control device
PM	Particulate matter
SCEM	Semi-continuous emissions monitor
SCR	Selective catalytic reduction
SDA	Spray dry absorber for flue gas desulfurization
SED	Solvent Emissions Directive
SNCR	Selective non-catalytic reduction
SO ₂	Sulfur dioxide
TOXECON	Advanced sorbent injection configuration licensed by EPRI
UBC	Unburned carbon
UNECE	United Nations Economic Commission for Europe
UNEP	United Nations Environment Programme
WFGD	Wet flue gas desulfurization
WID	Waste Incineration Directive
XAFS	X-ray absorption fine structure
XPS	X-ray photoemission spectroscopy

Part I
Mercury in the Environment: Origin, Fate, and Regulation

1

Mercury in the Environment

Leonard Levin

1.1 Introduction

Mercury is a naturally occurring chemical element found ubiquitously throughout both the natural and human environments. Mercury occurs throughout the earth's crust and is most commonly found in its geological occurrence as the mineral cinnabar (mercuric sulfide, HgS_2). Elemental mercury, the uncombined form, occurs at room temperature and sea level pressure as a liquid, the only chemical element so occurring. Due to its relatively high vapor pressure, liquid mercury will evaporate readily into the atmosphere.

Elemental mercury can be oxidized to the mercurous (Hg^{1+}) or mercuric (Hg^{2+}) inorganic form in the presence of hydroxyl radicals, ozone, or a number of other oxidizing agents. The more commonly occurring mercuric form readily recombines into either water-soluble forms, such as with halogens (e.g., HgCl_2), or insoluble salts (HgS_2).

Surface exposure of geological mercury minerals or elemental mercury concentrations led to the presence of both elemental and inorganic mercury in the global atmosphere, even prior to its enhanced release due to human activity after the onset of the Industrial Revolution (mid-eighteenth century). Indeed, this ubiquity of mercury, and its uptake by fauna via leaf stomata and root systems, leads to its association with fossil fuels such as oil and coal. These fuels derive from burial and metamorphosis of plant matter under anoxic conditions via stages starting with peat formation. Core sampling of peat formations in Arctic Canada by Givelet *et al.* [1] has shown transitory excursions of mercury deposition dating from before 1700 CE attributed to wildfires set by First Nations for land clearing.

One feature of interest to investigators is the relative increase in abundance of mercury in the environment from the pre-Columbian era to the present day, due to human mobilization of the substance. This mobilization has occurred in several ways, but primarily through either direct use of mercury in products or via combustion-related emissions of fuel-associated mercury. The use of elemental mercury in medical and consumer products has occurred over hundreds of years, in such instances as the forming of pelts and felts into chapeaux and

its use in electric switches. Fuel-associated mercury continues to be released globally in the production of power, space and process heat, process steam, and other uses.

This relative increase in global mercury cycling in the modern era can be determined by comparing mercury concentrations at both deep and shallow depths in cores of glacial ice or lake sediments, or by comparing global source inventories of mercury. In the case of inventory comparisons, the modern: preindustrial ratios are derived from separately calculating emission rates from undisturbed natural background sources (exposed mercuriferous deposits, surface, and undersea volcanism) with the total of those sources and human sources (atmospheric evasion from inactive mining sites, mineral recovery sites, point and area fuel combustion sources, and waste sites).

Each such method has both advantages and disadvantages. Core samples can represent localized conditions (e.g., lensing of lake sediments), while global inventories are subject to large uncertainties due to spatial scaling of local measurements, inaccurate extrapolation to unmeasured sources, and so on. Generally, results indicate that, globally, there is roughly three to four times as much mercury cycling through the biogeochemical and human environment currently as there was in pre-Columbian times (see Figure 1.1) [2]. This modern: preindustrial ratio, however, is a global average. There are many individual experimental samples in ice cores, peat bogs, lake-bottom sediments, and other environments globally exhibiting much higher ratios. For example, Schuster *et al.* [3] found a 20-fold enhancement ratio in ice core data from the Lower Fremont Glacier, Wind River Mountains, Wyoming, USA.

The atmospheric lifetime of vapor-phase elemental mercury is believed to be roughly 7–12 months, in bulk, although the mean lifetime of reactive oxidized mercury is more likely measured in days to weeks. Atmospheric oxidized mercury may undergo chemical reduction to the insoluble gaseous elemental form, or may be removed from the atmosphere by solution in precipitation or by dry deposition to the earth's surface.

Mercury concentrations in the planetary boundary layer appear to react to changes in global input within months to years (see, for example, [5]). There is a much longer period for aquatic systems to fully react to changes in mercury input via deposition and runoff, but this is somewhat dependent on the trophic depth of the ecosystem involved. Large piscivorous fish represent multiyear mercury reservoirs whose body burden of mercury (primarily as methylmercury) acts as multiyear transfers of an integrated record of mercury exposure from their feeding patterns.

1.2

Mercury as a Chemical Element

Mercury is a chemical element (atomic number 80, isotope-weighted atomic mass 200.59 amu) known as a *distinct substance* since the earliest days of civilization.

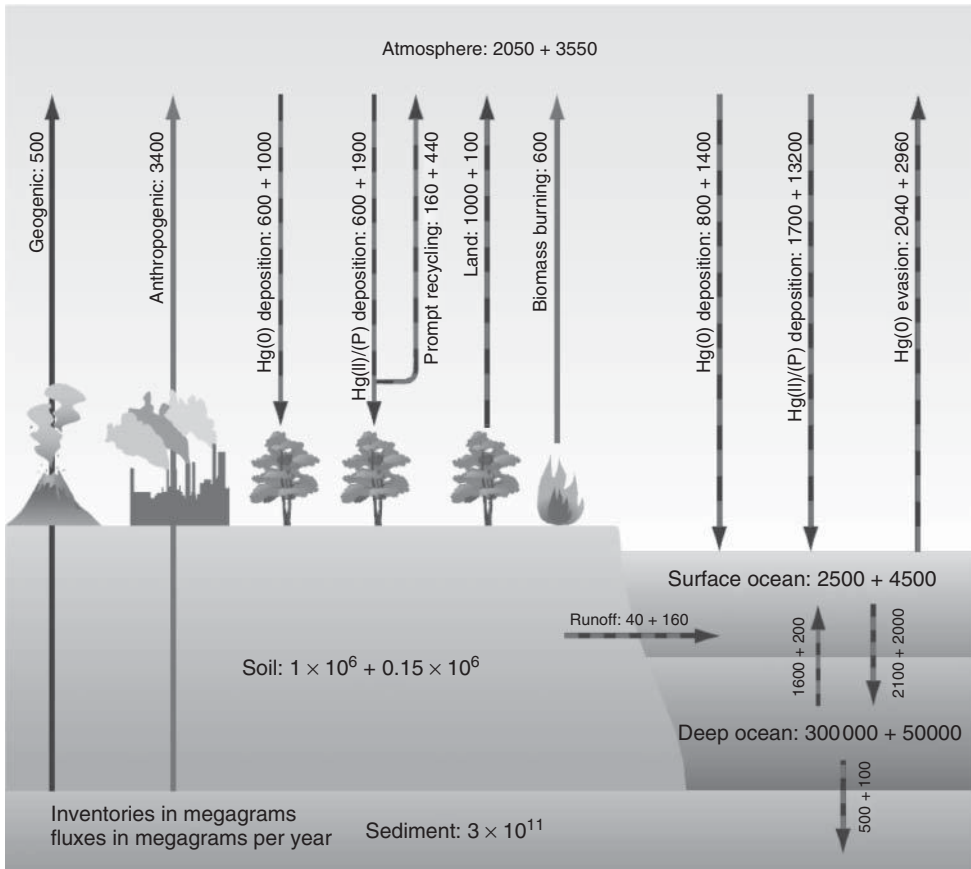


Figure 1.1 Global biogeochemical cycle for mercury. Natural (preindustrial) fluxes (megagrams (Mg) per year) and inventories, in megagrams, are noted in black. Anthropogenic contributions are in gray. Natural fluxes augmented by anthropogenic activities are noted by gray-and-black dashed lines.

(Modified from Selin *et al.* [4].) A mean enrichment factor of 3 between the preindustrial and present-day mercury deposition, based on remote sediment cores, is used as a constraint. (Figure from Selin [2] © 2009 by Annual Review.)

The Greek word for mercury, $\Upsilon\delta\rho\rho\alpha\rho\gamma\upsilon\rho\sigma$, means “water + silver.” This was adapted into the Latin *hydrargyros*, for “water–silver.” Both terms refer to the morphology of pure elemental mercury at room temperature, a silvery liquid, and the only chemical element occurring in pure form as a liquid at ambient temperatures.

The abundance of naturally occurring stable isotopes of mercury is shown in Table 1.1 [6]. In addition, several unstable isotopes of mercury are known. One of these, ^{203}Hg , is commonly used as a spiked tracer in, for example, experiments on mercury methylation in aquatic systems [7].

Table 1.1 Background natural abundance of stable mercury isotopes.

Isotope	¹⁹⁸ Hg	¹⁹⁹ Hg	²⁰⁰ Hg	²⁰¹ Hg	²⁰² Hg	²⁰⁴ Hg
Abundance (%)	10	17	23	13	30	7

1.2.1

Physical and Chemical Properties of the Forms of Mercury

A key variable of mercury and its chemically combined forms is its vapor pressure. The vapor pressure is of interest because one form of transference of mercury from the earth's surface to the overlying atmosphere is evasion, or net positive flux into the atmosphere [8].

1.2.2

Associations with Minerals and Fuels

Mercury is typically found in association with fossil fuels: coal, petroleum, and natural gas. Mercury associated with coal deposits ranges globally from 0.02 to 1.0 ppmw [9]. This range is similar to that found for the occurrence of mercury in background topsoil samples (<0.01–4.6 ppmw, [10]). Mercury association with coal is thought to be via diagenesis in coalbeds [11, 12]: during metamorphic processes, inclusions of pyritic minerals into coalbed fracture zones have brought with them mercury inclusions. This is in opposition to the obvious association of naturally occurring atmospheric mercury in surface vegetation later incorporated into sedimentary precursors to coalbed seams. The pyritic association of mercury in coal is primarily evident in bituminous and anthracite seams, while subbituminous and lignite coals tend to have mercury associated with organic constituents, perhaps the remnant of mercury ligands in surface vegetal deposits. The pyrite association is borne out by concentration enrichments of $\sim \times 100$ in analyses of pyrites from coal versus the concentrations in whole coal samples.

1.3

Direct Uses of Mercury

Mercury in medical treatment: Mercury in various chemical forms has long served as an artisanal medical treatment. Although liquid mercury is still used in scattered applications in the United States, it was more widely used in the early twentieth century for treatment of venereal disease; one documented example is the syphilis treatment of Karen Blixen ("Isaac Dinesen," *Out of Africa*) in Kenya by prescription of mercury pills [13]. Chinese herbal balls, with recommended doses of two balls swallowed per day, have been found to have mercuric sulfide added to

Table 1.2 Total mercury sold in pumps in the United States (pounds).

2001 Total mercury	2004 Total mercury	2007 Total mercury
12 745 (6.4 ton)	13 911 (7.0 ton)	10 383 (5.2 ton) ^{a)}

a) <http://www.newmoa.org/prevention/mercury/imerc/factsheets/pumps.cfm#4>
Source: NEWMOA [19].

their composition [14]. The daily dose of mercury can amount to 1200 mg. For a 70 kg consumer, this dose is equivalent to nearly 200 000 times the Environmental Protection Agency (EPA) mercury Reference Dose of $0.1 \mu\text{g kg}^{-1} \text{day}^{-1}$. More common uses of mercury have been in medical devices such as thermometers and sphygmomanometers; in the latter case, replacement of these devices where mercury is employed by aneroid or digital versions has produced problematic intercomparisons of readings [15].

Mercury in products: Mercury, particularly elemental mercury in liquid form, has often been directly used in consumer and industrial products and processes. In the United States, this was particularly the case for its use in batteries and switches [16]. Another common use was as a conductor in quiet mercury switches, which were commonly used in natural gas and petroleum distribution lines [17]. These uses have dropped significantly in recent years (Table 1.2). One of the last remaining large consumer uses for mercury is in fluorescent lamps, including compact fluorescent lamps (CFLs), each of which typically contains several milligrams of mercury [18].

1.4

Atmospheric Transport and Deposition

The concentration of mercury in ambient air is on the order of 1–5 ppt. Most of this occurs as gaseous elemental mercury (GEM), especially above the atmospheric boundary layer, although trace levels of the divalent form and even methylmercury have been measured [20]. A recurring public fallacy is that, as mercury is classified as a “heavy metal,” [21, 22], the substance “falls out of the sky” quickly upon being emitted to the atmosphere. Because the mercury from heated elevated sources disperses in the atmosphere, gravitational settling at the atomic or molecular level does not play a role in mercury dynamics – except for particulate-bound mercury (Hgp, primarily HgII bound to crustal and combustion particles), where particle deposition velocities do play a role. The high vapor pressure of elemental mercury serves to disperse it widely so that atmospheric turbulence keeps GEM in the atmosphere for a lifetime of 7–16 months (e-folding time). This long lifetime in the free troposphere classifies mercury, particularly elemental mercury, as a global pollutant [23].

1.5

Atmospheric Reactions and Lifetime

Mercury released to the atmosphere from natural sources, such as volcanoes or mercuriferous crustal deposits, is generally in the form of elemental mercury (Hg^0), commonly termed *gaseous elemental mercury* in its atmospheric occurrence. Anthropogenic emissions are, in general, a mix of GEM and divalent mercury (Hg^{II}), referred to as *reactive gaseous mercury* or *RGM* in its atmospheric occurrence. The lifetime of mercury species in the atmosphere is bounded by the reaction and removal rates of the two primary species, GEM and RGM. The oxidation of GEM to RGM by ozone, O_3 , has been studied by many investigators. An important removal mechanism for RGM is due to its relatively high solubility in precipitable water. Calvert and Lindberg [24] concluded that the single-stage reaction $\text{Hg} + \text{O}_3 \rightarrow \text{HgO} + \text{O}_2$ was less likely to occur than an intermediary unstable molecule HgO_3 , decaying to OHgOO , and then decomposing into $\text{HgO} + \text{O}_2$. Further removal reactions have been investigated; one such process, the oxidation of Hg^0 by hydroxyl radical, OH , was found by Goodsite *et al.* [25] to be a relatively unimportant step.

The atmospheric lifetime (average residence time) of GEM is normally assumed to be 7–15 months. Work by Selin *et al.* [4] tried to refine these numbers into the contributing factors: removal by dry deposition; oxidation to RGM by homogeneous- and heterogeneous-phase reactions in the atmosphere; additions by reduction reactions of RGM in the upper troposphere/lower stratosphere (UTLS); and evasion of GEM from surface reservoirs. Each of these processes is still poorly understood, particularly the subsidence and transport of UTLS mercury forms. The reservoir of RGM just above the tropopause plays an important role in nighttime subsidence peaks of RGM in the lower troposphere [26] and in Arctic mercury depletion events (AMDEs) [27].

1.6

Mercury Biogeochemical Cycling

Once deposited to the earth's surface, mercury may undergo a complex series of reactions that may result in one or more steps in its biogeochemical cycling: being re-evaded to the atmosphere, bound to organic compounds in the terrestrial understory; dissolved in seawater and removed by binding to marine "snow" [28].

One important study of mercury dynamics in an aquatic watershed was the Mercury Experiment to Assess Atmospheric Loading in Canada and the United States (METAALICUS) experiment [29]. During the METAALICUS experiment, solutions of mercuric chloride, each "tagged" with elevated concentrations of a different naturally occurring stable isotope of mercury, were deposited in segments of a test watershed in Ontario, Canada. This isotope spiking allowed tracing of the rate and partitioning of mercury introduced into each watershed compartment to be traced over both time and space. The isotope spikes were introduced into the

upland and wetland compartments as simulated precipitation: using fixed-wing aircraft, solutions of isotope-spiked HgNO_3 were distributed over each compartment just prior to or during periods of rainfall in the area. The wetland and upland spikes were added yearly for 3 years. The waterbody spike was applied by a small boat cruising a crisscross pattern on the lake itself; the water surface applications occurred every 2 weeks during the open-water seasons.

METAALICUS results from the first 3 years of the study showed that mercury movement from the application compartments (surfaces of wetlands, uplands, and waterbody) to sequestration in soils and sediments, respectively, was still underway at the end of the application period. Upland spike mercury was, by that time, preferentially found (areal mass distribution) in the underlying soil, but still progressing from the surface vegetation exposed to the original spike application. Wetland spike mercury exhibited the opposite distribution: that addition was still predominantly in the lowlands vegetation than in the underlying peat. Overall, there was a 2–5% increase in peat, soil, and sediment mercury concentrations from the 3 years' additions.

Lake water column mercury showed an overall 53% increase in concentration due to the introduction of the lake spike itself, while the upper layer of lake-bottom sediments revealed a 5% concentration increase. Since Lake 658 communicates with an adjacent shield lake via a narrow weired outflow, a 5% portion of the spike was itself lost through the outflow. The researchers estimated that 25–30% of the wetland and upland spikes, and 45% of the lake spike, were lost to the atmosphere via evasion over the 3-year period.

The METAALICUS findings are significant in several regards. As the only whole-ecosystem mercury study to date, the experiment demonstrates once more the relatively slow response of lake bodies to changes in atmospheric deposition. The authors conclude that lakes receiving all of their new mercury via deposition, such as perched seepage lakes, might respond to step changes in deposition (such as were simulated by the spike additions) over about a decade; that is, a proportional change in water column mercury to the deposition step would require that period of time to be reached. For drainage lakes, a longer adjustment period can be expected.

Additionally, the findings concerning evasion losses are a critical experimental check on assumptions used in mercury modeling. Generally, regional and global models of mercury assume a prompt re-emission of 50% of deposited mercury (see, e.g., [30]). This re-emitted or evaded mercury is the primary contributor to what is generally termed the *grasshopper effect* [31]: successive deposition and re-emission of mercury from lower to higher latitudes (down-gradient transport), leading to a successive and relatively high build-up rate of mercury (and other pollutants) in high temperate and boreal regions. The experiment at Lake 658 reveals that this effect is probably dominated by evasion from oceans and water bodies rather than terrestrial environments, and so is limited by the sum of deposition to and native mercury emissions from those marine and aquatic environments.

References

- Givelet, N., Roos-Barracough, F., Goodsite, M.E., Cheburkin, A.K., and Shotyk, W. (2004) Atmospheric mercury accumulation rates between 5900 and 800 calibrated years BP in the high arctic of Canada recorded by peat hummocks. *Environ. Sci. Technol.*, **38**, 4964–4972.
- Selin, N.E. (2009) Global biogeochemical cycling of mercury: a review. *Annu. Rev. Environ. Resour.*, **34**, 43–63.
- Schuster, P.F., Krabbenhoft, D.P., Naftz, D.L., Cecil, L.D., Olson, M.L., Dewild, J.F., Susong, D.D., Green, J.R., and Abbott, M.L. (2002) Atmospheric mercury deposition during the last 270 years: a glacial ice core record of natural and anthropogenic sources. *Environ. Sci. Technol.*, **36**, 2303–2310.
- Selin, N.E., Jacob, D.J., Yantosca, R.M., Strode, S., Jaeglé, L., and Sunderland, E.M. (2008) Global 3-D land-ocean-atmosphere model for mercury: present-day versus preindustrial cycles and anthropogenic enrichment factors for deposition. *Global Biogeochem. Cycles*, **22**, GB2011.
- Slemr, F., Brunke, E.-G., Ebinghaus, R., Temme, C., Munthe, J., Wängberg, I., Schroeder, W., and Steffen, A. (2003) Worldwide trend of atmospheric mercury since 1977. *Geophys. Res. Lett.*, **30** (10), 1516. doi: 10.1029/2003GL016954
- Roesmer, J. (1970) *Radiochemistry of Mercury*, National Academy of Sciences, Washington, DC.
- Gilmour, C.C. and Riedel, G.S. (1995) Measurement of Hg methylation in sediments using high-specific activity Hg-203 and ambient incubation. *Water Air Soil Pollut.*, **80**, 747–756. doi: 10.1007/BF01189726
- Denkenberger, J.S., Driscoll, C.T., Branfireun, B.A., Eckley, C.S., Cohen, M., and Selvendiran, P. (2012) A synthesis of rates and controls on elemental mercury evasion in the Great Lakes Basin. *Environ. Pollut.*, **161**, 291–298.
- Zheng, L., Liu, G., and Chou, C.-L. (2007) The distribution, occurrence and environmental effect of mercury in Chinese coals. *Sci. Total Environ.*, **384** (1–3), 374–383.
- Shacklette, H.T. and Boerngen, J.G. (1984) *Element Concentrations in Soils and Other Surficial Materials of the Conterminous United States*. U.S. Geological Survey Professional Paper 1270, Reston, VA.
- Larsen, G. and Chilingar, G.V. (eds) (1983) *Diagenesis in Sediments and Sedimentary Rocks*, vol. 2, Elsevier.
- Yudovich, Y.E. and Ketris, M.P. (2005) Mercury in coal: a review. Part 1. *Geochemistry. Int. J. Coal Geol.*, **62**, 107–134.
- Søgaard, I. (2002) Karen Blixen and her physicians. *Dan. Medicinhist. Arbog*, **2002**, 25–50.
- Espinoza, E.O., Mann, M.-J., and Bleasdel, B. (1995) Arsenic and mercury in traditional Chinese herbal balls. *N. Engl. J. Med.*, **333**, 803–804.
- O'Brien, E. (2000) Replacing the mercury sphygmomanometer : Requires clinicians to demand better automated devices. *Br. Med. J.*, **320** (7238), 815–816.
- Engstrom, D.R. and Swain, E.B. (1997) Recent declines in atmospheric mercury deposition in the upper midwest. *Environ. Sci. Technol.*, **31**, 960–967.
- NEWMOA (2008) *Trends in Mercury Use in Products*, Northeast Waste Management Officials' Association (NEWMOA)/IMERC. www.newmoa.org, (accessed June 2008).
- Stemp-Morlock, G. (2008) Mercury: cleanup for broken CFLs. *Environ. Health Perspect.*, **116** (9), A378.
- NEWMOA (2010) NEWMOA (2010), "IMERC Fact Sheet/Mercury Use in Pumps", <http://www.newmoa.org/prevention/mercury/imerc/factsheets/pumps.cfm#4>
- UNEP (2013) *Global Mercury Assessment 2013: Sources, Emissions, Releases and Environmental Transport*, UNEP Chemicals Branch, Geneva.
- Counter, S.A. and Buchanan, L.H. (2004) Mercury exposure in children: a review. *Toxicol. Appl. Pharmacol.*, **198**, 209–230.

22. Neustadt, J. and Pieczenik, S. (2007) Heavy-metal toxicity—with emphasis on mercury. *Integr. Med.*, **6**, 2.
23. Driscoll, C.T., Mason, R.P., Chan, H.M., Jacob, D.J., and Pirrone, N. (2013) Mercury as a global pollutant: sources, pathways, and effects. *Environ. Sci. Technol.*, **47** (10), 4967–4983.
24. Calvert, J.G. and Lindberg, S.E. (2005) Mechanisms of mercury removal by O₃ and OH in the atmosphere. *Atmos. Environ.*, **39**, 3355–3367.
25. Goodsite, M.E., Plane, J.M.C., and Skov, H. (2004) A theoretical study of the oxidation of Hg⁰ to HgBr₂ in the troposphere. *Environ. Sci. Technol.*, **38**, 1772–1776.
26. Lyman, S.N. and Jaffe, D.A. (2011) Formation and fate of oxidized mercury in the upper troposphere and lower stratosphere. *Nat. Geosci. Lett.*, **5**, 114–117, doi: 10.1038/NCEO1353.
27. Durnford, D. and Dastoor, A. (2011) The behavior of mercury in the cryosphere: a review of what we know from observations. *J. Geophys. Res.*, **116**, D06305. doi: 10.1029/2010JD014809
28. Sunderland, E.M., Krabbenhoft, D.P., Moreau, J.W., Strode, S.A., and Landing, W.M. (2009) Mercury sources, distribution, and bioavailability in the North Pacific Ocean: insights from data and models. *Global Biogeochem. Cycles*, **23**, GB2010. doi: 10.1029/2008GB003425
29. Harris, R.C., Rudd, J.W.M., Amyot, M., Babiarz, C.L., Beaty, K.G., Blanchfield, P.J., Bodaly, R.A., Branfireun, B.A., Gilmour, C.C., Graydon, J.A., Heyes, A., Hintelmann, H., Hurley, J.P., Kelly, C.A., Krabbenhoft, D.P., Lindberg, S.E., Mason, R.P., Paterson, M.J., Podemski, C.L., Robinson, A., Sandilands, K.A., Southworth, G.R., St. Louis, V.L., and Tatem, M.T. (2007) Whole-ecosystem study shows rapid fish-mercury response to changes in mercury deposition. *Proc. Natl. Acad. Sci. U.S.A.*, **104**, 42.
30. Lohman, K., Seigneur, C., Gustin, M., and Lindberg, S. (2008) Sensitivity of the global atmospheric cycle of mercury to emissions. *Appl. Geochem.*, **23**, 454–466.
31. UNEP Chemicals Branch (2008) *The Global Mercury Atmospheric Mercury Assessment: Sources, Emissions, and Transport*, UNEP Chemicals, Geneva.

2

Mercury and Halogens in Coal

Allan Kolker and Jeffrey C. Quick

2.1

Introduction

2.1.1

Mode of Occurrence of Mercury (Hg) in Coal

In bituminous coals, the iron disulfide, pyrite and its FeS_2 polymorph, marcasite, typically host the greatest fraction of Hg present [1–8], with lesser fractions of Hg associated with organic matter and with non- FeS_2 mineral hosts. Evidence for the occurrence of Hg and other trace metals in Fe disulfides in coal is reviewed by Kolker [9], including crystal chemistry and controls on element substitution in Fe disulfides and available data on Hg concentrations from direct determinations by microanalysis. In cases where individual Fe disulfide grains in coal have been analyzed, Hg contents are in the tens to hundreds of times those in the whole coal. But assuming that pyrite-rich coals are necessarily Hg-rich coals is an oversimplification. A good example to the contrary is the U.S. bituminous Illinois #6 coal. This commercially important coal has relatively high contents of total and pyritic sulfur widely attributed to marine influence, but low to moderate Hg (and As) contents [10–12], as the extent of substitution in Illinois #6 pyrite by impurities is relatively small [7, 12–14].

In low-rank coals, including lignite and subbituminous coals, Hg and S contents are generally lower overall than in bituminous coals, and the proportion of Hg occurring in association with organic material is greater [2, 15]. From the standpoint of Hg capture, compared to bituminous coals, the lower overall Hg content of low-rank coals is offset by the tendency of these coals to also have lower halogen contents, and, because of their lower calorific value, the requirement that greater amounts of low-rank coal are needed to achieve an equivalent energy output.

As shown elsewhere in this volume, the form of Hg in feed coal does not impact Hg speciation at boiler temperatures. In the furnace, Hg is present in the elemental form but it can combine to form compounds as the flue gas cools. Knowledge of the mode of occurrence of Hg in coal has important implications for the extent to

which pre-combustion Hg control might be possible (following section), whereas the halogen species present influence post-combustion Hg capture.

2.1.2

Effectiveness of Pre-Combustion Mercury Removal

Three approaches, coal preparation, selective mining, and upgrading low-rank coals by drying, offer the potential to reduce Hg input to the boiler. A detailed review of each is beyond the scope this chapter, but some of the major factors influencing the effectiveness of pre-combustion removal are highlighted in this section.

For coal preparation, the major factors influencing its effectiveness in Hg reduction are the mode of occurrence of Hg in coal, its particle size, and the approach taken in preparation. For bituminous coals having pyrite as the primary mineralogic host of Hg, preparation by density separation, such as in a heavy media cyclone, is more likely to be effective than methods that depend on differences in surface characteristics, such as froth flotation, because coal and pyrite have similar surface characteristics [16, 17]. Grain size is especially important in multi-stage preparation circuits because gravity concentration is the dominant cleaning method for coarse and intermediate size fractions of coal, whereas flotation is the dominant method for cleaning fine size fractions [18]. Where pyrite occurs primarily as framboids, their fine grain size (typically 10 μm) and presence of interstitial voids filled with non-pyrite material may make them especially difficult to remove by coal preparation. Low-rank coals having a greater fraction of organically bound Hg than bituminous coals are also less likely to be responsive to coal preparation for Hg reduction. Recent studies by Wang *et al.* [19, 20] show significant degrees of removal of Hg and/or associated elements in large-scale preparation plants processing Chinese coals. Huggins *et al.* [14] determined element concentrations, and modes of occurrence by spectroscopic methods, for a range of major and trace elements in fractions of an Illinois #6 coal produced by physical separation at a preparation plant. For Hg, results show a 25% reduction on a weight concentration basis for the cleaned product relative to the feed coal, with corresponding enrichment in the reject fractions. These investigations follow from previous work showing the effectiveness of coal preparation in reducing air toxics as a co-benefit to reducing ash and increased calorific value (e.g., [21–24]).

Effective reduction of Hg by selective mining requires characterization and analysis of the coal beds being mined. This approach has been used to better define the spatial distribution of Hg variation in bituminous coals of the Illinois Basin in Indiana, USA [25, 26], in the Appalachian Basin of eastern Kentucky, USA [27, 28], and in subbituminous coals of western Canada [29]. Where Hg is concentrated by geologic processes, such as along fault-controlled zones of mineralization, or controlled stratigraphically, such as by incursion of marine waters, detailed characterization can be effective in delineating Hg-rich zones to avoid in mining operations.

Various thermal pretreatment processes have been proposed or are in place for low-rank coals, for the purpose of enhancing power plant performance [30–32]. Thermal pretreatment can have the co-benefit of Hg reduction, as reported by Merriam [33] for a Powder River Basin subbituminous coal and subsequently, by Guffey and Bland [34], for a Powder River Basin coal, and a North Dakota lignite. These studies show Hg removals in the 70–80% range with heating of both coals to temperatures ranging from 150 to 290 °C. Mercury driven from these coals primarily enters the gas stream of the process.

2.1.3

Methods for Mercury Determination

Sub-parts per million levels of Hg in coal require methods with adequate sensitivity, but generally do not require the most sensitive methods used for low-level determinations of Hg in the environment ([35], this volume). The two methods most widely employed for analysis of Hg in coal are cold vapor atomic absorption spectrometry (CVAA; [36, 37]), and thermal decomposition, amalgamation, and atomic absorption spectrophotometry, otherwise known as direct mercury analysis (DMA; [38]). Mercury concentrations normally encountered in coal are well within the working range of either method. DMA has gained acceptance in recent years because sample digestion, required in CVAA analysis, is not necessary. In U.S. Geological Survey (USGS) databases discussed in this chapter, Hg data obtained before about 2005, including coal quality (COALQUAL) [11] were obtained by CVAA. Results for international coals in the World Coal Quality Inventory (WoCQI, [39]) include data obtained by both methods, depending on the date of sample acquisition.

Other methods that have been used to determine Hg in coal include instrumental neutron activation analysis (INAA; [10, 40]) and cold vapor atomic fluorescence spectrometry (CVAFS; [41]). INAA can be used directly on small samples, but requires sample irradiation by neutrons at a reactor facility and subsequent counting of gamma rays emitted at the energies of radionuclides present [40]. CVAFS offers better detection limits than either CVAA or DMA, with the potential to obtain higher precision total Hg results than by the other two methods. However, CVAFS has not been widely employed because low-level determinations in the parts per billion range are generally not required for coal. Furthermore, because total mercury contents are controlled to a large degree by Fe disulfide minerals, sample heterogeneity, especially in pyrite content, can result in total Hg variations for different sample splits that are larger than analytical uncertainties by CVAFS. Other methods for Hg analysis of coal have been used in specific applications. For example, multicollector inductively coupled plasma mass spectrometry (ICP-MS) methods with cold vapor Hg generation have been used in recent studies to determine variations in the natural Hg isotopic composition of coal [42, 12]. Synchrotron-based determinations of element speciation by X-ray absorption fine structure (XAFS), which have been very useful for As in coal, have limited applicability for Hg as only the most unusually Hg-rich coals

have sufficient Hg to apply this method (F.E. Huggins, personal communication, 2012) [43].

2.2

Mercury in U.S. Coals

2.2.1

U.S. Coal Databases

Three large databases, described here, and several smaller ones, provide detailed information on the Hg contents of U.S. coals. These are (i) the 1999 U.S. Environmental Protection Agency (EPA) Information Collection Request (ICR) database [44], (ii) the 2010 EPA Utility MACT ICR (MACT, maximum achievable control technology) [45, 46], and (iii) an extensive USGS database known as COALQUAL [11]. Each database provides coverage for a wide range of U.S. commercial coals, but with somewhat different emphases. The two EPA databases emphasize Hg contents of coals delivered to U.S. utility power stations, whereas the COALQUAL database reflects the composition of coal in the ground. As noted by Quick *et al.* [47], in a comparison of the COALQUAL and 1999 ICR data, sample frequency in these databases is not production weighted and therefore, mean values for each database are not accurate indicators of the Hg content of either in-ground or delivered U.S. coal. The databases nonetheless provide useful comparisons with international coal sample databases in which large numbers of samples are compiled and averaged.

2.2.1.1 USGS COALQUAL Database

The USGS COALQUAL database consists almost entirely of results for coal samples collected or calculated to represent the entire thickness of a coal bed in the ground [48, 11]. The COALQUAL data include analytical results for 7432 coal samples collected from 399 counties in 33 U.S. states. Up to 136 data fields listing the sample type, location, and assay results are included for each sample record. Nearly all records have complete proximate and ultimate assays as well as major, minor, and trace-element values. Excluding weathered coal and samples from non-producing counties, COALQUAL contains records for 4566 samples originating from 170 of the 198 counties that produced coal during 2009 (see comparison of databases). Most of the samples were collected as whole-bed or bench samples from working mines. These samples give an arithmetic mean of 0.17 ppm Hg ([48]; Table 2.1), almost twice the mean Hg content in the 1999 EPA ICR for coals delivered to utilities (following section). The difference in mean Hg contents between the USGS and EPA databases is a consequence of (i) COALQUAL data include the portion of Hg that is removed by coal preparation and (ii) compared to current U.S. coal production, in which the Power River Basin is the largest single producer, COALQUAL is weighted heavily toward eastern U.S. bituminous coals, with nearly 60% of its samples from the Appalachian Basin.

Table 2.1 Comparison of mercury, halogen, and trace-metal content of coal samples in the COALQUAL, 1999 ICR, and 2010 ICR data.

	Parts per million, ppm (dry)												
	Cl	F	Hg	Sb	As	Be	Cd	Cr	Pb	Mn	Ni	Se	Co
COALQUAL 4 566 in-ground samples													
Maximum	8 200	4 900	2.90	35.0	2200.0	18.0	150.0	190	1 900	1 100	190.0	150.0	180.0
Average	633	102	0.17	1.3	28.6	2.2	0.19	15	9.2	31	14.6	3.0	6.1
Median	360	60	0.11	0.8	9.4	1.9	0.07	13	5.9	17	12.0	2.4	4.8
Apparent detection limit	140	14	0.02	0.2	0.3	0.2	0.05	1	1.7	2	1.2	0.6	0.7
Number of records	3 161	4 557	4 564	4 555	4 546	4 469	4 559	4 548	4 564	4 561	4 561	4 543	4 545
% below detection limit	29	7	7	5	1	2	29	1	9	1	1	6	2
1999 ICR 37 916 shipment samples													
Maximum	11 000	—	1.30	—	—	—	—	—	—	—	—	—	—
Average	820	—	0.11	—	—	—	—	—	—	—	—	—	—
Median	628	—	0.09	—	—	—	—	—	—	—	—	—	—
Apparent detection limit	50	—	0.02	—	—	—	—	—	—	—	—	—	—
Number of records	37 916	—	37 916	—	—	—	—	—	—	—	—	—	—
% below detection limit	13	—	1	—	—	—	—	—	—	—	—	—	—

(continued overleaf)

Table 2.1 (Continued)

	Parts per million, ppm (dry)												
	Cl	F	Hg	Sb	As	Be	Cd	Cr	Pb	Mn	Ni	Se	Co
2010 ICR part 2 13 968 shipment samples													
Maximum	4 900	300	0.95	5.4	96.7	6.8	14.2	99	77.2	484	161.0	9.9	26.8
Average	980	90	0.12	1.0	9.5	1.5	0.32	16	7.6	29	14.1	2.5	5.5
Median	965	88	0.11	1.0	5.7	1.3	0.14	17	7.1	20	13.7	2.2	5.0
Apparent detection limit	—	—	0.04	1.0	1.0	2.0	0.20	—	2	—	—	1.0	—
Number of records	3 507	994	13 130	901	1 265	845	978	1 031	1 120	914	1 030	1 045	749
% below detection limit	—	—	1	26	5	3	22	0	6	0	0	11	0
2010 ICR part 3 1 590 feedstock samples													
Maximum	3 600	320	0.97	50.9	167.0	2.9	10.2	85	77.3	326	155.7	36.9	42.5
Average	576	74	0.12	1.1	6.7	0.8	0.35	14	7.8	31	11.7	2.4	5.1
Median	355	66	0.08	0.8	3.0	0.5	0.13	10	5.5	16	9.0	1.1	3.4
Apparent detection limit	10	45	0.02	2.0	1.0	1.0	0.40	5	2.0	0.1	10.0	1.0	1.0
Number of records	1 253	1 001	889	684	868	883	877	903	903	912	892	844	798
% below detection limit	7	7	4	48	17	18	44	3	6	3	3	32	11

Bold values — Averages of multiple analyses

COALQUAL: Compiled data exclude weathered coal as well as samples from counties that did not produce coal during 2009. Non-detects are reported in COALQUAL as 0.7 times a detection limit, but the actual detection limit and affected records are not identified. Instead, the percent of affected records for each element (called *qualified* data within COALQUAL) is noted in text that accompanies the data. We used this percent value to identify the apparent detection limit from the corresponding percentile distributions.

1999 ICR: Compiled data exclude non-coal fuels but include waste coal. We estimated the apparent detection limit as the median value of all values reported with a < symbol.

2010 ICR: Compiled data exclude duplicate records and non-coal fuels, but include waste coal. Values annotated with a < symbol were multiplied by 0.5 and included in the compilation. We estimated the apparent detection limit as the median value of results reported with a < symbol. The 2010 ICR part 2 data collection did not identify the Cl and F values that were below detection limits.

Whereas the EPA ICR databases are more representative of current U.S. steam coal production, COALQUAL is nonetheless useful as a reference in comparing U.S. and international coal samples, especially for the in-ground state.

2.2.1.2 1999 EPA ICR

The 1999 ICR coal quality data [44] Originated from an ICR issued by the EPA to inform its Section 112 rulemaking to regulate Hg emissions from electric utility steam generating units. The EPA required units of 25 MW or more to report coal origin, as well as dry-basis tonnages, ash, S, and heating value for every solid fuel shipment received during 1999, and to periodically report fuel Hg and Cl content. This systematic data collection effort produced analyses for 152 476 samples, which are available in four quarterly EXCEL files on an EPA website [44]. Excluding non-coal fuels and records without Hg or Cl values, the 1999 ICR includes results for 37 916 coal samples. Limitations of these data include erroneously low Hg values for most Gulf Coast coal, coal shipments of unknown origin (14% of records), inconsistent reporting bases (8%), and duplicate or nominal data (4%; [49]). Nonetheless, the 1999 ICR data were systematically collected and include coal from most coal-producing counties. Estimates based on the 1999 ICR coal analyses and corresponding emissions testing showed that coal burned in U.S. utility boilers during 1999 contained 75 ton of Hg, of which 48 ton (64%) was emitted to the atmosphere [50].

2.2.1.3 2010 EPA ICR

The 2010 ICR coal quality data originate from an ICR issued by the EPA in 2009 to inform its Mercury and Air Toxics Standards (MATS) rulemaking effort. The data were made available in two ACCESS databases, designated Part II [45] and Part III [46]. Limitations of these data include inconsistent reporting units for trace and minor elements and numerous duplicate records.

The Part II data include analyses reported by U.S. electric utilities for more than 14 000 coal samples. Most of the samples were collected from coal shipments delivered to power plants during 2009 and the corresponding data records include dry-basis ash, S, Hg, and heating values. About 25% of the records also include coal Cl content, and 10% include trace-metal content. Comparison of the Part II data with 2009 EIA-923 data [51] showed that about one-third of the ash, S, and heating values are actually on a moist basis, rather than the dry basis indicated in the Part II database [52]. State origins are listed for most samples and county origins are listed for about half of the samples.

The Part III data include analyses for over 1600 coal samples reported by electric utilities that were selected for mandatory emission testing to inform the MATS rulemaking. These were feedstock samples intended to represent the coal that was burned during the emission testing. Sample collection methods were not noted, but probably included automated or manual sampling from feed belts, as well as grab samples from stockpiles. Most of the data records include analytical results for Hg, Cl, F, and trace metals, and many also include complete proximate and ultimate analyses (moisture, ash, volatile matter, fixed carbon, heating value, C,

H, N, O, and S). The Part III data include numerous coal blends with multiple or uncertain origins. Nonetheless, state origins are listed for about half of the samples and county origins are listed for about a third.

In December 2011, results from the 2010 ICR were used in developing a final rule for MATS that limits emissions of Hg, other non-Hg metal air toxics, including As, Ni, Cr, and Se, as well as acid gasses (HCl, HF; [53]). The health-based rationale for MATS, the events leading to its approval, and the process of its implementation are covered in greater detail by Hutson [54], this volume.

2.2.2

Comparison of U.S. Coal Databases

Table 2.1 compares the halogen and trace-metal content of coal samples in the COALQUAL, 1999 ICR, and 2010 ICR data. Note that the Hg content of coal shipped to utilities (ICR data sets) is lower than the Hg content of the in-ground coal resource (COALQUAL data). This difference is a result of impurities removed from commercial coal during coal washing and selective mining of higher quality coal [47], as well as the greater proportion of Appalachian Basin coals in COALQUAL [11]. Similarly, Table 2.1 shows that delivered commercial coals contain less Sb, As, Be, Pb, and Se than indicated for in-ground coal by COALQUAL.

The lower apparent detection limit for Cl in the 2010 ICR Part III data compared to the 1999 ICR is noteworthy. Because Cl promotes Hg capture, the lower apparent detection limit for Cl should improve prediction of Hg capture for units burning low-Cl coal. Also notable is the relatively large number of Hg analyses in the 2010 Part II data (13 130 records) compared to other trace metals (~1000 records). The abundance of available Hg analyses for coal shipments is likely due to mandatory reporting of coal Hg content on the U.S. Energy Information Administration Form 923 [51]. Although the Hg content of U.S. coal shipments to electric utilities has been reported to the EIA since 2008, these data have not yet been published.

Publication of Hg assays collected with the EIA-923 data should eventually provide an accurate estimate of the Hg content of coal burned at U.S. electric utilities. In the meantime, the Hg content of coal burned at U.S. power plants can be reasonably estimated. This is done by assigning a Hg content to each coal shipment in the EIA-923 data according to the shipment origin using county-average Hg contents from the 1999 ICR [49]. The same estimation can be applied to Cl in coal. The resulting estimates of the Hg and Cl contents of coal shipped to electric utilities during 2009 are compared in Figure 2.1 with Hg contents of samples listed in the COALQUAL, 1999 ICR, and 2010 ICR databases. Heating values, ash yields, and sulfur contents of these databases are also compared. Note the lower ash, S, Cl, and Hg values for the 2009 EIA-923 data, which are weighted by delivered tons, compared to the other data sets. Comparison of the ash and S distributions helps to explain this difference. Figure 2.1 shows that the 2010 ICR coal samples have more S and more ash than coal delivered to U.S. power plants during 2009. This

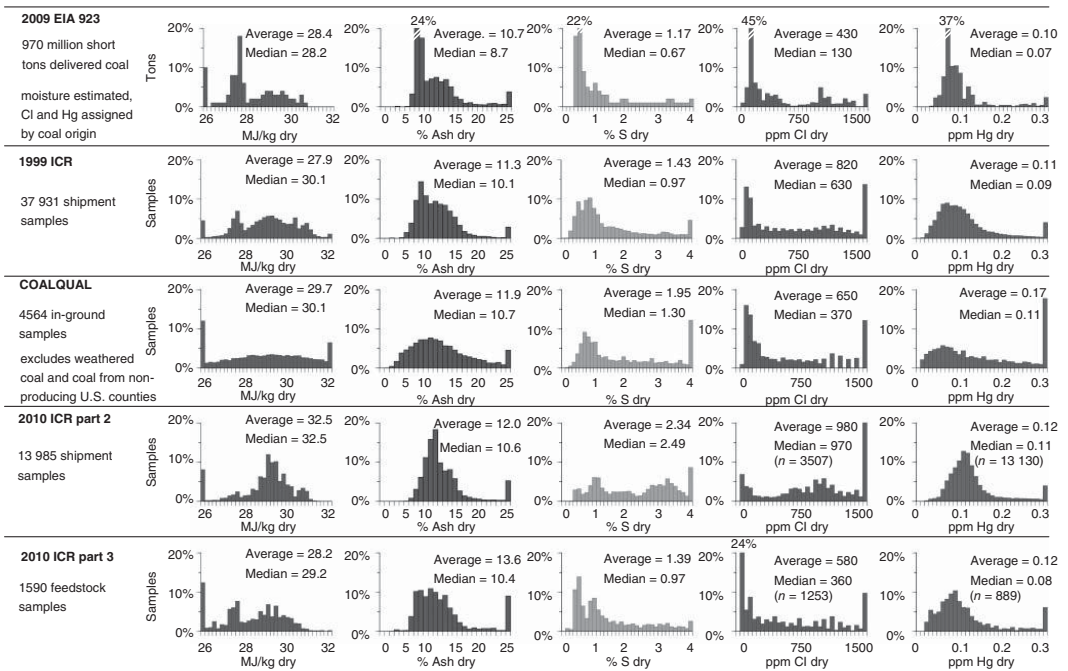


Figure 2.1 Comparison of megajoules per kilogram, ash, S, Cl, Hg distributions for shipped coal tons (EIA 923, 2009) with sample frequency distributions for in-ground (COALQUAL), shipped (1999 ICR; 2010 ICR part 2), and feedstock (2010 ICR part 3) samples. Notably, sample frequency distributions indicate higher ash, S, Cl, and Hg values than the shipped coal tons distributions shown at the top of the figure. Heat and ash values for the 2009 EIA 923 data [51] were adjusted to a dry basis using estimated moisture values, whereas Cl and Hg values were assigned to coal shipment tons by county origin based on compiled 1999 ICR data [49]. The data sets are described in the text. (Modified from Reference [47] Copyright © 2003, Springer.)

is consistent with the higher Hg content for the 2010 ICR coals, given that Hg is associated with pyritic S and is abundant in high-ash waste coal. More importantly, this comparison suggests that like COALQUAL, the 2010 ICR data are not representative of commercial U.S. coal. Consequently, the non-Hg trace-metal content of commercial U.S. coal will likely differ from the values listed in Table 2.1 and remains uncertain. Nonetheless, the 2010 ICR data are unique in that they are publicly available and include trace-element values for a wide range of commercial U.S. coals. Consequently, these data should assist efforts to understand the abundance, behavior, and fate of Hg and other trace metals in coal-derived gas streams.

2.3

Mercury in International Coals

2.3.1

Review of Mercury in Coal in the Largest Coal Producers

China, the United States, and India, listed in order of hard coal production rank, accounted for ~75% of 2010 world coal production [55]. If Australia, South Africa, the Russian Federation, and Indonesia are added, these countries accounted for more than 90% of 2010 hard coal production (Table 2.2). Of the major coal-producing countries, detailed nationwide surveys of Hg distribution are available only for the United States and China, as described below. For countries lacking comprehensive surveys of Hg distribution, brief summaries of available information are given below, together with the possible implications of these results for Hg output from coal combustion. Where applicable, results from the USGS WoCQI [39] are compared to other published results. WoCQI is a publicly available database that contains analyses of 1580 samples from 57 countries, including Hg, Cl, and other relevant coal quality determinations on a dry, whole-coal basis. For China, WoCQI contains 328 samples from 25 provinces

Table 2.2 Production data by country, listed in order of hard coal production (in megatons).^{a)}

	China	United States	India	Australia	South Africa	Russian Federation	Indonesia	Kazakhstan	Poland	Columbia	Others	World total
Hard coal	3162	932	538	353	255	248	173	105	77	74	269	6186
Brown coal	b)	65	33	67	0	76	163	6	57	0	576	1043

a) 2010 data.

b) Brown coal included in hard coal data. Countries shown in bold are discussed in the text.

Source: IEA [55] Copyright © 2011, OECD/IEA.

and autonomous regions, representing an estimated 80% of production at the time of sampling. For major coal producers India, Australia, South Africa, the Russian Federation, and Indonesia, WoCQI sampling is much less complete than for China. For India, Australia, and the Russian Federation, USGS sampling is limited to specific study areas.

2.3.1.1 China

China is both the world's largest producer and user of coal. Recent compilations confirm that Hg concentrations of coals used commercially in China are similar to those used elsewhere [56–59], with nationwide means from studies over the last 10+ years ranging from 0.10 to 0.22 ppm [59]. The most recent compilations show less variability and an overall value for Chinese commercial coal between 0.15 and 0.19 ppm is likely (Table 2.3). For example, Dai *et al.* [58] report a mean of 0.16 ppm Hg for 1666 samples, which is identical to that determined by the USGS (0.16 ppm) for 305 WoCQI samples, excluding 23 samples of prepared coal [60]. Streets *et al.* [56] used a merged dataset of USGS results and available data from the literature to determine a mean for China of 0.18–0.19 ppm. Ren *et al.* [61], as reported by Dai *et al.* [58] give a mean of 0.19 ppm for 1413 samples. A subset of 619 of the Ren *et al.* samples reported by United Nations Environment Programme (UNEP) [62], give a mean of 0.33 ppm where a large proportion (21%) of samples is from Guizhou Province. Zheng *et al.* [57] determined an arithmetic mean of 0.19 ppm for 1699 samples, but with 16% (276) of these from Guizhou Province, compared to only 5% (16 of 305) in the USGS dataset (see next section). Taken together,

Table 2.3 Compilation of results for Hg in Chinese coal (in microgram per gram).

Arithmetic mean (\pm s.d.)	Number of samples	Samples from Guizhou Province	References
0.22 ^{a)}	234	NA	[63]
0.1	1458	NA	[64]
0.19	NA	NA	[56] ^{b)}
0.19	1413	NA	[61] ^{c)}
0.33	619	133 (21%)	[61] ^{d)}
0.16 \pm 0.14	305	16 (5%)	[60]
0.19 \pm 1.22	1699	276 (16%)	[57]
0.154	1123	NA	[65]
0.18 ^{e)}	~900	NA	[66]
0.163	1666	NA	[58]
0.17 (U.S. mean)	7430	—	[11]

NA, not available.

- a) Value calculated from 14 provinces sampled and other published results.
- b) Data include USGS data and other published results merged.
- c) As reported by Dai *et al.* [58] Copyright © 2012, Elsevier.
- d) As reported in Ref. [62] Copyright © 2011, United Nations Environment Programme.
- e) Mean value noted in oral presentation.

Source: After Refs [58, 59, 62] Copyright © 2012, Elsevier; Copyright © 2006, DEStech Publications, Inc.

the result of various compilations of Hg in Chinese coal are comparable to the in-ground mean for U.S. coals (0.17 ppm; [11]) both in concentration value and numbers of samples, but unlike COALQUAL, are probably more representative of current production.

It is apparent in coal Hg compilations for China that some provinces, especially Guizhou, and to a lesser extent Shanxi, and Inner Mongolia, have greater variability in Hg contents than others [56, 59, 62, 67]. Furthermore, province-wide means for Guizhou are strongly influenced by the proportion of Hg-enriched samples included in the data. In an analysis of USGS data for Chinese coals, Wu *et al.* [67] showed that the distribution of Hg contents in Guizhou Province coals contains a tail of values in excess of 1 ppm Hg, giving an overall mean of 0.51 ppm for 46 samples. A similar trend in Hg distribution was shown for coals in Shanxi Province. The highest Hg values in Guizhou Province are associated with mineralized coals produced in small-scale mines and used primarily for domestic purposes [68, 69]. While various studies [69, 70–73] have drawn attention to health risks associated with the latter, inclusion of mineralized coal samples from small-scale workings in database compilations to assess Hg input to the utility sector is inappropriate and has resulted in over-estimates in the past. If mineralized coals are excluded from those produced on a commercial scale, the province-wide mean for Guizhou is comparable to current estimates of the nationwide mean (Figure 2.2). Consideration of Hg in Chinese coals on a production-weighted basis could help refine the estimate for China and keep pace with rapidly evolving utilization patterns.

2.3.1.2 India

India is the world's third largest coal producer after China and the United States, and coal accounted for 69% of India's electric power generating capacity in 2010 [55, 74]. Coals in the Indian subcontinent originated in the Gondwana supercontinent encompassing all or part of peninsular India, Australia, southern Africa, South America, and Antarctica. These coals are dominantly of Permian age, in contrast to Carboniferous coals of Europe and North America. Compared to Carboniferous coals in the northern hemisphere, Gondwana coals tend to be relatively high in ash and low in sulfur, with a greater proportion as organic sulfur, except where coal beds are overlain by marine sediments [75].

Unlike China and the United States, detailed studies of elemental concentrations, especially Hg, in Indian coals are lacking. For example, a recent report by Mukherjee *et al.* [76] on Hg emissions from industrial sources assumed a mean value of 0.376 ppm Hg for Indian coal, based on the average of coals sampled at eight (of about 80) operating power stations in India, whose range in Hg contents was from 0.18 to 0.61 ppm. In a study of global Hg flow from coal utilization, Mukherjee *et al.* [77] give a range from 0.11 to 0.80 ppm for Hg in coal from India, but note a much smaller variation (0.11–0.14 ppm) in results provided by the National Thermal Power Corporation of India. Rajagopalan [78] gives a range for Hg in Indian coal from 0.26 to 0.49 ppm that was reported by Mukherjee and Zevenhoven [79]. The number of samples on which these ranges are based, and the analytical methods employed, are not clearly stated.

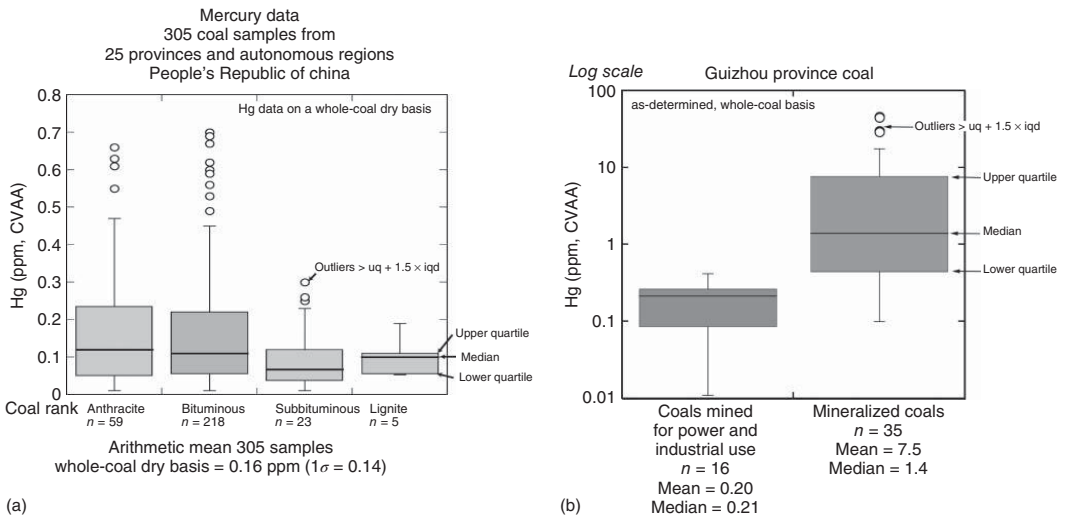


Figure 2.2 (a) Comparison of mercury content of Chinese coals by rank. (Results from Belkin *et al.* [60].) (b) Comparison of Guizhou Province, China, coals produced for power generation and industrial uses with mineralized coals. (Results from Ref. [60, 80].)

USGS sampling in India (102 samples; [39]) is limited to the Sohagpur Basin, an important Permian coal basin, together with reconnaissance sampling of younger, Tertiary coals having more limited commercial use. Together, these samples give a mean Hg value of 0.09 ppm. Additional sampling is required to determine an overall Hg content of Indian coals similar to values obtained by more comprehensive sampling in China and the United States. Coal washing is widely employed in India to reduce high-ash contents, a characteristic of some Gondwana coals. Additional characterization is needed to determine the effect of coal washing on Hg contents and to expand the information available on Hg in Indian coals.

2.3.1.3 Australia

Australia is the largest hard coal exporter (298 Mton in 2010) and the fourth largest producer [55]. Australia relied on coal for 77% of its 2010 power generation needs [55]. Mercury contents in Australian coals are low by international standards. In estimating Australia's atmospheric Hg emissions, Nelson [81] assumed a mean value of 0.05 ppm Hg for Australian hard coal, based on work by Dale [82] and Riley *et al.* [83], giving mean values of 0.045 and 0.040 ppm, respectively, on an as-received basis, for a suite of 100 Australian hard coals. A mean value of 0.08 ppm, on a dry basis, was assumed for Australian brown coals, as noted by Brockway *et al.* [84]. Most Australian hard coals are Permian in age, whereas brown coals are Tertiary. Mercury contents in Australian export coals are especially low, ranging from 0.01 to 0.08 ppm, with a mean of 0.02 ppm according to CSIRO [85]. Only 10 samples are included in WoCQI for Australia. Four export bituminous coals from the Bowen Basin, Queensland, have Hg contents ranging from 0.011 to 0.026 ppm on a dry, whole-coal basis [39]. One low-rank coal has a much higher Hg concentration (0.16 ppm), consistent with higher Hg values for low-rank coals suggested by Brockway *et al.* [84]. Of four bituminous coals investigated in detail in an international round robin study of methods for determining element affinities in coal [86], the Wyee (Australia) coal had the lowest pyritic S content (0.05 wt%) and the lowest Hg content (0.01 ppm; [87, 4]). As part of a more recent study of element modes of occurrence, Riley *et al.* [88] determined Hg contents by cold vapor atomic fluorescence for six Permian and Triassic Australian coals, including several blended coals. These six samples give a mean of 0.050 ppm Hg and a median of 0.022 ppm, reflecting one sample (GG) of high sulfur coal, formed under marine influence, having a Hg content of 0.16 ppm. Selective leaching studies of these six coals are consistent with pyrite as the predominant mineral association for Hg [88].

2.3.1.4 South Africa

South Africa is of particular interest from the standpoint of Hg emissions because it has the highest proportion of its electricity produced by coal combustion (93%; [74]), and is a major user of coal for liquid fuels. South Africa is also the world's fifth largest hard coal producer and a significant (68 Mton) coal exporter [55]. There is considerable range in coal products produced, both by natural variation in quality and by coal beneficiation, with the best quality (lowest ash, highest calorific

values) coals produced for export and higher ash coals retained for domestic use or rejected (C. van Alphen, personal communication, 2011) [89]. This variation likely contributes to a considerable range in Hg content, even for a single coal by a single producer, with export coals expected to be lowest by virtue of removal of mineral matter, including pyrite. A large portion of coal production and generation capacity has traditionally come from central coalfields within the main part of the Permian Karoo Supergroup in Mpumalanga Province, including the Witbank, Highveld, and Ermelo coals. The Witbank and Highveld coals are approaching exhaustion. The largest remaining coal reserves are in the Waterburg coalfield in Limpopo Province to the northwest; together these three coal fields constitute more than 70% of total reserves in South Africa [90].

Wagner and Hlatshwayo [91] determined a series of potentially hazardous trace elements in five Highveld coals, giving a range of 0.04–0.27 ppm Hg and a mean of 0.15 ± 0.05 ppm. These authors recognized that many of the element concentrations determined were either less than or comparable to global values for coal with the exception of Cr, which is noticeably higher. Bergh *et al.* [17] investigated the potential for trace-element reduction by beneficiation of the Witbank no. 4 coal. The no. 4 coal has a higher ash yield than the no. 2 coal, historically the most important producer in the Witbank coalfield, but whose reserves are declining. Bergh *et al.* [17] give a mean of 0.3 ppm Hg for an unspecified number of run-of-mine samples of the Witbank no. 4 coal. Extents of trace-element reduction by dense media and by froth flotation were investigated, with dense media beneficiation showing a greater reduction of pyrite-associated elements such as Hg.

Reconnaissance USGS sampling of South African coals (40 WoCQI samples, major coalfields represented; [39]), gives a mean of 0.20 ppm Hg for 11 samples of Highveld coal, comparable to findings of Wagner and Hlatshwayo [91]. But for 10 samples of Witbank coal, the mean is only 0.045 ppm, excluding one Witbank sample with 0.83 ppm Hg. The ash yield of the 10 USGS Witbank samples ranges from only 7.2% to 16.4%, suggesting these are export coals, whereas the outlier with 0.83 ppm Hg has an ash yield of 32.5% (Figure 2.3). USGS results confirm that Highveld coals are especially Cr-enriched, in agreement with Wagner and Hlatshwayo [91] and consistent with possible exposure of chromite-($\text{Fe}^{2+}\text{Cr}_2\text{O}_4$) bearing source rocks during Karoo sedimentation.

Wagner and Tlotleng [92] prepared and analyzed density fractionated mineral concentrates from four Waterburg coal samples. Results show a strong association of As with the most pyritic fractions for all four samples and a more variable mode of occurrence for Hg, which includes a pyritic association for three samples from the Grooteegeluk formation. These results suggest that Waterburg coals may be amenable to reduction of As and Hg by coal preparation.

2.3.1.5 Russian Federation

Russia has the world's second largest coal reserves, after the United States, and currently (2010) is the sixth largest hard coal producer (248 Mton) immediately following South Africa [55]. Thermal power stations account for nearly 70% of the power generation sector in the Russian Federation, but the majority of these

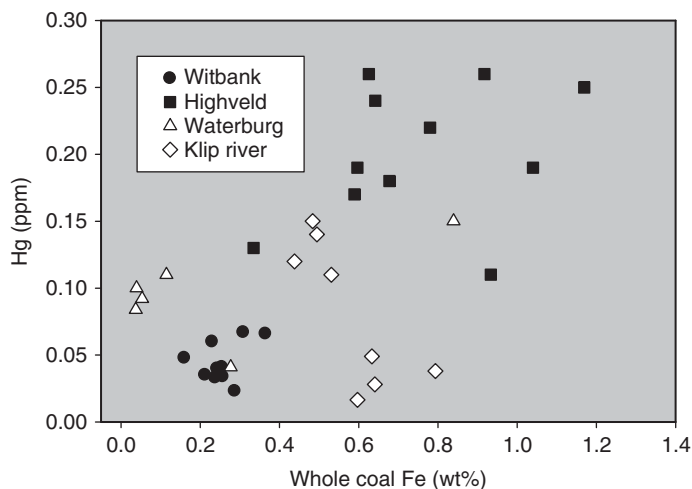


Figure 2.3 Plot showing variation in Hg content as a function of Fe content (a proxy for pyrite) for reconnaissance USGS sampling of South African coals from four coalfields. Both parameters are expressed on a dry, whole-coal basis. One Witbank sample with 1.24% Fe and 0.83 ppm Hg is omitted as well

as four other WoCQI samples – two with unidentified locations and two from other coalfields (Hg in these four samples ranges from detection limit to 0.62 ppm). Low-Hg Witbank samples (lower left) are probably export coals (see text).

plants are gas-fired. Coal accounts for nearly 30% of this capacity, comprising about 20% of overall electric power generation [93, 94]. Although coal is produced in several parts of the Russian Federation and adjacent areas of Ukraine and Kazakhstan, three coal basins, the Ekibastuzsk Basin in northeastern Kazakhstan bordering Siberia, the Kuznetsk Basin in southwestern Siberia, and the Kansk-Achinsk Basin, also in Siberia, accounted for about 60% of the coal used for power generation in 2007 [95, 94]. Of these, the Kuznetsk Basin is the primary source of coal produced for export, whereas in the Kansk-Achinsk Basin, brown coals are produced, with use outside of Siberia limited to small amounts that are shipped to European Russia [94].

Mercury contents of Russian coals show some variability within and between major coal basins, but available data for areas with the greatest production are well within international standards. Mercury contents of Kuznetsk coals tend to be on the low side, with an average of 0.06 ppm given by ACAP [96] for coal produced in 40 mines, similar to that reported by Meij and te Winkel [97] about 0.05 ppm for Kuznetsk coal exported to the Netherlands. Higher Hg contents have been reported for some basins. The Donets Basin (Donbas region) of eastern Ukraine and adjacent parts of the Russian Federation has historically been an important coal-producing region, especially for metallurgical coals. These coals are known to have relatively high Hg concentrations with Hg enrichment that is controlled geologically by faulting and other structures. Kolker *et al.* [98] report a mean content of 0.68 ppm Hg for 29 samples of commercial coal collected from active mines in

the vicinity of Donetsk, Ukraine, but this is reduced to 0.43 ppm for 17 samples if 11 samples from the mining district closest to the geologic Hg source, and one outlier with 3.5 ppm Hg, are excluded. On a nationwide basis, the proportion of Hg-enriched coals used for power generation in the Russian Federation is likely to be small, as commercial coal production is dominated by three main sources, each having low to moderate Hg contents.

2.3.1.6 Indonesia

Indonesia is the world's largest producer of brown coal (163 Mton), the second largest hard coal exporter (162 Mton) after Australia, and the seventh largest hard coal producer (173 Mton; [55]). Indonesia's production is likely to increase as new coal fields are developed. Coal in Indonesia is present in a series of shallow, geologically young basins that are distributed across the archipelago. As a result, 85% of coal produced in Indonesia is lignite or subbituminous in rank. In a study of trace elements in coal imported to the Netherlands, Indonesian coal is at the lower end of the range of Hg concentrations in coal from 14 countries, with a mean value <0.10 ppm [97]. In an effort to better define the environment of deposition of coals in Kutai Basin, East Kalimantan, Widodo *et al.* [99] examined the distribution of pyrite in these coals and found excellent correlations between the occurrence of pyrite and total iron content, which likely extends to Hg.

Detailed geochemistry for eight samples of in-ground Indonesian coal is given by Belkin and Tewalt [100]. These are the only Indonesian samples in the USGS WoCQI database, but give a range in rank (lignite B to semi-anthracite) and geographic distribution. Most of these samples are low in S, as is typical of Indonesian coals. These eight samples give a mean Hg content of 0.10 ppm with a range of 0.02–0.19 ppm, and Cl contents ranging from <150–300 ppm, with a mean of 260 ppm.

2.4

Halogens in Coal

2.4.1

Introduction

Information on the controls and natural variation of halogens in coal is provided here as background to their impact on mercury capture in combustion systems. In general, halogen contents of coals used for power generation increase with rank, which, in the absence of localized thermal sources, corresponds to depth of burial or paleo-depth in coal-forming sedimentary basins. This is because the salinity of formation waters and the concentration of dissolved constituents such as halogens increase with depth in sedimentary basins, and halogen concentrations are influenced by exchange between formation waters and coal.

2.4.1.1 Chlorine (Cl)

Elemental Hg is a semi-noble metal, exceedingly water insoluble, and difficult to capture by adsorption on unpromoted activated carbons, or by absorption in wet scrubbers. Compounds of mercury, such as mercuric chloride, have some water solubility, and are more amenable to capture by sorbents or scrubbers. Halogens such as Cl can also facilitate the oxidation of mercury by selective catalytic reduction (SCR) catalysts located upstream of wet scrubbers. At flue gas temperatures, the Cl content of coal strongly influences Hg speciation, converting Hg^0 present at boiler temperatures to oxidized forms that can react with Cl species in the flue gas to form Hg–Cl complexes or compounds. These Hg–Cl complexes or compounds can be captured by air pollution control devices or taken up by halogen-doped sorbents (“[100], [101,102], this volume” or equivalent.). The proportion of oxidized Hg formed in combustion systems increases with increasing Cl, for coals having Cl contents between about 100 and 1000 ppm Cl [7, 104].

The range in coal Cl values shown to be effective in enhancing Hg capture is rank-dependent and corresponds to values typically found in bituminous coals [105, 106]. Yudovich and Ketris [105] compiled Cl data for coals throughout the world and their ashes. This compilation gives a median Cl concentration in hard coals (340 ± 40 ppm) that is roughly three times that for lignites (brown coals; 120 ± 20 ppm). The world value for hard coal and the mean for Chinese coal (255 ppm; [58]) are comparable. Both values are lower than the U.S. mean (614 ppm; [11, 107]) that is elevated by the predominance of eastern U.S. bituminous coals in COALQUAL.

U.S. coals show rank dependence of Cl concentration (Figure 2.4a) and considerable variation within and between U.S. coal basins [106]. In the Appalachian Basin, Bragg *et al.* [106] have shown that chlorine contents have a pronounced stratigraphic dependence with the highest mean concentrations found in the lowermost coals sampled (Table 2.4). A similar variation in Cl contents with depth has been observed in the Illinois Basin (USA), with concentrations ranging from below detection at outcrop to 0.8 wt% in the deepest part of the basin [108, 109]. Some of the highest Cl values shown in Figure 2.4a for the U.S. Interior Province correspond to deep-basin samples from the Illinois Basin. Variation in Cl contents with depth in the Illinois Basin is attributed to equilibration with groundwater whose salinity increases with depth. For 13 mines in which Cl was determined for both coal and ground water, a correlation coefficient of 0.93 was obtained for these two parameters [108]. Elsewhere, proximity to geologic structures that have acted as pathways for influx of Cl-bearing fluids can result in localized Cl enrichment. This is thought to be the case in the Southwestern reserve district of eastern Kentucky, USA, where the major coal beds present have higher mean Cl contents than their equivalents elsewhere in eastern Kentucky [28]. Whereas Cl is desirable for its capacity to enhance Hg capture, at high concentrations it can be deleterious. Chlorine contents greater than about 0.3 wt% are known to cause significant fouling and corrosion of boilers [109]. Moreover, HCl emissions from Cl in coal are regulated under the new MATS rule.

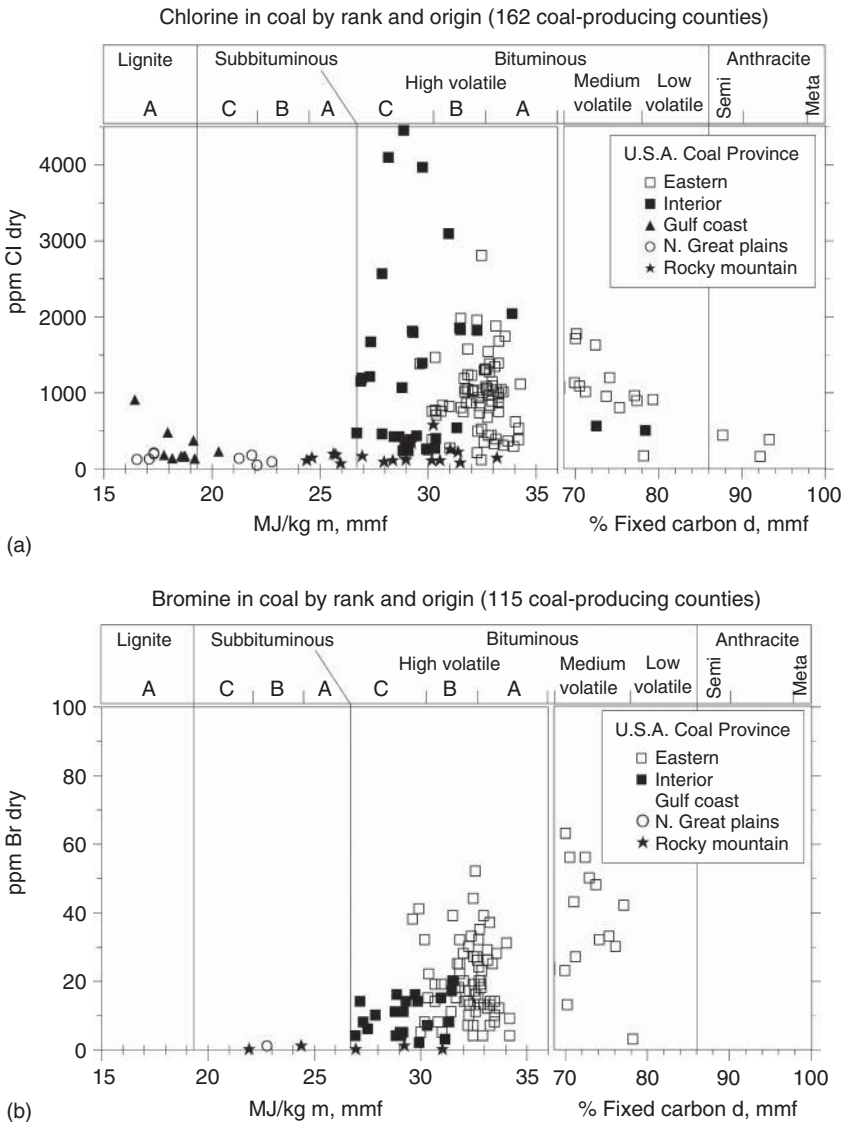


Figure 2.4 (a,b) Plots showing variation of county-average Cl and Br contents of U.S. coal with ASTM [110] coal rank and geographic origin. County-average values were calculated from at least five samples. With a few exceptions, Cl values are from the 1999 ICR, Br values are from COALQUAL, mega-joules per kilogram values are mostly from year 2005 EIA-423 coal shipment assays with a few from the 1999 EIA-423 data, and fixed

carbon values are mostly from COALQUAL with a few from Keystone. Additional data from the Illinois Geological Survey, which include Br and Cl values for coal from 12 counties in Illinois, were also used. The data sets have been described elsewhere [111]. Compared to Cl, relatively few data are available for Br in lower rank U.S. coal. (Modified from Reference [7] Copyright © 2006, Elsevier.)

Table 2.4 Mean chlorine content of coal by formation in the central Appalachian Basin, Pennsylvania, and West Virginia, USA.

Age	Formation	Number of samples	Mean (ppm) ^{a)}
Permo-Pennsylvanian	Dunkard Group	44	162
Upper Pennsylvanian	Monongahela	73	477
Upper Pennsylvanian	Conemaugh	41	828
Middle Pennsylvanian	Allegheny	709	1097
Middle Pennsylvanian	Kanawha ^{b)}	36	1408
Lower Pennsylvanian	New River ^{b)}	56	1503

Formations are listed in order of increasing age.

a) Detection limit is 100 ppm. In calculating mean, non-detects are assumed to contain 70% of the detection limit.

b) Samples from southern West Virginia; other samples are from Pennsylvania.

Source: Ref. [106].

The mode of occurrence of Cl in coal has drawn considerable attention in part because of boiler corrosion problems caused by coals with excessive Cl contents and in part because multiple forms of Cl have been suggested, which has led to considerable disagreement. Major forms recognized or suggested include inorganic Cl in mineral chlorides or other mineral matter in coal, organically bound Cl, and chloride anions present within moisture in coal [105, 112, 113]. Huggins and Huffman [112] used Cl K-edge XAFS spectroscopy to investigate the mode of occurrence of Cl in bituminous and low-rank coals and compare Cl in raw coals with that in cleaned coals, and before and after aqueous leaching treatments. These authors found that hydrated chloride species provided a much better fit to the Cl K-edge X-ray absorption near edge structure (XANES) spectra obtained for a range of U.S. and U.K. coal samples than either a series of organochlorine compounds or crystalline NaCl. They concluded that in coals with typical Cl contents, Cl is present as chloride anions associated with coal moisture and weakly bound to the surfaces of micropores in coal macerals by organic–ionic complexes [112]. A similar model was advanced for Br (following section).

2.4.1.2 Bromine (Br)

Compared to Cl, on a molar equivalent basis, Br is a much more effective oxidizer of Hg in power plant flue gas ([102], this volume). As a result, the native Br content in coals may be even more important than Cl in determining the extent of spontaneous Hg oxidation and self-capture in combustion systems [104, 114–117]. For coals that are low in halogens, including many low-rank coals, this has led to the suggestion that limited addition of Br would effectively enhance Hg oxidation and capture [117]. As a result, a range of Br-based commercial sorbents has been developed, particularly for use with subbituminous coal ([103], this volume).

Like Cl, the absolute concentration of Br in coal is rank-dependent (Figure 2.4b). However, the proportions of Br and Cl are relatively constant. Vosteen *et al.* [117] reviewed the native halogen content of coals in the United States, China, and several other countries, and determined that Br/Cl mass ratios of 0.01–0.04 were

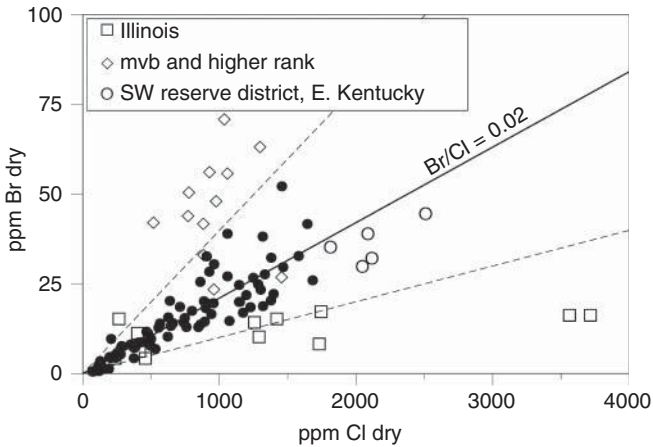


Figure 2.5 Average Cl and Br contents for coal produced in 110 U.S. counties showing that most have Br/Cl mass ratios near 0.02. Points show county-average values calculated from selected COALQUAL records where there were at least five Cl and Br analyses. Dashed lines show Br/Cl ratios of 0.04 (top) and 0.01 (bottom). Data for non-producing counties are included in the figure but weathered coal and samples collected from outcrop have been ignored. Additional data from the Illinois Geological Survey were also used. The data sets have been described elsewhere [80, 111].

typical, even in coals having low overall halogen contents (i.e., regardless of rank). For U.S. coals, most scatter about a Br/Cl ratio of 0.02 (Figure 2.5). Exceptions include high-rank coals (above high volatile bituminous rank) and coals influenced by saline formation waters, including coal from the Southwestern reserve district in eastern Kentucky, and some Illinois coals (Figure 2.5). Using a Br/Cl ratio of 0.02 as a guide, Br concentrations near 2 ppm might be expected for a subbituminous coal with 100 ppm Cl, and 8 ppm Br for a bituminous coal having 400 ppm Cl. In some cases, for example, in selected coals from Bulgaria and parts of the Ukraine Donbas, exceptionally high Br concentrations are present, with Br contents in excess of those for Cl for some samples ([113, 117]; Figure 2.6). Inclusion of these highly Br-enriched coals in results for 34 world coal deposits [113] gives a mean Br value in excess of 100 ppm that is probably not representative. Excluding seven deposits with Br contents >50 ppm gives a mean Br/Cl ratio of 0.05 for the 27 remaining deposits, which is more in line with typical Br/Cl proportions. In a review of Cl and Br in U.K. coals, Spears [118] found that means for both elements were enriched proportionally in a representative suite of 24 samples.

Bromine/chlorine ratios are potentially of use in distinguishing the processes controlling halogen distribution in coal. In the simplest cases, this ratio is controlled by pore waters present during coal formation or by formation waters presently in equilibrium with coal. At the peat stage, halogens are enriched in peat and its pore water relative to atmospheric deposition [119, 120] and the proportion of Br to Cl is higher than that of modern seawater, which has a consistent Br/Cl ratio of 0.0035 on a weight concentration basis [121]. Typical Br/Cl ratios

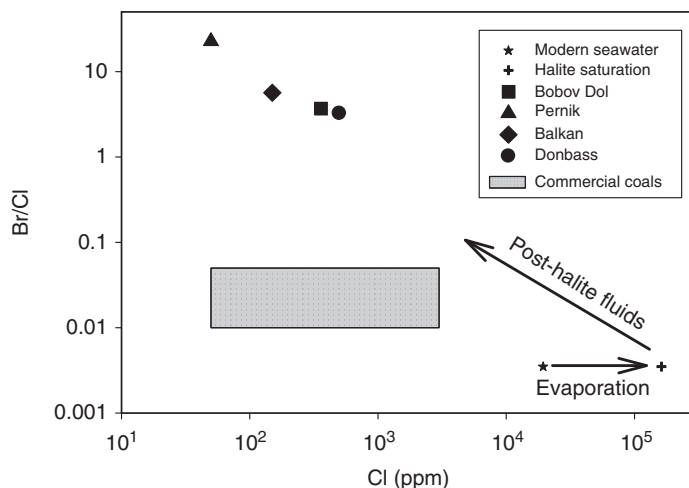


Figure 2.6 Generalized Br–Cl systematics for coals and brines, showing compositions typical of commercial coals (gray swath) and results from Vassilev *et al.* [113] for four coal deposits with extreme Br enrichment including Bobov Dol, Pernik, and Balkan, in Bulgaria, and Donbass in Ukraine. Halite precipitation enriches residual fluids in Br, thereby

increasing Br/Cl. Actual trajectory is dependent on conditions present in a particular basin. Range for commercial coals assumes a Br/Cl from 0.01 to 0.05, 50 ppm Cl as a minimum and 3000 ppm as a maximum, based on boiler corrosion problems using more Cl-rich coals.

in coal are approximately 5–10 times that of seawater (Figure 2.6), reflecting either inheritance from the peat stage, exchange with formation waters, or both. As seawater evaporates and salinity increases, Br/Cl remains relatively constant until halite (NaCl) precipitates, which excludes Br. As a result, halite precipitation in saline formation waters enriches the residual fluids in Br, increasing the Br/Cl ratio ([122], expressed as lowering Cl/Br; Figure 2.6). Halite-bearing “salt coals” in a number of countries have unusually high Cl concentrations and atypical Br/Cl ratios [113, 120], which may be inherited in part from the peat stage or a consequence of halite precipitation. Conversely, halite dissolution by less saline formation waters serves to decrease Br/Cl ratios ([122], expressed as raising Cl/Br).

Like Cl, the mode of occurrence of Br in coal has been difficult to ascertain with certainty. In Cl-enriched coals containing discrete mineral chlorides such as halite (NaCl), sylvite (KCl), or other Cl-bearing minerals such as chlorapatite ($\text{Ca}(\text{PO}_4)_3(\text{Cl}, \text{F}, \text{OH})$), limited inclusion of Br may be expected. But as suggested by Huggins and Huffman [112], mineral occurrence of halogens in coal may be the exception rather than the rule. Based on more limited XAFS spectroscopy at the Br K-edge showing many features in common with the Cl data, Huggins and Huffman concluded that the dominant mode of occurrence for Br is in association with coal moisture, similar to that for Cl. Based on the similarity of Cl and Br, Spears [118] concluded that moisture-hosted Cl and Br were consistent with results for U.K.

coals showing (i) correlation between Cl in coal with that in adjacent groundwater; (ii) correlation between coal Cl content and moisture content; and (iii) brine-like water extracted from coal moisture by centrifugation.

2.4.1.3 Iodine (I)

Various studies have found I and its compounds such as potassium iodide to be effective oxidants and sorbent promoters for capture of Hg^0 in flue gas from coal combustion [104, 123–125]. On a volume-equivalent basis, Chi *et al.* [125] determined I to be even more effective than Br in promoting Hg^0 oxidation, whereas Cao *et al.* [104] found Br (as HBr) to be more effective, and both HBr and HI more effective on a per volume basis than either HCl or HF. These results follow a general trend that the heavier halogens (Br, I) are more effective oxidants than the lighter halogens (Cl, F), a surprising result given that oxidizing ability decreases in the group with increasing atomic weight.

Information on the naturally occurring I content of coals is limited. However, several recent studies have introduced methods to quantify I content, particularly in Chinese coals [126–128]. Wu *et al.* found a range in I content from 0.04 to 39.5 ppm for 305 samples of coal from throughout China, with an arithmetic mean of 2.6 ppm and a geometric mean of 1.27 ppm. Iodine content was found to be positively correlated with coal rank and with depositional environment, with anthracite having the highest values. Chinese coals deposited under the influence of marine or brackish conditions have a higher mean I content than those deposited in non-marine settings and this is likely to be applicable elsewhere, analogous to other marine-associated elements such as B [129]. Bettinelli *et al.* [130] give a range of 0.15–12.8 ppm I by ICP-MS for 158 commercial coal samples imported to Italy from China, Columbia, Poland, South Africa, the United States, and Venezuela. This study confirms that median I concentrations in the 1–3 ppm range are typical from various sources. Wang *et al.* [126] report I contents (by INAA) ranging from 2.2 to 15.7 ppm for a series of coals from Guizhou Province, China. There, the most I-enriched coals reflect post-coalification interaction with hydrothermal fluids and are not representative of values for coals used commercially. Wang *et al.* [126] (their Figure 1) and Zheng *et al.* [73] argue that domestic use of I-enriched coal in Guizhou Province limited the incidence of iodine deficiency disorders in the Province to wood-burning areas, prior to its virtual elimination by introduction of iodized salt throughout China.

2.4.1.4 Fluorine (F)

Comparison of the impact of F addition on oxidation of Hg^0 with addition of Br, I, and Cl indicates that the effect of F is similar to or less than that of Cl [104]. As a result, there has been less interest in addition of F, the lightest halogen, as a means to promote Hg capture from combustion systems. However, because its behavior is comparable to that of Cl, in coals with naturally high F contents, the sum of F and Cl may be a more important indicator of the potential for Hg self-capture than Cl itself.

Like other halogens, F concentrations in coal show considerable variation. Values in the 50–100 ppm range are typical, with similar means estimated for world coal (88 ppm; [131]), U.S. coal (98 ppm; [11, 107]), and coal in China (82 ppm; [71, 132]), although Dai *et al.* [58] later give a higher mean value for China (130 ppm). Unusually F-enriched coals (mean of 286 ppm for 29 samples) in Inner Mongolia, described by Wang *et al.* [133], are thought to be the result of introduction of Al- and F-bearing solutions to the mire during coal formation. These solutions are likely derived from an adjacent geologically ancient, deeply weathered, bauxite-bearing terrane. This history is reflected by the presence of boehmite ($\text{AlO}(\text{OH})$) in these coals and a strong correlation between F concentration and the volume percentage of boehmite [133]. Elsewhere in China, high F contents are known in some stone coals (carbonaceous mudstone), and in manufactured coal briquettes that use F-rich clay as a binder. Domestic use of these materials is thought to contribute to endemic fluorosis in China [71, 73, 133], but based on the moderate F contents typical of Chinese coals, the contribution of coal itself to the fluorosis problem is considered to be secondary [71].

2.5

Summary

As discussed elsewhere in this volume, interaction of coal-derived Hg and halogens in the flue gas of combustion systems provides a fundamental mechanism for mercury capture. Variation in the concentrations of these parameters in coal is a consequence of geologic processes, and as a result, to some extent, every coal is unique. In general, low-rank coals have lower contents of both Hg and halogens than bituminous coals, and when combined with their lower energy output and higher moisture content, may offset some of the advantage of being low in Hg. At the other end of the spectrum, bituminous coals generally have higher Hg content but also have halogen concentrations in a range that promotes a greater degree of Hg self-capture. Compared to low-rank coals, bituminous coals have a greater fraction of Hg occurring within Fe disulfides, which potentially allows for pre-combustion removal of Hg to some extent. Concentrations of halogens in coal are influenced by the interaction of coal with associated fluids that may include pore water present during various stages of coal formation, formation waters present in a coal basin, or thermally or structurally driven brines. Where coals are in equilibrium with deep-basin brines, halogen contents may be especially high, and this may limit their commercial usefulness due to corrosion of boilers and emission of acid gasses. The content of Br in coal is typically only a small percentage of the Cl content, but even so, this proportion is enriched relative to that of seawater. As shown elsewhere in this volume, the capacity of Br to promote Hg oxidation is substantially greater and disproportionate to that of Cl.

Of the major coal-producing countries, database compilations sufficient to estimate Hg input to the boiler on a nationwide basis are available only for the United States and China. More detailed sampling and analysis of Hg in coal are

needed, especially for the next largest coal-producing countries such as India, South Africa, the Russian Federation, and Indonesia. In the absence of available detailed compilations, extrapolation of limited datasets to estimate Hg input to the utility sector on a nationwide basis is unlikely to be representative.

Acknowledgments

We thank the editors of this volume for inviting us to contribute a chapter on mercury in coal. The editors are acknowledged for their insightful comments on the manuscript. Additional reviews by Harvey Belkin and Susan Tewalt, on behalf of the USGS, and by David Tabet and Mike Hylland for the Utah Geological Survey, helped improve the manuscript. Harvey Belkin is acknowledged for his help in interpreting USGS mercury data for Chinese coals.

References

1. Finkelman, R.B. (1994) Modes of occurrence of potentially hazardous elements in coal: levels of confidence. *Fuel Process. Technol.*, **39**, 21–34.
2. Palmer, C.A., Mroczkowski, S.J., Finkelman, R.B., and Crowley, S.S. (1998) The use of sequential leaching to quantify the modes of occurrence of elements in coals. Proceedings of the 15th Annual International Pittsburgh Coal Conference, CD-ROM, 28 p.
3. Kolker, A. and Finkelman, R.B. (1998) Potentially hazardous elements in coal: modes of occurrence and summary of concentration data for coal components. *Coal Prep.*, **19**, 133–157.
4. Goodarzi, F. (2002) Mineralogy, elemental composition and modes of occurrence of elements in Canadian feed coals. *Fuel*, **81**, 1199–1213.
5. Diehl, S.F., Goldhaber, M.B., and Hatch, J.R. (2004) Modes of occurrence of mercury and other trace elements in coals from the warrior field, Black Warrior Basin, Northwestern Alabama. *Int. J. Coal Geol.*, **59**, 193–208.
6. Yudovich, Y.E. and Ketris, M.P. (2005) Mercury in coal: a review. Part 1. Geochemistry. *Int. J. Coal Geol.*, **62**, 107–134.
7. Kolker, A., Senior, C.L., and Quick, J.C. (2006) Mercury in coal and the impact of coal quality on mercury emissions from combustion systems. *Appl. Geochem.*, **21**, 1821–1836.
8. Zheng, L., Liu, G., Qi, C., Zhang, Y., and Wong, M. (2008) The use of sequential extraction to determine the distribution and modes of occurrence of mercury in Permian Huaibei coal, Anhui Province, China. *Int. J. Coal Geol.*, **73**, 139–155.
9. Kolker, A. (2012) Minor element distribution in iron disulfides in coal: a geochemical review. *Int. J. Coal Geol.*, **94**, 32–43.
10. Ruch, R.R., Gluskoter, H.J., and Kennedy, E.J. (1971) *Mercury Content of Illinois Coals*, Illinois State Geological Survey Environmental Geology Notes, vol. 43, Illinois State Geological Survey, 15 p.
11. Bragg, L.J., Oman, J.K., Tewalt, S.J., Oman, C.L., Rega, N.H., Washington, P.M., and Finkelman, R.B. (1998) Coal Quality (COALQUAL) Database – Version 2.0. Open-File Report 97–134, U.S. Geological Survey, Energy Resources Program, Reston, VA.
12. Lefticariu, L., Blum, J.D., and Gleason, J.D. (2011) Mercury isotopic evidence for multiple mercury sources in coal from the Illinois Basin. *Environ. Sci. Technol.*, **45**, 1724–1729.
13. Kolker, A. and Huggins, F.E. (2007) Progressive oxidation of pyrite in

- five bituminous coal samples: an As XANES and ^{57}Fe Mössbauer study. *Appl. Geochem.*, **22**, 778–787.
14. Huggins, F.E., Seidu, L.B.A., Shah, N., Huffman, G.P., Honaker, R.Q., Kyger, J.R., Higgins, B.L., Robertson, J.D., Pal, S., and Seehra, M.S. (2009) Elemental modes of occurrence in an Illinois #6 coal and fractions prepared by physical separation techniques at a coal preparation plant. *Int. J. Coal Geol.*, **78**, 65–76.
 15. Palmer, C.A., Mroczkowski, S.J., Kolker, A., Finkelman, R.B., and Bullock, J.H. Jr., (2000) Chemical Analysis and Modes of Occurrence of Selected Trace Elements in a Powder River Basin Coal and Its Corresponding Simulated Cleaned Product. U.S. Geological Survey Open File Report 00–323, U.S. Geological Survey, 53 p.
 16. Akers, D.J. and Harrison, C.D. (1995) Precombustion control options for air toxics. Preprints of Symposia, American Chemical Society, Division of Fuel Chemistry, ACS Fall Meeting, Chicago, IL, vol. 40 (4), pp. 823–827.
 17. Bergh, J.P., Falcon, R.M.S., and Falcon, L.M. (2011) Trace element concentration reduction by beneficiation of Witbank Coalfield no. 4 Seam. *Fuel Process. Technol.*, **92**, 812–816.
 18. Laskowski, J.S. (2001) *Coal Flotation and Fine Coal Utilization (Developments in Mineral Processing)*, vol. 14, Chapter 1, Elsevier.
 19. Wang, W., Qin, Y., Wei, C., Li, Z., Guo, Y., and Zhu, Y. (2006) Partitioning of elements and macerals during preparation of Antaibao coal. *Int. J. Coal Geol.*, **68**, 223–232.
 20. Wang, W.-F., Qin, Y., Wang, J.-Y., and Li, J. (2009) Partitioning of hazardous trace elements during coal preparation. *Procedia Earth Planet. Sci.*, **1**, 838–844.
 21. Demir, I., Ruch, R.R., Damberger, H.H., Harvey, R.D., Steele, J.D., and Ho, K.K. (1998) Environmentally critical elements in channel and cleaned samples of Illinois coals. *Fuel*, **77** (1/2), 95–107.
 22. Hower, J.C., Blandchard, L.J., and Robertson, J.D. (1998) Magnitude of minor element reduction through beneficiation of central Appalachian coals. *Coal Prep.*, **19**, 213–229.
 23. Toole-O'Neil, B., Tewalt, S.J., Finkelman, R.B., and Akers, D.J. (1999) Mercury concentrations in coal: unraveling the puzzle. *Fuel*, **78**, 47–54.
 24. Quick, W.J. and Irons, R.M.A. (2002) Trace element partitioning during the firing of washed and untreated power station coals. *Fuel*, **81**, 665–672.
 25. Mastalerz, M. and Drobnik, A. (2005) Vertical variations in Pennsylvanian coal beds from Indiana. *Int. J. Coal Geol.*, **63**, 36–57.
 26. Mastalerz, M., Drobnik, A., and Filippelli, G. (2006) Mercury content and petrographic composition in Pennsylvanian coal beds of Indiana, USA. *Int. J. Coal Geol.*, **68**, 2–13.
 27. Sakulpitakphon, T., Hower, J.C., Schram, W.H., and Ward, C.R. (2004) Tracking mercury from the mine to the power plant: geochemistry of the Manchester coal bed, Clay County, Kentucky. *Int. J. Coal Geol.*, **57**, 127–141.
 28. Hower, J.C., Eble, C.F., and Quick, J.C. (2005) Mercury in Eastern Kentucky coals: geologic aspects and possible reduction strategies. *Int. J. Coal Geol.*, **62**, 223–236.
 29. Goodarzi, F. and Goodarzi, N.N. (2004) Mercury in Western Canadian subbituminous coal- a weighted average study to evaluate potential mercury reduction by selective mining. *Int. J. Coal Geol.*, **58**, 251–259.
 30. Merriam, N.W., Sethi, V., and Brecher, L.E. (1994) Process for clean-burning fuel from low-rank coal. US Patent 5,322,530, 7 p.
 31. Nunes, S. (2009) Review of Coal Upgrading. Report CCC/156, IEA Clean Coal Centre, London, 45 p.
 32. Dong, N. (2011) Utilisation of Low Rank Coals. Report CCC/182, IEA Clean Coal Centre, London, 92 p.
 33. Merriam, N.W. (1993) Removal of Mercury from Powder River Basin Coal by Low-Temperature Thermal Treatment. Report to U.S. Department of Energy DOE/MC/30126-3916; WRI-93-R021

- under Cooperative Agreement DE-FC21-93MC30126, U.S. Department of Energy, 23 p. doi: 10.2172/10189789.
34. Guffey, F.D. and Bland, A.E. (2004) Thermal pretreatment of low-ranked coal for control of mercury emissions. *Fuel Process. Technol.*, **85** (6–7), 521–531.
 35. Levin, L. (2015) Mercury in the environment, in *Mercury Control – for Coal-Derived Gas Streams* (eds E.J. Granite, H.W. Pennline, and Constance Senior), Wiley-VCH GmbH & Co KGaA, Weinheim.
 36. Aruscavage, P.J. and Moore, R. (1989) in *Methods for Sampling and Inorganic Analysis of Coal*, U.S. Geological Survey Bulletin 1823 (eds D.W. Golightly and F.O. Simon), USGS, pp. 55–57.
 37. O’Leary, R.M. (1997) in *The Chemical Analysis of Argonne Premium Coal Samples*, U.S. Geological Survey Bulletin 2144 (ed. C.A. Palmer), USGS, pp. 51–55.
 38. U.S. EPA (2007) Mercury in Solids and Solutions by Thermal Decomposition, Amalgamation, and Atomic Absorption Spectrophotometry, U.S. EPA Method 7473, 17 p.
 39. Tewalt, S.J., Belkin, H.E., SanFilipo, J.R., Merrill, M.D., Palmer, C.A., Warwick, P.D., Karlsen, A.W., Finkelman, R.B., and Park, A.J. (2010) Chemical Analyses in the World Coal Quality Inventory, vers. 1. U.S. Geological Survey Open File Report 2010–1196, U.S. Geological Survey, 4 p.
 40. Palmer, C.A. and Baedeker, P.A. (1989) in *Methods for Sampling and Inorganic Analysis of Coal*, U.S. Geological Survey Bulletin 1823 (eds D.W. Golightly and F.O. Simon), USGS, pp. 27–34.
 41. Bloom, N.S. and Prestbo, E.M. (1994) A new survey of mercury in U.S. coals. Proceedings of the 11th Annual International Pittsburgh Coal Conference, vol. 1, pp. 563–568.
 42. Biswas, A., Blum, J.D., Bergquist, B.A., Keeler, G.J., and Xie, Z. (2008) Natural mercury isotope variation in coal deposits and organic soils. *Environ. Sci. Technol.*, **42**, 8303–8309.
 43. Brownfield, M.E., Affolter, R.H., Cathcart, J.D., Johnson, S.Y., Brownfield, I.K., and Rice, C.A. (2005) Geologic setting and characterization of coals and the modes of occurrence of selected elements from the Franklin coal zone, Puget Group, John Henry No. 1 mine, King County, Washington, USA. *Int. J. Coal Geol.*, **55**, 139–150.
 44. U.S. EPA (2003) U.S. Environmental Protection Agency, Electric Utility Steam Generating Units Section 112 Rule Making – Coal Analysis Results, epa.gov/ttn/atw/combust/utiltox/utoxpg.html (accessed December 2011), four zipped EXCEL files.
 45. U.S. EPA (2011) U.S. Environmental Protection Agency, Air Toxics Standards for Utilities – MATS ICR Data (EGU_ICR_PartI_and_PartII). epa.gov/ttn/atw/utility/utilitypg.html (accessed March 2011).
 46. U.S. EPA (2011) U.S. Environmental Protection Agency, Air Toxics Standards for Utilities – MATS ICR Data (EGU ICR Part III). epa.gov/ttn/atw/utility/utilitypg.html (accessed March 2011).
 47. Quick, J.C., Brill, T.C., and Tabet, D.E. (2003) Mercury in U.S. coal: observations using the COALQUAL and ICR data. *Environ. Geol.*, **43**, 247–259.
 48. Tewalt, S.J., Bragg, L.J., and Finkelman, R.B. (2001) Mercury in U.S. Coal-Abundance, Distribution, and Modes of Occurrence. U.S. Geological Survey Fact Sheet FS-095-01, 4 p.
 49. Quick, J.C., Tabet, D. E., Wakefield, S., and Bon, R. L. (2005) Optimizing Technology to Reduce Mercury and Acid Gas Emissions from Electric Power Plants – A GIS Study of Coal Chemistry. Final Report for DOE Contract DE-FG26-03NT41901, Utah Geological Survey, Salt Lake City, 91 p, geology.utah.gov/emp/mercury/index.htm (accessed 18 March 2014).
 50. EPRI (2000) An Assessment of Mercury Emissions from U.S. Coal-Fired Power Plants. Report 1000608, Electric Power Research Institute, Palo Alto, CA, 191 p.
 51. U.S. EIA (2011) Energy Information Administration Form-923 (Schedule

- 2) – Monthly Utility and Nonutility Fuel Receipts and Fuel Quality Data. eia.gov/cneaf/electricity/page/eia423.html (accessed March 2011).
52. Quick, J.C. (2011) Comment on the Proposed Mercury and Air Toxics Rule. Document EPA-HQ-OAR-2009-0234-12991. 21 p. www.regulations.gov (accessed 31 March 2014).
53. U.S. EPA (2011) Mercury and Air Toxics Standards (MATS), <http://www.epa.gov/mats/pdfs/20111216MATSfinal.pdf> (accessed December 2011).
54. Hutson, N. (2015) Regulations, in *Mercury Control – for Coal-Derived Gas Streams* (eds E.J. Granite, H.W. Pennline, and Constance Senior), Wiley-VCH GmbH & Co KGaA, Weinheim.
55. International Energy Agency (IEA) (2011) Key World Energy Statistics, 80 p, http://www.iea.org/textbase/nppdf/free/2011/key_world_energy_stats.pdf (accessed 18 March 2014).
56. Streets, D.G., Hao, J., Wu, Y., Jiang, J., Chan, M., Tian, H., and Feng, X. (2005) Anthropogenic mercury emissions in China. *Atmos. Environ.*, **39**, 7789–7806.
57. Zheng, L., Liu, G., and Chou, C.-L. (2007) The distribution, occurrence and environmental effect of mercury in Chinese coals. *Sci. Total Environ.*, **384**, 374–383.
58. Dai, S., Ren, D., Chou, C.-L., Finkelman, R.B., Seredin, V.V., and Zhou, Y. (2012) Geochemistry of trace elements in Chinese coals: a review of abundances, genetic types, and impacts on human health and industrial utilization. *Int. J. Coal Geol.*, **94**, 3–21.
59. Qiu, G., Feng, X., and Jiang, G. (2012) Synthesis of current data for Hg in areas of geologic resource extraction contamination and aquatic systems in China. *Sci. Total Environ.* doi: 10.1016/j.scitoenv.2011.09.024
60. Belkin, H.E., Zheng, B., and Finkelman, R.B. (2006) Mercury in Coal from the People's Republic of China. 8th International Conference on Mercury as a Global Pollutant, Madison, WI, August, 2006 (abstract), pp. 83–84.
61. Ren, D., Zhao, F., Dai, S., Zhang, J., and Luo, K. (2006) *Geochemistry of Trace Elements in Coal*, Science Press, Beijing, 556 pp. (in Chinese with English abstract (not seen; cited in [58, 62])).
62. UNEP (2011) Reducing Mercury Emissions from Coal Combustion in the Energy Sector. United Nations Environment Programme Project Report prepared by Department of Environmental Science and Engineering, Tsinghua University, Beijing, February, 2011, 58 p., (in China), http://www.unep.org/hazardoussubstances/Portals/9/Mercury/Documents/coal/FINAL%20Chinese_Coal%20Report%20-%2011%20March%202011.pdf (accessed February 2012).
63. Wang, Q., Shen, W., and Ma, Z. (2000) Estimation of mercury emission from coal combustion in China. *Environ. Sci. Technol.*, **34**, 2711–2713.
64. Tang, X. and Huang, W. (2004) *Trace Elements in Chinese Coals*, The Commercial Press, Beijing, pp. 6–11, in Chinese (not seen; cited in [58]).
65. Bai, X., Li, W., Chen, Y., and Jiang, Y. (2007) The general distributions of trace elements in Chinese coals. *Coal Qual. Technol.*, **1**, 1–4, in Chinese with English abstract (not seen; cited in [58]).
66. Zhang, L., Wang, S., Wu, Y., and Hao, J. (2009) Synergistic mercury removal by conventional pollutant control strategies for coal-fired power plants in China. 9th International Conference on Mercury as a Global Pollutant, Guiyang, Guizhou Province, China [Hg data given in oral presentation] (abstract).
67. Wu, Y., Streets, D.G., Wang, S.X., and Hao, J.M. (2010) Uncertainties in estimating mercury emissions from coal-fired power plants in China. *Atmos. Chem. Phys.*, **10**, 2937–2947.
68. Ding, Z., Zheng, B., Long, J., Belkin, H.E., Finkelman, R.B., Chen, C., Zhou, D., and Zhou, Y. (2001) Geological and geochemical characteristics of high arsenic coals from endemic arsenosis areas in southwestern Guizhou

- Province, China. *Appl. Geochem.*, **16**, 1353–1360.
69. Belkin, H.E., Zheng, B., Zhou, D., and Finkelman, R.B. (2008) in *Environmental Geochemistry- Site Characterization, Data Analysis and Case Histories* (eds B. De Vivo, H.E. Belkin, and A. Lima), Elsevier, Amsterdam, pp. 401–420.
 70. Finkelman, R.B., Belkin, H.E., and Zheng, B. (1999) Health impacts of domestic coal use in China. *Proc. Natl. Acad. Sci. U.S.A.*, **96**, 3427–3431.
 71. Dai, S., Ren, D., and Ma, S. (2004) The cause of endemic fluorosis in western Guizhou Province, Southwest, China. *Fuel*, **83**, 2095–2098.
 72. Zheng, B., Wang, B., Ding, Z., Zhou, D., Zhou, Y., Zhou, C., Chaochang, C., and Finkelman, R.B. (2005) Endemic arsenosis caused by indoor combustion of high-As coal in Guizhou Province, P.R. China. *Environ. Geochem. Health*, **27**, 521–528.
 73. Zheng, B., Wang, B., and Finkelman, R.B. (2010) in *Medical Geology- A Regional Synthesis* (eds O. Selinus, R.B. Finkelman, and J.A. Centeno), Springer, pp. 303–327.
 74. World Coal Institute (2011) Coal in Electricity Generation, <http://www.worldcoal.org/coal/uses-of-coal/coal-electricity/> (accessed 18 March 2014).
 75. Taylor, G.H., Teichmüller, M., Davis, A., Diessel, C.F.K., Littke, R., and Robert, P. (1998) *Organic Petrology, A New Handbook Incorporating Some Revised Parts of Stach's Textbook of Coal Petrology*, Gebrüder Borntraeger, Berlin, 704 p.
 76. Mukherjee, A.B., Bhattacharya, P., Sarkar, A., and Zevenhoven, R. (2008) in *Mercury Fate and Transport in the Global Atmosphere: Measurements, Models, and Policy Implications*, Interim Report of the UNEP Global Mercury Partnership, Mercury Air Transport and Fate Research Area, July 14, 2008, Chapter 4 (eds N. Pirrone and R. Mason), UNEP, 450 p.
 77. Mukherjee, A.B., Zevenhoven, R., Bhattacharya, P., Sajwan, K.S., and Kikuchi, R. (2008) Mercury flow via coal and coal utilization by-products: a global perspective. *Resour. Conserv. Recycl.*, **52**, 571–591.
 78. Rajagopalan, R. (2003) Monitoring and regulation of the use of mercury: government perspective. National Conference on Mercury Pollution in India, New Delhi, November, 2003 (not seen; cited in [79]).
 79. Mukherjee, A.B. and Zevenhoven, R. (2006) Mercury in coal ash and its fate in the Indian subcontinent: a synoptic review. *Sci. Total Environ.*, **368**, 384–392.
 80. Kolker, A., Quick, J.C., Senior, C.L., and Belkin, H.E. (2006), Mercury and Halogens in Coal: Their role in determining mercury emissions from coal combustion: USGS Fact Sheet 2012–3122, 6 p.
 81. Nelson, P.F. (2007) Atmospheric emissions of mercury from Australian point sources. *Atmos. Environ.*, **41**, 1717–1724.
 82. Dale, L.S. (2003) *Review of Trace Elements in Coal*. Project Number C11020, Australian Coal Association Research Program, p. 65 (not seen; cited in [80]).
 83. Riley, K., Dale, L., Devir, G., Williams, A., and Holcolmbe, D. (2005) *Background Information for Web Site on Trace Elements in Coal*. Project number C12060, Australian Coal Association Research Program, p. 55 (not seen; cited in [80]).
 84. Brockway, D.J., Ottrey, A.L., and Higgins, R.S. (1991) in *The Science of Victorian Brown Coal: Structure, Properties, and Consequences for Utilization* (ed. R.A. Durie), Butterworth-Heinemann, Oxford, pp. 598–650, (not seen; cited in [80]).
 85. CSIRO (2011) Mercury in Australian Export Thermal Coals, <http://www.csiro.au/en/Outcomes/Energy/Energy-from-coal/MercuryInExportCoals.aspx#a1> (accessed 17 March 2014).
 86. Davidson, R.M. (2000) Modes of Occurrence of Trace Elements in Coal-Results of An International Collaborative Programme. Report CCC/36, IEA Clean Coal Centre, London, 36 p.

87. Querol, X., Klika, Z., Weiss, Z., Finkelman, R.B., Alastuey, A., Juan, R., Lopez-Soler, A., Plana, E., Kolker, A., and Chenery, S.R.N. (2001) Determination of element affinities by density fractionation of bulk coal samples. *Fuel*, **80**, 83–96.
88. Riley, K.W., French, D.H., Farrell, O.P., Wood, R.A., and Huggins, F.E. (2012) Modes of occurrence of trace and minor elements in some Australian coals. *Int. J. Coal Geol.*, **94**, 214–224.
89. Pretorius, C.C., Boshoff, H.P., and Pinheiro, H.J. (2002) *Analyses of Coal Product Samples of South African Collieries, 2001–2002*, Bulletin 114, Energy Branch, Department of Minerals and Energy, 25 p.
90. Jeffrey, L.S. (2005) Characterization of the coal resources of South Africa. *J. S. Afr. Inst. Min. Metall.*, **105** (2), 95–102.
91. Wagner, N.J. and Hlatshwayo, B. (2005) The occurrence of potentially hazardous trace elements in five Highveld coals, South Africa. *Int. J. Coal Geol.*, **63**, 228–246.
92. Wagner, N.J. and Tlotleng, M.T. (2012) Distribution of selected trace elements in density fractionated Waterburg coals from South Africa. *Int. J. Coal Geol.*, **94**, 225–237.
93. EFA, Energy Forecasting Agency (Russian Federation) (2009) Scenario Conditions of Electric Power Industry Development for the Period up to 2030, Moscow, 2009, (not seen; cited in [93]).
94. UNEP (2011) Reducing Mercury Emissions from Coal Combustion in the Energy Sector in the Russian Federation. United Nations Environment Programme Project Report prepared by Scientific Research Institute for Atmospheric Air Protection (SRI Atmosphere, JSC), Saint-Petersburg, November, 2011, 61 p, http://www.unep.org/hazardoussubstances/Portals/9/Mercury/Documents/coal/Report_Coal_Russia_20FINAL_2016_20Nov2011.pdf (accessed February 2012).
95. VTI (2009) Mercury Content of Russian Coals. Draft Report, All-Russia Thermal Engineering Institute (VTI) (not seen, cited in [93]).
96. ACAP, Arctic Council Action Plan to Eliminate Pollution of the Arctic (2005) Assessment of Mercury Releases from the Russian Federation, 332 p.
97. Meij, R. and te Winkel, B.H. (2009) Trace elements in world steam coal and their behavior in Dutch coal-fired power stations: a review. *Int. J. Coal Geol.*, **77**, 289–293.
98. Kolker, A., Panov, B.S., Panov, Y.B., Landa, E.R., Conko, K.M., Korchemagin, V.A., Shendrik, T., and McCord, J.D. (2009) Mercury and trace element contents of Donbas coals and associated mine water in the vicinity of Donetsk, Ukraine. *Int. J. Coal Geol.*, **79**, 83–91.
99. Widodo, S., Oschmann, W., Bechtel, A., Sachsenhofer, R.F., Anggayana, K., and Puettmann, W. (2010) Distribution of sulfur and pyrite in coal seams from Kutai Basin (East Kalimantan, Indonesia): implications for paleoenvironmental conditions. *Int. J. Coal Geol.*, **81**, 151–162.
100. Belkin, H.E. and Tewalt, S.J. (2007) Geochemistry of Selected Coal Samples from Sumatra, Kalimantan, Sulawesi, and Papua, Indonesia. U.S. Geological Survey Open File Report 2007–1202, U.S. Geological Survey, 34 p.
101. Davidson, R.M., 2005, Chlorine in Coal Combustion and Cofiring. Report CCC/105, IEA Clean Coal Centre, London, 32 p.
102. Senior, C. (2015) Mercury behavior in combustion systems, in *Mercury Control – for Coal-Derived Gas Streams* (eds E.J. Granite, H.W. Pennline, and Constance Senior), Wiley-VCH GmbH & Co KGaA, Weinheim.
103. Nebergall, R. (2015) Halogenated carbon sorbents, in *Mercury Control – for Coal-Derived Gas Streams* (eds E.J. Granite, H.W. Pennline, and Constance Senior), Wiley-VCH GmbH & Co KGaA, Weinheim.
104. Cao, Y., Gao, Z., Zhu, J., Wang, Q., Huang, Y., Chiu, C., Parker, B., Chu, P., and Pan, W.-P. (2008) Impacts of halogen additions on mercury oxidation, in a slipstream selective catalyst

- reduction (SCR), reactor when burning sub-bituminous coal. *Environ. Sci. Technol.*, **42**, 256–261.
105. Yudovich, Y.E. and Ketris, M.P. (2006) Chlorine in coal: a review. *Int. J. Coal Geol.*, **67**, 127–144.
 106. Bragg, L.J., Finkelman, R.B., and Tewalt, S.J. (1991) in *Chlorine in Coal* (eds J. Stringer and D.D. Banerjee), Elsevier, Amsterdam, pp. 3–10.
 107. Finkelman, R.B. (1993) in *Organic Geochemistry* (eds M.H. Engel and S.A. Macko), Plenum Press, New York, pp. 593–607.
 108. Gluskoter, H.J. and Rees, O.W. (1964) *Chlorine in Illinois Coal*, Illinois State Geological Survey Circular, vol. 372, Illinois State Geological Survey, Urbana, IL, 23 p.
 109. Demir, I., Chou, C.-L., and Chaven, C. (1990) in *Recent Advances in Coal Geochemistry*, Special Paper 248 (eds L.L. Chyi and C.-L. Chou), Geological Society of America, pp. 73–86.
 110. ASTM Method D388-99. (2000) *Standard Classification of Coals by Rank. Annual Book of ASTM Standards v.05.06*, American Society for Testing and Materials, West Conshohocken, PA, pp. 33-38.
 111. Quick, J.C. (2010) Supporting information for: carbon dioxide emission factors for U.S. coal by origin and destination. *Environ. Sci. Technol.*, **44** (7), 2709–271468 p, <http://pubs.acs.org/doi/abs/10.1021/es9027259> (accessed 18 March 2014).
 112. Huggins, F.E. and Huffman, G.P. (1995) Chlorine in coal: an XAFS spectroscopic investigation. *Fuel*, **74**, 556–569.
 113. Vassilev, S.V., Eskenazy, G.M., and Vassileva, C.G. (2000) Contents, modes of occurrence and origin of chlorine and bromine in coal. *Fuel*, **79**, 903–921.
 114. Van Otten, B., Buitrago, P.A., Senior, C.L., and Silcox, G.D. (2011) Gas-phase oxidation of mercury by bromine and chlorine in flue gas. *Energy Fuels*, **25**, 3530–3536.
 115. Liu, S.-H., Yan, N.-Q., Liu, Z.-R., Qu, Z., Wang, H.P., Chang, S.-G., and Miller, C. (2007) Using bromine gas to enhance mercury removal from flue gas of coal-fired power plants. *Environ. Sci. Technol.*, **41**, 1405–1412.
 116. Niksa, S., Pakak, B., Krishnakumar, B., and Naik, C.V. (2010) Process chemistry of Br addition to utility flue gas for Hg emissions control. *Energy Fuels*, **24**, 1020–1029.
 117. Vosteen, B.W., Winkler, H., and Berry, M.S. (2010) Native halogens in coals from USA, China and elsewhere- Low chlorine coals need bromide addition for enhanced mercury capture. Proceedings, 2010 Power Plant Air Pollutant Control “MEGA” Symposium, Baltimore, MD, Paper 103, 22 p.
 118. Spears, D.A. (2005) A review of chlorine and bromine in some United Kingdom coals. *Int. J. Coal Geol.*, **64**, 257–265.
 119. Biester, H., Selimović, D., Hemmerich, S., and Petri, M. (2006) Halogens in pore water of peat bogs- the role of peat decomposition and dissolved organic matter. *Biogeosciences*, **3**, 53–64.
 120. Vainikka, P. and Hupa, M. (2012) Review on bromine in solid fuels. Part I: natural occurrence. *Fuel*, **95**, 1–14.
 121. Drever, J.I. (1988) *The Geochemistry of Natural Waters*, 2nd edn, Prentice-Hall, Englewood Cliffs, NJ, 437 p.
 122. Walter, L.M., Stueber, A.M., and Huston, T.J. (1990) Br-Cl-Na systematics in Illinois basin fluids: constraints on fluid origin and evolution. *Geology*, **18**, 315–318.
 123. Lee, S.J., Seo, Y.-C., Jurng, J., and Lee, T.G. (2004) Removal of gas-phase elemental mercury by iodine- and chlorine-impregnated activated carbons. *Atmos. Environ.*, **38**, 4887–4893.
 124. Li, Y., Daukoru, M., Suriyawong, A., and Biswas, P. (2009) Mercury emissions control in coal combustion systems using potassium iodide: bench-scale and pilot-scale studies. *Energy Fuels*, **23**, 236–243.
 125. Chi, Y., Yan, N., Qu, Z., Qiao, S., and Jia, J. (2009) The performance of iodine on the removal of elemental mercury from the simulated coal-fired gas. *J. Hazard. Mater.*, **166**, 776–781.
 126. Wang, B., Jackson, J.C., Palmer, C., Zheng, B., and Finkelman, R.B.

- (2005) Evaluation on determination of iodine in coal by energy dispersive X-ray fluorescence. *Geochem. J.*, **39**, 391–394.
127. Yun-Chuan, G., Qin-Fen, G., Ming-Xing, S., Zhi-Xiu, Z., and Zong-Hong, C. (2007) Simultaneous measurements of arsenic, bromine, and iodine in coal and coke by inductively coupled plasma-mass spectrometer. *Chin. J. Anal. Chem.*, **35** (8), 1175–1178.
128. Wu, D., Deng, H., Zheng, B., Wang, W., Tang, X., and Xiao, H. (2008) Iodine in Chinese coals and its geochemistry during coalification. *Appl. Geochem.*, **23**, 2082–2090.
129. Goodarzi, F. and Swaine, D.J. (1994) The influence of geological factors on the concentration of boron in Australian and Canadian coals. *Chem. Geol.*, **118**, 301–318.
130. Bettinelli, M., Spezia, S., Minoia, C., and Ronchi, A. (2002) Determination of chlorine, fluorine, bromine, and iodine in coals with ICP-MS and I.C. *At. Spectrosc.*, **24** (4), 105–110.
131. Ketris, M.P. and Yudovich, Y.E. (2009) Estimations of Clarkes for Carbonaceous biolithes: world averages for trace element contents in black shales and coals. *Int. J. Coal Geol.*, **78**, 135–148.
132. Luo, K., Ren, D., Xu, L., Dai, S., Cao, D., Feng, F., and Tan, J. (2004) Fluorine content and distribution pattern in Chinese coals. *Int. J. Coal Geol.*, **57**, 143–149.
133. Wang, X., Dai, S., Sun, Y., Li, D., Zhang, W., Zhang, Y., and Luo, Y. (2011) Modes of occurrence of fluorine in the Late Paleozoic No. 6 coal from the Haerwusu Surface Mine, Inner Mongolia, China. *Fuel*, **90**, 248–254.

3 Regulations

Nick Hutson

3.1 U.S. Regulations

3.1.1 Background

The enactment of the Clean Air Act of 1970 (1970 CAA) resulted in a major shift in the federal government's role in air pollution control. This legislation authorized the development of comprehensive federal and state regulations to limit emissions from both stationary (industrial) and mobile sources. At this time, the National Emission Standards for Hazardous Air Pollutants (NESHAP) program was initiated to limit emissions of toxic or hazardous air pollutants (HAPs) from stationary sources. CAA Section 112 addresses emissions of HAPs, which are those pollutants which are hazardous to human health or the environment but are not specifically covered under another portion of the CAA. These pollutants are typically carcinogens, mutagens, or reproductive toxins. In 1990, the U.S. Congress, believing that the 1970 CAA and subsequent amendments had failed to provide substantial reductions of air toxic pollutants, passed the Clean Air Act Amendments of 1990 (1990 CAAA). The 1990 CAAA authorized, among other things, the incorporation of the NESHAP into a greatly expanded program for controlling toxic air pollutants.

The new law included a list of 189 toxic air pollutants (including mercury and its compounds) for which emissions must be reduced. Congress then mandated that the Environmental Protection Agency (US EPA) publish a list of source categories that emit certain levels of these pollutants within 1 year of the law's passage. For major sources (those emitting more than 10 ton of any single HAP or more than 25 ton cumulatively of all the listed HAPs), Section 112 mandates that the EPA establish emission standards that require the maximum degree of reduction in emissions of HAPs. These emission standards are commonly referred to as *maximum achievable control technology* or *MACT* standards. These standards are to be based on the best demonstrated control technology or practices within the regulated industry.

Eight years after issuance of the technology-based standards, the EPA is required to review those standards to determine whether any residual risk exists for that source category and must, if necessary, revise the standards to address such risk.

3.1.2

Electric Generating Units (EGUs)

Congress established a specific structure for determining whether to regulate electric generating units (EGUs) under CAA Section 112. Specifically, Congress required the EPA to conduct a study to evaluate the remaining public health hazards that are reasonably anticipated to occur as a result of EGUs' HAP emissions after imposition of other CAA requirements. The EPA was required to report the results of that study – referred to as *the Utility Study* [1] – to Congress, and to regulate EGUs “if the Administrator finds such regulation is appropriate and necessary,” after considering the results of that study.

The Utility Study included numerous analyses. The EPA first collected HAP emissions test data from 52 EGUs, including a range of coal-, oil-, and natural gas-fired units, and the test data along with facility-specific information were used to estimate HAP emissions from all 684 utility facilities. The EPA determined that 67 HAP were potentially emitted from EGUs. EPA conducted a screening level assessment of all 67 HAP to prioritize the HAP for further analysis. Six HAPs (mercury, radionuclides, arsenic, cadmium, lead, and dioxins) were considered a priority for multi-pathway assessment of exposure and risk. Based on these analyses, EPA determined that Hg from coal-fired EGUs was the HAP of greatest potential concern.

Congress also directed the EPA to conduct a study specifically on mercury emissions from EGUs, municipal waste combustion units, and other sources. This is referred to as *the Mercury Study*. In this study, the EPA was directed to consider the rate and mass of mercury emissions, the health, and environmental effects of such emissions, available control technologies, and the costs of those technologies. Congress also directed the National Institute of Environmental Health Sciences (NIEHS) to conduct a study to determine the threshold for mercury concentrations in the tissue of fish which may be consumed (including consumption by sensitive populations) without adverse effects to public health. In addition, Congress directed the EPA to fund the National Academy of Sciences (NAS) to perform an independent evaluation of the available data related to the health impacts of methylmercury (MeHg). Specifically, Congress required the NAS to advise the EPA as to the appropriate reference dose (RfD) for MeHg. The RfD is the amount of a chemical which, when ingested daily over a lifetime, is anticipated to be without adverse health effects to humans, including sensitive subpopulations.

As directed by Congress through different vehicles, the NAS Study and the NIEHS Study evaluated the same issues. The NIEHS completed their study in 1995 and the NAS study was completed in 2000.

On 20 December 2000, the EPA issued a finding that it was “appropriate and necessary” to regulate coal- and oil-fired EGUs under CAA Section 112 and added such units to the list of source categories subject to regulation. Once the source category was listed, the EPA was then required to establish technology-based emission standards. More specifically, the EPA was required to establish emission standards that reflect the “MACT” level of control. By statute, the MACT standards for existing sources must be at least as stringent as the average emission limitation achieved by the best performing 12% of existing sources in the category (for which the Administrator has emissions information). This level of minimum stringency is referred to as the *MACT floor*, and the EPA cannot consider cost in setting the floor. For new sources, MACT standards must be at least as stringent as the control level achieved in practice by the best controlled similar source. The EPA must also consider more stringent “beyond-the-floor” control options, but must take into account costs, energy, and nonair quality health and environmental impacts when doing so.

The EPA did issue standards for Hg emissions from coal- and oil-fired power plants. However, instead of issuing emission standards under CAA Section 112 (covering HAPs), the Agency, on 29 March 2005, issued the Section 112(n) Revision Rule that removed EGUs from the list of sources subject to regulation under CAA Section 112. This Revision Rule essentially reversed the Agency’s previous finding and determined that it was neither appropriate nor necessary to regulate such units under CAA Section 112.

Subsequently, on 18 May 2005, the EPA issued the Clean Air Mercury Rule (CAMR). That rule established standards of performance for emissions of Hg from new and existing coal-fired EGUs under CAA Section 111 (New Source Performance Standards, NSPS).

A collection of environmental groups, states, and tribes challenged the Section 112 delisting action and the legality of the CAMR. On 8 February 2008, the D.C. Circuit Court vacated both the 2005 delisting action and the CAMR. The D.C. Circuit held that the EPA had failed to comply with the requirements for delisting source categories from Section 112. Thus, CAMR and the 2005 delisting action became null and void and the rule was never implemented.

On 18 December 2008, several environmental and public health organizations filed a complaint in the U.S. District Court for the District of Columbia. They alleged that the EPA had failed to perform a nondiscretionary duty by failing to promulgate final CAA Section 112(d) standards for HAP from coal- and oil-fired EGUs by the statutorily-mandated deadline. The EPA settled the litigation and agreed to issue final MACT emission standards for coal- and oil-fired EGUs by 16 December 2011.

3.1.3

Mercury and Air Toxics Standards (“MATS”) – Existing Sources

On 16 December 2011, the EPA Administrator signed the Mercury and Air Toxics Standards (or “MATS”) which requires that coal- and oil-fired EGUs meet HAP

Table 3.1 Final mercury emission limits in the U.S. EPA “Mercury and Air Toxics Standards (MATS)” for existing fossil fuel power plants.

Sources	lb TBtu ⁻¹ (input)	lb GWh ⁻¹ (output)	~μg m ⁻³
<i>Existing plants</i>			
Coal > 8300 Btu lb ⁻¹	1.2	0.013	1.40
Coal < 8300 Btu lb ⁻¹	4.0	0.04	4.70
Solid oil-derived fuel	0.2	0.002	0.23
IGCC units	2.5	0.03	2.90

The emission limits for existing units are provided in pounds of mercury per trillion British thermal unit of heat input or alternatively in units of pounds of mercury per gigawatt-hour of power output, both based on a 30 day rolling average. The measured emission in micrograms per cubic meter is an approximate value only; the affected units must show compliance with the input or output based standard. The EPA did not set emission limits for natural gas-fired power plants. Solid oil-derived fuel is commonly known as *petroleum coke* or *pet coke*.

standards reflecting the performance of the MACT. The rule [2] established uniform emissions-control standards that affected sources can meet with proven and available technologies and operational processes. The rule set emission limits for mercury and other toxic metals (such as arsenic, cadmium, lead, and nickel), for hazardous acidic gases (such as hydrochloric and hydrofluoric acids) and set work practice standards to limit the emissions of toxic organic pollutants, including benzene and dioxins.

The specific limits for subcategories of existing EGUs are given in Table 3.1. The emission limits are provided for mine-mouth units designed for and burning low rank, virgin coal with a calorific value <8300 Btu lb⁻¹ (this will represent primarily units utilizing lignite coal), all other coals, solid oil-derived fuel (petroleum coke), and integrated gasification combined cycle (IGCC) units (regardless of fuel source). If an EGU burns coal (either as a primary fuel or as a supplementary fuel) or any combination of coal with another fuel (except for solid waste) where the coal accounts for more than 10.0% of the average annual heat input during any three consecutive calendar years or for more than 15.0% of the annual heat input during any one calendar year after the applicable compliance date, the unit is considered to be coal-fired.

For coal-fired, IGCC, and solid oil-derived fuel-fired units, operators must use a Hg continuous emissions monitoring system (CEMS) or a sorbent trap monitoring system for both initial and continuous compliance.

CAA Section 112 specifies the dates by which affected sources must comply with this rule. New or reconstructed units must be in compliance immediately upon startup or the effective date of this rule, whichever is later. Existing sources may be provided up to 3 years after the effective date to comply with the final rule; if an existing source is unable to comply within 3 years, a permitting authority (usually the state) has the ability to grant such a source up to a 1 year extension, on a case-by-case basis, if such additional time is necessary for the installation

of controls. The EPA's Office of Enforcement and Compliance Assurance (OECA) also issued a memorandum describing the Agency's "intended approach regarding the use of administrative orders ("AOs") for sources that must operate in noncompliance with MATS for up to 1 year to address a specific and documented reliability concern."

3.1.4

Mercury and Air Toxics Standards ("MATS") – New Sources

On 16 December 2011, the final "MATS" also contained standards for new fossil fuel-fired EGUs (i.e., those that commence construction after 3 May 2011). The rule set emission limits for mercury and other toxic metals (such as arsenic, cadmium, lead, and nickel), for hazardous acidic gases (such as hydrochloric and hydrofluoric acids) and set work practice standards to limit the emissions of toxic organic pollutants, including benzene and dioxins. The CAA specifies that, for new sources, the emission limitation "shall not be less stringent than the emission control achieved in practice by the best controlled similar source."

Following promulgation of the final MATS rule, the EPA received several petitions for reconsideration of numerous provisions of both the MATS rules, including the achievability of the final new source standards. The EPA Administrator agreed to reconsider certain aspects of the final MATS rule and the reconsideration proposal was published on 30 November 2012 [3]. The reconsidered emission limits for new sources were finalized in March 2013.

The mercury emission limits for subcategories of new EGUs are given in Table 3.2. The original final emission limits are given along with final reconsideration emission limits. As with existing sources, the emission limits are provided for mine-mouth units designed for and burning low rank, virgin coal with a calorific value $<8300 \text{ Btu lb}^{-1}$ (this will represent primarily units utilizing lignite

Table 3.2 Final mercury emission limits in the U.S. EPA "Mercury and Air Toxics Standards (MATS)" for new fossil fuel power plants.

Sources	MATS original (lb GWh ⁻¹) (output)	MATS revised (lb GWh ⁻¹) (output)	Revised (~ $\mu\text{g m}^{-3}$)
<i>New plants</i>			
Coal $> 8300 \text{ Btu lb}^{-1}$	0.0002	0.003	0.35
Coal $< 8300 \text{ Btu lb}^{-1}$	0.04	0.04	4.70
Solid oil-derived fuel	0.002	0.002	0.23
IGCC units	0.003	0.003	0.35

The emission limits for new coal-fired or IGCC power plants are provided only in units of pounds of mercury per gigawatt-hour of power output, based on a 30 day rolling average. The measured emission in micrograms per cubic meter is an approximate value only; the affected units must show compliance with the output based standard. The EPA did not set emission limits for natural gas-fired power plants. Solid oil-derived fuel is commonly known as *petroleum coke* or *pet coke*.

coal), all other coals, solid oil-derived fuel (petroleum coke), and IGCC units (regardless of fuel source). New sources may only meet an output based emission limitation.

References

1. U.S. EPA (1998) Study of Hazardous Air Pollutant Emissions from Electric Utility Steam Generating Units—Final Report to Congress. EPA-453/R-98-004a, Environmental Protection Agency, February 1998.
2. EPA (2012) National Emission Standards for Hazardous Air Pollutants From Coal and Oil-Fired Electric Utility Steam Generating Units and Standards of Performance for Fossil-Fuel-Fired Electric Utility, Industrial-Commercial-Institutional, and Small Industrial-Commercial-Institutional Steam Generating Units. Federal Register, Vol. 77, No. 32, February 16, 2012 (77 FR 9304).
3. EPA (2012) Reconsideration of Certain New Source and Startup/Shutdown Issues: National Emission Standards for Hazardous Air Pollutants From Coal- and Oil-Fired Electric Utility Steam Generating Units and Standards of Performance for Fossil-Fuel-Fired Electric Utility, Industrial-Commercial-Institutional, and Small Industrial-Commercial-Institutional Steam Generating Units. Federal Register, Vol. 77, No. 231, November 30, 2012 (77 FR 71323).

4

International Legislation and Trends

Lesley L. Sloss

4.1

Introduction

Some regions and countries in Europe, Australia, and Asia are actively monitoring and controlling mercury emissions. However, they are currently doing so without the apparent urgency incurred by national and regional binding legislation and specific mercury reduction targets that are being applied in Canada and introduced in the United States at the moment. That is not to say that mercury is not being controlled outside North America. Rather that this control of mercury is largely being achieved as a result of co-benefit effects.

There were a number of international treaties, set by the United Nations Environment Programme (UNEP), which included mercury. These were not challenging with respect to mercury limits and therefore did not require any action to be taken at coal-fired utilities. The UNEP Governing Council made a decision in February 2009 to further strengthen international action on mercury and initiated negotiations toward producing a “Global legally binding instrument on mercury.” This instrument, is known as the *Minamata Convention*, was completed in February 2013. The convention promotes BAT at all new coal-fired power plants and requires a national action plan, with options for BAT, emission limits, reduction targets and so on, to be taken at all existing plants. There is enough flexibility in the wording to allow signatory countries to determine their own best approach to reducing mercury emissions from this sector.

Concern has been expressed that the rapid increase in coal use in countries such as those in Asia may override reductions in emissions achieved elsewhere. It is therefore essential that any international mercury legislation is made both technically and economically viable in developing countries to ensure that the current upward trend in global mercury emissions is controlled effectively. These are the kind of issues which have been addressed within the flexibility of the UNEP convention.

This chapter will summarize both international and national legislation (excluding the United States). Mercury legislation is currently in a state of extreme flux and, as a result, the information included in this chapter can only be regarded as a

snapshot of the issue as this document goes to print. However, it is clear that many countries, not just those in North America, are moving toward stringent control of all toxic emissions and so legislation for mercury control can be regarded as somewhat inevitable. It remains only to be seen what form this legislation may take in different regions and how soon it will be initiated.

4.2

International Legislation

There are a number of international agreements and action plans to co-ordinate activities to reduce mercury emissions. These include [1]

<i>UNECE</i>	The United Nations Economic Commission for Europe (UNECE) has a convention on long-range trans-boundary air pollution (LRTAP). This convention was published in 1998 and covers heavy metals including mercury. The protocol has been signed by Canada, Europe, Russia, and the United States. Although the protocol calls for the installation of BAT at new stationary sources, it does not go so far as to define BAT for coal-fired plants or to specify any reduction strategies.
<i>OSPAR</i>	Oslo and Paris Commission's program on reduction of land-based pollutants transported to the North Sea.
<i>HELCOM</i>	The Helsinki Commission program covering the North Sea.
<i>Barcelona Convention</i>	A program similar to OSPAR and HELCOM covering the Mediterranean Sea.
<i>MEPOP</i>	European political initiative studying the atmospheric cycling of mercury and persistent organic pollutants.
<i>Nordic</i>	Co-ordination of projects between Denmark, Finland, Norway, and Sweden to reduce mercury emissions.
<i>Arctic</i>	The Arctic Council's Environmental Protection Strategy includes mercury.
<i>NARAP</i>	North American Regional Action Plan between Canada, the United Mexican States, and the United States to reduce mercury fluxes.
<i>Binational Toxics</i>	Canada and the United States have a project for cleaning up substances, including mercury, in the Great Lakes Basin Area.

None of these agreements or programs includes guidelines on how the proposed reductions in emissions or concentrations should be achieved other than by recommending "best practices." The agreements rely on the individual governments of each signatory country to produce a successful strategy to reduce mercury emissions. They therefore do not necessarily guarantee results. Action is rarely, if ever, taken against countries that are not as successful as others in

reducing emissions. For the moment, there is no international treaty that requires specific mercury control at coal-fired utilities. However, this may change with the introduction of the UNEP “Minamata Convention.”

4.2.1

UNEP International Legally Binding Instrument on Mercury (“Minamata Convention”)

In February 2009, the Governing Council of the UNEP agreed on Decision 23/9 defining the need to develop a global legally binding instrument on mercury. The convention was completed in February 2014. The final text requires that signatory parties take measures to control and, where feasible, reduce emissions. New plants will have to apply BAT/BEP and BAT/BEP is an option, alongside emission limit values, reduction targets, multi-pollutant strategies or “alternative measures”, for existing sources. The definition of BAT within the convention is to be determined by the conference of the parties but must take geographical, technical and economic considerations into account. And so, at this stage, it is up to each signatory country to determine how the convention will be applied to sources within their jurisdiction.

4.2.2

European Union (EU)

There are three established directives which are currently relevant to coal-fired utilities in the European Union (EU) member states:

- the Integrated Pollution Prevention and Control (IPPC) Directive;
- the Large Combustion Plant Directive (LCPD); and
- the Waste Incineration Directive (WID, applicable to plants co-firing waste with coal).

All these directives will continue to apply until they are replaced by

- the Industrial Emissions Directive (IED), which comes into force for coal-fired power plants in 2016.

It is therefore necessary to discuss each of these directives in turn to appreciate the ramifications for utilities in Europe. Although none of these Directives specifies emission limits or control requirements for mercury, the technologies that plants must install to meet SO₂ and NO_x limits will have a significant effect on mercury emissions.

EU-Directive on IPPC (2008/1/EC) (EC, European Commission) applies an integrated environmental approach to the regulation of around 45 000 industrial facilities, including large combustion plants, in the EU. The directive is based on a plant-specific permit which details the requirements relevant to each individual facility and can therefore take into account not only any international and national requirements (such as reduction targets for UNECE protocols and EU emission limits) but also regional and local considerations such as preservation of sensitive

watershed areas. For particulates, the BAT options are electrostatic precipitator (ESP) (99.5% efficiency) in combination with wet flue gas desulfurization (FGD); or bag houses (fabric filters) (99.95% efficiency) in combination with wet FGD. For SO₂, the BAT options are either low-sulfur fuel, wet FGD, spray dry FGD, seawater FGD, or combined SO₂ and NO_x systems. For NO_x, the BAT options are primary measures (air/fuel staging, low NO_x burners, re-burn) in combination with SCR (selective catalytic reduction) or SNCR (selective non-catalytic reduction) in some cases; or combined SO₂ and NO_x systems. However, the choice of which control combination is suitable as BAT for each individual plant has to be defined on a case-by-case basis under each permit and is based on extensive BAT reference documents (BREFs) provided by the EC.

The revised LCPD (2001/80/EC) applies to combustion plants with a thermal output of >50 MW. According to the directive, by 1 January 2008, all large combustion plants in Europe had to opt for one of the following three compliance options:

- 1) meet emission limit values (ELVs) for particulates, SO₂ and NO_x;
 - a. 200 mg m⁻³ SO₂ for new plant and 400–2000 mg m⁻³ for existing plant (based on size);
 - b. 200–400 mg m⁻³ NO_x for new plant and 500–600 mg m⁻³ for existing plant (based on plant size)
- 2) sign up to lower SO₂ and NO_x “bubbles” that are equivalent to the ELV reductions and which are part of a National Emission Reduction Plan (NERP); or
- 3) “opt-out” of ELVs and NERP and commit to close by 2015, operating for no more than 20 000 h over that period.

Therefore, to meet both the IPPC BAT requirements and the LCPD ELV with fuel switching alone, plants would need to be firing very low-sulfur coal to avoid having to install FGD [2]. In simple terms, the IPPC and LCPD together mean that all plants must install wet FGD (or a technology with similar or greater SO₂ control) and make at least combustion modifications to reduce NO_x (some plants will require SCR in addition to combustion modifications). Plants which could not comply with either option 1 or 2 above were to close by 2016 and run limited operating hours until that date.

Many plants within Europe regarded the ELVs defined by the LCPD as too challenging. Before the LCPD was replaced by the IED, almost 25 GW of coal units and 10 GW of lignite units decided not to install FGD, particularly in Spain, France, and the United Kingdom in Western Europe. These plants chose to opt-out of the LCPD and close by 2016 [3].

If co-combustion of other waste is to be applied at an existing coal-fired plant, the emission limits must be revised according to the EU WID (2000/76/EC). Table 4.1 includes a summary of the EU emission limits under the WID alongside the emission limits in Germany (*see below*) [4].

The WID limits are more stringent than those in the LCPD. Under the “mixing rule,” plants firing waste materials defined under the WID must calculate a specific emission limit based on the amount of waste material being co-fired. However, this

Table 4.1 German emission limits for waste incineration plant and power plant [4].

Compound	Thirteenth BImSchv ^{a)}		Seventeenth BImSchv ^{a)}		EU-Directive	
	Power plants		Waste incineration		Power plants >300 MW th	
	Daily average (6% O ₂)	Daily average (11% O ₂)	Daily average (11% O ₂)	Half-hour average (11% O ₂)	Daily average (6% O ₂)	Daily average (10% O ₂)
CO (mg m ⁻³)	250	50	100	100	Mixing rule	—
Organic compounds as total C (mg m ⁻³)	—	10	20	20	Mixing rule	10
Particulate matter (mg m ⁻³)	50	10	30	30	30	30
SO ₂ /SO ₃ as SO ₂ (mg m ⁻³)	400	50	200	200	200	50
Sulfur emission factor (%)	15	—	—	—	5	—
NO _x (mg m ⁻³)	500	200	400	400	200	800
HCl (mg m ⁻³)	100	10	60	60	10	10
HF (mg m ⁻³)	15	1	4	4	Mixing rule	1
Σ TI + Cd (mg m ⁻³)	—	0.05	—	—	0.05	0.05
Hg (µg m ⁻³)	—	0.03	0.05	—	0.05	0.05
Σ Sb, As, Pb, Cr, Co, Cu, Mn, Ni, V, Sn (mg m ⁻³)	—	0.5	—	—	0.5	0.5
PCDD/PCDF (ng m ⁻³)	—	0.1	—	—	0.1	0.1

a) Bundesimmissionschutz-Verordnung or BImSchv limits.

does not apply to mercury and its compounds, for which the limit is 0.050 mg m^{-3} for all co-incineration plants. The WID is far more challenging with respect to compliance than the LCPD and so existing coal-fired plants are generally reluctant to co-fire waste material that falls under the remit of the WID. In addition to the more stringent emission limits, the WID also has more demanding monitoring requirements.

In 2007, in recognition that the EU legislation at that time was somewhat piecemeal and confusing, the EC launched a review of the existing legislation with the aim of merging seven different directives into one. The directives which were merged were

- the Large Combustion Plant directive (LCPD);
- the Integrated Pollution Prevention and Control Directive (IPPC);
- the Waste Incineration Directive (WID);
- the Solvent Emissions Directive (SED); and
- the three existing directives on Titanium dioxide on (i) disposal (78/176/EEC), (ii) monitoring and surveillance (82/883/EEC), and (iii) programs for the reduction of pollution (92/112/EEC).

These directives were all merged into the new IED which was published by the EC in December 2010. The IED was to be drafted into national legislation within each of the Member States by 6 January 2013.

For coal-fired plants, the IED is effectively a combination of the IPPC and LCPD discussed above, containing aspects of both permitting and plant-specific requirements along with ELVs or equivalent reduction strategies. Each plant must have its own plant-specific permit with performance, based on a combination of BAT and ELVs.

The new IED allows some flexibility in the definition of BAT, according to the decisions of the local competent authority, and requires continued work at the EC level on BREFs. The IED also includes potential derogations where BAT is considered to be of a disproportionately high cost, as long as the ELV are still met. There is also still the option of a minimum desulfurization rate for plants which cannot comply with ELVs due to specific fuel characteristics.

As with the original LCPD, the IED allows the same three options for compliance: the ELV, the NERP (now referred to as the *National Action Plan*), or opt-out (eventual closure).

The new ELVs for SO_2 for combustion plants granted permits before 7 January 2013 are as follows:

Emission limit for SO_2 for plants permitted pre-2013 (mg m^{-3})

Plant size (MWt)	Coal, lignite, and other solid fuels	Biomass	Peat	Liquid
50–100	400	200	300	350
100–300	250	200	300	250
>300	200	200	200	200

The remaining plants must then meet more stringent SO₂ limits after 2016.

Emission limit for SO₂ for plants permitted post-2013 (mg m⁻³)

Plant size (MWt)	Coal, lignite, and other solid fuels	Biomass	Peat	Liquid
50–100	400	200	300	350
100–300	200	200	300	200
>300	150	150	150	150

For those plants, originally permitted prior to 2013, which cannot meet the prescribed ELV due to specific fuel characteristics, there is still the option of meeting a minimum rate of desulfurization, shown below.

Desulfurization rate for SO₂ for plants with challenging fuel, permitted pre-2013

Plant size (MWt)	Plants permitted before 27 November 2002 (%)	Other plants (%)
50–100	80	92
100–300	90	92
>300	96	96

All other plants must meet tighter reduction requirements.

Desulfurization rate for SO₂ for plants with challenging fuel, permitted post-2013

Plant size (MWt)	(%)
50–100	93
100–300	93
>300	97

Both these reduction requirements and the ELVs listed above would require, in most if not all instances, the use of FGD technologies.

For those plants firing low-sulfur fuel, there is a potential derogation period of 6 months, which will be permitted during instances of interruption in the supply of low-sulfur fuel (such as that resulting from a serious shortage).

The new NO_x limits (milligrams per cubic meter) for combustion plants granted permits before 7 January 2013 are as follows:

Emission limit for NO_x for plants permitted pre-2013 (mg m⁻³)

Plant size (MWt)	Coal	Lignite	Biomass and peat	Liquid
50–100	300	450	300	450
100–300	200	200	250	200
>300	200	200	200	150

Plants not permitted before 7 January 2013 must meet the following limits after 2016:

Emission limit for NO_x for plants permitted post-2013 (mg m⁻³)

Plant size (Mwt)	Coal	Lignite	Biomass and peat	Liquid
50–100	300	400	250	300
100–300	200	200	200	150
>300	150	200	150	100

For most plants, low NO_x burning systems may not be able to reach these limits and additional SCR or SNCR technologies will be required.

As with the original LCPD, under the new IED, plants may be exempt from the ELV if they agree to the following:

- to operate no more than 17 500 h between 1 January 2016 and 31 December 2023 (a more forgiving timescale than the LCPD);
- to report hours of operation on an annual basis; and
- ELVs prescribed in the plant permit on 31 January 2015 shall be maintained for the remaining operation period of the plant.

The IED carries with it requirements for continuous emission monitoring (CEM) of particulates/dust, SO₂, and NO_x on all plants. Although the IED does not set an ELV for mercury from coal-fired utilities, it does introduce a requirement for annual monitoring of mercury emissions.

Although this monitoring requirement for mercury is the only mention of mercury in the new IED, this does not mean that mercury is not under control. Studies carried out in the EU and elsewhere have consistently shown that the installation of control technologies for particulates, SO₂ and NO_x on coal-fired power plants can effectively reduce mercury emissions. For most plants and coals, the combination of particulate controls and wet FGD systems will mean at least 70% mercury reduction [5, 6]. If SCR is also included, as will be the case at many EU plants, mercury capture can be up to and over 90%. While this significant reduction rate is certainly not guaranteed, especially for some challenging coals, most plants will still achieve some co-benefit mercury control. By introducing the requirement for mercury monitoring at all plants, the EC will gather data on just how effective the control systems required under the IED are for mercury control and, based on this, may or may not set mercury specific legislation in the future. Although, for the moment, mercury emissions are regarded as largely under control, the new IED BREFs (currently being updated to include mercury) may well define BAT levels for mercury based on available information and reductions achieved so far and this could mean requirements for mercury on some plants in the future.

4.3

Regional and National Legislation

The following sections summarize the situation in several example countries and regions (excluding North America) that either have legislation for mercury control or have monitoring and compliance regimes that are potentially moving toward mercury specific legislation.

4.3.1

Europe

As discussed earlier, the existing IPPC and LCPD and their replacement, the IED, will not target mercury directly but are still likely to result in significant mercury reductions as a result of co-benefit effects.

Individual member states within the EU must adopt EU legislation as national legislation within a set time period. Over and above this, each country may set its own legislation or reduction targets based on more local environmental challenges or concerns. Countries such as Germany and the Netherlands often go above and beyond what is required by EU legislation.

4.3.1.1 Germany

The Thirteenth Ordinance of the Federal Immission Control Act (13 BImSchV) set an emission limit of $30 \mu\text{g m}^{-3}$ for mercury at all coal-fired utility plants, and continuous emission monitors for mercury are also required at all plants. Daily average and half-hour average values are required. As all plants have FGD and SCR fitted, mercury is also captured efficiently and, as yet, no mercury specific control technologies have been required at any plants firing coal alone (H. Thorwarth, Personal Communication, 2008). Germany has around 20 plants co-firing sewage sludge with coal, as summarized by Fernando [7]; these plants face a significant challenge with respect to mercury emissions and control.

Under the IPPC/IED permitting scheme, individual plants may be granted a permit that sets emission limits or control requirements which are more challenging than those for other national plants. Unpublished information suggests that a new coal-fired plant (Staudinger) in Germany will be facing a mercury emission limit in the order of $15 \mu\text{g m}^{-3}$. No more details are available at this time.

4.3.1.2 Netherlands

Similar to Germany, the Dutch Government takes a pro-active approach to emission control and often sets national and regional legislation, which is significantly more stringent than that set by the EU. Although the current IED for the EU specifies BAT requirements only for particulates, SO_2 and NO_x , permits for Dutch coal-fired plants must also consider BAT for mercury. This is based on an estimated mercury input (fuel content) and the yearly average removal efficiency of the air pollution control devices (APCDs), as measured during monitoring campaigns.

KEMA in the Netherlands have developed the KEMA TRACE MODEL[®] (KTM), an empirical and statistical model developed from mass balance studies

at all the coal-fired plants in the Netherlands over 25 years. The model can cope with co-firing secondary fuels such as biomass up to 30% on a mass base. The model covers 46 elements, including mercury. The calculated emissions, based on the fuel data, are compared to relevant emission regulations such as the LCPD or IED and any national regulations. The KTM is well trusted and is used in the impact statements and permit applications of coal-fired plants in the Netherlands (H. Te Winkel, Personal Communication, 2011).

Although there has been nothing published as yet, it would appear that three new coal-fired plants in the Netherlands, including units at Maasvlakte and Datteln, could face plant-specific mercury regulations that would limit mercury emissions to around $3 \mu\text{g m}^{-3}$ on an annual basis.

4.3.2

Asia

Asia contains some of the cleanest and some of the dirtiest coal-fired plants in the world. Several areas of Asia, such as Japan and South Korea, have already retrofitted most if not all of their plants with state-of-the-art emission control systems. Other areas, such as China and India, have such rapidly growing populations and economies that bringing all plants up to satisfactory emission limit standards is a challenge. The majority of environmental work being undertaken in India under a national government program is to improve the efficiency of existing coal-fired plants. Significant improvements in efficiency can be achieved, resulting in extended plant lifetime, reduced fuel consumption, increased energy output, and reduced emissions. For most of the plants studied, this rehabilitation makes more economic sense than the construction of new plants.

China has a range of plans and programs to reduce emissions of SO_2 based on limits and emission fees. The Chinese Government has recently introduced a new policy based on the phasing out of smaller, less-efficient coal-fired units. Other Asian nations face their own local challenges. To date, the environmental performance of each plant in many developing Asian nations depends on the location (for example, whether it is causing noticeable local effects) or on the operator/utility (depending on the level of pro-activeness). Emission monitoring is not common in most of Asia and therefore it is hard to determine compliance with any applicable emission standards. It is also difficult to determine which plants should receive priority when it comes to investment for rehabilitation or retrofitting without emission information. A move toward increased measurement and monitoring in these areas would help evaluate areas of concern to produce the most effective national policies.

The following sections summarize the situation in selected countries in Asia.

4.3.2.1 China

Chinese emission legislation is defined within 5- and 10-year plans. These plans are not law, but are rather targets that are achieved through agreements, performance, incentives, or existing laws [8]. Recently, the Chinese government's

efforts have concentrated on sulfur emissions. Despite some missed reductions in the past, the reduction target for SO₂ under the Eleventh 5 year plan (2006–2010; 10% reduction below 2005 levels) was met early and exceeded (a 14% reduction was achieved). This reduction was achieved largely due to the installation of FGD. The success of this Eleventh plan may be due to the strengthening of the approach with binding agreements with provinces and key emitters, economic and administrative incentives, performance audits, and stronger enforcement of existing laws. There has also been an unprecedented installation rate of FGD in China. In 2005, only 14% of the installed coal-fired generating capacity had been fitted with FGD but this had increased to 86% by the end of 2010 [9]. This would no doubt have resulted in significant co-benefit mercury reduction.

The *Emission Standard of air pollutants for thermal power plants* (GB 13223-2011) was adopted by the Chinese Ministry for Environmental Protection (MEP) on 18 July 2011 and should be effective starting 1 January 2012 [10]. The standard applies to particulate, SO₂, NO_x, and mercury emissions from coal-fired plants but does not apply to plants co-firing waste or biomass. Emissions of mercury will be controlled from 1 January 2015. The limit for mercury is set at 0.03 mg m⁻³. However, because of known co-benefit effects, the limits for SO₂ and NO_x are also relevant. The full emission limits are listed in the table below.

Emission limits for coal-fired boilers in China, from 2011 (for particulates, SO₂ and NO_x) to 2015 (for mercury)

Pollutant	Conditions	Limit (mg m ⁻³)
Soot	All units	30
	Plants in “key regions” ^{a)}	20
SO ₂	New boiler	100
		200 ^{b)}
	Existing boiler	200
		400 ^{b)}
NO _x (as NO ₂)	Plants in “key regions” ^{a)}	50
		All
	Plants in “key regions” ^{a)}	400 ^{c)}
		All
Hg and compounds	All	100
		0.03

^{a)}Plants in “key regions” are defined as those situated where development is concentrated and environmental capacity is low (such as existing weak environmental capacity, vulnerable ecological environment, and major air pollution problems, as defined by the MEP).

^{b)}Applies in Guangxi Zhuang Autonomous Region, Chongqing Municipality, Sichuan Province, and Guizhou Province.

^{c)}W-type thermal power generation boilers, furnace chamber flame boilers, circulating fluidized bed boilers, and boilers in operation before 31 December 2003.

The limit set for mercury, 30 µg m⁻³, is equivalent to the general emission limit for coal-fired units in Germany (see below) and applies to both existing and new

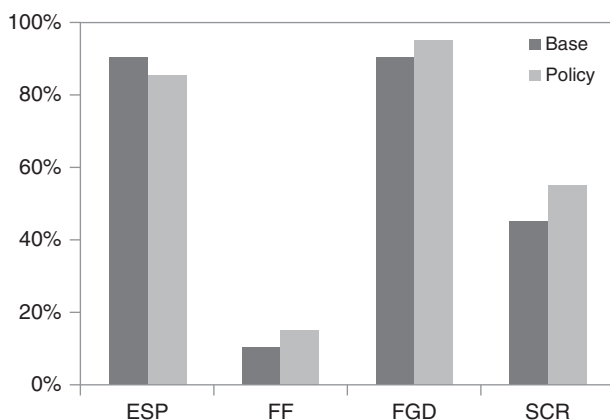


Figure 4.1 Chinese projections: application rate of emission controls in 2020.

plants. It is therefore significantly less stringent than the limits set in the United States and would be achieved by most modern plants fitted with ESP or baghouse systems firing standard coals. However, the limits set for SO_2 and NO_x will be challenging and are likely to result in FGD on all plants and upgrades on many existing FGD systems, SCR on almost all plants, and upgrading of ESPs with potential retrofitting of fabric filters in some cases. This will mean that, although the mercury limit will not itself result in mercury control, the co-benefit effects of the new SO_2 , NO_x , and particulate limits are likely to result in significant mercury reduction.

A report produced by Tsinghua University for MEP under a UNEP Coal Partnership project included emission estimates for mercury from coal-fired utilities in China for 2005 and 2008 along with predictions for mercury reduction under future energy scenarios in 2020 [11]. The scenarios are summarized in Figure 4.1 and the predicted reductions as a result of each of these are summarized in Figure 4.2. It is important to note that these scenarios were produced prior to the new 2011 standards and so the predicted mercury reduction may be even more significant.

The new Chinese limits are challenging and are predicted to cost the Chinese economy at least 260 billion yuan (\$40.74 billion) [12]. It is not clear whether this cost will include potential new monitoring requirements including CEM systems to ensure compliance. It therefore remains to be seen whether the Chinese coal sector can afford to comply with the new limits, bearing in mind the current increase in coal prices.

4.3.2.2 Japan

Environmental legislation in Japan is set on an individual company/plant basis and it is not simple to summarize the requirements that apply. There is a very high priority based on social responsibility and most companies wish to enhance their public credibility by not exceeding any requirements set. Most, if not all, coal-fired

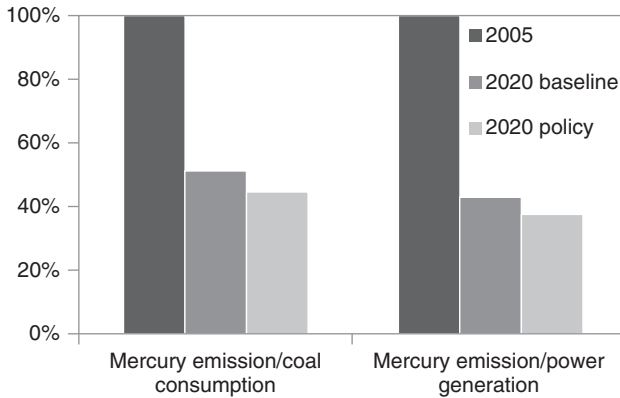


Figure 4.2 Chinese projections: mercury emission intensities in 2020.

units in Japan already have FGD and deNO_x systems in place and many plants pride themselves in fitting the most up-to-date systems [1]. By 2000, over 90% of plants had wet scrubber systems installed and <3% had no flue gas treatment for sulfur. Over 75% of plants have both low NO_x burners and SCR systems installed and the remainder had one or the other [13].

4.3.2.3 Other Asian Countries

The Philippines have a mercury emission limit from any source of 5 mg m⁻³. At the moment, there are 12 coal-fired plants in the country, four of which are FBC systems (fluidized bed combustion) systems. New plants are required to install FGD systems and low NO_x burners. There is also a fee levied, which is proportional to emissions. However, some plants obtained a “grace period” from these fees to help fund the installation of control technologies, for which tax credits are also available [14].

Prior to 2010, there was no limit for mercury from coal-fired plants in *Korea* other than the general limit for mercury emissions for all industrial emissions set at 5 mg m⁻³. However, the new standards, promulgated in 2010, set an emission limit for mercury and its compounds for all coal-fired facilities at 0.1 mg m⁻³. As can be seen in Figure 4.3, this limit can easily be met by almost any plant fitted with an ESP system. New legislated emission limits for SO₂ are set at 100 ppm for existing plants >100 MW (in operation before 1996) and 80 ppm for new plants. The limit for NO_x is 150 ppm for existing plants and 80 ppm for new plants. This is equivalent to around 300 mg m⁻³. This may require SCR systems on some plants, which will improve mercury capture due to co-benefit effects. However, it has been proposed that mercury CEMs be introduced at plants in Korea to monitor the effectiveness of the potential co-benefit effects of the SO₂ and NO_x control systems, which would provide information for a future review of the legislation by policy makers to potentially tighten mercury emission limits [15].

NB – the limit cited for Germany in this figure may be lower in practice as the standards are currently 50 µg m⁻³ for 30 min averages and 30 µg m⁻³ for 24 h

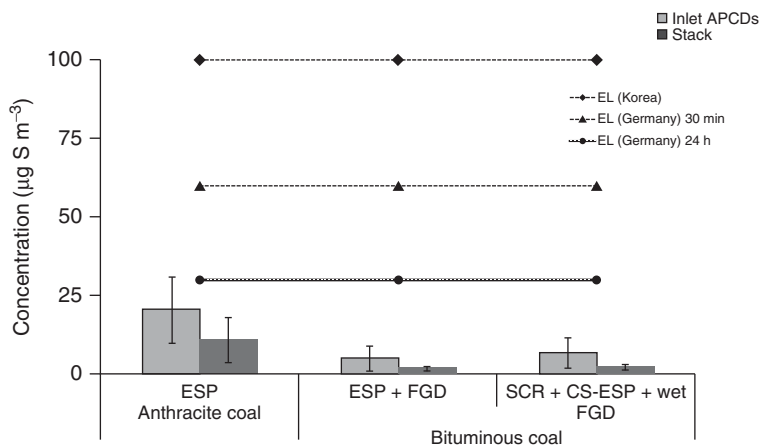


Figure 4.3 Measured mercury emission concentration and the permissible emission limit in current Korean and German regulations [15].

averages. However, the standards are still well above that which can be achieved in most plants fitted with APCD.

4.3.3

Other Countries

The following short sections summarize the situation on mercury emissions and control in selected countries.

4.3.3.1 Australia

Individual states in Australia have the jurisdiction to set their own emission legislation, including targets for greenhouse gas reduction. Over and above this, National Environmental Protection Measures (NEPM) can be set, based on goals, standards, protocols and/or guidelines. At the moment, although there is a National Pollutants Inventory (NPI) for the quantification of emissions, there are no binding national emission standards for SO_2 or NO_x . Emission guidelines for SO_2 and NO_x have been issued by the National Health and Medical Research Council (NHMRC). However, the limits are very general and were set at levels which could be met relatively easily. Australian coals are generally low in sulfur and therefore SO_2 emissions are not regarded as a high priority for control and there are, to date, no FGD or similar controls on any Australian coal-fired plants. Although NO_x limits have been specified in some states, it is thought that these are relatively lenient and have not required the installation of any NO_x control technologies [1].

The focus of Australian emission legislation is very much on the development of new clean coal technologies and low carbon options. So, for the moment at least, existing coal-fired power plants are not facing any retrofit requirements. Morrison and Nelson [16] have looked at future strategies for energy in Australia toward 2050. Most of the strategies considered relate to the reduction of mercury

and CO₂ emissions through the use of brown coal in IGCC (integrated gasification combined cycle) with and without CCS (carbon capture and storage). Australia's future energy strategies appear more concerned with greenhouse gas reductions and energy efficiency while SO₂ and NO_x emissions have much lower priority. It can therefore be assumed that there will be limited co-benefit reductions in mercury emissions, based on current legislation.

4.3.3.2 Canada

When the United States first introduced its Clean Air Mercury Rule (CAMR), Canada was quick to follow suit. However, the format the Canadian standard took differs from the CAMR and therefore, although the CAMR has now been abandoned, the Canada-Wide Standard (CWS) still applies. The CWS sets stringent emission reduction targets. There are provincial caps for each province, which apply to existing plants that require a total reduction of 60–70%. BAT is required on new plants. Individual provinces must decide the most appropriate means of meeting the required reduction targets and the approaches vary from enhanced co-benefit controls to activated carbon injection, and even complete plant closure [1].

4.3.3.3 Russia

In 1991, a national emissions charge system was introduced in Russia, which applied to over 300 air and water pollutants from a large number of stationary sources. However, monitoring and administrative capabilities are limited and the final charge is often open to negotiation between the source and the local authority. It is not uncommon for fees to be waived for sources experiencing financial problems. There does not appear to be any imminent move toward requirements for SO₂, NO_x, or mercury control [1].

4.3.3.4 South Africa

In March 2010, the South African Government established updated requirements for sulfur emission control. The limits are 3500 mg m⁻³ for SO₂ from existing coal-fired power plants and 500 mg m⁻³ for new plants (>50 MW). The emission limits for NO_x are 1100 and 750 mg m⁻³ for existing and new plants respectively [17]. There is also a move toward requiring the installation of FGD on all large coal-fired units in the country. However, the financial constraints and, perhaps more importantly, the limited availability of water in the country, will make the installation of FGD within the required time period a significant challenge. However, once FGD or equivalent sulfur control is required, some level of co-benefit mercury control can be expected.

4.4

Summary

At the moment, the majority of mercury control requirements apply in North America. Although there are international and national mercury emission limits

outside North America, the majority of these are not currently set at levels that require any significant action to be taken. This does not, however, mean that mercury is not being controlled. In fact, mercury reduction rates of over 50% and even over 95% are being achieved in countries which require state-of-the-art technologies for particulate, SO₂ and NO_x control as a result of co-benefit effects. Significant reduction in mercury emissions from the coal combustion sector have been achieved and are continuing in the EU and in countries such as Japan, Korea and, more recently, in China. And so, as a result, there is currently no real urgency to take specific action to control mercury. This may well change in the future if international and national bodies decide that current rates of mercury reduction in these regions are not sufficient.

References

- Sloss, L.L. (2003) *Trends in Emission Standards*, CCC/77, IEA Clean Coal Centre, London.
- Adams, E. (2006) Opting out of the LCPD – where to next? IPG 2006, Conference on Implementing EC Emission Directives, Leipzig, Germany, November 15–16, 2006, www.ipgconference.net, pp. 49–62.
- Kramarchuk, R. and Brunetti, B. (2008) New Emission Rules to Weigh on EU ETS. Environmental Finance, February 2008, p. 22.
- Richers, U., Scheurer, W., Seifert, H., and Hein, K.R.G. (2002) *Present Status and Perspectives of Co-Combustion in German Power Plants*, University of Karlsruhe, Germany, Wissenschaftliche Berichte FZKA, vol. 6686, Forschungszentrum Karlsruhe GmbH, Karlsruhe, pp. 19–20.
- Sloss, L.L. (2002) *Mercury – Emissions and Control*, CCC/58, IEA Clean Coal Centre, London.
- Sloss, L.L. (2008) *Economics of Mercury Control*, CCC/134, IEA Clean Coal Centre, London.
- Fernando, R. (2007) *Cofiring of Coal with Waste Fuels*, IEA Clean Coal Centre, London, CCC/126.
- Guttman, D. and Song, Y. (2007) Making central-local relations work: comparing America and China environmental governance systems. *Front. Environ. Sci. Eng. China*, **1**, 418–433.
- Zhang, X. and Schreifels, J. (2011) Continuous emission monitoring systems at power plants in china: improving SO₂ emission measurement. *Energy Policy*, **39** (11), 7432–7438.
- GB 13223–2011. (2011) *Emission Standard of Air Pollutants for Thermal Power Plants*, MEP (Ministry of Environmental Protection), http://www.zhb.gov.cn/gkml/qt/201109/t20110921_217526.htm (accessed 19 March 2014).
- United Nations Environment Programme (2011) *Reducing Mercury Emissions from Coal Combustion in the Energy Sector (China)*. UNEP, Geneva, http://www.unep.org/hazardoussubstances/Portals/9/Mercury/Documents/coal/FINAL%20Chinese_Coal%20Report%20-%202011%20March%202011.pdf (accessed 19 March 2014).
- PEI (2011) Tighter Chinese emission rules could trigger \$41bn investment. *Power Eng.*, <http://www.powerengineeringint.com/articles/2011/09/tighter-chinese-emission-rules-could-trigger-41bn-investment.html> (accessed 1 October 2011).
- Ito, S., Yokoyama, T., and Asakura, K. (2006) Emissions of mercury and other trace elements from coal-fired power plants in Japan. *Sci. Total Environ.*, **368**, 397–402.
- Findsen, J. (2008) Results of APEC study: environmental regulations to promote clean coal in developing APEC economies. *Cleaner Coal Asia 2008*, Ha Long Bay, Vietnam, August 19–21, 2008, <http://www.egcfe.ewg.apec.org/publications/proceedings/CleanerCoal/>

- HaLong_2008/Day%201%20Session%201A%20-%20Jette%20Findsen%20Environmental%20Regulations.pdf.*
15. Pudasainee, D., Kim, J.-H., and Seo, Y.-C. (2009) Mercury emission trend influenced by stringent air pollutants regulation for coal-fired power plants in Korea. *Atmos. Environ.*, **43** (39), 6254–6259.
 16. Morrison, A.L. and Nelson, P.F. (2004) Emission consequences of transformation of Australia's energy generation portfolio to 2050. CCSD Industry Steering Committee Meeting, Brisbane, Australia, December 14–15 December, 2004.
 17. GG (2010) Government Gazette (Staatskoerant) Republic of South Africa, Vol. 537, issue 33064, Government Gazette Staatskoerant, pp. 1–40.

Part II

Mercury Measurement in Coal Gas

5

Continuous Mercury Monitors for Fossil Fuel-Fired Utilities

Dennis L. Laudal

5.1

Introduction

Instrumentation to measure mercury has been available for many years. However, until recently, these monitors were designed to measure ambient mercury and mercury in liquids. It has only been since about 1990 that the concept of using mercury instrumentation to measure mercury in flue gas generated by burning fossil fuels, such as coal, has been considered. Until that time, mercury measurements were made using wet-chemistry methods such as U.S. Environmental Protection Agency (EPA) Method 29, EPA Method 101A and, later, the Ontario Hydro method. Although these methods could be highly accurate, they were expensive and difficult to apply. As a result, a serious effort was made to further develop and optimize continuous mercury monitors (CMMs). CMMs have the following advantages over traditional wet-chemistry methods:

- Yield real- or near-real-time results
- Able to assess process variability
- May be used for system optimization
- Provide feedback for Hg control strategies
- Have the potential to be less costly and are less labor-intensive
- Give direct measure of pollutants
- May promote better public relations.

Before these monitors could be reliably used in utility applications, many challenges had to be overcome:

- Reliability
- Ability to accurately measure low mercury concentrations
- Measurement environment
- Dynamic range
- National Institute of Standards and Technology (NIST) traceability for calibration.

To resolve some of these issues, as well as others, CMMs have become complex, with multiple parts, and new definitions were needed. For the purposes of this chapter, the entire mercury measurement system is called a *CMM*. The section of the CMM that actually analyzes the mercury in the gas steam is referred to as a *mercury analyzer*. Even this is a bit of a misnomer in that these instruments are not actually continuous. With the exception of a few *in situ* systems, all mercury monitors draw flue gas into an analyzer utilizing a pump and there is a time lag between instrument readings, which can be minutes or seconds depending on the instrument. The exact number of CMMs installed is unknown because many of the CMMs that were installed were not verified and/or removed following the vacature of the Clean Air Mercury Rule (CAMR). However, it is known that about 600 CMMs have been sold to the utility industry with about two-thirds

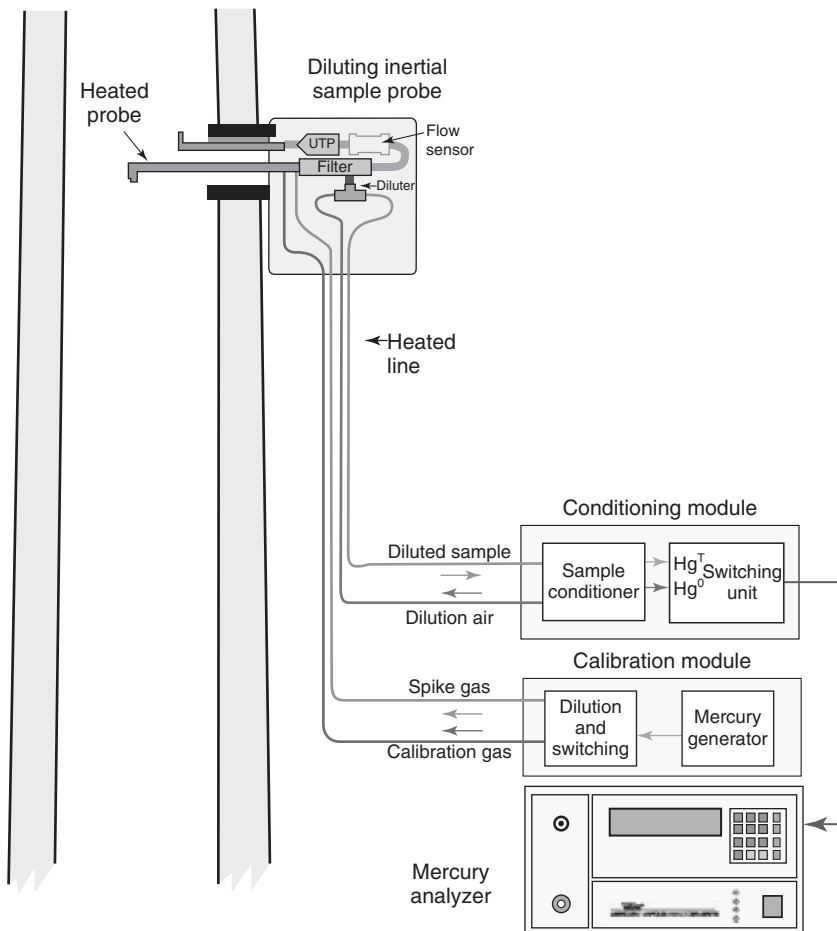


Figure 5.1 Diagram of a CMM.

manufactured by Thermo Scientific and about one-third by Tekran, with a small number supplied by other CMM vendors [1].

5.2

Components of a CMM

In general, a CMM designed for combustion flue gas has four main sections: the probe, the pretreatment and conversion system, the mercury analyzer, and the calibration system. How each of these sections is configured is highly dependent on the vendor. A diagram illustrating this is shown in Figure 5.1.

5.2.1

Mercury Analyzer

With several exceptions, all mercury analyzers measure mercury using either cold-vapor atomic absorption spectroscopy (CVAAS) or cold-vapor atomic fluorescence spectroscopy (CVAFS).

5.2.1.1 Cold-Vapor Atomic Absorption Spectrometry

The most popular method for determining mercury in almost any type of sample in the past has been based on CVAAS and the technique is still widely used today. Mercury is unique among metals in that it has a very high vapor pressure at relatively low temperatures and can be introduced quantitatively to the spectrometer as a vapor without difficulty. Absorption at 253.65 nm in the ultraviolet (UV) region has been measured with the use of mercury vapor lamps as well as hollow cathode lamps as the light source. Such methods are quite old; mercury vapor meters were first developed in the 1930s [2]. A typical CVAAS scheme is shown in Figure 5.2. CVAAS systems typically are considered to have detection limits somewhere in the 0.05–1.0 $\mu\text{g m}^{-3}$ range, depending on the design of the system.

When mercury concentration in a mixed gas stream is measured, a number of gases such as SO_2 can interfere with a CVAAS detector. A number of approaches have been taken to either remove these interference gases or greatly reduce their impact [3]. These include the use of a dual path with two detectors, gold amalgamation of the mercury, and the Zeeman effect.

In the dual-path method, the gas stream is split, with one of the streams having the mercury removed using a gold or activated carbon cartridge. The absorbance of the two streams is then subtracted, resulting in the absorbance due to the mercury. The second technique, gold amalgamation, is based on the selective adsorption of mercury on a gold surface at room temperature. Mercury is released from the gold trap by heating and then introduced into the spectrometer using an inert gas. As a result, the only gas analyzed is the mercury. The method has the advantage of not only removing interferences but also allowing for the mercury to be concentrated, making it possible to achieve increased sensitivity without actually

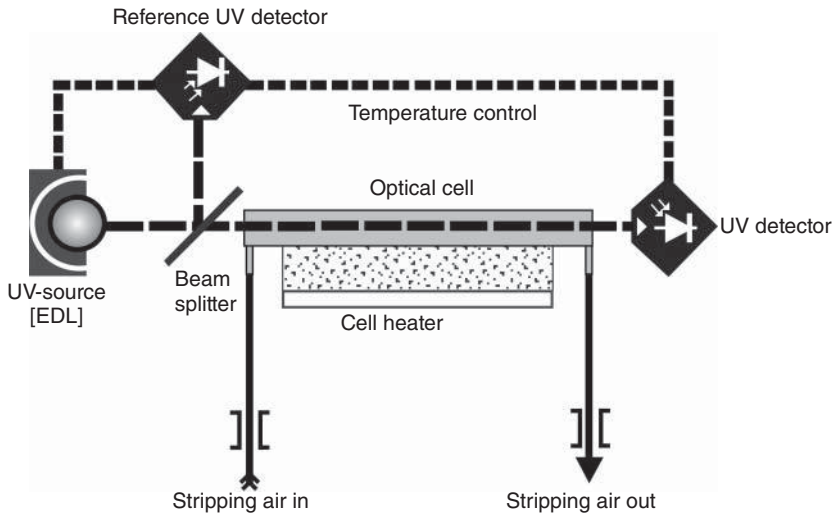


Figure 5.2 Simplified diagram of a CVAAS analyzer with dual beam (EDLs, electrodeless discharge lamps).

changing the detection limit. Because of this concentration effect, it is possible to use dilution to help minimize gases that could poison the gold trap, which is a concern when this technique is used.

As stated previously, one of the flue gas constituents that greatly reduces the sensitivity of CVAAS for mercury is SO_2 , particularly in concentrations >100 ppm. Unfortunately, the UV absorption peak for SO_2 is a broad band that partially overlaps the mercury absorption peak of 253.65 nm. As a result, several mercury analyzers use the Zeeman effect to offset this. The Zeeman effect was first used as a background correction in the mid-1960s. The radiation source (mercury lamp) is placed in a permanent magnetic field, resulting in a frequency splitting. The total absorbance of the sample gas is measured at the center frequency. The absorbance of everything except mercury is measured on the slightly shifted frequency. The results are then subtracted, providing the absorbance due to the mercury present in the gas stream. Although this has proved effective, there is still a dependence on the concentration of the interfering gases [4].

5.2.1.2 Cold-Vapor Atomic Fluorescence Spectrometry

CVAFS makes use of the unique characteristic of mercury that allows measurement at room temperature. Free mercury atoms in a carrier gas are excited by a collimated UV source at a wavelength of 253.65 μm [5]. The excited atoms reradiate their absorbed energy (fluoresce) at this same wavelength. The fluorescence is omnidirectional and can be detected with a photomultiplier tube. The excitation path and viewing path are perpendicular to each other to allow separation. The CVAFS technique differs from the CVAAS technique in that it is more sensitive, more selective, and linear over a wide range of concentrations. However, any

molecular species, particularly diatomic molecules such as O₂ and N₂ present in the carrier gas, will quench the fluorescence signal. One method of circumventing this is to use gold-coated traps to collect mercury from the flue gas stream. The traps are then heated, releasing the mercury from the gold and using an inert carrier gas such as argon to carry the mercury to the detector. The method is highly sensitive, with a detection limit of <0.1 pg m⁻³, and inherently linear (greater than five orders of magnitude) [6].

However, several CMM vendors have taken the approach of simplifying the process by not using gold traps but directly analyzing the flue gas after diluting with N₂ to reduce the interfering gases. In this approach, the resulting quenching of the fluorescence is not considered significant when measuring mercury in combustion flue gases. The detection limit is still generally considered to be <0.03 μg m⁻³ [7].

5.2.1.3 Other Analytical Methods

Although almost all of the CMMs that have been developed for measuring mercury in fossil fuel-fired flue gases use either CVAAS or CVAFS, other techniques have been developed. One such method is plasma emission spectroscopy (PES). This method is the basis for the EnviroMetrics Argus-Hg CMM. In this process, a plasma source is generated using microwave technology. Because the plasma emits light that is characteristic of the induced molecule, a low-resolution spectrometer can then identify that molecule based on the UV spectrum [8].

At one point, Opsis introduced a true *in situ* analyzer based on differential optical atomic spectroscopy. However, this analyzer could only measure elemental mercury, with no possibility of measuring total mercury. Therefore, this analyzer had very limited application for measuring mercury in fossil fuel combustion streams [9].

Cooper Environmental has developed a CMM based on X-ray fluorescence (XRF). When materials are exposed to short-wavelength X-rays or gamma rays, ionization of their component atoms takes place. Ionization consists of the ejection of one or more electrons from the atom. The removal of an electron in this way renders the electronic structure of the atom unstable and electrons in higher orbitals “fall” into the lower orbital to fill the hole left behind. In falling, energy is released in the form of a photon, the energy of which is equal to the energy difference of the two orbitals involved. Thus the material emits radiation, which has an energy output that is characteristic of the atoms present. With a solid-state detector, the concentration of the atoms present in the gas can be determined, based on the emitted radiation [10]. This type of detector has the advantage of not only measuring the mercury concentrations but also other metals.

5.2.2

Pretreatment/Conversion Systems and Probe

For all CMMs, essential parts of the system are the pretreatment/conversion system and the probe. These have four major functions, which are as follows:

- 1) To provide a stinger and probe that is inserted into the flue gas to sample the flue gas.
- 2) To convert all mercury forms into elemental mercury.
- 3) To remove or greatly reduce gases that may interfere with the mercury analyzer.
- 4) To provide mercury speciation for some CMMs.

5.2.2.1 Sampling Probe

During the early development stage of CMMs, the probe consisted only of the stinger, the filter, and the filter holder. Some type of filter was necessary to prevent the fly ash from ruining the optics of the analyzer. However, depending on the flue gas and fly ash, it was discovered in the early 1990s that the fly ash captured on the filter could adsorb mercury and/or change the speciation [11]. As a result, methods were developed to remove the fly ash but minimize the contact between the collected fly ash and the mercury-containing flue gas. The most successful method was a concept called an *inertial separation probe (ISP)* [12]. A diagram of an ISP developed by ADA-ES is shown in Figure 5.3. As shown in Figure 5.3, a large amount of flue gas ($>20 \text{ l min}^{-1}$) is pulled through the annulus of the ISP using an eductor. Typically, only about 0.5 l min^{-1} (may vary depending on the CMM) is needed for the CMM. The analyzer pump pulls the small amount of needed gas through the sintered-metal filter portion of the ISP, removing the particulate matter. The high velocity of flue gas passing through the annulus of the ISP continually removes the particulate matter, resulting in minimal contact between the particulate matter and flue gas passing into the mercury analyzer. A detailed diagram of the sintered-metal portion of the ISP is shown in Figure 5.4.

Although most of the CMMs currently available use some type of ISP, there have been several design changes over the past several years. One of the major changes occurred as a result of wet stacks [13]. The ISPs were being corroded by the acidic flue gas (see Figure 5.5) and also had severe plugging problems. As a result, more exotic alloys such as Hastelloy[®] are being used. Also, the flue gas flow rates through the ISP have been changed to help prevent plugging.

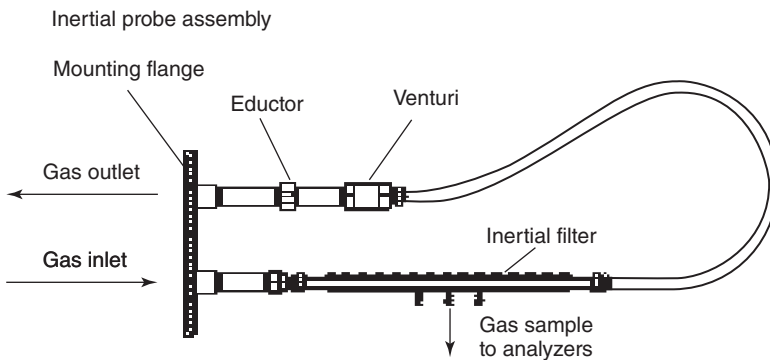


Figure 5.3 Diagram of an ISP. (Courtesy of ADA-ES, Littleton, CO.)

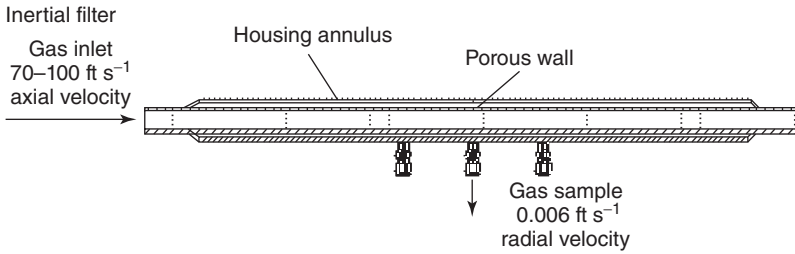


Figure 5.4 Detailed diagram of the inertial filter portion of the ISP. (Courtesy of ADA-ES, Littleton, CO.)

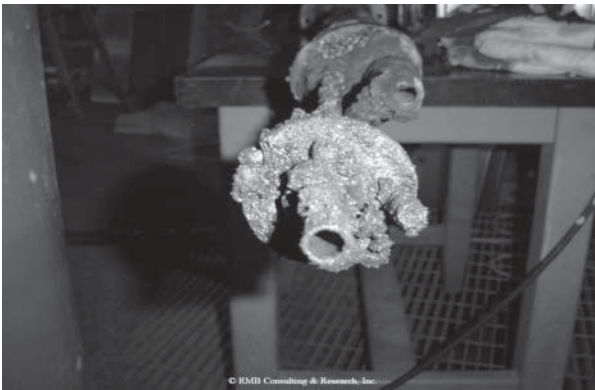


Figure 5.5 Photograph of a sampling probe after 1 month in a wet stack.

5.2.2.2 Pretreatment and Mercury Conversion

Pretreatment/conversion systems are essentially classified into two main types. The first are those based on wet chemistry and the second are those based on thermal decomposition. Almost all of the mercury research done in the 1990s and early 2000s used wet-chemistry systems. These systems can be utilized with either CVAAS- or CVAFS-based CMMs. A diagram of a typical wet-chemistry pretreatment conversion unit is shown in Figure 5.6 [14].

Because of the research nature of most of the work being done prior to the introduction of CAMR, it was also necessary that a CMM provide mercury speciation data. Therefore, the wet-chemistry pretreatment/conversion systems were designed such that the CMM would provide speciated data. As shown in Figure 5.6, the speciation was done by splitting the gas flow and passing each gas stream through a separate solution. To measure total mercury, the flue gas passed through a solution of $\text{SnCl}_2/\text{NaOH}$, which removed the acid gases and reduced all mercury forms to elemental mercury. To measure only elemental mercury, the flue gas passed through a solution of KCl or other Hg^{2+} solution, which removed oxidized forms of mercury. The difference between the two measurements is the concentration of oxidized mercury. For CVAAS mercury analyzers, it has been

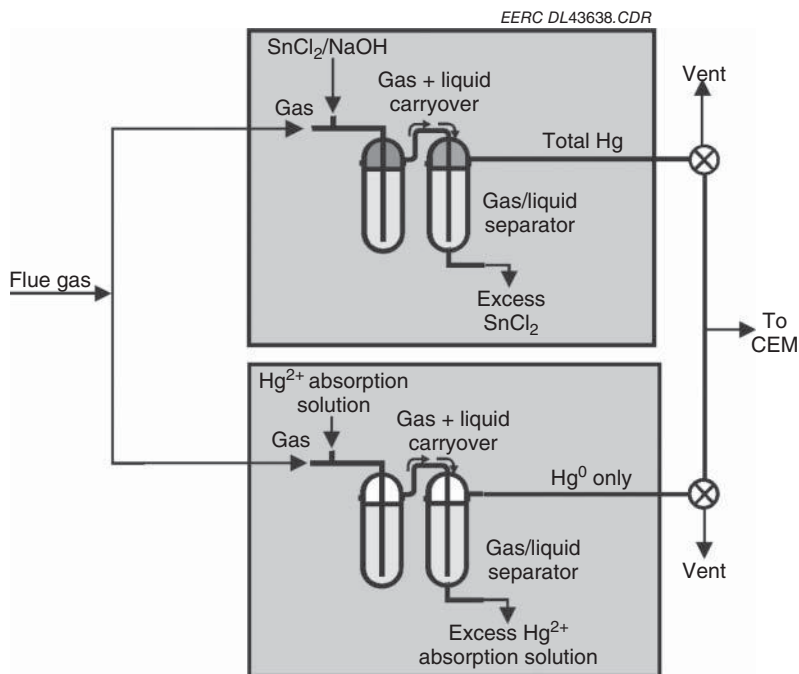


Figure 5.6 Diagram of a wet-chemistry pretreatment/conversion system for a CMM.

reported [15] that the efficiency of mercury conversion is greatly decreased by high levels (>500 ppm) of SO_2 in the gas stream. For a CVAFS mercury analyzer using gold traps, the acid gases must also be removed but for a different reason. If HCl and NO_2 are present in the flue gas, the gold trap is permanently poisoned [16]. To prevent this, it is necessary that the HCl (much easier to remove than NO_2) be removed prior to the flue gas passing through the gold trap.

Although the wet-chemistry pretreatment/conversion systems have worked well for research, they are not suited for long-term compliance monitoring for the following reasons:

- Extensive engineering or technician support is required.
- The NaOH solution will remove CO_2 from the sample gas, requiring that the CO_2 flue gas concentration be known.
- Tin plating and crystallization of solutions can cause problems.
- It is difficult to ensure that no cold spots accumulate mercury, which will show up as mercury spikes in the data.

For these reasons, the mercury CMM vendors developed other pretreatment/conversion systems that did not rely on wet chemistry.

Currently, almost all CMM pretreatment/conversion systems are based on thermal reduction of the Hg^{2+} forms of mercury to Hg^0 . Because very high temperatures (near 900°C) are needed to ensure complete reduction, it is

SO₂ or NO_x that are routinely used in power plants, calibration is done using certified calibration gas cylinders. However, because of the low mercury concentrations and the stability required, the development of these calibration gases has been difficult. NIST has been working with Spectra Gases in an attempt to certify calibration gases [18]. Because of the cost and volume of gas needed to conduct a CMM calibration prescribed by Performance Specification (PS)-12A, most likely these calibration gases will have limited uses. As a result, all CMM systems sold today provide an elemental mercury calibrator. These calibrators are either internal to the mercury analyzer or a separate unit. The elemental mercury calibration gas is generated either by heating a pool of elemental mercury so that a carrier gas is saturated and then the concentration is determined, based on the mercury vapor pressure curves or by using permeation devices. In either case, it is critical that the temperature and flow rates of the calibration devices be maintained very precisely. In most CMMs, the generated elemental mercury calibration gas can be sent to a variety of points within the system, from the probe tip to directly into the mercury analyzer. This allows not only for instrument calibration but also for troubleshooting the instrument and providing quality control checks. A diagram of a typical elemental mercury calibration system is shown in Figure 5.8.

When the CAMR was promulgated, the calibration requirements for CMMs stated that the calibrators were to be NIST-traceable. The same NIST traceability is also part of the new National Emission Standards for Hazardous Air Pollutants (NESHAPs) for coal-fired power plants as NIST traceability is required under PS-12A. In 2005, with funding from EPA, NIST began developing protocols for producing vendor prime calibration systems. To date, NIST has certified and recertified its NIST Prime elemental Hg generator and has certified the first round of the vendor prime generators. Vendor prime generator recertification is

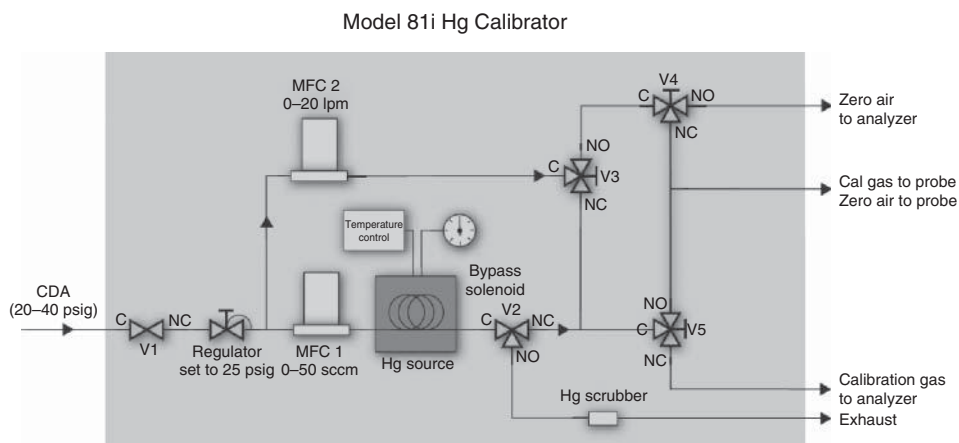


Figure 5.8 Diagram of the Thermo Scientific elemental calibrator.

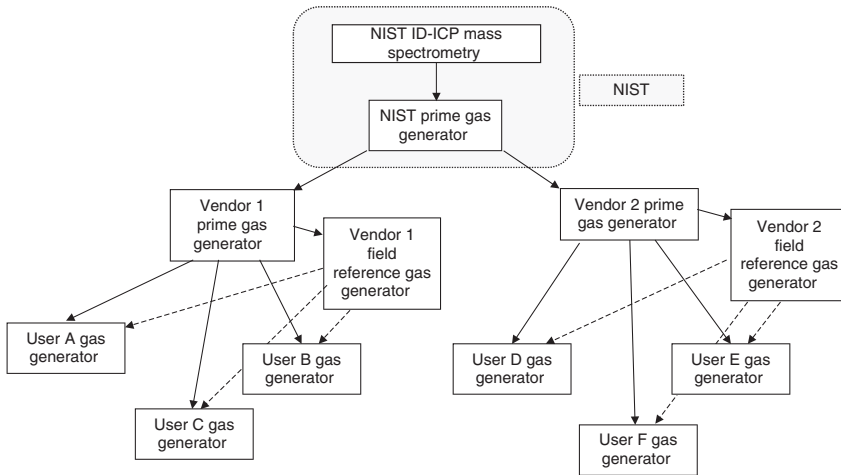


Figure 5.9 NIST traceability scheme for CMM calibration.

expected to begin in the near future [18]. The overall NIST traceability scheme for CMMs is shown in Figure 5.9.

PS-12A requires that compliance CMMs be calibrated using both NIST-traceable elemental mercury calibrators and oxidized mercury calibrators. The primary purpose of the oxidized mercury calibrator is to ensure that the conversion system is converting all mercury to Hg^0 and not creating a low bias. Rather than actually providing vendor prime NIST-traceable oxidized mercury calibrators, it was determined by EPA that NIST-traceability would be accomplished by certifying that all parts of the system be NIST-traceable. For example, the source of mercury, mass flow controllers, and temperature controllers would need to be NIST-traceable. As a result, NIST-traceable protocols for oxidized mercury calibrators were not needed.

There have been essentially two approaches to the manufacture of oxidized mercury calibrators. The first approach is to use the HovaCal[®] gravimetric approach. A NIST-traceable HgCl_2 solution is made or bought and weighed precisely on a continuous basis. A small amount of the HgCl_2 solution is continuously pumped in an evaporator, resulting in gaseous HgCl_2 . Using mass flow controllers, a mercury-free carrier gas is then mixed with the HgCl_2 vapor, which is introduced into the CMM. This is the procedure used by Tekran and also by Cemtrex. A diagram of the technique is shown in Figure 5.10.

The second approach is to convert the mercury generated by a NIST-traceable elemental mercury calibrator to HgCl_2 . This is done by passing the output of the elemental mercury calibrator over a heated catalyst and introducing Cl_2 . This the procedure used by Thermo Scientific for its oxidized mercury calibrator. Spectra Gases also has patented a version of this calibrator called *MerCal*[™] [19].

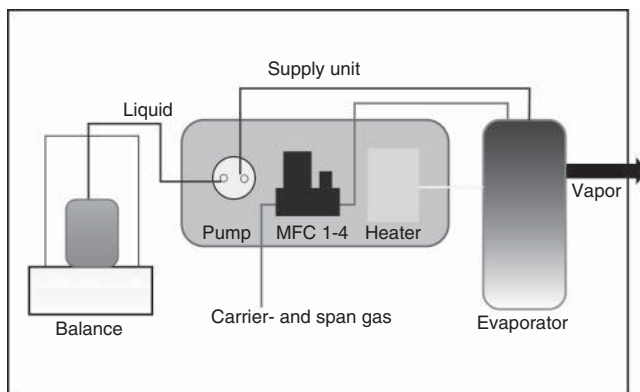


Figure 5.10 Basic diagram of a gravimetric oxidized mercury generator.

5.3

Installation and Verification Requirements

Installation and verification of CMMs for power plants are detailed in PS-12A. The following is a brief summary of PS-12A, which assumes that the vendor recommendations for installation are also being followed.

5.3.1

Installation

Obviously, for compliance purposes, the CMM must be installed following the last air pollution control device. This most often will be at stack location. However, it is important that the CMM probe be installed in a location that is readily accessible, as some maintenance will be required. Therefore, a duct location may also be considered. Because a CMM is a single-point monitor, it is required that the location be chosen such that the flue gas is representative with little or no stratification. As such, the chosen location must follow the requirements of EPA Method 1 and be at least two equivalent diameters downstream of the nearest control device or any other point at which a change in gas flow or mercury concentration could occur. This may require mercury stratification testing using EPA Method 30B or, alternatively, SO₂ stratification testing.

Once the sampling location has been chosen, the stinger is inserted such that it is no <1.0 m from the stack wall or duct. Also, it must be within the centroidal velocity traverse area of the stack or duct cross section.

5.3.2

CMM Verification

Three tests must be performed to certify a CMM installation:

- 1) Measurement error (ME)

- 2) Seven-day calibration drift (CD)
- 3) Relative accuracy test audit (RATA).

5.3.2.1 Measurement Error

This test requires that three levels (zero, midlevel, and high) of a mercury reference gas be sequentially injected into the CMM such that all sections of the CMM are challenged. This test is done in triplicate. Using the average CMM value, the ME for each of the three reference gas concentrations is calculated using the following equation:

$$ME = \frac{|R - A|}{\text{Span}} \times 100\% \quad (5.1)$$

where R is the reference gas concentration and A is the average of the CMM reading for the three injections at that reference gas level. The span gas is defined in PS-12A as gas concentration no greater than twice the emission limit. To pass the ME test, each of the values calculated using Equation 5.1 must be $\leq 5\%$.

5.3.2.2 Seven-Day Calibration Drift

The purpose of the CD test is to verify the ability of the CMM to conform to the established response used for determining emission concentrations. The test is conducted with a zero gas and either the mid-level or high-level gas used for the ME test. The gases are added to the probe sequentially. The CD is calculated using Equation 5.2. This test is done for seven consecutive operation days.

$$CD = \frac{|R - A|}{\text{Span}} \times 100\% \quad (5.2)$$

To pass the CD test, each of the values calculated using Equation 5.2 must be $\leq 5\%$ for each of the 7 days.

5.3.2.3 Relative Accuracy Test Audit

The third CMM verification test that must be performed is a RATA. This test involves comparison of the mercury concentration measured using a reference method (RM) to the average CMM concentration measured over the same time period. Although an instrumental RM (EPA Method 30A) can be used in almost all cases, the procedures outlined in EPA Method 30B (sorbent traps) are used.

A RATA using EPA Method 30B requires that nine paired sorbent samples (C_a and C_b) be taken at a representative location in the same duct or stack as the CMM. Depending on the potential for the flue gas to be stratified, this may or may not involve traversing. To be a valid pair, the relative difference between the two paired samples (Equation 5.3) must be $\leq 10\%$ at Hg concentrations $\geq 1.0 \mu\text{g m}^{-3}$. If the average Hg concentration is $\leq 1.0 \mu\text{g m}^{-3}$, then the relative difference between the paired samples must be $\leq 20\%$ or have an absolute difference of $\leq 0.2 \mu\text{g m}^{-3}$.

$$RD = \frac{|(C_a - C_b)|}{(C_a + C_b)} \times 100\% \quad (5.3)$$

The relative accuracy (RA) is calculated using Equation 5.4. Note that the mercury concentrations for the CMM and RM must be on the same basis, either wet or dry.

$$RA = \frac{|\bar{d}| + |cc|}{\overline{RM}} \times 100\% \quad (5.4)$$

where \bar{d} is the sum of the difference between the RM concentrations and the corresponding CMM concentration, cc is the value of the confidence coefficient (Equation 5.5), and \overline{RM} is the mean of the RM values.

$$cc = t_{0.025} \frac{S_d}{\sqrt{n}} \quad (5.5)$$

where $t_{0.025}$ is the Student t value based on n (from statistical tables), S_d is the standard deviation (Equation 5.6), and n is the number of paired RM tests.

$$S_d = \sqrt{\frac{\sum_{i=1}^n d_i^2 - \frac{\left(\sum_{i=1}^n d_i\right)^2}{n}}{n-1}} \quad (5.6)$$

To pass the RATA, the calculated value RA in Equation 5.4 must not exceed 20%. Alternatively, if an average RM concentration is $<5.0 \mu\text{g m}^{-3}$, the results are acceptable if the absolute value of the difference between the mean RM values and CMM does not exceed $1.0 \mu\text{g m}^{-3}$.

5.4

Major CMM Tests

Over the last 15 years, a number of tests have evaluated the ability of CMMs to measure mercury at fossil fuel-fired boilers. These tests have been conducted by the vendors themselves and/or the utilities as well as by independent agencies such as the U.S. Department of Energy (DOE), EPA, and the Electric Power Research Institute (EPRI). Below is a summary of some of these tests.

One of the first systematic tests was funded by EPA and DOE at a cement plant in Holly Hills [20]. Three different CMMs were tested at the Holly Hills cement plant in 1995. The installed CMMs were compared to the RM, EPA Method 29. In general, these tests were not very successful for a number of reasons. The cement plant burned a wide variety of fuel, including hazardous wastes and, as such, the flue gas constituents changed widely during the testing. Because the effects of these flue gas constituents were not very well known at the time, the CMM mercury measurements were not very accurate. Also, there were several mechanical and engineering problems because these instruments were still in the development stage.

EPA's Environmental Technology Verification Program's Advanced Monitoring Systems Center, operated by Battelle under a cooperative agreement with EPA, between 2001 and 2007, evaluated 10 different instrumental CMMs and a sorbent trap CMM. The verification testing was conducted in three phases. It should be noted that not all CMMs were tested in all three phases. In the first phase, four CMMs were tested under conditions simulating (i) coal-fired flue gas and (ii) municipal incinerator flue gas. The tests took place at a pilot-scale incinerator in Research Triangle Park, North Carolina, over a 3-week period. In the second phase, five CMMs (including two of the technologies tested in the first phase) were evaluated at a full-scale hazardous waste incinerator in Oak Ridge, Tennessee. The third phase was conducted at a coal-fired power plant. The reports for each of these systems are available on EPA's Web site at www.epa.gov/etv/vt-ams.html#mcem. As would be expected, the results were mixed. Some of the systems compared very well to the RM, while others had more difficulties.

One of the more extensive field tests was completed at Tennessee Valley Authority's Trimble County Power plant, Unit 1 [21]. This plant burns an eastern bituminous coal, utilizes selective catalytic reduction for NO_x removal (operates during the ozone season), an electrostatic precipitator, and a wet scrubber. As a result, the mercury concentration at the outlet of Unit 1 was low, typically $<2.0 \mu\text{g Nm}^{-3}$. Testing began in November 2004 and continued through September 2005. The purpose of this field test program was to collect data to assess the ability of commercially available CMMs to provide reliable and accurate data over an extended time period while meeting certification, durability, data availability, and setup/maintenance requirements. In particular, data were collected to assess the ability of the CMMs to satisfy the requirements of PS-12A. The testing was divided into two phases (Phases 1 and 2). Phase 1 consisted of the setup and verification of four different CMMs at the power plant. In addition, some data were gathered as to the maintenance requirements. In Phase 2, two additional CMMs (plus the original four) were added and verified. Phase 2 saw 7 months of testing.

The results of this test program demonstrated that the source characteristics can have a significant effect on CMM performance. Regardless of the vendor supplying the CMMs, it is clear that CMMs should be appropriately modified for the source. For instance, the source sampled for this demonstration project had a wet stack and thus required a CMM with efficient sample transfer and conditioning capabilities in order to function properly. Detailed results of this test program can be found at www.epa.gov/ttn/emc/cem/hgcemsdemo.pdf.

With the promulgation of the Utility NESHAPs Mercury and Air Toxics (MATs), mercury limits are based on maximum achievable control technology (MACT). Obtaining this level of control will often require measuring mercury at concentrations $<1.0 \mu\text{g m}^{-3}$. There is little data in the literature as to the validity of using CMMs to consistently and accurately measure mercury concentrations $<1.0 \mu\text{g m}^{-3}$. As a result, the Energy & Environmental Research

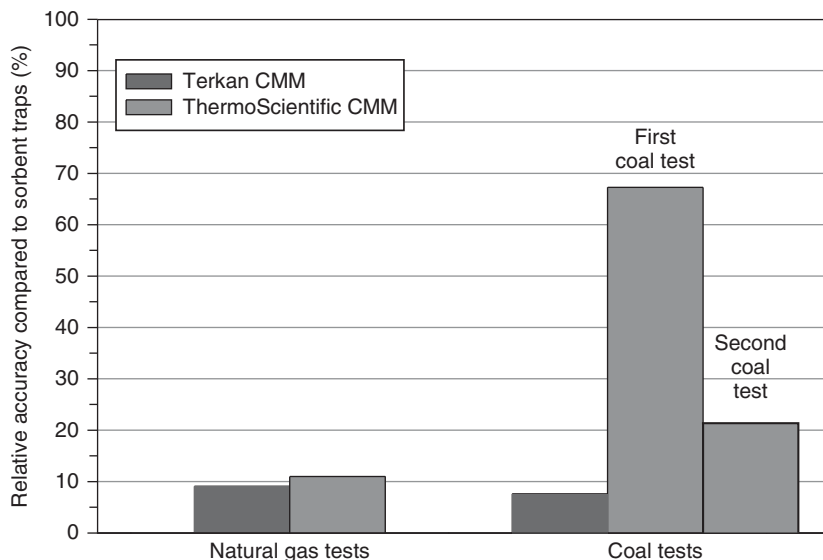


Figure 5.11 Summary of the low-level mercury testing at the EERC.

Center (EERC), with funding from the Illinois Clean Coal Institute (ICCI), DOE, EPRI, and the EERC Center for Air Toxic Metals®, conducted a pilot-scale test program to systematically determine the precision and accuracy of the two most widely used CMMs by the utility industry – Tekran and Thermo Scientific CMMs – when measuring mercury at these levels [22]. The first portion of the test was conducted firing natural gas with $0.5\text{--}1.0\ \mu\text{g Nm}^{-3}$ of elemental and oxidized mercury spiked into the flue gas. The second portion of the test involved firing an Illinois bituminous coal with a baghouse and wet scrubber in operation. Again, the outlet mercury concentration was $<1.0\ \mu\text{g Nm}^{-3}$. A summary of the results are shown in Figure 5.11. As can be seen in Figure 5.11, the results for the Thermo Scientific CMM were problematic. This was believed to be a result of a software error; therefore, a second week firing coal was conducted using only the Thermo Scientific CMM. The results were considerably better the second week. In general, it was concluded that both instruments provided quite good agreement with the RM even at these low mercury concentrations. Detailed results of this test program can be found at the ICCI Web site at www.icci.org/reports/10Laudal6A-1.pdf.

Under the MATs rule, the reliability of CMMs will be a critical issue as utilities will be penalized for incomplete or missing data. Although the experiences of the utilities with CMMs have been varied, in general, once these instruments have been installed, are operating correctly, and properly maintained, they are highly reliable. Figure 5.12 shows the percent availability for 10 different Tekran monitors over the year 2009 [23]. As can be seen, the average reliability was $>91\%$, with the lowest being about 87% . This is typical of many of the CMM installations.

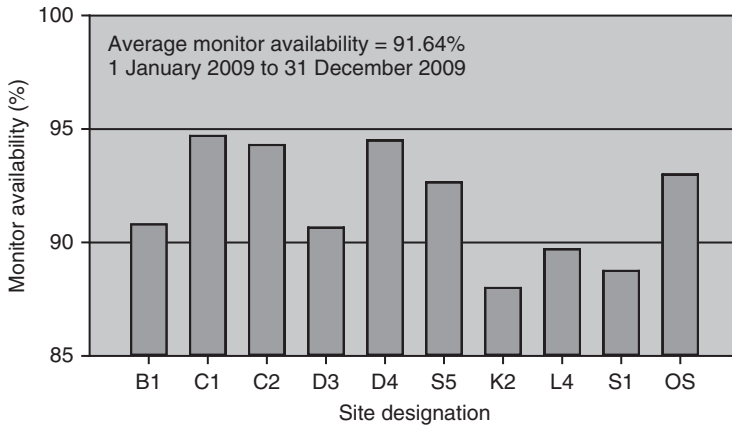


Figure 5.12 Availability of Tekran CMM during the 2009 calendar year.

5.5

CMM Vendors

As stated earlier, most of the CMM sales to the utility industry have been either Tekran or Thermo Scientific. However, a number of other vendors are also offering complete systems. Table 5.1 provides a listing of vendors that have the potential to provide complete mercury measurement systems to the utility industry as of 2011. Currently, these other instruments have primarily been used to measure mercury for non-utility industries such as incineration, natural gas refining, mining, or the manufacture of cement. For a detailed description of the CMMs, Web sites are provided in Table 5.1.

Table 5.1 List of vendors offering CMM systems to the utility industry.

Vendor	Instrument	Analysis method	Web site
Thermo Scientific	Mercury Freedom System	CVAF	www.thermoscientific.com/
Tekran Instrument Corp.	Series 3300	CVAF	www.tekran.com/
Envimetrics	Argus-Hg	PES	www.envimetrics.com/
PS Analytical	PSA 10.665 System	CVAF	www.psanalytical.com/
Gasmert	Gasmert CMM	CVAF	www.gasmert.fi/
Cemtrex	SM-4	CVAA	www.cemtrex.com/
Sick Maihak GmbH	MERCEM300Z	CVAA	www.sick.com/
Durag Group	HM 1400 TR	CVAA	www.durag.com/
Pall Corporation	Xact 645	XRF	http://pall.com/

References

1. Amar, P., Senior, C.L., Afonso, R., and Staudt, J. (2010) Technologies for Control and Measurement of Mercury Emissions from Coal-Fired Power Plants in the United States: A 2010 Status Report, Northeast States for Coordinated Air Use Management (NESCAUM), July 2010, www.nescaum.org/documents/hg-control-and-measurement-techs-at-us-pps_201007.pdf (accessed 31 March 2014).
2. Slavin, M. (1978) *Atomic Absorption Spectroscopy*, 2nd edn, John Wiley & Sons, Inc., New York, p. 193.
3. Morita, M., Yoshinaga, J., and Edmonds, J.S. (1998) The determination of mercury species in environmental and biological samples. *Pure Appl. Chem.*, **70** (8), 1585–1615.
4. Pomfrey, L. (2007) Investigating the Zeeman Effect in Mercury, November 2007, http://media.lukepomfrey.org/docs/Zeman_Effect_in_Mercury_1.pdf (accessed October 2011).
5. U.S. Environmental Protection Agency (2001) EPA Draft Method 245.7: Mercury in Water by Cold-Vapor Atomic Fluorescence, Spectrometry, EPA-821-R-01-008, January 2001
6. Tekran Instrument Corporation (2014) Experts Corner: Comparison of CVAA and CVAFS Analytical Systems, www.tekran.com/wp-content/uploads/2011/02/FAQ_AA_vs_AFr101.pdf (accessed October 2011).
7. Thermo Scientific (2014) Resource Library, Thermo Scientific Mercury Freedom System, www.thermoscientific.com/ecomm/servlet/techresource?storeId=11152&langId=-1&taxonomy=4&resourceId=93834&contentType=%5bRadation%5d&productId=11961825 (accessed October 2011).
8. Efthimion, P.C. and Morozov, A. (2014) Commercialization of a Continuous Emissions Monitor for Mercury in Flue Gas, www.envimetrics.com/Env_Papers.htm (accessed October 2011).
9. Opsis <http://opsis.se/Techniques/UVDOSTechnique/tabid/632/Default.aspx> (accessed October 2011).
10. Cooper, J.A., Johnsen, B.E., Peterson, K., Yanca, C.A., Nakanishi, M., Barth, D., and Fry, S. (2007) Candidate Conditional Method ZZ: Determination of Metal Concentration in CES' Xact CEMS Stilling Chamber Using Filters and Solid Sorbents with X-Ray Fluorescence Analysis, Prepared for U.S. Environmental Protection Agency, June 2007.
11. Pavlish, J.H., Sondreal, E.A., Mann, M.D., Olson, E.S., Galbreath, K.C., Laudal, D.L., and Benson, S.A. (2003) Status review of mercury control options for coal-fired power plants. *Fuel*, **82**, 89–165.
12. Sjostrom, S., Amrhein, G., Bustard, J., Starns, T., and Merrit, R. (2007) Performance evaluation of inertial separation probes for vapor-phase mercury measurements. Presented at the 4th International Conference on Air Quality, Crystal City, VA, September 2007.
13. McRanie, R. (2007) Mercury CEMs significant and technical issues and recent results. Presented at EPRI Hg Measurements Workshop, January 24, 2007, www.rmb-consulting.com/papers/Hg%20Presentation%20for%20Utility%20Users%20Group%20at%20EUEC.pdf (accessed October 2011).
14. Laudal, D.L. and French, N.B. (2000) State-of-the-art of mercury continuous emission monitors for coal-fired systems. Presented at the Air Quality II Conference, McLean, VA, September 2000.
15. Kilgroe, J.D., Sedman, C.B., Srivastava, R.K., Ryan, J.V., Lee, C.W., and Thornloe, S.A. (2002) Control of Mercury Emissions from Coal-Fired Electric Utility Boilers: Interim Report, Prepared for the U.S. Environmental Protection Agency Office of Air Quality Planning, EPA-600/R-01-109, April 2002.
16. Chu, P., Roberson, R., Laudal, D., Brickett, L., and Pan, W. (2003) Characterization of "Longer-Term" mercury emissions from coal-fired power plants. Proceedings of the Combined Power

- Plant Air Pollution Control Mega Symposium, Washington, DC, May 2003.
17. Bashlov, N.L., Milenin, V.M., Panasyuk, G.Y., and Timofeev, N.A. (1995) Study of mercury discharge plasma during initial warmup. *Tech. Phys.*, **40** (3), 242–247.
 18. Schabron, J.F., Kalberer, E.W., Boysen, R.B., Schuster, W.C., and Rovani, J.F. (2009) Mercury Continuous Emission Monitor Calibration. Topical Report for U.S. Department of Energy Cooperative Agreement, DE-FC26-98FT40323, April 2009.
 19. Spectragases Spectra Environmental Division, www.spectragases.com/content/upload/AssetMgmt/PDFs/environmental/ENV_MerCalDataSheet_030107.pdf (accessed October 2011).
 20. Constans, D.L., Jameson, R., and Raynor, G. (1997) Observations and comments on EPA/DOE mercury CEMs demonstration at Holnam's Holly Hill. SC Facility. Presented at AWMA International Specialty Conference on Waste Combustion in Boilers and Industrial Furnaces, April 1997.
 21. Hosenfeld, J. (2006) Long-Term Field Evaluation of Mercury (Hg) Continuous Emission Monitoring Systems: Coal-Fired Power Plant Burning Eastern Bituminous Coal and Equipped with Selective Catalytic Reduction (SCR), Electrostatic Precipitator (ESP), and Wet Scrubber: Field Activities from November 2004 to September 2005. Final Report for U.S. Environmental Protection Agency, EPA Contract GS-10F-0127J MRI, Project No. 110489, November 29, 2006.
 22. Laudal, D.L. and Thompson, J.S. (2011) Determining the Variability of Continuous Mercury Monitors (CMMs) at Low Mercury Concentrations. Final Report for AAD Document Control, U.S. Department of Energy; Cooperative Agreement DE-FC26-08NT43291 Subtask 4.10; June 2011.
 23. Ryan, J.V. (2010) Update on Hg CEMS. Presented at OAQPS Measurement Technology Workshop 2010, Research Triangle Park, NC, December 6, 2010.

6 Batch Methods for Mercury Monitoring

Constance Senior

6.1

Introduction

The previous chapter discussed continuous emissions monitoring systems (CEMS) for quantifying mercury concentrations in combustion flue gas. In this chapter, several batch methods for quantifying mercury concentration are discussed. A number of batch, wet-chemistry based methods are available for measuring mercury in flue gas. Recently, dry batch methods, also known as *sorbent trap methods*, have been preferred for many applications. In the United States, sorbent trap methods have been specified by the U.S. Environmental Protection Agency (EPA) as being acceptable for compliance with federal mercury emissions standards for a number of industrial combustion sources.

6.2

Wet Chemistry Batch Methods

6.2.1

Early EPA Total Hg Methods

EPA developed several wet chemistry methods for measuring mercury in industrial stack gases in order to quantify emissions. Descriptions of these methods can be found at the EPA website [1]. EPA Method 101A was developed for determination of gaseous and particulate mercury emissions from sewage sludge incinerators, but is often applied to coal-fired boilers to measure total mercury emissions. EPA Method 29 was developed to measure mercury and other metals in stack emissions.

Figure 6.1 gives a schematic of Method 101A. A probe is inserted into the flue gas with a nozzle designed for isokinetic sampling of the flue gas. A pitot tube probe and a thermocouple are also inserted into the duct. The size of the nozzle is matched to the gas velocity in the flue gas. The probe is traversed in the flue gas during the test in order to collect a representative sample. The sample is

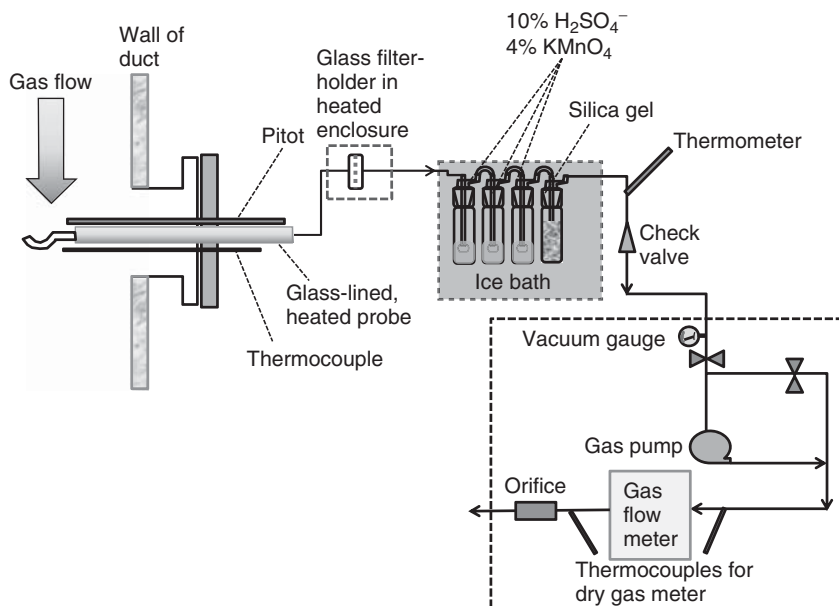


Figure 6.1 Schematic of EPA Method 101A.

withdrawn through the probe and into a heated filter. The filter collects the particulate matter (PM). After the filter, the sample gas is pulled through a series of four glass impingers in an ice bath. The first three impingers contain a solution of 4% KMnO_4 –10% H_2SO_4 (wt% basis). The fourth impinger contains silica gel to dry the gas. Following the impingers, there is a pump and dry gas meter.

EPA Method 29 is designed to measure the solid particulate and gaseous emissions of mercury and 16 other trace elements (antimony, arsenic, barium, beryllium, cadmium, chromium, cobalt, copper, lead, manganese, nickel, phosphorus, selenium, silver, thallium, and zinc). The equipment and sampling train are similar to that for Method 101A, with the exception of the impingers. In Method 29, gaseous metals and mercury are collected in two impingers in series containing an acidic peroxide solution (5% HNO_3 /10% H_2O_2). An empty impinger follows the first two impingers in the train. Elemental mercury that passes through the first three impingers is collected in the two following impingers in series containing acidified permanganate (10% H_2SO_4 /4% KMnO_4). A final impinger containing silica gel is used to dry the sample gas. After the measurement, the contents of the peroxide impingers are saved separately from the contents of the permanganate impingers in an attempt to quantify mercury speciation.

A minimum sampling time of 2 h is recommended for Method 101A. Similar sampling time is usually used for Method 29. The limits of detection of the methods may be improved by increasing the sample time. In Method 101A, if there is an excess of oxidizable organic matter in the gas stream, it may be impossible to

sample for the minimum time. This problem will be indicated by the loss of the purple color of the KMnO_4 solution.

Both methods require leak-checking before and after the test. Post-test, the glassware, including the glass-lined probe, must be rinsed, and the rinsate saved for analysis. The method also requires the use of blanks for the impinger solutions and the filter in the field. After the test, the filter, collected solutions, and blanks are analyzed in a commercial laboratory using cold-vapor atomic absorption (CVAA) spectroscopy.

Three replicate measurements are usually conducted for these methods. These can be done in 1 day, but are often completed over 2 days. The methods require considerable time to set up and recover samples from each measurement. A high level of quality assurance/quality control (QA/QC) and well-trained personnel are needed for these wet chemistry methods.

6.2.2

Development of Wet Chemistry Methods to Speciate Hg

EPA Method 29 was not originally designed for mercury speciation analysis. In the 1980s, various research groups evaluated the method for mercury speciation, because it was thought that the gaseous oxidized (Hg^{2+}) and elemental (Hg^0) species would be selectively absorbed in the separate acidified hydrogen peroxide and acidified permanganate solutions, respectively. However, experience from data validation experiments showed that the two different impinger solutions were not effective for reliably separating the Hg^{2+} and Hg^0 species in a coal-combustion flue gas containing high levels of SO_2 . As a consequence, several groups proposed modifications to the impinger solutions used in EPA Method 29. These included the Ontario Hydro, Tris buffer, and Research Triangle Institute (RTI) methods. All three methods used the framework of Method 29, but substituted different impinger solutions for the speciation of mercury [2].

The Ontario Hydro method was developed by Dr. Keith Curtis and colleagues at Ontario Hydro Technologies in late 1994. In this method, three aqueous 1 N potassium chloride (KCl) impinger solutions were substituted for one of the HNO_3 - H_2O_2 solutions. Originally, no acidified peroxide impingers were included in the sampling train. However, it was discovered that when SO_2 concentration in the flue gas was $>\sim 750$ ppm, the SO_2 reacted with the KMnO_4 neutralized, which meant that sampling time had to be very short. To avoid this problem, an impinger of acidified peroxide solution was used directly after the KCl impingers in order to absorb the SO_2 . It is assumed that any mercury collected in the acidified peroxide solution was Hg^0 , as the KCl solutions would collect all of the Hg^{2+} . Early testing also showed a substantial portion of the mercury was lost from the solutions [3]. To prevent this, acidified permanganate, dichromate, or acidified peroxide solution was added to the KCl solution immediately following sampling.

Formal evaluation of the Ontario Hydro method was completed with dynamic spiking of Hg^0 and HgCl_2 into a flue gas stream [3]. The Ontario Hydro method

Table 6.1 Comparison of wet chemistry methods.

Method	Sampling train configuration		Impinger configuration (number of impingers – impinger set solution)			Analytical method
	Front-half collection (PM and Hg _p)	Back-half collection (gaseous Hg)	First set	Second set	Third set	
EPA Method 101A	Glass fiber filter	Impinger solutions	3H ₂ SO ₄ – KMnO ₄	None used	None used	CVAA
EPA Method 29	Glass fiber filter	Impinger solutions	2HNO ₃ – H ₂ O ₂	1 dry	2H ₂ SO ₄ – KMnO ₄	CVAA
Ontario-Hydro Method	Glass fiber filter	Impinger solutions	3KCl	1HNO ₃ – H ₂ O ₂	3H ₂ SO ₄ – KMnO ₄	CVAA

is now ASTM Method D6784-02 [4]. The method outlines QA/QC procedures, including leak-checking, calibration, and the use of blanks. The three wet chemistry methods discussed are compared in Table 6.1.

6.2.3

Method Application and Data Quality Considerations

The precision of measurement of particulate, oxidized, and elemental mercury is influenced by many factors: flue gas concentration, source, procedural, and equipment variables. To ensure that precise results are achieved, the sampling system must be leak-free, system components must be accurately calibrated, the proper sampling locations must be selected, glassware must be thoroughly cleaned, and prescribed sample recovery, preparation, and analysis procedures must be followed.

In the ASTM method description [4], $0.5 \mu\text{g m}^{-3}$ is estimated as the lower limit for most applications. Ryan and Keeney [5] stated that, assuming a 50–50 split between oxidized and elemental mercury in a flue gas, the lower limit of quantitation for total mercury in the Ontario Hydro Method ranges from 0.31 to $0.62 \mu\text{g m}^{-3}$. The lower limit of quantitation can be reduced by using low mercury calibration standards. However, at such low concentrations, achieving adequate blank samples may be difficult.

The impinger-based methods were designed to be used downstream of the plant's particulate control device. In many cases (for research or survey purposes), these wet methods are used before the particulate control device, when there is a lot of particulate matter present in the flue gas. In these situations, reactive particulate matter can bias the speciation. This bias can be manifest as either artificially high oxidized mercury (in the case of the Ontario Hydro Method) or high particulate mercury. All the sample gas must pass through the filter. Gaseous mercury species in flue gases can interact with fly ash particles collected

on the filter and can produce a positive particulate mercury bias. In some cases, particulate-bound mercury collected on the filter can volatilize because of flue gas exposure, and be collected in the impingers. Such vaporization losses of mercury result in a negative particle-bound mercury bias.

There are practical limitations to the impinger-based methods arising from the complex sample trains, which are composed of relatively large amounts of glassware and tubing. Furthermore, the glass impingers contain strongly oxidizing and acidic reagents requiring labor-intensive sample recovery and analytical procedures. Usually, these solutions must be shipped to a laboratory quickly. In some cases, testing contractors have brought complete analytical laboratories on-site for analysis. This reduces the turnaround time for obtaining results, but can substantially increase the cost of the measurements.

6.3

Dry Batch Methods

6.3.1

Sorbent Trap Method History

In this section, the general concept of sorbent trap methods will be discussed, in addition to specific methods such as Performance Specification 12B (PS-12B) and Method 30B. In addition, speciation sorbent traps, which are used for research and demonstrations, will also be discussed.

Sorbent trap methods for measuring mercury in combustion gas were developed in the early 1990s in the United States and have been used, in one form or another, for the last 20 years. The first method was developed by Frontier Geosciences and was called the *mercury speciation adsorption (MESA)* method [6]. The MESA method was used in a number of pilot and field demonstrations of mercury control technology on coal-combustion systems in the mid- to late-1990s [7]. Improvements were made to the method, under sponsorship of the Electric Power Research Institute (EPRI), and the resulting method was known as *QuickSEM*. In 2004, U.S. EPA adopted the method as part of the draft Utility Mercury Reduction Rule and called it *Method 324*. In 2005, EPA proposed a different utility regulation on mercury emissions called the *Clean Air Mercury Rule (CAMR)*; CAMR utilized a sorbent trap method known as the *Appendix K method*. CAMR was ultimately not promulgated by EPA. In 2010, EPA included PS-12B in the compliance monitoring procedures promulgated as part of the Portland Cement Maximum Achievable Control Technology (MACT) rulemaking [8]. In February 2012, EPA finalized the Mercury and Air Toxics Standard (MATS) rule for utility boilers, and this rule included PS-12B as an acceptable method for mercury measurement for compliance with the rule.

Total mercury measurement is needed for compliance with regulations. However, scientists and engineers need to measure speciated mercury in flue

gas in order to evaluate control technology options. As discussed above, the wet method, the Ontario Hydro Method, provides speciated mercury information, but this method is complicated and time-consuming to implement. Therefore, speciation sorbent trap methods have been developed.

The MESA sorbent trap method uses a trap containing KCl/soda lime to collect oxidized mercury. It has been used for measurement of both total Hg and speciated Hg in flue gas as for the EPRI PISCES program [9, 10] and performance-tested for total mercury using EPA Method 301 [11, 12]. It was evaluated for speciated Hg in coal flue gas [13, 14]. Total Hg results were within acceptable limits for sensitivity, accuracy, and precision [13, 15].

Frontier Geosciences developed the flue gas mercury sorbent speciation (FMSS) method in which a semi-isokinetic sample was pulled from the flue gas through a mini-particulate filter and a heated solid sorbent sample train, consisting of parallel sorbent traps. Analysis of the filter was carried out for particulate mercury and the sorbents were analyzed for gaseous Hg species. In the sorbent trap section, the first trap contained dry KCl-coated quartz chips and was used to capture the oxidized mercury. The second trap contained iodine-impregnated activated carbon to capture the elemental mercury. The FMSS method was validated according to the modified EPA Method 301 [16]. EPA Method 301 [17] specifies procedures for determining the precision and bias of measured emissions using a specific method at the concentrations typical of the specific standard for the source.

Currently, the most widely used speciated Hg sorbent trap method is the flue gas adsorption for mercury speciation (FAMS) method [18], which uses the KCl/quartz trap to remove oxidized mercury and an activated carbon trap to remove elemental mercury. The FAMS method was also developed by Frontier Geosciences.

As both CEMS and sorbent trap methods for compliance with mercury emissions regulations were being developed, there was a need for a reference method (RM) to verify the performance of the measurement system once installed at a specific plant. This performance verification was initially conducted using wet chemical methods, such as the Ontario Hydro Method (ASTM D6784) as the RM. However, such methods proved to be complex, slow, and cumbersome. In 2007, the EPA issued a direct final rule to add two reference measurement methods for coal-fired power plants. The two methods, Method 30A and Method 30B, were intended for use in relative accuracy audits (RATAs) of mercury emissions monitoring systems installed in combustion systems. Method 30A was based on a continuous monitoring instrument, while Method 30B was a sorbent trap method [19].

Monitoring of mercury emissions from coal-combustion systems for compliance purposes in the United States can be carried out using either a continuous emission monitoring system (CEMS) (as specified in EPA's PS-12A) or a sorbent trap (PS-12B). A part of the certification process for either emissions monitoring system is a RATA, which can be performed using the Ontario Hydro Method, Method 30A (instrumental RM) or Method 30B (sorbent trap RM).

6.3.2

Method Overview

In a sorbent trap method, a known volume of flue gas is pulled through paired, pre-spiked traps located in the stack or duct. The exposed traps can be analyzed by any method that meets the specified QA/QC criteria. The collection of paired samples is needed to determine the method precision.

Figure 6.2 shows a general schematic of the sampling set-up for sorbent trap methods. Two sorbent traps are located in the flue gas duct (detail not shown in figure). Gas is drawn through the traps in parallel. The sample is not isokinetic. Sorbent trap methods are intended for use only under conditions of relatively low particulate loading (i.e., sampling after particulate control devices); in cases where significant amounts of particle-bound Hg may be present, an isokinetic sampling method for Hg should be used.

The rest of the sampling system consists of a system to remove moisture, a pump, and dry gas meter. The measurement of the temperature and pressure at the dry gas meter (sampling console) is critical for calculating an accurate sample volume. The actual temperature and pressure of the sampled (flue) gas is not required. For a continuous mercury monitor, the flow rate is adjusted to maintain sample flow rate in proportion with total flue gas flow rate in the duct.

6.3.3

Total Hg Measurements

6.3.3.1 PS-12B

The purpose of this method is continuous monitoring of mercury from combustion stacks. Each trap must have the sorbent configured into three sections

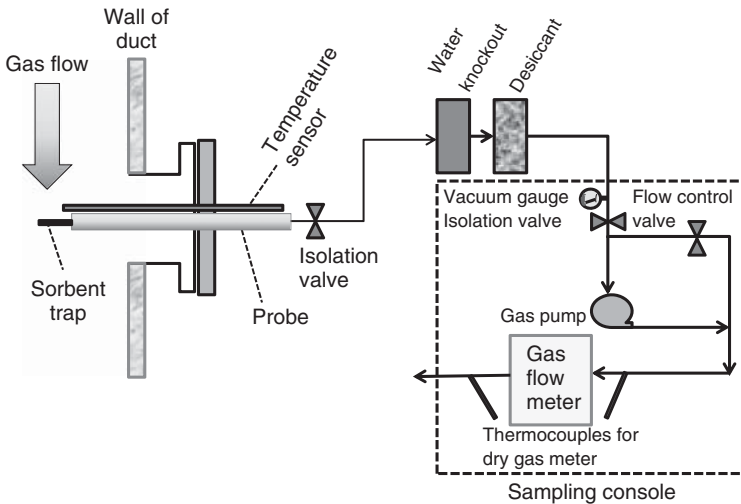


Figure 6.2 Schematic diagram of sorbent trap sampling system.

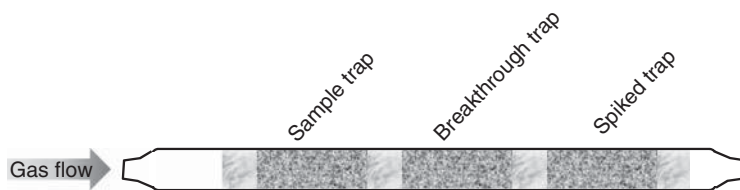


Figure 6.3 Three-section trap for PS-12B.

that can be tested independently (Figure 6.3). Plugs of quartz wool separate the sections. There is also a quartz wool plug before the first section and after the last section. A common trap sorbent material is activated carbon impregnated with a halogen such as iodine or bromine. The first section is for primary mercury collection. The second section is to provide an indication of mercury breakthrough. If there is too much breakthrough (i.e., too much mercury in the second trap), the sample could be invalidated. The third section is for spike recovery testing.

The spiked section is prepared in advance, using a mercury sample gas, which is flowed through the section. The method allows the use of any method for generating a known mass of gaseous elemental mercury as long as National Institute of Standards and Technology (NIST)-traceable standards are used. For example, an elemental mercury gas generator or cylinder of mercury calibration gas can be used to generate the mercury for the spike.

6.3.3.2 Method 30B

For RATA testing, Method 30B is used. The Method 30B trap has two sections, as shown in Figure 6.4. Quartz wool plugs separate the sections and an initial quartz wool plug removes any particles in the sample gas. There is no separate section for spiking but the first section of one of the paired traps is spiked with elemental mercury to assess the measurement bias and to verify data acceptability in the field.

6.3.4

Speciation Measurements

Speciation traps have been developed as an alternative to the Ontario Hydro Method for speciation of mercury in flue gas. As noted above, the most widely



Figure 6.4 Two-section trap for Method 30B.

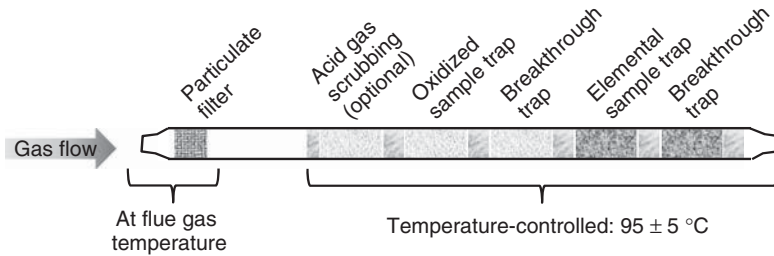


Figure 6.5 Sorbent trap configuration for speciated Hg measurement.

used speciation sorbent trap method is based on Method 30B [18]. Figure 6.5 shows a schematic of the sections in each trap.

In this method, there is a particulate collection section, followed by two sections to collect oxidized mercury (primary and breakthrough), which contain KCl on quartz chips, and two sections to collect elemental mercury (primary and breakthrough), which contain iodated or brominated carbon. An acid-gas scrubbing trap may also be used to remove acid gases like SO_2 . In some implementations of speciation traps, the particulate collection section of the trap is at the temperature of the flue gas being sampled, and in other implementations, a quartz wool plug is used upstream of the first trap. In any case, the other sections of the traps are controlled to $95 \pm 5^\circ\text{C}$ to prevent breakthrough of mercury on the KCl sections. One manufacturer of speciation traps also recommends that the trap should be kept $20\text{--}30^\circ\text{C}$ above the dew point of the sample gas in the duct [20].

Speciation sorbent traps use the same sampling apparatus as that for the total mercury methods, with the exception of a special probe to control the temperature of the sections intended to collect gaseous mercury.

6.3.5

Sampling Protocol

6.3.5.1 Procedure and Apparatus

The assembled system is leak-checked before the sampling begins and after the sampling ends. After a period of sampling, the traps are removed and the individual sections are analyzed to measure the total amount of mercury in the traps. The mass of mercury collected in the traps divided by the total gas volume over the period of the sampling indicates mercury concentration in the gas.

As noted above, the speciation trap method requires a temperature-controlled probe, which the total mercury trap methods do not.

During the sampling period, it is important to measure the characteristics of the flue gas, for example, the oxygen content, flue gas velocity, and the moisture content. These will be used to determine the sample rate (for proportional sampling) and to convert the results to the units of emissions (pound per trillion British thermal unit or pound per gigawatt hour). To compare the sorbent trap result to that

of a mercury CEMS, the results might have to be converted to concentration on a wet volume basis, because this is how some CEMS measure mercury in flue gas.

The sampling period is not specified in the methods. There are several factors that influence the sampling period. The total amount of mercury collected on an individual trap depends on the concentration in the flue gas, the sampling time, and the sample flow rate. The amount of mercury collected on a trap must fall within the range of the calibration curve for the analytical method. Furthermore, the spikes of mercury added to section 3 (PS-12B) or section 1 (Method 30B) must have a mass of mercury that is in the expected range of mercury to be collected in the sample (section 1). For Method 30B, the spiked amount of mercury must be within $\pm 15\%$ of the expected mass of mercury on section 1. Method 30B is not intended for long sample times, as is PS-12B. If the sample period for PS-12B is too long (days to weeks), there may be breakthrough of mercury from section 1 to section 2, which will invalidate the run. Finally, if the sampling time is too short (< 30 min), then small errors in the start and end times might result in substantial errors in the measured concentration.

6.3.6

Trap Analysis

The two most widely used approaches to analyzing the traps for mercury are (i) a wet digestion method using cold vapor atomic fluorescence (CVAF) spectroscopy and (ii) direct pyrolysis into a CVAA analyzer. The latter approach can be done on site with the proper equipment, adherence to standards of cleanliness, and proper calibration. Analysis of the traps is destructive; if there is a problem with the analysis, it cannot be repeated. Elemental mercury will absorb 253.7 nm UV light, and a CVAA detector will have exquisite low detection limits for mercury. However, contaminants such as sulfur dioxide, water, oxygen, halogens, and organic species can interfere with the determination of elemental mercury by CVAA.

6.3.7

Relative Accuracy and Quality Assurance/Quality Control

The sorbent trap methods are performance-based, which means that while some specifics of the method are not dictated (e.g., sample time, trap composition), the method must meet rigorous QA/QC criteria. The QA/QC criteria for PS-12B [8] and Method 30B [19] are similar, as seen in Tables 6.2 and 6.3.

For PS-12B, initial certification of the system requires a RATA using an RM. Acceptable RMs are the Ontario Hydro Method, Method 30A, or Method 30B. Twelve RM samples must be taken and the best nine samples compared to corresponding sorbent traps. The average relative difference between the sorbent trap measurements and the RM can be no $> 20\%$. If the RM concentration is $\leq 5 \mu\text{g m}^{-3}$, then the relative accuracy (RA) criterion is satisfied, if the difference between the average values of the continuous measurement and the RM is not $> 1 \mu\text{g m}^{-3}$.

Table 6.2 QA/QC criteria for PS-12B.

QA/QC test or specification	Acceptance criteria	Frequency	If criteria not met
Pre-monitoring leak check	$\leq 4\%$ of target sampling rate	Prior to monitoring	Cannot start sampling
Post-monitoring leak check	$\leq 4\%$ of target sampling rate	After monitoring	Data from pair traps invalidated, or if certain conditions met, report adjusted data from a single trap
Ratio of stack gas flow rate to sample flow rate	Hourly ratio may not deviate from the reference ratio by more than $\pm 25\%$	Every hour throughout the monitoring period	Data from pair traps invalidated, or if certain conditions met, report adjusted data from a single trap
Sorbent trap section 2 breakthrough	$\leq 5\%$ of section 1 Hg mass	Every sample	Data from pair traps invalidated, or if certain conditions met, report adjusted data from a single trap
Paired sorbent trap agreement	$\leq 10\%$ relative deviation (RD) if the average concentration is $> 1.0 \mu\text{g m}^{-3}$	Every sample	Either invalidate the data from the paired traps or report the results from the trap with the highest Hg concentration
	$\leq 20\%$ relative deviation (RD) if the average concentration is $\leq 1.0 \mu\text{g m}^{-3}$		
	Results also acceptable if absolute difference between concentration from parallel traps is $\leq 0.03 \mu\text{g m}^{-3}$		
Spike recovery	Average recovery between 85% and 115% for each of the three spikes' concentration levels	Prior to analyzing field samples and prior to the use of new sorbent media	Field samples must not be analyzed until the percent recovery criteria are met
Multipoint analyzer calibration	Each analyzer reading within $\pm 10\%$ of true value and $r^2 \geq 0.99$	On the day of analysis, before analyzing any sample	Recalibrate until successful

(continued overleaf)

Table 6.2 (Continued)

QA/QC test or specification	Acceptance criteria	Frequency	If criteria not met
Analysis of independent calibration standard	Within $\pm 10\%$ of true value	Following daily calibration, prior to analyzing field samples	Recalibrate and repeat independent standard analysis until successful
Spike recovery from section 3 of both sorbent traps	75 – 125% of spike amount	Every sample	Data from pair traps invalidated, or if certain conditions met, report adjusted data from a single trap
Relative accuracy (RA)	RA $\leq 20.0\%$ of reference method (RM) value; or if RM value $\leq 5.0 \mu\text{g m}^{-3}$, absolute difference between RM and sorbent trap monitoring system mean values $\leq 1.0 \mu\text{g m}^{-3}$	RA specification must be met for initial certification	Data from the system are invalid until an RA test is passed
Gas flow meter calibration	An initial calibration factor (Y) has been determined at three settings; for mass flow meters, initial calibration with stack gas has been performed. For subsequent calibrations, Y within $\pm 5\%$ of average value from the most recent three-point calibration	At three settings prior to initial use and at least quarterly at one setting thereafter	Recalibrate meter at three settings to determine a new value of Y
Temperature sensor calibration	Absolute temperature measured by sensor within $\pm 1.5\%$ of a reference sensor	Prior to initial use and at least quarterly thereafter	Recalibrate; sensor may not be used until specification is met
Barometer calibration	Absolute pressure measured by instrument within ± 10 mm Hg of reading with a NIST-traceable barometer	Prior to initial use and at least quarterly thereafter	Recalibrate; sensor may not be used until specification is met

Table 6.3 QA/QC criteria for Method 30B.

QA/QC test or specification	Acceptance criteria	Frequency	If criteria not met
Pre-monitoring leak check	≤4% of target sampling rate	Prior to monitoring	Cannot start sampling
Post-monitoring leak check	≤4% of target sampling rate	After monitoring	Data from pair traps invalidated, or if certain conditions met, report adjusted data from a single trap
Sorbent trap section 2 breakthrough	≤10% of section 1 Hg mass for Hg concentration is $>1.0 \mu\text{g m}^{-3}$ ≤20% of section 1 Hg mass for Hg concentration is $\leq 1.0 \mu\text{g m}^{-3}$	Every sample	Sample invalidated
Paired sorbent trap agreement	≤10% relative deviation (RD) if the average concentration is $>1.0 \mu\text{g m}^{-3}$ >1.0 $\mu\text{g m}^{-3}$ ≤20% relative deviation (RD) or $\leq 0.2 \mu\text{g m}^{-3}$ if the average concentration is $\leq 1.0 \mu\text{g m}^{-3}$ Each analyzer reading within $\pm 10\%$ of true value and $r^2 \geq 0.99$ Within $\pm 10\%$ of true value	Every sample	Run invalidated
Multipoint analyzer calibration		On the day of analysis, before analyzing any sample	Recalibrate until successful
Analysis of independent calibration standard		Following daily calibration, prior to analyzing field samples	Recalibrate and repeat independent standard analysis until successful
Temperature sensor calibration	Absolute temperature measured by sensor within $\pm 1.5\%$ of a reference sensor	Prior to initial use and at least quarterly thereafter	Recalibrate; sensor may not be used until specification is met
Barometer calibration	Absolute pressure measured by instrument within ± 10 mm Hg of reading with a NIST-traceable barometer	Prior to initial use and at least quarterly thereafter	Recalibrate; sensor may not be used until specification is met

(continued overleaf)

Table 6.3 (Continued)

QA/QC test or specification	Acceptance criteria	Frequency	If criteria not met
Sample analysis	Within valid calibration range (within calibration curve)	All section 1 samples where stack Hg concentration is $\geq 0.5 \mu\text{g m}^{-3}$	Reanalyze at more concentrated levels if possible, samples invalidated if not within calibrated range
Sample analysis	Within bounds of Hg^0 and HgCl_2 analytical bias test	All section 1 samples where stack Hg concentration is $\geq 0.5 \mu\text{g m}^{-3}$	Expand bounds of Hg^0 and HgCl_2 analytical bias test; if not successful, samples invalidated
Field recovery test (spiked trap)	Average recovery between 85% and 115%	Once per field test	Field sample runs not validated without successful field recovery test
Gas flow meter calibration (at three settings)	Calibration factor Y within $\pm 2\%$ of average value of Y	Prior to initial use and when post-test check is not within $\pm 5\%$ of Y	Recalibrate at three points until acceptance criteria met
Gas flow meter calibration, post-test (single-point)	Calibration factor Y within $\pm 5\%$ of average value from the most recent three-point calibration	After each field test. For mass flow controllers must be done on-site using stack gas	Recalibrate at three points to determine new Y . For mass flow meters, must be done on-site using stack gas. Apply new Y values to field test data
Analytical matrix interference test (wet chemical analysis only)	Establish minimum dilution (if any) needed to eliminate sorbent matrix interferences	Prior to analyzing any field samples; repeat for each type of sorbent used	Field sample results not validated
Analytical bias test	Average recovery between 90% and 110% for Hg^0 and HgCl_2 at each of the two spike levels	Prior to analyzing field samples and prior to use of new sorbent media	Field samples shall not be analyzed until the percent recovery criteria has been met
Analysis of continuing calibration verification standard	Within $\pm 10\%$ of true value	Following daily calibration, after analyzing ≤ 10 field samples, and at end of each set of samples	Recalibrate and repeat independent standard analysis, reanalyze samples until successful, if possible; for destructive techniques, samples invalidated
Test run sample volume	Within $\pm 20\%$ of total volume sampled during field recovery test	Each individual sample	Sample invalidated

6.4

Recommendations

For long-term monitoring of mercury emissions or for short-term testing of mercury control technologies, CEMS or batch methods can be used. The two types of methods have advantages and disadvantages. Consideration should be given to some of the following factors when choosing a mercury measurement method.

6.4.1

Particulate Matter

If there is a need to sample a gas that has a high dust loading and there is an expectation that there will be a significant component of mercury in the particulate matter, the best option is one of the wet chemistry methods, which collect an isokinetic sample on a filter (bearing in mind the potential for bias because of the particulate matter on the filter). When sampling after the particulate control device, the mercury in the flue gas will be almost entirely gaseous mercury and a CEMS or sorbent trap will give representative results.

6.4.2

Total Versus Speciated Mercury

For evaluating emissions from a combustion source for compliance purposes, only total mercury is required. This can be measured with a CEMS or with one of the batch methods that measure total mercury (Method 101A, Method 29, PS-12B). For research or testing reasons, it is sometimes necessary to measure gaseous speciation; for example, if there is a need to quantify re-emission of elemental mercury across a wet scrubber, speciated mercury measurements (CEMS, Ontario Hydro Method, FAMS) should be made at the inlet and outlet of the scrubber.

6.4.3

Expected Mercury Concentration in the Flue Gas

The Ontario Hydro Method is generally accurate above a total mercury concentration in the flue gas of $0.5 \mu\text{g m}^{-3}$, although the lower limit of detection can be higher, depending on the care taken by the test personnel. At present, NIST-traceable calibration gases for Hg CEMS provide concentrations from ~ 0.2 to $>40 \mu\text{g m}^{-3}$. Most commercial CEMS can accurately measure mercury in flue gas down to the lower concentration of $0.2 \mu\text{g m}^{-3}$. Sorbent traps can measure even lower concentrations of mercury in flue gas, because the sampling time can be increased to ensure that an adequate mass of mercury is collected in the traps. When very low levels of mercury are expected in the flue gas, sorbent traps are preferred.

6.4.4

Need for Real-Time Data

In some instances, a concentration of mercury averaged over 30 min to several hours (or even days) will suffice. In this case, batch sampling methods can be used. However, in some cases (for example, process control or short-term technology demonstrations), a continuous mercury measurement is required, and a CEMS must be used. Furthermore, batch methods use destructive analysis; if a measurement is lost or invalidated, there are no data for a specific period. CEMS provide data every 1–2 min typically.

6.4.5

Complexity of Installation and Operation

Sorbent trap methods are less expensive and complicated to install than CEMS or wet chemistry methods. Sorbent trap systems are less complex than CEMS and do not require as much training of technical personnel over long-term operation. Wet chemistry methods are not used for continuous monitoring of a source. These methods require specifically trained personnel and great care in preparation, set-up, and post-test sample collection and stabilization.

References

1. U.S. EPA (2012) Technology Transfer Network, Emission Measurement Center, <http://www.epa.gov/ttn/emc/> (accessed 16 December 2012).
2. Electric Power Research Institute (1999) A State-of-the-Art Review of Flue Gas Mercury Speciation Methods. Final Report TR-107080, EPRI, United States Department of Energy, Palo Alto, CA, Pittsburgh, PA.
3. Electric Power Research Institute (1999) Evaluation of Flue Gas Mercury Speciation Methods. Final Report TR-108988, EPRI, United States Department of Energy, Palo Alto, CA, Pittsburgh, PA.
4. ASTM International (2002) D 6784. *Standard Test Method for Elemental, Oxidized, Particle-Bound and Total Mercury in Flue Gas Generated from Coal-Fired Stationary Sources (Ontario Hydro Method)*, June 2002, American Society for Testing and Materials.
5. Ryan, J.V. and Keeney, R.M. (2004) The Ontario hydro method for speciated mercury measurements: issues and considerations. Presented at the Symposium on Air Quality Measurement Methods and Technology-2004, Research Triangle Park, NC, April 19–22, 2004.
6. Prestbo, E.M. and Bloom, N.S. (1995) Mercury Speciation Adsorption (MESA) method for combustion flue gas, methodology, artifacts, intercomparison and atmospheric implications. *Water Air Soil Pollut.*, **80**, 145.
7. Haythornthwaite, S., Sjostrom, S., Ebner, T., Ruhl, J., Slye, R., Smith, J., Hunt, T., Chang, R., and Brown, T. (1997) Demonstration of dry carbon-based sorbent injection for mercury control in utility ESPs and Baghouses. EPRI-DOE-EPA Combined Utility Air Pollution Control Symposium, EPRI TR-108683-V1-V3, Washington, DC, August 25–29, 1997.
8. U.S. EPA (2010) Performance Specification 12B – Specifications and Test Procedures for Monitoring Total Vapor Phase Mercury Emissions from Stationary Sources Using a Sorbent Trap Monitoring System,

- <http://www.epa.gov/ttn/emc/perfspec/ps-12B.pdf> (accessed 20 March 2014).
9. Prestbo, E.M. and Bloom, N.S. (1994) Mercury Speciation Adsorption (MESA) Method intercomparison results in combustion flue gas. Proceedings Coal-Energy and the Environment, 11th Annual Pittsburgh Coal Conference, Pittsburgh, PA, September 12–16, 1994.
 10. Chu, P. and Porcella, D. (1995) Mercury stack emissions from U.S. electric utility power plants. *Water Air Soil Pollut.*, **80**, 137.
 11. Nott, B.R., Huyck, K.A., DeWees, W., Prestbo, E.M., Olmez, I., and Tawney, C.W. (1994) Evaluation and comparison of methods for mercury measurement in utility stack gas. Presented at the Air and Waste Management Association Annual Meeting, Paper #94-MP6.02.
 12. Nott, B. (1985) Intercomparison of stack gas mercury measurement methods. *Water Air Soil Pollut.*, **80**, 1311.
 13. Laudal, D., Nott, B., Brown, T., and Roberson, R. (1997) Mercury speciation methods for utility flue gas. *Fresenius J. Anal. Chem.*, **358**, 397.
 14. Laudal, D.L., Heidt, M.K., Brown, T.D., Nott, B.R., and Prestbo, E.M. (1996) Mercury speciation: a comparison between EPA method 29 and other sampling methods. Presented at the Air and Waste Management Association Annual Meeting, Paper #96-WA64A.04.
 15. Prestbo, E.M. and Tokos, J.S. (1997) Mercury speciation in coal combustion flue gas: MESA method. Presented at Air and Waste Management Association Annual Meeting, Paper 97-WP72B.02.
 16. Laudal, D.L., Thompson, J.S., Dunham, G.E., Pavlish, J.H., Galbreath, K.E., Weber, G.F., and Sondreal, E.A. (2002) Mercury Studies, Appendix B. Final Report for U.S. Environmental Protection Agency Cooperative Agreement No. R-828323-01, U.S. Department of Energy National Energy Technology Laboratory Cooperative Agreement, No. DE-FC26-98FT40321, and Ontario Power Generation; Energy & Environmental Research Center, Grand Forks, ND, November 2002.
 17. U.S. EPA (2011) Method 301–Field Validation of Pollutant Measurement Methods from Various Waste Media. Code of Federal Regulations, Title 40, Parts 63, Appendix A.
 18. Wright, J. (2012) Low level mercury monitoring using sorbent traps to meet MATS monitoring requirements. Presented at Reinhold Environmental 2012 APC Round Table, Baltimore, MD, July 16–17, 2012.
 19. U.S. EPA (2009) Method 30B – Determination of Total Vapor Phase Mercury Emissions from Coal-Fired Combustion Sources Using Carbon Sorbent Traps, <http://www.epa.gov/ttn/emc/promgate/Meth30B.pdf> (accessed 20 March 2014).
 20. Ohio Lumex Company (2009) Testing and Analyzing Speciation Traps, http://www.ohiolumex.com/download/Speciation_Traps_SOP_090409.pdf (accessed 13 January 2013).

Part III
**Mercury Chemistry in Coal Utilization Systems and Air
Pollution Control Devices**

7

Mercury Behavior in Coal Combustion Systems

Constance Senior

7.1

Introduction

Control of mercury emissions from coal combustion systems relies on an understanding of the chemistry of mercury and its interactions with various elements in the combustion system. In coal utilization systems, mercury can take on different chemical forms in flue gas: gaseous elemental (Hg^0), gaseous oxidized (Hg^{2+}), and particulate-bound (Hg_p). As discussed in Chapter 1, the form in which mercury is emitted to the atmosphere determines its fate and transport in the environment. In this chapter, the factors influencing the forms of mercury found in coal combustion flue gas are elucidated.

Coal combustion systems that are used in electricity generating unit (EGU) boilers or industrial, commercial, and institutional (ICI) boilers have a variety of designs. The compositions of coals, which are burned to generate electricity and/or steam in these boilers, vary considerably. Finally, there are different types of air pollution control devices (APCDs) in use on coal-fired boilers to control emissions of NO_x , SO_x , and particulate matter (PM). These three factors – combustion system, coal type, and existing APCD configuration – affect the form and speciation of mercury that is emitted to the atmosphere and the degree of difficulty in controlling the emission of mercury to the atmosphere.

Later chapters in this book will discuss control technologies that are specific to mercury capture from coal-fired boilers. In this section, the groundwork will be laid for understanding mercury control technologies applied to coal combustion systems. The characteristics of coal combustion boilers and APCDs will be described. Then, the chemistry of mercury in coal combustion systems will be discussed. Finally, the behavior of mercury in the existing APCDs on coal-fired boilers will be explored.

7.2

Coal Combustion Boilers

The purpose of EGU or ICI boilers is to generate steam, which is used to generate electricity in EGU boilers and certain ICI boilers or to generate steam for chemical processes or heating in ICI boilers. Generating steam from coal combustion is accomplished by creating a high temperature gas and then transferring energy from the gas to water or steam, first in a radiant zone and then in a convective zone [1]. After this heat has been transferred, the flue gas has a temperature of 340–370 °C (650–700 °F). The combustion air is preheated in a gas–gas heat exchanger, called an *air preheater (APH)*. The flue gas that exits the convective heat exchangers then passes through the APH, and its temperature drops to 135–175 °C (275–350 °F) as illustrated in Figure 7.1. The temperature of the flue gas drops rapidly from the combustion temperatures in the range of 900–1500 °C (1650–2750 °F) to post-APH temperatures in a few seconds [2]. The peak combustion temperature depends on the type of combustion system. This rapid quench of the flue gas has consequences for the chemistry of mercury in the gas, as discussed below.

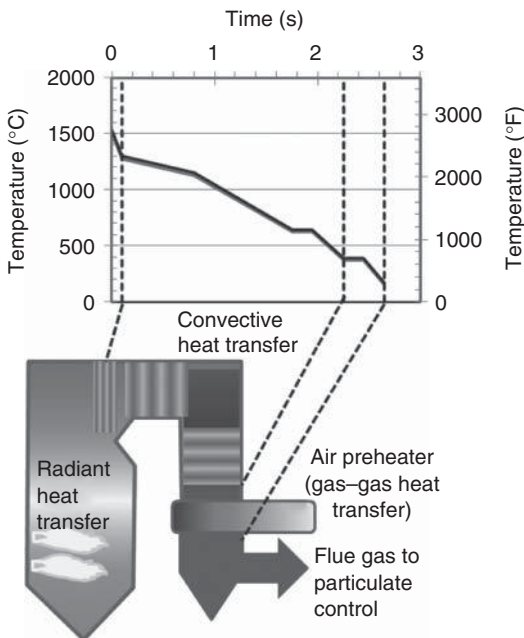


Figure 7.1 Time–temperature history in a coal-fired boiler from radiant section to air pre-heater.

7.3

Mercury Chemistry in Combustion Systems

Mercury is present in coal in low concentrations, on the order of $0.1 \mu\text{g g}^{-1}$, as discussed in Chapter 2. In the combustion zone of a coal-fired boiler, all the mercury in coal is vaporized as elemental mercury, yielding vapor concentrations of mercury in the range of $5\text{--}40 \mu\text{g m}^{-3}$. At furnace exit temperatures, all of the mercury is expected to remain as the thermodynamically favored elemental form in the gas. As the gas cools in the convective heat transfer zone, oxidation reactions can occur, significantly reducing the concentration of elemental mercury by the time the post-combustion gases reach the stack. Measurements of the concentration of mercury species taken in the stacks of pilot and full-scale coal combustion systems show that the range of the values of the fraction of oxidized mercury is broad: studies have reported anywhere from almost no Hg^{2+} to 95% Hg^{2+} upstream of the particulate control device (PCD) [3]. Laboratory experiments [4] have shown that mercury is not oxidized in the gas phase by O_2 at temperatures up to 700°C (1290°F). Combustion experiments in laboratory combustion systems have shown an increase in oxidized mercury post-combustion with increasing chlorine or bromine content [5–8]. Quench rate has been shown to affect the degree of homogeneous oxidation [6, 7].

Comparison of mercury speciation data from full-scale coal-fired boilers with those from particle-free laboratory combustion studies [9] shows higher amounts of oxidized Hg in the former, for similar amounts of chlorine in the fuel. Two conclusions arise from such comparisons:

- Oxidation of mercury by chlorine in practical coal combustion systems must be kinetically limited [10, 11].
- Heterogeneous oxidation of mercury on fly ash particles in coal-fired boilers is as important, or more important, than homogeneous oxidation of mercury [12, 13].

Gas-phase oxidation relies on the reaction between elemental mercury and halogen radicals. The inherent concentrations of these halogens in coal as well as the specific halogen species formed in the combustion system affect homogeneous mercury oxidation.

The range of concentrations of chlorine and bromine species in coal combustion flue gas depends on the concentrations in the coal. In U.S. coal-fired power plants, the concentration of HCl in the flue gas is on the order of $1\text{--}10$ ppmv when low-rank coals (subbituminous and lignite) are burned, but HCl concentrations can be as high as 150 ppmv when bituminous coals are burned. These estimates assume coal chlorine concentrations of up to $100 \mu\text{g g}^{-1}$ in subbituminous and lignite coals and up to $2000 \mu\text{g g}^{-1}$ in bituminous coals. Bromine concentrations in coals are significantly less than chlorine concentrations, as discussed in Chapter 2. The concentrations of bromine (expressed as HBr) in the flue gas of coal-fired combustion systems is estimated to be <0.5 ppmv in boilers firing subbituminous or lignite coals and up to 3.5 ppmv in bituminous-fired boilers.

The differences between the speciation of chlorine and bromine in combustion flue gas have implications for the oxidation of mercury by halogens. As flue gases cool in a practical combustion system, most of the chlorine is predicted to be HCl, with a very minor amount as the free radical Cl, the species thought to be responsible for the homogeneous oxidation of elemental mercury [2]. Recent kinetic modeling [12] results suggest that bromine speciation is different from chlorine speciation in coal combustion flue gases. In contrast, the concentrations of HBr and Br are comparable at flame temperatures and, as the flue gases cool, the concentration of Br is on the same order as that of HBr.

Experiments on the gas-phase oxidation of mercury by halogens were conducted in a bench-scale, laminar, methane-fired (300 W), quartz-lined reactor in which gas composition (HCl, HBr, NO_x , SO_2) was varied [7]. In the experiments, the post-combustion gases were quenched from flame temperature to about 350 °C, and then speciated mercury was measured using a wet conditioning system and continuous emissions monitor system (CEMS). Bromine was shown to be much more effective than chlorine in the post flame, homogeneous oxidation of mercury, on an equivalent molar basis, as illustrated in Figure 7.2.

In these experiments, the addition of NO to the flame (up to 400 ppmv) had no impact on mercury oxidation by chlorine or bromine. Addition of SO_2 had no effect on mercury oxidation by chlorine at SO_2 concentrations below about 400 ppmv; some increase in mercury oxidation was observed at SO_2 concentrations of 400 ppmv and higher. The addition of chlorine caused minor increases in the extent of oxidation by bromine.

Smith *et al.* [8] obtained similar results in a different methane-fired laboratory furnace: homogeneous oxidation of mercury was <30% when the concentration of HCl was as much as 500 ppmv. The researchers observed inhibition or enhancement of mercury oxidation by chlorine when SO_2 was added, and

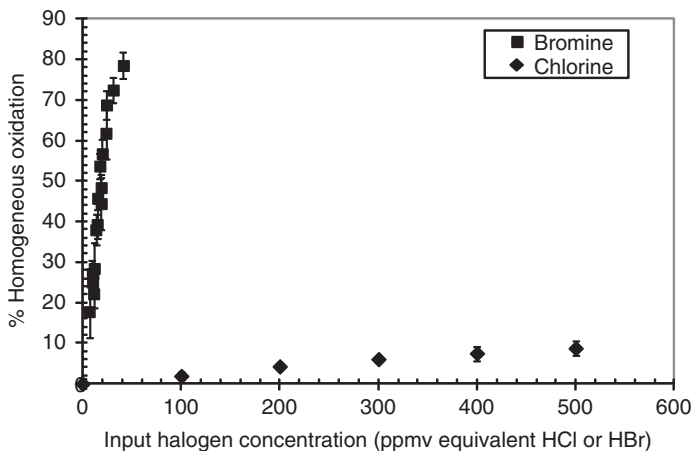


Figure 7.2 Homogeneous oxidation of mercury by halogens in a laboratory combustor as a function of initial halogen concentration [7].

the effect depended on the concentrations of SO_2 and HCl. There was little effect when the concentration of SO_2 was 400 ppmv with up to 550 ppmv HCl. However, at an HCl concentration of 200 ppmv and lower concentrations of SO_2 (100–200 ppmv), SO_2 did affect the level of mercury oxidation observed.

A detailed chemical kinetic mechanism for mercury oxidation by chlorine species in flue gas was applied to pilot-scale coal combustion results by Niksa and Fujiwara [13], but was unable to predict the extent of mercury oxidation. The authors concluded, based on gas-phase kinetic modeling, that the quench rate in the pilot-scale system was not high enough to produce sufficient chlorine radicals to oxidize elemental mercury. A heterogeneous pathway, utilizing the interaction of mercury and HCl on carbon surfaces, was suggested to explain the results.

In coal-fired boilers, concentrations of HCl are expected to be <150 ppmv, which means that the contribution from homogeneous oxidation of mercury by chlorine in practical combustion systems should be 10% or less. The concentration of bromine native to coal is too low to promote significant gas-phase oxidation, although the addition of bromine to the coal or the flue gas does yield increased oxidation, as discussed in Chapter 14.

Gas-phase oxidation of mercury by chlorine has been shown to be inadequate for explaining the observed mercury oxidation in coal-fired furnaces (see Part VI for details of gas-phase mercury models). Heterogeneous oxidation (that is, catalyzed by surfaces) must be responsible for much of the mercury oxidation observed in coal combustion systems.

Transition metal oxides have been shown to oxidize mercury in coal flue gas. Studies have shown that vanadium oxide can oxidize mercury in simulated coal combustion flue gas, and that mercury oxidation increases with increasing concentration of HCl in the gas [14–16]. Studies on V_2O_5 have been carried out at temperatures on the order of 350 °C, which is the temperature of selective catalytic reduction (SCR) reactors in power plants. (This is discussed in more detail in Chapter 15.) At these temperatures, other oxides also catalyze mercury oxidation in the presence of HCl. Kamata *et al.* [17] reported that the activity for mercury oxidation was as follows: $\text{MoO}_3 \sim \text{V}_2\text{O}_5 > \text{Cr}_2\text{O}_3 > \text{Mn}_2\text{O}_3 > \text{Fe}_2\text{O}_3 > \text{CuO} > \text{NiO}$.

Metal oxides have been demonstrated to oxidize mercury in simulated flue gas at post-APH temperatures (120–180 °C) in many different published works. For example, in fixed-bed experiments with simulated ash (mixtures of oxides), Ghoshri *et al.* [18] showed that the transition metal oxides, CuO and Fe_2O_3 , acted as catalysts for the oxidation of Hg^0 in the presence of HCl. Galbreath *et al.* [19] flowed coal combustion flue gas from a pilot-scale combustor through a fixed bed of $\gamma\text{-Fe}_2\text{O}_3$ at 150 °C and observed the conversion of Hg^0 to Hg^{2+} and/or Hg_p . Smith *et al.* [8] injected either $\alpha\text{-Fe}_2\text{O}_3$ or montmorillonite clay particles into combustion flue gas from a methane flame doped with mercury and HCl. Mercury oxidation increased in the flue gas with respect to pure homogeneous oxidation when iron oxide particles were injected, but not when the clay particles were injected.

Efforts to find such a relationship between oxidation and metal oxides have produced ambiguous results when using actual coal fly ash (containing mixed inorganic oxides and unburned carbon).

In fixed-bed studies using simulated flue gas and fly ash from two different coal combustion boilers, Norton *et al.* [20] concluded that HCl and NO₂ were of primary importance to mercury oxidation, with NO and SO₂ being of secondary importance. Tests were performed at 120 and 180 °C (248 and 356 °F). The extent of mercury oxidation generally correlated well with the surface areas of the different ash samples. One iron-rich ash sample did not show significantly more oxidation than a low-iron ash sample.

Ash samples from a variety of sources and coal types were tested by Dunham *et al.* [21] in a fixed-bed reactor using elemental mercury in simulated flue gas mixtures at 121 and 177 °C (250 and 350 °F). Oxidation of elemental mercury increased with increasing amounts of magnetite in the fly ash. However, one high-carbon subbituminous ash with no magnetite showed considerable mercury oxidation that may have been due to the carbon surface area. Galbreath *et al.* [22] also noted that the presence of maghemite ($\gamma\text{-Fe}_2\text{O}_3$) in fly ash and HCl in flue gas promoted oxidation of elemental Hg. These works suggest that an iron oxide with a spinel-type structure is active in fly ash with respect to mercury oxidation. The importance of surface area suggests that unburned carbon and/or soot (which have much higher surface areas than inorganic ash particles) dominate the oxidation of mercury at these temperatures.

Fly ash can adsorb elemental and oxidized mercury, in addition to catalyzing the oxidation of elemental mercury. Early experimental work by Hall and coworkers [4] on the adsorption of mercury by activated carbon or fly ash in the presence of O₂ suggested that physisorption of mercury dominated at temperatures below 100 °C (212 °F), but that chemisorption dominated between 100 and 300 °C (212 and 572 °F). The rate of mercury adsorption peaked at a temperature of 200 °C (392 °F) in their experiments, and there was no mercury adsorption observed above 350 °C (662 °F).

A large body of work (much of it summarized by Hower *et al.* [23]) suggests that the unburned carbon in fly ash from coal combustion systems can adsorb mercury in flue gas. For example, in the fixed-bed study of Dunham *et al.* [21], all the fly ash samples that acted as oxidation catalysts for elemental mercury also adsorbed elemental mercury in simulated flue gas mixtures. The adsorption capacity of the ash for elemental mercury was similar to that for HgCl₂. There was a correlation between fly ash surface area and adsorption of elemental Hg and HgCl₂, although the correlation was better for HgCl₂. The adsorption capacity had an inverse dependence on temperature, over the range studied (121–177 °C). Most of the fly ash surface area is due to the presence of unburned carbon and/or soot, which seems to dominate the adsorption process.

Fly ash, and in particular the unburned carbon in fly ash, has been observed to both oxidize mercury and adsorb mercury. Most of the theoretical and experimental work carried out to date on the fundamental mechanisms of mercury–carbon reactions in combustion systems has focused on activated

carbon, instead of unburned carbon in fly ash. Part VI of this book discusses mechanisms and models for the interaction of mercury and carbon surfaces in detail, and these will be discussed only briefly here.

The review by Hower *et al.* [23] provides detailed information on the properties of unburned carbon as related to mercury adsorption in flue gas. Acid gases in flue gas – for example, HCl, Cl₂, H₂SO₄ – promote the oxidation of mercury in the presence of carbon surfaces at post-APH temperatures. However, some of these species are not oxidants; therefore, other species in the flue gas must be responsible for oxidation of mercury on carbon surfaces. As discussed in Chapter 25, a mechanism has been hypothesized and validated in which acid gas species such as HCl bind to the carbon surface, forming a site at which elemental mercury can bind and subsequently be oxidized, principally by NO₂. Furthermore, there is a competition for these active carbon sites between mercury species and H₂SO₄, which has profound implications for capture of mercury by carbon in practical combustion systems. Sulfuric acid can occupy surface sites either by adsorption of gaseous SO₃ or H₂SO₄ or by adsorption of SO₂ and subsequent oxidation by NO₂ on the surface. As H₂SO₄ accumulates on the surface, the bound, oxidized mercury species are displaced and desorbed, probably as HgCl₂. The rate of mercury adsorption decreases as temperature increases, but the rate of oxidation of elemental mercury increases as temperature increases [24].

Alkaline species in fly ash, particularly calcium oxide, if present, have been shown to adsorb oxidized mercury in flue gas. As discussed above, mercury–halogen compounds are the most likely gas-phase oxidized mercury species present in combustion flue gas. Chapter 13 provides a detailed discussion of the interaction between mercury and calcium species in combustion flue gas.

The coal combustion boiler represents a series of chemical reactors, which change the elemental mercury produced in the flame to gaseous oxidized mercury and particulate-bound mercury. The transformations of mercury in coal combustion flue gases are influenced by gas-phase species (halogens, NO_x, SO_x) and the PM (unburned carbon, inorganic ash) suspended in the gas as well as the quench rate and gas temperatures. The most significant of these transformations take place in the APCDs downstream of the boiler. Therefore, an understanding of the APCDs used on coal-fired boilers is essential for understanding the mercury emissions and the potential for control of mercury on a wide variety of combustion systems.

7.4

Air Pollution Control Devices on Utility and Industrial Boilers

Before discussing the chemistry of mercury in APCDs, a brief overview will be presented of the major pollution control equipment in use on coal-fired boilers. These APCDs have been installed to control the major pollutants NO_x, SO₂, and

Table 7.1 Air pollution control devices for PM, NO_x, and SO₂.

<i>Particulate control</i>	
C-ESP	Cold-side electrostatic precipitator
H-ESP	Hot-side electrostatic precipitator
FF	Fabric filter (baghouse)
WPS	Wet particulate scrubber (venturi scrubber)
Cyclone	Sometimes known as <i>mechanical collector</i>
<i>NO_x control</i>	
LNB	Low-NO _x burner
OFA	Overfire air
SNCR	Selective non-catalytic reduction
SCR	Selective catalytic reduction
<i>SO₂ control</i>	
DSI	Dry sorbent injection
dFGD	Dry flue gas desulfurization
wFGD	Wet flue gas desulfurization

PM. In this section, the major types of APCDs for coal-fired boilers are introduced. Table 7.1 contains a glossary of the processes.

7.4.1

PM Control

Combustion processes emit both primary and secondary PM. Primary PM emissions are called *fly ash* (e.g., non-combustible inorganic matter and unburned solid carbon). Secondary PM emissions are the result of substances that condense in the stack, such as sulfuric acid, to produce PM in the atmosphere. PM control technologies include fabric filters (FFs) or “baghouses,” wet and dry electrostatic precipitators (ESPs), venturi scrubbers, and mechanical collectors (cyclones). ESPs are the most widely used PM control device on coal-fired boilers. Most ESPs are located after the APH (see Figure 7.1) and operate at temperatures of 120–190 °C (250–370 °F); these are called *cold-side electrostatic precipitators* (C-ESPs). A small fraction of ESPs are located upstream of the APH at temperatures in the range of 350–400 °C (650–750 °F); these are called *hot-side electrostatic precipitators* (H-ESPs). ESPs charge fly ash particles and then collect the charged particles in an electric field. Particles are collected on electrically charged plates and periodically removed by mechanical means. The particles drop from the plate into a hopper. FFs, in contrast, collect particles on a filter or bag, such that the flue gas must pass through the “cake” of collected particles. Periodically, the dust cake is removed by agitating the bag so that the cake falls off into a hopper. FFs operate in the same temperature range as C-ESPs. FFs and ESPs represent about 97% of the PM control devices on EGU boilers. Other PM control devices, like wet particulate scrubbers and cyclones, are more commonly found on ICI boilers.

7.4.2

NO_x Control

Emission control strategies for NO_x fall into two categories: combustion controls and post-combustion technologies. Combustion control technologies minimize the formation of NO_x in the furnace and include combustion tuning, low-NO_x burners (LNBs), and overfire air (OFA). LNBs (or staged combustion conditions) may introduce higher carbon monoxide and unburned carbon in fly ash, which reflect lower plant efficiency. In an OFA system, the primary combustion zone is operated at less than a stoichiometric air/fuel ratio, and additional air is added in the upper furnace. Unburned carbon in ash can still increase in boilers using OFA, depending on the type of fuel and design of the system.

Post-combustion technologies reduce the amount of NO_x that has been formed during combustion. In selective non-catalytic reduction (SNCR), a nitrogen-containing reagent is injected into the furnace in the temperature range of 900–1100 °C (1600–2000 °F). NO_x reduction with SNCR is in the range of 30–50%, depending on the residence time and degree of mixing achieved. Higher NO_x reduction (80–90%) is achieved using SCR. In this process, ammonia is injected over a vanadia-based catalyst at temperatures in the range of 350–400 °C (650–750 °F) in order to chemically reduce NO_x to nitrogen and water.

7.4.3

SO₂ Control

SO₂ emission control technologies are post-combustion devices that remove SO₂ by reacting it with an alkaline reagent. The two most commonly used SO₂ controls are dry flue gas desulfurization (FGD) units and wet FGD units. In the former, an aqueous slurry (usually lime) is sprayed into a contacting vessel in order to contact the alkaline reagent with SO₂. The reagent dries and is collected in a PCD (usually a FF). A lower-cost version of a dry process is dry sorbent injection (DSI) in which there is no dedicated contacting vessel; instead, the dry reagent (sodium carbonate or sodium sesquicarbonate) is injected into the flue gas duct and then collected in the PCD. Dry FGDs can achieve 90–95% reductions, although they are used when the coal sulfur content is less than about 2 wt%. DSI results in more modest SO₂ reductions, but the low capital cost of this technology makes it attractive for some boilers.

In a wet FGD, a solution of water and limestone or lime contacts the flue gas. The scrubbing solution is sprayed into the gas and collected as a liquid in the bottom of the scrubber; in some designs, the flue gas is bubbled through a liquid solution. Wet FGDs turn SO₂ into either calcium sulfite or calcium sulfate. The end product is either a sludge or gypsum, depending on the oxidation potential in the solution. Wet FGDs are the most efficient for removal of SO₂ and are typically used when the coal sulfur content is higher than 1–2 wt%; removals of >95% can be achieved.

7.4.4

Boiler Populations in the United States

There are ~1100 coal-fired EGU boilers in the United States with capacities >25 MW at more than 500 facilities [25]. The generating capacities of EGU boilers are generally in the range of 150–1300 MW. According to a survey of industrial and commercial boilers in the United States in 2005 [26], there were about 2600 coal-fired industrial and commercial boilers. The fuel firing rate of these coal-fired boilers averaged 37 MJ s^{-1} ($125 \text{ million Btu h}^{-1}$), which is much smaller than the firing rate of EGU boilers; for comparison, the firing rate of a 500 MW EGU boiler is about 1700 MJ s^{-1} .

The distribution of APCDs on EGU boilers is summarized in Table 7.2 [27]. The table indicates the number of APCDs in individual categories. Some boilers have only a PCD, while other boilers have scrubbers and SCRs in addition to PCDs. Those boilers with both an SCR and a scrubber are called out separately in Figure 7.3, because, as discussed below, this combination of APCDs can remove a significant fraction of mercury from the flue gas.

Bituminous coals have higher sulfur contents than low-rank coals (i.e., subbituminous and lignite), which results in a different distribution of APCD equipment on bituminous plants as compared to low-rank plants. Many bituminous-fired plants are located in the Eastern half of the United States, where NO_x emissions are regulated in order to reduce the formation of ground-level ozone. Thus, bituminous-fired boilers are more likely to have a combination of SCR for

Table 7.2 Air pollution control devices on EGU boilers in the United States [27] in terms of number of boilers.

APCD	Coal rank				Total
	Bituminous	Subbituminous	Lignite	Other ^{a)}	
<i>Particulate control</i>					
Cold-side ESP ^{b)}	454	257	17	1	729
Fabric filter ^{c)}	120	112	12	31	275
Hot-side ESP	78	23	0	0	101
Other	16	14	1	0	31
<i>Post-combustion NO_x</i>					
SNCR	146	22	2	15	185
SCR	208	84	2	1	295
<i>SO₂ control</i>					
Fluidized bed ^{d)}	20	4	7	29	60
Dry sorbent injection	29	7	1	0	37
Dry FGD	54	31	3	0	88
Wet FGD	255	89	16	1	361

a) Includes waste coal and petcoke.

b) Includes combinations of cold-side and hot-side.

c) Includes combinations of ESP and FF.

d) Includes in-bed capture in fluidized bed.

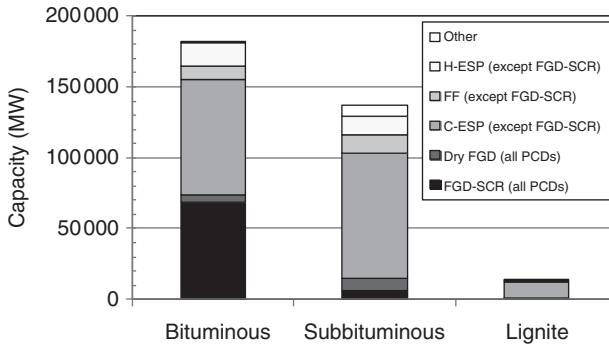


Figure 7.3 Distribution of APCDs on EGU boilers in the United States by boiler capacity [27].

NO_x control and wet FGD for SO_2 control. Subbituminous-fired plants have a larger share of dry FGDs, because the fuels have <1% sulfur. For all types of fuel, the largest category of APCDs is a C-ESP alone, with no scrubber and no post-combustion NO_x control. (Most boilers have some form of combustion control of NO_x , whether or not they have post-combustion NO_x controls.)

New APCD equipment will be installed by 2015 on EGU boilers in the United States as a result of the new Mercury and Air Toxics Standards (MATSS) regulation and the Cross-State Air Pollution Rule (CSAPR). US EPA's analysis of EGU boilers [25] projects an additional 20 GW of dry FGD, 44 GW of DSI, 102 GW of additional FFs, 63 GW of scrubber upgrades, and 34 GW of ESP upgrades by 2015.

ICI boilers tend to have less pollution control equipment than EGU boilers. For example, a survey of ICI boilers firing wood or coal in four states in Northeastern USA [28] showed that about half the boilers had no air pollution controls, 40% of the boilers had only PM control, and 8% of the boilers had a combination of NO_x control and PM control. There were no boilers with SO_2 controls in this population.

7.5

Mercury Behavior in Coal-Fired Boilers

7.5.1

Data Sources

Understanding the behavior of mercury in full-scale coal-fired boilers requires a large body of data from the field. Laboratory and pilot-scale data can provide useful information but the complexity of coal combustion boilers necessitates full-scale data. Over the past 15 years, a large body of data has been generated in the United States and it is largely from these data that the mechanisms and pathways presented here have been drawn.

Table 7.3 Types of coal-fired boilers sampled in 1999 ICR by coal type and APCD, compared with total boiler population [29].

APCD equipment	Coal type	% units tested	% existing units
Cold-side ESP	Bituminous	7.2	48.3
Cold-side ESP	Low rank	7.1	11.7
Hot-side ESP	Bituminous	7.2	6.6
Hot-side ESP	Low rank	3.6	2.4
Cold-side ESP + wet FGD	Bituminous	6	8.8
Cold-side ESP + wet FGD	Low rank	9.2	2.5
Hot-side ESP + wet FGD	Bituminous	4.8	0.7
Hot-side ESP + wet FGD	Low rank	3.6	1
FF	Bituminous	3.6	2.9
FF	Low rank	7.2	2.7
FF + wet FGD	Bituminous	7.2	1.6
FF + wet FGD	Low rank	3.6	1.6
Dry FGD + FF	Bituminous	3.6	2.9
Dry FGD + FF	Low rank	7.2	1.3
Dry FGD + ESP	Bituminous	2.4	0.2
Dry FGD + ESP	Low rank	3.6	0.3
FF + FBC	Bituminous	3.6	2.9
Other	Other	9.3	1.6

US EPA has carried out two Information Collection Requests (ICRs) as part of rulemaking for the electric utility industry. These ICRs have provided much data on the speciation and removal of mercury in various APCD configurations.

The first ICR was carried out in 1999. Part 3 of the ICR consisted of measurements of mercury speciation from 83 coal-fired power plants. Plants were selected based on the configurations of air pollution control equipment and fuel type. For each plant, the mercury content of the coal was measured (along with other coal composition data). Mercury measurements were made at the stack and at the inlet to the last APCD using the Ontario Hydro method (see Part II for a description of the method); the result was a set of gaseous elemental, gaseous oxidized, and particulate-bound mercury at the inlet and outlet of APCDs. Table 7.3 summarizes the configurations for the ICR data sets, comparing the distribution of units tested with the distribution of the boiler population in the United States. As the table shows, a wide range of APCD configurations were tested, which proved valuable for understanding mercury behavior.

The 1999 ICR was used to support the creation of the Clean Air Mercury Rule (CAMR), which was proposed in 2005. The CAMR was ultimately vacated by the courts. EPA decided to issue another ICR in order to support development of a new rule for EGU boilers, because there had been considerable changes in the APCD configurations since the original ICR. At the end of 2009, EPA issued another ICR to the electric utility industry, requesting information on emissions of mercury and other hazardous air pollutants (HAPs) from EGUs firing coal or

oil. In 2010, a subset of coal-fired EGUs was required to conduct measurements of mercury and non-mercury HAP metals (antimony, arsenic, beryllium, cadmium, chromium, cobalt, lead, manganese, nickel, and selenium) in the boiler stack. Mercury was measured using CEMS or sorbent traps (see Part II for descriptions of methods) at the stack, as well as measured in a coal sample taken concurrently with each stack test. This ICR data set represents a range of fuel types and APCD types, as shown in Table 7.4.

There were many changes in APCD configurations in the industry in the 11 years between the two ICRs. The 1999 ICR dataset contained very few boilers that had post-combustion NO_x control (SCR and SNCR) and no boilers that had activated carbon injection (ACI) for mercury control or DSI for acid gas control. Furthermore, the 2010 ICR dataset contains more data from fluidized bed combustors (FBCs) as compared to the 1999 dataset.

Part IV of this book discusses the substantial research and development efforts undertaken by US DOE, EPA, and EPRI in the mercury control area. Sampling campaigns and technology demonstrations at coal-fired power plants sponsored by these organizations have also provided much valuable information on mercury behavior in coal-fired power plants.

7.5.2

Mercury Behavior in APCDs

In this section, the reader will follow the path of mercury through a coal-fired boiler, using full-scale data from DOE- and EPRI-sponsored mercury measurement campaigns at coal-fired utility boilers [30], unless otherwise noted.

As discussed above, mercury is released from the coal in the flame as gaseous Hg⁰ and halogens present in the gas are the primary pathway for gas-phase oxidation. In an evaluation of homogeneous models and data for mercury oxidation by chlorine in combustion systems, Krishnakumar and Helble [11] concluded that oxidation of Hg⁰ occurs at temperatures below 625 °C (1160 °F) and the chlorine radical is the most important reactive species for mercury oxidation in the gas phase. Halogens are also involved in the heterogeneous oxidation of mercury, catalyzed either by SCR catalysts or by fly ash.

Oxidation of mercury by SCR catalysts is discussed in detail in Chapter 15. The primary variables that affect the oxidation of mercury across SCR catalysts are halogen content of flue gas, temperature, space velocity (residence time), and catalyst design. Without the injection of additional halogens (Chapter 14), the halogen content of the flue gas is primarily related to the chlorine content of the coal. As Figure 7.4 shows, mercury oxidation across SCR reactors is strongly correlated with the chlorine content of the coal.

All coal-fired utility boilers and most coal-fired industrial boilers have a gas–gas heater exchanger to preheat the combustion air by contacting it with the flue gas. This APH decreases the flue gas temperature from typically 350 to 150 °C, while heating the combustion air to ~300 °C. There are two types of APHs: regenerative and tubular. The majority of APHs are drum-type regenerative heat exchangers,

Table 7.4 Number of coal-fired boilers sampled in 2010 ICR by coal type and APCD.

	Bituminous	Subbituminous	Lignite	Waste coal
<i>Units with cold-side ESPs</i>				
C-ESP only	42	51	1	—
SNCR, C-ESP	5	1	—	—
SCR, C-ESP	—	9	—	—
C-ESP, wet FGD	14	5	2	—
SNCR, C-ESP, wet FGD	8	1	—	—
SCR, C-ESP, wet FGD	25	2	—	—
Dry FGD, C-ESP	—	1	—	—
DSI, C-ESP	—	1	—	—
SNCR, DSI, C-ESP	—	1	—	—
<i>Units with fabric filters</i>				
FF only	8	14	3	—
SNCR, FF	—	1	1	—
FE, wet FGD	7	6	—	—
SNCR, FE, wet FGD	1	—	—	—
SCR, FE, wet FGD	4	2	—	—
Dry FGD, FF	14	7	1	—
SNCR, dry FGD, FF	2	—	2	—
SCR, dry FGD, FF	7	2	—	—
SNCR, DSI, FF	1	—	—	—
<i>Units with hot-side ESPs</i>				
H-ESP only	5	5	—	—
SNCR, H-ESP	1	—	—	—
SCR, H-ESP	1	—	—	—
H-ESP, wet FGD	2	2	—	—
SNCR, H-ESP, wet FGD	2	—	—	—
H-ESP, SCR, wet FGD	1	—	—	—
<i>Units with venturi scrubbers</i>				
Venturi, wet FGD	—	1	—	—
<i>Units with activated carbon injection (ACI)</i>				
ACI, C-ESP	1	15	—	—
SNCR, ACI, C-ESP, wet FGD	1	—	—	—
ACI, FF	3	6	—	—
ACI, FE, wet FGD	—	4	—	—
SCR, ACI, FE, wet FGD	1	—	1	—
ACI, dry FGD, FF	—	2	—	—
SCR, ACI, dry FGD, FF	1	6	—	—
ACI, venturi, wet FGD	—	1	—	—
<i>Fluidized bed combustors (FBCs)</i>				
FBC, FF	1	—	—	2
FBC, SNCR, FF	5	—	—	6
FBC, DSI, FF	—	—	—	1
FBC, SNCR, dry FGD, C-ESP	1	—	—	—
FBC, SNCR, dry FGD, FF	5	—	—	3
	169	146	11	12

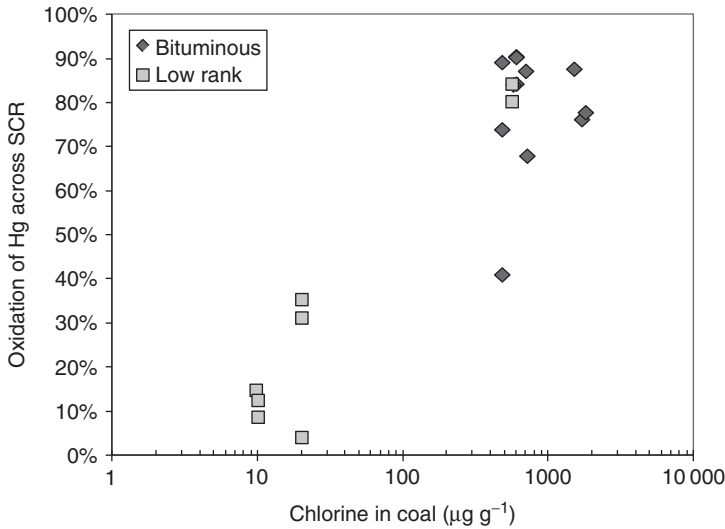


Figure 7.4 Oxidation of mercury across full-scale SCRs as a function of coal chlorine content.

in which a large wheel containing metal surfaces rotates through the flue gas path, alternating contact with the hot flue gas and the cold combustion air. Tubular APHs are shell-and-tube heat exchangers in which the flue gas passes through tubes and the combustion air flows outside the tubes. In either case, there is a lot of cold metal surface area, which can become coated with ash particles. The large surface area in APHs can promote oxidation of elemental mercury. Figure 7.5 shows full-scale data on the oxidation of elemental mercury across APHs as a function of coal chlorine content. Chlorine is not the only important parameter for mercury oxidation across APHs; the unburned carbon in the fly ash (which can act as a catalyst), the temperature, and the quench rate (determined by the design of the APH) are also important for mercury oxidation. The variation in unburned carbon in fly ash can be large, because the amount of unburned carbon depends on the coal rank and on the combustion system [23]. Unless the chlorine content of the coal is very low, a significant amount of mercury oxidation can be expected across an APH.

In almost all coal-fired boilers, a PCD follows the APH. The exceptions to this are a boiler with a H-ESP in which the ESP is located upstream of the APH or a boiler with a spray dryer (dry FGD) for SO_2 control in which the spray dryer is located between the APH and the PCD. Only about 9% of coal-fired utility boilers employ a H-ESP as the only PCD and about 8% of coal-fired utility boilers have a dry FGD (Table 7.2). C-ESPs are the most common PCD on coal-fired utility boilers. These devices remove mercury that has been converted to a particulate form upstream of the ESP by reaction with unburned carbon in fly ash. There is little contact between the flue gas and the ash collected in the ESP; therefore, mercury does not oxidize or adsorb on fly ash within the ESP.

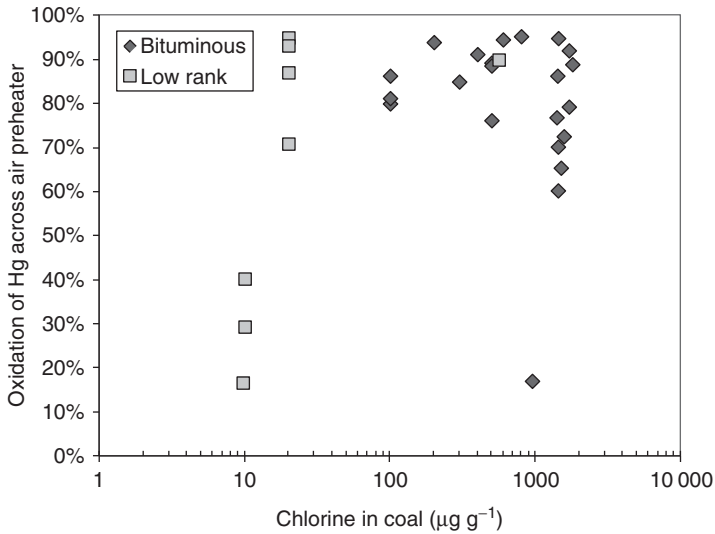


Figure 7.5 Oxidation of mercury across air preheaters on full-scale, coal-fired boilers as a function of coal chlorine content.

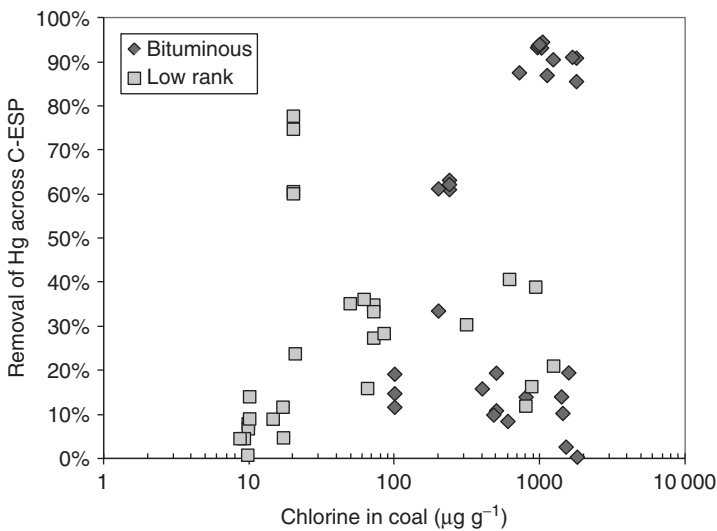


Figure 7.6 Removal of Hg across cold-side ESP as a function of coal chlorine content.

The chlorine content of the coal has an influence on how much of the mercury is converted to a particulate form via reaction with the fly ash upstream of the ESP. However, as Figure 7.6 illustrates, chlorine is not the only factor that determines how much mercury is removed across C-ESPs. There are other factors that influence how much mercury adsorbs on the fly ash [18–24] as was noted previously in the discussion of fixed-bed experiments on mercury interactions with fly

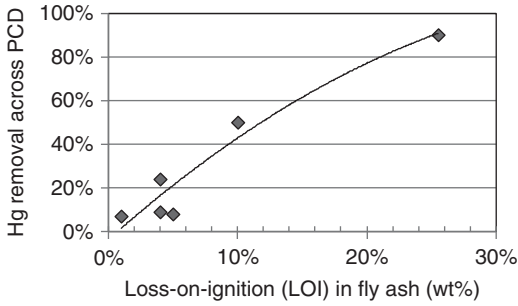


Figure 7.7 Mercury removal across cold-side ESPs as a function of LOI, for bituminous pulverized-fired boilers [31].

ash. The amount of unburned carbon in the fly ash is also important. Figure 7.7 shows mercury removal at full-scale bituminous coal-fired boilers as a function of loss-on-ignition (LOI), that is, unburned carbon, in the fly ash [31]. For pulverized coal-fired boilers with C-ESPs, there is a good correlation between LOI and mercury removal.

In FFs, there is more contact between the flue gas and the fly ash, because the fly ash builds up on the filter over a period of several hours before being removed. Thus, in addition to removing particulate-bound mercury, which is formed upstream of the PCD, FFs also remove oxidized elemental mercury and gaseous mercury. The fixed-bed experiments using fly ash and simulated flue gas discussed previously [18–21] are similar to a FF in that the gas must pass through a layer of ash. The temperature, composition of the flue gas, unburned carbon in the fly ash, and baghouse cleaning frequency all affect the removal of mercury across FFs.

Figure 7.8 illustrates the removal of both gaseous mercury and total (gas plus particulate-bound) mercury across the FF on a 170 MW tangential boiler burning a low-sulfur bituminous coal [32]. The unburned carbon in ash was varied by changing combustion conditions and the FF temperature was 130 °C (265 °F).

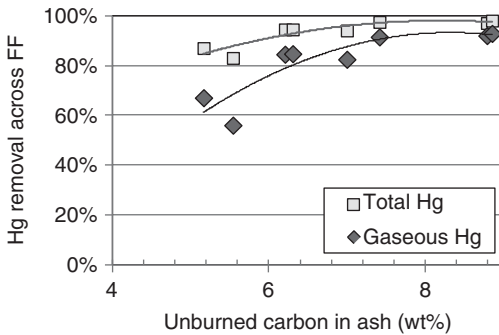


Figure 7.8 Mercury removal across fabric filter as a function of unburned carbon in fly ash [32].

The FF removed both gaseous and particulate mercury, and the mercury removal increased with increasing unburned carbon in ash. In certain situations (temperature, gas composition), unburned carbon in fly ash can be effective at capturing mercury. However, reliance on unburned carbon alone as a mercury control strategy is not without risk of non-compliance, because changes in combustion conditions affect the amount of unburned carbon, and such changes are not always predictable or controllable. Furthermore, increasing the amount of unburned carbon in ash means decreasing the efficiency of the combustion process, which is not desirable.

Thus, both C-ESPs and FFs can remove mercury from the flue gas. H-ESPs operate at too high a temperature to remove significant amounts of mercury. Particulate-bound mercury that has formed upstream of the PCD is removed by a C-ESP; in contrast, FFs remove both particulate-bound mercury and gaseous mercury. The degree to which mercury is removed in PCDs depends on the amount of unburned carbon in the fly ash, the halogens present in the flue gas, and the temperature of the PCD. The design and operation of a FF can also have an effect on its ability to remove mercury.

Both wet and dry FGD scrubbers remove mercury, if it is in the oxidized form. Mercuric halides (such as HgCl_2) are soluble in water but elemental mercury is not. Thus, the removal of mercury across FGD scrubbers depends on how much oxidized mercury enters the scrubber, as illustrated in Figure 7.9. The removal of mercury across wet FGD scrubbers is complicated by the aqueous reactions that take place in the scrubbing solution [33], as discussed in Chapter 16. The complex aqueous chemistry can result in some of the absorbed Hg^{2+} being reduced back to

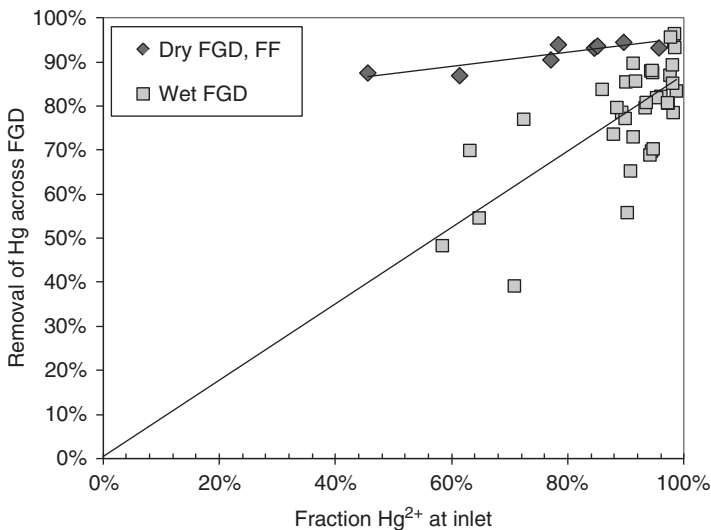


Figure 7.9 Mercury removal across dry and wet FGD scrubbers on bituminous-fired boilers as a function of the fraction of oxidized mercury at the inlet.

Hg^0 . This re-emission of Hg^0 can reduce the efficiency of mercury capture across wet FGD scrubbers.

7.6 Summary

The transformations of mercury in coal-fired boilers and APCDs are summarized in Figure 7.10. Although Hg leaves the combustion zone as gaseous elemental mercury, varying amounts can be transformed to gaseous oxidized mercury and particulate-bound mercury as the flue gas passes through the economizer and air heater. The efficiency of Hg capture by APCDs depends on the gas-phase speciation as well as on the partitioning between gaseous and particulate forms. In turn, the coal composition (Cl and S content, ash composition) and boiler operation (unburned carbon content, gas cooling rate, and residence time) affect the Hg speciation and partitioning in the flue gas. Existing APCDs provide a range of “native” Hg removals; FFs and scrubbers have the highest Hg removals, as much as

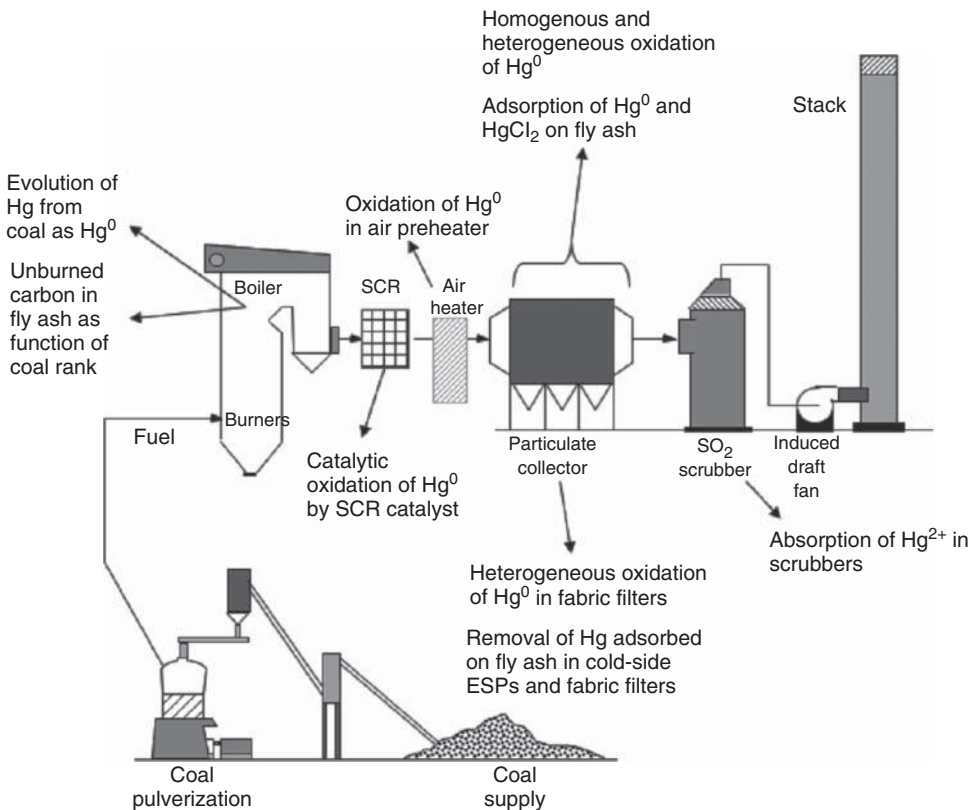


Figure 7.10 Summary of mercury behavior in coal-fired boilers.

90%, for units burning bituminous coal. Moderate to low levels of natural capture are typically found in units that burn either subbituminous coals or lignites.

References

1. Stultz, S.C. and Kitto, J.B., (eds) (1992) Performance calculations, in *Steam Its Generation and Use*, 40th edn, The Babcock and Wilcox Company, Barberton, OH.
2. Senior, C.L., Sarofim, A.F., Zeng, T., Helble, J.J., and Mamani-Paco, R. (2000) Gas-phase transformations of mercury in coal-fired power plants. *Fuel Process. Technol.*, **63** (2-3), 197–213.
3. Chu, P., Behrens, G., and Laudal, D. (2011) Estimating total and speciated mercury emissions from U.S. coal-fired power plants. Proceedings of the Air and Waste Management Association Specialty Conference on Mercury Emissions: Fate, Effects, and Control, Chicago, IL, August 21–23, 2001.
4. Hall, B., Schager, P., and Weesmaa, J. (1995) The homogeneous gas phase reaction of mercury with oxygen, and the corresponding heterogeneous reactions in the presence of activated carbon or fly ash. *Chemosphere*, **30**, 611–627.
5. Slinger, R.N., Kramlich, J.C., and Marinov, N.M. (2000) Towards the development of a chemical kinetic model for the homogeneous oxidation of mercury by chlorine species. *Fuel Process. Technol.*, **65-66**, 423–438.
6. Fry, A., Cauch, B., Lighty, J.S., Silcox, G.D., and Senior, C.L. (2007) Experimental evaluation of the effects of quench rate and quartz surface area on homogeneous mercury oxidation. *Proc. Combust. Inst.*, **31**, 2855–2861.
7. Van Otten, B., Buitrago, P.A., Senior, C.L., and Silcox, G.D. (2011) Gas-phase oxidation of mercury by bromine and chlorine in flue gas. *Energy Fuels*, **25**, 3530–3536.
8. Smith, C., Krishnakumar, B., and Helble, J. (2011) Homogeneous and heterogeneous mercury oxidation in a bench-scale flame-based flow reactor. *Energy Fuels*, **25**, 4367–4376.
9. Kilgroe, J.D., Sedman, C.B., Srivastava, R.K., Ryan, J.V., Lee, C.W., and Thorneloe, S.A. (2002) Control of Mercury Emissions From Coal-Fired Electric Utility Boilers: Interim Report Including Errata Dated 3-21-02, EPA-600/R-01-109, NTIS, Springfield, VA.
10. Senior, C.L., Chen, Z., and Sarofim, A.F. (2002) Mercury oxidation in coal-fired utility boilers: validation of gas-phase kinetic models. Proceedings of Air and Waste Management Association 94th Annual Conference and Exhibition, Baltimore, MD, June 2002.
11. Krishnakumar, B. and Helble, J.J. (2007) Understanding mercury transformations in coal-fired power plants: evaluation of homogeneous Hg oxidation mechanisms. *Environ. Sci. Technol.*, **41**, 7870–7875.
12. Niksa, S., Padak, B., Krishnakumar, B., and Naik, C.V. (2010) Process chemistry of Br addition to utility flue Gas for Hg emissions control. *Energy Fuels*, **24**, 1020–1029.
13. Niksa, S. and Fujiwara, N. (2005) Predicting extents of mercury oxidation in coal-derived flue gases. *J. Air Waste Manage. Assoc.*, **55**, 930–939.
14. Richardson, C., Machalek, T., Miller, S., Dene, C., and Chang, R. (2002) Effect of NOx control processes on mercury speciation in utility flue gas. *J. Air Waste Manage. Assoc.*, **52**, 941–947.
15. Lee, C.W., Serre, S.D., Zhao, Y., and Hastings, T. (2008) Mercury oxidation promoted by a selective catalytic reduction catalyst under simulated powder river basin coal combustion conditions. *J. Air Waste Manage. Assoc.*, **58**, 484–493.
16. Kamata, H., Ueno, S., Naito, T., and Yukimura, A. (2008) Mercury oxidation over the V₂O₅(WO₃)/TiO₂ Commercial SCR Catalyst. *Ind. Eng. Chem. Res.*, **47**, 8136–8141.
17. Kamata, H., Ueno, S., Sato, N., and Naito, T. (2009) Mercury oxidation by hydrochloric acid over TiO₂ supported

- metal oxide catalysts in coal combustion flue gas. *Fuel Process. Technol.*, **90**, 947–951.
18. Ghorishi, S.B., Lee, C.W., Josewicz, W., and Kilgroe, J.D. (2005) Effects of fly ash transition metal content and flue gas HCl/SO₂ ratio on mercury speciation in waste combustion. *Environ. Eng. Sci.*, **22**, 221–231.
 19. Galbreath, K.C., Zygarrlicke, C.J., Tibbetts, J.E., Schultz, R.L., and Dunham, G.E. (2004) Effects of NO_x, alpha-Fe₂O₃, gamma-Fe₂O₃, and HCl on mercury transformations in a 7-kW coal combustion system. *Fuel Process. Technol.*, **86**, 429–448.
 20. Norton, G.A., Yang, H., Brown, R.C., Laudal, D.L., Dunham, G.E., and Erjavec, J. (2003) Heterogeneous oxidation of mercury in simulated post combustion conditions. *Fuel*, **82**, 107–116.
 21. Dunham, G.E., DeWall, R.A., and Senior, C.L. (2003) Fixed-bed studies of the interactions between mercury and coal combustion fly ash. *Fuel Process. Technol.*, **82**, 197–213.
 22. Galbreath, K.C., Zygarrlicke, C.J., Tibbetts, J.E., Schultz, R.L., and Dunham, G.E. (2004) Effects of NO_x, alpha-Fe₂O₃, gamma-Fe₂O₃, and HCl on mercury transformations in a 7-kW coal combustion system. *Fuel Process. Technol.*, **86**, 429–448.
 23. Hower, J.C., Senior, C.L., Suuberg, E.M., Hurt, R.H., Wilcox, J.L., and Olson, E.S. (2010) Mercury capture by native fly ash carbons in coal-fired power plants. *Prog. Energy Combust. Sci.*, **36**, 510–529.
 24. Olson, E.S. and Mibeck, B.A. (2005) Oxidation kinetics of mercury in flue gas. *Prepr. Pap. – Am. Chem. Soc., Div. Fuel Chem.*, **50** (1), 68–70.
 25. U.S. EPA (2011) Regulatory Impact Analysis for the Final Mercury and Air Toxics Standards, EPA-452/R-11-011, U.S. Environmental Protection Agency, December 2011.
 26. Energy and Environmental Analysis, Inc. (2005) Characterization of the U.S. Industrial Commercial Boiler Population, May 2005.
 27. Amar, P., Senior, C.L., Afonso, R., and Staudt, J. (2010) Technologies for Control and Measurement of Mercury Emissions from Coal-Fired Power Plants in the United States: A 2010 Status Report, NESCAUM, Boston, MA, July, 2010.
 28. Amar, P., Senior, C.L., and Afonso, R. (2009) Applicability and Feasibility of NO_x, SO₂, and PM Emissions Control Technologies for Industrial, Commercial, and Institutional (ICI) Boilers, NESCAUM, Boston, MA, January 2009.
 29. Afonso, R.E., and Senior, C.L. (2001) Assessment of mercury removal by existing air pollution control devices in full scale power plants. Proceedings of A&WMA Specialty Conference on Mercury Emissions: Fate, Effects and Control, Chicago, IL, August 21–23, 2001.
 30. Senior, C., Fry, A., Montgomery, C., Sarofim, A., and Wendt, J. (2006) Modeling tool for evaluation of utility mercury control strategies. Proceedings of DOE-EPRI-U.S. EPA -A&WMA Combined Power Plant Air Pollutant Control Symposium – The Mega Symposium, Baltimore, MD, August 28–31, 2006.
 31. Senior, C.L. and Johnson, S.A. (2005) Impact of carbon-in-ash on mercury removal across particulate control devices in coal-fired power plants. *Energy Fuels*, **19**, 859–863.
 32. La Marca, C., Bianchi, A., Cioni, C., and Malloggi, S. (2006) Impact of combustion system on mercury speciation and removal in coal-fired units. Proceedings of the 29th Meeting of the Italian Section of the Combustion Institute, Pisa, Italy, June 14–17, 2006.
 33. Senior, C.L. (2007) Review of the role of aqueous chemistry in mercury removal by acid gas scrubbers on incinerator systems. *Environ. Eng. Sci.*, **24**, 1128–1133.

8

Gasification Systems

Nicholas Lentz

8.1

Principles of Coal Gasification

Coal gasification processes employ fixed-bed, fluidized-bed, or entrained-flow reactor systems to react coal with air or oxygen and steam over a range of temperatures from 650 °C (1202 °F) for fixed- and fluidized-bed gasification to about 1500 °C (2732 °F) for entrained flow gasifiers. The ash byproducts are dry, agglomerated, or slagging ash, depending on the gasifier type, operating pressure, and operating temperature. Process pressures range from near atmospheric to up to 82 bar (1200 psig). Gasification reactions can be classified into the following groups: pyrolysis, combustion, steam gasification, and secondary reactions among gaseous products and with carbon. Each reaction group produces a significantly different gas composition. The common coal gasification reactions and enthalpy energies are presented below:

*Pyrolysis and tar cracking*Coal → char + tar, light oil, H₂O, H₂, CO, CO₂, and hydrocarbon gasesTar, light oil → CH₄ and other HC gases + CO + H₂ + CO₂*Combustion* ΔH (Btu lbmol⁻¹)C + O₂ → CO₂ -169 300C + (1/2)O₂ → CO -47 600CO + (1/2)O₂ → CO₂ -121 700*Steam gasification*C + H₂O → CO + H₂ +56 490*Secondary reactions*C + CO₂ → 2CO +74 200H₂ + (1/2)O₂ → H₂O_(g) -104 000C + 2H₂O_(g) → CO₂ + 2H₂ +38 780*Water-gas shift reaction*CO + H₂O_(g) → CO₂ + H₂ -17 700*Mercury Control: for Coal-Derived Gas Streams*, First Edition.

Edited by Evan J. Granite, Henry W. Pennline and Constance Senior.

© 2015 Wiley-VCH Verlag GmbH & Co. KGaA. Published 2015 by Wiley-VCH Verlag GmbH & Co. KGaA.

Methanation reactions

$C + 2H_2 \rightarrow CH_4$	-32 200
$CO + 3H_2 \rightarrow CH_4 + H_2O$	-88 700
$CO + H_2 \rightarrow (1/2)CH_4 + (1/2)CO_2$	-53 200

(-) indicates exothermic and (+) indicates endothermic.

The primary products of gasification are CO, H₂, and CH₄, along with some carbon dioxide and nitrogen when air is used as the oxidant. If water–gas shift catalysts are being used, the shift catalysts will convert the majority of the CO into CO₂ so that the main syngas products are H₂ and CO₂. This is desirable when carbon capture is required. Other byproducts produced during gasification can include tars, oil, phenols, chars, hydrogen sulfide, carbonyl sulfide, ammonia, and hydrogen cyanide. The primary reactions involving pyrolysis and steam gasification are endothermic and heat must be provided either externally or by the combustion of carbon. Smaller bench and pilot-scale systems typically require external heat sources to maintain consistent gasification conditions due to their small size and increased thermal effects related to scaling of the equipment. Heat from combustion can also be supplied indirectly by recycling bed material to provide either sensible heat or chemical energy (e.g., the CO₂ acceptor process). The water–gas shift and methanation reactions are exothermic and contribute to the energy balance at lower temperatures and high pressures where CH₄ is a principal product. The particular gas composition obtained from various types of gasifiers depends on the effects of temperature, pressure, flow patterns (e.g., cocurrent vs countercurrent), fluid dynamic intensity, solid and gas residence times, and catalysis on chemical kinetics and equilibrium.

8.2

Gasification Technologies Overview and Gasifier Descriptions

Different gasifiers are utilized for different applications and fuel sources. A comprehensive review of the different gasifier types is provided by Sondreal and Benson [1]. Table 8.1 summarizes the different gasifier types and characteristics. Gasifiers are typically categorized into three main classes: entrained-flow, fixed-bed, or fluidized-bed systems followed by describing the system as either a slurry or dry coal feed. Another classification can be if the system has a dry ash, or a slab byproduct discharge. Designs and classifications are typically based on the type of coal to be gasified and the desired syngas exit conditions for subsequent downstream processes and desired syngas conditions.

Figure 8.1 shows the diagrams and temperature profiles for the fixed bed (moving bed), fluidized bed, and entrained flow gasifiers. Each gasifier has a very unique temperature profile which affects the fuel types and ranks that provide optimal performance as well as the syngas composition. Entrained flow gasifiers exhibit the highest temperature profile and also have the hottest syngas exiting the gasifier.

Table 8.1 Gasifier types and characteristics [2].

Gasifier type	Fixed bed	Fluidized bed	Entrained flow
Coal feed size	6–50 mm	6–10 mm	<100 μm
Acceptability of fines	Limited	Good	Unlimited
Oxidant demand	Low	Moderate	High
Outlet temperature	Low (425–600 °C)	Moderate (900–1050 °C)	High (1250–1600 °C)
Ash conditions	Dry ash or slagging	Dry ash or agglomerating	Slagging
Other characteristics	Methane, tars, and oils are present in the syngas	Low carbon conversion	Pure syngas and a high carbon conversion

8.3

Gasification Applications and Downstream Gas Cleanup and Processing

Syngas produced as a result of coal gasification can be a very flexible feedstock for a wide range of applications and manufacturing processes. Electrical power output is oftentimes not the primary function of a gasification plant. In addition to chemical production, syngas can also be directly used to produce power and/or steam for municipal purposes. Syngas is commonly comprised mainly of H_2 and CO and the ratio between H_2 and CO can be adjusted via water gas shift catalyst reactions in order to provide a specific syngas composition to a downstream process such as a Fischer Tropsch reactor. Gasification plants often are equipped with multiple product production streams and can sometimes modify the syngas composition to shift product stream yields in order to maximize profit as commodity prices and/or outlooks change. A list of potential products from syngas includes

- Gaseous fuels
- Synthetic natural gas
- Liquid fuels
- Chemicals
- Fertilizers
- CO_2 for use in enhanced oil recovery (EOR) applications
- Hydrogen as a fuel and/or for power generation.

8.4

Mercury Transformations and Fate

Mercury has been measured for over 20 years from stationary sources to assess emissions, develop control technologies, and set appropriate mercury regulations. Mercury is present in three different forms, particulate bound, oxidized, and

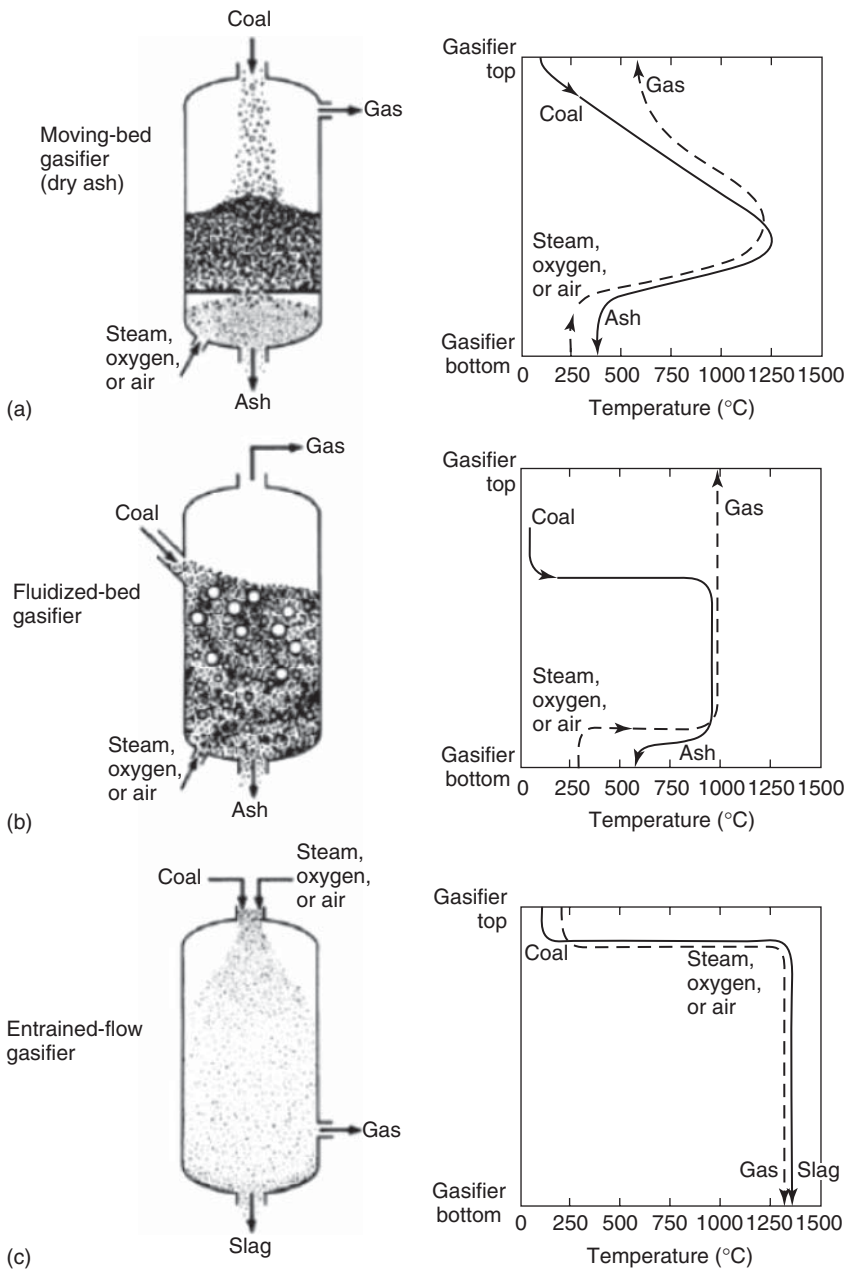


Figure 8.1 (a–c) The three major types of gasifiers [3].

elemental ($\text{Hg}[p]$, Hg^{2+} , and Hg^0), which greatly complicates the measurement process. The low mercury concentrations (low-parts per billion by volume range) also make measuring mercury difficult.

Five measurement methods are used to measure mercury from combustion sources: continuous mercury monitors (CMMs), the Ontario Hydro (OH) method, EPA M30B, EPA M29, and EPA M101A (EPA, U.S. Environmental Protection Agency) (see Chapters 5 and 6). Of these methods, the OH method is the only method validated to obtain speciated mercury measurements. Each method is able to provide accurate and reliable data, provided that the mercury concentrations are within the range of the method. All of the methods require samplers who are extremely familiar with the methods and their corresponding biases and/or interferences. Most mercury measurement methods were developed for combustion applications and later tested on gasification systems. Further discussion will show their applicability in gasification systems.

Under gasification conditions, mercury typically only exists in the elemental form due to the reducing conditions in the gasifier. Research conducted at the Energy and Environmental Research Center (EERC) confirmed the presence of elemental Hg during simulated gasification conditions and speculated that CH_3Hg may also be possible [4, 5]. In combustion systems, mercury can exist in both the elemental and oxidized forms with a wide range depending on the fuel type, boiler type, and place in the pollution control system. Elemental Hg is usually found in the higher temperature regions of combustion systems and is also likely why elemental Hg is the predominant form in gasification systems. The high gasification temperatures and reducing environment make it challenging for any oxidized forms to remain stable and favor the formation of Hg^0 . Erickson *et al.* [6] investigated the volatility of elements under gasification conditions. They found that the majority of elements behaved similar to combustion systems but arsenic, lead, and cadmium were found to volatilize in the finer sized particle fractions.

8.5

Hg Measurement in a Reducing Environment

In previous chapters, Laudal and Senior have provided extensive reviews of mercury measurement technologies. Mercury measurements in a reducing (gasification) environment present a significant challenge, especially for any method that utilizes liquid impingers or scrubbing systems such as a CMM wet conversion system. Syngas constituents such as H_2 , H_2S , CO , and CO_2 often react with the chemical solutions and render them ineffective at either capturing the Hg or performing their specific function [7]. The result is that there can be very fast mercury breakthroughs that invalidate the test. Traditional 2 h EPA impinger tests exhibit breakthrough and render the tests invalid. Shorter sampling times often do not capture enough mercury for a good data point with the tests that utilize

impingers. Measurement methods such as M29, OH, and CMMs with wet conversion systems all have exhibited challenges in obtaining consistent mercury data in reducing environments [8].

The most favorable mercury measurement methods are the methods that do not utilize liquid solutions and impinger trains. Dry conversion CMM systems and sorbent traps are the most widely used systems that do not use liquids as a part of their sampling process and are the most widely used methods on gasification systems. Sorbent traps are not able to provide continuous data, but suffer the least interferences in a gasification environment and have provided the most accurate values [9].

8.6

Hg Control Technologies for Gasification

Mercury control technologies for gasification are commonly a part of the cold, warm, or hot gas cleanup system that is designed to remove an array of pollutants including Hg, H₂S, halogens, and other trace metals such as As and Se. Currently, hot gas cleanup technologies are not mature and most of the focus through Department of Energy (DOE) and National Energy Technology Laboratory (NETL) has subsequently concentrated on warm gas cleanup systems. Warm gas cleanup systems are also favorable because they operate at temperatures that are suitable for phase shift catalysts, such as Fischer Tropsch catalysts, which allow the syngas stream to be converted into numerous useful byproducts. A hot gas filter vessel is commonly utilized for gasification particulate removal upstream of the gas cleanup system. The filter vessel is able to remove most of the particulates as well as the particulate bound Hg. The mercury control technologies are typically fixed beds and can be grouped into two main categories: carbon-based sorbents and metal-based sorbents. Chapter 22 discusses these in more detail; a brief description is provided here.

Carbon-based sorbents are commonly utilized in cold or warm gas cleanup systems and have a very high capacity with respect to mercury. Carbon-based sorbents have been extensively used at municipal waste-to-energy facilities for many years and have demonstrated the ability to cost effectively remove high levels of mercury. The carbons are typically either iodine or sulfur impregnated in order to facilitate Hg capture. Select tests under integrated gasification combined cycle (IGCC) conditions have utilized sulfur impregnated sorbents to successfully remove mercury and other contaminants [10]. A Parsons-GTI group conducted a study that demonstrated a carbon bed mercury capacity as high as 20 wt%, which correlates to a bed lifetime of ~2 years [11]. Often, pressure drop across the bed, water buildup, and other operating factors determine when a bed is replaced, rather than the Hg capacity of the sorbent bed [12].

Metal-based sorbents are another mercury control technology that has been tested. Metal-based sorbents are designed to target warm gas and hot gas cleanup systems. Most of the developed sorbents are precious metal based, with Pd, Pt, Au, Ir, and Rh being the most widely used metals. Of these, Pd has been identified as the best absorber of mercury [13, 14]. Even though metal-based sorbents have shown some promise, the technology is currently not a cost effective option for mercury capture, largely due to the cost of the precious metals required for the sorbents. Further research is required to identify cheaper surrogate metals that will also maintain sufficient activity and capture rates in warm and hot gas cleanup systems.

8.7

Hg and the MATS Rule for Gasifiers

The Mercury and Air Toxics Standards commonly called the *MATS rule* was recently finalized with the latest version published in the Federal Register on 16 February 2012. The MATS rule regulates filterable particulate matter (PM) (as a trace metal surrogate), mercury, and HCl (as an acid gas surrogate) emissions from coal-fired electricity generating units (EGUs), including IGCC units. The gasifier emission limits (PM, HCl, and Hg) for new and existing sources are presented in Table 8.2.

The data for existing units is based on a limited dataset because there are very few operating IGCC gasifiers in the United States. The only two IGCC plants in operation are the Polk Power Station operated by TECO Energy, and the Wabash River Generating Station operated by Duke Energy. These gasifiers have shown high native mercury captures of around 60%, with most of the mercury emitted in the elemental form [15]. The emission limits for the new IGCC units were based on permit data for some of the units that are either in the planning phase or the construction phase. An example is the Kemper County IGCC plant that is currently in the construction phase.

Table 8.2 Emission limits for coal-fired IGCC EGUs.

Subcategory	Filterable PM	HCl	Mercury
Existing IGCC	4.0E-2 lb MMBtu ⁻¹ (4.0E-1 lb MWh ⁻¹)	5.0E-4 lb MMBtu ⁻¹ (5.0E-3 lb MWh ⁻¹)	2.5E0 lb TBtu ⁻¹ (3.0E-2 lb GWh ⁻¹)
New IGCC	7.0E-2 lb MWh ^{-1a)} 9.0E-2 lb MWh ^{-1b)}	2.0E-3 lb MWh ^{-1c)}	3.0E-3 lb GWh ^{-1d)}

a) Duct burners on syngas; based on permit levels in comments received.

b) Duct burners on natural gas; based on permit levels in comments received.

c) Based on best-performing source.

d) Based on permit levels in comments received.

References

1. Benson, S.A. and Sondreal, E.A. (2010) Gasification of Lignites of North America. North Dakota Industrial Commission Summary Report.
2. Higman, C. and van der Burgt, M. (2003) *Gasification*, Elsevier.
3. Holt, N. (2004) Gasification process selection – tradeoffs and ironies. Gasification Technologies Conference, Washington, DC.
4. Zygarlicke, C.J., McCollor, D.P., and Benson, S.A. (1994) Transformations of trace metals in coal gasification. Presented at the Pacific Rim International Conference on Environmental Control of Combustion Processes, Maui, Hawaii, October 1994.
5. Galbreath, K.C. and Zygarlicke, C.J. (1996) *Environ. Sci. Technol.*, **30** (8), 2421–2426.
6. Erickson, T.A., Galbreath, K.C., Zygarlicke, C.J., Hetland, M.D., and Benson, S.A. (1998) Trace Element Emissions Project. Final Technical Report (Aug 5, 1992 – Dec 31, 1998) for U.S. Department of Energy Contract No. DE-AC21-92MC28016, Energy & Environmental Research Center, Grand Forks, ND, October 1998.
7. Zhuang, Y., Pavlish, J.H., Lentz, N.B., and Hamre, L.L. (2011) *Int. J. Greenhouse Gas Control*, **5-1**, S136.
8. Swanson, M. (2010) DOE AAD Document Control. Cooperative Agreement No. DE-FC26-98FT40320.
9. Pavlish, J.H., Lentz, N.B., Martin, C.L., Ralston, N.V.C., Zhuang, Y., and Hamre, L.L. (2011) DOE AAD Document Control. Cooperative Agreement No. DE-FC26-08NT43291.
10. Rutkowski, M.D., Klett, M.G., and Maxwell, R.C. (2002) The cost of mercury removal from coal-based IGCC relative to a PC plant. Presented at Gasification Technologies 2002, San Francisco, CA.
11. Newby, R.A., Lippert, T.E., Slimane, R.B., Akpolat, O.M., Pandya, K., Lau, F.S. *et al.* (2001) DOE AAD Document Control. Cooperative Agreement No. DI-AC26-99FT40674.
12. Pavlish, J.H., Hamre, L.L., and Zhuang, Y. (2010) *Fuel*, **89**, 838.
13. Granite, E.J., Myers, C.R., King, W.P., Stanko, D.C., and Pennline, H.W. (2006) *Ind. Eng. Chem. Res.*, **45** (13), 4844.
14. Jain, A., Seyed-Reihani, S.A., Fischer, C.C., Couling, D.J., Ceder, G., and Green, W.H. (2010) *Chem. Eng. Sci.*, **65** (10), 3025.
15. Miller, P.J. and Atten, C.V. *North American Power Plant Air Emissions*, Commission for Environmental Cooperation of North America, 2004, www.cec.org/files/PDF/POLLUTANTS/PowerPlant_AirEmission_en.pdf (accessed July 2013).

9

Mercury Emissions Control for the Cement Manufacturing Industry

Robert Schreiber Jr., Shameem Hasan, Carrie Yonley, and Charles D. Kellett

9.1

Introduction

The manufacturing of portland cement is performed in a large industrial process that is raw material and fuel intensive. The industry is considered as one of the anthropogenic contributors of mercury to the environment. During the pyroprocessing step that occurs in the cement kiln system, the mercury compounds are vaporized from the fuels and raw materials due to the very high temperatures achieved inside the kiln. There are different types of pyroprocessing systems used in the cement industry, and the specifics of each system have been shown to have an effect on reactions and emissions/emissions control of mercury. However, the state of knowledge on the fate of mercury, speciation of emissions from the kiln system, and potential for control is still in the early stages of development and testing, although knowledge is being amassed more rapidly over recent years. This chapter describes the specifics of the cement manufacturing process and the corresponding effects of the process chemistry and temperatures within the kiln system on mercury speciation. The discussion includes the current state of the study of mercury in the industry and knowledge on mercury control.

9.2

Cement Manufacturing Process Description

Portland cement (hereinafter, cement) is the gray powder that is the active chemical binder used to produce concrete by mixing it with sand, gravel, and water. Cement manufacturing is performed in a large-scale industrial production process using large volumes of raw materials and fuels. The basic steps of cement production are generally as follows:

- Raw material procurement
- Raw material feed preparation

Mercury Control: for Coal-Derived Gas Streams, First Edition.

Edited by Evan J. Granite, Henry W. Pennline and Constance Senior.

© 2015 Wiley-VCH Verlag GmbH & Co. KGaA. Published 2015 by Wiley-VCH Verlag GmbH & Co. KGaA.

- Pyroprocessing of raw material in the kiln system (formation of cement “clinker”)
- Clinker cooling
- Clinker grinding and cement packaging.

The basic raw materials used to manufacture cement include sources of calcium carbonate, silica, alumina, and iron, with trace amounts of other compounds such as alkalis (sodium, potassium), sulfur, chlorine, and metals naturally occurring in the raw materials. Typical raw feed to a kiln contains about 80–85% calcium carbonate, 10–15% silica, and small amounts of alumina and iron. Maintaining the quality of raw feed is an important step in manufacturing quality cement. Traditional mineralogical sources of the cement ingredients include the calcareous component such as limestone, marl, or chalk; the argillaceous components such as clay, shale, slate, or sand which provide the silica and alumina; and iron components, in some cases provided by mill scale or a similar material. Cement plants are generally located in areas that have an abundant supply of readily available raw materials. With about 80–85% of the raw materials being limestone, plants are usually located at or near abundant limestone quarries for economics related to raw material transportation costs.

Raw material feed preparation involves sizing through crushers and mixing and grinding raw materials in a raw mill(s) to obtain correct size and chemical composition for kiln feed, also termed as *raw mix* or *raw meal* (Figure 9.1). The process used to prepare raw meal is dependent on the type of pyroprocessing system being used.

The main types of systems used in the cement industry include the wet process and the dry process. The dry process is further subdivided into the

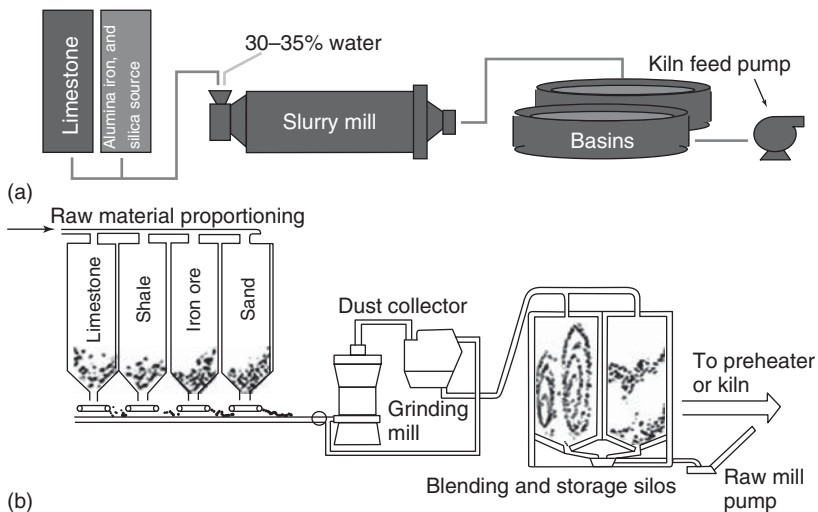


Figure 9.1 Schematic of raw meal preparation for (a) wet kiln and (b) dry kiln.

long dry process, the preheater process, and the most recent technology – a preheater/precalciner system. Each type of system is further described below.

For use in the wet process, the raw materials are mixed and ground with water (~30–35 wt%) to produce slurry, which simplifies the blending of the kiln feed to produce a uniform chemical composition. The dry process involves mixing a calculated proportion of raw materials, drying, and grinding the mixture to a powdered form, blending the materials together in silos, and feeding the raw meal to the kiln in a dry state. For the preheater and preheater/precalciner processes, heat to dry the raw material may be recovered from the kiln system and utilized in an in-line raw mill system. For a continuous operation, the raw mill must grind more raw materials than can be used in the kiln system in a given time frame; otherwise, sufficient kiln feed would not be available on a consistent basis as the raw mills require more down time for maintenance and repair than the kiln. Normally, raw mill systems are designed to grind enough material such that they can be taken off-line once a week for repair and maintenance. Under most circumstances, raw mills are designed to operate about 85–90% of the kiln operational time. For the in-line raw mill design, this phenomenon is known as *raw mill on* and *raw mill off* operating conditions.

The kiln system is where the key process step occurs, where a specific combination of minerals is heated to a temperature of about 1500° C in a large, cylindrical, rotating, refractory-lined kiln, and associated equipment, depending on the type of kiln system. The raw materials are fed counter-current to the gases from burning fuel in the combustion zone of the kiln and undergo the chemical and physical reactions required to produce quality cement. Inside the kiln, the minerals are partially fused at high temperatures, resulting in the formation of clinker nodules, which is the intermediate product of cement. Cement kiln dust (CKD) is generated during raw materials processing inside the kiln system. CKD includes thermally changed and unchanged raw feed that becomes entrained in the counter-current gas flow through the kiln system. Gases that exit the cement kiln system are vented to an air pollution control device (APCD) where the CKD is removed, followed by the exhaust stack. Traditionally, an electrostatic precipitator (ESP) or baghouse is used as the APCD in the cement industry. New APCD technologies are beginning to be studied and tested as regulations are becoming increasingly stringent for additional pollutants.

Large amounts of fuel are necessary to drive the pyroprocessing that occurs in the kiln system. Typical fuels used in cement kilns are coal, petroleum coke, natural gas, oil, and/or alternative materials used for energy recovery, such as used tires, plastics, and oil. The most significant quantity of traditional fuel continues to be solid fuel, including coal and coke. In a typical kiln, ~2–6 million British thermal units of heat value are required to produce a ton of clinker [1]. Fuels fired in the hot end generally need to have a relatively high heat value as fired to maintain the high flame temperature required at the front of the kiln. Fuel fired at the hot end of the kiln also must be finely atomized to promote rapid combustion, which is important to clinker quality. The most important factor for fuel is the consistency. If each load has a different consistency, maintaining stable kiln

operations, maximum kiln production, and product quality is challenging. Also, an accurate control of energy input is required for the critical clinkering step. Insufficient energy input in the kiln will not allow necessary chemical reactions to occur during the clinkering process, which may result in unreacted lime in the clinker, thereby producing poor quality cement. Too much energy input will shorten the life of the kiln refractory lining, which may damage the kiln shell. It can also cause molten clinker to drop into the clinker cooler, causing significant damage and shutting down the system.

The clinker exits the hot end of the kiln, and is cooled from ~ 1500 to 90°C in the clinker cooler where ambient air is forced through a slowly moving bed of clinker for rapid cooling to stabilize its molecular structure. Typically, the air used to cool the clinker is recovered and used as preheated combustion air in the kiln. The cooled clinker is conveyed to a finishing mill (e.g., ball mill) for grinding. In the finishing mill system, the clinker is interground with a small amount of gypsum ($\text{CaSO}_4 \cdot 2\text{H}_2\text{O}$), an agent that controls the setting time of the concrete, and grinding aid, a material used to make the grinding process more efficient (too varied to describe within the context of this chapter) into the powder known as *portland cement*. At this point, the product is ready for commercial distribution.

Typical portland cement clinker comprises 67% CaO , 22% SiO_2 , 5% Al_2O_3 , 3% Fe_2O_3 , and other minor components such as MgO , K_2O , TiO_2 , and Mn_2O_3 . Four major phases, including $3\text{CaO} \cdot \text{SiO}_2$ (50–70%), $2\text{CaO} \cdot \text{SiO}_2$ (15–30%), $3\text{CaO} \cdot \text{Al}_2\text{O}_3$ (5–10%), $4\text{CaO}, \text{Al}_2\text{O}_3 \cdot \text{Fe}_2\text{O}_3$ (5–15%), also termed *alite*, *belite*, *aluminite*, and *ferrite*, respectively, are present in clinker [2]. The phases in portland cement clinker are important as they function as a strength development agent in cement when mixed with water. The American Society for Testing and Materials (ASTM) specifies different types of portland cement based on the mineralogical properties of the clinker [3]. Among them, normal portland cement (Type I), modified portland cement (Type II), high-early-strength portland cement (Type III), low-heat portland cement (Type IV), and sulfate-resisting portland cement (Type V) are most common.

9.2.1

Wet Process Kiln

In the wet process, the blended raw feed is introduced to the “cold end” of the rotary kiln and tumbles down the length of the kiln toward the flame in the lower “hot end” of the kiln. In general, a rotary kiln is 400–700 ft in length, and has a 3–4% slope with the horizontal and rotates at $1\text{--}2\text{ rev min}^{-1}$ during operation. Figure 9.2 shows the temperature profile of a typical wet kiln [4]. There are essentially four stages to the pyroprocessing – evaporation and preheating, calcining, clinkering (sintering), and cooling. Fuel normally is fired at the hot end of the kiln, although some kilns are equipped with a secondary mid-kiln firing location. Evaporation and preheating remove moisture from the raw feed and raise the feed temperature to about 870°C . At 760°C , calcination of the material takes

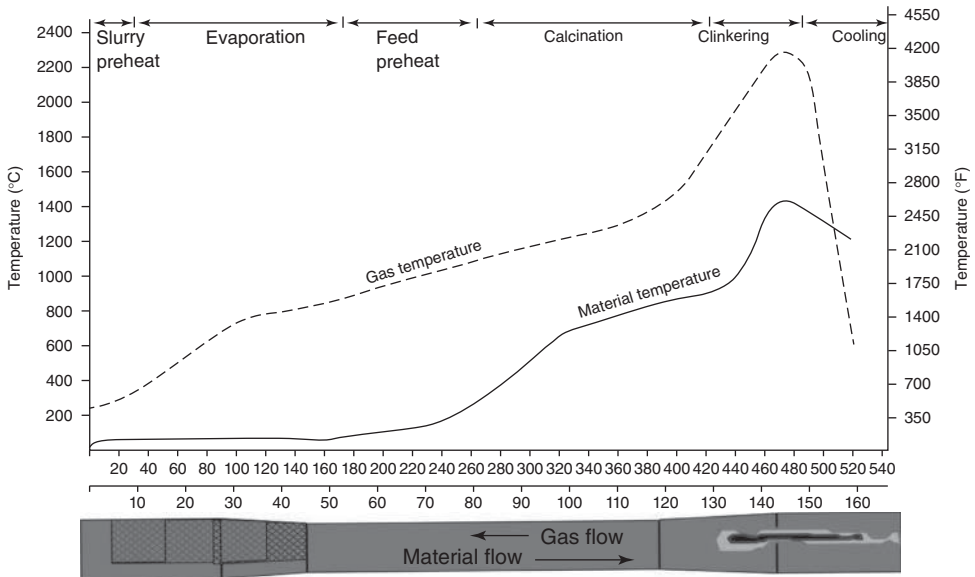


Figure 9.2 Typical temperature profile of wet kiln system in cement industry [4]. (Reproduced from Ref [4] © (1986) with permission from Chemical Publishing Co. Inc.)

place, breaking the calcium carbonate down into calcium oxide and carbon dioxide. At 1500°C , $\sim 20\text{--}30\%$ of the load melts and the formation of calcium silicate occurs. At this stage, the material forms the clinker nodules due to gravitational flow and the rotating effect of the kiln. The clinkering process occurs in the hottest zone of the kiln, called the *burning zone*, where the material temperature reaches about 1500°C and in which the material spends $\sim 10\text{--}15$ min.

Due to the nature of raw feed preparation, the wet process offers more uniform feed blending and generates less dust particles. Wet kilns require more combustion energy per ton of clinker produced than the dry process kiln systems as the water must be evaporated from the slurry feed.

9.2.2

Dry Process Kiln

More than 80% of the U.S. cement industry uses dry process kilns in which raw meal is prepared without adding any water. Dry process kilns are further divided into three types – long dry, preheater, and preheater/precalciner systems, with those built over the last two to three decades typically being the modern preheater/precalciner design. A long dry kiln is similar to a wet kiln with the exception that the raw materials are fed to the kiln as a dry powder, therefore requiring less combustion energy to produce clinker than a wet kiln but more electrical energy to blend the dry raw materials. The preheater kiln system uses dry raw meal that passes through a tower containing one or more cyclone-type vessels that simulate

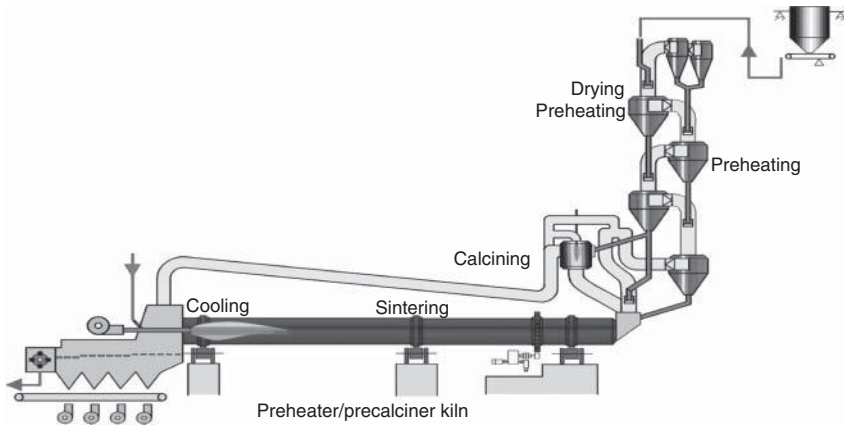


Figure 9.3 Schematic of a typical preheater/precalciner dry kiln in cement industry.

a fluidized bed heat transfer mechanism before entering the rotary kiln. The raw feed is suspended by the hot counter-current kiln gases prior to entering the kiln, and the preheating phase of the process is accomplished in the tower in a few seconds. This allows a rapid and more efficient energy transfer between the hot kiln (flue) gases and raw meal than a typical long dry or wet process kiln.

A preheater/precalciner kiln system has a tower with preheater vessels but also contains a secondary combustion vessel, called a *calciner*, near the lower stages of the preheater tower. (Figure 9.3 shows a typical preheater/precalciner kiln system, and Figure 9.4 documents the temperature profile of a preheater/precalciner kiln.) Fuel is introduced into the calciner and about 90% of the kiln feed is calcined within a few seconds in the hottest zone of that vessel. In this type of process, drying, preheating, and most of the calcining take place before the feed enters the rotary kiln. Preheater and preheater/precalciner systems require shorter rotary kilns, and the process is the most energy-efficient from a fuel standpoint. Approximately 60% of the overall fuel requirements for a precalciner system is at the calciner versus the main burner in the rotary kiln [5]. Therefore, the addition of a precalciner also extends the refractory service life of the kiln by reducing the heat load inside the rotary kiln. A variety of fuels with larger particle sizes and lower heat values can be accommodated in the calciner as the temperature required for calcination is much lower than sintering (clinkering) the raw meal into clinker. Most of the preheater/precalciner kiln systems are equipped with in-line raw mills usually located between the preheater tower and the APCD, allowing the exhaust gas from the preheater to be further used to dry the raw material in the raw mill. The gases exit the raw mill and pass through the APCD before being released from the stack to the atmosphere. APCDs employed for these types of systems are primarily fabric filters, or baghouses; however, some kilns do use ESPs.

Modern large kilns produce 4000–5000 tons of clinker per day or ~1.5 million tons of clinker per year. This requires processing between 6000 and 8000 tons of raw materials daily. Due to the large amounts of fuel and raw materials required to

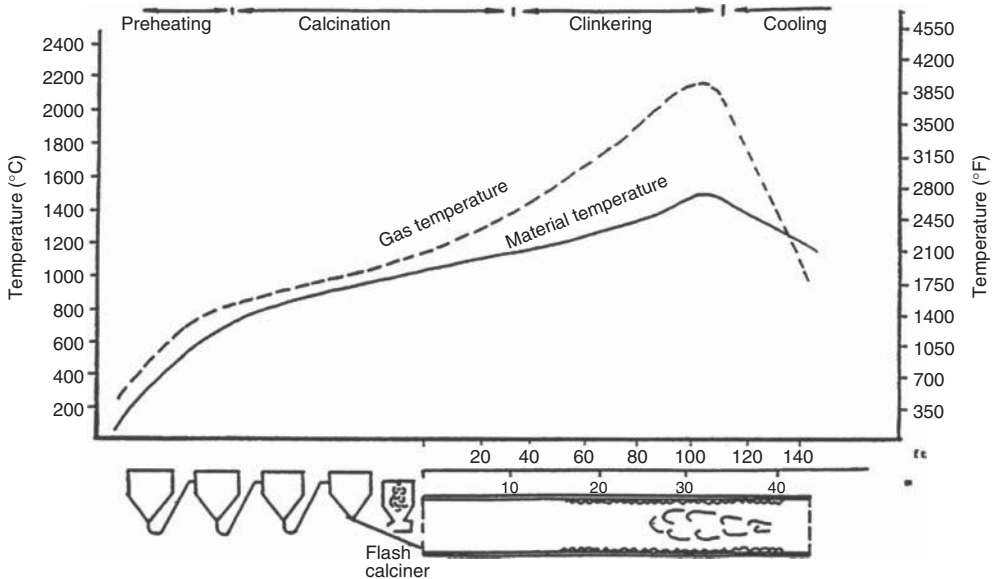


Figure 9.4 Temperature profile of a typical preheater/precalciner dry kiln system [4]. (Reproduced from Ref [4] © (1986) with permission from Chemical Publishing Co. Inc.)

produce cement clinker, there is a production incentive in the cement industry to find alternate fuels and raw materials compatible with the manufacturing process, where cost-effectiveness of the operations can be improved and quarrying of naturally occurring materials can be reduced.

9.3

State of Knowledge on the Source and Behavior of Mercury in the Cement Kiln System

Mercury can enter the kiln system from two sources – the raw material and the fuel – both of which inherently contain trace amounts of mercury as naturally occurring substances and are used in large quantities in manufacturing cement. The mass and chemical composition of the raw material and fuel and the type of pollution abatement technology ultimately determine the quantity of the mercury emissions from a cement kiln system. Studies have been conducted to determine the mercury content of cement manufacturing raw materials and fuels. The studies have revealed mercury concentrations ranging from 0.01 to >1.0 ppm in raw materials [6]. The amount of mercury in the raw feed is highly dependent on the quarry characteristics. The mercury input from fuel can also be significant. The concentration and distribution of mercury content in coal has been documented through U.S. Geological Survey research over the last 20 years. The study results show concentrations ranging from 0.058 to 0.362 ppm [6]. It is also important to note there are several constituents in raw materials that can have an effect on the kiln operations/chemistry and resulting air emissions.

These include sulfur content, alkali content, chlorine content, and other minor constituents (e.g., fluorine). The understanding of the chemistry can also play an important part in the understanding of potential mercury reactions in the cement kiln system and the form of the mercury in the exhaust gas from the kiln.

All mercury and mercury compounds in the fuel or raw material are volatilized and converted completely to the elemental form (Hg^0) at temperatures above 500°C in the kiln system. The volatilized mercury is subsequently carried through the kiln system toward the raw feed end of the kiln along with combustion gases, where it is subject to cooling from $\sim 1900^\circ\text{C}$ down to $\sim 200^\circ\text{C}$. Generally, once mercury enters a cement kiln system, it has five potential fates [7]:

- It may remain unchanged and exit the kiln as part of the clinker (very small amount).
- It may react with raw materials and exit the kiln as part of the clinker (very small amount).
- It may vaporize in the high temperature zone of the kiln and/or preheater.
- It may condense or react with the CKD and be removed by the APCD.
- It may exit the kiln system in vapor form or be adsorbed to a dust particle as emitted from the stack.

If the primary source of mercury is the raw feed, studies have shown that it is likely to be in the form of mercury sulfate (HgSO_4) or mercury sulfide (HgS) in the raw material [7]. If the mercury is primarily from the fuel, then it is most likely in the mercuric chloride (HgCl_2) or HgS form, or already existing as mercuric oxide (HgO). Also, during combustion, oxidizing agents that may be present in the fuel, such as chlorine and sulfur, are released. These oxidizing agents play an important role in the speciation of mercury emitted from cement kiln systems.

Mercury is reported to be present in the combustion gas (or flue gas) comprising varying percentages of Hg^0 , oxidized (Hg^{2+}), or particle-bound (Hg_p) form [8]. Hg^0 is considered as less reactive, highly volatile, and also insoluble in water. It passes through the entire kiln system and exits the stack in the vapor phase. Hg^0 and a minor proportion of HgO can be present in the flue gas at high temperatures; however, only Hg^0 is stable at the high temperatures. As the flue gas cools, mercury is oxidized through the reaction with compounds from the raw materials and fuel (e.g., chlorinated compounds, oxygen, bromine, etc.). Hg^0 and Hg^{2+} comprise the vapor-phase mercury. Organomercury compounds would be minuscule in comparison to inorganic mercury or not likely to be found in the emissions of a cement kiln as these compounds would be destroyed in the presence of the high temperatures in the kiln system. In the cooler zones of the kiln system, the Hg^{2+} may adsorb or condense onto CKD particles in flue gas to form Hg_p . Much of the dust containing mercury would then be captured by the APCD and, for most kiln systems, returned to the kiln. A portion of the CKD is often removed from the system in order to lower the alkali content of the clinker to meet product specifications. The removal of CKD is a mechanism to bleed the kiln system of alkali salts that build up as they circulate through the system. Mercury adsorbed onto the dust would also be removed in the same way.

A number of complex thermo-chemical gas-phase reactions control the speciation of mercury associated with cement kilns. The presence of hydrogen chloride (HCl) in the exhaust (flue gas with a range of HCl from 1 to 120 ppm or greater), which may accelerate the mercury oxidation reaction in the kiln through the Decon reaction, can result in the formation of HgCl_2 [9–12]. The oxidation of mercury occurs when the elemental mercury reacts with chlorine to form HgCl_2 below the gas temperature range of 480–590 °C due to a thermo-chemical process [6, 13]. The possible mercury oxidation in the kiln system is reported to be a homogeneous- or heterogeneous-phase reaction [14]. The homogeneous oxidation may occur in the gas phase whereas the heterogeneous oxidation occurs on the interface of solid particles inside the kiln system or APCD. As the flue gas passes through the APCD, temperatures continue to drop below 200 °C, allowing some of the Hg^0 to be adsorbed onto the CKD. Some of the Hg^{2+} compounds also adsorb and condense onto the CKD. The remaining mercury compounds pass through the stack and are emitted. Mercury oxidation reactions in the cement kiln system are as follows:



There has been a limited, but recently increasing amount of sampling and analysis of mercury speciation in U.S. cement kiln stack emissions. Figure 9.5 shows the averages for Hg^0 , Hg^{2+} , and Hg_p emissions for wet kilns, long dry kilns, and preheater/precalciner kilns with both raw mill on and off conditions [15]. Due to the limited data, the results shown in Figure 9.5 may not be representative. However, this limited data indicates that wet kilns predominantly emit higher concentrations of Hg^0 compared to long dry and preheater/precalciner kiln systems. This may be explained by kiln system heat profile differences between wet kilns and long dry or preheater/precalciner kilns. More data are needed to be more definitive on mercury speciation from different kiln systems.

In a long wet or dry kiln, the raw materials are introduced through the kiln feed end where they encounter gas temperatures of ~200–300 °C. In the long kiln, the evaporation of water from the slurry (wet kiln) or kiln feed (dry kiln) must first occur, with the raw meal being maintained in the 50–100 °C range, with gas temperatures being as high as 300 °C (Figure 9.2). Hg^0 that may form during drying and subsequent calcination of raw meal will reach the APCD with a very limited interaction with CKD. For long dry kilns, as there is little water to evaporate, the temperature profile may be sufficiently different compared to the long wet kiln that oxidation may be more pronounced. In consideration of the limited data and knowledge of other influencing factors that may be present, additional long-term data are necessary to confirm the assumed mechanisms of formation.

In contrast, in a preheater/precalciner kiln system, the raw meal passes through the preheater cyclones and calciner before entering the rotary kiln. The heat profile of this system, as shown in Figure 9.4, allows sufficient time and temperature for the oxidation of mercury to occur in the presence of an oxidizing agent (e.g., chlorine, sulfur, and oxygen). In the preheater/precalciner system, the formation of

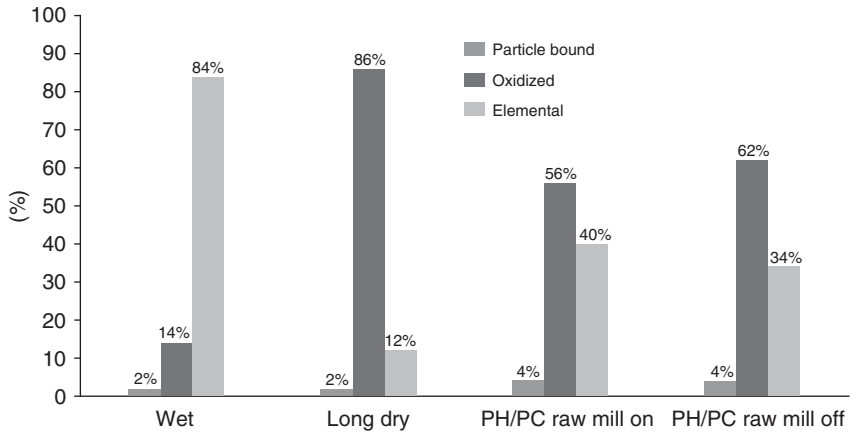


Figure 9.5 Mercury speciation percentages – averages for all kiln types [15]. (Reproduced from Ref [15] © (2009) with permission from Portland Cement Association.)

Hg⁰ occurs when the temperature of the raw meal reaches in excess of 500 °C as it descends through the preheater tower.

Figures 9.5 and 9.6 show mercury speciation data for all kiln types and for preheater/precalciner systems with the raw mill on-line and off-line conditions. The data for preheater/precalciner systems is derived from tests on seven different kiln systems. The studies have shown that, during the raw mill off-condition, the gas stream delivered directly to the system’s APCD is found to have a higher concentration of mercury as compared to the raw mill on-condition [16]. When the mill is on-line, exhaust gas exits the top of the preheater tower and is introduced into the raw mill to dry the raw meal. The temperature of the mercury-laden hot flue gas exiting the preheater tower prior to entering the in-line raw mill ranges from 315 to 398 °C. The preheater tower exit gas typically contains ~100–150 g nm⁻³ of fine

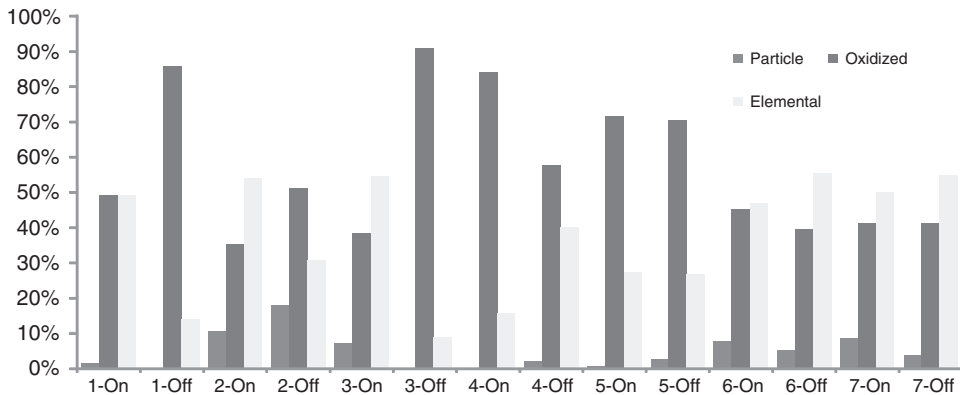


Figure 9.6 Mercury speciation percentages – raw mill on and raw mill off [15]. (Reproduced from Ref [15] © (2009) with permission from Portland Cement Association.)

dust particles [15] containing volatilized Hg^0 . In this scenario, the operating raw mill acts as both a dry scrubber and condenser. The gas temperature is reduced through heat exchange in the raw mill to the exit temperature of 90–120 °C. The larger surface area of the finer dust particles in the gases allows adsorption of condensed material containing mercury to occur at the lower temperatures.

The gas stream exiting the raw mill with mercury-laden fine particles is ducted to cyclones in most system designs prior to the APCD, thus removing 85–90% of the coarser particles (10–50 μm range) from the gas stream. The finer particulate (0–5 μm) is carried to the APCD where further gas/particulate separation occurs. In essence, with the raw mill operating, mercury-laden particulate is captured by both the raw mill system and the APCD and is transported to the blend silos where it is re-blended into the raw meal and used as kiln feed, creating the opportunity for a significant mercury recycle loop. The cleaned gas stream is exhausted out the stack. When the re-blended raw meal reaches temperatures in the preheater cyclones of ~ 400 °C, the captured mercury is again volatilized and returned in the gas stream to the raw mill, only to be recaptured in the particulate. The repeated volatilization and adsorption of mercury in the preheater tower, raw mill, and APCD create an enriching mercury loop in the kiln system during the raw mill on operating condition.

For illustrative purposes, Figure 9.7 shows a mercury loop in a cement kiln for the raw mill off and on conditions. When the mill is off, the kiln flue gas stream continues to be cleaned by the APCD. This stream has particulates, in the form of CKD, with elevated levels of mercury. In general, the mercury-laden CKD

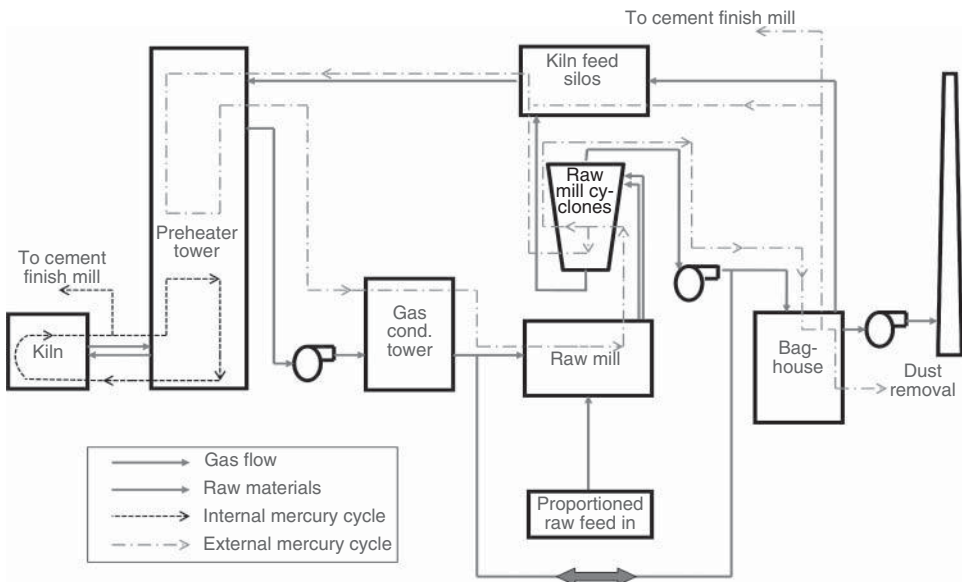


Figure 9.7 Possible internal mercury pathways in cement kiln system and external cycle during raw mill off and on condition.

captured by the APCD would be returned to the kiln. As the CKD is returned to the system, a circulation of mercury will be created through the preheater, raw mill, and APCD. Depending on the APCD inlet temperature, some of the mercury may be in the gaseous state due to higher operating temperatures in the mill off condition, will not be attached to the CKD, and will be released to the environment. The net effect of raw mill on and off is simply accumulation of mercury in the kiln system. Eventually, the mercury will be released to the environment over time [17].

The release and form of mercury in cement kiln systems is not completely understood. In general, the form of mercury in the system will be dependent on the cooling rate, temperature, and opportunities for the oxidation/chemical reaction to occur. These conditions correspond to the gas-phase chemistry relevant to the specific kiln characteristics, which are driven by the raw materials, gas conditions, and operating conditions. For example, the concentration of chlorine in the flue gas depends on a complex series of gas-phase reactions involving oxygen, water vapor, hydrocarbons, chlorine, and sulfur compounds present in the flue gas in the kiln system [18, 19].

Without significant data on mercury speciation in cement kilns, it is difficult to make definitive statements about the types of mercury compounds. However, the gas-phase equilibrium studies for coal-based flue gas suggest that HgCl_2 is the dominant oxidized species in flue gas at temperatures below 480–590 °C [19, 20]. The equilibrium of the oxidation reaction also depends on the concentration of chlorine and the degree of flue gas cooling [19]. It is generally assumed that the oxidation of mercury may have a similar pattern in the cement kiln system. Therefore, the degree of oxidation of mercury in the cement kiln system would be expected to decrease with increased flue gas cooling rates. As the flue gas temperatures continue to cool to the mercury boiling point (~357 °C), some of the mercury reacts to form HgO , which may further react with chlorine to form HgCl_2 . However, the gas-phase homogeneous oxidation of Hg^0 is kinetically limited because of the short residence time [10], on the order of ~2 s. At gas temperatures below ~325 °C, some of the mercury may react with sulfur dioxide (SO_2) to form HgSO_4 and its subsequent reaction with gaseous HCl produces volatile dichloride which remains within the flue gas [21]. Therefore, the presence of SO_2 compounds in the flue gas may limit the concentration of chlorine and subsequent conversion of Hg^0 to HgCl_2 .

The formation of complex silicates in a kiln system is also possible due to the high silica content in typical raw feed (13–15% by weight) and sufficient residence time for reactions to take place as vaporized mercury cycles through a kiln system. Owens *et al.* [22] stated that the formation of mercury silicates is possible based on the estimated thermodynamic data at temperatures ranging between 225 and 325 °C. However, the formation of mercury silicate may be inhibited by the presence of chlorine and sulfur. Additional research and alternative laboratory methods for clinker analysis will be required to confirm that mercury silicates are stable above temperatures of 325 °C. As the flue gas passes through the APCD, the temperature continues to drop below 200 °C, allowing some of the Hg^0 to adsorb

Table 9.1 Potential mercury transformation within cement kiln systems [15]. (Reproduced from Ref [15] © (2009) with permission from Portland Cement Association.)

System temperature (°C)	Chemical species influencing reactions	Resulting mercury compounds
2200	—	Hg (elemental, vapor)
<480–590	Chlorine	HgCl ₂
<350	Oxygen, chlorine	HgO, HgCl ₂
<325	Sulfur	HgSO ₄
225–325	Silica	HgSiO ₃

onto CKD particles. Also, some of the Hg²⁺ compounds (i.e., HgCl₂, HgO, HgSO₄) adsorb onto the CKD particles as mentioned already. It is evident that a lower flue gas temperature would produce more Hg_p, which would be efficiently removed by the APCD [23] with the remaining mercury compounds exiting the stack. The mercury reactions that can take place at different temperatures in a cement kiln system are summarized in Table 9.1.

It is postulated that nearly all forms of mercury exiting the kiln system will be gaseous or condensed on the fine particulate that exits with the gas stream. However, there is some very limited data that shows the presence of low but detectable levels of mercury in cement clinker. As cement manufacturing is a large industrial process that involves complicating factors such as raw mill on versus raw mill off and accumulation of mercury in the feed silo or accumulation at different parts of the system, it is important to note that a short-term stack emission test is not necessarily representative of actual annual emissions.

9.4

Mercury Emissions Control Solutions in the Cement Industry

U.S. Environmental Protection Agency (EPA) recently set a new limit for maximum mercury emissions from U.S. cement kiln stacks at 55 lb MM ton⁻¹ clinker for an existing kiln, and 21 lb MM ton⁻¹ clinker for a new kiln [24]. Therefore, reductions of mercury from cement kiln stacks will need to be further accomplished in the near future, in addition to those reductions already being implemented.

As described earlier, the source of mercury emissions from cement kiln systems are trace amounts of mercury in the raw materials and fuel that are inherently introduced into the kiln system as a part of the cement manufacturing process. The behavior of mercury in cement kiln systems is very complex as mercury can exist in various forms depending on the type of system and the chemical reactions that occur in that specific system. The following possible approaches can be considered for mercury control, which are based on the current state of mercury

control knowledge as applied to the cement process. Further study is ongoing and may provide additional approaches or variations to the following.

Option 1: The mass of mercury entering the kiln system can be reduced by using different raw materials or different fuels containing smaller trace amounts of mercury, although this option is limited.

Option 2: Some of the CKD captured in the APCD that contains elevated mercury concentrations can be removed from the system and wasted, treated, or mixed with clinker.

Option 3: The gas stream can be treated to remove the mercury before it is exhausted out the kiln stack.

Each of these options is further described in the following paragraphs.

Option 1: Although this option may sound the most practical, reducing mercury emissions by reducing mercury concentrations in the raw materials may be difficult to accomplish without profound economic consequences. Cement plants are located in areas where raw materials are readily available. Therefore, changing sources of raw materials, if possible, could impose a huge economic burden on a cement plant. In a situation where the fuel is found to contain relatively high trace levels of mercury, the economics, and practicality of reducing mercury inputs may also be difficult. Transportation costs for fuel can be very significant and the location of a potential alternate source of fuel with lower mercury content may significantly increase costs of fuel acquisition.

Option 2: In cement kiln operations, a portion of the CKD is often removed from the system in order to lower the alkali content of the clinker to meet U.S. product specifications. This mode of operation is also known in the cement industry as wasting CKD. This practice is minimized as much as possible to keep from wasting material that has already been partially calcined, thus continuing to have economic value as a partially processed raw material. As a matter of fact, the U.S. cement industry has made significant reductions in dust wastage rates over the last few decades. The removal of CKD is a mechanism to bleed the kiln system of alkali salts that build up as they circulate through the system in a pattern similar to mercury. If a portion of the dust from the APCD is not wasted, the mercury remains in the system and is recirculated, with the concentration of mercury in the external loop of a preheater/precalciner system (shown in Figure 9.7) increasing over a period of time. If the raw mill exhaust is equipped with cyclones to separate coarse dust particles that are transported to the blending silo, then the mercury concentration in the APCD may not be significantly different between raw mill off versus raw mill on operating modes. If the raw mill exhaust is not equipped with cyclones, then diverting APCD dust with the raw mill on will not be as efficient for removing mercury from the system because of the dilution effect of the large mass of dust captured by the APCD. The amount of CKD generated in a typical kiln system when the raw mill is off can be

significant at 8–15 ton h⁻¹. Wasting all the CKD would not be economically viable due to its value as a raw material to the process.

A patent-pending, mercury-laden, kiln CKD roasting technology has been identified as a possible mercury removal mechanism for the cement industry [25]. In the roasting system, the mercury-laden CKD is heated above the boiling point of mercury. While mercury is in the gas phase, an ESP is used to separate the dust from the gas-phase mercury, which can then be removed by various techniques such as activated carbon injection (ACI). The cleaned dust is taken back to the blending silo to be used as kiln feed.

Another practice possible for cement plants is called *dust shuttling*. This practice is utilized currently at some facilities, and is being considered by others as a potentially viable option to remove mercury from the kiln system by shuttling dust from the APCD. For this practice, the facility maintains a specific mix chemistry to allow incorporating a small quantity (3–5% of product) of CKD in the finish mill, intermixing the CKD with cement [25–27].

For those cement kilns that do not waste or shuttle CKD, it is reasonable to assume that essentially all the mercury in the raw material and fuel will end up as stack emissions over the course of a year. However, if a portion of the dust is shuttled, this will lower mercury stack emissions, as some of the mercury becomes bound up in the cement product matrix. This is a viable mercury reduction option to the extent the CKD can be interground with the clinker while still maintaining a quality product. Since only a portion of the collected CKD from the APCD can be diverted, the mercury reduction capability is limited. It is reported that the efficiency of mercury removal of APCD dust is dependent on site-specific conditions, including the flue gas composition, operating temperature at the inlet of APCD, and dust loading in the systems [25]. Thus, dust shuttling is expected to have a limited impact on mercury emission reductions. However, in the event, as the shuttled CKD has a high mercury content, dust shuttling may present an effective method of removing mercury from the system, subsequently being a significant mercury control option.

Option 3: When considering cement industry options for treating the gas stream for mercury removal before exhausting the gas through the kiln stack, the majority of the controls require tailpipe treatment after the existing APCD. In fact, as described below, control technologies being currently considered would require an additional APCD between the existing APCD and the stack.

Mercury control technologies currently being considered as options for cement kiln system emissions include

- Activated carbon injection (ACI)
- Wet scrubbing
- Selective catalytic reduction (SCR) and wet scrubbing.

9.4.1

Activated Carbon Injection (ACI)

Activated carbon is a widely used adsorbent in several industries due to its unique physical and chemical properties. The large surface area, pore volume, and pore size distribution of activated carbon make it a potential adsorbent to accomplish mercury removal from the cement kiln flue gas. ACI applications have been used historically for mercury control in municipal waste incinerators, hazardous waste incinerators, and power plant applications. However, there are some factors that make direct transfer of this technology to the cement industry less effective. For example, the variable SO_2 and HCl concentrations along with a high dust loading of calcium and alkali materials may interfere with the absorption sites on the activated carbon. The percent mercury removal using ACI in the cement industry will be dependent on the temperature and composition of kiln flue gas and the amount and type of activated carbon used. Cement kiln APCD operating temperatures are usually at the high end of absorption temperatures of activated carbon, being effective up to 204°C . It has been found that typical mercury reduction ranges from 20% to 90% using ACI rates of 2–10 lb MMacf⁻¹. It is reported that the mercury adsorbed onto activated carbon is stable. It does not readily desorb, nor is it leachable (based on toxicity characteristic leaching procedure (TCLP) results) [28, 29]. This becomes an important factor as the carbon and CKD captured in the APCD must be appropriately managed for final disposal.

There are at least two cement kilns in the United States currently using ACI technology for mercury control. However, there are additional issues to study and resolve as described in the following paragraphs.

The new EPA MACT (maximum achievable control technology) standard for HCl in an existing cement kiln is 3 ppm [24]. When facilities comply with the HCl standard concurrently with the Hg standard, there may be an impact on the effectiveness of mercury control technologies. This correlation needs to be taken into account for determining the final control mechanism for a particular kiln. Moreover, chlorine in the cement kiln may combine with the alkalis (sodium and potassium) prevalent in the raw materials, resulting in insufficient chlorine to convert Hg^0 to Hg^{2+} . In addition, the presence of SO_2 in the flue gas may interfere with the carbon absorption efficiency [30].

In employing ACI technology to a cement kiln system, an additional APCD may be required to be constructed between the existing APCD and the kiln stack for further polishing. Activated carbon would be injected into the gas stream between the first and second APCDs. By capturing the remaining mercury from the flue gas in the second APCD before it is exhausted through the stack, mercury can be effectively removed from the system, as the mercury-laden activated carbon is separated from the kiln flue gas stream prior to the gases being released to the environment through the stack. This activated carbon can be wasted typically to a sanitary landfill as non-hazardous solid waste, which would effectively remove mercury from the kiln system.

Another approach to collecting and removing mercury from a cement kiln would be to use the absorption capacity of the kiln system, which could also be enhanced by using activated carbon. In a current kiln system configuration, the CKD is typically recycled to the maximum extent possible back to the kiln as part of the kiln feed, with most of the Hg_p being absorbed by the dust recycled back to the kiln. However, in some kiln systems, activated carbon could be injected into the main baghouse, depending upon the mercury carbon absorption properties of the collected dust. Some of this collected dust could be shuttled to the finished mill, with the remainder sent to the blend silos. This would work where the dust shuttled material would be small enough not to impact product quality. The material from the blend silos would re-enter the kiln system, destroying the carbon, and releasing the mercury to be once again collected on new carbon that is injected into the baghouse. This would have the effect of increasing the mercury concentration of the baghouse dust, which would make the removal of that dust a more efficient mechanism for mercury removal from the kiln system.

For an in-line raw mill system, ACI might be a mercury control option when the raw mill is off-line. However, the adsorption of mercury onto activated carbon is temperature-dependent. It is reported that ACI can work effectively only at temperatures below 160 °C [31]. This may be a problematic temperature for some existing systems as the flue gas temperature is comparatively high when the raw mill is not operating. Some halogenated powdered activated carbon (PAC) is reported to reduce mercury emission by more than 70% at APCD inlet temperatures up to 343 °C, but further investigation is needed to test the PAC performance for a longer period of time at various cement plants. As an example of potential issues, the brominated PACs could cause operational issues in a kiln system if they are reintroduced, causing an imbalance in the alkali–halogen ratio in the kiln.

As described above, both temperature and mercury concentrations in the flue gas may be issues that render the use of ACI technology less effective in the cement kiln system environment. Moreover, the baghouse dust with activated carbon may be problematic when used in clinker grinding or dust shuttling, but this issue will be site-specific. Activated carbon negatively impacts the air entrainment capabilities of the final cement product [25, 32]. Although ACI has the potential for mercury control in a cement kiln system, the industry still faces the significant economic issues of an additional large capital cost to construct a second APCD and to deal with disposal of the mercury-laden carbon material.

9.4.2

Wet Scrubbing

Wet scrubbing has been used in several industrial processes such as the electric power generation industry to reduce the SO_2 content of flue gases. In this process, a slurry of limestone or lime is sprayed into the gas stream, usually after the APCD, and the acidic SO_2 content of the gas reacts with the basic lime content to form gypsum. Therefore, the soluble components within the gas stream are removed in the scrubber, and a clean gas stream results. The solid residue that is

formed is removed and discarded. Wet scrubbers have not been used extensively in the cement industry historically due to lime inherently being in the kiln system. This creates a natural dry scrubbing process that removes much of the SO_2 content from gaseous effluents, nullifying the need for additional SO_2 control. It is reported that wet scrubbers have the capability of capturing soluble forms of mercury [33]. The oxidized mercuric compounds such as HgCl_2 are generally soluble in water, whereas Hg^0 is not soluble in water. EPA has reported that the electric power generation industry has had some success in mercury removal in wet scrubbers, especially in plants burning medium to high sulfur bituminous coals that tend to produce a larger amount of the Hg^{2+} species.

A limited number of cement kiln systems in the United States (five known installations to date) have installed wet scrubbers primarily for SO_2 and acid gas control. It is reported that the wet scrubber can capture more than 80% of SO_2 and HgCl_2 from the cement kiln flue gases [25]. However, there are several problems in transferring the process from electric power generation to the cement industry for mercury control. The effectiveness of wet scrubbing is highly dependent on the temperature of the gas stream, and the scrubber is normally located after the APCD. In many cases, the cement kiln gas stream exiting the APCD is $>204^\circ\text{C}$ when the raw mill is off-line. Wet scrubbers have been shown to be effective in capturing up to 90% of the Hg^{2+} in the kiln flue gases. Hg_0 not captured in the APCD will likely be captured in the wet scrubbers. However, Hg^0 is not removed from the flue gases due to its non-solubility.

As described, the effectiveness of wet scrubbers for mercury removal mainly depends on the mercury species present in the flue gas. In addition, the reemission of mercury may occur with wet scrubbers. Reemission is a result of mercury reduction chemistry in wet scrubbers, where Hg^{2+} is reduced to insoluble Hg^0 . Thus, the overall effectiveness of wet scrubbing for cement kiln emissions is unclear [34]. Studies based on the coal-fired power plant flue gases have shown that the amount of mercury retained in the scrubber solids may range from 40% to 85% [35]. The primary reported factor affecting mercury retention by a wet scrubber is the liquid to gas ratio, which may limit the mass transfer of pollutants. In addition, the scrubber solids must be properly managed and the water chemistry must be controlled to prevent reemission of the captured mercury.

9.4.3

Selective Catalytic Reduction (SCR) and Wet Scrubbing

SCR has been developed to remove NO_x emissions from flue gas. In an SCR system, the reducing agent of ammonia or urea is injected into the flue gas at the upstream side of the catalyst bed. The flue gas is passed through the catalyst bed containing oxides of vanadium or titanium where NO_x is reduced to form elemental nitrogen and water vapor. The SCR system is generally installed before the primary APCD in a cement plant for NO_x control as temperatures in the

range of 288–460 °C are required for the catalyst to be effective. A wet scrubber is installed after the APCD to control SO₂ emissions. A co-benefit of the SCR process is reported to be its ability to convert Hg⁰ to Hg²⁺, primarily HgCl₂ [36]. As described earlier, HgCl₂ is water soluble and can be captured in a wet scrubber along with SO₂. EPA has reported data from its Mercury Information Collection Request (ICR) showing that some electric power generation facilities use a combination of SCR and wet scrubber technologies to control the oxides of nitrogen and sulfur, which is also very effective in removing mercury from flue gases. The oxidation of mercury by the SCR process appears to be dependent on the type of coal combusted, furnace conditions, and physical and chemical properties of the catalyst [37, 38].

The catalyst used in an SCR system has the potential to catalyze the formation of sulfur trioxide (SO₃) from SO₂ and gas-phase chlorine (Cl₂) from HCl that are present in the flue gas [37]. Cl₂ in the flue gas will affect the overall conversion of Hg⁰ to HgCl₂. Bituminous coal typically contains higher Cl₂ and sulfur than the low-ranking sub-bituminous and lignite coals that are abundant with high calcium [37–40]. Higher quantities of Cl₂ result in greater conversion of Hg⁰ to Hg²⁺ in an SCR system and subsequently increase the removal of mercury in the wet scrubber. Conversely, the flue gas from the combustion of sub-bituminous and lignite coal appears to reduce the effectiveness of the SCR in converting mercury. This is due to the Cl₂ in the power plant flue gas from coal combustion tending to react with the alkaline materials in ash resulting in little, if any, Cl₂ being available for the oxidation of mercury. In a power plant SCR application, ~80–90% Hg⁰ in the flue gases from bituminous coal use is reported to be oxidized to HgCl₂. When the gas stream passes through the wet scrubber, the soluble HgCl₂ is dissolved in the solution sprayed into the wet scrubber. Therefore, the wet scrubber would then be expected to remove ~90% of the soluble mercury. The reduction of mercury from the flue gases of a power plant utilizing sub-bituminous and lignite coals is found to be only 20% with or without SCR [40]. However, the use of an SCR system at a cement plant will be dependent on site-specific conditions. The SCR catalyst bed must be located in an area where the flue gas temperature is in the appropriate range. There may be catalyst poisons such as alkali metals and calcium oxide in the cement kiln flue gas that will deactivate the catalyst by reacting with active sites. The catalyst may also become plugged in the high dust installations associated with preheater/precalciner kiln systems.

9.5

Conclusions

The cement manufacturing industry is a raw material-driven industry with demanding combustion conditions a part of the pyroprocessing portion of the process. As such, the study of mercury sources, forms, and emissions are unique in this industry. With the wide range of temperatures existing within a kiln system, mercury can be present in several chemical forms at different locations within the system. It can pass through the system as Hg⁰ or a volatile mercury

compound. It can condense or adsorb onto CKD in cooler parts of the system, such as in the APCD or raw mill (for preheater/precalciner kilns), when the temperature falls below 200° C. It has been shown that there are mercury recycle loops within the kiln system. CKD generated during processing of raw meal is recycled back to the kiln as kiln feed, with some systems being designed to continuously bleed some portion of the CKD from the APCD to maintain cement quality. This process inherently helps break the mercury accumulation cycle in the kiln, subsequently reducing the mercury load in the system and therefore reducing annual emissions.

As increased regulatory controls have just been put in place, and corresponding control of mercury emissions is currently being evaluated for future installations, the status of proven mercury control technologies used in cement kiln systems to treat the kiln exit gas stream is not yet clearly established. There are several technologies, including the use of ACI, a wet scrubber, and SCR; all of which are currently used to control mercury from flue gases in the electric power generation industry and for municipal and hazardous waste incinerators. These technologies may potentially be transferable to a cement kiln system, although the gas streams that exit the kiln are different than those industries currently using these technologies for mercury control. Current mercury control technologies used in other industries and transferred to cement kilns would require the installation of an additional APCD for an ACI installation or wet scrubber for particulate control downstream of the existing APCD. Another mercury control solution may be through wasting or shuttling some of the mercury-enriched CKD collected in the APCD when the raw mill of a preheater/precalciner kiln is off-line.

Regardless of the control system(s) used for mercury in a cement plant, additional data collection on the variation of mercury emissions over time needs to be conducted. This is especially true of emissions under the raw mill on/off scenarios of a preheater/precalciner kiln. Additional data collection is also needed to determine the speciation of mercury emissions from cement kiln stacks and within the kiln process. As described in this chapter, and throughout this book, many of the control technologies are dependent on the exact form of mercury. There are limited definitive studies on the speciation of mercury in a cement kiln system, and there is yet much to learn on mercury control for this industry. It is anticipated that much knowledge will be gained over the next few years and that additional control technologies currently being developed and tested will become additional solutions for the industry.

References

1. Tahsin, E. and Vedat, A. (2005) Energy auditing and recovery for dry type cement rotary kiln systems- a case study. *Energy Conserv. Manag.*, **46**, 551–562.
2. Taylor, H.F.W. (1997) *Cement Chemistry*, 2nd edn, Thomas Telford Publishing, London.
3. ASTM (2011) C150/C150M-11 *Standard Specification for Portland Cement*, American Society for Testing and Materials, <http://www.astm.org/Standards/C150.htm> (accessed 21 December 2014).

4. Peray, K.E. (1986) *The Rotary Cement Kiln*, 2nd edn, Chemical Publishing Co. Inc, New York.
5. Battye, R., Walsh, S., and Lee-Greco, J. NOx Control Technologies for the Cement Industry, Final Report EPA-457/R00-002, September 19, 2000, www.epa.gov/.../200009_nox_epa457_r-00-002_cement_industry.p (accessed 26 September 2000).
6. Johansen, V.C. and Hawkins, G.J. (2003) Mercury Speciation in the Cement Kiln: A Literature Review, PCA R&D Serial No. 2567, Portland Cement Association, Skokie, IL, 16 p.
7. Schreiber, R.J., Kellet, C.D., and Joshi, N. (2005) Inherent Mercury Controls Within the Portland Cement Kiln System, PCA R&D Serial No. 2841, Portland Cement Association, Skokie, IL, 29 p.
8. Yang, H., Xu, Z., Fan, M., Bland, A.E., and Judkins, R.R. (2007) Adsorbents for capturing mercury in coal-fired boiler flue gas. *J. Hazard. Mater.*, **146** (1-2), 1–11.
9. Olson, E.S., Mibeck, B.A., Benson, S.A. *et al.* (2004) The mechanistic model for flue gas-mercury interactions on activated carbons: the oxidation site. *Prepr. Pap. -Am Chem. Soc., Div. Fuel Chem.*, **49** (1), 279.
10. Li, Y., Daukoru, M., Suriyawong, A., and Biswas, P. (2009) Mercury emissions control in coal combustion systems using potassium iodide: bench-scale and pilot-scale studies. *Energy Fuel*, **23**, 236–243.
11. Murakami, A., Uddin, M.A., Ochiai, R., Sasaoka, E., and Wu, S. (2010) Study of the mercury sorption mechanism on activated carbon in coal combustion flue gas by the temperature-programmed decomposition desorption technique. *Energy Fuel*, **24** (8), 4241–4249.
12. Diamantopoulou, I., Skodras, G., and Sakellariopoulos, G.P. (2010) Sorption of mercury by activated carbon in the presence of flue gas components. *Fuel Process. Technol.*, **91**, 158–163.
13. Wang, S.X., Zhang, L., Li, G.H., Wu, Y., Hao, J.M., Pirrone, N., Sprovieri, F., and Ancora, M.P. (2010) Mercury emission and speciation of coal-fired power plants in China. *Atoms. Chem. Phys.*, **10**, 1183–1192.
14. Cao, Y., Gao, Z., Zhu, J., Wang, Q., Huang, Y., Chiu, C., Parker, B., Chu, P., and Pan, W.-P. (2008) Impacts of halogen additions on mercury oxidation, in a slipstream Selective Catalyst Reduction (SCR), reactor when burning sub-bituminous coal. *Environ. Sci. Technol.*, **42** (1), 256–261.
15. Schreiber, R.J. and Kellet, C.D. (2009) Compilation of Mercury Emissions Data, PCA R&D Serial No. 3091, Portland Cement Association, Skokie, IL.
16. Linero, A.A. (2011) Synopsis of mercury controls at florida cement plants. Presented at AWMA 104th Annual Conference and Exhibition, Orlando, Florida, June 22, 2011.
17. EPA (2006) National Emission Standards for Hazardous Air Pollutants From the Portland Cement Manufacturing Industry, Federal Register, Vol. 71, 76523, 40 CFR Part 63.
18. Pudasainee, D., Kim, J.-H., Lee, S.-H., Cho, S.-J., Song, G.-J., and Seo, Y.-C. (2009) Hazardous air pollutants emission characteristics from cement kilns Co-burning wastes. *Environ. Eng. Res.*, **14** (4), 212–219.
19. Senior, C., Sarofim, A., and Eddings, E. (2003) Behavior and measurement of mercury in cement kilns. IEEE-IAS/PCA Cement Industry Technical Conference, Dallas, Texas, May 4-9, 2003.
20. Senior, C., Montgomery, C.J., and Sarofim, A. (2010) Transient model for behavior of mercury in portland cement kilns. *Ind. Eng. Chem. Res.*, **49**, 1436–1443.
21. Abu-Daibes, M.A. (2004) Synthesis and characterization of nano-structured chelating adsorbents for the direct removal of mercury vapor from flue-gases. PhD Dissertation. University of Cincinnati, Ohio.
22. Owens, T.M., Chang-Yu, W., and Biswas, P. (1995) An equilibrium analysis for reaction of metal compounds with sorbents in high temperature systems. *Chem. Eng. Commun.*, **133**, 31–52.
23. Mlakar, T.L., Horvat, M., Vuk, T., Stergarsek, A., Konik, J., Tratnik, J., and Fajon, V. (2010) Mercury species,

- mass flows and processes in a cement plant. *Fuel*, **89**, 1936–1945.
24. EPA (2010) Procedure 5. Quality Assurance Requirements for Vapor Phase Mercury Continuous Emissions Monitoring Systems and Sorbent Trap Monitoring Systems Used for Compliance Determination at Stationary Sources Section 63.1343. Federal Register, Vol. 75, 55051-55066, September 9, 2010.
 25. Paone, P. (2010) Mercury controls for the cement industry. IEEE-1AS/PCA 52nd IEEE Cement Industry Technical Conference, Colorado Springs, CO, March 28 to April 1, 2010.
 26. Adaska, W.S. and Taubert, D.H. (2008) Beneficial uses of cement kiln dust. Presented at 2008 IEEE/PCA 50th Cement Industry Technical Conference Miami, Florida, May 19–22, 2008.
 27. Crowley, D. (2010) Cement kiln mercury reduction strategies a case study in materials management. IEEE-1AS/PCA 52nd IEEE Cement Industry Technical Conference, Colorado Springs, CO, March 28–April 1, 2010.
 28. Graydon, J.W., Zhang, X., Kirk, D.W., and Jia, C.Q. (2009) Sorption and stability of mercury on activated carbon for emission control. *J. Hazard. Mater.*, **168** (2-3), 978–982.
 29. Luo, Z., Hu, C., Zhou, J., and Cen, K. (2006) Stability of mercury on three activated carbon sorbents. *Fuel Process. Technol.*, **87** (8), 679–685.
 30. EPA (1997) *Mercury Study Report to Congress, An Evaluation of Mercury Control Technologies and Costs*, U.S. Environmental Protection Agency, vol. 8, p. ES-11, <http://www.epa.gov/mercury/report.htm> (accessed 19 March 2014).
 31. Durham, M., Bustard, J., Starns, T., *et al.* (2003) Full-scale results of mercury control by injecting activated carbon upstream of ESPs and fabric filters. Presented at ICAC Forum 2003, Nashville, Tennessee October 14–15, 2003.
 32. Laudal, D.L., Kay, J.P., Jones, M.L., and Pavlish, J.H. (2010) Issues associated with the use of activated carbon for mercury control in cement kilns. IEEE-1AS/PCA 52nd IEEE Cement Industry Technical Conference, Colorado Springs, CO, March 28–April 1, 2010.
 33. Kilgore, J. and Senior, C. (2003) Fundamental science and engineering of mercury control in coal-fired power plants. Presented at the Air Quality IV Conference, Arlington, Virginia, September 22–24, 2003.
 34. Portland Cement Association's Comments on EPA's Proposed (2009) National Emission Standards for Hazardous Air Pollutants for the Portland Cement Manufacturing Industry, Federal Register, Vol. 74, 21136, Docket Number: EPA-HQ-OAR-2002-0051.
 35. Niksa, S. and Fujiwara, N. (2005) The impact of wet flue gas desulfurization scrubbing on mercury emissions from coal-fired power stations. *J. Air Waste Manage. Assoc.*, **55**, 970–977.
 36. (2010) Summary of Environmental and Cost Impacts for Final Portland Cement NESHAP and NSPS, 40CFR Part 63, Subpart LLL, August 6, 2010. Docket Number EPA-HQ-QAR-2002-0051. Environmental Protection Agency (EPA).
 37. Lee, C.W., Srivastava, R.K., Ghorishi, S.B., Karwowski, J., Hasting, T.W., and Hirschi, J.C. (2006) Pilot-scale study of the effect of selective catalytic reduction catalyst on mercury speciation in Illinois and powder river basin coal combustion flue gases. *J. Air Waste Manage. Assoc.*, **56**, 643–649.
 38. Feeley, T.J. III, Murphy, J.T., Hoffmann, J.W., Granite, E.J., and Renninger, S.A. (2003) DOE/NETL's Mercury Control Technology Research Program for Coal-Fired Power Plants, EM Feature, pp. 16–23.
 39. Lee, C.W., Srivastava, R.K., Ghorishi, S.B., Hasting, T.W., and Stevens, F.M. (2004) Investigation of selective catalytic reduction impact on mercury speciation under simulated NOx emission control. *J. Air Waste Manage. Assoc.*, **54**, 1560–1566.
 40. Monroe, L.S. (2003) The Status of Mercury Control Technology, EM Feature, pp. 26–31.

Part IV

Mercury Research Programs in the United States

10

DOE's Mercury Control Technology Research, Development, and Demonstration Program

Thomas J. Feeley III, Andrew P. Jones, James T. Murphy, Ronald K. Munson, and Jared P. Ciferno

10.1

Introduction

The U.S. Department of Energy's (DOE's) National Energy Technology Laboratory (NETL) managed a comprehensive, collaborative program from the mid-1990s to 2008 that focused on the research, development, and demonstration (RD&D) of cost-effective mercury (Hg) control technologies, including investigating the potential impact of Hg control on the use and disposal of coal combustion byproducts. The overall goal of the program was to significantly lower the cost and increase the capture efficiency of advanced systems to remove Hg from coal combustion flue gas, should coal-fired power plants be regulated. NETL achieved this ambitious goal and ultimately was successful in bringing Hg control technology from what was only a concept in the early 1990s to a commercial product. As of 2010, pollution control equipment vendors have sold nearly 150 full-scale activated carbon injection (ACI) systems, a signature technology of the NETL program, to U.S. coal-fired power generators. These sales represent more than 56 GW of coal-fired electric generating capacity. The U.S. Environmental Protection Agency (EPA) projects that 146 GW of ACI will be installed on U.S. power plants by 2015 in order to comply with proposed Federal Hg emission control regulations [1]. The Hg control systems developed under the NETL program that are currently being deployed by the electric-utility industry have the potential to achieve 80–90% or more Hg reduction at a cost that can dip below \$10 000 per pound of Hg removed, compared to baseline costs of \$50 000–70 000 per pound of Hg.

10.2

Background

Coal is one of the United States' most abundant and secure energy resources and coal-based power systems generated ~45% of the nation's electricity in 2009 [2]. Coal is projected to continue to be an important component of the U.S. energy

Mercury Control: for Coal-Derived Gas Streams, First Edition.

Edited by Evan J. Granite, Henry W. Pennline and Constance Senior.

© 2015 Wiley-VCH Verlag GmbH & Co. KGaA. Published 2015 by Wiley-VCH Verlag GmbH & Co. KGaA.

portfolio well into the twenty-first century. While coal-based power plants have made significant strides since the early 1970s in substantially reducing emissions of particulate matter (PM), sulfur dioxide (SO₂), and nitrogen oxide (NO_x), environmental challenges still exist. One of those challenges is Hg. Mercury is found in trace amounts in coal, and much of it escapes capture by technologies designed to remove PM, SO₂, and NO_x. Today, coal-fired utility boilers represent the largest source of anthropogenic Hg emissions in the United States, accounting for about 50% of all man-made emissions [1].

Mercury is present in dilute concentrations in power plant flue gases. Liquid at room temperature and pressure, Hg, when heated, is volatile and easily vaporized. Depending on the type or mix of coal being burned and the downstream emissions control systems being employed by a power plant, Hg is released to the atmosphere in varying percentages in two primary gaseous forms – elemental Hg and oxidized Hg. It can also be emitted as particulate-bound Hg.

As part of the 1990 Clean Air Act Amendments (CAAAAs), Congress mandated that EPA assess the potential health impacts of Hg and other hazardous air pollutants and, if necessary, set standards that would reduce these impacts. In 2000, EPA determined that there was sufficient evidence of a link between Hg emitted from stationary sources and certain adverse health effects and began crafting regulations. In March 2011, EPA proposed new Federal Hg standards (known as *Maximum Achievable Control Technology (MACT)*) that would reduce Hg emissions from coal- and oil-fired power plants by more than 90%. The new proposed rule will replace the vacated Clean Air Mercury Rule (CAMR) that was issued by EPA in March 2005. The proposed MACT standards would establish plant-specific numerical emission limits for Hg, PM (a surrogate for toxic, non-Hg metals), and hydrochloric acid (a toxic acid gas). The final MACT rule was promulgated in November 2011. Due in part to EPA's delay in setting Federal Hg emission standards, state regulatory agencies began implementing Hg standards. As of February 2011, at least 14 states had laws or regulations requiring Hg emission reductions at coal-fired power plants [3].

10.2.1

NETL's Hg Control Technology R&D

Paralleling EPA's assessment of the health effects of Hg, NETL initiated an ambitious Hg control technology research and development (R&D) program in the mid-1990s [4]. The program was driven by concerns that cost-effective Hg capture technology did not exist should EPA conclude that Hg emissions from coal-fired power plants and other stationary sources needed to be regulated. Under DOE's Office of Fossil Energy's (FEs) Innovations for Existing Plants (IEP) Program, NETL worked collaboratively with EPA, the Electric Power Research Institute (EPRI), the University of North Dakota Energy and Environmental Research Center (UNDEERC), power plant operators, and state and local agencies, as well as a host of research organizations, technology developers, and academic institutions, to bring to commercial readiness both reliable techniques for measuring the

different chemical forms of Hg in coal-based flue gas and cost-effective technologies and approaches for reducing Hg emissions from power plants.

More than \$120 million in Federally funded extramural and in-house research was conducted under the IEP Hg Program – including more than \$30 million in private-sector cost sharing – directed at five interrelated research areas:

- Emissions characterization.
- Development and testing of measurement devices.
- Speciation research.
- Development and field testing of control technologies.
- Coal utilization byproducts (CUBs) characterization.

The overall short-term goal of the NETL Hg R&D Program was to develop Hg control technologies that would be ready for commercial demonstration by 2007 and that could achieve 50–70% Hg capture at 50–75% of the cost of state-of-the-art ACI estimated to be between \$50 000 and \$70 000 per pound of Hg removed. The NETL Hg R&D Program had a longer-term goal of developing advanced Hg control technologies that could achieve 90% or greater capture at 50–75% of the cost of state-of-the-art ACI technology for commercial demonstration by 2010. However, in 2008, it was determined that DOE had successfully achieved its goal of bringing efficient, cost-effective Hg control technologies to commercial readiness and that further development and refinement of Hg control systems should be carried out by the private sector.

10.2.2

Mercury Speciation

Analysis of flue gas samples conducted early in the NETL program revealed that the trace amount of Hg present in coal is volatilized during combustion and converted to gaseous elemental mercury (Hg^0). Subsequent cooling of the coal combustion flue gas and interaction of the gaseous Hg^0 with other flue gas constituents, such as chlorine (Cl) and unburned carbon (UBC), result in a portion of the Hg^0 being converted to gaseous oxidized forms of mercury (Hg^{2+}) and particulate-bound mercury (Hg_p) [5].

The initial research conducted by NETL and other organizations, such as EPRI and UNDEERC, further showed that the varying percentages of Hg_p , Hg^{2+} , and Hg^0 had a profound effect on the Hg capture efficiency of existing air pollution control devices (APCDs) designed to control PM, SO_2 , and NO_x emissions, ranging from 0% to more than 90% removal [6]. The Hg_p fraction typically was captured by a power plant's particulate control system, such as an electrostatic precipitator (ESP) or fabric filter (FF). The Hg^{2+} portion is water-soluble, and therefore a relatively high percentage was shown to be removed in a plant's wet flue gas desulfurization (FGD) unit designed to remove SO_2 . The Hg^0 fraction is generally not captured by any existing APCD. In addition, operation of a selective catalytic reduction (SCR) system for control of NO_x emissions was shown to promote Hg^0 oxidation and enhance Hg capture across a downstream FGD [7].

In summary, NETL's Hg speciation research revealed that (i) several key factors influence Hg speciation in coal combustion flue gas; (ii) Hg speciation impacts the level of Hg control achieved by existing APCD configurations; and (iii) Hg capture across existing APCD configurations could be enhanced.

10.2.3

Mercury Control Technologies

The Hg speciation research set the stage for the development of a suite of Hg control technologies that would be needed for the diverse fleet of U.S. coal-fired power plants. The research was directed at two general approaches for controlling Hg: (i) Hg^0 oxidation concepts that maximize co-benefit removal of Hg^{2+} in wet FGD systems and (ii) Hg-specific control technology, such as ACI. In a typical ACI configuration, powdered activated carbon (PAC) is injected downstream of the power plant's air heater and upstream of the particulate control device – either an ESP or FF (Figure 10.1). The PAC adsorbs the Hg from the combustion flue gas and is subsequently captured along with the fly ash in the ESP or FF.

In 2000, following laboratory-through pilot-scale development of these approaches, NETL launched a three-phase field testing program. The program called for full-scale and slip-stream testing of Hg control technologies over a limited test period at operating coal-fired power plants. The initial field testing (Phase I) focused on both slip-stream and larger-scale testing of conventional (untreated) PAC and on improving the capture of Hg across wet FGD systems. Phase II, which began in 2003, included longer duration, full-scale field testing of chemically treated ACI, sorbent enhancement additives (SEAs), and sorbent-based technologies designed to preserve fly ash quality. Phase II also included evaluations of chemical additives and Hg^0 oxidation catalysts to enhance FGD Hg capture. The goal of Phase I and Phase II was to develop Hg control technologies that could achieve 50–70% Hg capture at costs 25–50% less than

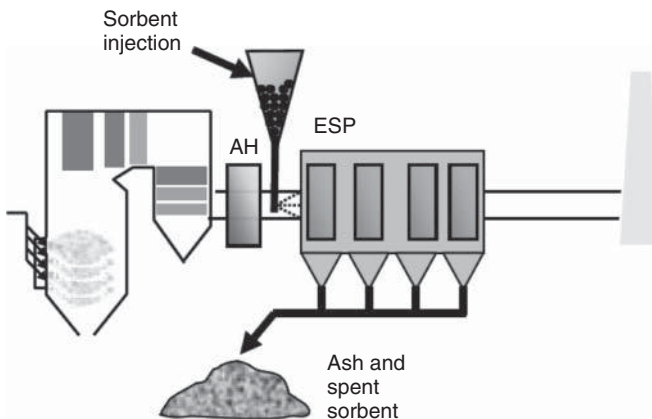


Figure 10.1 Activated carbon injection technology schematic.

the baseline (1999) estimate of about \$60 000 per pound of Hg removed (\$/lb Hg removed).

While the 30-day-long tests conducted in Phase II yielded significant information on the performance of the advanced Hg control technologies, the testing period was not always sufficient to answer all of the questions about the impact these systems might have on power plant operations. To better understand potential balance-of-plant impacts and to further push the capture effectiveness of the Hg control technologies, NETL initiated nine new projects in 2006 to conduct longer duration field tests. The Phase III projects supported the NETL Hg R&D Program's longer-term goal of developing advanced Hg control technologies that could achieve at least 90% Hg capture and be available for commercial demonstration by 2010.

10.2.4

Results from Field Testing Program

Between 2000 and 2008, the NETL Hg R&D Program managed full-scale field tests of Hg control technologies at nearly 50 U.S. coal-fired power generation facilities. The flexibility of the Hg R&D Program allowed NETL to quickly incorporate insights and lessons learned into the development of advanced Hg control technologies tailored to specific areas of need. For instance, a determination that Cl released during coal combustion promotes Hg oxidation in flue gas led to field testing of technologies designed to provide a halogen "boost" for coals such as subbituminous and lignite. NETL had observed a step-change improvement in both the cost and performance of Hg control during full-scale field tests of coal treatment with an aqueous calcium bromide (CaBr_2) solution at plants equipped with a wet FGD system, and during tests using chemically treated (or brominated) ACI upstream of a particulate control device.

10.2.5

Oxidation Enhancements

Oxidation of flue gas Hg^0 followed by absorption of Hg^{2+} across a wet FGD system has the potential to be a reliable and cost-effective Hg control strategy for some coal-fired power plants. To optimize Hg capture across FGD systems, NETL funded field tests of technologies, such as chemical additives and Hg^0 oxidation catalysts that promote Hg^0 oxidation in coal combustion flue gas. The impacts of combustion modification, such as coal reburn, on flue gas Hg^0 oxidation were also examined under the NETL Hg R&D Program [8]. In addition, NETL evaluated FGD additives designed to suppress Hg^0 re-emissions across an FGD system. Originally thought to be a sampling artifact, Hg^0 re-emissions were observed at several coal-fired units to occur when Hg^{2+} captured by a wet FGD is chemically reduced within the vessel and reemitted as Hg^0 .

10.2.6

Chemical Additives

The ability of chemical additives, sprayed onto the coal as an aqueous salt solution, to promote flue gas Hg^0 oxidation and enhance FGD Hg capture was evaluated during a full-scale field test at Luminant Power's Monticello Station Unit 3 [9]. During a 2-week trial conducted at Monticello Station, which burns a 50:50 blend of Powder River Basin (PRB) subbituminous and Texas lignite (TxL) coals, total Hg capture across the ESP/FGD configuration averaged 86% with a CaBr_2 injection rate equivalent to 113 ppm Br in the dry coal. Greater than 90% total Hg capture was observed during a short-term test with a CaBr_2 injection rate equivalent to 330 ppm Br in the coal.

NETL also conducted pilot- and full-scale field tests of wet FGD additives designed to limit Hg^0 reemissions through the formation of insoluble salts with Hg^{2+} [10]. The effectiveness of Degussa Corporation's TMT-15 additive in suppressing Hg^0 reemissions was also evaluated at the Monticello Station and at Southern Company's bituminous-fired Plant Yates. The results were inconclusive due to (i) the absence of reemissions, even without chemical addition, at Monticello Station and (ii) Hg measurement issues at Plant Yates. However, TMT-15 had the anticipated impact on FGD byproducts as the FGD liquor Hg concentrations were significantly reduced during both tests. During a full-scale field test at Indianapolis Power and Light's Petersburg Station, which burns high-sulfur bituminous coal, a modest decline in Hg^0 reemissions was observed during an 8-day TMT-15 injection test, but the additive did not impact the partitioning of Hg in FGD byproducts at this site. Meanwhile, full-scale results obtained during a 30-day evaluation of Nalco Company's 8034 additive at Plant Yates were confounded by low baseline Hg^0 reemission levels. A third wet FGD additive to reduce Hg reemission, Babcock and Wilcox's Absorption Plus (Hg)TM, was evaluated at E.ON America's high-sulfur bituminous-fired Mill Creek Station after parametric trials revealed that untreated ACI had little, if any, impact on Hg removal [11]. During long-term testing, total Hg removal averaged about 92% with the addition of Absorption Plus (Hg). Note that more than 80% of total Hg removal was observed under baseline conditions.

10.2.7

Catalysts

The ability of fixed-bed catalysts to promote flue gas Hg^0 oxidation was evaluated at pilot-scale, and a full-scale field test of a gold-based catalyst was conducted in 2008/2009 at Lower Colorado River Authority's Fayette Unit 3 [12]. The catalysts were designed for installation downstream of an ESP or FF to (i) minimize fly ash deposition on the catalysts; (ii) prevent or minimize catalyst erosion; and (iii) ensure a low flue gas temperature and flow rate, which reduces the catalyst space velocity and minimizes the length of catalyst required. The full-scale catalyst test was planned for 24 months to provide catalyst life data. However, the test

was terminated after 17 months because of continual increases in pressure drop across the catalyst. The adverse effects of the fly ash buildup on oxidation catalyst performance, along with variable Hg reemissions across the Unit 3 wet FGD absorbers, led to an increase in Hg removal averaging only 27–30% during the demonstration.

During pilot-scale testing at Great River Energy's (GREs) North Dakota lignite-fired Coal Creek Station, about 67% Hg⁰ oxidation was measured across a palladium-based (Pd#1) catalyst after 20 months of operation. Following thermal regeneration, Hg⁰ oxidation across the Pd#1 catalyst increased from 67% to 88% (near the 95% activity of the fresh catalyst). Meanwhile, nearly 80% total Hg capture was observed across the pilot-scale wet FGD, with 84% Hg²⁺ at the FGD inlet. At Luminant Power's Monticello Station, severe fly ash buildup was observed on the catalyst surfaces, likely caused by frequent pilot unit outages during the test campaign. Following catalyst cleaning, Hg⁰ oxidation was ~72% across the regenerated Pd#1 catalyst (transferred from Coal Creek) and 66% across a gold-based catalyst after about 20 months of pilot-scale operation. Total Hg capture across a pilot-scale wet FGD ranged from 76% to 87%, compared with only 36% removal under baseline conditions. This equates to about 70% incremental Hg capture due to the catalysts.

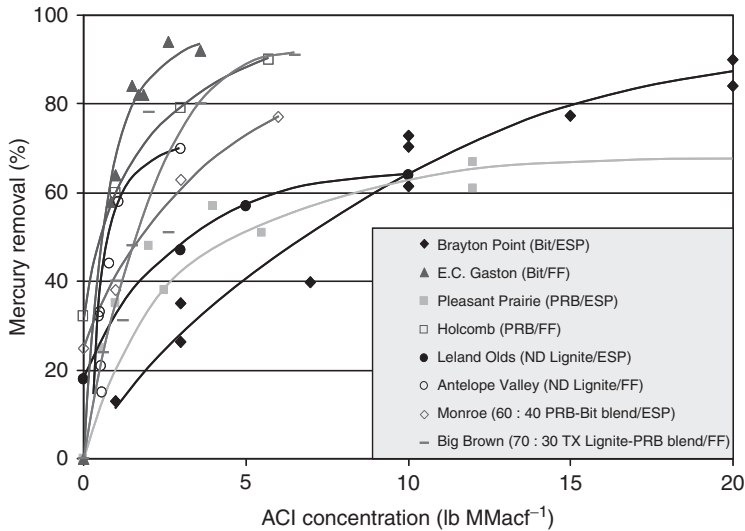
10.2.8

Activated Carbon Injection

DOE/NETL's portfolio of full-scale field testing projects encompassed several variations of sorbent injection technology: untreated PAC, untreated PAC with chemical additives, chemically treated PAC, EPRI's toxic emissions control (TOXECON™) configuration, TOXECON II™, and non-carbon and "concrete-friendly" PAC sorbents. The development, and subsequent field testing, of ACI with chemically treated PAC and chemical additives, in conjunction with untreated PAC, represented a concerted effort to enhance Hg capture at units firing low-rank coal after Phase I results at the PRB-fired Pleasant Prairie Unit 2 showed total Hg removal via untreated PAC was limited to about 65%. These advanced, Hg-specific control technologies were designed to introduce excess halogens into the Cl-deficient flue gas emitted from low-rank coals to promote Hg⁰ oxidation and adsorption. Meanwhile, minimizing the impact of ACI on fly ash utilization was the driving force behind field testing of the TOXECON configurations and non-carbon/"concrete-friendly" sorbent injection.

10.2.8.1 **Untreated PAC**

NETL's initial field testing using ACI with untreated PAC was conducted by ADA-ES at four coal-fired power plants (E.C. Gaston, Pleasant Prairie, Brayton Point, and Salem Harbor) in 2001–2002 [13]. Testing included parametric tests using several commercially available PAC products at various feed rates and operating



* All data generated using NORIT Americas' DARCO® Hg.

Figure 10.2 Test results for untreated activated carbon injection.

conditions, followed by a 1–2 week short-term test with a PAC selected from the parametric testing. Test results for E.C. Gaston, Pleasant Prairie, and Brayton Point are shown in Figure 10.2. The ACI test results at Salem Harbor were inconclusive because average Hg capture was already at 90% during baseline testing without PAC injection. The high baseline Hg removal was attributed to high levels of UBC and low flue gas temperature.

Untreated PAC was also evaluated during two 30-day long-term tests at Plant Yates Unit 1 during subsequent field testing during Phase II of NETL's R&D Program. URS selected RWE Rhinebraun's Super HOK sorbent and total Hg capture varied from 50–86%, with injection rates ranging from 4.5 to 9.5 lb MMacf⁻¹ [14]. Plant Yates was selected for long-term testing, in part, to gain a better understanding of the effect of ACI on small specific collection area (SCA) ESP (173 SCA) and wet FGD operation. URS observed an increase in the ESP arcing rate during continuous ACI, particularly at high load. While the 30-day long-term injection test caused no visible physical damage to the ESP, it was unclear what effect the increased arcing rate would have on ESP performance over longer time periods.

ADA-ES chose DARCO® Hg PAC for the 30-day long-term test conducted at DTE Energy's Monroe Station Unit 4, which burns a 60% PRB and 40% bituminous coal blend and is equipped with an SCR and cold-side-electrostatic precipitator (CS-ESP) [15]. Total Hg removal averaged 78% with DARCO Hg injection at 4.9 lb MMacf⁻¹. The performance of untreated DARCO Hg during select full-scale field tests is presented in Figure 10.2.

10.2.8.2 Chemically Treated PAC

The limited Hg removal achieved by untreated ACI at Pleasant Prairie spurred the development and full-scale field testing of alternatives, such as PAC chemically treated with Br. Two brominated PACs – NORIT Americas' DARCO Hg-LH and Sorbent Technologies' B-PAC™ – were consistently top performers at field testing units burning lower-rank coals. In fact, the outstanding performance (see Figure 10.3) of these brominated sorbents accelerated the commercialization of Hg-specific control technologies and drastically reduced the estimated cost of Hg control due to a reduction in the ACI rate required to achieve a given level of control, which offsets the higher cost of these sorbents.

ADA-ES selected brominated DARCO Hg-LH for 30-day long-term field tests at two PRB-fired units: Sunflower Electric's Holcomb Station Unit 1 and AmerenUE's Meramec Station Unit 2. At Meramec, 93% average total Hg removal was achieved across the CS-ESP with DARCO Hg-LH injection at 3.3 lb MMacf⁻¹ [16]. Total Hg capture averaged 93% across the spray dryer absorber (SDA)/FF configuration at Holcomb with DARCO Hg-LH injection at 1.2 lb MMacf⁻¹ [17]. UNDEERC also conducted a 30-day evaluation of DARCO Hg-LH at GRE's North Dakota lignite-fired Stanton Station Unit 10. With DARCO Hg-LH injection at 0.7 lb MMacf⁻¹, total Hg capture across the SDA/FF configuration averaged 59% [18]. However, >90% Hg capture was achieved at this unit during parametric trials with both DARCO Hg-LH and B-PAC injection at 1.5 lb MMacf⁻¹.

The brominated B-PAC sorbent was also selected for 30-day long-term trials at three of NETL's field testing sites. At GRE's PRB-fired Stanton Station Unit 1, URS observed 85% average total Hg removal across the CS-ESP with B-PAC injection at 1.7 lb MMacf⁻¹ [19]. Sorbent Technologies conducted long-term field tests with B-PAC at DTE Energy's St. Clair Station Unit 1 that burned an 85% PRB and 15% bituminous coal blend, and at Progress Energy's bituminous-fired Lee Station

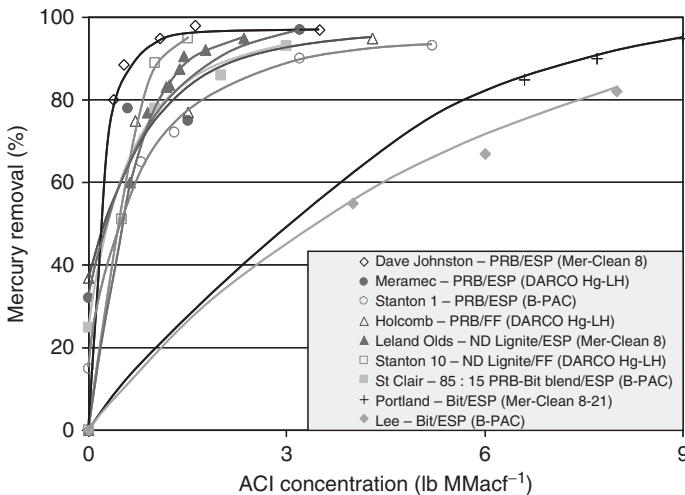


Figure 10.3 Test results for treated activated carbon injection.

Unit 1. At St. Clair, 94% average total Hg removal was achieved across the CS-ESP with B-PAC injection at 3 lb MMacf⁻¹ [20]. Total Hg capture averaged 85% across the CS-ESP at Lee with B-PAC injection at 8 lb MMacf⁻¹ [19]. Note that the 30-day long-term test at Lee was conducted with the sulfur trioxide (SO₃) flue gas conditioning (FGC) system idled and opacity levels remained acceptable.

ADA-ES conducted field testing at Rocky Mountain Power's PRB-fired Hardin Generating Station to evaluate the Hg removal performance, long-term emissions variability, and associated operating and maintenance costs of PAC injection for >90% Hg control during a year-long, full-scale demonstration. Baseline Hg capture at Hardin ranged from 20–30% across the SCR and SDA/FF configuration [21]. During parametric testing, an injection rate of about 1 lb MMacf⁻¹ was required to attain slightly more than 90% total Hg removal with DARCO Hg-LH and Calgon Carbon's brominated FLUEPAC™-MC Plus. In addition, injection of a DARCO Hg and FLUEPAC-MC Plus mixture achieved 90% total Hg at 0.14 lb MMacf⁻¹, with a low KNX™ additive rate.

URS conducted field testing at NRG Texas Power LLC's Limestone Electric Generating Station Unit 1 that fired a 70:30 blend of TxL and PRB coals and was equipped with a CS-ESP and wet FGD. Baseline Hg removal was highly variable, ranging from about 5–50%. Since this unit markets its fly ash for reuse, two Hg control technologies designed to preserve ash quality were evaluated during parametric tests: low-ash impact sorbent injection and TOXECON II [22]. During injection upstream of the ESP, the brominated B-PAC and DARCO Hg-LH sorbents performed similarly, with about 90% ACI Hg removal at 2–3 lb MMacf⁻¹. Untreated DARCO Hg also achieved 90% ACI Hg removal with injection at slightly <6 lb MMacf⁻¹. Injection of the "concrete-friendly" C-PAC™ sorbent at about 1.5 lb MMacf⁻¹ resulted in ~73% ACI Hg removal. During parametric trials with the TOXECON II configuration, ACI Hg removal was limited to about 60% with DARCO Hg and DARCO Hg-LH injection at about 5–6 lb MMacf⁻¹. Note that DARCO Hg-LH injection into the TOXECON II configuration took place with the unit firing 100% PRB coal. A 2-month continuous injection test was completed with DARCO Hg-LH injection at 2 lb MMacf⁻¹, and results indicated that the project goal of 50–70% ACI Hg removal across the ESP was achieved. In addition, URS was confident that the low DARCO Hg-LH injection rate would not prohibit fly ash reuse.

Another chemically treated ACI technology tested under the NETL Hg Program, ALSTOM Power, Inc.–U.S. Power Plant Laboratories' (ALSTOM–PPLs) Mer-Cure™ process, is unique in that injection takes place in the high-temperature region upstream of the air preheater (APH) and the process employs a proprietary "processor" to prevent chemically treated Mer-Clean™ sorbent agglomeration and to ensure uniform sorbent dispersion [23]. Three 30-day long-term field tests of Mer-Cure were completed at sites equipped with a CS-ESP: (i) PacifiCorp's PRB-fired Dave Johnston Unit 3; (ii) Leland Olds Unit 1; and (iii) Reliant Energy's medium-sulfur (2%) bituminous-fired Portland Station Unit 1. Chemically treated Mer-Clean eight injection rates of 0.63 and 1.4 lb MMacf⁻¹ achieved average total Hg removals of 92% and 90% at Dave

Johnston and Leland Olds, respectively. At Portland, about 95% average total Hg capture was observed with chemically treated Mer-Clean 8–21 injection at $8.5 \text{ lb MMacf}^{-1}$. The reduced efficiency of the Mer-Clean sorbents at Portland might have been caused by elevated levels of flue gas SO_3 , resulting from the combustion of medium-sulfur bituminous coal.

An evaluation of Mer-Cure was completed at LCRA's Fayette Unit 3 in April 2007 [24]. Baseline Hg capture was $\sim 50\%$ across the CS-ESP and wet FGD. ALSTOM–PPL evaluated three sorbents (eSorb™ 11, eSorb™ 13, and eSorb™ 18) designed to preserve fly ash quality, along with Mer-Clean 8, during parametric testing. Excluding eSorb 18, 80% ACI Hg capture was achieved with injection at $0.4\text{--}0.5 \text{ lb MMacf}^{-1}$. At an injection at about $0.8 \text{ lb MMacf}^{-1}$, eSorb 11, and Mer-Clean 8 attained 90% ACI Hg capture. Test results indicate that fly ash remains marketable with eSorb 13 at about $0.5 \text{ lb MMacf}^{-1}$ (85% ACI Hg capture).

10.2.8.3 Conventional PAC with Chemical Additives

As an alternative to using chemically treated PAC, NETL also sponsored field tests using conventional PAC supplemented with chemical additives – known as *sorbent enhancement additives* (SEA) – applied to the coal and/or flue gas to overcome the poor performance of conventional PAC in low-rank coal applications. Through funding provided by NETL, UNDEERC conducted two 30-day long-term field tests at full-scale units firing North Dakota lignite coal to determine whether SEA coal treatment enhances the performance of untreated ACI at units burning lower-rank coals [18]. Indeed, SEA coal treatment improved the Hg capture efficiency of untreated ACI at both of these field testing sites. During the 30-day trial at Basin Electric's Leland Olds Station Unit 1, 58% average total Hg capture was observed across the CS-ESP with DARCO Hg injection at $2.7 \text{ lb MMacf}^{-1}$, coupled with the addition of an aqueous CaCl_2 solution to the North Dakota lignite coal at a rate of $2.9 \text{ lb MMacf}^{-1}$. UNDEERC also evaluated this advanced, Hg-specific control technology at Basin Electric's Antelope Valley Station Unit 1. Total Hg removal averaged 92% across the SDA/FF configuration with the addition of SEA2 to the North Dakota lignite coal at a rate of $0.033 \text{ lb MMacf}^{-1}$ and DARCO Hg injection at $0.81 \text{ lb MMacf}^{-1}$.

UNDEERC conducted additional field testing at Montana-Dakota Utilities Company's Montana lignite-fired Lewis and Clark Station that was equipped with a mechanical collector and wet venturi scrubber. Parametric tests evaluated the Hg capture efficiency of SEA1 and SEA2 addition to the coal with and without ACI upstream of the wet venturi scrubber [25]. With SEA1 injection at 600 ppm coal equivalent, about 90% Hg removal was achieved with untreated DARCO Hg injection at 3 lb MMacf^{-1} . Slight improvements in performance were observed with higher SEA1 and DARCO Hg injection rates. Ninety percent Hg removal was also observed with SEA2 injection at 100 ppm coal equivalent and DARCO Hg injection at 1 lb MMacf^{-1} . Note that in the absence of PAC injection, Hg removal was limited to about 55% with SEA2 injection at 100 ppm coal equivalent.

UNDEERC evaluated PAC and SEA injection, as well as the SEA2 technique 2 (SEA2 T2) technology that involves co-injection of the proprietary SEA2 additive and PAC upstream of the particulate control device. Full-scale field testing was conducted at Kansas City Power & Light's Hawthorn Unit 5 that burns PRB coal and was equipped with an SCR and SDA/FF configuration. During parametric testing at Hawthorne, >90% total Hg capture was achieved with SEA1 added to the coal at 1200 ppm and DARCO Hg-LH injection at 3 lb MMacf⁻¹ [26]. With the SEA2 T2 technology, the co-injection of DARCO Hg at 2.8 lb MMacf⁻¹ and SEA2 at 0.14 lb/lb of PAC resulted in about 85% total Hg removal.

10.2.8.4 ACI Upstream of a Hot-Side ESP

NETL also evaluated Hg control technologies designed specifically for hot-side electrostatic precipitator (HS-ESP) applications where the elevated flue gas temperature limits the Hg capture efficiency of ACI. A 4-day trial conducted at Duke Energy's low-sulfur bituminous coal-fired Buck Plant achieved ~70% total Hg removal with the injection of Sorbent Technologies' chemically treated H-PAC™ at 10 lb MMacf⁻¹ [20]. Sorbent Technologies conducted additional field testing at Midwestern Generation's PRB-fired Will County Unit 3. A high-temperature version of the brominated, "concrete-friendly" C-PAC sorbent was evaluated as fly ash from this unit is marketed for reuse. Using a newly developed X-a-Lance distributing lance design, 73% Hg removal was achieved during a parametric trial with C-PAC injection at 5 lb MMacf⁻¹ [27]. During a 6-day continuous test, Hg removal ranged from about 60–73% with C-PAC injection at 5 lb MMacf⁻¹.

Under a separate project, ADA-ES evaluated the impact of adding high-temperature liquid sorbents to the pre-combusted coal and/or upstream of the HS-ESP on Hg control at MidAmerican's PRB-fired Louisa Station Unit 1 [28]. While Alstom's brominated KNX coal additive promoted Hg⁰ oxidation, the lack of a downstream FGD at this unit led to no increase in Hg removal.

10.2.9

Remaining Technical Issues

Although the development of chemically treated ACI, oxidation additives, and catalysts under NETL's R&D Program has significantly improved the cost and performance of Hg control for coal-based power plants, two primary technical issues remain – impacts on fly ash and sulfur trioxide interference.

10.2.9.1 Impacts on Fly Ash

The typical ACI system is located upstream of a particulate control device to enable simultaneous capture of the spent sorbent and fly ash. This Hg control strategy leads to commingling of the sorbent and fly ash that can prohibit certain fly ash recycling efforts. In 2009, U.S. power plants generated 63 million tons of fly ash, with nearly 25 million tons put to beneficial use. One of the highest-value reuse applications for fly ash is as a substitute for Portland cement in concrete

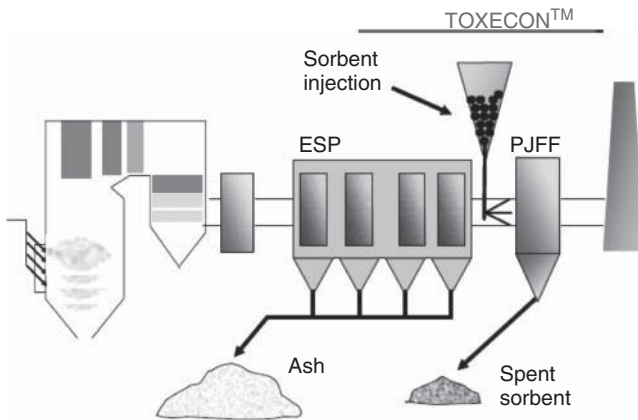


Figure 10.4 EPRI's TOXECON™ process configuration.

production [29]. The utilization of fly ash in concrete production is particularly sensitive to carbon content as well as the surface area of the carbon present in the fly ash.

NETL's Hg control technology portfolio included alternative sorbent injection technologies designed to minimize fly ash carbon contamination caused by ACI upstream of a particulate control device. The TOXECON configuration, developed by EPRI, is designed not to impact fly ash utilization because the ash is removed by an ESP upstream of the sorbent injection location, whereas the spent sorbent is captured by a downstream FF (Figure 10.4). EPRI's TOXECON II technology injects sorbents directly into the downstream collecting field(s) of an ESP. Because the majority of fly ash (~90%) is collected in the upstream ESP fields, only a small portion of the total collected ash contains spent sorbent. During full-scale TOXECON II testing at Entergy's PRB-fired Independence Station Unit 1, DARCO Hg-LH injection at $5.5 \text{ lb MMacf}^{-1}$ achieved 90% total Hg removal [30]. A remaining concern with any Hg control strategy involving sorbent injection, particularly the TOXECON II configuration that limits ESP residence time, is the potential for inefficiencies in the existing particulate control system that could trigger New Source Review.

Activated carbon passivated during production can potentially allow coal-fired power generators to continue marketing fly ash commingled with the spent sorbent as a suitable replacement for Portland cement in concrete. Sorbent Technologies conducted a 30-day evaluation of their brominated, "concrete-friendly" C-PAC sorbent at Midwest Generation's PRB-fired Crawford Station Unit 7 [31]. Total Hg removal averaged 81% with C-PAC injection upstream of the ESP at about $4.6 \text{ lb MMacf}^{-1}$. A high-temperature version of C-PAC was tested at Midwest Generation's PRB-fired Will County Unit 3 that is equipped with an HS-ESP [32]. During a 6-day continuous test, Hg removal ranged from about 60–73% with C-PAC injection at 5 lb MMacf^{-1} . Most importantly, test results indicated that fly

ash collected during C-PAC injection at these sites remained suitable for reuse in concrete production.

During testing at Lower Colorado River Authority's PRB-fired Fayette Unit 3, Alstom evaluated three sorbents (eSorb 11, eSorb 13, and eSorb 18) designed by Envergen to preserve fly ash quality [33]. Results indicated that fly ash remains marketable with eSorb 13 at about $0.5 \text{ lb MMacf}^{-1}$ (~85% ACI Hg capture).

10.2.9.2 Sulfur Trioxide Interference

Field testing showed that SO_3 in the flue gas, even at low concentrations, can impede the performance of ACI. It appears that SO_3 competes with Hg for adsorption sites on the sorbent surface, thereby limiting its performance [34]. During field testing at American Electric Power's (AEP's) high-sulfur (3–4%) bituminous-fired Conesville Station Unit 6, total Hg removal was limited to ~30% with chemically treated ACI at 12 lb MMacf^{-1} [35]. Consequently, a long-term field test was not conducted at this unit; instead, NETL evaluated the impact of SO_3 FGC on ACI performance at AmerenUE's PRB-fired Labadie Station Unit 2 [36]. As shown in Figure 10.5, turning the SO_3 FGC system off at Labadie increased total Hg removal from about 50–80% with DARCO Hg-LH injection at 8 lb MMacf^{-1} . Greater than 90% Hg removal was observed with no SO_3 injection and DARCO Hg-LH injection upstream of the APH at about 5 lb MMacf^{-1} . The performance of brominated B-PAC was also impacted by SO_3 FGC at Progress Energy's Lee Station Unit 1 [37]. With B-PAC injection at 8 lb MMacf^{-1} , Hg capture increased from 32% to 82% when SO_3 FGC was idled.

One possible solution to the SO_3 issue that was considered was dual injection of Hg sorbents and alkaline materials. This approach was explored during a field test

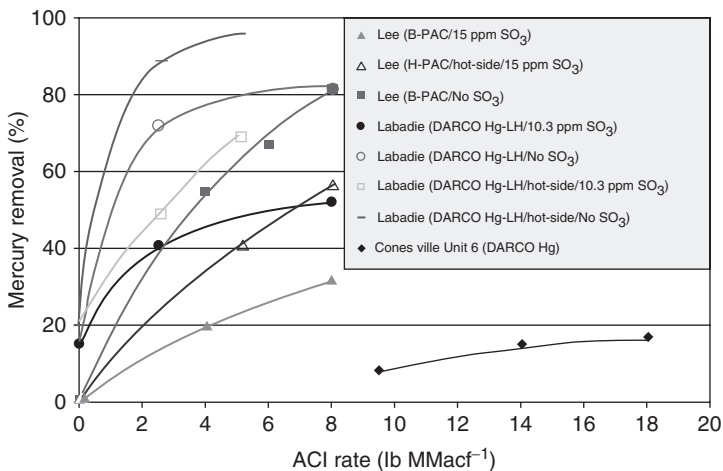


Figure 10.5 Impact of flue gas SO_3 on ACI performance.

at Public Service of New Hampshire Company's Merrimack Station Unit 2 that utilized a cyclone-fired boiler to burn a blend of bituminous coals (~1% sulfur) and is equipped with an SCR system followed by two ESPs in series [38]. During parametric testing, several Hg sorbents were evaluated both with and without the injection of two potential SO₃ mitigation additives – magnesium oxide (MgO) and sodium sesquicarbonate (trona). Results indicated that trona injection enhanced ACI performance to a greater degree than MgO; however, the sodium content of trona could limit fly ash recycling opportunities. Without SO₃ mitigation, Hg removal was limited to about 22% with brominated DARCO Hg-LH injection between the two ESPs at 8 lb MMacf⁻¹. During a continuous injection test completed in March 2008, 50% Hg removal was achieved with trona injection upstream of the APH at 500 lb h⁻¹ and DARCO Hg-LH injection between the two ESPs at about 4 lb MMacf⁻¹.

10.2.10

NETL In-House Development of Novel Control Technologies

In addition to the technologies developed in partnership with private sector companies, researchers from NETL's Office of Research and Development (ORD) also developed and patented technologies for capturing and detecting mercury from coal-based power systems. In one case, ultraviolet light near the wavelength of 254 nm was found to oxidize elemental mercury [39]. The oxidized form of mercury is much more readily removed by the more traditional capture techniques than elemental mercury. This method was unique not only because the photochemical technique enhances the capture of mercury, but also because, as a spinoff, it can be used as the basis for mercury detection. Another patented technique that had been developed uses a lance or "thief" to extract a partially combusted coal from the combustion section of a pulverized coal-fired combustor [40]. This material acts very similarly to that of activated carbon and will remove mercury when injected into the flue gas ductwork. Not only can the thief process be used to capture mercury, the carbon-based material itself, and a few other materials were also found able to catalytically convert elemental mercury to the oxidized form.

Recognizing the need for a low-cost technique to remove Hg from coal-based integrated gasification combined cycle (IGCC) power plants, ORD researchers invented a new palladium (Pd)-based sorbent that works on fuel gas at elevated temperatures [41]. IGCC plants will be affected by the new mercury regulation. Although electricity in the United States is primarily a product of combusting coal, IGCC may be the power generation method in the future if mitigation of the greenhouse gas carbon dioxide is imposed on the power industry. Unlike conventional sorbents such as activated carbon, which operate at a lower temperature, high-temperature Pd sorbents remove Hg and arsenic at temperatures above 500 °F, resulting in a major improvement in overall thermal energy efficiency of the IGCC power process.

10.2.11

Hg Control Technology Commercial Demonstrations

A key component of the overall success of NETL's Hg Program was the full-scale commercial demonstration of Hg control technology under DOE's Clean Coal Power Initiative (CCPI). CCPI was part of DOE's Major Demonstration Program directed at accelerating advanced coal technology adoption, thus rapidly moving promising new concepts to a point where private-sector decisions on deployment could be made.

In the first project, EPRI's TOXECON was selected for demonstration on a 270-MW slipstream at We Energies' Presque Isle Power Plant in Marquette, Michigan. During initial operation in 2006, the TOXECON configuration maintained >90% total Hg removal for 48 consecutive days. Sorbent injection rates of about 1.7 and 1.2 lb MMacf⁻¹ were required to achieve at least 90% total Hg removal with untreated DARCO Hg and brominated DARCO Hg-LH, respectively [42]. Over a 3-year demonstration period (2006–2009), We Energies consistently demonstrated more than 90% Hg removal based on monthly averages while maintaining acceptable baghouse pressure drops of 5–6 in. of water and providing significant opacity improvements. The TOXECON installation at Presque Isle cost \$128 per kilowatt (kW) and increased the cost of electricity by about 0.3–0.5 cents kWh⁻¹ [43].

In the second project, NeuCo, Inc., a developer of power plant control and optimization technologies, demonstrated the capability to optimize Hg speciation and control Hg emissions from an existing power plant. This demonstration took place at an 890 MW utility boiler in Jewett, Texas, that was completed in 2010 and is owned by NRG Energy. NeuCo utilized state-of-the-art sensors and neural, network-based optimization and control technologies to maximize the proportion of Hg²⁺ species in order to increase the rate of co-benefit Hg capture. Artificial intelligence and simulation technologies were used to control and optimize appropriate operational parameters. Critical sensing devices were added to the unit to monitor inputs and emissions from the plant. Data from these sensors was analyzed by the neural network to optimize plant operations, while simultaneously minimizing Hg emissions [44].

10.2.12

Mercury Control Cost Estimates

NETL has conducted in-depth economic analyses for both ACI and wet FGD enhancement technologies for Hg control, based on the results of its field testing program. The increase in cost resulting from Hg control via ACI is primarily determined by annual PAC consumption costs that are dependent on the required ACI rate, delivered PAC price, and the volume of flue gas being treated. Chemical composition also affects PAC price since manufacturers charge a higher price for chemically treated PAC to offset the additional production costs required to alter the sorbent's molecular structure. The ACI rate required to achieve a given level

of Hg control can be impacted by a host of plant-specific dynamics, including, but not limited to, Cl and sulfur contents of the coal being burned, APCD configuration, flue gas temperature, boiler efficiency, UBC content of the fly ash, and ductwork geometry in proximity to the ACI location.

10.2.12.1 Economic Analyses for ACI

In 2003, NETL prepared an economic assessment of ACI with untreated PAC based on the results of its Phase I field testing program [45]. The report developed “study-level” costs for Hg control using ACI at representative 500 MW bituminous- and subbituminous-fired power plant units equipped with an existing CS-ESP. Costs were estimated for ACI into an existing CS-ESP, as well as a TOXECON configuration. The cost estimates were developed for equipment designed to achieve Hg control at low (50%), mid-range (60–70%), and high (90%) levels. It is important to note that the costs developed here were based on the current state of knowledge and understanding of ACI technology at three of the Phase I field test sites. The incremental cost of Hg control for this analysis, excluding impact to fly ash sales and disposal practices, was estimated to range from \$33 000/lb Hg removed to \$131 000/lb Hg removed for the bituminous-fired unit, and from ~\$18 000/lb Hg removed to \$55 000/lb Hg removed for the subbituminous-fired unit.

A follow-up NETL economic analysis released in May 2007 indicated that the high Hg capture efficiency of chemically treated sorbents drastically reduced the estimated cost of Hg control due to the lower injection rate required to achieve a given level of control that offsets the higher cost of these treated sorbents [46]. As shown in Figure 10.6, the 20-year levelized incremental cost of 90% ACI Hg control ranged from about \$30 000 to <10 000/lb Hg removed (without considering impacts on CUBs) for seven of NETL’s field testing sites where chemically treated ACI was evaluated. The May 2007 report provides “study-level,” plant-specific cost estimates and gives NETL a gage to measure its success in achieving the target of reducing the baseline Hg control cost estimate of \$60 000/lb Hg removed by 25–50%.

10.2.12.2 Economic Analyses for Wet FGD Enhancement

In May 2008, NETL released a report that provided cost estimates for technologies developed to enhance co-benefit Hg capture for wet FGD systems [47]. The report provides “study-level” cost estimates for two such technologies: fixed-bed Hg^0 oxidation catalysts, and coal treatment with a CaBr_2 solution. The economics were developed for an average Hg control level of 73% at “representative” 500 MW units burning three types of low-rank coal: North Dakota lignite, PRB subbituminous, and a blend of 50% TxL and 50% PRB subbituminous coals. The report estimated an incremental cost of control <\$17 000 per pound of Hg removed (\$/lb Hg removed) using the Hg^0 oxidation catalysts. Addition of CaBr_2 solution at an injection rate of about 5.90 lb h^{-1} was required to achieve 73% total Hg removal at the “representative” PRB-fired unit equipped with an SCR, resulting in a cost of \$2200/lb Hg removed. Without an SCR in-service, a CaBr_2 injection rate of

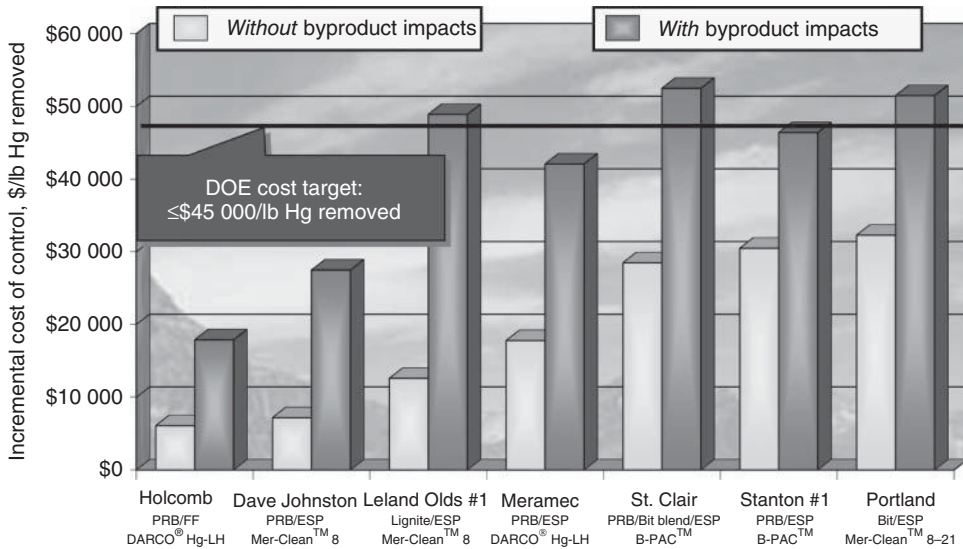


Figure 10.6 Six-year levelized incremental cost of 90% Hg control with chemically treated ACI.

322 lb h⁻¹ was required to achieve the same level of control and the levelized costs rise to \$21 200/lb Hg removed.

10.2.13

Coal Utilization Byproducts (CUB) R&D Program

In addition to developing cost-effective control technologies for coal-fired power plants, NETL's program also investigated the potential implication of Hg control on the use and disposal of CUB [48, 49]. CUB are the solid materials resulting from the combustion of coal and the removal of air pollutants from coal-based flue gas that include bottom ash, fly ash, boiler slag, and FGD gypsum. U.S. power plants produced 134.7 million tons of CUB in 2009, with nearly 42% put to beneficial use in applications such as concrete, flowable fill, road base, snow and ice control, blasting grit, fertilizer, and wallboard [29]. Put another way, this was 56 million tons of material that did not have to be landfilled or placed in an impoundment.

The CUB research was directed at better understanding the transfer and ultimate fate of Hg and other trace metals from the flue gas to the power plant's solid and liquid effluent streams as a result of implementing Hg control systems. Although the NETL CUB program was ended in 2008, it was determined that DOE had successfully achieved its goal of bringing efficient, cost-effective Hg control technologies to commercial readiness and that further research into the fate of Hg and other trace metals in fly ash, scrubber solids, and other byproducts should be carried out by the private sector.

ACI Hg control leads to commingling of the PAC and fly ash that can prohibit certain fly ash recycling efforts. As part of the economic analyses noted above

[42, 43], NETL evaluated the 20-year levelized costs of Hg control both with and without the inclusion of byproduct impacts. The analyses assumed that for units equipped with a CS-ESP, the utility was able to sell all fly ash collected in the ESP hoppers for \$18/ton prior to ACI. Following installation of an ACI system, it was assumed that the fly ash could no longer be sold; instead, the utility must pay \$17/ton for non-hazardous fly ash disposal. For an SDA/FF system, it was assumed that solids that were given away prior to ACI would have to be disposed of at a price of \$17/ton (non-hazardous). Using these assumptions, NETL estimated that the cost for Hg control, with chemically treated ACI and accounting for the cost of byproduct disposal, ranged from \$52 500/lb Hg removed to \$17 900/lb Hg removed for seven of NETL's field testing sites, as shown in Figure 10.6.

While CUB were, and still are, regulated as non-hazardous under the Resource Conservation and Recovery Act, EPA is considering alternative regulatory approaches for CUB, including a hazardous designation due in part to concerns over the partitioning of Hg to these materials. Such a designation would significantly increase the cost of Hg control because the cost of hazardous waste disposal can be more than five times more expensive than non-hazardous disposal. Therefore, it was extremely important to evaluate the potential for leaching and volatilization of Hg and other trace metals from CUB to the environment as part of the NETL Hg Program.

10.2.14

Determining the Fate of Hg in FGD Byproducts

NETL's ORD conducted research directed at determining the fate of Hg in FGD materials [50]. This activity focused on Hg stability during FGD gypsum drying, Hg stability during wallboard production using FGD gypsum, Hg leachability from FGD gypsum, and the Hg-binding phase in FGD gypsum. The stability of Hg during FGD gypsum drying was studied by collecting samples before and after natural gas-fired heating that reduces the moisture content of the FGD solids for ease of handling during the wallboard manufacturing process. Results indicated that within analytical precision, no Hg desorbed during the drying process.

The stability of Hg in FGD gypsum during wallboard production was also analyzed by collecting samples of FGD gypsum feedstock and the corresponding wallboard products from five wallboard manufacturing plants. The Hg present in the unprocessed FGD gypsum and the finished wallboard product ranged from 0.04 to 1.5 ppm on a dry basis. The quantity of Hg retained in the finished wallboard product varied, with three samples showing nearly complete Hg retention during the wallboard manufacturing process. For the other two samples, Hg losses were 12% and 58%, suggesting that the quantity and thermal stability of Hg in FGD gypsum and wallboard depends on the origin of the gypsum and/or the nature of processing.

Research was also performed using FGD slurry samples in an attempt to isolate the Hg-binding phase from bulk gypsum. During settling, Hg partitioned almost exclusively to the top, slower-settling layer of the FGD slurry. Analysis of this

residue revealed that both Hg and iron (Fe) were enriched in the top layer by factors of about 20 and 10, respectively. Meanwhile, Hg was not mobilized during FGD slurry leaching experiments using a continuous, stirred-tank extractor. This is indicative of a strong chemisorption rather than physical adsorption of Hg. As a result, it is believed that Hg sequestered in FGD gypsum is primarily bound to an iron-rich phase, such as iron-coated clay materials or iron oxide/hydroxide particles, probably introduced with the limestone used as the FGD reagent. Additional research [51] also showed that some Hg retained in FGD gypsum requires hydrogen peroxide oxidation for release, such as a phase containing sulfides or carbonaceous materials.

Leach testing was also used to evaluate the impacts of pH and oxidation–reduction potential (ORP) on Hg mobility in FGD byproducts. Leaching of six FGD materials to pH > 2 under aerobic conditions failed to mobilize appreciable amounts of Hg. While no Hg was released to the leachate during experiments with pH > 4 and ORP > 100 mV, dissolution of the major immobilized form of Hg was complete with pH < 1 and an ORP of ~350 mV. Consequently, ORD researchers concluded that the Hg-retaining phase will immobilize Hg in many reuse applications, with one possible exception being placement in mine-land reclamation areas where the FGD byproducts could be exposed to acidic, anaerobic conditions.

As part of NETL's CUB research, the Tennessee Valley Authority (TVA) evaluated Hg retention in FGD gypsum from three sources: an Hg-amended commercial calcium sulfate, a laboratory-scale wet FGD system, and a full-scale wet FGD system [52]. TVA researchers concluded that no Hg would evolve from disposed FGD byproducts up to a maximum temperature of 140 °F, although thermal desorption of Hg from FGD gypsum did occur at ~400 °F.

USG Corporation provided data on the extent and location of Hg loss during the wallboard production process, and also provided information on the potential for Hg leaching at the end of the wallboard life cycle, when it is disposed in municipal landfills [53]. FGD gypsum evaluation tests from six different power plant/FGD feedstock variations were completed to investigate the impact of different configurations on the stability of Hg during wallboard production. Testing included the use of FGD gypsum produced during TMT-15 injection into a power plant scrubber. Test results indicated that use of fines blowdown in wet FGD systems significantly reduced Hg content in the FGD gypsum. For FGD gypsum generated without fines blowdown, Hg loss amounted to <8%, while tests using FGD gypsum from power plants employing fines blowdown indicated Hg loss of 46–55%.

10.2.15

Determining the Fate of Hg in Fly Ash

NETL awarded a contract to Frontier Geosciences, Inc. (Frontier) to conduct independent laboratory analysis of CUB generated during NETL's Phase II full-scale Hg control technology field testing program [54]. The purpose of the independent

laboratory analysis was to ensure accurate and consistent laboratory procedures were used to determine the environmental fate of Hg in CUB. NETL's ORD also conducted in-house leaching experiments with fly ash collected from ACI field testing sites.

The Frontier work included leaching studies using the Synthetic Precipitation Leaching Procedure (SPLP, EPA Method 1312); low-temperature (40 °C for 30 days), medium-temperature (190 °C for 1 h), and high-temperature (900–1200 °C for 5 min) Hg volatility tests; microbial methylation experiments; and halide analysis. The SPLP results indicated that little to no Hg would be released under normal disposal conditions. In addition, Hg bound to PAC sorbents, particularly those that were chemically treated, appeared to be more stable than the UBC-bound Hg. During the low-temperature volatility tests, essentially no Hg was emitted from the fly ash samples. Thermal desorption of Hg was observed during the medium- and high-temperature volatility tests conducted by Frontier.

A pure culture of sulfate-reducing bacteria known to methylate Hg or produce methyl-mercury, was monitored over a 30-day period to assess the methylation potential of Hg present in CUB. Results from this “worst-case-scenario” microbial mobilization study indicated an increase in methyl-mercury production. However, microbial activity also stabilized a number of target metals.

NETL's ORD researchers also conducted leaching experiments on the Phase II byproducts using the modified SPLP, the NETL Serial Batch Leaching Procedure (SBLP), and NETL Column Leaching on a select number of sample pairs. During a 5-month continuous column experiment using four leachants, water (pH = 5.7), dilute sulfuric acid (pH = 1.2), dilute acetic acid (pH = 2.9), and sodium carbonate (pH = 11.1) [55], the PAC/ash mixtures were generally found to effectively immobilize the captured Hg over a range of laboratory conditions. Overall, very little of the Hg (always below 0.5% and often under 0.1%) contained in the ash samples was solubilized during leaching. Neither the pH nor the nature of the anion had a noticeable effect on the leachate Hg.

Not only have the Hg control technologies demonstrated capture of Hg that would otherwise be released into the environment, but the Hg has generally been shown to be retained in the control technology byproducts under conditions of laboratory leaching tests. For some of these materials, the tests performed show these control technology byproducts, in spite of their higher Hg content, to be environmentally more stable with respect to Hg release than the corresponding baseline ashes of lower Hg content [56].

10.3

Summary

Working closely with key stakeholders, NETL's Hg RD&D program successfully brought Hg control technology from what was a concept in the early 1990s to a commercial product by 2008. As of June 2010, nearly 150 full-scale ACI systems,

a signature technology of the NETL Hg R&D Program, have been ordered by U.S. coal-fired power generators [57]. These contracts represent more than 56 GW of coal-fired electric generating capacity. This includes ~43 GW of existing capacity (almost 15% of total U.S. coal-fired capacity) that will be retrofit with ACI systems to control Hg emissions. EPA projects that 146 GW of ACI will be installed on U.S. power plants by 2015 in order to comply with proposed Federal Hg regulations [1].

The ACI systems have the potential to remove up to 90% or more of the Hg in many, but not all, applications based on results from NETL's field testing program, at a cost estimated to be as low as \$10 000/lb Hg removed in some situations. However, although the results achieved during NETL's field tests met or exceeded the program goals, only through experience gained during long-term continuous operation of these advanced technologies in a range of full-scale commercial applications will their actual costs and performance be determined.

Disclaimer

Neither the United States Government nor any agency thereof, nor any of their employees, makes any warranty, express or implied, or assumes any legal liability or responsibility for the accuracy, completeness, or usefulness of any information, apparatus, product, or process disclosed, or represents that its use would not infringe privately owned rights. Reference therein to any specific commercial product, process, or service by trade name, trademark, manufacturer, or otherwise does not necessarily constitute or imply its endorsement, recommendation, or favoring by the United States Government or any agency thereof. The views and opinions of authors expressed herein do not necessarily state or reflect those of the United States Government or any agency thereof.

References

1. EPA (2011) Reducing Toxic Pollution from Power Plants, U.S. EPA, March 2011, <http://www.epa.gov/airquality/powerplanttoxics/pdfs/presentation.pdf> (accessed 21 March 2014).
2. EIA (2011) Annual Energy Outlook 2011, Energy Information Administration, April 2011, <http://www.eia.gov/forecasts/aeo/index.cfm> (accessed 21 March 2014).
3. NACAA (2011) State/Local Mercury/Toxics Programs for Utilities, National Association of Clean Air Agencies, February 2011, <http://www.4cleanair.org/> (accessed 21 March 2014).
4. Feeley, T. and Jones, A. (2008) An update on DOE/NETL's mercury control technology field testing program. Prepared for the U.S. Department of Energy National Energy Technology Laboratory, 2008, <http://www.netl.doe.gov/technologies/coalpower/ewr/mercury/pubs/netl%20Hg%20program%20white%20paper%20FINAL%20Jan2008.pdf> (accessed 21 March 2014).
5. Srivastava, R., Hutson, N., Martin, B., Princiotta, F., and Standt, J. (2006) Control of mercury emissions from coal-fired electric utility boilers. *Environ. Sci. Technol.*, **40**, 1385.
6. Kilgroe, J., Sedman, C., Srivastava, R., Ryan, J.V., Lee, C.W., and Thorneloe, S.A. (2002) Control of Mercury Emissions from Coal-Fired Electric Utility Boilers. Interim Report Including Errata Dated 3-21-02, EPA-600/R-01-109, U.S.

- Environmental Protection Agency U.S. Government Printing Office, Washington, DC.
7. Laudal, D.L., Thompson, J.S., Pavlish, J.H., Brickett, L., Chu, P., Srivastava, R.K., Lee, C.W., and Kilgroe, J. (2003) The evaluation of mercury speciation at power plants using SCR and SNCR control technologies, *Environ. Manager* 53 (2), 16.
 8. Lissianski, V. and Marquez, A. (2004) Preliminary Field Evaluation of Mercury Control Using Combustion Modifications. Quarterly Report to the U.S. Department of Energy under Cooperative Agreement No. DE-FC26-03NT41725, GE Energy and Environmental Research Corporation, Irvine, CA, <http://www.osti.gov/scitech/servlets/purl/825582>. Accessed 2014-07-27.
 9. Benson, S.A., Holmes, M.J., McCollor, D.P., Mackenzie, J.M., Kong, L., and Crocker, C.R. (2007) Large-Scale Mercury Control Technology Testing for Lignite-Fired Utilities – Oxidation Systems for Wet FGD. Final report to the U.S. Department of Energy under Cooperative Agreement No. DEFC26-03NT41991, URS Corporation, Austin, TX, <http://www.netl.doe.gov/File%20Library/Research/Coal/ewr/mercury/41991-Final-Report.pdf>. Accessed 2014-07-27.
 10. Richardson, M., Blythe, G., Owens, M., Miller, C., and Rhudy, R. (2007) Wet FGD additive for enhanced mercury control. Presented at the DOE/NETL Mercury Control Technology Conference, Pittsburgh, PA, http://www.netl.doe.gov/publications/proceedings/07/mercury/presentations/Richardson_Pres.pdf (accessed 21 March 2014).
 11. Laumb, J., Laudal, D., Dunham, G., Martin, C., and Galbreath, K. (2007) Long-Term demonstration of sorbent enhancement additive technology for mercury control. Presented at the DOE/NETL Mercury Control Technology Conference, Pittsburgh, PA, 2007, http://www.netl.doe.gov/publications/proceedings/07/mercury/presentations/Laumb_Pres.pdf (accessed 21 March 2014).
 12. Blythe, G. (2006) Pilot testing of mercury oxidation catalysts for upstream of wet FGD systems. Presented at the DOE/NETL Mercury Control Technology Conference, Pittsburgh, PA, 2006, http://www.netl.doe.gov/publications/proceedings/06/mercury/presentations/Blythe_presentation_Pilot_121206.pdf (accessed 21 March 2014).
 13. NETL (2005) Field Test Program to Develop Comprehensive Design, Operating, and Cost Data for Mercury Control Systems. ADA-ES Final Report to DOE/NETL, March 2005, NETL <http://www.netl.doe.gov/technologies/coalpower/ewr/mercury/control-tech/comp-design.html>. (accessed 21 March 2014).
 14. Dombrowski, K., Richardson, C., Chapman, D., Chang, R., Monroe, L., Berry, M., Glessman, S., Campbell, T., and McBee, K. (2005) Full-scale evaluation of activated carbon injection. Proceedings of the Air Quality V Conference, Arlington, Virginia, September 19–21, 2005.
 15. Sjostrom, S. (2005) Evaluation of Sorbent Injection for Mercury Control. Quarterly Technical Report to the U.S. Department of Energy under Cooperative Agreement No. DE-FC26-03NT41986, ADA-ES, Inc., Littleton, CO, <http://www.netl.doe.gov/technologies/coalpower/ewr/mercury/control-tech/pubs/41986/41986%20Q093005.pdf>.
 16. Sjostrom, S. (2005) Evaluation of Sorbent Injection for Mercury Control: AmerenUE's Meramec Station Unit 2. Topical Report to the U.S. Department of Energy under Cooperative Agreement No. DE-FC26-03NT41986, ADA-ES, Inc., Littleton, CO, <http://www.netl.doe.gov/technologies/coalpower/ewr/mercury/control-tech/pubs/Topical%20Report%20for%20Meramec%20Station.pdf>.
 17. Sjostrom, S. (2005) Evaluation of Sorbent Injection for Mercury Control: Sunflower Electric's Holcomb Station. Topical Report to the U.S. Department of Energy under Cooperative Agreement No. DE-FC26-03NT41986, ADA-ES, Inc., Littleton, CO, <http://www.netl.doe.gov/>

- technologies/coalpower/ewr/mercury/control-tech/pubs/Topical_Report_for_Holcomb_Station.pdf*.
18. Holmes, M.J. and Brickett, L.A. (2006) Enhancing carbon reactivity for mercury control in coal-fired power plants: results from Ieland Olds, Stanton, and Antelope Valley stations. Presented at the DOE/NETL Mercury Control Technology Conference, Pittsburgh, PA, December 11–13, 2006, http://www.netl.doe.gov/publications/proceedings/06/mercury/presentations/Holmes_presentation_121106.pdf (accessed 21 March 2014).
 19. Landreth, R., Nelson, S., Liu, X., Tang, Z., Miller, J., Hoefflich, P., Moore, G., and Brickett, L. (2006) New full-scale results from B-PAC control trials. Proceedings of the A&WMA/EPA/DOE/EPRI Combined Power Plant Air Pollutant Control Mega Symposium, Baltimore, MD, August 28–31, 2006.
 20. Landreth, R. and Brickett, L. (2006) Advanced utility mercury-sorbent field-testing program. Presented at the DOE/NETL Mercury Control Technology Conference, Pittsburgh, PA, December 11–13, 2006, http://www.netl.doe.gov/publications/proceedings/06/mercury/presentations/Landreth_presentation_121206.pdf (accessed 21 December 2014).
 21. Sjostrom, S. (2007) Long-Term Carbon Injection Field Test for >90% Mercury Removal for a PRB Unit with a Spray Dryer and Fabric Filter. Quarterly Progress Report to the U.S. Department of Energy under Cooperative Agreement No. DE-FC26-06NT42774, ADA-ES, Inc., Littleton, CO.
 22. Dombrowski, K., Padilla, J., Richardson, C., Fisher, K., Campbell, T., Chang, R., Eckberg, C., Hudspeth, J., and Pletcher, S. (2007) Evaluation of low-ash impact sorbent injection technologies at a Texas lignite/PRB fired power plant. Proceedings of the Air Quality VI Conference, Arlington, VA, September 24–27, 2007.
 23. Kang, S.G. and Brickett, L.A. (2006) Field demonstration of enhanced sorbent injection for mercury control. Presented at the DOE/NETL Mercury Control Technology Conference, Pittsburgh, PA, December 11–13, 2006, http://www.netl.doe.gov/publications/proceedings/06/mercury/presentations/Kang_presentation_121106.pdf.
 24. Kang, S.G. (2007) Demonstration of Mer-Cure™ Technology for Enhanced Mercury Control. Quarterly Technical Progress Report to the U.S. Department of Energy under Cooperative Agreement No. DE-FC26-07NT42776, ALSTOM-PPL, Windsor, CT.
 25. Brickett, L. (2007) An update of DOE's phase II & III mercury control technology program. Presented at the Air Quality VI Conference, Arlington, VA, September 24–27, 2007.
 26. Laumb, J. and Pavlish, B. (2007) Long-term demonstration of sorbent enhancement additive technology for mercury control. Presented at the Electric Utilities Environmental Conference, Tucson, AZ, January 22–24, 2007.
 27. Landreth, R., Nelson, S., Liu, X., Tang, Z., Donochod, D., Kulpinski, K., Wanninger, K., and Brickett, L. (2007) Additional B-PAC™, H-PAC™, and C-PAC™ trial results. Proceedings of the Air Quality VI Conference, Arlington, VA, September 24–27, 2007.
 28. Campbell, T. and O'Palko, A. (2006) Low cost options for moderate levels of mercury control – Toxecon II™ and high temperature sorbents. Presented at the DOE/NETL Mercury Control Technology Conference, Pittsburgh, PA, December 11–13, 2006, http://www.netl.doe.gov/publications/proceedings/06/mercury/presentations/Campbell_presentation_121106.pdf (accessed 21 March 2014).
 29. American Coal Ash Association (2009) Coal Combustion Product (CCP) Production and Use Survey, American Coal Ash Association, Aurora, CO, February 2011, <http://www.acaa-usa.org/> (accessed 21 March 2014).
 30. Campbell, T. (2007) Low cost options for moderate levels of mercury control—2007 update on TOXECON II™. Presented at the DOE/NETL Mercury Control Technology Conference, Pittsburgh, PA, <http://www.netl.doe.gov/publications/proceedings/07/mercury/>

- presentations/Campbell_Pres.pdf* (accessed 21 March 2014).
31. Brickett, L., Nelson, S., Landreth, R., Liu, X., Tang, Z., and Miller, J. (2006) Brominated sorbents for small cold-side ESPs, hot-side ESPs, and fly ash use in concrete. Presented at the DOE/NETL Mercury Control Technology Conference, Pittsburgh, PA, 2006, http://www.netl.doe.gov/publications/proceedings/06/mercury/presentations/Nelson_presentation_121106.pdf (accessed 21 March 2014).
 32. Brickett, L., Nelson, S., Landreth, R., Liu, X., Tang, Z., and Miller, J. (2007) Brominated sorbents for small cold-side ESPs, hot-side ESPs, and fly ash use in concrete. Presented at the DOE/NETL Mercury Control Technology Conference, Pittsburgh, PA, 2007, http://www.netl.doe.gov/publications/proceedings/07/mercury/presentations/Landreth_Pres.pdf (accessed 21 March 2014).
 33. Kang, S., Edberg, C., Rebula, E., and Noceti, P. (2007) Demonstration of mer-cure™ technology for enhanced mercury control. Presented at the DOE/NETL Mercury Control Technology Conference, Pittsburgh, PA, 2007, http://www.netl.doe.gov/publications/proceedings/07/mercury/presentations/Kang_Pres.pdf.
 34. Presto, A., Granite, E., and Karash, A. (2007) Further investigation of the impact of sulfur oxides on mercury capture by activated carbon. *Ind. Eng. Chem. Res.*, **46**, 8273; <http://www.netl.doe.gov/technologies/coalpower/ewr/mercury/pubs/Hg-SO3-AC-IECR-2007.pdf>.
 35. Sjostrom, S. (2006) Full-scale evaluation of carbon injection for mercury control at a unit firing high sulfur coal. Presented at the DOE/NETL Mercury Control Technology Conference, Pittsburgh, PA, 2006, http://www.netl.doe.gov/publications/proceedings/06/mercury/presentations/Sjostrom_presentation_121106.pdf (accessed 21 March 2014).
 36. Dillon, M. (2007) Evaluation of sorbent injection for mercury control. Presented at the DOE/NETL Mercury Control Technology Conference, Pittsburgh, PA, 2007, http://www.netl.doe.gov/publications/proceedings/07/mercury/presentations/Dillon_Pres%20.pdf (accessed 21 March 2014).
 37. Landreth, R., Nelson, S., Liu, X., Tang, Z., Miller, J., Hoefflich, P., Moore, G., and Brickett, L. (2006) New full-scale results from B-PAC control trials. Presented at Proceedings of the A&WMA/EPA/DOE/EPRI Combined Power Plant Air Pollutant Control Mega Symposium, Baltimore, MD, 2006.
 38. Campbell, T. (2007) Evaluation of sorbent injection for mercury control. Presented at the DOE/NETL Mercury Control Technology Conference, Pittsburgh, PA, 2007, http://www.netl.doe.gov/publications/proceedings/07/mercury/presentations/Campbell1_Pres.pdf (accessed 21 March 2014).
 39. Granite, E.J. and Pennline, H.W. (2002) Photochemical removal of mercury from flue gas. *Ind. Eng. Chem. Res.*, **41** (22), 5470–5476.
 40. O'Dowd, W.J., Pennline, H.W., Freeman, M.C., Granite, E.J., Hargis, R.A., Lacher, C.J., and Karash, A. (2006) A technique to control mercury from flue gas: the thief process. *Fuel Process. Technol.*, **87**, 1071–1084.
 41. Granite, E.J., Myers, C.R., King, W.P., Stanko, D.C., and Pennline, H.W. (2006) Sorbents for mercury capture from fuel gas with application to gasification systems. *Ind. Eng. Chem. Res.*, **45**, 4844–4848.
 42. Derenne, S., Stewart, R., Bustard, J., Sjostrom, S., Johnson, P., Sartorelli, P., McMillan, M.H., and Sudhoff, E.A. (2007) TOXECON™ clean coal demonstration for mercury and multi-pollutant control at the presque isle power plant. Presented at Proceedings of the Air Quality VI Conference, Arlington, VA, 2007.
 43. NETL (2011) TOXECON™ Retrofit for Mercury and Multi-Pollutant Control on Three 90 MW Coal-Fired Boilers, DOE-NETL, May 2011, <http://www.netl.doe.gov/technologies/coalpower/cctc/ccpi/index.html> (accessed 21 March 2014).

44. DOE-NETL (2011) Mercury Specie and Multi-Pollutant Control Project, May 2011, <http://www.netl.doe.gov/technologies/coalpower/cctc/ccpi/index.html> (accessed 21 March 2014).
45. DOE/NETL (2003) Preliminary Cost Estimate of Activated Carbon Injection for Controlling Mercury Emissions from an Un-Scrubbed 500 MW Coal-Fired Power Plant, November 2003, http://www.netl.doe.gov/technologies/coalpower/ewr/mercury/pubs/ACI_Cost_Final.pdf.
46. DOE/NETL (2007) DOE/NETL's Phase II Mercury Control Technology Field Testing Program: UPDATED Economic Analysis of Activated Carbon Injection, May 2007, http://www.netl.doe.gov/technologies/coalpower/ewr/mercury/pubs/Phase_II_UPDATED_Hg_Control_Economic_Analysis.pdf.
47. DOE/NETL (2008) Preliminary Economic Analysis of Wet FGD Co-Benefit Enhancement Technologies, May 2008, <http://www.netl.doe.gov/energy-analyses/pubs/Enhanced%20FGD%20Hg%20Capture%20Economics%20FINAL%20May2008.pdf>.
48. Aljoe, W., Feeley, T., Murphy, J., and Brickett, L. The Fate of Mercury in Coal Utilization Byproducts. EM Magazine (May 19-26, 2005).
49. DOE/NETL (2004) A Review of DOE/NETL's Coal Utilization By-Products Environmental Characterization Research, July 2004, http://www.netl.doe.gov/technologies/coalpower/ewr/pubs/Final_CUB%20Environmental%20Research.pdf.
50. Kairies, C.L., Schroeder, K.T., and Cardone, C.R. (2006) Mercury in gypsum produced from flue gas desulfurization. *Fuel*, **85** (17-18), 2530–2536.
51. Schroeder, K., Beatty, L., Cardone, C., Hreha, D., Kairies, C., Rohar, P., Thompson, R., and White, F. Leach testing of FGD materials. Presented at the DOE/NETL Mercury Control Technology Conference, Pittsburgh, PA, December 11-13, 2006, http://www.netl.doe.gov/publications/proceedings/06/mercury/presentations/Schroeder_presentation_121206.pdf (accessed 21 March 2014).
52. Meischen, S. (2004) The Effect of Mercury Controls on Wallboard Manufacture. Final Report to the combustion byproducts recycling consortium under sub-contract no. ECM-01-CBRC-M12, Tennessee Valley Authority, Muscle Shoals, AL, http://www.wri.org/wp-content/uploads/2012/05/01CBRCM12_final1.pdf.
53. Sanderson, J., Blythe, G., Richardson, M., and Miller, C. (2006) Fate of mercury in synthetic gypsum. Presented at the DOE/NETL Mercury Control Technology Conference, Pittsburgh, PA, December 11-13, 2006, http://www.netl.doe.gov/publications/proceedings/06/mercury/presentations/Sanderson_presentation_121206.pdf (accessed 21 March 2014).
54. Hensman, C., Dahl, A., McIntosh, B., Hawkins, L., Kilner, P., Hien, J., Prestbo, E., Gilmour, C., and Brickett, L. (2007) The impact of Hg control technologies on mobility pathways for Hg, Ni, As, Se, Cd and Pb from coal utilization byproducts. Proceedings of the Air Quality VI Conference, Arlington, VA, September 24–27, 2007.
55. Schroeder, K., Cardone, C., White, F., Rohar, P., and Kim, A. (2007) Long-term column leaching of phase ii mercury control technology by-products. Proceedings of the 2007 World of Coal Ash Conference, Covington, KY, May 7–10, 2007.
56. Hesbach, P. and Kachur, E. (2007) Leaching of phase II mercury control technology by-products. Proceedings of the 2007 World of Coal Ash Conference, Covington, KY, May 7–10, 2007.
57. Institute of Clean Air Companies (2010) Commercial Electric Utility Mercury Control Technology Bookings, June 2010, <http://www.icac.com/>.

11

U.S. EPA Research Program

Nick Hutson

11.1

Introduction

The U.S. Environmental Protection Agency (EPA) has maintained a broad research program examining the emissions and control of hazardous air pollutants (HAPs), including mercury, from stationary sources. The EPA has also maintained research programs studying the fate and transport of mercury and the resulting impacts, including health impacts, on the environment. There is considerable documentation of the studies of the fate and transport and the resulting effects of mercury on the environment. This section focuses exclusively on the EPA research program dealing with emissions of mercury from coal combustion. This work includes studies that were mandated by Congress to evaluate the emissions and hazards of mercury emissions from fossil-fuel-fired electricity generating units. It also includes fundamental work focused on development and evaluation of control technologies for mercury control. The EPA has also conducted considerable and significant work on the fate of mercury and other toxic metals in coal combustion residuals (CCRs) and other process effluents. That work is summarized in full in another section. The EPA has also played a leading role in the development and testing of technologies and techniques for continuous measurement and monitoring of mercury emissions in the very low concentrations (parts per trillion) and in the harsh environments that are seen in typical coal combustion flue gas streams. That work is also summarized in another section and is thus not covered here.

11.2

Congressionally Mandated Studies

In the 1990 Clean Air Act (CAA) amendments, Congress established a specific structure for determining whether to regulate HAP emissions from electric generating units (EGUs). Congress required that various reports concerning HAP emissions from EGUs be completed.

Mercury Control: for Coal-Derived Gas Streams, First Edition.

Edited by Evan J. Granite, Henry W. Pennline and Constance Senior.

© 2015 Wiley-VCH Verlag GmbH & Co. KGaA. Published 2015 by Wiley-VCH Verlag GmbH & Co. KGaA.

The first report, the Utility Study, required the EPA to evaluate the hazards to public health reasonably anticipated to occur as the result of HAP emissions from EGUs after imposition of the requirements of the CAA. The EPA issued the Utility Study, which included numerous analyses, in February 1998. The EPA first collected HAP emissions test data from 52 EGUs, including a range of coal-, oil-, and natural-gas-fired units. The test data along with facility specific information were used to estimate HAP emissions from all 684 utility facilities. The EPA determined that 67 HAPs were potentially emitted from fossil-fuel-fired EGUs.

The EPA evaluated exposures, hazards, and risks due to HAP emissions from coal-, oil-, and natural-gas-fired EGUs. The EPA conducted a screening-level assessment of all 67 of the potentially emitted HAPs to prioritize the pollutants for further analysis. A total of 14 were identified as priority HAPs that would be further assessed. Twelve HAPs (arsenic (As), beryllium (Be), cadmium (Cd), chromium (Cr), manganese (Mn), nickel (Ni), hydrochloric acid (HCl), hydrofluoric acid (HF), acrolein, dioxins, formaldehyde, and radionuclides) were identified as priority pollutants for further assessment based on inhalation exposure and risk. Six HAPs (Hg, radionuclides, As, Cd, Pb, and dioxins) were considered a priority for multipathway assessment of exposure and risk. On the basis of the multipathway assessments, the EPA determined that Hg from coal-fired EGUs was the HAP of greatest potential concern.

The second report directed the EPA to “conduct a study of mercury emissions from EGUs, municipal waste combustion units, and other sources, including area sources.” This is referred to as the *Mercury Study*. In conducting the Mercury Study, Congress directed the EPA to “consider the rate and mass of emissions, the health and environmental effects of such emissions, technologies which are available to control such emissions, and the costs of such technologies.” The EPA issued the Mercury Study in December 1997. The Mercury Study assessed the magnitude of U.S. Hg emissions by source, the health and environmental implications of those emissions, and the availability and cost of control technologies.

The last required report was to be completed by the National Institute of Environmental Health Sciences (NIEHS). Congress directed NIEHS to conduct “a study to determine the threshold level of Hg exposure below which adverse human health effects are not expected to occur.” In conducting this study, NIEHS was to determine “a threshold for mercury concentrations in the tissue of fish which may be consumed (including consumption by sensitive populations) without adverse effects to public health.” In addition, Congress, in the conference report language associated with EPA’s fiscal year 1999 appropriations, directed the EPA to fund the National Academy of Sciences (NAS) to perform an independent evaluation of the available data related to the health impacts of methyl mercury (MeHg). Specifically, NAS was tasked with advising the EPA as to the appropriate reference dose (RfD) for MeHg, which is the amount of a chemical which, when ingested daily over a lifetime, is anticipated to be without adverse health effects to humans, including sensitive subpopulations.

The EPA completed the Mercury Study and the Utility Study by 1998. The NIEHS study was completed in 1995, and the NAS study was completed in 2000.

In December 2000, after considering public input, the results of the required studies described and other relevant information, including Hg emission data from EGUs, EPA determined that it was appropriate and necessary to regulate EGUs under CAA Section 11.2.

11.3

Control Technology from Work on Municipal Waste Combustors (MWCs)

There has been significant public and scientific concern over the risks of air pollution emissions from municipal waste combustors (MWCs). Historically, the primary pollutants of concern have been dioxins/furans (e.g., polychlorinated dibenzo-*p*-dioxins (PCDDs) and polychlorinated dibenzofurans (PCDFs)), and mercury (Hg). The potential emissions of each of these toxic pollutants can vary considerably depending on the composition of the waste and the control technologies used. The EPA conducted work in the mid-1990s to examine the effectiveness of typical air pollution control (APC) technologies for mitigation of emissions of PCDDs/PCDFs and Hg from MWC [1]. Much of this knowledge was later applied to the initial development and testing of similar controls for mercury emissions from coal-fired electricity generating units. EPA researchers noted that powdered activated carbon (PAC) can be injected into MWC flue gas to reduce Hg emissions from SD/FF (spray dryer/fabric filter) and SD/ESP (electrostatic precipitator) systems and that it can also be used to improve PCDD/PCDF capture in these systems. The researchers also identified fundamental Hg properties that affect capture in flue gas cleaning equipment.

EPA researchers also conducted bench-scale experiments under conditions simulating MWCs and coal-fired units to study Hg capture by dry sorbents, including PAC [2]. The focus of the work was specifically to evaluate the effects of reaction temperature on the capture of different Hg species (Hg^0 and Hg^{2+}) by various types of dry sorbents.

Ghorishi *et al.* [3] followed with tests designed to better understand the transformation of mercury species (elemental and oxidized forms) in stationary waste combustion sources. Elemental mercury (Hg^0) poses a challenging flue gas control issue, and oxidized forms of mercury (Hg^{2+}) are of concern because of the potential for local deposition. Gas-phase studies indicated that homogeneous oxidation of Hg^0 in the presence of hydrogen chloride (HCl) is slow, proceeding at measurable rates only at temperatures $>700^\circ\text{C}$ and with HCl concentrations of 100 ppm or more. The effect of fly ash composition on heterogeneous Hg^0 oxidation was investigated using a fixed-bed reactor containing different synthetic model fly ash components such as alumina (Al_2O_3), silica (SiO_2), ferric oxide (Fe_2O_3), copper oxide (CuO), and calcium oxide (CaO). The transition metal oxides, CuO and Fe_2O_3 , exhibited significant catalytic activity in the surface-mediated oxidation of Hg^0 in the presence of HCl. This was suggested to be possibly caused by the Deacon process in which chlorine gas (Cl_2) is produced via catalytic oxidation of HCl over these two oxides. The researchers also studied the effect of the sulfur dioxide

to HCl ratio ($\text{SO}_2 : \text{HCl}$) on Hg^0 oxidation. The addition of SO_2 to the moist flue gas at high $\text{SO}_2 : \text{HCl}$ ratios (from 10 : 1 to 4 : 1) caused a notable decrease in oxidation of Hg^0 . This was attributed to a scavenging effect of SO_2 and H_2O on Cl_2 . Addition of CaO to the synthetic fly ashes also caused a drop in Hg^0 oxidation – likely due to the neutralization of HCl by reaction with CaO .

11.4

Mercury Chemistry, Adsorption, and Sorbent Development

Most of the larger scale mercury control demonstration projects have been sponsored or cosponsored by the Department of Energy (DOE), by the Electric Power Research Institute (EPRI), and by the electric utilities. By contrast, the EPA focused its research efforts on smaller scale experimental work with the goal of better understanding the fundamental aspects of mercury control.

Much of the early work originated from results obtained from studies aimed at controlling organic emissions and mercury from MWCs (as just described). Other work looked at sorbent injection technology to reduce emissions of trace air toxic metals (including Hg) from coal combustion facilities. Gullett and Raghunathan [4] conducted pilot-scale tests of high-temperature furnace injection using hydrated lime, limestone, kaolinite, and bauxite sorbents. They found that the impact of sorbent injection on trace metal emissions is a function of metal type, sorbent type, and injection mode. Reductions in submicron concentrations of antimony, arsenic, mercury, and selenium were observed when hydrated lime and limestone were injected.

Krishnan *et al.* [5] studied the mechanisms and rate of elemental mercury (Hg^0) capture by activated carbons using a bench-scale apparatus. Three types of activated carbons were chosen to study the effects of surface area, sorption temperature (from room temperature to 140°C), and varying Hg^0 concentration. The results suggested the sorption mechanism to be a combination of physisorption and chemisorption at lower temperature and primarily via chemisorption at 140°C .

Additional bench-scale experiments were conducted in a flow reactor to simulate entrained-flow capture of elemental mercury (Hg^0) by activated carbon [6, 7]. Mercury adsorption by several commercial activated carbons was examined at different carbon-to-Hg mass ratios, particle sizes, Hg^0 concentrations, and temperatures (from room temperature to 250°C). Increasing the carbon-to-Hg mass ratio increased mercury removal in some cases and capture increased with a decrease in the particle size of the sorbent.

Efforts were made to use detailed chemical models to better understand and explain mercury reaction and control mechanisms in a coal combustion flue gas environment. Mercury speciation in combustion-generated flue gas was modeled using a detailed chemical mechanism consisting of 60 reactions and 21 species [8]. The model confirmed a strong sensitivity to reaction temperature. Starting

with pure HCl, at higher reactor temperatures (more than 630 °C), model predictions were in good agreement with experimental data. But, at lower reactor temperatures, the model tended to underpredict Hg chlorination compared with experimental data, indicating that Hg oxidation at lower temperatures is dominated by heterogeneous mechanisms.

EPA researchers also conducted considerable bench-scale work to understand binding mechanisms of mercury on activated carbon sorbents. Li *et al.* [9] conducted experiments to examine the effect of surface moisture on low-temperature Hg adsorption on activated carbons. A bituminous coal-based activated carbon and an activated carbon fiber were tested for Hg⁰ adsorption capacity. Tests showed that Hg⁰ adsorption decreased considerably when the sorbent moisture was removed by heating at 110 °C before the adsorption experiments. These observations suggested that moisture contained in activated carbons may play an important role in retaining Hg⁰ under these conditions. This effect of moisture on Hg adsorption was observed for both carbon sorbents, despite extreme differences in their ash contents. Temperature programmed desorption (TPD) experiments performed on the two mercury-containing carbons indicated that chemisorption of Hg is the predominant process over physisorption for the moisture-containing samples. The nature of the mercury binding on the carbon surface was examined by X-ray absorption fine structure (XAFS) spectroscopy. XAFS results provided evidence that mercury binding on the carbon surface was associated with oxygen. The results of the study suggested that surface oxygen complexes provide the active sites for mercury binding. The adsorbed H₂O is closely associated with surface oxygen complexes and the removal of the H₂O from the carbon surface by low-temperature heat treatment reduces the number of active sites that can chemically bind Hg⁰ or eliminates the reactive surface conditions that favor Hg⁰ adsorption.

Li *et al.* [10] studied the effect of varying physical and chemical properties of activated carbons on adsorption of elemental mercury (Hg⁰) by treating two activated carbons to modify their surface functional groups and pore structures. Heat treatment (to 927 °C) in nitrogen (N₂), air oxidation (at 420 °C), and nitric acid treatment (6 N HNO₃) of two activated carbons were conducted to vary their surface oxygen functional groups. Adsorption experiments of Hg⁰ by the activated carbons were conducted using a fixed-bed reactor at a temperature of 125 °C and under a N₂ atmosphere. The pore structures of the samples were characterized by N₂ and carbon dioxide (CO₂) adsorption. TPD and acid–base titration experiments were conducted to determine the chemical characteristics of the carbon samples. Characterization of the physical and chemical properties of activated carbons in relation to their Hg⁰ adsorption capacity can provide important mechanistic information on Hg⁰ adsorption. The results suggested that oxygen surface complexes, possibly lactone and carbonyl groups, are the active sites for Hg⁰ capture. The carbons having a lower carbon monoxide (CO)/CO₂ ratio and a low phenol group concentration tended to have a higher Hg⁰ adsorption capacity, suggesting that phenol groups may inhibit Hg⁰ adsorption. The high Hg⁰ adsorption capacity of one carbon sample was also found to be associated with a low ratio of

the phenol/carbonyl groups. The EPA concluded that a possible Hg^0 adsorption mechanism may involve an electron-transfer process in which the carbon surfaces act as an electrode for Hg^0 oxidation.

11.4.1

Halogenated Activated Carbon Sorbents

Ghorishi *et al.* [11] conducted studies in an effort to discern the role of an activated carbon's surface functional groups on the adsorption of Hg^0 vapor and gaseous mercuric chloride (HgCl_2). The results demonstrated that chlorine (Cl) impregnation of a virgin activated carbon using dilute solutions of HCl leads to increased (by a factor of 2–3) fixed-bed capture of these mercury species. A commercially available activated carbon was Cl impregnated and tested for entrained flow, short-time-scale capture of Hg^0 . In the entrained-flow reactor, the chlorine-impregnated powdered activated carbon (Cl-PAC) was introduced in Hg^0 -laden synthetic flue gases (containing 86 ppb of Hg^0) of varying compositions with gas/solid contact times of about 3–4 s. The results indicated significant Hg^0 removal (80–90%), compared to virgin activated carbon (10–15% Hg removal). These levels of Hg^0 removal were observed across a wide range of very low carbon-to-Hg weight ratios. Variation of the natural gas combustion flue gas composition, by doping with nitrogen oxides and sulfur dioxide, and the flow reactor temperature (ranging from 100 to 200 °C) had minimal effect on Hg^0 removal by the Cl-PAC in the studied carbon-to-Hg weight ratios. The results demonstrated significant enhancement of activated carbon reactivity with minimal halogen treatment.

Brominated powdered activated carbon (Br-PAC) sorbents have been shown to be quite effective for Hg capture when injected into the flue gas duct at coal-fired power plants and are especially useful when burning western subbituminous and other low-chlorine coals. Hutson *et al.* [12] used X-ray absorption spectroscopy (XAS) and X-ray photoelectron spectroscopy (XPS) to determine information about the speciation and binding of Hg on two commercially available brominated activated carbons. The results were compared with similar analysis of a conventional (nonhalogenated) and chlorinated activated carbon. Both the XAS and XPS results indicated that the Hg, although introduced as elemental vapor, was consistently bound on the carbon in an oxidized form. The conventional and chlorinated activated carbons appeared to contain mercury bound to chlorinated sites and possibly to sulfate species that have been incorporated onto the carbon from adsorbed SO_2 . The Hg-containing brominated sorbents appeared to contain Hg bound primarily at bromination sites. The researchers concluded that the mechanism of capture for the sorbents likely consists of surface-enhanced oxidation of the Hg^0 vapor via interaction with surface-bound halide species with subsequent binding by surface halide or sulfate species.

With the use of halogenated PACs, concerns were raised about the potential for these PACs to assist in the formation and emission of brominated and/or chlorinated dioxins and furans. To evaluate this, Hutson *et al.* [13] conducted

sampling campaigns at two U.S. DOE demonstration sites where Br-PAC was being injected for control of mercury emissions. The results of the studies showed that injection of the Br-PAC upstream of the ESP did not increase the emissions of total and Toxic Equivalent (TEQ) chlorinated and brominated dioxin compounds. Rather, the data suggested that the sorbent may capture these compounds and reduce their concentration in the flue gas stream. This effect, when seen, was small, and independent of the type of plant emission controls, temperature at the point of injection, or fuel-chlorine content. The addition of the brominated-PAC sorbent resulted in slight increases in the total content of chlorinated dioxins and furan in the particulate matter (ash) collected in the ESP, but did not increase its overall toxicity.

11.4.2

Non-Carbonaceous Sorbents

Efforts to develop multipollutant control strategies have demonstrated that adding certain oxidants to different classes of Ca-based sorbents leads to a significant improvement in elemental Hg vapor (Hg^0), SO_2 , and NO_x removal from simulated flue gases. Ghorishi *et al.* [14] studied the multipollutant capacity of two classes of Ca-based sorbents (hydrated limes and silicate compounds). A number of oxidizing additives at different concentrations were used in the Ca-based sorbent production process. The Hg^0 , SO_2 , and NO_x capture capacities of the oxidant-enriched sorbents were evaluated and compared to those of a commercially available activated carbon in bench-scale fixed- and fluidized-bed experimental systems. Calcium-based sorbents prepared with two unspecified oxidants exhibited Hg^0 sorption capacities ($\sim 100 \mu\text{g g}^{-1}$) comparable to that of the activated carbon; and they showed far superior SO_2 and NO_x sorption capacities.

Meyer *et al.* [15] studied the use of copper-doped Fe nanoaggregates silanized with organic sulfur as bis-(triethoxy silyl propyl)tetrasulfide for the capture of Hg^0 vapor for potential power plant applications. Silanization procedures resulted in 70% deposition of the targeted sulfur level, with particles containing $\sim 4 \text{ wt}\% \text{ S}$. The addition of copper was found to increase the fixed-bed (total) capacity of the sorbent from $170 \pm 20 \mu\text{g Hg/g-sorbent}$ with no copper doping to $2730 \pm 80 \mu\text{g Hg/g-sorbent}$ at 1.2 wt% Cu loading. When no S was deposited, the capacity of Fe/Cu nanoaggregates was only $180 \mu\text{g Hg/g-sorbent}$. The findings suggested that a combined Cu–S mechanism is responsible for Hg capture using these sorbents. Moving-bed (injection) testing of the Fe-based sorbents in a simulated flue gas stream showed that the 1.2 wt% Cu sample was able to achieve significant removal of Hg.

Meyer *et al.* [16] conducted additional work to examine the use of Cu–S sites for Hg capture from the gas phase for a silica-based platform using an S4 organic polysulfane and copper sulfate. The maximum fixed-bed equilibrium capacity achieved when using these materials was for a sorbent material with 2.5 wt% Cu and 6 wt% S. When compared to two other platforms, commercially available brominated-PAC and the previously tested Fe–Cu–S4 nanoaggregates, the Si-1

material performed the best in fixed-bed testing. During entrained-flow testing, the performance of Si-1 was only diminished 10% when exposed to 20 ppm SO_3 , an encouraging result for flue gas applications where SO_3 levels range from 1 to 40 ppm.

Hutson and Attwood [17] studied Hg capture using adsorbent material derived from the bauxite residue (red mud) from two North American aluminum refineries. The red mud, a seawater-neutralized red mud, and an acid-treated red mud were evaluated for their mercury adsorption capacity and compared with other, more conventional sorbent materials. Two different seawater-neutralized red mud samples were treated with HCl and HBr in an effort to increase the mercury sorption capacity. In all cases, the acid treatment resulted in a significant increase in the total surface area and an increase in the total pore volume. The fixed-bed mercury capture experimental results showed that the HBr activation treatment was effective in increasing the mercury capture performance of both sorbent samples. The HCl treatment, however, had no effect on the mercury capture performance; and entrained-flow experiments revealed that the bromine-containing red mud sorbent was much less effective for in-flight mercury capture.

11.4.3

Mercury Control in a Wet-FGD Scrubber

Experimental data from a laboratory-scale wet scrubber simulator confirmed that oxidized mercury, Hg^{2+} , can be reduced by aqueous S(IV) (sulfite and/or bisulfite) species and result in elemental mercury (Hg^0) emissions under typical wet flue gas desulfurization (FGD) scrubber conditions [18]. The S(IV)-induced Hg^{2+} reduction and Hg^0 emission mechanism was described by a model which assumed that only a fraction of the Hg^{2+} can be reduced, and that the rate-controlling step of the overall process is a first-order reaction involving the Hg–S(IV) complexes. Experimental data and model simulations predicted that Hg^{2+} in the flue gas can cause a rapid increase of Hg^0 concentration in the flue gas across a wet-FGD scrubber. The researchers also noted that forced oxidation enhanced Hg^{2+} reduction and Hg^0 emission by decreasing the S(IV) concentration in the scrubbing liquor. The model predictions also indicated that flue gas Hg^0 increases across a wet-FGD scrubber can be reduced by decreasing the pH, increasing the S(IV) concentration in the scrubber liquor, and lowering the temperature.

Chang and Zhao [19] discussed additional observations of elemental mercury (Hg^0) reemissions from a pilot-scale limestone wet scrubber. In those studies, simulated flue gas was generated by burning natural gas in a down-fired furnace and doped with 2000 ppm of SO_2 . A solution of mercuric chloride (HgCl_2) was delivered to the scrubber at a controlled rate to simulate the absorption of ionized mercury (Hg^{2+}). The testing results indicated that, after Hg^{2+} was injected, elevated Hg concentrations were soon detected both in the flue gas exiting the scrubber and in the hold tank air, indicating the occurrence of Hg^0 reemissions in both places. When the HgCl_2 feed was stopped, the Hg^0 reemission continued

for more than 2 h. In addition, a significant Hg^0 reemission was also detected outside the scrubber loop. In an attempt to understand the Hg^0 reemission increase across the wet scrubber system under transient and steady-state conditions and to understand the underlying relationship with the mercury complexes retained in the wet scrubber system, a mercury reemission model was developed. With this model, the researchers determined that the Hg^0 reemission rate under the current testing conditions could be simulated by a first-order reaction, and only a portion of Hg-S(IV) complexes retained in the slurry were participating in the reemission reaction.

Hutson *et al.* [20] and Krzyzyska *et al.* [21, 22] conducted a series of bench- and pilot-scale studies to examine the simultaneous control of SO_2 , NO_x , and mercury (both Hg^0 and Hg^{2+}) from a coal combustion flue gas in a multipollutant wet scrubber. The multipollutant capacity of a calcium-carbonate-based wet scrubber was enhanced with the addition of the oxidizing salt, sodium chlorite. The initial bench-scale results showed a maximum scrubbing of 100% for SO_2 and Hg species and near complete NO oxidation with about 60% scrubbing of the resulting NO_x species. The chlorite additive was less effective as an oxidant in the absence of SO_2 and NO in the flue gas. Oxidation of NO and mercury were only about 50% and 80%, respectively, when no SO_2 was present in the simulated flue gas. The mercury oxidation was similarly affected by the absence of NO in the flue gas.

Parametric studies investigating the effects of flue gas components, temperature, and oxidant addition rate were completed with the bench- and pilot-scale experimental facilities. Various process configurations were examined to optimize the addition of sodium chlorite. Additional studies by Krzyzyska and Hutson [23] showed that the location of the sodium chlorite application (before, in, or after the wet scrubber) greatly influences which pollutants are removed and the amount removed. This effect is related to the chemical conditions (pH, absence/presence of particular gases) that are present at different positions throughout the flue gas cleaning system profile. The results indicated that there is a potential to achieve very high SO_2 , NO_x , and Hg removals from the flue gas when sodium chlorite was applied before the wet limestone scrubber. However, applying the oxidizer after the wet limestone scrubber was the most effective configuration for Hg and NO_x control for extremely low chlorite concentrations (below 0.002 M) and therefore appears to be the best configuration for Hg control or as an additional step for NO_x polishing (after other NO_x control technologies).

Krzyzyska and Hutson [24] further examined the role of slurry pH on the multipollutant capacity of the oxidant-enhanced wet scrubber. The results showed that the slurry strongly influenced the chemical mechanism in the scrubber and, therefore, affected pollutant removal. Different NO_x removal efficiencies and mechanisms were found in acidic and alkaline slurry in the multipollutant scrubber. The acidic solution was favorable for NO and Hg^0 oxidation, while increasing the slurry pH above 7.0 was disadvantageous for NO and Hg oxidation/removal.

11.4.4

Effect of SCR on Mercury Oxidation/Capture

Selective catalytic reduction (SCR) technology is increasingly being applied for controlling emissions of nitrogen oxides (NO_x) from coal-fired boilers. Field and pilot studies suggested that the operation of SCR could affect the chemical form of mercury in coal combustion flue gases. The speciation of Hg is an important factor influencing the control and environmental fate of Hg emissions from coal combustion. The vanadium and titanium oxides, used commonly in the vanadia–titania SCR catalyst for catalytic NO_x reduction, promote the formation of oxidized mercury (Hg^{2+}).

Lee *et al.* [25] conducted bench-scale experiments to investigate Hg^0 oxidation in the presence of simulated coal combustion flue gases and under SCR reaction conditions. Flue gas mixtures with different concentrations of hydrogen chloride (HCl) and sulfur dioxide (SO_2) for simulating the combustion of bituminous coals and subbituminous coals were tested. The tests showed that HCl is the most critical flue gas component contributing to conversion of Hg^0 to Hg^{2+} under SCR reaction conditions.

Lee *et al.* [26] followed the bench-scale work with pilot-scale studies to investigate the effect of SCR catalyst on mercury (Hg) speciation in bituminous and subbituminous coal combustion flue gases. Three different Illinois Basin bituminous coals (from high to low sulfur and chlorine) and one Powder River Basin (PRB) subbituminous coal with very low sulfur and very low Cl were tested in a pilot-scale combustor equipped with an SCR reactor for controlling nitrogen oxide (NO_x) emissions. The SCR catalyst induced high oxidation of Hg^0 , decreasing the percentage of Hg^0 at the outlet of the SCR to values <12% for the three Illinois coal tests. The PRB coal test indicated a low oxidation of Hg^0 by the SCR catalyst, with the percentage of Hg^0 decreasing from similar to 96% at the inlet of the reactor to similar to 80% at the outlet. The low Cl content of the PRB coal and corresponding low level of available flue gas Cl species were believed to be responsible for low SCR Hg oxidation for this coal type. The test results indicated a strong effect of coal type on the extent of Hg oxidation.

Additional studies were conducted in a bench-scale reactor consisting of a natural gas burner and an electrically heated reactor housing an SCR catalyst that was constructed for studying elemental mercury (Hg^0) oxidation under SCR conditions [27]. A subbituminous coal combustion fly ash was injected into the entrained-flow reactor along with SO_2 , nitrogen oxides, HCl, and trace Hg^0 . Concentrations of Hg^0 and total mercury upstream and downstream of the SCR catalyst were measured using an online Hg monitor. The effects of HCl concentration, SCR operating temperature, catalyst space velocity, and feed rate of PRB fly ash on Hg^0 oxidation were evaluated. It was observed that HCl provides the source of chlorine for Hg^0 oxidation under simulated PRB coal-firing conditions. The decrease in Hg mass balance closure across the catalyst with decreasing HCl concentration suggests that transient Hg capture on the SCR catalyst occurred during the short test exposure periods and that the outlet

speciation observed may not be representative of steady-state operation at longer exposure times. Increasing the space velocity and operating temperature of the SCR led to less oxidized mercury. Introduction of PRB coal fly ash resulted in slightly decreased outlet oxidized mercury as a percentage of total inlet Hg and correspondingly resulted in an incremental increase in Hg capture. The injection of ammonia (NH_3) for NO_x reduction was found to have a strong effect to decrease Hg oxidation. The observations suggest that Hg^0 oxidation may occur near the exit region of commercial SCR reactors. Passage of flue gas through SCR systems without NH_3 injection, such as during the low-ozone season, may also impact Hg speciation and capture in the flue gas.

11.5

Coal Combustion Residues and By-Products

Flue gas from coal combustion contains significant amounts of volatile toxic trace elements such as arsenic (As), selenium (Se), and mercury (Hg). The capture of these elements in the FGD scrubber unit has resulted in generation of a metal-laden residue. With increasing reuse of the FGD residues in beneficial applications, it is important to determine metal speciation and mobility to understand the environmental impact of its reuse. Al-Abed *et al.* [28] reported the solid-phase speciation of As, Se, and Hg in FGD residues using XAS, X-ray fluorescence spectroscopy (XRF), and sequential chemical extraction (SCE) techniques. The SCE results combined with XRF data indicated a strong possibility of As association with iron oxides, whereas Se was distributed among all geochemical phases. The Hg appeared to be mainly distributed in the strong-complexed phase. XRF images also suggested a strong association of Hg with Fe oxide materials within FGD residues. XAS analysis indicated that As existed in its oxidized state (As(V)), whereas Se and Hg were observed in primarily reduced states as selenite (Se(IV)) and Hg(I), respectively. The results from the SCE and variable pH leaching tests indicated that the labile fractions of As, Se, and Hg were fairly low and thus suggestive of their stability in the FGD residues. However, the presence of a fine fraction enriched in metal content in the FGD residue suggested that size fractionation is important in assessing the environmental risks associated with their reuse.

Changes in emissions control at U.S. coal-fired power plants will shift metal content from the flue gas to the APC residues. To determine the potential fate of metals that are captured through use of enhanced APC practices, the leaching behavior of 73 APC residues was characterized following the approach of the Leaching Environmental Assessment Framework [29]. Materials were tested over pH conditions and liquid solid ratios expected during management via land disposal or beneficial use. Leachate concentrations for most metals were highly variable over a range of coal rank, facility configurations, and APC residue types. Liquid–solid partitioning (equilibrium) as a function of pH showed significantly different leaching behavior for similar residue types and facility configurations. Within a facility, the leaching behavior of blended residues was shown to follow

one of four characteristic patterns. Variability in metal leaching was greater than the variability in total concentrations by several orders of magnitude, inferring that total content is not predictive of leaching behavior. The complex leaching behavior and lack of correlation to total contents indicates that release evaluation under likely field conditions is a better descriptor of environmental performance than total content or linear partitioning approaches.

11.6

EPA SBIR Program

With support from EPA's Small Business Innovation Research (SBIR) Program and the U.S. DOE, Albemarle Mercury Control Division (formerly Sorbent Technologies Corporation) developed gas-phase bromination, a proprietary treatment, for PACs that can increase cost effectiveness for mercury control significantly when compared to non-brominated PAC.

With support from EPA's SBIR Program and the EPRI, Apogee Scientific, Inc. developed an advanced dry-catalytic gas sample conditioning system for use in the determination of in-duct mercury concentrations in coal-fired utility boilers. The Apogee Dry Sample Conditioning System (DSCS) represents a breakthrough in real-time mercury measurement technology.

EPA's SBIR Program also supported Advanced Fuel Research, Inc. (AFR) in the development of a technology to address both (i) removal and recovery of mercury from combustion/incineration flue gas and (ii) reprocessing of waste tires into value-added products. AFR's approach is based on mercury adsorption on low-cost, sulfur-rich activated carbons derived from scrap tires. The sulfur added to tire rubber in the process of vulcanization makes the tire-derived sorbents particularly effective in mercury removal. The first step in the waste-tire-processing scheme is pyrolysis, which involves thermal decomposition of tire rubber in an oxygen-free atmosphere. The solid product of pyrolysis (tire char) is subsequently converted into activated carbon. The sulfur content increases during tire processing, which is believed to facilitate mercury-capture efficiency. The cost-performance characteristics of tire-derived carbons are excellent and more favorable than those of the benchmark commercial carbon, Norit FGD.

References

1. Kilgroe, J.D. (1996) Control of dioxin, furan, and mercury emissions from municipal waste combustors. *J. Hazard. Mater.*, **47** (1), 163.
2. Krishnan, S.V., Gullett, B.K., and Jozewicz, W. (1997) Mercury control in municipal waste combustors and coal-fired utilities. *Environ. Prog.*, **16** (1), 47.
3. Ghorishi, S.B., Lee, C.W., Jozewicz, W.S., and Kilgroe, J.D. (2005) Effects of fly ash transition metal content and flue gas HCl/SO₂ ratio on mercury speciation in waste combustion. *Environ. Eng. Sci.*, **22** (2), 221.
4. Gullett, B.K. and Raghunathan, K. (1994) Reduction of coal-based metal emissions

- by furnace sorbent injection. *Energy Fuel*, **8** (5), 1068.
5. Krishnan, S.V., Gullett, B.K., and Jozewicz, W.S. (1994) Sorption of elemental mercury by activated carbons. *Environ. Sci. Technol.*, **28** (8), 1506.
 6. Ghorishi, S.B. and Gullett, B.K. (1999) Sorption of mercury species by activated carbons and calcium-based sorbents: effect of temperature, mercury concentration and acid gases. *Waste Manage. Res.*, **17** (4), 324.
 7. Serre, S.D., Gullett, B.K., and Ghorishi, S.B. (2001) Entrained-flow adsorption of mercury using activated carbon. *J. Air Waste Manage. Assoc.*, **51** (5), 733.
 8. Edwards, J.R., Srivastava, R.K., and Kilgroe, J.D. (2001) A study of gas-phase mercury speciation using detailed chemical kinetics. *J. Air Waste Manage. Assoc.*, **51** (6), 869.
 9. Li, Y.H., Lee, C.W., and Gullett, B.K. (2002) The effect of activated carbon surface moisture on low temperature mercury adsorption. *Carbon*, **40** (1), 65.
 10. Li, Y.H., Lee, C.W., and Gullett, B.K. (2003) Importance of activated carbon's oxygen surface functional groups on elemental mercury adsorption. *Fuel*, **82** (4), 451.
 11. Ghorishi, S.B., Keeney, R.M., Serre, S.D., Gullett, B.K., and Jozewicz, W.S. (2002) Development of a Cl-impregnated activated carbon for entrained-flow capture of elemental mercury. *Environ. Sci. Technol.*, **36** (20), 4454.
 12. Hutson, N.D., Attwood, B.C., and Scheckel, K.G. (2007) XAS and XPS characterization of mercury binding on brominated activated carbon. *Environ. Sci. Technol.*, **41** (5), 1747.
 13. Hutson, N.D., Ryan, S.P., and Abderrahmane, T. (2009) Assessment of PCDD/F and PBDD/F emissions from coal-fired power plants during injection of brominated activated carbon for mercury control. *Atmos. Environ.*, **43** (26), 3973.
 14. Ghorishi, S.B., Singer, C.F., Jozewicz, W.S., Sedman, C.B., and Srivastava, R.K. (2002) Simultaneous control of Hg⁰, SO₂, and NO_x by novel oxidized calcium-based sorbents. *J. Air Waste Manage. Assoc.*, **52** (3), 273.
 15. Meyer, D.E., Sikdar, S.K., Hutson, N.D., and Bhattacharyya, D. (2007) Examination of sulfur-functionalized, copper-doped iron nanoparticles for vapor-phase mercury capture in entrained-flow and fixed-bed systems. *Energy Fuel*, **21** (5), 2688.
 16. Meyer, D.E., Meeks, N., Sikdar, S., Hutson, N.D., Hua, D., and Bhattacharyya, D. (2008) Copper-doped silica materials silanized with bis-(triethoxy silyl propyl)-tetra sulfide for mercury vapor capture. *Energy Fuel*, **22** (4), 2290.
 17. Hutson, N.D. and Attwood, B.C. (2008) Binding of Vapour-phase Mercury (Hg⁰) on Chemically Treated Bauxite Residues (Red Mud). *Environ. Chem.*, **5** (4), 281.
 18. Chang, J.C.S. and Ghorishi, S.B. (2003) Simulation and evaluation of elemental mercury concentration increase in flue gas across a wet scrubber. *Environ. Sci. Technol.*, **37** (24), 5763.
 19. Chang, J.C.S. and Zhao, Y. (2008) Pilot plant testing of elemental mercury reemission from a wet scrubber. *Energy Fuel*, **22** (1), 338.
 20. Hutson, N.D., Krzyzyska, R., and Srivastava, R.K. (2008) Simultaneous removal of SO₂, NO_x, and Hg from coal flue gas using a NaClO₂-enhanced wet scrubber. *Ind. Eng. Chem. Res.*, **47** (16), 5825.
 21. Krzyzyska, R., Zhao, Y., and Hutson, N.D. (2010) Absorption of NO_x, SO₂ and mercury in a simulated additive-enhanced wet flue gas desulphurization scrubber. *Pol. J. Environ. Stud.*, **19** (6), 1255.
 22. Krzyzyska, R., Zhao, Y., and Hutson, N.D. (2011) Bench- and pilot-scale investigation of integrated removal of sulphur dioxide, nitrogen oxides and mercury in a wet limestone scrubber. *Rocznik Ochrona Srodowiska (Poland)*, **13** (1), 29.
 23. Krzyzyska, R. and Hutson, N.D. (2012) The importance of the location of sodium chlorite application in a multipollutant flue gas cleaning system. *J. Air Waste Manage. Assoc.*, **62** (6), 707.
 24. Krzyzyska, R. and Hutson, N.D. (2012) Effect of solution pH on SO₂, NO_x and

- Hg removal from simulated coal combustion flue gas in an oxidant-enhanced wet scrubber. *J. Air Waste Manage. Assoc.*, **62** (2), 212.
25. Lee, C.W., Srivastava, R.K., Ghorishi, S.B., Hastings, T.W., and Stevens, F.M. (2004) Investigation of selective catalytic reduction impact on mercury speciation under simulated NO_x emission control conditions. *J. Air Waste Manage. Assoc.*, **54** (12), 1560.
26. Lee, C.W., Srivastava, R.K., Ghorishi, S.B., Karwowski, J., Hastings, T.W., and Hirschi, J.C. (2006) Pilot-scale study of the effect of selective catalytic reduction catalyst on mercury speciation in Illinois and powder river basin coal combustion flue gases. *J. Air Waste Manage. Assoc.*, **56** (5), 643.
27. Lee, C.W., Serre, S.D., Zhao, Y., and Lee, S.J. (2008) Mercury oxidation promoted by a selective catalytic reduction catalyst under simulated powder river basin coal combustion conditions. *J. Air Waste Manage. Assoc.*, **58** (4), 484.
28. Al-Abed, S.R., Jegadeesan, G., Scheckel, K.G., and Tolaymat, T. (2008) Speciation, characterization, and mobility of As, Se, and Hg in flue gas desulphurization residues. *Environ. Sci. Technol.*, **42** (5), 1693.
29. Thorneloe, S.A., Kosson, D.S., Sanchez, F., Garrabrants, A.C., and Helms, G. (2010) Evaluating the fate of metals in air pollution control residues from coal-fired power plants. *Environ. Sci. Technol.*, **44**, 19.

12

The Electric Power Research Institute's Program to Control Mercury Emissions from Coal-Fired Power Plants

Ramsay Chang

12.1

Introduction

The Electric Power Research Institute (EPRI) draws on decades of research to help member companies operate electric power plants in an efficient and cost-effective manner, in compliance with state and federal environmental regulations. This chapter describes EPRI's research and development program to control mercury (Hg) emissions from power plants firing different coals under various configurations and operating conditions. EPRI gratefully acknowledges the participation of stakeholders who have made this research possible, and the work of others who have contributed specific information on the many aspects of mercury control.

12.2

Co-Benefits of Installed Controls

At coal-fired electric generating units, mercury control co-benefits occur when installed control equipment, combustion conditions, and mercury pathways offer a baseline level of flue gas mercury removal that does not depend on adding new controls. Using the co-benefits of installed controls for nitrogen oxides (NO_x) and sulfur oxides (SO_x) is the first key, near-term technology for controlling mercury emissions. Co-benefits assume new importance as power plant owners seek all avenues of compliance with the Mercury and Air Toxics Standards (MATS) rule.

12.2.1

Selective Catalytic Reduction/Flue Gas Desulfurization

When flue gas passes through a selective catalytic reduction (SCR) system, the SCR converts elemental mercury to oxidized mercury, the form most easily captured in a downstream wet or dry flue gas desulfurization (FGD) system. The resulting baseline mercury removal is a co-benefit of SCR operation to control NO_x and FGD operation to control SO_x .

Mercury Control: for Coal-Derived Gas Streams, First Edition.

Edited by Evan J. Granite, Henry W. Pennline and Constance Senior.

© 2015 Wiley-VCH Verlag GmbH & Co. KGaA. Published 2015 by Wiley-VCH Verlag GmbH & Co. KGaA.

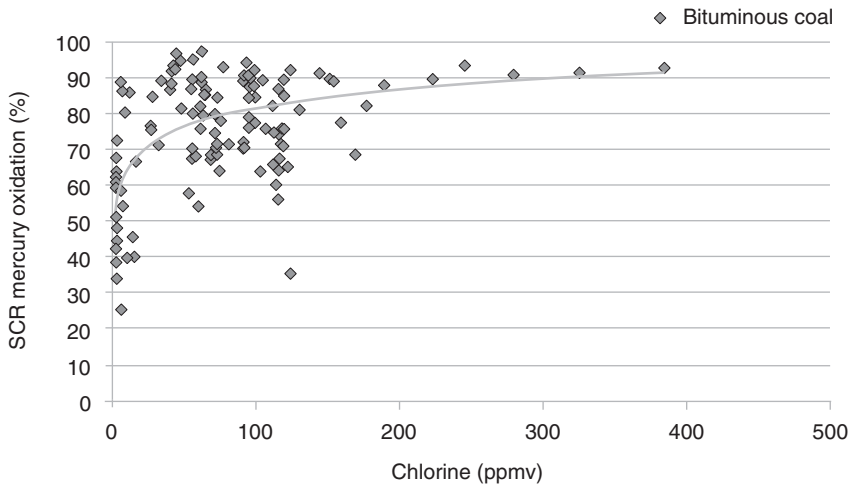


Figure 12.1 SCR mercury oxidation for bituminous coal-fired units.

Some eastern bituminous (EB)-fired units with combined SCR/FGD operation experience baseline mercury removals exceeding 90% [1]. However, many such units fail to achieve 90% control, especially over extended periods of time. For consistent, long-term regulatory compliance, these co-benefit units may require operational adjustments to counter excursions above the 1.2 lb Tbtu⁻¹ MATS mercury emission limit, and a significant number may require supplemental mercury controls, such as activated carbon injection (ACI) and boiler halogen addition, to meet the limit.

A recent analysis of 240 datasets collected by EPRI at EB-fired co-benefit units shows highly variable mercury oxidation, with an average oxidation of 75% across the SCR; only about one-third of the datasets describe 90% or greater mercury oxidation (Figure 12.1) [2]. In research that will contribute to stable, high mercury removal at these co-benefit units, EPRI is working to enhance mercury oxidation across the SCR by evaluating high-mercury-oxidation SCR catalysts, improving catalyst management, and optimizing flue gas conditions such as halogen (chloride, bromide) content and temperature. EPRI is also pursuing a full characterization and understanding of wet flue gas desulfurization (wFGD) chemistry with the goal of enhancing reliable, continuous mercury removal by managing wFGD processes.

12.2.2

Unburned Carbon

When coal combustion is incomplete, unburned carbon (UBC) particles in fly ash remain available to adsorb flue gas mercury. Capture of the UBC-laden ash in particulate control devices provides a modest level of baseline mercury removal.

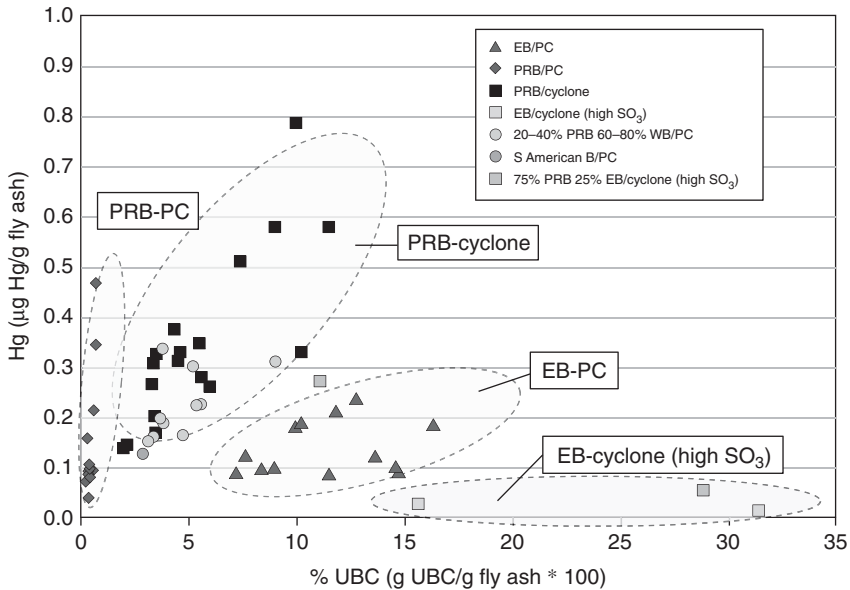


Figure 12.2 Influence of coal type, UBC concentration, and boiler type on fly ash mercury adsorption. (EB, eastern bituminous coal; WB, western bituminous coal; PRB, Powder River Basin coal; and PC, pulverized coal.)

The amount of mercury adsorbed on fly ash depends on coal type, the concentration of UBC in the ash, and boiler type. As shown in Figure 12.2, UBC in fly ash derived from western Powder River Basin (PRB) coal adsorbs much more mercury than does UBC in fly ash derived from high-sulfur eastern bituminous (HSEB) coal [1]. For a given coal, increasing UBC in fly ash enhances mercury capture. Increasing halogen levels in flue gas can enhance UBC affinity for elemental mercury.

12.3

Sorbent Injection

Sorbent injection – in particular, the use of ACI and BACI (brominated activated carbon injection) – is the second key, near-term technology for controlling mercury emissions.

In 2011, EPRI reported that ACI was installed at more than 60 U.S. power plants (more than 100 units) on coal-fired boilers rated from 73 to 1375 MWe [3]. Most of these ACI installations have operated since 2009, in compliance with state regulations and consent decrees. During site visits in 2010–2011, EPRI conducted detailed surveys of 11 ACI installations representing a broad cross section of the industry. EPRI member companies have hosted numerous ACI field studies.

12.3.1

Units Equipped with Electrostatic Precipitators

12.3.1.1 Western Coals

At electrostatic precipitator (ESP)-equipped units firing western coals, ACI removes about 75% of flue gas mercury at an injection rate of 5 lb MMacf⁻¹ (Figure 12.3) [1]. This poor performance results from the low halogen content of the flue gas environment created by western coal combustion. Fundamental studies to date show that elemental mercury adsorption is enhanced by halogens that oxidize mercury and form halogen–mercury–carbon bonds. Use of BACI at injection rates similar to those for ACI removes more than 90% of flue gas mercury (Figure 12.3). BACI does not perform significantly better than ACI for EB coals, where a significant fraction of vapor-phase mercury is in the oxidized form [1].

12.3.1.2 Eastern Bituminous Coals and High-Sulfur Flue Gases

At ESP-equipped units firing EB coals, ACI mercury removals vary widely (Figure 12.4) [1]. Although the flue gas environment created by EB coal combustion contains more halogen (chloride) than western coal flue gas, it also contains more sulfur – especially if the coal fired is HSEB (S > 3%). Under these conditions, researchers postulate that sulfur trioxide (SO₃) in the flue gas competes with mercury for active adsorption sites on injected carbon or forms sulfuric acid (H₂SO₄) that blocks carbon pores. High concentrations of SO₃ in flue gas can form during combustion of high-sulfur coal, SCR conversion of sulfur dioxide (SO₂) to SO₃, or the use of SO₃ flue gas conditioning to improve ESP performance.

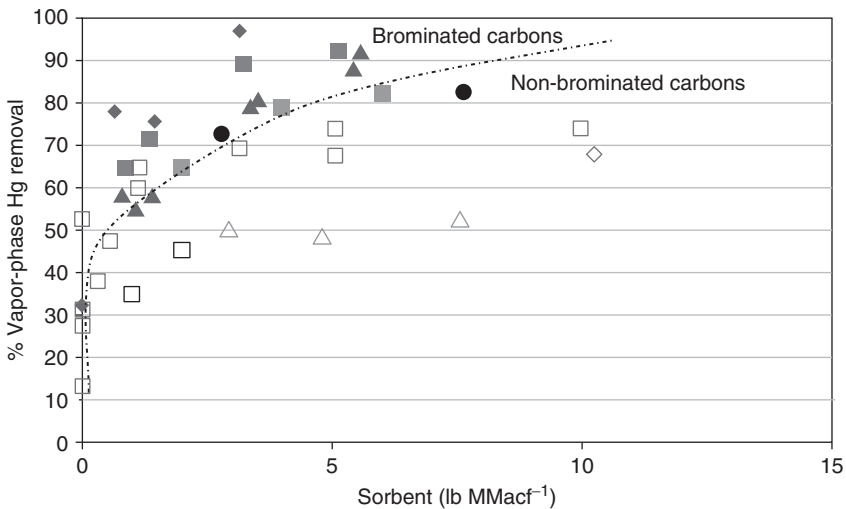


Figure 12.3 ACI mercury removal across ESPs for western coals. (Symbol shapes denote different sorbents, with solids representing BACs and outlines representing ACs.)

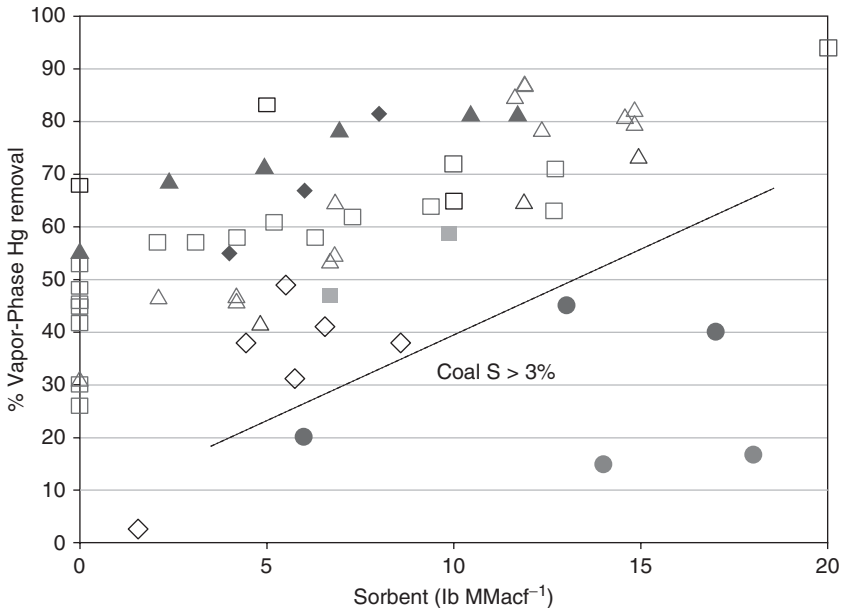


Figure 12.4 ACI mercury removal across ESPs for EB coals. (For LSEB coal ($S < 3\%$), symbol shapes denote different sorbents, with solids representing BACs and outlines representing ACs.)

Figures 12.4 and 12.5 illustrate the impact of flue gas SO_3 concentration on mercury removal across an ESP when using ACI for mercury control [1]. EPRI is evaluating various options to mitigate SO_3 impacts, including the use of SO_3 -tolerant sorbents, alkali injection to reduce flue gas SO_3 concentrations, and alternate ESP flue gas conditioning agents.

12.3.2

Units Equipped with Fabric Filters or TOXECON[®]

To date, results show that using ACI or BACI with fabric filters (FFs) – including TOXECON[®] [4] (an ESP followed by a polishing FF) – can effectively remove mercury from western and low-sulfur eastern bituminous (LSEB) coal flue gases (Figure 12.6) [1]. Few ACI or BACI results are available for HSEB coal flue gas, as very few FFs are installed on HSEB-fired units; most of these units are equipped with an ESP and wFGD. EPRI is investigating whether ACI before an FF can effectively remove mercury from HSEB coal flue gas and whether mercury removals can be enhanced with alkali injection to reduce SO_3 levels.

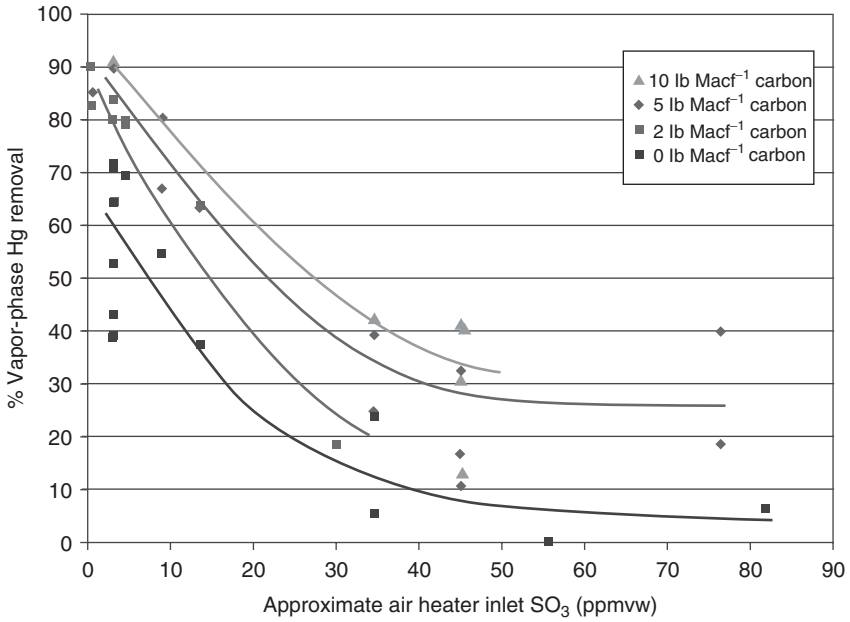


Figure 12.5 Influence of flue gas SO₃ concentration on ACI mercury removal across an ESP.

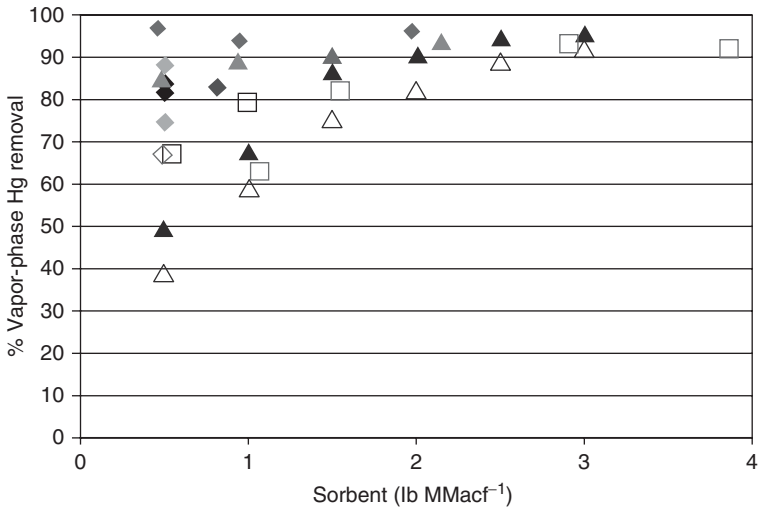


Figure 12.6 ACI mercury removal across FFs for western and LSEB coals. (Symbol shapes denote different carbons, with solids representing brominated and outlines representing non-brominated carbons.)

12.3.3

Challenges and Responses

Potential balance-of-plant impacts associated with ACI and BACI present challenges that must be addressed to contain the cost of regulatory compliance and, hence, the cost of electricity.

12.3.3.1 Preserving Fly Ash Sales

Preserving fly ash sales and avoiding ash disposal costs are important economic goals for many power plants. But these goals are thwarted if ACI or BACI increases the carbon content of fly ash, making it unsuitable for sale as a replacement for Portland cement in concrete.

Even small amounts of activated carbon (AC) in fly ash can adsorb the organic, air-entraining agents (AEAs) that fabricators add to improve concrete expansion and contraction over freeze/thaw cycles. To avoid this problem while continuing to use ACI for mercury control, power plant owners have evaluated mitigation measures such as minimizing the amount of injected AC, treating carbon-laden fly ash with chemicals to block AEA adsorption, injecting specially treated ash compatible carbons or non-carbon sorbents, or installing TOXECON. In EPRI's TOXECON configuration, an initial ESP captures 99% of the fly ash before carbon injection occurs between the ESP and an FE, or secondary particulate collector. Because fly ash collects in the ESP hoppers before it is exposed to AC, the ash remains uncontaminated and suitable for sale.

Some wholesalers purchase fly ash with relatively consistent concentrations of carbon, allowing them to predict the amount of AEA needed for concrete fabrication. Thus, another option to preserve ash sales is to maintain a relatively stable and predictable ratio of AC to fly ash [1].

12.3.3.2 Optimizing Electrostatic Precipitator Performance

- *Particulate matter emissions and opacity:* Although ACI increases the carbon burden in flue gas, EPRI found no significant ACI-related changes in particulate matter (PM) mass emissions or opacity monitored at the stacks of 12 ESP units surveyed in 2010 [5]. With or without ACI, historical data indicate that PM mass emissions from large ESPs and TOXECON units fall below the 0.03 lb MMBtu⁻¹ new source performance standard for power plant emissions, which is identical to the MATS limit for filterable PM. However, some small ESPs (specific collection area ~300 ft² kacfm⁻¹ or lower) do have PM mass emissions above this limit [5]. The electric power industry is evaluating low-cost performance upgrades for these small ESPs.
- *Mercury removal in the presence of flue gas conditioning:* Units firing either EB or western coals may employ both ACI and SO₃ flue gas conditioning to reduce ash resistivity and improve ESP collection efficiency. However, because SO₃ adversely impacts mercury adsorption on AC in flue gas, EPRI has tested the performance of alternative flue gas conditioners.

At a PRB-fired unit equipped with an ESP, researchers replaced SO_3 with an alternative liquid flue gas conditioner (LFGC) in tests of ACI mercury control. The LFGC proved to be as effective as SO_3 conditioning in controlling particulate emissions across the ESP. Furthermore, it did not interfere with mercury removal [3].

12.3.3.3 Optimizing Fabric Filter and TOXECON Performance

- *Optimal ash-to-carbon ratio:* In the TOXECON configuration, if the ESP is too efficient in removing fly ash from flue gas during ACI, PM entering the FF is largely carbon. As observed at one unit, fine carbon particles can clog filter bags – increasing pressure drop and cleaning pulse frequency while decreasing actual mercury removal. To solve this problem, plant operators at the unit detuned the ESP to allow more fly ash to enter the FF [5]. Thus, there may be an optimal ash-to-carbon ratio that must be determined empirically for some TOXECON installations to optimize mercury capture in the FF while maintaining reasonable pressure drop and cleaning frequency.
- *Hopper fires:* The high carbon content of ash in TOXECON FF hoppers also creates the possibility of hopper fires. At one TOXECON installation where fires were reported, researchers modeled combustion of the carbon-rich ash and suggested mitigation measures. These measures included installing temperature sensors and ash level detectors in the hoppers, as well as implementing an aggressive hopper cleaning schedule [6].
- *Influence of flue gas temperature:* AC adsorbs mercury more readily at lower flue gas temperatures. Figure 12.7 illustrates the response of ACI mercury removal to temperature variations from 330 to 360 °F at a PRB-fired unit equipped with an FF. To maintain stable mercury removal at this unit, plant operators must adjust the ACI rate for seasonal variations in temperature from winter to summer months [1].

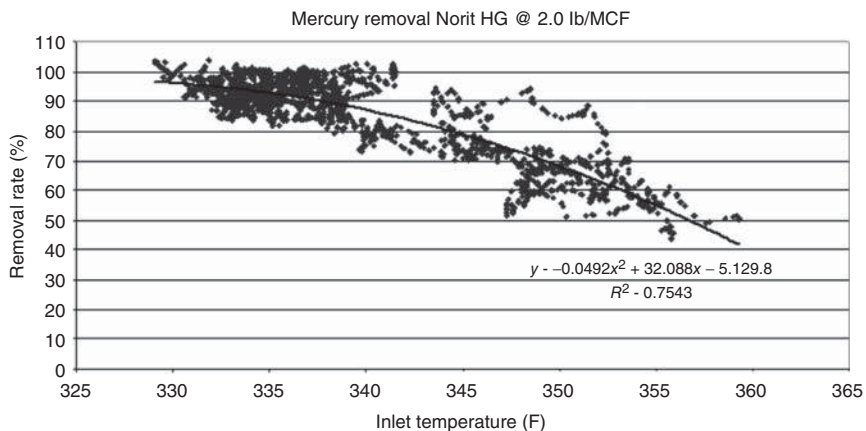


Figure 12.7 Influence of temperature on ACI mercury removal across an FF for PRB coal.

12.4

Boiler Chemical Addition

Boiler chemical addition (BCA) is the third key, near-term technology for controlling mercury emissions. BCA introduces halogens – usually bromide salts, such as calcium bromide (CaBr) – in solid or liquid form to the coal feed [7, 8]. Plant operators may also inject hydrogen bromide (HBr) into flue gas upstream of the air heater. Figure 12.8 shows the locations of these treatments, along with potential bromine balance-of-plant impacts on fly ash, the SO₂ scrubber, and stack emissions.

Since 2004, EPRI has conducted several full-scale demonstrations of boiler bromide addition (BBA) at units firing western coals (PRB and Texas lignite). In these demonstrations, more than 90% of flue gas mercury was oxidized at BBAs equivalent to 25–300 ppm by weight in coal [1]. This oxidizing effect is enhanced at units with SCR. For example, BBA (25 ppm Br) removed 90% of flue gas mercury in a 2-month test at a PRB-fired unit equipped with an SCR, ESP, and a downstream wFGD to capture the bromine-oxidized mercury (Figure 12.9) [9].

In a continuous 12-day test at an EB-fired unit equipped with an ESP and wFGD, BBA failed to achieve more than 90% mercury oxidation and did not improve total mercury removal [3]. At another EB-fired unit, researchers determined that BBA took several weeks to equilibrate in the wFGD; this reduced mercury reemissions and improved total mercury removal (Unpublished EPRI field test data). EPRI continues to study BBA at EB-fired units.

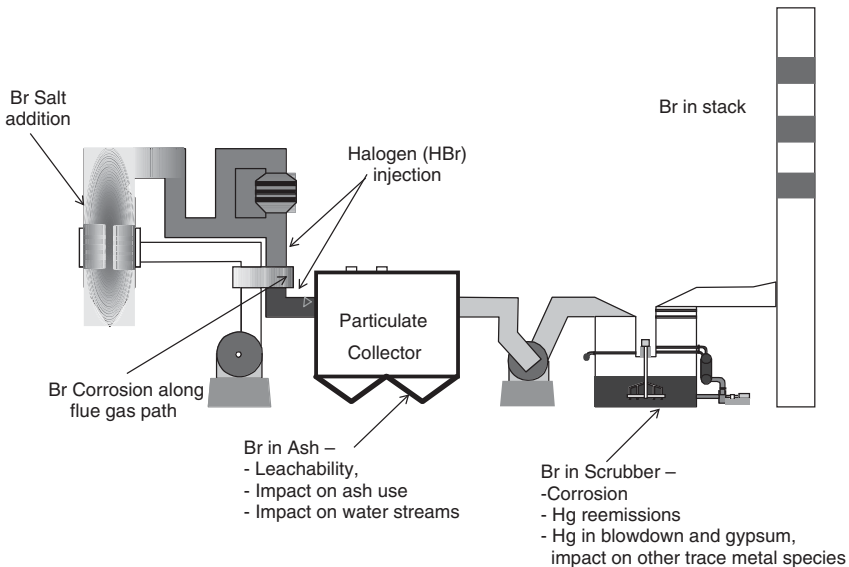


Figure 12.8 BCA options and potential balance-of-plant impacts.

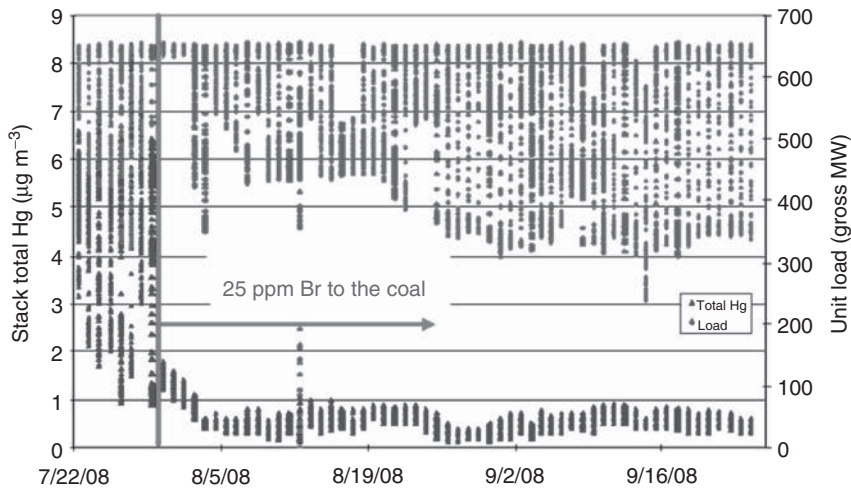


Figure 12.9 BBA promotes SCR mercury oxidation and removal across a wFGD for PRB coal.

12.4.1

Combined Technologies

Recently, several power plants have combined BBA with ACI. Combined technologies may offer an advantage over BACI at western coal-fired units because they reduce the amount of AC needed to achieve a given level of mercury control. At a North Dakota lignite-fired unit equipped with an ESP and wFGD, researchers tested the relative effectiveness of ACI (Norit Darco Hg) and BACI (Norit Darco Hg-LH) used as sole technologies or in combination with varying concentrations of BBA (CaBr). BACI was not as effective as BBA plus ACI in controlling mercury emissions, requiring an injection rate of 2 lb MMacf^{-1} or more to meet the 4.0 lb TBtu^{-1} MATS mercury emission limit for lignite coal-fired units (Figure 12.10). BBA (75 ppm Br) paired with ACI was the most effective treatment, meeting the emission limit at even the lowest sorbent injection rate (Unpublished EPRI field test data). This reduced use of AC can be an important consideration in preserving fly ash sales.

BBA can enhance the mercury removal effectiveness of ACI at units with FFs or TOXECONs, as well as ESPs. In one field test at a TOXECON unit firing PRB coal, the use of BBA (CaBr) alone supported 70–85% mercury removal across the TOXECON FF without ACI. Combining BBA with ACI delivered an average of 90% removal at an ACI rate of about $0.75 \text{ lb MMacf}^{-1}$. On the other hand, several days of continuous BACI offered 90% mercury removal at a rate of $1.26 \text{ lb MMacf}^{-1}$ [5]. The decision to use BBA plus ACI versus BACI will depend on cost, including any potential balance-of-plant impacts.

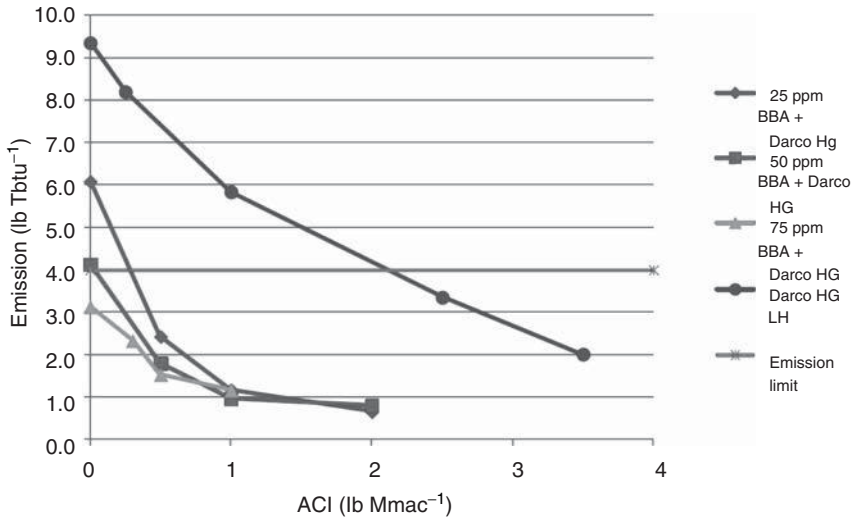


Figure 12.10 Combined BBA and ACI for mercury control.

12.4.2

Challenges and Responses

EPRI pursues a comprehensive research program to clarify potential balance-of-plant impacts associated with BBA to control mercury emissions at coal-fired units (Figure 12.11). This section describes challenges encountered during power plant operation and responses offered by EPRI research.

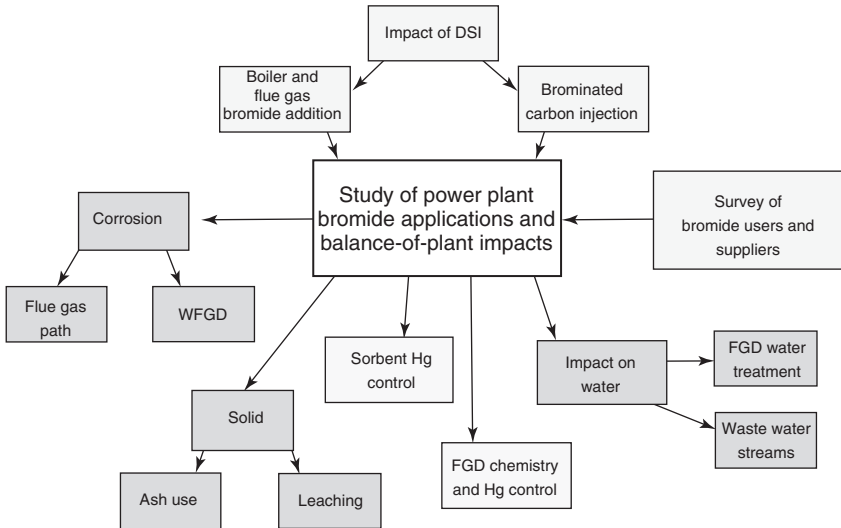


Figure 12.11 EPRI research program to clarify potential balance-of-plant impacts associated with BBA.

12.4.2.1 Wet Flue Gas Desulfurization Chemistry and Mercury Partitioning

Clarity about wFGD chemistry may allow researchers to partition mercury (and other trace metals such as selenium) to the most advantageous liquid or solid waste stream for a given unit. EPRI is conducting fundamental studies of chemical reactions within the scrubber that influence mercury and selenium (Se) partitioning, including mercury reemissions. These reactions involve constituents that concentrate in the FGD, such as limestone (CaCO_3) used in forced oxidation scrubbers and the inert materials the limestone contains, ferric chloride (FeCl_3) added for water treatment, and trace metals.

In one study at a PRB-fired unit equipped with an SCR, ESP, and wFGD, researchers observed no impact of BBA (CaBr) on mercury reemissions from the FGD. At this unit, most of the scrubbed mercury reported to the FGD solids under baseline conditions and BBA [1].

In contrast, most of the mercury reported to the FGD liquor during BBA at an EB-fired unit equipped with an ESP and wFGD. Under baseline conditions, about 67% of the wFGD mercury partitioned to the liquor. With BBA, these results remained basically unchanged (74%). However, adding AC to the sump liquor decreased wFGD mercury in the liquor to about 5%. This dramatic decrease demonstrated that added carbon was adsorbing mercury from the wFGD liquor. No other trace metals, including selenium, were significantly adsorbed by the added carbon [3].

12.4.2.2 Corrosion along Flue Gas Path and in the wFGD

Bromides formed with BBA are scrubbed and can reach high concentrations (500 to >30 000 ppm) in the wFGD over time, depending on scrubber design and the amount of recirculation that occurs [3]. There is concern that such high bromide concentrations may corrode FGD metal surfaces, especially in conjunction with high chloride levels.

In EPRI-sponsored laboratory studies, researchers exposed various metal alloys to simulated FGD liquors, creating corrosive environments reflecting the operation of a PRB-fired unit equipped with an SCR, ESP, and wFGD. The halogen content of the simulated liquors was based on chlorine already present and BBA rates needed for 90% mercury removal with SCR operation (25 ppm Br) or without SCR operation (100 ppm Br). Under these test conditions, alloys 2205, 317LM, and 316L experienced corrosion at 100 ppm BBA, as shown by the pitting potential in Figure 12.12, where lower voltages indicate greater susceptibility to corrosion [1]. These results suggest that careful selection of FGD construction materials may mitigate corrosion at units employing BBA for mercury control.

In addition to potential corrosion in wFGD scrubbers, corrosion along the flue gas path – for example, in air heater baskets – appears to occur at some full-scale units using BBA [10]. EPRI is conducting field and laboratory studies to determine whether bromide in flue gas causes the observed corrosion, or whether other factors and flue gas constituents are involved.

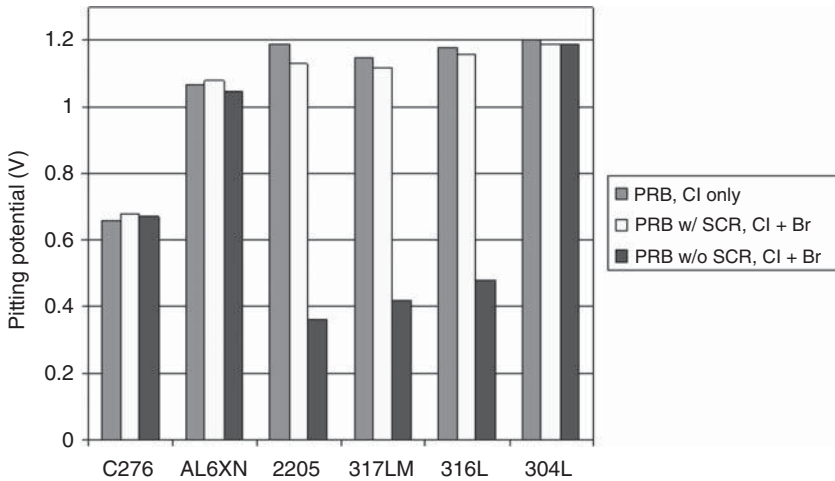


Figure 12.12 Corrosion of alloys in simulated FGD liquor for PRB coals, with and without SCR operation. (Lower pitting potential voltages indicate greater susceptibility to corrosion.)

12.4.2.3 Preserving Fly Ash Sales

At a PRB-fired unit equipped with an SCR, ESP, and FGD, 95% of bromide added to the boiler was scrubbed in the FGD unit. Fly ash adsorbed only 1–2% of the added bromide after 2 weeks of continuous treatment. This bromide concentration in fly ash did not affect physical properties of prepared concrete mixes, such as air content, compressive strength, set time, slump, or unit weight [1].

12.4.2.4 Selenium Partitioning in Wet Flue Gas Desulfurization Systems

Tracking selenium through a unit may alert operators to possible waste disposal issues. EPRI investigated selenium partitioning with BBA at an EB-fired unit equipped with an ESP and wFGD. Under baseline conditions, about 70% of the selenium appeared in the fly ash. BBA displaced this selenium from the fly ash to the FGD liquor, whose selenium concentration increased fourfold – from 151 $\mu\text{g}/100\text{ g}$ of liquor at baseline to 590 $\mu\text{g}/100\text{ g}$ of liquor at test [3]. This displacement may occur because selenium and bromide react to form selenium bromide (SeBr), a highly volatile compound that is not easily adsorbed on fly ash.

Selenium in the FGD liquor was largely selenate (SeO_4^{2-}), the form most difficult to remove with traditional wastewater treatments. Selenate displacement to the FGD liquor is an undesirable outcome, given the more stringent effluent guidelines proposed by the U.S. Environmental Protection Agency for fluid waste streams from coal-fired power plants.

12.4.2.5 Bromide Leaching from Fly Ash

As reported, 1–2% of bromide added to the boiler was adsorbed by fly ash at a PRB-fired unit equipped with an SCR, ESP, and FGD. In Synthetic Precipitation

Leaching Procedure tests on fly ash samples from the unit, 60–100% of total bromide content leached from the fly ash, confirming bromide's high water solubility [1]. Companies disposing of fly ash in landfills should consult state and local regulations to determine whether specific limits apply to bromide concentrations in landfill leachate.

12.5

Novel Concepts for Mercury Control

Novel concepts address the need to contain capital and operating costs while offering the most effective and efficient controls for mercury and other air pollutants.

12.5.1

TOXECON II®

This adaptation offers many of the advantages of TOXECON, without the expense of installing a compact FF. In the TOXECON II® configuration, sorbent is injected between the fields of an ESP [11]. Most of the fly ash collects in the inlet fields, before carbon injection, and can be sold. About 10% of the remaining fly ash collected in the final fields is contaminated and requires disposal. TOXECON II flue gas mercury removals of about 80% are possible for western coal-fired units without SO₂ scrubbers [1].

12.5.2

Gore® Carbon Polymer Composite Modules

W. L. Gore & Associates, Inc. has developed a carbon polymer composite (CPC) material made of AC granules embedded in a Teflon™ polymer matrix and formed into sheets [12]. When a CPC sheet is placed in the flue gas path, its carbon granules adsorb mercury and oxidize SO₂ to SO₃. Both elemental and oxidized mercury remain bound to the embedded carbon granules, while the SO₃ reacts with flue gas moisture to form sulfuric acid droplets that drain from the surface of the hydrophobic sheet. CPC modules can be placed above the mist eliminator at the top of a wFGD (Figure 12.13) [13]. The goal is to capture residual mercury and SO₂ downstream of the wFGD, where flue gas temperature is low (ensuring maximal mercury adsorption) and moisture is high. Depending on SO_x levels, a CPC reactor could be an alternative to an upgraded or new FGD system.

In 2010, EPRI demonstrated the feasibility of the Gore® CPC concept at an EB-fired unit equipped with an ESP and wFGD. In these tests on slipstream flue gas sampled after a limestone wet scrubber, mercury removal efficiency remained high (80–95%) over the entire 180 days of testing (Figure 12.14), resulting in outlet emissions of <1 lb TBtu⁻¹ mercury. About 60% of SO₂ was removed from slipstream flue gas during the same test period [14]. EPRI is conducting further

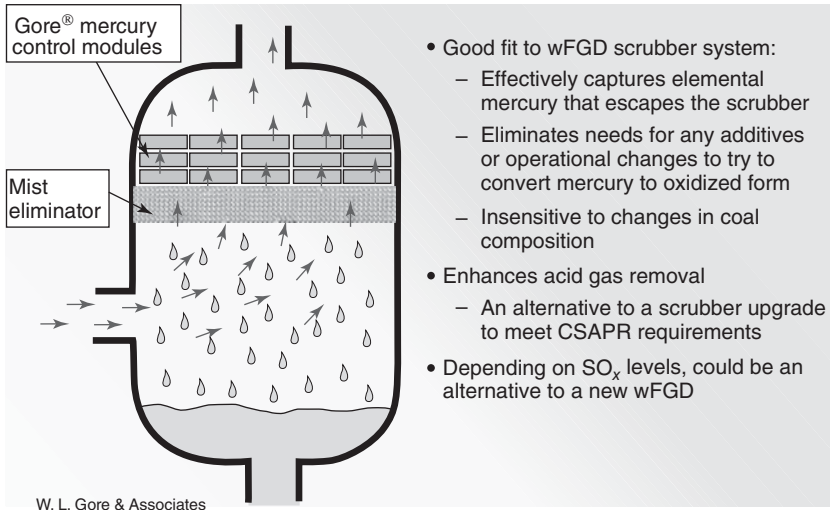


Figure 12.13 CPC modules placed above the mist eliminator in a wFGD.

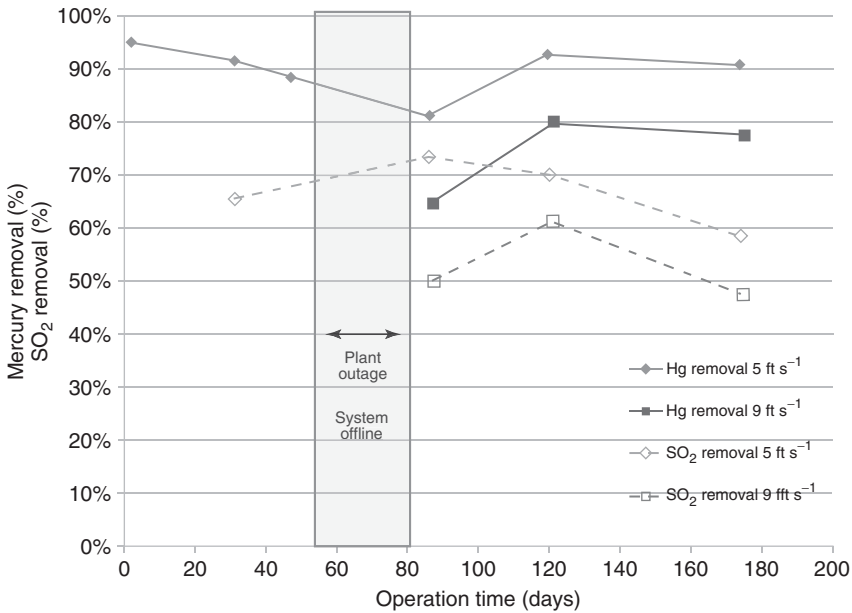


Figure 12.14 Mercury and SO₂ removal by CPC during 180 test days for EB coal.

pilot- and full-scale evaluations at other power plant sites to assess the potential for full-scale applications of CPC technology. Gore has recently renamed the CPC as Gore Mercury Control System (GMCS).

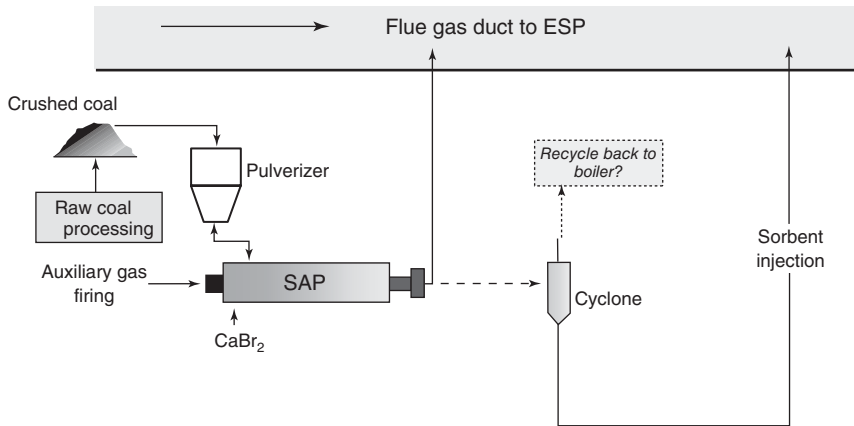


Figure 12.15 SAP process schematic.

12.5.3

Sorbent Activation Process

The Sorbent Activation Process (SAP[®]) [15, 16] reduces AC cost by more than 50% using on-site feedstocks to produce AC for mercury removal via a much simplified production process. Patented by EPRI and the University of Illinois at Urbana-Champaign, SAP uses a high-temperature reaction chamber to convert pulverized coal feedstock to AC in a matter of seconds (Figure 12.15) [17]. The AC is then injected directly into flue gas before an ESP or other particulate control device. Alternately, SAP flue gas and product AC are separated by a cyclone. The gas is recirculated to the boiler and the AC is injected into the flue gas. SAP uses the coal burned at the power plant site, together with activating agents and other chemicals, to create sorbents with unique surface areas, pore structures, and surface chemistries.

Field tests at a PRB-fired unit and an EB-fired unit confirmed that SAP ACs made from these coals are comparable to commercially available ACs used for mercury control. For example, both a commercial brominated activated carbon (BAC) and an SAP BAC removed about 80% to more than 90% of the mercury from flue gas across an FF (TOXECON configuration) at the PRB-fired unit (Figure 12.16) [17].

Further field tests at the EB-fired unit equipped with an ESP and wFGD offered proof of concept that SAP also can produce lime from limestone co-injected with pulverized coal for acid gas removal [17]. EPRI is demonstrating the cost-effectiveness of SAP at a Texas lignite-fired unit equipped with an ESP and wFGD.

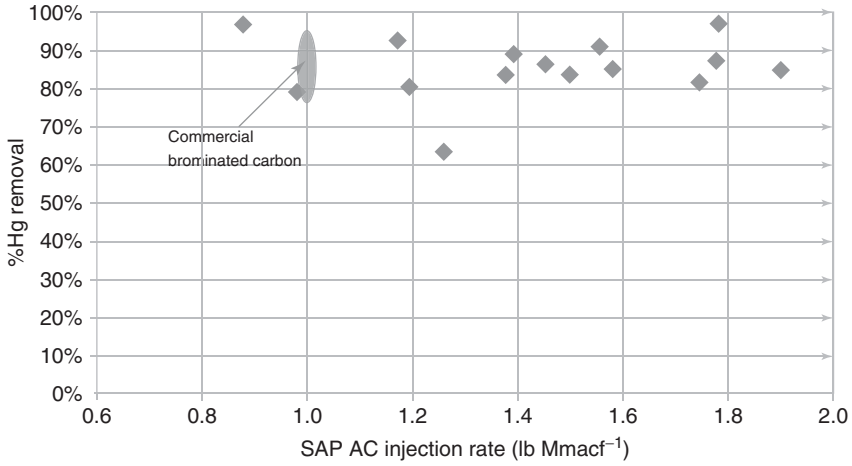


Figure 12.16 Mercury removal for PRB coal using SAP-produced BAC compared to commercial BAC.

12.6

Integration of Controls for Mercury with Controls for Other Air Pollutants

In the era of compliance with strict MATS limits and other pollution control regulations, such as the Cross-State Air Pollution Rule (CSAPR), mercury control technologies must work effectively with other pollution control technologies, such

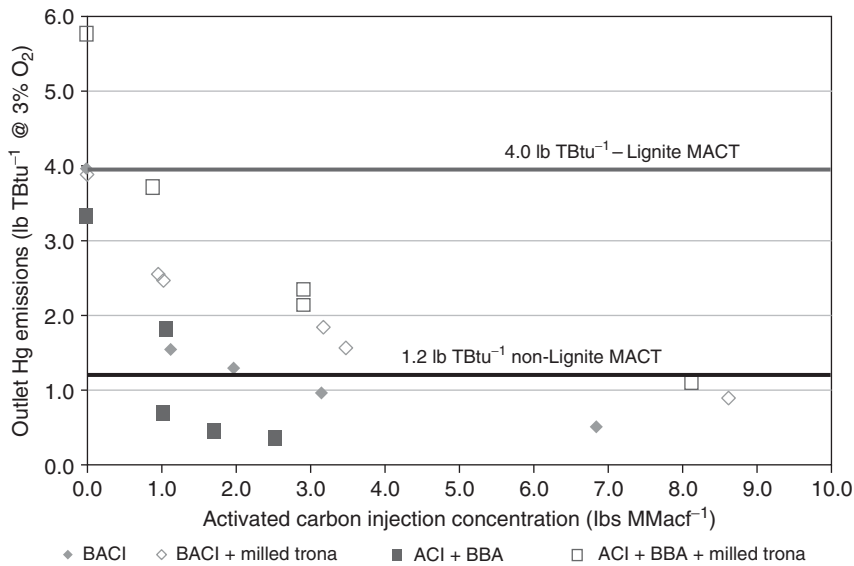


Figure 12.17 DSI (Trona) impact on ACI plus BBA mercury removal across an ESP for PRB coal.

as dry sorbent injection (DSI) for FGD. Many power plants are investigating DSI as a low capital cost, interim solution to meet acid gas control requirements. Tests are being conducted with Trona, sodium bicarbonate, or hydrated lime.

However, evidence suggests that alkali sorbents may reduce the effectiveness of ACI for mercury control. They may interact with BBA for mercury control by removing bromide and other halogens from flue gas. Injection of sodium-based alkali also produces nitrogen dioxide (NO₂), a compound that can reduce ACI mercury removal effectiveness. An example of these interactions is shown in Figure 12.17, where DSI and ACI were tested at a PRB-fired unit equipped with an ESP (Unpublished EPRI field test data). In these tests, milled Trona was simultaneously injected upstream of the air heater with either BAC or AC (paired with BBA in some runs). Co-injecting Trona had a significant, negative impact on mercury control effectiveness with ACI plus BBA.

12.7

Summary

This chapter presents results of EPRI's research and development program to support technologies that offer the most effective flue gas mercury removal at the lowest capital and operating cost. It reviews the achievements, balance-of-plant challenges, and research responses associated with near-term mercury control technologies, and describes novel, longer term concepts.

References

1. EPRI (2009) Mercury Control Update 2009, Product ID: 1017564, Palo Alto, CA.
2. EPRI (2011) Database of Selective Catalytic Reduction System Mercury Oxidation, Product ID: 1022065, Palo Alto, CA.
3. EPRI (2011) Mercury Control Update 2011, Product ID: 1022076, Palo Alto, CA.
4. Chang, R. (1996) Method for removing pollutants from a combustor flue gas and system for same. US Patent 5,505,766, Apr. 9, 1996.
5. EPRI (2010) Mercury Control Update 2010, Product ID: 1019720, Palo Alto, CA.
6. EPRI (2007) Field Mercury Control Testing Update, Product ID: 1012676: Palo Alto, CA.
7. Vosteen, B., Beyer, J., Bonkhofer, T.-G., Fleth, O., Wieland, A., Pohontsch, A., Kanefke, R., Standau, E., Mueller, C., Nolte, M., and Koeser, H. (2005) Process for removing mercury from flue gases. US Patent 6,878,358 B2, Apr. 12, 2005.
8. Oehr, K.H. (2004) Enhanced mercury control in coal-fired power plants. US Patent 6,808,692, Oct. 26, 2004.
9. EPRI (2008) Mercury Control Update, Product ID: 1015761, Palo Alto, CA.
10. Zhuang, Y., Chen, C., Timpe, R., and Pavlish, J. (2009) Investigations on bromine corrosion associated with mercury control technologies in coal flue gas. *Fuel*, **88**, 1692–1697.
11. Chang, R. (2006) Method and apparatus for removing particulate and vapor phase contaminants from a gas stream. US Patent 7,141,091 B2, Nov. 28, 2006.
12. Lu, X-C. and Wu, X. (2008) Flue gas purification process using a sorbent

- polymer composite material. US Patent 7,442,352 B2, Oct. 28, 2008.
13. Machalek, T., Richardson, C., Paradis, J., Chang, R., Lu, X-C., Stark, S., Xu, Z., Gebert, R., Looney, B., and Mathews, M. (2011) Field investigations of fixed-structure sorbents for mercury emission control. Paper Presented at Air Quality VIII, Arlington, VA, October 24–27, 2011.
 14. Lu, X.S. (2012) A flue gas Hg and SO_x control technology using fixed sorbent bed. Paper presented at the Energy, Utility and Environment Conference, Phoenix, AZ, January 30–February 1, 2012.
 15. Chang, R., Rostam-Abadi, M., and Chen, S. (2002) Apparatus and method for removal of vapor phase contaminants from a gas stream by in-situ activation of carbon-based sorbents. US Patent 6,451,094 B1, Sept. 17, 2002.
 16. Chang, R., Rostam-Abadi, M., and Sjostrom, S. (2003) Method for removal of vapor phase contaminants from a gas stream by in-situ activation of carbon-based sorbents. US Patent 6,558,454 B1, May 6, 2003.
 17. Chang, R., Shaban, C., Ebner, T., Fisher, K., Slye, R., Lu, H., Sugiyono, I., Rostam-Abadi, M., Sy, G., White, C., Lindsay, C., and Smith, D. (2011) Sorbent activation process for mercury control. Paper Presented at Air Quality VIII, Arlington, VA, October 24–27, 2011.

Part V

Mercury Control Processes

13

Mercury Control Using Combustion Modification

Thomas K. Gale

13.1

Mercury Speciation in Coal-Fired Power Plants without Added Catalysts

13.1.1

Mercury is all Liberated and Isolated in the Furnace

The predominant forms of mercury in coal-fired flue gas are elemental (Hg^0) and oxidized (HgCl_2) [1–3]. The percentage of oxidized mercury in the stack effluent of a particular power plant depends on the coal type, combustion efficiency, and the pollution control equipment used. Essentially, all of the mercury entering the furnace with the coal is vaporized and exists in the elemental form until the flue gases cool below $\sim 600^\circ\text{C}$ ($\sim 1000^\circ\text{F}$) [1–3]. The oxidation of mercury in coal-fired boiler systems is kinetically limited [1–3]. Because the concentration of mercury is exceedingly small at around 1 ppb in flue gas, any favorable mercury-oxidation reaction does not have the ability to promulgate itself. In virtually every conceivable competitive reaction, the competing gas component, much in excess of mercury, dominates. Where the formation of mercuric compounds is thermodynamically favored, the kinetically controlled oxidation requires the oxidant to be in vast abundance compared with mercury.

13.1.2

Chlorine Speciation in Coal-Fired Power Plants

Chlorine (Cl_2) is more reactive for the oxidation of mercury compared to hydrogen chloride (HCl). Chlorine gas (Cl_2) is not thermodynamically promoted at high temperatures. However, below 370°C (644 K or 700°F), a significant driving force toward the formation of Cl_2 develops. This driving force begins to dominate over the formation of HCl below 260°C (533 K or 500°F). Chlorine speciation is governed by equilibrium in furnace sections of coal-fired boilers and limited by kinetics and residence time downstream. Therefore, several statements can be made relative to chlorine speciation in coal-fired power stations. Chlorine gas

injection through the burner or entering with the coal will be entirely converted to HCl and Cl^- in the furnace. Any form of chlorine injected through the primary-air line will be converted in the furnace to HCl and a smaller amount of Cl^- , as long as it vaporizes in the flame. The result downstream ($\sim 600^\circ\text{F}$) will be to increase the total amount of chlorine in the flue gas by the amount injected through the burner. The form of chlorine will be primarily HCl. However, as more total chlorine is injected through the burner, a small but higher concentration of Cl^- may persist a short distance downstream of the furnace. Although a driving force toward the formation of Cl_2 begins to form below 370°C (644 K or 700°F), the formation of Cl_2 is expected to be limited by kinetics at this point. Thus, the majority of the HCl is expected to remain in that form for the residence times that exist in full-scale power plants. Furthermore, if Cl_2 gas was injected at a lower temperature location downstream, where the thermodynamic driving force was more favorable to its formation (i.e., after the economizer), then it would remain in the form in which it was injected.

13.1.3

Mechanisms Governing Mercury Speciation

The following mechanism [4] was proposed whereby carbon, in the form of unburned carbon (UBC), activated injected carbon, or other carbon types could oxidize mercury by effectively removing the activation barrier, preventing HCl from directly reacting with elemental mercury atoms in the flue gas:



Equations 13.2–13.6 describe how UBC can effectively catalyze mercury oxidation by reacting with HCl to form chlorinated carbon sites, which then react with mercury on the surface of the carbon to form adsorbed HgCl, which finally desorbs as oxidized mercury. The oxidized mercury may in turn readsorb onto open UBC sites.

Equation 13.2 describes the formation of chlorinated carbon sites.



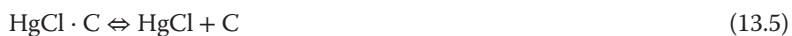
Equation 13.3 allows for desorption of chlorine, thus providing some moderation of chlorine accumulation on the carbon surface.



Equation 13.4 describes the capture of elemental mercury by reaction with chlorinated carbon sites located on the surface of ash particles.

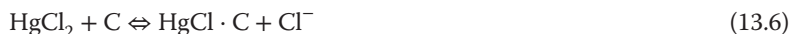


Equation 13.5 allows for the desorption of oxidized mercury.



Various homogeneous pathways can convert HgCl to HgCl_2 , such as reaction of HgCl with Cl^- or Cl_2 . The conversion is assumed to be very fast, and thermochemical equilibrium calculations predict nearly all mercury to be in the HgCl_2 form in flue gas downstream of the airheater [1, 5].

Equation 13.6 allows for the re-adsorption of oxidized mercury onto open carbon sites (as in the dissociative adsorption of mercuric chloride shown here).



13.2

Role of Unburned Carbon in Mercury Oxidation and Adsorption

13.2.1

UBC is the Only Catalyst with Enough Activity in Coal-Fired Power Plants

Extensive parametric investigations of mercury speciation in coal-fired flue gas and coal-fired power plants *without selective catalytic reductions (SCRs) installed* (or other catalysts or reagents introduced for the purpose of enhancing mercury oxidation or capture) have shown [1, 5, 6] that variable parameters such as exposed iron-oxide surfaces in the convection pass, flue-gas concentrations of O_2 , N_2 , H_2O , NO , NO_2 , SO_2 , CO , and CO_2 , or the concentrations of Fe, Al, Si, Na, or derivatives of iron in the flyash have little impact on mercury oxidation or removal under conditions that exist within actual coal-fired power plants. What has been shown to have an impact on mercury oxidation and capture within the flue gas of coal-fired power plants (without SCR or other catalysts or reagents) is the type and extent of carbon in the flyash.

As mentioned earlier, the HCl concentration of the flue gas will have little impact on mercury oxidation if the UBC is low. Figure 13.1, previously published elsewhere [6], compares the relationship between Hg oxidation across a baghouse, HCl concentration in the flue gas, and UBC in the flyash, during a pilot-scale [7] mercury-speciation study. The HCl and UBC concentrations were varied by injecting chlorine gas through the burner while firing Powder River Basin (PRB) coal (a low-chlorine, high-calcium ash, sub-bituminous coal) and by blending PRB with higher chlorine bituminous coals.

A mass balance on coal-mercury suggested that the majority of mercury at the baghouse inlet was in the gas phase for all blend conditions. As shown, chlorine injection alone (i.e., resulting in HCl addition in the back pass) had some impact on mercury oxidation. However, much more mercury oxidation was realized as a result of coal blending, even though there was less chlorine. Adding bituminous coal also yielded more UBC in the ash, which catalytically enhanced mercury oxidation. The chlorine and UBC levels shown in Figure 13.1 are low relative to the levels produced from most eastern bituminous coals. Nevertheless, UBC clearly plays a significant role in catalyzing the oxidation of elemental mercury with hydrochloric acid vapor in the flue gas, and the concentration of UBC in flue

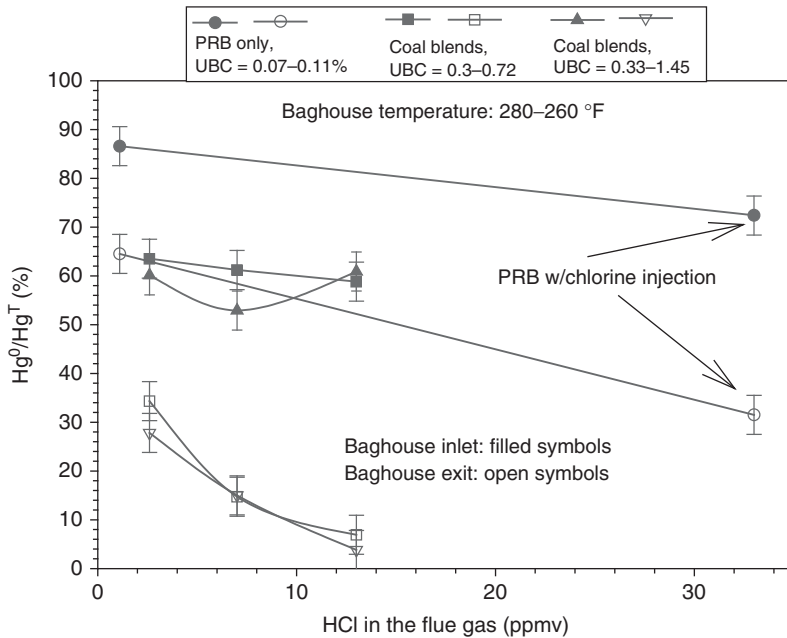


Figure 13.1 Effect of flue-gas–chlorine on mercury oxidation ahead of and across a baghouse [6] (shown as a decrease in the elemental mercury (Hg^0) concentration at

the measurement location relative to total mercury (Hg^T) at the baghouse inlet). (Reproduced with permission from Ref [6]. Copyright © 2009, Elsevier Limited.)

gas will be as important, or more important, than the concentration of HCl in the flue gas for many plants relative to mercury oxidation.

13.2.2

UBC can Remove Hg or Oxidize Hg, Depending on the UBC Concentration

It is known [8] that the desorption rate of HgCl from carbon at a given temperature decreases with increasing available carbon sites, as the desorption rate depends primarily on the HgCl concentration deposited on the carbon surface and the concentration of vacant carbon sites per unit mass of carbon. Furthermore, for a given temperature, the adsorption rates of Hg^0 and HgCl_2 increase with an increase in the number of sites available for sorption – that is, the UBC sites for activation by HCl and adsorption of HgCl_2 (i.e., through the mechanisms described in Equations 13.2 and 13.6, respectively) and the Cl-C sites (see Equation 13.4) for adsorption of Hg^0 . Hence, the speciation and removal of mercury by particulate, produced by a given coal and firing condition, depend on the amount (and surface activity) of the carbon (in the flue gas) available to adsorb mercury, keep it adsorbed, and to re-adsorb oxidized mercury.

With sufficient carbon (i.e., high enough C/Hg ratio), the overall adsorption rate of mercury may be overwhelmingly greater than the overall desorption rate, in

which case significant mercury removal will be observed. On the other hand, if sufficient carbon (activated carbon or UBC) is present to yield significant mercury adsorption on chlorinated carbon sites, but not enough carbon is available to slow the desorption of HgCl and to allow significant re-adsorption of HgCl_2 , then extensive mercury oxidation may be observed without significant mercury removal.

13.2.3

Nature of Carbon Type Depends on Parent Coal and Combustion Efficiency

Activated carbon used for mercury control is often made from coal, typically a low-rank coal or lignite, and less often from coconut or walnut shell or other biomass feedstock such as wood. The feedstock, be it biomass or coal based, is subjected to thermal decomposition with strategic oxidation (often with steam) in order to produce an active sorbent for mercury adsorption with a high internal surface area. The carbon–steam reaction, shown here, is typically used to generate internal porosity and high-surface-area carbons.



If the temperature is too hot, the heating rate too slow, or if too much oxygen is present and not enough steam, then the resulting activated carbon will be less active than that produced under optimized conditions. Similarly, UBC in flyash has gone through a thermal decomposition process and been subject to reactions with steam, carbon dioxide, and oxygen. Although coal-fired boilers are clearly not optimized to produce UBC with a high activity for mercury adsorption, the activity of the carbon for mercury adsorption may differ significantly from one plant to another, depending on the coal type fired, the efficiency of the boiler, the furnace exit oxygen of the furnace, and moisture content of the coal and humidity of the secondary air.

The impact of the coal type on the resulting carbon activity can be determined from the coalification curve. Peat, although not coal, is the first material that plant matter was converted into as it began the coalification process. Peat consists of high moisture content, high volatile content, and will produce a highly active carbon type when thermally decomposed. Graphite, although not coal, sits on the other end of the coalification curve and is the end product of material passing through the coalification curve. Graphite has little moisture and no volatiles, and consists of an unreactive carbon type before and after heat treatment. In between these two endpoints are the different types of coal we burn in power plants at present, with the more reactive carbon types produced from the younger coals (i.e., lignites and sub-bituminous coals) and the less reactive carbon types being produced from the older coals (low-volatile bituminous and anthracite coals).

The order of coals from youngest to oldest from the coalification curve is maintained in the heating value and proximate analysis charts produced by Hendrickson in 1975 [9], reproduced in Perry's Chemical Engineers' Handbook [10]. As shown in those charts, the younger the coal, the more moisture content, the more

volatiles, the less fixed carbon, and the lower the heating value. It is also true that the char produced from the initial stages of combustion known as *devolatilization* (which takes place in <25 ms in pulverized coal (PC) boilers) is more reactive for younger coals and less reactive for older coals. The char produced from younger coals is more reactive for essentially two reasons. First, the solid organic network comprising the char structures contain more aliphatic material (i.e., attachments to organic rings, such as methane and toluene and components that can easily be released as light gases), and the aromatic structures are less ordered and graphitic in nature (i.e., the rings contain fewer inclusions and the ring structures tend to be more planar with respect to each other) [11, 12]. Second, in large part due to the first reason (i.e., the nature of the solid carbon structure), the char produced from the younger coals tends to have a higher porosity and internal surface area than char produced from the older coals.

The higher moisture content of the younger coals also tends to yield higher medium-sized pores or mesopores, through which increase the reaction rate of chars with oxygen would, if the chars survived, yield more active carbon structures for mercury capture.

Firing a coal that yields char with a high reactivity results in two trends that tend to cancel each other out in terms of yielding highly active UBC, outlined as follows: The higher reactivity does indeed relate to a higher activity for mercury capture. However, the higher reactivity also means that more of the carbon will be burned out in the furnace by oxygen and will not survive to serve as an actor for mercury adsorption or oxidation. A good example of this is PRB coal. PRB coal yields a highly reactive char type that is very effective for oxidizing and adsorbing mercury. However, most power plants that burn PRB coal have very low UBC in their flyash, because most of the carbon burns out in the boiler, before reaching the backpass.

It has been shown that high oxygen contents tend to decrease the reactivity of coal chars by consuming the outer surface of the char (eating the char particles from the outside in), while high-steam concentrations tend to increase the char reactivity by increasing the char mesoporosity and Brunauer–Emmett–Teller (BET) surface area [13]. The water molecules, with orders of magnitude lower reaction rate than oxygen with carbon, are able to penetrate the micropores of the coal char and react with their inner walls, thus widening the micropores and creating mesopores, without reducing the particle diameter. Hence, higher moisture contents in the furnace may increase the carbon activity for mercury if the active carbon produced is not all consumed by oxygen in the furnace.

13.2.4

Concentration of UBC Needed to Oxidize or Remove Mercury from Flue Gas

The mechanism of carbon enhancement of mercury oxidation is consistent with bench-, pilot-, and full-scale Hg-adsorption and speciation data, which have shown a direct relationship between mercury adsorption and carbon concentration [1, 5, 14]. At low carbon concentrations, the rate of Hg adsorption

is of the same magnitude as the rate of mercury desorption. As the carbon concentration increases, assuming at least some chlorine in the flue gas, mercury adsorption begins to dominate over mercury desorption, until most of the mercury is observed to be removed from the flue gas. The mechanism is observed even more clearly for mercury speciation. At very low concentrations of carbon in the flue gas (i.e., PRB-fired power plants with high carbon burnout), the mercury will neither be oxidized nor adsorbed. For slightly higher concentrations of UBC (i.e., up to about 4.0% in the ash) in the absence of much calcium, extensive mercury oxidation will be observed, and for still higher concentrations of UBC, mercury removal will dominate even without much calcium present (as observed at power plants with high levels of UBC in the ash, that is, 20–50% UBC).

If firing conditions can be changed to increase the UBC in the flyash from PRB coal by just 0.2%, a significant increase in mercury oxidation will likely be observed, while an increase in UBC to several percent may result in high removals of mercury in the flyash (calcium content of the ash will also have an impact on removal for PRB coals). On the other hand, UBC concentrations as much as 10% in the flyash from bituminous coal may not produce high mercury removals or complete mercury oxidation.

In the same pilot-scale system [7] from which the data shown in Figure 13.1 were obtained, the concentration of UBC in the flyash needed to oxidize mercury across a baghouse was also measured (see Figure 13.2 published previously [6]). Combustion modifications were used to increase the concentration of UBC from the PRB coal, which is a highly reactive carbon type. As shown in Figure 13.2, the resulting increase in UBC was highly effective at oxidizing mercury. The coal blends were primarily of PRB and bituminous coals, where the average UBC type produced was also effective for oxidizing mercury.

13.3

Synergistic Relationship between UBC and Calcium in Flyash

13.3.1

Calcium Enhances the Retention of Mercury on Carbon

A fundamental investigation by Gale *et al.* [6] on the impact of calcium on mercury removal in power plants found that the presence of calcium, in the form of PRB flyash, injected hydrated lime, calcium carbonate, or calcium, enhanced mercury removal from the flue gas under certain conditions. Among other things, it was demonstrated that adding different forms of calcium to the baghouse collecting bituminous coal flyash changed the measured form of mercury at the baghouse outlet from about 90% oxidized with about 25% removed across the baghouse, to over 80% of the mercury removed across the baghouse. It was further shown [6] that calcium powders would only increase mercury removal across the baghouse if they were mixed with the UBC in the flyash. Without UBC from flyash, the

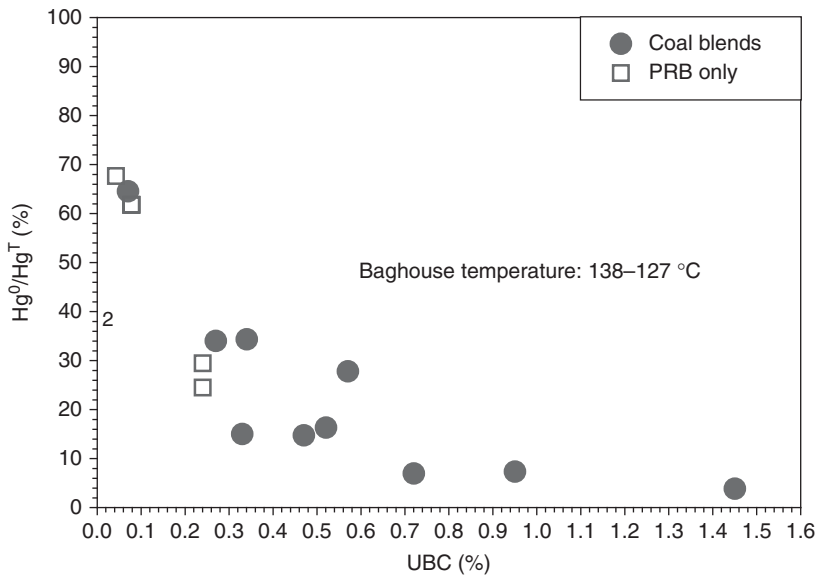


Figure 13.2 Mercury oxidation versus UBC [6]. (Reproduced with permission from Ref [6]. Copyright © 2009, Elsevier Limited.)

calcium powders had no effect, even for flue gas containing a high percentage of oxidized mercury.

The synergistic relationship of calcium and UBC for the removal of mercury also extends to mercury removal across an electrostatic precipitator (ESP) [6]. Contour lines showing the concentration of calcium and UBC necessary to achieve different mercury removal percentages derived in this work are reproduced here in Figures 13.3–13.5. All of this work was performed on low-sulfur coals, with SO₃ concentrations <2 ppmv, so the impact of calcium on protecting the carbon from deactivation by SO₃ was not significant.

As shown in Figures 13.3–13.5, different combinations of calcium and carbon concentrations can be used to obtain the same mercury removal percentages at the inlet and outlet of an ESP. The contour lines shown in these figures were created from data interpolation. No extrapolations were made. Therefore, all of the points on each of the contour lines are achievable.

13.3.2

Calcium/Carbon Synergism is Limited to a Range of Conditions

Synergism between calcium and UBC in flyash or injected activated carbon was found to be effective only for UBC concentrations in the flyash that would otherwise yield significant mercury oxidation with moderate mercury capture. If a large concentration of UBC was present, such that mercury removal was already high, the impact of adding calcium would be far less effective or not effective at all.

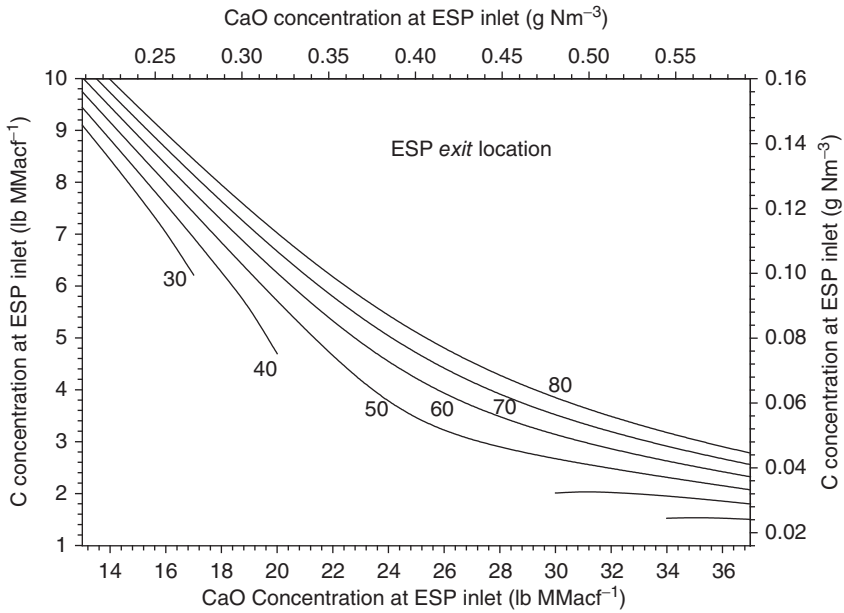


Figure 13.3 Predicted Hg removal contours for PRB/eastern bituminous blend tests (ESP exit) [6]. (Reproduced with permission from Ref [6]. Copyright © 2009, Elsevier Limited.)

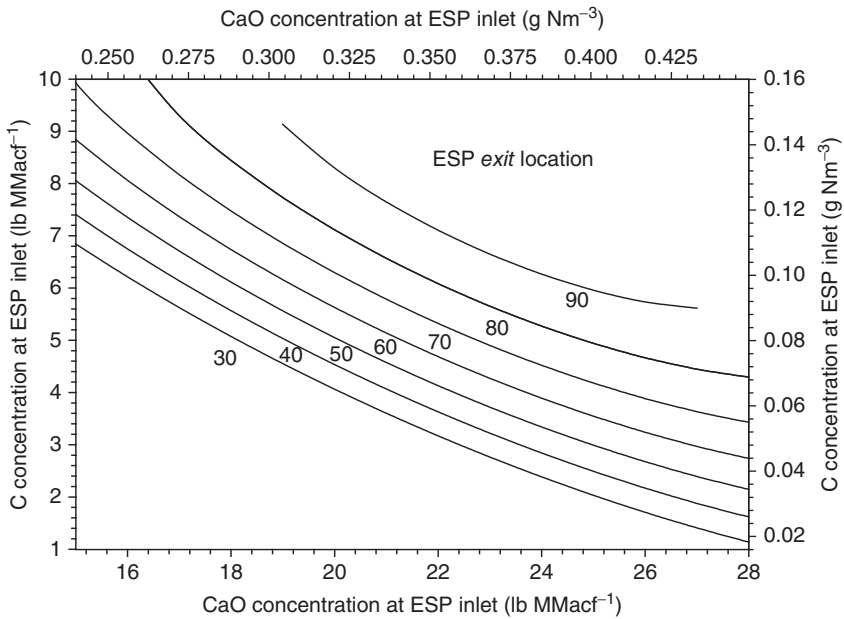


Figure 13.4 Predicted Hg removal contours for PRB/West Elk blend tests (ESP exit) [6]. (Reproduced with permission from Ref [6]. Copyright © 2009, Elsevier Limited.)

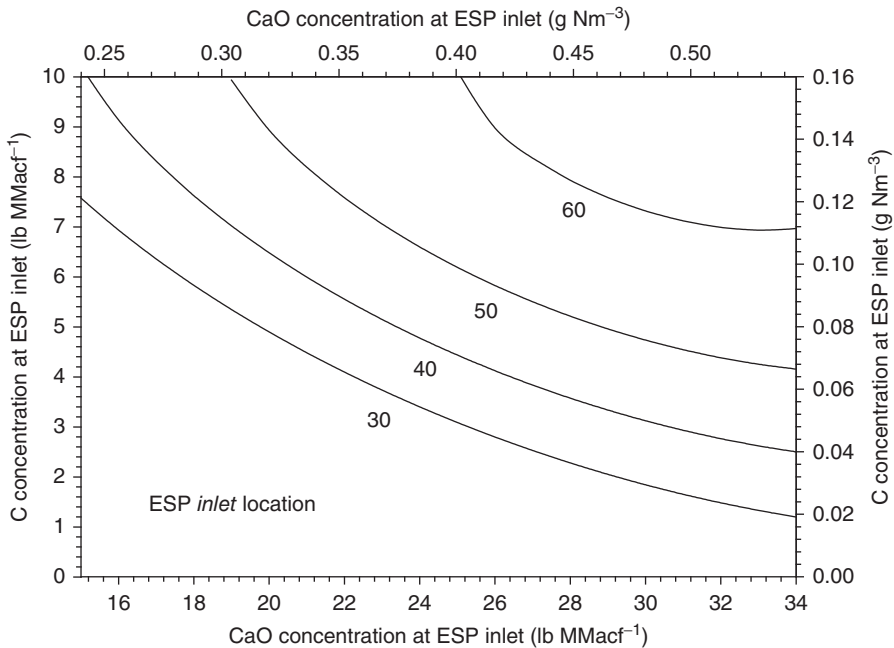


Figure 13.5 Predicted Hg removal contours for PRB/West Elk blend tests (ESP inlet) [6]. (Reproduced with permission from Ref [6]. Copyright © 2009, Elsevier Limited.)

Furthermore, the calcium/carbon synergism work by Gale *et al.* [1, 5, 6], was confined to relatively low-chlorine coals, that is, with flue-gas concentrations below 50 ppmv.

13.4

Potential Combustion Modification Strategies to Mitigate Mercury Emissions

Coal blending, although technically not a combustion modification, is a way to change the nature of the combustion by burning a different fuel type with a more or less active carbon type, more or less moisture, and more or less calcium than normally fired, all of which have the potential to impact the overall mercury removal strategy. The specific application of this method will vary significantly from plant to plant, depending on the plant configuration, coal type currently being burned, efficiency of the boiler, and availability and cost of different coal types.

Several specific examples are provided for clarification.

In a power plant that currently fired PRB coal, did not have an SCR or wet scrubber, and had a fairly high furnace efficiency, such that the UBC in the flyash was 0.1% or less, co-firing with a higher rank coal, well up on the coalification curve would likely increase the mercury capture to perhaps 80% or 90% across the ESP or even more across a baghouse.

A similar but much less efficient power plant that burned bituminous coal, resulting in >10% UBC in the flyash, may be able to significantly reduce mercury emissions by blending with or switching completely to PRB coal. If so, the power plant would have the added benefit of a much lower UBC concentration in their flyash.

Although these examples are realistic, it is not likely that the anticipated regulatory standards can be met through coal blending alone, as most standards are anticipated to require >95% removal of the mercury from the flue gas, which is unlikely to be achievable by coal blending for most power plants.

Reduced combustion efficiency is another way to increase the UBC concentration in the flyash and thereby increase the mercury removal in the particulate collection device (PCD). This would be most effective while burning PRB coal or lignite and would provide the least problem with high UBC concentrations in the ash. However, increasing the UBC in the flyash while firing PRB or lignite is quite difficult, because of the highly active carbon type.

It should be understood that if this approach is taken to increase the UBC in the flyash, it must be done in a way so as to only increase the UBC from the char. If radical measures are taken to produce a highly unstable flame or channeling of gases that are not completely burned, there is a possibility that some of the UBC produced will be from unburned volatile matter. Carbon produced in the ash from unburned volatile matter, or soot, will not produce the desired results. Soot once formed through incomplete combustion of volatiles is unreactive and will not provide an active carbon concentration in the flyash for the promotion of either mercury oxidation or capture.

Reburning is a technology where fuel is fired in the furnace downstream of the main burners to reduce NO_x that were formed in the primary combustion zone, by creating a reducing zone at the location of the reburning. As the objective of reburning is to create a reducing zone, there will be less oxygen needed to burn all of the solid fuels and so provides a great opportunity to combine this technology with production of activated carbon types for mercury adsorption in the flyash. Reburning can be done with natural gas, but it can be done with a variety of different solid fuels, including the same coal that is fired through the main burners. If the reburning system is designed for both the reduction of NO_x and for limited burnout and activation by steam, the cost should be reasonable to solve both the NO_x and Hg emissions problems. This may be a possible approach for smaller plants that are trying to extend their life and cannot afford to add an SCR unit for deNO_x .

Furnace intrusion modifications is the final area of combustion modification possibilities for existing coal-fired power plants. This broad area of modification requires intrusion into the furnace itself to either add equipment or redirect part of flame flow downstream of the furnace. An example of such a modification would be a highly isolated jet of inert gas that was directed through part of a flame or the whole furnace, sweeping unburned char out of the flame zone, and transporting it downstream unreacted and quenched so that it would not continue to burn. Another example would be a mechanical device or high-temperature vanes in a

boiler that would extract some of the char from the flame zone downstream before it was completely burned out.

The Thief Process is an example of a commercial Furnace Intrusion Modification [15]. The Thief Process extracts coal out of the flame zone through a pipe outside the furnace and then reinjects the UBC downstream where it can be used as a sorbent to capture mercury.

13.5

Effects of Combustion Modifications on Mercury Oxidation across SCR Catalysts

13.5.1

Inhibition of Mercury Oxidation can Occur in Low-Chlorine Flue Gas

Although it is unlikely that combustion modifications would be used as a mercury mitigation strategy at a power plant where an SCR was installed for deNO_x , combustion modifications, or tuning for other reasons can have a significant effect on mercury oxidation across the SCR catalyst. Walsh *et al.* [16] showed that as little as 10 ppmv of CO can significantly inhibit the oxidation of mercury across an SCR catalyst in flue gas with an HCl concentration of 2.0 ppmv, which is typical of the HCl concentration at some plants firing PRB coal. Hence, care should be taken when considering combustion modification that might increase the CO concentration when firing a low-chlorine coal and using an SCR to oxidize mercury.

At chlorine concentrations as high as 50 ppmv, there was no effect of the CO concentration on mercury oxidation.

Although ammonia slip can inhibit mercury oxidation across SCR catalysts in low-chlorine flue gas, the concentration of NO treated has little impact [17]. Nevertheless, efforts to change UBC or lower NO through combustion modifications could have negative impacts on mercury oxidation across an SCR by increasing the concentration of carbon monoxide.

References

1. Gale, T.K. (2005) Mercury Control with Calcium-Based Sorbents and Oxidizing Agents. Final Report – DE-PS26-05NT41183, United States Department of Energy, July 2005.
2. Senior, C.L., Chen, Z., and Sarofim, A.F. (2002) Mercury oxidation in coal-fired utility boilers: validation of gas-phase kinetic models. A&WMA 95th Annual Conference, Baltimore, MD.
3. Niksa, S., Helble, J.J., and Fujiwara, N. (2001) Kinetic modeling of homogeneous mercury oxidation: the importance of NO and H₂O in predicting oxidation in coal-derived systems. *Environ. Sci. Technol.*, **35**, 3701–3706.
4. Niksa, S. and Fujiwara, N. (2003) Predicting mercury speciation in coal-derived flue gases. EPRI-DOE-EPA-A&WMA Combined Utility Air Pollution Control Symposium: The MEGA Symposium, May 2003.
5. Gale, T.K. (2006) Understanding Mercury Chemistry in Coal-Fired Boilers. Final Report No. 1014418, EPRI, Palo Alto, CA.

6. Gale, T.K., Lani, B.W., and Offen, G.R. (2008) Mechanisms governing the fate of mercury in coal-fired power systems. *Fuel Process. Technol.*, **89** (2), 139–151.
7. Southern Research (2004) The 1.1 MWth (3.6 MMBtu/hr thermal) Pilot-Scale Combustion Research Facility, Southern Research Institute in Birmingham, Alabama, www.southernresearch.org (accessed 20 March 2014).
8. Smith, J.M. (1981) *Chemical Engineering Kinetics*, 3rd edn, McGraw-Hill, pp. 361–363.
9. Hendrickson, T.A. (ed.) (1975) *Synthetic Fuels Data Handbook*, Cameron Engineer, Inc., Denver, CO.
10. Perry, R.H., Green, D.W., and Maloney, J.O. (1984) *Perry's Chemical Engineers' Handbook*, 6th edn, McGraw-Hill, pp. 9–4.
11. Gale, T.K., Bartholomew, C.H., and Fletcher, T.H. (1996) Effects of pyrolysis heating rate on intrinsic reactivities of coal chars energy. *Fuels*, **10**, 766–775.
12. Hurt, R.H. and Gibbins, J.R. (1995) Residual carbon from pulverized coal fired boilers: 1. Size distribution and combustion reactivity. *Fuel*, **74** (4), 471–480.
13. Gale, T.K., Fletcher, T.H., and Bartholomew, C.H. (1995) Effects of pyrolysis conditions on internal surface areas and densities of coal chars prepared at high heating rates in reactive and non-reactive atmospheres. *Energy Fuels*, **9**, 513–524.
14. Behrens, G. (2000) Final Report: An Assessment of Mercury Emissions from U. S. Coal-Fired Power Plants. EPRI Report No.1000608, EPRI, Palo Alto, CA.
15. Pennline, H.W., Granite, E.J., Freeman, M.C., Hargis, R.A., and O'Dowd, W.J. (2003) Thief process for the removal of mercury from flue gas, U.S. Patent 6,521,021, Feb. 18, 2003.
16. Walsh, P.M., Tong, G., Bhopatkar, N.S., Gale, T.K., Blankenship, G. A., Ingram, C.W., Blavo, S., Mehreteab, T., Banjoko, V., Ghirmazion, Y., Ban, H., and Sibley, A.F. (2009) Oxidation of Mercury in Products of Coal Combustion. DOE Final Report DE-FG26-04NT42195. United States Department of Energy.
17. Gale, T.K., Blankenship, G.A., Hinton, W.S., Cannon, J.W., and Lani, B.W. (2006) Hg oxidation compared for three different commercial SCR catalysts. EPRI-DOE-EPA-A&WMA MEGA Symposium, Baltimore, MD, August 28–31, 2006.

14

Fuel and Flue-Gas Additives

John Meier, Bruce Keiser, and Brian S. Higgins

14.1

Background

The primary mercury oxidation pathway during coal combustion occurs as a function of coal halogen content and subsequent release during the combustion process. Native oxidation occurs [1] through the reaction of mercury with HCl (or Cl^- or Cl_2 produced by the Deacon reaction [2]), utilizing the inherent chlorine in the coal.

The easiest and most readily available method to increase mercury oxidation is through the introduction of halogen-containing material to the fuel before combustion. Typical methods include treating the coal with a liquid solution containing halogen salts, such as CaBr_2 or CaCl_2 . These salt compounds vaporize and dissociate, or react during combustion, to form molecular halogen compounds or precursors in the flue gas, primarily forming HBr, Br_2 , HCl, and Cl_2 . These halogen species then oxidize elemental mercury to its oxidized form, which is readily capturable across downstream air quality control devices.

Additives to promote enhanced mercury capture were first implemented to augment mercury capture by activated carbon. Initial generic-powdered activated carbon injection (ACI) studies noted that with low chlorine fuels (e.g., $<200 \mu\text{g g}^{-1}$) there was poor mercury removal relative to units burning higher chlorine coal (e.g., $>500 \mu\text{g g}^{-1}$) [3]. Because of this result, manufacturers began impregnating the activated carbon with various halogen additives (i.e., iodine, chlorine, or bromine). While all of these halogens are effective in oxidizing mercury and facilitating activated carbon mercury capture [4], bromine-based additives have often exhibited the best cost performance.

An additional factor affecting mercury capture by activated carbon is the flue-gas temperature. At elevated flue-gas temperatures, approaching 200°C , activated carbon efficiency is reduced, specifically for elemental mercury [5]. By increasing the portion of oxidized mercury in the gas stream, high-temperature mercury capture is improved with activated carbon.

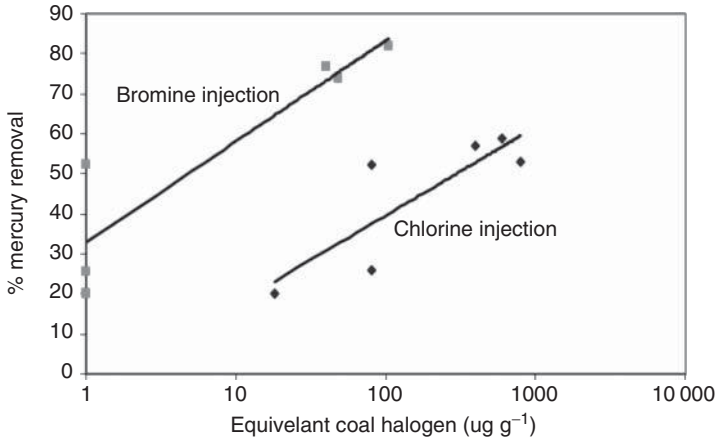


Figure 14.1 Mercury oxidation in coal-fired boilers with bromine and chlorine addition .

The effect of the concentration of several halogen-based oxidants have been considered by Senior *et al.* [6] Figure 14.1 illustrates the difference in native capture as a function of halogen concentration in the coal, where the halogen concentration is artificially augmented. Increased mercury removal is directly attributed to higher halogen concentration before coal combustion. In this study, bromine addition reaches 80% mercury removal ($\text{Br} \sim 100 \mu\text{g g}^{-1}$), while the peak mercury removal with chlorine ($\text{Cl} \sim 1000 \mu\text{g g}^{-1}$) does not exceed 60%, even with a concentration 10-fold larger.

14.1.1

Bromine-Salt Mercury Oxidation

The case studies presented here show results from injecting a bromine salt solution into a boiler to produce a molecular halogen or molecular halogen precursor, which promotes mercury oxidation. The proprietary bromine salt solution injected by Nalco is branded as MerControl[®] 7895 technology. In the results that follow, the data is presented as micrograms per gram, representing the number of micrograms of MerControl 7895 solution per gram of coal. This is equivalently referred to as milligrams per kilogram or parts per million weight.

14.1.2

Fuel Additive Injection Equipment

The application of halogen salt solutions is typically to the coal before injection into the furnace. The point of application is usually at the coal feeders just before the pulverizers. Permanent injection systems include a bulk storage tank, metering pumps, and injection assemblies. The pumps are controlled relative to plant operational data; for example, coal flow, gross mega watts, and/or

outlet mercury speciation (when a plant continuous mercury monitor (CMM) is available). The injection point is a simple lance comprising an open-ended stainless steel tube, without a nozzle, or a constriction, which may plug. An even distribution of the product across the coal flow is not required at the application point as the additive will be well mixed with coal during the pulverization process.

Different precombustion application locations have been investigated, at various points from the coal yard to the burners. The application equipment is less expensive the further upstream the chemistry is added. Alternatively, the control response to a downstream feedback control parameter (e.g., a stack mercury measurement) is faster the further downstream the chemistry is added. However, these differences are slight and neither approach appears to have a strong advantage over the other.

Alternative injection strategies include injecting the oxidizer additives directly into the boiler or in the back-pass through a grid injection system.

Injection into the boiler can be performed by using compressed or fan-boosted air to facilitate mixing. Often, this is performed by combining the oxidizer injection with other air or chemical injection systems such as over-fired air or a selective noncatalytic reduction (SNCR) system. The key point is to confirm that there is good mixing with all of the flue gas. One reason to pursue this approach is to remove the bromine from the coal handling and milling systems; however, an operational performance advantage to doing this has not been established.

Halogen-containing solutions can also be injected into the flue gas downstream of the economizer using a grid injection system. The decreased flue-gas temperature at this injection point may require the use of a larger quantity and/or a more hazardous reagent, such as hydrobromic acid. Either may raise the costs and safety concerns with handling and storage. Again, good mixing needs to be confirmed. It has not been demonstrated that injection downstream of the economizer is more effective or more economical than precombustion addition of halogen salts.

14.1.3

Case Study Results

The following two sections present results from different case studies. The first section summarizes conditions where an halogen based fuel additive will likely lead to advantageous performance and the second summarizes conditions where there is likely not an advantageous performance.

Note that every boiler application must be individually analyzed, as results are heavily dependent on flue-gas temperatures, coal constituents, post combustion temperatures, mixing, residence time, metal surface characteristics, and, most importantly, the operation of downstream air pollution control devices. Nalco commonly demonstrate the effectiveness of fuel additives, with and without activated carbon, through field trials to help our clients fully understand the cost–benefit of various operational scenarios.

14.1.3.1 Case Studies where Halogen-containing Fuel Additives are Advantageous

Nalco has performed a number of demonstrations with fuel additives with the specific goal of reducing mercury compliance costs. In this section, the results from three case studies are reviewed:

Case Study One: Optimized carbon and halogen-containing additive for preservation of fly ash quality in concrete reuse

Case Study Two: Bituminous coal with performance shortfalls and SCR (selective catalytic reduction)/wFGD (wet flue-gas desulfurization)

Case Study Three: Subbituminous coal with high fly ash unburned carbon.

Case Study One: Optimized Carbon and Halogen Oxidizer for Concrete Applications

The demonstration site for this case study was a 615-MW boiler, burning low-sulfur subbituminous coal. The boiler was equipped with low-NO_x burners and a cold-side electrostatic precipitator (CS-ESP) for particulate control. No desulfurization equipment was installed [7]. The coal chlorine content averaged 100 μg g⁻¹ during the demonstration, resulting in only 30–35% native mercury oxidation during baseline measurements.

The goal of this demonstration was to achieve 90% mercury capture, with <2 lb MMacf⁻¹ activated carbon addition rates. Through previous testing, the client had determined that at <2 lb MMacf⁻¹ activated carbon addition, the fly ash integrity was sufficient to permit economic reuse as a concrete feedstock.

A temporary MerControl 7895 technology injection system was installed, with injection occurring at the coal feeders before the pulverizer. ACI was injected both before and after the air heater. However, the injection before the air heater produced much better results and therefore only these data are presented.

Case Study One: Results Two temporary CMMs were installed at the exit of the economizer and at the stack. The inclusion of the inlet CMM was to provide information regarding changing coal conditions and was considered representative of the coal mercury concentration.

In Figure 14.2, injection of over 2.5 lb MMacf⁻¹ of a standard halogenated activated carbon, introduced before the air heater, resulted in about 91% mercury capture. Also, in Figure 14.2, two nonhalogenated activated carbons were injected with the application of a fuel additive, MerControl 7895 technology. ACI-I is a higher reactivity carbon designed to be used in conjunction with fuel additives. ACI-II is a standard nonhalogenated activated carbon. The significant difference in performance between the two activated carbons emphasizes that all activated carbons are not equal in terms of performance when used in conjunction with fuel additives.

ACI-I required 50% less carbon than ACI-II to reach 91% mercury capture, using the same fuel additive injection rate (168 μg g⁻¹). ACI-I, with a fuel additive concentration of 168 μg g⁻¹ in coal, required 80% less carbon to reach 91% mercury capture, when compared to results obtained with a standard halogenated activated carbon alone.

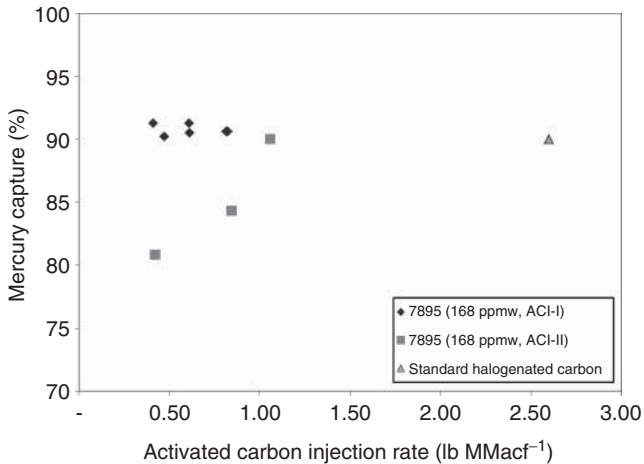


Figure 14.2 Mercury capture as a function of the activated carbon injection rate, with and without MerControl 7895 technology injection.

The 2.5 lb MMacf⁻¹ injection rate with the halogenated activated carbon did not meet the initial requirements of 90% mercury capture at <2 lb MMacf⁻¹ injection rates to preserve fly ash quality. The application of halogen-containing fuel additive and a greatly reduced activated carbon flow rate met both of the client's goals and resulted in the lowest annual compliance cost.

Case Study Two: Bituminous Coal with Performance Shortfalls and SCR/wFGD Typically, halogen-containing fuel additives are discussed with respect to application on low-chlorine, subbituminous, fuels [8]. The reason is that bituminous coals usually have sufficiently high levels of chlorine to oxidize most of the mercury. This is particularly true when there is also an SCR present. However, as shown earlier, even with high levels of chlorine, mercury oxidation is limited, and cannot reach as high a level of mercury oxidation as a bromine-based fuel additives.

Oxidized mercury is readily soluble in water, specifically in wFGD systems. Elemental mercury is not readily soluble in wFGD water. Units with a wFGD system are limited in mercury capture by their mercury oxidation rate. If 80% of the mercury entering the wFGD is oxidized and reemission is controlled, 80% mercury capture across the wFGD is expected. Because bromine-based fuel additives increase the oxidation of mercury, it also increases the unit overall mercury capture in a wFGD.

Case Study Two: Results The case study outlines the application of a bromine-based fuel additive on a 195-MWe high-chlorine bituminous-coal-fired boiler, equipped with an SCR for NO_x control, a wFGD for SO₂ control, and a CS-ESP for particulate control. The typical coal chlorine level was around 1600 μg g⁻¹ of fuel, which in combination with the SCR should have resulted in excess of 90% mercury oxidation and subsequent capture in the wFGD. SCR catalysts typically increase the oxidation rate of mercury in the presence of high concentrations of chlorine.

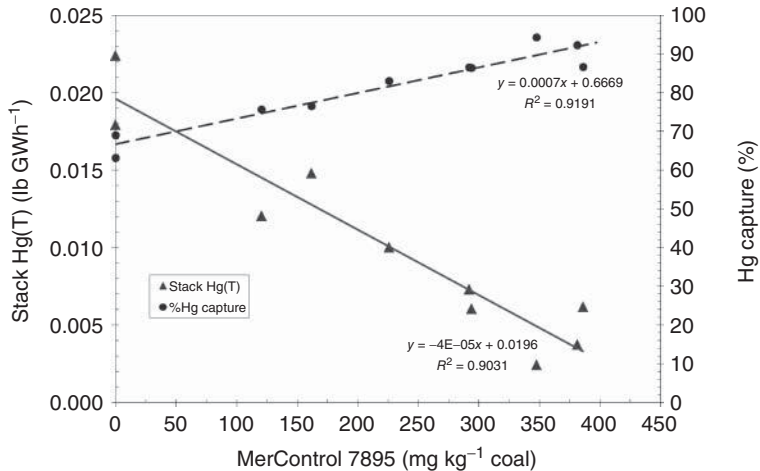


Figure 14.3 Decreasing stack emissions (left) and increasing mercury capture (right) shown for increasing MerControl 7895 technology concentration.

However, owing to the catalyst type and age, mercury oxidation was limited to 70% as observed in previous testing and validated with Ontario Hydro (OH) measurements [9] performed during the baseline observation.

In order to increase the mercury oxidation, a MerControl 7895 solution was applied using a temporary injection system. OH measurements were performed daily, and were validated against Environmental Protection Agency (EPA) Method 30B [10] carbon traps. As with CMMs, halogens can result in fouling of the OH impinger trains, so it is important to validate measurements with an alternative reference method to ensure data accuracy.

The results of the addition of MerControl 7895 technology are shown in Figure 14.3. The mercury oxidation rate during baseline measurements was suggested to be about 80% and the overall mercury capture rate was about 70%. The wFGD was estimated to be nearly 100% efficient in removing oxidized mercury and showed no evidence of reemission. The reason the mercury capture rate is less than the mercury oxidation rate is due to an estimated 5–10% of the flue gas bypassing the wFGD through a leaking flue gas bypass damper.

With increasing dosage rates of MerControl 7895 technology, there is a linear decrease in stack emissions, as shown in Figure 14.3. With the addition of at least 265 mg MerControl 7895 technology per kg coal, the client was able to maintain their required emission rate of 0.008 lb GWh⁻¹, equal to a net 85% mercury capture rate, which includes the bypass damper leakage.

Using the wFGD as the primary mercury removal mechanism was highly desired by the client relative to the injection of activated carbon. High-sulfur bituminous coal burning units with SCRs result in formation of high levels of SO₃ in the flue gas. The deleterious effect of SO₃ on activated carbon performance is well known, resulting in greatly increased ACI rates required to maintain high levels of mercury removal. We estimate that 5–7 lb MMacf⁻¹ of ACI would

be required to reach the same removal rate as $265 \mu\text{g g}^{-1}$ of MerControl 7895 technology because of the CS-ESP as the primary particulate control device and the high levels of SO_3 . Because of this, the MerControl 7895 technology application resulted in substantial savings compared to an option with ACI alone.

Case Study Three: Subbituminous Coal with High Fly Ash Unburned Carbon[†] For units that are not equipped with a wFGD, the primary mercury removal mechanism is formation of particulate mercury. Mercury absorbs on the surface of a carbonaceous material, such as injected activated carbon or unburned carbon from the combustion process. Units with high unburned carbon in the fly ash, typically >2% loss on ignition (LOI), do not require much, if any, activated carbon to be injected because the carbon in the fly ash is adequate to achieve high levels of mercury capture when in the presence of high levels of oxidized mercury. For units that produce a high fraction of elemental mercury (e.g., >20%), the addition of an halogen-containing fuel additive can increase total mercury capture through oxidation and adsorption onto the unburned carbon in the fly ash.

Not all unburned carbon is created equal in terms of oxidized mercury capture efficiency. Owing to high volatility and moisture content, subbituminous coals typically produce higher quality unburned carbon in terms of capturing mercury, relative to bituminous coals. Subbituminous fly ash has better performing pore size, better carbon distribution throughout the ash, more favorable alkali content, and higher surface area resulting from the thermal activation processes that occur during combustion.

If no activated carbon is required, the total capital cost for a halogen-containing fuel additive mercury can be 20% that of an ACI system. Typically, annual operating and maintenance (O&M) costs are substantially lower as well.

Case Study Three: Results The injection of a halogen salt solution was demonstrated on a tangentially fired, 400-MW boiler burning subbituminous coal. The boiler was equipped with low NO_x burners and a CS-ESP, for particulate control. Before the demonstration, the unit was in compliance with their mercury regulation ($0.008 \text{ lb GWh}^{-1}$) by injecting approximately $1.7 \text{ lb MMacf}^{-1}$ ($\sim 61 \text{ kg h}^{-1}$ at full load) of a relatively concrete-friendly halogenated activated carbon. The injection location during normal operation occurred after the air heater through eight injection lances. The goals of the fuel additive demonstration were as follows:

- Reduce ACI flow rates to permit high-value fly ash resale for concrete manufacture. High amounts of activated carbon present in the fly ash causes discoloration when used for concrete manufacture, and also increases the amount of air entrainment chemicals required.
- Decrease overall compliance costs, while maintaining their regulated mercury emission limit.

Selling fly ash for concrete manufacturing can be a significant revenue stream for coal-fired utilities. If the fly ash is unsuitable for concrete, the utility will be

[†] These results have not yet been independently published.

forced to landfill their ash off site at considerable cost. Therefore, poor fly ash quality impacts the utility's profitability by both the loss of sale and the price to landfill. Two main concerns with the quality of fly ash are air entrainment and structural integrity. Activated carbon, while not the only factor, will negatively affect the quality of fly ash by preventing proper air entrainment of the concrete. By reducing the amount of activated carbon used during normal operations, halogen-containing fuel additives can help produce fly ash suitable for concrete manufacturing.

Given the client's goals, we implemented an approach to (i) determine the effect of MerControl 7895 technology on reducing activated carbon consumption rates and (ii) determine the effect of changing the injection location of the activated carbon to upstream of the air heater to further reduce the activated carbon flow with and without MerControl 7895 technology. Gas-phase measurements were provided by an independent third party using two CMMs, one placed at the inlet of the ESP and the other at the stack. CMMs can become fouled during the addition of halogen-containing fuel additives. In order to verify the CMM accuracy, EPA Method 30B carbon trap sampling should always be performed to validate the CMM.

We have found that inlet CMM measurements provide essential information related to process variation and changes in coal mercury concentration. By monitoring the inlet mercury concentration, we can account for process variables that otherwise could systematically affect the results and lead to incorrect conclusions. When coal analyses are solely used to determine inlet mercury concentration, we have found that this does not work as well and does not illuminate process variable effects.

We applied a liquid-based bromine salt solution (MerControl 7895) to all five of the coal feeders. The MerControl 7895 product was delivered to site in 240-gal Schutz totes. A pump-and-control skid provided product pressure, flow control, and flow rate measurements. Temporary injection lines were provided from the pump skid to the injection nozzles, installed on the coal mill feeders. As part of this project, we also provided movable ACI lances to be able to inject carbon before the air heater. The demonstration was completed in under 2 weeks.

Fly ash samples acquired during the demonstration showed LOI values over 2.0%. This level of LOI provided adequate sites for mercury adsorption during application of MerControl 7895 technology. As shown in Figure 14.4, the addition of $10 \mu\text{g g}^{-1}$ of MerControl 7895 technology produced mercury emissions $<0.005 \text{ lb GWh}^{-1}$, below the required emission rate of $0.008 \text{ lb GWh}^{-1}$. The application of MerControl 7895 technology reduced overall compliance cost by over 90% compared to the application of activated carbon.

14.1.4

Case Studies where Conditions Are Disadvantageous to Fuel Additive

There are several conditions in which the utilization of fuel additives is unlikely to provide economic justification. These need to be considered on a case-by-case basis.

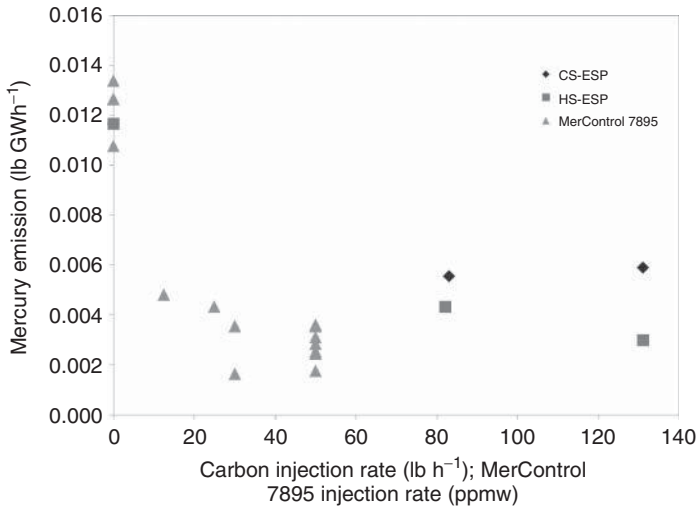


Figure 14.4 Decrease in mercury emissions for increasing carbon and MerControl 7895 technology injection rate.

14.1.4.1 Units Burning High Chlorine Fuel with an SCR

SCR systems have a synergistic effect with available chlorine in the combustion gas in oxidizing mercury. Units burning fuels containing chlorine over $800 \mu\text{g g}^{-1}$ and employing an SCR will typically result in over 90% mercury oxidation. Addition of halogen-containing fuel additives is unlikely to show benefit for these conditions because of the high inherent mercury oxidation rates. Some catalysts contained in the SCRs are less effective than others in oxidizing mercury, and application of fuel additives may still be beneficial.

Generally, the combination of high chlorine and an SCR should not require fuel additives. However, additives can be used to augment deficiencies in fuel chlorine content or SCR function.

14.1.4.2 Subbituminous Fired Units with Flue Gas Conditioning (SO_3 Injection)

A significant fraction of subbituminous fired units inject SO_3 into the ductwork to modify ash resistivity. This, in turn, increases the collection efficiency of the ESP. The injection of SO_3 reduces the performance of activated carbon, requiring relatively high levels of ACI compared to similar configurations without SO_3 injection. These high levels of ACI virtually always spoil the ash for resale.

We have found for these cases that the benefits from applying a bromine oxidizer are rarely economical. This is primarily due to specialty activated carbons that are better suited for high SO_3 applications without the co-benefit of using halogen-containing fuel additives.

For boilers that have high SO_3 concentrations, injected to improve ESP function, and also have a wFGD, the use of halogen-containing fuel additives would be economically justified. These configurations are infrequent because of low sulfur content traditionally found in subbituminous coals.

14.1.4.3 Units without Acid Gas Scrubbing and a Fabric Filter (FF)

Units employing a FF for particulate control, but without a spray dry absorber (SDA) or wFGD, will see little benefit from the application of a bromine-containing fuel additive. Compliance costs are generally low for this condition, typically requiring $<1 \text{ lb MMacf}^{-1}$ halogenated ACI to reach around 90% mercury capture. Compliance costs are so low for this configuration that there is typically not enough economic opportunity to reduce the ACI rates to justify the use of a halogen-containing fuel additive.

There are other considerations that can make the addition of halogen-containing fuel additives attractive for these configurations, such as increased fly ash quality because of reduced ACI rates with addition of halogen-containing fuel additives or the inclusion of an SCR, reducing the typically required dosage rates of halogen-containing fuel additives.

14.2

Summary

Elemental mercury can be difficult to remove using existing air pollution control equipment. The addition of halogen-containing fuel or flue-gas additives to promote mercury oxidation can increase overall mercury capture, decrease compliance costs, and/or reduce activated carbon requirements. The efficacy of halogen-based oxidizers is subject to a number of operational parameters (e.g., flue-gas temperature, unburned carbon, and ash alkalinity), and as such, low-cost trial demonstrations are often used to show results.

References

- Ghorishi, S.B. (1998) Fundamentals of Mercury Speciation and Control in Coal-Fired Boilers. EPA-600/R-98-014, February 1998.
- Kilgroe, J. and Senior, C. (2003) Fundamental science and engineering of mercury control in coal-fired power plants. Air Quality IV Conference, Arlington, VA, September 22-24, 2003.
- Strivastava, R. (2010) Control of Mercury Emissions from Coal Fired Electric Utility Boilers: An Update. EPA/600/R-10/006, February 2010.
- Olson, E.S., Laumb, J.D., Benson, S.A., Dunham, G.E., Sharma, R.K., Miller, S.J., and Pavlish, J.H. (2003) The multiple site model for flue gas-mercury interactions on activated carbons: the basic site. *Fuel Chem. Divi. Prepr.*, **48** (1), 31.
- Pavlish, J.H., Sondreal, E.A., Mann, M.D., Olson, E.S., Galbreath, K.C., Laudal, D.L., and Benson, S.A. (2003) Status review of mercury control options for coal-fired power plants. *Fuel Process. Technol.*, **82**, 89–165.
- Senior, C., Fry, A., Montgomery, C., Silcox, G., Cauch, B., and Bozzelli, J. (2007) Impact of halogen injection on mercury speciation and capture in coal-fired power plants. Presented at Air Quality VI, Arlington, VA, September 24–26, 2007.
- Meier, J., Keiser, B., and Higgins, B. (2011) Demonstrating mercury emissions

- reduction cost management. Air Quality VIII, Arlington, VA, October 24-27, 2011.
8. Keiser, B., Meier, J., Shah, J., Lu, J., and G. Finigan (2010) Mercury emissions: demonstration of air and water quality management. MEGA Symposium, Paper #145, August 2010.
 9. ASTM D6784-02. *Ontario Hydro Method*, American Society for Testing and Materials, www.epa.gov/ttnemc01/guidlnd/gd-051.pdf (accessed 21 March 2014).
 10. EPA EPA Method 30B, www.epa.gov/ttn/emc/promgate/Meth30B.pdf (accessed 21 March 2014).

15

Catalysts for the Oxidation of Mercury

April Freeman Sibley

15.1

Introduction

In December of 2011, the United States Environmental Protection Agency (EPA) issued an emissions standard aimed primarily at mercury but an extensive list of other hazardous air pollutants as well. The regulation was finalized in February of 2012. Targeted toward coal and oil-fired electric generating units, this rule requires applied and potentially newly installed emission control technologies to meet these standards using a maximum achievable control technology application as stemming from the Clean Air Act. In response to this regulation, it has been noted that an approach of utilizing existing emissions control systems retrofitted in the current fleet and capitalizing on a co-benefit strategy as a likely option.

This section discusses the applicability of selective catalytic reduction (SCR) catalysts in the oxidation of mercury contained within the flue gas from coal combustion as it pertains to mercury control using existing technology. Through various operating conditions, multiple responses to varying levels of mercury oxidation can be observed. Factors that affect mercury oxidation include temperature, halogen concentration in the flue gas (from the coal type burned), flow rate, and rate of deNO_x (or ammonia concentration in the flue gas). By optimizing the rate of mercury oxidation, co-benefit capture can be observed downstream in the wet FGD (flue gas desulfurization) vessel and this could make it easier to comply with potential future mercury emissions regulations. Contained within this section are various tables, figures, and data to substantiate this application.

15.1.1

Process Overview

Mercury emissions from coal-fired boilers can be characterized into three main forms: elemental mercury (Hg⁰), oxidized mercury (Hg²⁺), and particle-bound mercury (Hg^p). The concentration of Hg⁰, Hg²⁺, and Hg^p primarily depends on coal composition and combustion conditions. During combustion, Hg⁰ is liberated from coal. In the high-temperature regions of coal-fired boilers, mercury

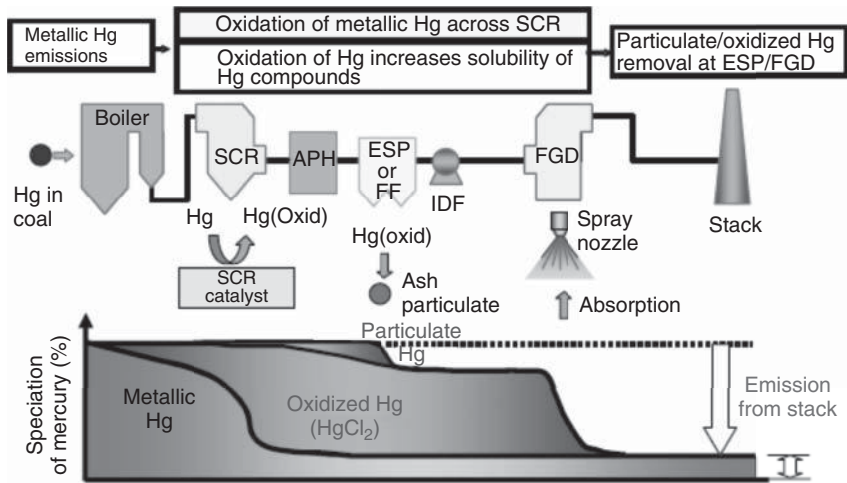


Figure 15.1 Typical behavior of mercury.

in coal is volatilized and converted into the elemental form. However, depending on the coal type, a significant fraction of the mercury can be oxidized, as well as become associated with the fly ash particles in the post-combustion environment of a coal-fired boiler. Relative to Hg^0 , Hg^{2+} , and Hg^p are more effectively captured in conventional pollution control systems, such as FGD systems, fabric filters, and electrostatic precipitators (ESPs). The identification of a process for converting Hg^0 to Hg^{2+} and/or Hg^p forms would improve the mercury removal efficiencies of existing pollution control systems. Mercuric chloride compounds are soluble and can be captured in FGD systems used for SO_2 removal. It is known that the catalysts used for SCR of NO_x compounds can exhibit the co-benefit of promoting mercury oxidation. In addition to catalyzing the decomposition of NO_x compounds to form nitrogen and water, the metal contents of the SCR catalysts have been shown to aid in the oxidation of elemental mercury into a water-soluble compound form. Figure 15.1 depicts the behavior of Hg through a typical eastern bituminous SCR-ESP-wFGD (wet flue gas desulfurization) system [1].

15.2

Hg Oxidation and Affecting Parameters

Upon focusing on the operations of the SCR and its affect on the oxidation of mercury, it is important to note some key areas. The potential contributing factors that can affect mercury oxidation across the SCR reactor include reaction with the catalyst, increased residence time, change in flue gas chemistry (including, but not limited to, the reduction in NO_x concentration), and reaction with NH_3 . Some tests conducted within various electric generating fleets show clearly that for low-halogen flue gases, increases in flue gas chlorine and/or bromine levels will have beneficial effects on SCR mercury oxidation. To capitalize on this effect, facilities

may consider the artificial adjustment of halogens, through direct injection or fuel additives. In addition, tests have shown that direct injection of hydrogen chloride before an SCR can enhance mercury oxidation across the SCR and this will likely enhance the overall mercury removal at sites equipped with an SCR-ESP-wFGD. The data show that lower temperature operation of the SCR will help maximize SCR mercury oxidation. Thus, in designing both retrofit and green-field facilities, lower SCR operating temperatures aid in mercury oxidation and capture. For green-field installations, boiler/SCR designs that provide for generally lower SCR temperatures will help maximize the achievable mercury oxidation through the SCR, at least with conventional catalysts. Lower operating temperatures also have potential benefits in terms of minimizing SO₂ oxidation to SO₃, but the benefits of lowering the SCR temperature must be weighed against the possible loss of catalytic activity for NO_x decomposition (removal).

15.2.1

Hg⁰ Oxidation Reaction Mechanism

On the basis of experimental data available, theories suggest that elemental mercury conversion can occur either through a homogeneous or heterogeneous oxidation. In terms of rate order, it appears that the heterogeneous reaction occurs at a faster rate than the homogeneous reaction. Both reactions, however, have a commonality of kinetics limitation. Factors affecting oxidation reaction kinetics include any of the following: fuel type, halogen content of coal, SCR catalyst age and/or type, SCR reactor temperature, and space velocity.

15.2.2

Homogeneous Oxidation of Mercury

During the homogeneous oxidation reaction, elemental gas-phase mercury reacts with other gas-phase constituents, primarily halogens, to achieve oxidation. There is a very specific temperature window of 400–700 °C in which this occurs. This temperature range is key to the abundance of halogen radicals, namely, chlorine, allowing for sufficient oxidation to occur. It is then that the mercury undergoes two steps to reach a more favorable oxidized state, in the form of water-soluble HgCl₂. The following equations represent what chemically occurs during the homogeneous oxidation of mercury.



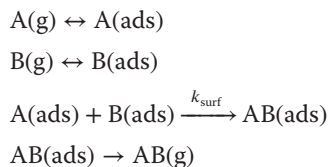
15.2.3

Heterogeneous Oxidation of Mercury over SCR Catalysts

We can propose numerous reaction mechanisms to describe heterogeneous catalytic reactions. The mechanism described as a catalytic reaction will

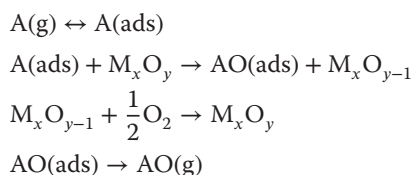
often fall into one of these three categories: (i) Langmuir–Hinshelwood; (ii) Mars–Maessen/Mars–van Krevelen; or (iii) Eley–Rideal.

The Langmuir–Hinshelwood mechanism involves reaction of two adsorbed species on the catalyst to form the product, as shown:

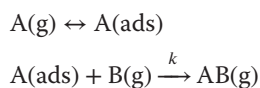


where A could represent mercury and B could represent a halogen such as chlorine.

The Mars–Maessen or Mars–van Krevelen mechanism involves reaction between an adsorbed species (in our case, mercury) and lattice oxygen, or halogen from the catalyst to form the product. The oxygen or halogen is replenished from the gas. The mechanism is depicted here for oxidation of species A by lattice oxygen of the catalyst.



The Eley–Rideal mechanism involves a gas-phase species reacting with an adsorbed species to form the product. The mechanism is depicted here.



where A could represent mercury and B could represent a halogen atom such as chlorine.

Niksa and Fujiwara [2] suggest that ammonia and HCl strongly adsorb to the surface of the SCR catalyst, thus creating an environment for surface site adsorption competition. The elemental mercury either in the gas phase contained within the flue gas itself, or as a weakly adsorbed species, eventually contacts the chlorinated sites and the oxidation reaction occurs. The form of this reaction follows the Eley–Rideal rate expression describing the mercury oxidation rate as a function of the ammonia/NO_x ratio and concentrations of elemental mercury and HCl at the inlet of the SCR as well as catalyst pitch and channel shape, SCR temperature, and the gas space velocity [2]. Other mechanisms suggest that elemental mercury reacts with other constituents either in the gas phase or on the surface of the catalyst or some other solid particle (such as unburned carbon or fly ash), before converting to the more stable HgCl₂ form. No one mechanism, however,

has been verified as the primary reaction mechanism for mercury oxidation, possibly because of the multiple components comprising both the catalysts and the flue gas in a real power plant setting. For example, although we may speculate that the tungsten and vanadium species of the SCR catalyst comprise the active phase for mercury oxidation, we must note that there will also typically be catalytically active fly ash particles (containing carbon and numerous metal oxides) present on the catalyst. In addition, if we suggest that a halogen such as adsorbed chlorine on the surface of the catalyst is primarily responsible for the oxidation of mercury, we must note the possibilities (likelihood) of adsorbed oxygen and bromine participating in the oxidation of mercury as well.

15.2.4

SCR Operation-Hg⁰ Reaction Effects

Because of the limited knowledge of the exact reaction that occurs during mercury oxidation, little information is available with regard to the effect of operational conditions within the SCR itself. To better understand operational effects, some data has been collected during an array of laboratory and pilot scale tests. One particular test conducted between Southern Company and Gulf Power, Electric Power Research Institute (EPRI) and W.S Hinton and Associates, investigated the mercury oxidation behavior of several different commercial SCR catalysts across various operating conditions. The testing occurred at the 5 MWe Mercury Research Center (MRC) located in Pensacola, FL. at Gulf Power's Plant Crist. Parameters such as halogen content in the flue gas, flue gas flow rate, temperature, and ammonia injection, were all varied to measure the mercury oxidation response to these changes.

Research has demonstrated the inhibitive effect of ammonia on the process of oxidizing mercury. Tests have demonstrated that in a low-ammonia concentration environment, the vast majority of the mercury oxidation was observed to have occurred across the first two layers of the three-layer SCR. In the instance of increasing and subsequent high-ammonia concentrations, the reaction zone for the mercury oxidation tended to shift further down in the SCR reactor occurring in the third layer. In one test program performed at the Mercury Research Center in particular, there was a marked increase in the amount of oxidized mercury further down in the SCR catalyst layers, particularly at lower ammonia injection rates.

Owing to the host unit's fuel source containing a very low level of native chlorine in the coal, opportunity existed to vary the levels of halogens into the flue gas to measure the response of mercury oxidation. For the sake of this particular test, chlorine was injected as HCl gas directly into the flue gas. Injection levels ranged from 0 to 150 ppm of chlorine and to ensure minimal interference from ammonia being injected, a constant alpha ratio of 0.9 (or 90% deNO_x) was maintained. It was observed that there was indeed a positive response to mercury oxidation levels as the injection rate of chlorine increased.

A key component of any chemical reaction, temperature was varied to observe the response of the mercury oxidation levels. DeNO_x activity tends to improve as

temperature increases. In addition, the conversion of SO_2 to SO_3 also increases with increasing temperature. Conversely, the rate of mercury oxidation decreases as the temperature increases. Typically, for a constant rate of gas flow, given a certain geometry of the catalyst pitch, the temperature change will also result in a volumetric flow change. High- and low-temperature operating conditions were created in conjunction with slightly different ammonia injection rates while increasing the chlorine concentration in the flue gas. Although there were varying conditions affecting data collection, the data do show a decline in mercury oxidation as the temperature is increased. It is noted that mercury is a semi-noble metal, and the thermal decomposition temperatures of its compounds, such as mercuric chloride, are relatively modest, possibly explaining this observed effect.

Although it is observed to not have as large an effect on mercury oxidation as other parameters, the flow rate through the SCR was varied and response to mercury oxidation measured. It was noted that flow rate changes in addition have an effect on residence time (gas contact time across the catalyst), mass transfer, and ammonia slip, thus ultimately affecting mercury oxidation. As the flow rate increased, the rate of mercury oxidation decreased, which could be linked to the lowered residence (contact) time and increased ammonia slip throughout the reactor.

On the basis of the research conducted, some general conclusions can be drawn from the data collected. They include (i) chlorine content has no apparent effect on deNO_x rate, (ii) chlorine concentrations are effective from 0 to 50 ppm, (iii) mercury oxidation is a function of specific surface area of the catalyst, and (iv) lower temperatures within the SCR reactor increase mercury oxidation rates.

15.2.5

Hg⁰ Oxidation and SO₂/SO₃ Conversion

In addition to the deNO_x and mercury oxidation properties that SCR catalysts possess, there is the ability to oxidize SO_2 (present in the flue gas) to SO_3 , with conversion being represented by the following equation:



The SO_3 produced can then combine with water vapor in the flue gas to produce sulfuric acid. Other potential side reactions that can occur in the presence of excess ammonia include the formation of ammonium sulfate and ammonium bisulfate, which can have adverse reactions on both catalyst performance as well as downstream equipment performance (namely, the air preheater). Through proper operation of the SCR (including minimizing ammonia slip, minimizing SO_2 conversion through catalyst formulations, controlling temperature, etc.), ammonium sulfate and ammonium bisulfate formation can be reduced. Formation reactions are described here:





In an ideal situation, the SCR catalyst would promote the oxidation of mercury and removal of NO_x in the flue gas while minimizing the conversion of SO_2 to SO_3 . Typical SCR operating conditions have made this balance difficult, especially when it has been observed that SO_2 strongly reduces elemental mercury oxidation at high temperatures ($>662^\circ\text{F}$) [4]. In laboratory operations, catalyst manufacturer Hitachi has observed that while SO_2 conversion rates of conventional SCR catalysts have decreased, corresponding rates of mercury oxidation have decreased. This suggests a close correlation between both mercury oxidation activity and SO_2 conversion activity. It is noted that vanadium oxides are well-known commercial catalysts for the oxidation of sulfur dioxide to sulfur trioxide, and are also a key component of the SCR catalysts.

By changing the active composition of catalysts, one could also control activity of the catalyst, which would affect all of the chemical reactions. Research has shown that the active metal components contained in the SCR catalyst have demonstrated this direct effect on both the conversion of SO_2 to SO_3 and mercury oxidation. In a test conducted by Schwaemmle *et al.* [5] V_2O_5 and WO_3 concentrations were varied to measure the effects on deNO_x and SO_2 – SO_3 conversion. By reducing the amount of V_2O_5 in the catalyst, a decrease in SO_2 conversion was observed. In addition, the removal of WO_3 and subsequent addition of Cu to the catalyst composition resulted in an increased SO_2 – SO_3 conversion and a higher deNO_x activity. By altering the active catalyst compositions while noting performance, such data can aid manufacturers in catalyst development, achieving high deNO_x and high mercury oxidation while keeping SO_2 – SO_3 conversion relatively low. Both the removal of NO_x as well as oxidation of elemental mercury occur on the surface of the catalyst, and the SO_2 conversion is a diffusion-limited reaction that occurs within the catalyst itself. According to Gretta *et al.* [4], the reaction rate of SO_2 to SO_3 conversion is slower than the diffusion velocity of SO_2 through the catalyst and the reaction rate of mercury oxidation is faster than the diffusion velocity of the mercury through the catalyst owing to its molecular weight. This means that the SO_2 conversion is controlled by the oxidation rate, which is controlled by the active composition of the SCR catalyst. In order to develop the area of optimizing mercury oxidation using SCR catalysts, design must take into account the amount of active components in the catalyst. By altering the catalyst based on the reaction mechanism, allowing the more active sites to oxidize mercury instead of converting SO_2 to SO_3 , higher oxidation rates can be achieved while maintaining low conversion rates [4].

15.3

Conclusions and Future Research

While much research has been done to understand the impacts of SCR operations on mercury oxidation, there is still a need to gain better insight on the actual

reaction mechanism. This need is the key to being able to predict oxidation performance given a plethora of catalyst types and formulations. Given certain SCR inlet conditions as well as catalyst properties, one could essentially predict the fate of the mercury across the SCR as well as in downstream equipment, namely, the ESP and eventually the wFGD.

In terms of operations, it is noted that changes in flow rate did not appear to have significant impact upon mercury oxidation. This is important to note because in the case of a load change, the change in temperature is expected to have the greatest impact, rather than any effects due to flow rate. This holds given a moderate turndown in load (roughly 60%). More extreme turndowns may see larger effects in which flow rate does play a significant role, but facilities should not assume that low load conditions are necessarily beneficial in terms of mercury oxidation, especially in cases where the flue gas temperatures do not change significantly [3]. The data also indicate that changes in ammonia will affect the amount of mercury oxidation through the SCR. From the results found, the total effect of SCR reactor conditions is not well noted, but the relationship between ammonia concentration and mercury oxidation performance has been identified.

Available data can be used in a relative sense to determine how various operational changes will affect mercury-related parameters; however, the industry would benefit from information from other catalyst formulations, such as newer formulations designed to enhance the oxidation of elemental mercury, ultralow SO₂ conversion catalysts, and regenerated and spent catalysts. New information will help utilities develop catalyst management strategies to maximize and maintain high levels of oxidized mercury from outage to outage. From a compliance perspective, being able to predict and optimize mercury oxidation using current air pollution control equipment, namely, the SCR, would provide cost-effective options for electric generating fleets, avoiding higher installation costs of more capital-intensive control technologies in an effort to meet a stringent standard.

References

1. (a) Diagram courtesy of BHK as presented by: Gretta, W.J. (2007) Mercury oxidation by SCR catalyst. Reinhold Environmental NOx-Combustion/PCUG Conference, Cincinnati, OH, February 5–6, 2007.
2. Niksa, S. and Fujiwara, N. (2005) A predictive mechanism for mercury oxidation on selective catalytic reduction catalysts under coal derived flue gas. *J. Air Waste Manage. Assoc.*, **55**, 1866–1875.
3. Hinton, W.S., Sibley, A.F., Jimenez, A., and Dene, C. (2008) Pilot scale studies of mercury oxidation by SCR catalysts. Power Plant Air Pollutant Control “Mega” Symposium, Baltimore, MD, August 25–28, 2008.
4. Kai, K., Kikkawa, H., Kato, Y., Nagai, Y., and Gretta, W. (2006) SCR catalyst with high mercury oxidation and low SO₂ to SO₃ conversion. Combined Power Plant Air Pollutant Control Mega Symposium, Baltimore, MD, August 28–31, 2006.
5. Schwaemmle, T., Heidel, B., Brechtel, K., and Scheffknecht, G. (2010) Study of the effect of newly developed mercury oxidation catalysts on the deNO_x-activity and SO₂-SO₃ conversion. *Fuel*, doi: 10.1016/j.fuel.2010.11.043.

16

Mercury Capture in Wet Flue Gas Desulfurization Systems

Gary Blythe

16.1

Introduction

This section discusses mercury removal by wet flue gas desulfurization (FGD) systems installed to remove sulfur dioxide (SO_2) from coal flue gas. This is often called *co-benefit* mercury removal because wet FGD systems are generally installed to remove SO_2 , but many achieve a substantial amount of mercury removal from the flue gas as well.

Wet FGD systems work by circulating an alkaline slurry that contains lime or limestone, or a sodium-based alkaline solution, through a flue gas contactor or “absorber vessel” to remove SO_2 and other acid gases from the flue gas. Figure 16.1 is an illustration of a limestone forced oxidation (LSFO) wet FGD process, showing the main components of reagent preparation, flue gas handling and SO_2 absorption, and by-product dewatering. While most wet FGD systems were not originally designed to remove mercury from flue gas, there can be considerable co-benefit capture of mercury under favorable conditions.

As described in earlier sections, mercury in the gas phase of coal flue gases is present in two main forms: elemental or metallic mercury (Hg^0) and oxidized or ionic mercury (Hg^{2+}), with a small amount present as particulate-bound mercury. Oxidized mercury is believed to be present primarily as mercuric chloride (HgCl_2) under most circumstances, but may include mercuric bromide if bromide is added to the coal or flue gas to enhance mercury oxidation.

Of the two major mercury forms in flue gas, the elemental form is exceedingly insoluble in aqueous solutions and therefore is not removed at significant percentages in wet FGD absorbers. In contrast, the oxidized forms, as mercuric chloride or mercuric bromide, are very soluble and absorbed into the FGD scrubbing slurry at high efficiency – at or near the gas-film mass transfer limit of the FGD absorber. In most modern FGD systems, the gas-film limit represents 95–99+% capture of soluble gas-phase species from the FGD inlet flue gas.

Thus, ideally, of the oxidized mercury in the FGD inlet flue gas, a high percentage should be absorbed into the scrubbing slurry. For example, if the total mercury at the FGD inlet is 60% in the oxidized form, approximately 57% to greater than

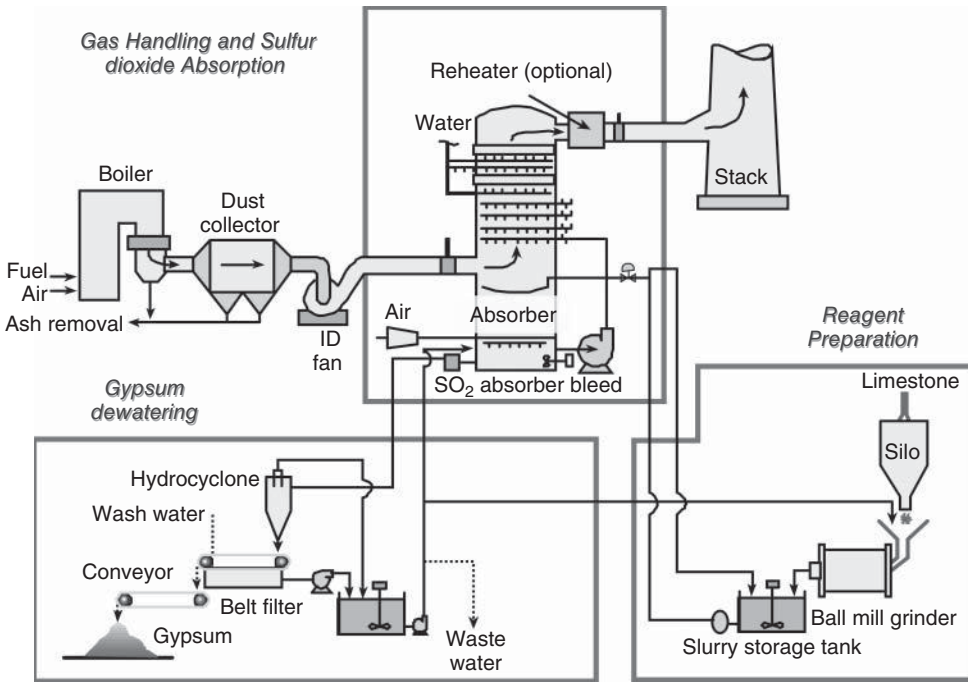


Figure 16.1 Typical limestone forced oxidation wet FGD process.

59% of the total mercury should be absorbed. However, the net removal of oxidized mercury across the FGD system is often limited to lower percentages by a phenomenon called *mercury reemission*, or *reemissions*. In this phenomenon, a portion of the absorbed oxidized mercury undergoes chemical reduction reactions while dissolved in the aqueous phase, and is converted to the relatively insoluble elemental form. Once converted, it is released from the aqueous phase back into the flue gas. Evidence of reemission is seen when the FGD outlet or stack flue gas elemental mercury concentration is measured to be greater than the FGD inlet elemental mercury concentration. Reemissions are discussed in greater detail later in this section.

In the remainder of this section, the capture of oxidized mercury by wet FGD systems is described using two different terminologies to account for the effects of reemissions in limiting net mercury removal. Mercury “absorption” or “capture” is used to describe the transfer of oxidized mercury in the flue gas into the dissolved state in the absorber recirculating slurry, before any reemission reactions. This could be considered the gross capture or removal of oxidized mercury by the FGD system. In contrast, the term *net removal* describes how much oxidized mercury is removed from the inlet flue gas across the FGD system after considering the limitations imposed by reemissions. The initial mercury absorption or capture into the FGD slurry liquor is typically in the range of 95–99+% of the oxidized mercury in the FGD inlet flue gas, while the net removal could be

anywhere in the range of 0–99+%, depending on how significant the reemissions might be. In some cases, the mercury removal across an FGD system can appear to be negative, when in a transient circumstance the inlet mercury concentration to the absorber(s) is lower than the concentration produced by the reemission of mercury from the FGD slurry liquor.

16.2

Fate of Net Mercury Removed by Wet FGD Systems

16.2.1

Phase Partitioning

Mercury is initially absorbed from the flue gas into the liquid phase of the absorber slurry. Once absorbed, it can either remain in the liquor, undergo reemission reactions and be released back into the flue gas as elemental mercury, or be adsorbed or precipitated into the slurry solids.

After being absorbed and dissolved into the aqueous phase of a wet FGD recirculating slurry, oxidized mercury becomes a cationic (positively charged ionic) species. Considering the mercuric salts of the major FGD anionic (negatively charged ionic) species such as sulfate, sulfite, chloride, and carbonate, mercury would be expected to remain in the liquid phase of an FGD slurry; all of these mercuric salts are very soluble. However, the many trace elements present in FGD slurries enter the FGD system by absorption from the flue gas, by capture of fly ash from the flue gas, or from the lime or limestone reagent. Some of these, such as iron (Fe^{3+}) precipitate in FGD slurries, form fine (small particle size) ferri-hydroxides ($\text{Fe}_x(\text{OH})_y$) that can adsorb and/or coprecipitate heavy metals such as mercury. Others such as reduced forms of sulfur (sulfide) and selenium (selenide) form very insoluble salts with oxidized mercury and can result in the precipitation of mercury salts from the aqueous phase into the slurry solid phase. Any or all of these species could be present in FGD slurries in concentrations sufficient to cause a significant phase change of oxidized mercury from the aqueous phase to the solid phase.

The actual mechanism for mercury adsorption/coprecipitation into the solids is not well understood. A number of theories have been considered, and include mercury adsorption/coprecipitation with iron hydroxide fines [1], precipitation as mercuric sulfides [2], or precipitation as mercuric selenides (Bloom, N. (2011) URS Corporation. Personal communication with Gary Blythe, August 2011) and others.

Whether the mercury is found in the slurry solids or liquor is often called the *mercury phase partitioning*. Electric Power Research Institute (EPRI) investigated the phase partitioning of mercury in U.S. wet FGD systems and found that the absorbed mercury can be partitioned over a wide range, from primarily in the slurry liquor to primarily in the slurry solids [3]. Two decades ago, Gutberlet *et al.*, observed that mercury was found primarily dissolved in the liquor phase of LSFO

or gypsum ($\text{CaSO}_4 \cdot 2\text{H}_2\text{O}$) producing wet FGD systems, but primarily in the solid phase of low-oxidation FGD systems that produce calcium sulfite hemihydrate ($\text{CaSO}_3 \cdot \frac{1}{2}\text{H}_2\text{O}$) as a by-product [4]. At first, this was puzzling to EPRI researchers collecting mercury phase partitioning data on U.S. wet FGD systems, because as mentioned a wide range of mercury partitioning was measured in LSFO systems.

However, on further analysis of the data collected, it was observed that the mercury phase partitioning in forced oxidation FGD systems correlated with the oxidation-reduction potential (ORP) measured in the absorber recirculating slurry. ORP is measured in millivolts and provides a measure of how electrochemically oxidizing or reducing is the chemical environment in an aqueous solution. The more positive the ORP the more oxidizing the environment, while the more negative (or closer to zero) the ORP the more reducing the environment.

ORP measurements are relative to a reference electrode also inserted into the aqueous environment, and each electrode type has its own characteristic electrochemical potential. A “standard hydrogen electrode” (SHE) is defined as having a potential of 0 mV, and this is the defined basis for ORP measurements. Field measurements require a more rugged reference electrode than the SHE, so most FGD ORP measurements are made with a silver/silver chloride electrode in a solution of potassium chloride (Ag/AgCl in KCl), with the KCl solution either 4-M or saturated in concentration. The ORP measurements discussed in this section were all made relative to an Ag/AgCl reference electrode in 4-M KCl, and are reported as measured. These measurement results should have approximately 200-mV added to them to make them equivalent to measurements with a SHE.

Figure 16.2 shows EPRI data for mercury phase partitioning in U.S. wet FGD systems as a function of ORP measured in the absorber slurry. The data for LSFO systems show a consistent trend of increasing percentage of mercury in the liquor phase of the slurry as the ORP increases, although with a few outliers. The linear least-squares fit of the data shown in the plot has an R^2 value of 0.9, indicating a relatively good fit. The LSFO systems show a wide range of mercury partitioning, from virtually all in the solids to greater than 80% in the liquor, over a relatively wide range of ORP from less than 100 to over 600 mV. The underlying mechanism for this apparent correlation with ORP in LSFO systems is not yet fully understood.

The data for low-oxidation (calcium sulfite producing) FGD systems show ORP values of approximately +50 to -50 mV, and the mercury is found primarily in the solid phase. However, the data do not fit the linear correlation made for the LSFO systems, and the reason for the different response to ORP is not apparent.

16.2.2

Mercury in FGD By-product Streams

The recirculating slurry in wet FGD systems contains mostly by-product solids (gypsum in LSFO systems and calcium sulfite in low-oxidation systems) with a small amount of lime or limestone reagent present to provide alkalinity. The reactions with flue gas SO_2 produce solid by-products that must be purged periodically

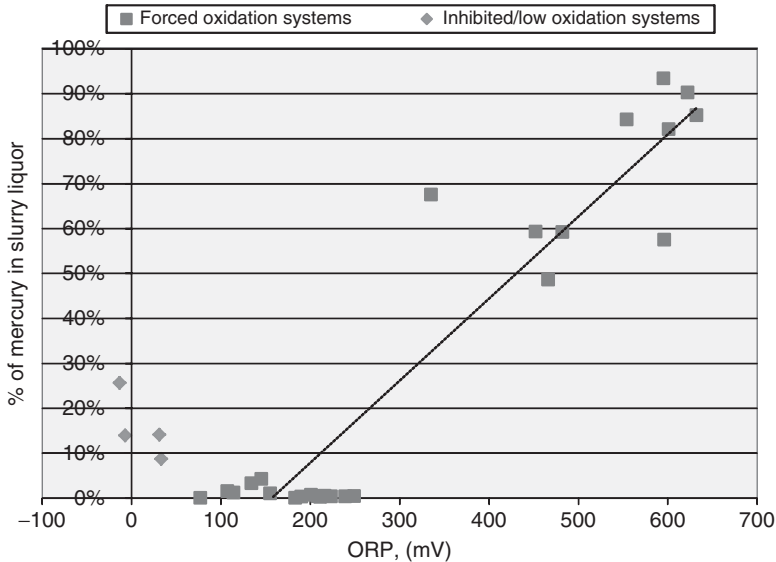


Figure 16.2 Apparent relationship between ORP and phase partitioning of mercury in an FGD absorber slurry. (Reference [5].)

to limit the concentration of suspended solids in the recirculating slurry. This absorber purge stream is dewatered in up to two stages, to produce a damp solid by-product and a low-solid-content liquor stream. In LSFO systems, a portion of the low-solid-content liquor stream is commonly purged to bleed soluble chlorides from the FGD system to prevent excessive chloride concentrations, while the remainder is returned to the absorber. In sulfite-producing wet FGD systems, the sulfite by-product does not dewater as well as gypsum; a separate chloride stream may not be needed, as the water leaving with the dewatered calcium sulfite by-product may adequately control chloride concentrations.

Generally, LSFO systems use hydrocyclones for the first dewatering step, whereas sulfite-producing systems use thickeners (sometimes called *clarifiers*) for the first dewatering step. Figures 16.3 and 16.4 illustrate these two primary dewatering processes. Some early LSFO systems use thickeners for the first step, but hydrocyclones are almost never used in sulfite-producing systems. Both device types produce a low-solid-content liquor overflow and a high-solid-content underflow that can be further dewatered in secondary dewatering processes such as horizontal vacuum belts, drum vacuum filters, or centrifuges. Hydrocyclones produce an overflow that contains approximately 1–5 wt% fine suspended solids, whereas well-performing thickeners produce an overflow with only part-per-million levels of very fine suspended solids. Correspondingly, the two devices produce a different distribution of solids between their overflow and underflow streams.

Hydrocyclones tend to send most of the fine solids in the feed stream to their overflow and most of the coarser solids to their underflow. In contrast,

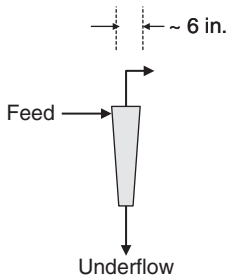


Figure 16.3 Illustration of a hydrocyclone-type FGD primary dewatering system (one of ~10 to 20 per unit is illustrated).

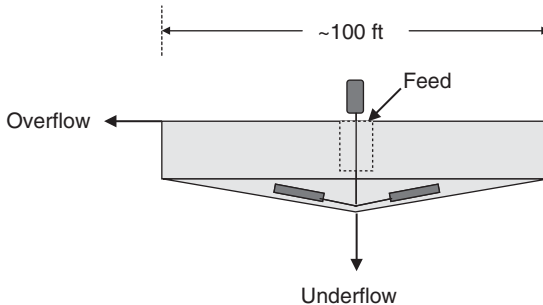


Figure 16.4 Illustration of a thickener-type FGD primary dewatering system (typically one per unit).

well-performing thickeners send almost all of the solids in the feed stream, both fine and coarse, to the underflow. Thus, FGD systems with hydrocyclones tend to recycle an appreciable percentage of fine solids back to the absorber, whereas in systems with thickeners the solids are essentially once through (i.e., no recycle of fine solids).

The sulfite oxidation mode and the types of dewatering devices used in wet FGD systems are described here because they can have a significant impact on how mercury distributes among the solid and liquid by-product streams leaving a wet FGD system. It has generally been observed that mercury is enriched in fine (<20- μm -diameter) solids and is found in a lower concentration in larger solids [5]. This means that in FGD systems with hydrocyclones, the mercury in fine solids tends to get recycled back to the absorber. Because the fine solids have a higher concentration of mercury, the absorber slurry tends to have a higher mercury concentration than the gypsum by-product (hydrocyclone underflow). In systems with thickeners for primary dewatering, the absorber solids tend to have nominally the same mercury concentration as the solid by-product, as the solids are essentially passed through with no size separation.

In systems where most of the mercury is found in the slurry liquor (mostly LSFO systems operated at high ORP), there can be considerable mercury recycle back to the absorber in the hydrocyclone overflow slurry, which is mostly liquor rich in mercury and mostly returned to the absorber. Such a recycle is less common in FGD systems with thickeners, because most are sulfite-producing FGD

systems that operate at low ORP where mercury mostly partitions to the solids, and because it has been observed that liquid-phase mercury concentrations tend to decrease across the thickener. This is likely due to the long residence time in a thickener, during which mercury adsorption and/or precipitation into the solids (or possibly reemission to the atmosphere) can occur.

Correspondingly, in systems that use thickeners for primary dewatering, particularly sulfite-producing wet FGD systems, nearly all of the mercury removed by the wet FGD system leaves with the solid by-product stream. This is largely because in sulfite-producing wet FGD systems, most of the mercury captured by the FGD system is found in the solids. Also, calcium sulfite hemihydrate does not dewater as well as gypsum, so sulfite-producing FGD systems may not require a separate chloride purge stream to control chloride concentrations in the FGD absorber slurry liquor. Thus, there is not a second by-product stream in which mercury can leave the FGD system.

In gypsum-producing wet FGD systems, the mercury removed can be distributed between the gypsum by-product, the chloride purge liquor, and the chloride purge suspended solids. The distribution of mercury among these by-products depends primarily on the ORP at which the absorber(s) operate, the type of primary dewatering device employed, and the weight percent solids in the chloride purge stream. For example, in LSFO systems with a thickener as the primary dewatering device and that operate at low ORP, nearly all of the mercury leaves the FGD system in the gypsum by-product. In contrast, in FGD systems with hydrocyclones for primary dewatering, which operate at high ORP, and/or contain significant fine solids content in the chloride purge stream (e.g., several weight percent solids), the solid and/or liquid portion of the chloride purge stream can represent a significant percentage of the mercury discharge.

16.3

Mercury Reemissions

16.3.1

Definition and Reporting Conventions

As described earlier in this section, mercury reemission describes a phenomenon where oxidized mercury in the flue gas is absorbed in the wet FGD scrubbing slurry, then chemically reduced to the relatively insoluble elemental form and released back into the FGD outlet flue gas. Evidence of reemission is seen when the FGD outlet elemental mercury concentration is greater than the inlet flue gas elemental mercury concentration, when the two concentrations are expressed on a comparable basis (e.g., lb TBtu^{-1} or $\mu\text{g Nm}^{-3}@ 3\% \text{ O}_2$).

However, it should be noted that making mercury concentration and speciation measurements is sometimes difficult, and FGD inlet and outlet flue gas conditions are much different in terms of temperature and moisture content. Reemissions

are quantified by subtracting one measurement result from another, which often involves subtracting one large number from another to quantify a smaller number by difference. This measurement by difference between two significantly different flue gas matrices can lead to measurement errors. Consequently, it is the author's opinion that reemission levels $<0.5 \mu\text{g Nm}^{-3}@3\% \text{ O}_2$ (less than about 0.3 lb TBtu^{-1}) difference between the FGD inlet and outlet elemental mercury concentrations may be within measurement error. Only if such apparent reemission levels are seen consistently in a series of measurements might such levels be considered "real." Even if the measurement data are consistent, it is possible that apparent reemissions are actually measurement bias artifacts.

Several conventions are used to express reemission levels across an FGD system besides the elemental mercury concentration increase across the FGD system, as described earlier. One is to calculate an observed elemental mercury removal percentage based on FGD inlet and outlet elemental mercury concentrations:

$$\text{Reemission percentage} = (\text{inlet Hg}^0 - \text{outlet Hg}^0) \div \text{inlet Hg}^0 \times 100$$

with reemission being represented by a negative value. However, this percentage can be deceiving because the size of the result is dependent on how large is the inlet elemental mercury concentration. Instead, the author prefers to express reemission levels as a percentage of the inlet oxidized mercury concentration, as it is the oxidized mercury that is removed by the wet FGD system and reduced to the elemental form:

$$\text{Reemission percentage} = (\text{outlet Hg}^0 - \text{inlet Hg}^{2+}) \div \text{inlet Hg}^{2+} \times 100$$

Also, this percentage is a reasonably accurate measure of how much reemission has reduced the overall net mercury removal across the FGD system. However, this percentage result can be misleadingly high when the inlet flue gas contains mostly elemental mercury and/or the inlet oxidized mercury concentration is low. In general, it is best to show reemission levels both as a concentration increase and as a percentage of the inlet oxidized mercury concentration. The two conventions for reporting together provide the best overall measure of how significant the observed reemissions might be.

Table 16.1 illustrates mercury measurements made across an LSFO wet FGD system that was experiencing significant levels of reemissions, both when expressed as an elemental mercury concentration increase across the absorber and as a percentage of the inlet oxidized mercury [6]. In this example, the FGD inlet mercury is 76% in the oxidized form; therefore, in the absence of reemissions approximately 72% to nearly 76% overall mercury capture across the FGD system would be expected. The measured capture percentage of oxidized mercury was high at 95%. However, the measured reemissions (by the Ontario Hydro method [7]) were significant, representing an increase in elemental mercury concentration across the FGD system of $3.4 \mu\text{g Nm}^{-3} @ 3\% \text{ O}_2$, or reemission of 49% of the inlet oxidized mercury. Thus, the net overall mercury capture across the FGD system was limited to only 34% of the FGD inlet total mercury instead of the expected 72–76%.

Table 16.1 Example of reemissions from an LSFO wet FGD system.

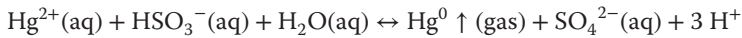
Parameter (all Hg concentrations corrected to 3% O ₂)	FGD inlet flue gas	Stack flue gas
Hg ⁰ (μg Nm ⁻³)	2.2	5.7
Hg ⁺² (μg Nm ⁻³)	6.9	0.38
% Oxidized Hg	76	—
Total Hg (μg Nm ⁻³)	9.2	6.1
Hg ⁺² capture (%)	—	95
Hg ⁰ reemissions (μg Nm ⁻³)	—	3.4
Hg ⁰ reemissions, % of inlet Hg ⁺²	—	49
Overall Hg removal (%)	—	34

Source – Ref. [6].

16.3.2

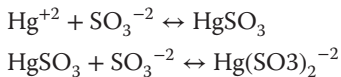
Reemission Chemistry

The primary reaction that produces reemission from FGD systems is believed to be an aqueous oxidation-reduction reaction between absorbed SO₂ and absorbed oxidized mercury. The overall reaction is shown as follows:



where HSO₃⁻ (bisulfite ion) represents absorbed SO₂ in an ionic form at lower pH. However, this reaction is actually the net result of a number of reactions that appear to be kinetically limited at FGD conditions (i.e., they do not always proceed to chemical equilibrium).

The U.S. Department of Energy and EPRI funded a research project to investigate the kinetics of mercury reactions in the aqueous phase of wet FGD slurries, and fundamental studies were conducted in both an ultraviolet/visible spectrophotometer and in a bench-scale wet FGD simulator [8]. Those results showed that in simple simulated FGD solutions, reemission rates slowed as sulfite concentrations increased. This was determined to be the result of the formation of a disulfite complex with oxidized mercury that is more stable than a monosulfite complex with oxidized mercury, according to the following reactions:



It was determined that the monosulfite complex decomposes to produce the reemission reaction, as follows:



However, with the addition of chloride to the synthetic FGD liquor, the reemission reaction rates slowed markedly, in proportion to the chloride concentration in the liquor. The effect is apparently the result of the formation of mercuric chloride complexes that are more stable (less likely to produce reemission reactions)

than the mercury-sulfite complexes. Figure 16.5 provides an illustration of the proposed reactions involved in mercury reemissions in a relatively simple aqueous environment containing only mercuric ion, sulfite, and chloride. Bromide and iodide anions were found to form increasingly stronger complexes than chloride (in that order) when compared on a molar concentration basis, but these halogens are much less abundant in U.S. coals than chloride, and are correspondingly found in lower concentrations in wet FGD liquors.

Other FGD variables such as pH were found to have a complex relationship with sulfite and chloride concentration in their effects on reemission rates (i.e., no consistent trends over the typical range of values for FGD systems). Some species found in FGD systems were found to have a direct impact on reemission rates, most likely because they are reducing species themselves and may directly reduce oxidized mercury in the FGD liquor. Examples of this phenomenon include thio-sulfate ion (present in inhibited oxidation FGD systems) and some sulfur-nitrogen species (present in many FGD systems, particularly those that do not have a high-efficiency NO_x control system upstream of the FGD).

This research also identified that reemission rates are directly proportional to FGD liquor mercury concentrations. As described, there are mechanisms that result in the transfer of mercury from the liquid phase to the solid phase of the FGD slurry. Reemission reactions occur predominantly in the liquid phase, so mercury precipitated or adsorbed into the solid phase is less likely to reemit. Current research funded by EPRI is focused on developing kinetics for mercury precipitation or adsorption from the liquid phase to the solid phase in FGD slurries, and on identifying the mechanisms for this phase transfer [5].

The species that cause mercury to transfer to the solid phase (e.g., iron hydroxides, sulfide, or selenide) have limited capacity to precipitate or adsorb mercury.

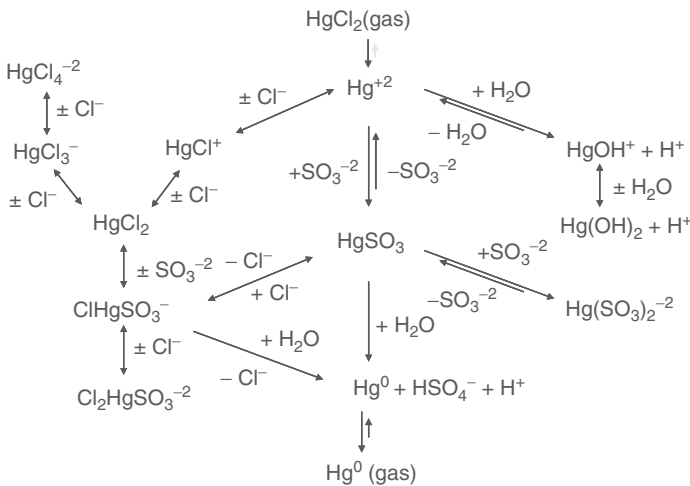


Figure 16.5 Illustration of proposed chemical reactions for mercuric ion, sulfite, and chloride in an aqueous environment [8].

Thus, the ratio of oxidized mercury concentration in the FGD liquor to the concentrations of these species may impact the amount of mercury that remains in the FGD liquor rather than transferring to the solid phase.

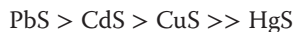
The phase change from the liquor to the solids serves as the basis for the so-called FGD reemission additives, which are added to FGD slurries to control reemissions and improve overall co-benefit capture of mercury. Reemission additives are discussed subsequently.

16.3.3

Reemission Additives

A number of vendors offer additives that can be used to limit or even completely eliminate reemissions. Most reemission additives are compounds that contain sulfide (R-S) or thiol (R-S-H) groups (where R represents the remainder of the molecule). Some are based on sodium or calcium molecules, while others have an organic base molecule. Of the organic-based molecules, the base species can either be a single molecule or a polymer.

The principle of operation of reemission additives is that they either precipitate or form very strong complexes with ionic mercury in aqueous solutions. Several of these additives are commonly used in industrial wastewater treatment processes to remove mercury and other metals from waters, and have been adapted for use directly in FGD processes to precipitate mercury. An example is Evonik Degussa's TMT-15, a 15 wt% solution of trimercapto-s-triazine, which has a molecular weight of 243 and has three sulfide groups attached. Evonik Degussa literature cites how extremely insoluble mercuric sulfides are, and that this is the principle of operation of their additive. The additive has been used for some time in industrial wastewater treatment and Evonik Degussa reported its use in European wet FGD systems for reemission control in 2003 [9]. Sulfide-based additives can also precipitate other metals, mostly divalent transition metals, but mercuric sulfide is the least soluble sulfide salt. Degussa cites the relative solubilities of several metal sulfides in the following order:



Besides lead (Pb), cadmium (Cd), copper (Cu) and mercury, nickel (Ni) and zinc (Zn) are also precipitated as low-solubility sulfides. All of these metals tend to be present in FGD liquors, many in concentrations higher than mercury. Thus, these metals can compete with the reemission additives when they are first injected into an FGD system. Over time, with mercury being the least soluble sulfide salt, mercury in the liquor will preferentially precipitate with the additives. But, depending on how fast the reemission reactions occur, these reactions could still produce reemissions before the mercury is precipitated. Therefore, additive dosage and location of injection must be optimized to ensure rapid precipitation of oxidized mercury as it is absorbed into the FGD liquor.

Besides TMT-15, other vendors have reported considerable testing results on U.S. coal plant FGD systems, including Babcock and Wilcox, and the Nalco

Company [10, 11]. Several other companies offer sulfide- or thiol-based reemission additives; one such example is Pravo [12]. Other approaches for controlling reemissions are being offered. For example, Steag offers a technology to add activated carbon to FGD systems to adsorb mercury as it is absorbed from the flue gas [13]. CH2MHill has a patent for a technology to add iron salts to FGD absorbers to remove mercury from the liquor by iron coprecipitation [14]. All of these technologies are adaptations of technologies commonly used to remove mercury and other heavy metals from industrial wastewaters.

Another approach for controlling reemissions from FGD systems may be to optimize FGD operating conditions to minimize reemission rates. However, more research and development is needed to establish this as a well-defined and controllable approach. FGD parameters that could be optimized to control reemissions might include (but may not be limited to) the following:

- ORP (Mitsubishi Heavy Industries has a patent covering ORP control to optimize net mercury capture [15]),
- Iron content in the limestone reagent, and/or process configurations that maximize iron fines recycle to the absorber as part of the slurry dewatering process,
- Chloride concentrations in the FGD liquor (impacts mercury complexation, indirectly impacts the recycle of iron-based mineral fines in FGD reclaim water in systems that employ hydrocyclones),
- Concentrations of other halogens (bromide and iodide) in the FGD liquor that form strong complexes with mercury, and
- Weight percent suspended solids in the absorber slurry (impacts fines concentrations and surface area available for mercury adsorption).

16.4

Effects of Flue Gas Mercury Oxidation Technologies on FGD Capture of Mercury

One way to increase the co-benefit removal of mercury by wet FGD systems is to increase the percent oxidation of the mercury in the flue gas. Other chapters discuss the effects of fuel and flue gas additives, several of which enhance mercury oxidation, and the effects of catalysts, which also can enhance mercury oxidation. Of course, these technologies are not as effective if reemissions limit the net removal of oxidized mercury across the FGD system.

One additive that has been demonstrated to increase mercury oxidation in flue gas is the bromide ion, which can be added to the coal as a salt or injected into the flue gas as a salt or an acid. One impact of bromide injection is that bromine compounds in the flue gas are scrubbed at high efficiency in the FGD system, and the bromide ion is highly soluble in calcium- and sodium-based solutions. Thus, bromide builds up in the FGD system in a manner similar to chloride, to a concentration at which the bromide rate leaving in the water purged from the FGD system equals the rate entering with the coal and the bromide additive.

As the bromide builds to steady-state concentrations in wet FGD systems, it can affect mercury chemistry in the system. One effect was mentioned earlier in this section: bromide forms a relatively strong aqueous complex with oxidized mercury. This complexation can have further effects. As the bromide concentration builds, the mercury tends to remain in the liquor phase rather than transfer to the solids, and is available to participate in aqueous reemission reactions. However, the strength of the mercury–bromide complex tends to slow reemission reaction rates. The net effect of increased bromide concentrations on mercury reemission tendencies can be site specific – in some cases, reemissions are significant, while in one account the presence of elevated bromide concentrations appears to have stopped reemissions [16].

FGD system operators should keep in mind their system's liquid residence time when conducting tests with the bromide additive, as the true performance of the FGD system for net mercury capture may not be realized until steady-state bromide concentrations are achieved. The data plotted in Figure 16.6 show that it took almost 1 week of bromide addition testing at one full-scale wet FGD system to experience a change in mercury partitioning between the FGD liquor and solids. The change was not realized until the liquor bromide concentration exceeded 100 mg l^{-1} . FGD systems with hydrocyclones for primary dewatering, which operate with relatively low chloride concentrations in the FGD liquor and do not have a lot of slurry or liquor storage volume incorporated (e.g., no filter feed tanks or no large reclaim water tanks), tend to reach steady state rapidly, within a matter of days. The FGD liquid residence time is affected by factors such as the total volume of process water in the FGD system, the chloride concentration in the coal, and the chloride concentration in the FGD liquor at blow down. Systems that fire low-chloride coal but operate with elevated chloride concentrations in the absorber liquor, have thickeners for primary dewatering (which have a large liquid volume), and/or systems with other large volumes of water that get returned to the FGD system (e.g., from ponds) can take many days, weeks, or months to reach steady-state bromide concentrations.

Oxidation catalysts that enhance mercury oxidation percentages in the FGD inlet flue gas have generally not been observed to impact mercury behavior in wet FGD systems. That is, catalytically oxidized mercury is generally captured from the flue gas at as high an efficiency as is native oxidized mercury, and is no more or less likely to be reemitted.

However, one possible adverse effect is that by increasing the concentration of oxidized mercury in the flue gas, the ratio of oxidized mercury to species that enhance the transfer of mercury to the solid phase is increased. As this ratio increases, mercury may tend to remain in the liquor, and thus be available for reemission reactions. In contrast, selective catalytic reduction (SCR) catalysts can also oxidize mercury and may have a beneficial effect on mercury chemistry in wet FGD systems. By lowering NO_x concentrations in the FGD inlet flue gas, SCR systems may reduce the formation of “sulfur-nitrogen” compounds in FGD liquors [18]. Some of these compounds are chemically reducing species, and in bench-scale tests have been observed to contribute to mercury reemission

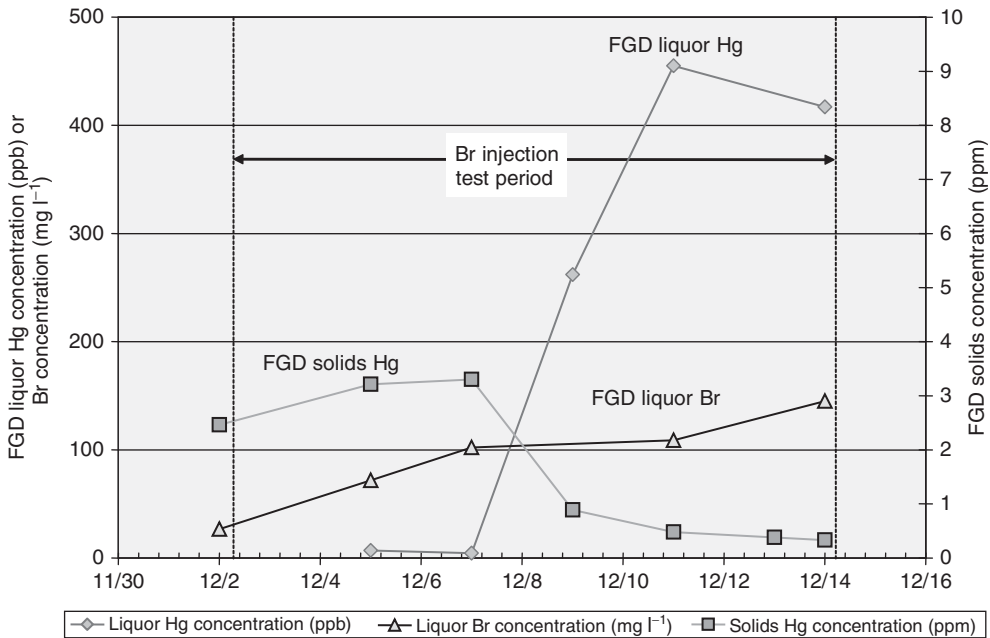


Figure 16.6 Example data showing time dependency of bromide concentration and effects on mercury partitioning in a full-scale wet FGD system. (Reference [17].)

reactions [8]. Thus, SCR catalysts may indirectly lower mercury reemission rates by lowering sulfur-nitrogen compound concentrations.

Some researchers are developing technology to enhance mercury capture by wet FGD systems by *in situ* oxidation of the small amount of elemental mercury that is soluble in wet FGD solutions [19]. Another technology being investigated would use replaceable carbon composite panels in the upper portion of an absorber vessel to absorb mercury from the flue gas [20]. These development efforts may represent future directions for maximizing co-benefit mercury capture by wet FGD systems. At present, these technologies are being investigated at laboratory to demonstration scale.

References

1. Schroeder, K., *et al.* (2006) Leach testing of FGD materials. Paper Presented at the DOE/NETL Mercury Control Technology Conference, Pittsburgh, PA, December 11-13, 2006.
2. Ghorishi, B., Bill, D., and Scott, R. (2006) Role of sulfides in the sequestration of mercury by wet scrubbers. Paper #116 Presented at the 2006 Power Plant Air Pollutant Control "Mega" Symposium, Baltimore, MD, August 28-31, 2006.
3. Richardson, M., Gary, B., and Rhudy, R. (2008) Field study of mercury partitioning in wet FGD byproducts. Paper Presented at the Power Plant Air Pollutant Control "Mega" Symposium, Baltimore, MD, August 25-28, 2008.

4. Gutberlet, H. *et al.* (1992) Behaviour of the trace element mercury in bituminous coal furnaces with flue gas cleaning plants. *VGB Kraftwerkstechn.*, **72** (7), 586–591.
5. Blythe, G.M., *et al.* (2011) Investigation of mercury control by wet FGD systems. Paper Presented at the Symposium on Air Quality VIII, Arlington, VA, October 24–27, 2011.
6. Blythe, G. and Owens, M. (2008) Field Testing of a Wet FGD Additive for Enhanced Mercury Control, Final Report, Cooperative Agreement DE-FC26-04NT42309, U.S. Department of Energy National Energy Technology Center, Pittsburgh, PA, March 2008.
7. ASTM International (2002) D 6784 – 02. *Standard Test Method for Elemental, Oxidized, Particulate-Bound and Total Mercury in Flue Gas Generated from Coal-Fired Stationary Sources (Ontario Hydro Method)*, ASTM International, West Conshohocken, PA, June 2002.
8. Blythe, G., Currie, J., and DeBerry, D. (2008) Bench-scale Investigation of the Kinetics of Mercury Reactions in FGD Liquors. Final Report, Cooperative Agreement DE-FC26-04NT42314, U.S. Department of Energy National Energy Technology Center, Pittsburgh, PA, August 2008.
9. Tarabocchia, J. and Peldszus, R. (2003) Mercury separation from flue gas and scrub water with Trimercapto-s-triazine (TMT). Paper Presented at the Combined Power Plant Air Pollutant Control Mega Symposium, Washington, DC, May 19–22, 2003.
10. Ghorishi, S.B., *et al.* (2005) Effects of SCR catalyst and wet FGD additive on speciation and removal of mercury within a forced-oxidized limestone scrubber. Paper Presented at the ICAC Clean Air Technologies and Strategies Conference 05, Baltimore, MD, March 7–10, 2005.
11. Keiser, B., Meier, J., and Higgins, B. (2011) Demonstrating mercury emissions reduction cost management. Paper Presented at the Symposium on Air Quality VIII, Arlington, VA, October 24–27, 2011.
12. Vosteen, B.W., D. Ing. *et al.* (2008) KNX™ and PRAVO® – a perfect duo for mercury capture; recent industrial applications in waste incineration. Paper Presented at the 11th Annual EUEC Conference 2008, Tucson, AZ, January 30, 2008.
13. Elliott, P. (2011) Midwest utility and evonik energy services successfully perform full-scale mercury capture test. Paper Presented at the Symposium on Air Quality VIII, Arlington, VA, October 24–27, 2011.
14. Higgins, T.E. (2009) Methods and systems for enhancing mercury, selenium and heavy metal removal from flue gas. US Patent Application Number 20090130013, May 21, 2009.
15. Shintaro, H. *et al.* (2009) Method for removing mercury in exhaust gas and system therefor. US Patent US7572420, Aug. 11, 2009.
16. Tyree, C., Looney, B., and Vosteen, B. (2011) Effect of precombustion bromide addition on mercury emissions from full-scale bituminous coal unit equipped with cobenefit controls. Paper Presented at the Symposium on Air Quality VIII, Arlington, VA, October 24–27, 2011.
17. Dombrowski, K. (2005) Data Collected as Part of U.S. Department of Energy Cooperative Agreement DE-FC26-04NT41991. URS Corporation, Austin, TX, December 2005.
18. Gutberlet, H. and Gabriele, B. (2005) The influence of induced oxidation on the operation of wet FGD systems. Paper presented at the Air Quality V, Arlington, VA, September 19–21, 2005.
19. Stergarsek, A., Horvat, M., Frkal, P., and Stergarsek, J. (2010) Removal of Hg⁰ from flue gases in wet FGD by catalytic oxidation with air – An experimental study. *Fuel*, **89** (11), 3167–3177.
20. Machalek, T., *et al.* (2011) Field investigation of fixed-structure sorbents for mercury emission control. Paper Presented at the Symposium on Air Quality VIII, Arlington, VA, October 24–27, 2011.

17

Introduction to Carbon Sorbents for Pollution Control

Joe Wong

17.1

Carbon Materials

Carbon materials occur in various forms owing to the arrangement of the carbon atom in the structural lattice, which can be characterized as either crystalline or amorphous. Crystalline carbons represent a class of materials whereby the carbon atoms are highly ordered and show a high degree of symmetry in their structural features (Figure 17.1). Crystalline carbon materials include diamond, graphite, and fullerenes. Diamond is considered the most highly ordered crystalline carbon material, having tetrahedrally bonded carbon atoms (sp^3) that form a face-centered cubic structure (Figure 17.2) [1]. Graphite is a highly ordered layered carbon structure with “sheets” of graphene planes (Figure 17.3) [1]. Carbon bond lengths and structural features of crystalline carbons are very regular and well defined.

In contrast, amorphous carbons are carbon materials with less order and/or more defects in the carbon structures. As there is never total disorder of the structure, there exist micro-regions of order or micro-crystallinity in the structure. The irregular carbon arrangement and structural defects give rise to the carbon material's pore structure, surface, and surface area features. Amorphous carbons are further classified into materials derived from coal, charcoal, or lamp black. Activated carbons possess many of the crystal structural features of amorphous carbon materials, and thus are characterized as predominantly amorphous solids.

17.2

Carbon Activation

Activated carbon can be produced from a variety of raw materials, including coal (predominantly bituminous and lignite), lignocellulose (sawdust, nut shells, lignin, pits, etc.), peat, plastics, resins, and petroleum residue. Essentially, any raw material that can be converted to a carbonaceous form can be activated.

Mercury Control: for Coal-Derived Gas Streams, First Edition.

Edited by Evan J. Granite, Henry W. Pennline and Constance Senior.

© 2015 Wiley-VCH Verlag GmbH & Co. KGaA. Published 2015 by Wiley-VCH Verlag GmbH & Co. KGaA.

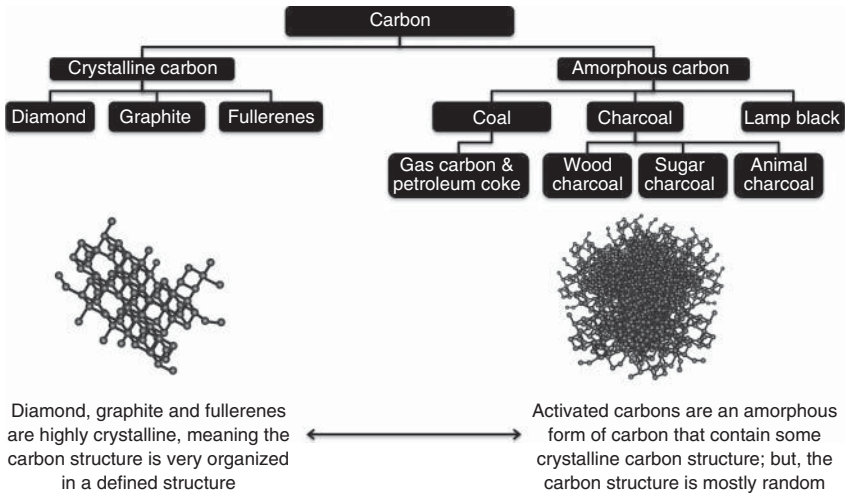


Figure 17.1 Crystalline and amorphous carbon materials.

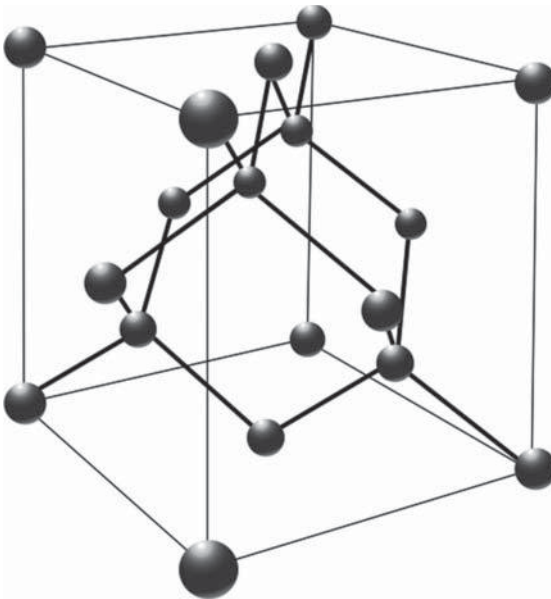


Figure 17.2 Crystalline structure of diamond.

Activation of the carbonaceous raw material is typically conducted either by thermal means or with chemical reactants. Heat treatment equipment ranging from rotary kilns, multihearth furnaces, fluid bed reactors, and batch ovens are employed under a variety of temperature, residence time, and gas composition conditions to achieve desired activated carbon properties. As one can imagine,

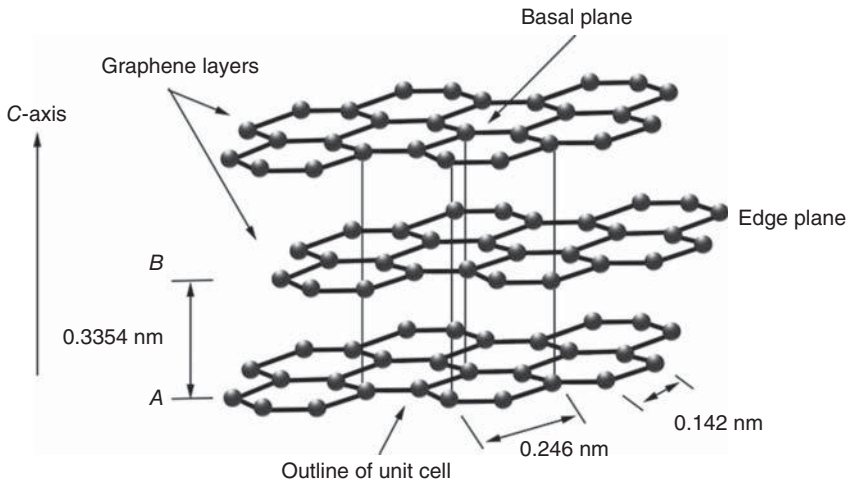


Figure 17.3 Crystalline structure of graphite.

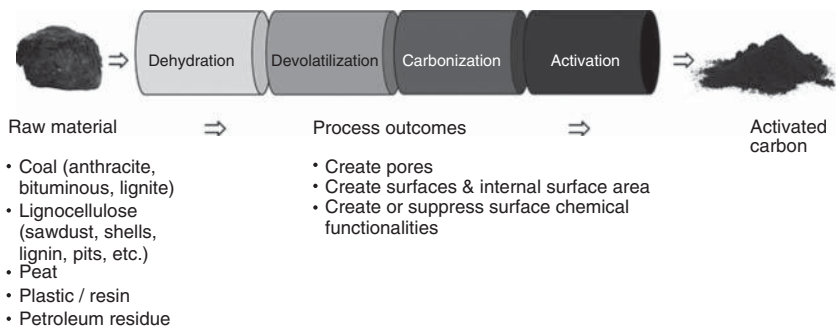


Figure 17.4 Carbon activation.

those in academia and industry and entrepreneurs have defined many activated carbon processing conditions. An Internet search of “Activated Carbon Activation” will return over 37 million hits. Baker, *et al.* [2] describe the various commercial manufacturing processes.

Despite the plethora of activation conditions, there are predominant basic processes occurring in activation, consisting of dehydration, devolatilization, carbonization, and finally activation itself. Figure 17.4 depicts a generalized view of these basic process steps in a thermal activation process. These basic steps are not necessarily discrete steps with fine lines of demarcation, but instead can overlap each other significantly. The first step consists of “dehydration.” Most raw materials contain moisture, essentially in the form of free and some bound water, that is initially removed upon heating to about 100–150 °C. The next step is termed *devolatilization* and occurs above 150 °C, whereby free or weakly bound volatile organic constituents begin to evolve from the raw material into the gas phase.

“Carbonization” begins to occur around about 350 °C and proceeds to slightly below 800 °C in an inert or nonoxidizing atmosphere [3]. During carbonization, the non-carbon constituents containing heteroatoms, including oxygen, hydrogen, sulfur, and nitrogen, decompose or volatilize. Some of the organic constituents are not removed and remain in the carbon material as partially charred matter. Elemental carbon is essentially concentrated in the carbon material during carbonization. In addition, the carbon atoms begin to arrange into semirandom amorphous structures. Spaces or interstices of various sizes and shapes begin to form, giving rise to the beginning formation of the material’s pores and surfaces. This carbonized material is sometimes referred to as *char*.

Typically, above about 800 and below 1000 °C in the presence of air, steam, carbon dioxide, or another oxidizing agent, the char begins to “activate.” During activation, the initial pore structure from carbonization is further developed through oxidation or “burn-off” of the carbon structure and charred organics. Depending on the desired activated carbon “activity,” pore development is a trade-off to carbon yield.

During activation and in subsequent cooling steps, the surface chemical functionalities can be manipulated. The oxidative atmosphere during activation typically results in a high oxygen-containing carbon surface. The injection of a “reductive” gas is sometimes employed to cap these oxygen functional groups to obtain desired carbon surface properties.

17.3

Carbon Particle Shapes and Forms

Activated carbons produced from thermal or chemical activation are typically in a combination of powdered and granular particulate form with particle sizes of less than about 2–3 mm in diameter. Additional processing employed by manufacturers can provide smaller or larger particles or shaped forms. Figure 17.5 describes typical activated carbon shapes and forms, which can consist of powdered activated carbon (PAC), granular activated carbon (GAC), shaped carbon, and carbon cloths.

17.3.1

Powdered Activated Carbon (PAC)

The American Society for Testing and Materials (ASTM) classifies PAC as activated carbon material passing through an 80-mesh sieve (0.177 mm or 177 μm) [4]. PAC is produced commercially by comminuting larger activated carbon particles produced during the activation process through one or more types of grinding equipment, including roller mill, hammer mill, ball mill, jet mill, and so on. The comminuted particle is sometimes classified to attain desired sieve mesh size fractions for different application requirements.

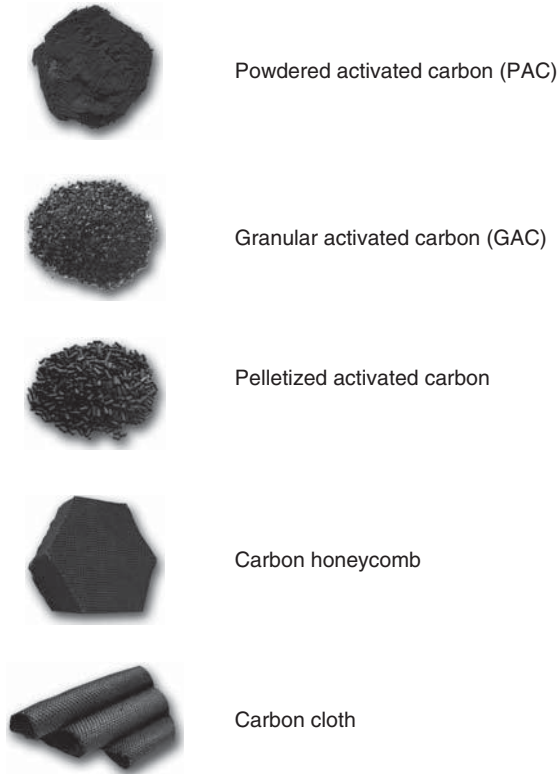


Figure 17.5 Activated carbon shapes and forms.

PAC is used prevalently in liquid-phase purification applications, such as in water treatment and food purification. By the nature of its small particle size, PAC is also a leading candidate for dispersed gas-phase applications. PAC can be designed to be highly dispersible in the gas phase, which allows for enhanced probability of contacting with dilute concentration gaseous pollutants and for rapid capture and uptake of pollutant molecules.

17.3.2

Granular Activated Carbon (GAC)

GAC particles are larger in size than PAC. ASTM classifies GAC as activated carbon particles that are retained on an 80-mesh sieve. The larger particle sized GAC is often used in gas- and liquid-phase applications, whereby the process stream flows through a packed bed of activated carbon. The GAC provides a lower pressure drop, thus allowing higher process stream flow rates, simpler equipment design, and lower energy requirements.

17.3.3

Shaped Activated Carbon

PAC can be mixed with a binder and shaped into different forms, including pellets, beads, honeycombs, and so on. Typical binders include carboxyl methylcellulose, clays, phenolic resins, ceramics, coal tar pitch, or combinations thereof. Depending on the manufacturing process, the binder addition and shaping of the raw material may occur before or after activation.

The manufacture of shaped carbons requires additional equipment and processing beyond carbon activation, thus adding cost to the final activated carbon product. Additional steps include (i) mixing and mulling of the PAC and binder, (ii) extrusion/briquetting/shaping, (iii) low-temperature heat treatment to achieve “green” strength, and (iv) high-temperature heat treatment to “set” the binder.

Shaped activated carbons, including honeycombs (Figure 17.5), are used extensively in gas-phase purification and catalyst support applications. The binder system provides the activated carbon its shape integrity, high mechanical strength, and low dust properties.

17.3.4

Other Activated Carbon Forms

Activated carbons can be impregnated into cloths and fabric, either physically bound or via a coating. These cloths find utility in air filters, chemical warfare suits, or applications requiring a conformal shape.

Other activated carbon forms include fibers and aerogels, which typically tend to be used for high-value, specialized applications.

17.4

Activated Carbon Applications

Activated carbon is a proven, versatile technology for a host of purification and other applications. The ability to tailor performance properties is a key, enabling feature of activated carbons. Although not an encompassing list, Baker, Global Industry Analyst, Freedonia and Roskill [2, 5–7] each describe industrial markets for activated carbon. Figure 17.6 lists some of the larger established and emerging market areas for activated carbon.

The use of activated carbons is well established for waste and potable water treatment, food and pharmaceutical separations and purifications and industrial processes, including solvent recovery. Other specialty applications are also well established, such as for catalyst and catalyst supports. The versatility of activated carbons has garnered much interest in applications for electrode materials for electrical energy storage markets. Other applications in the medical and consumer products arena are also prevalent. Carbon dioxide capture and sequestration are rapidly expanding R&D sectors for activated carbon sorbents.

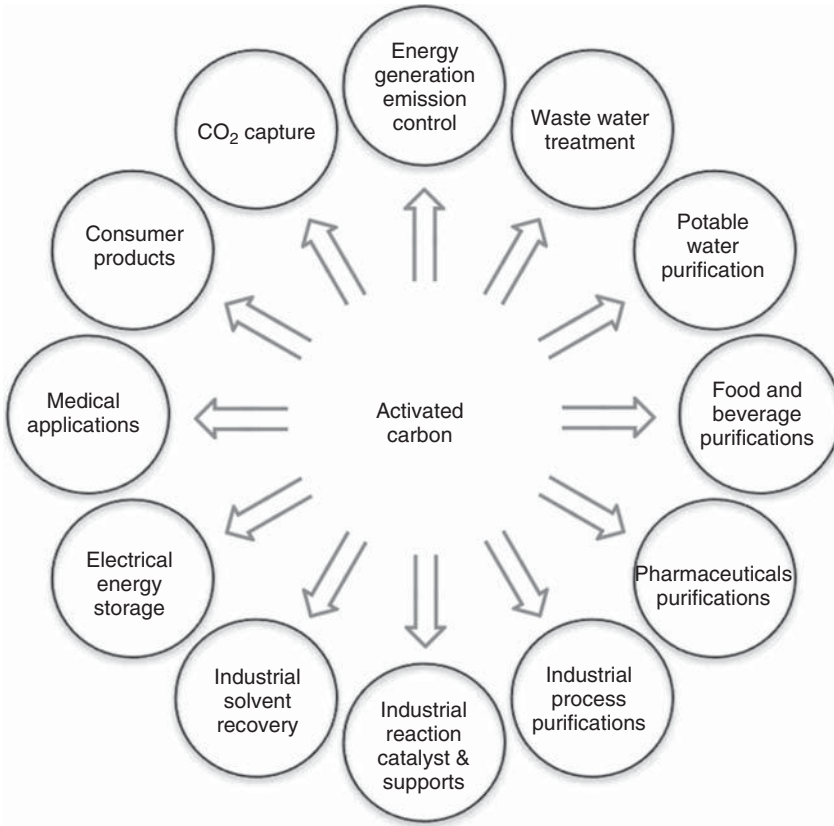


Figure 17.6 Activated carbon market applications.

A significant market interest in activated carbon has come from the energy generation industries, such as coal- and waste-fired power plants, industrial boilers, and cement kilns. These industries are in their initial commercial stages of applying activated carbons in their flue gas treatment steps and are conducting plant trials of improved, specialty activated carbons for mercury and other emission controls. This specialized application of activated carbon technology is establishing ground as the best available, cost-effective technology for mercury capture from flue gas.

17.5

Activated Carbon Properties in Emission Systems

Activated carbons are highly adaptable and can serve multiple purposes in removing organic and inorganic pollutants. Their innate ability to attract and capture

targeted molecules has made activated carbon a viable solution for removing mercury from flue gas streams.

The removal of mercury from power plant flue gas is a complex process, with consideration, to name a few, of the effects of chemical reaction kinetics, flue gas constituents and activated carbon surface interactions, and carbon adsorption capacity, diffusion kinetics, and adsorptive energy distribution. In addition, power plant flue gas emission trains are typically set up differently and thus present a variety of operating conditions from which the activated carbon must perform. Unfortunately, there is no reliable computational model to estimate the individual or collective nature of these factors on mercury removal. However, much work has been conducted to start painting a scientific-based fundamental picture of an ideal model system from which to build upon [8]. Later chapters in this book describe in detail the recent work on mechanisms and models for mercury interaction with carbon surfaces.

It is acknowledged widely that the removal of mercury from flue gas is represented by three predominant mechanisms.

- Conversion of elemental mercury, Hg^0 , to an electron-receptive, oxidized state, either Hg^+ or preferably Hg^{2+} to enhance mercury's receptivity to activated carbon;
- Contact of the mercury compound, which is in a very dilute concentration in the flue gas, with the activated carbon;
- Diffusion and capture of the mercury compound in the activated carbon structure by physical adsorption and chemisorption.

The order and influence of these mechanisms and the rate-limiting step have been studied, proposed, and debated; however, it is plausible that all occur in a parallel manner, with one being more pronounced than the others in certain emission train conditions.

Given these mechanisms, activated carbon has three key properties or capabilities that make it effective for emission control applications (Figure 17.7). A meaningful specification for activated carbon for mercury removal in flue gas should factor in each of these characteristics.

- Activated carbons provide a **SURFACE** to host chemical reactants and other functionalities that interact with or affect the pollutant species, both chemically and physically.
- Carbons have **PORES** that adsorb, meaning attract, transport, and capture, molecules to be removed.
- Carbons are **PARTICLES** that are highly dispersible and provide a transport medium to deliver all the desired properties to the right place and at the right time in the emission system.

Each of these properties is discussed here.

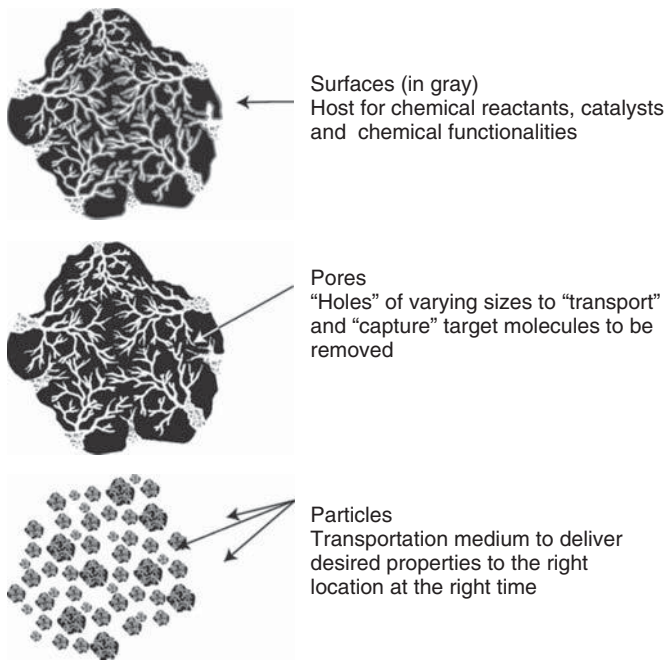


Figure 17.7 Activated carbons are multifunctional.

17.5.1

Activated Carbon Surface

A typical activated carbon designed for power plant flue gas mercury capture contains 500–700 m² of surface area per gram of activated carbon. In other words, 1 lb of activated carbon per million actual cubic feet of flue gas (lb/actual cubic feet per minute (ACFM)) injection rate provides enough carbon surface area to cover about 50 football fields if each carbon particle is unfolded completely flat to expose all surfaces. At this level of potential surface area, it is evident that not all of the activated carbon's surfaces are accessible to the mercury and that there are other factors involved. Accordingly, in developing activated carbon specifications specific to mercury capture, specifying surface area alone is insufficient.

Consideration of the role of an activated carbon surface in mercury removal reveals other key surface activities that occur (Figure 17.8).

The carbon surface provides bromine or other halogen forms or an oxidant to facilitate oxidation of elemental mercury to an oxidized, more “adsorbable/soluble” state.

The surface contains and exposes minerals to catalyze the oxidation of mercury. It is well documented that heterogeneous catalysis of mercury in the presence of halogens by precious metals and other minerals is on order of 100 000 times faster than the oxidation of mercury by halogens in a homogeneous gas phase [9, 10]. Having certain minerals present is particularly important when there are only

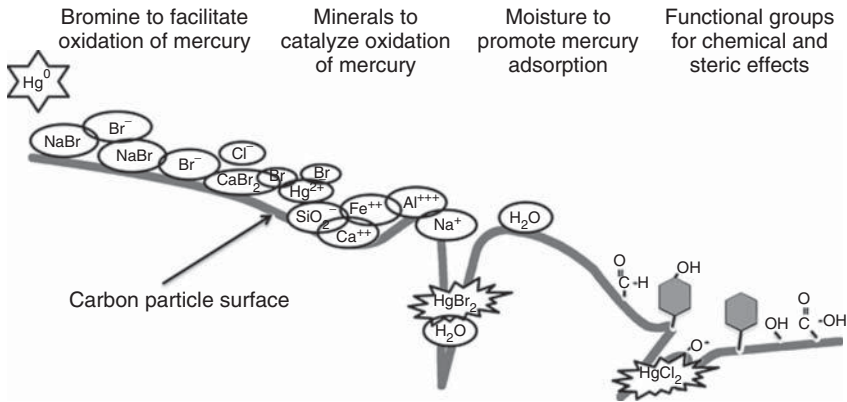


Figure 17.8 Activated carbon surfaces.

seconds of exposure time of the mercury to the halogen in most plant emission systems.

The surface contains moisture to promote mercury adsorption into the pores. The effects of carbon moisture levels have been studied and cited in literature [11]. Moisture plays a role in improving the adsorption of oxidized mercury.

The surface exposes certain chemical functional groups. It is well known that activated carbon surfaces contain a variety of chemical functions, including acidic carboxylic acid functions, phenyl and phenol groups, reactive free radicals, and polar hydroxyl and carbonyl groups [12, 13]. These surface functionalities can enhance or reduce the affinity of the activated carbon for the mercury species [14].

Evaluation of the binding energies of mercury and oxidized mercury species with simulated carbon surfaces has offered insights as to potential surface complex mechanisms, but a definitive or dominate pathway has not been elucidated [15]. However, it has been demonstrated that activated carbon surface features can be tuned to enhance or block specific surface mechanisms to enhance pollutant capture.

17.5.2

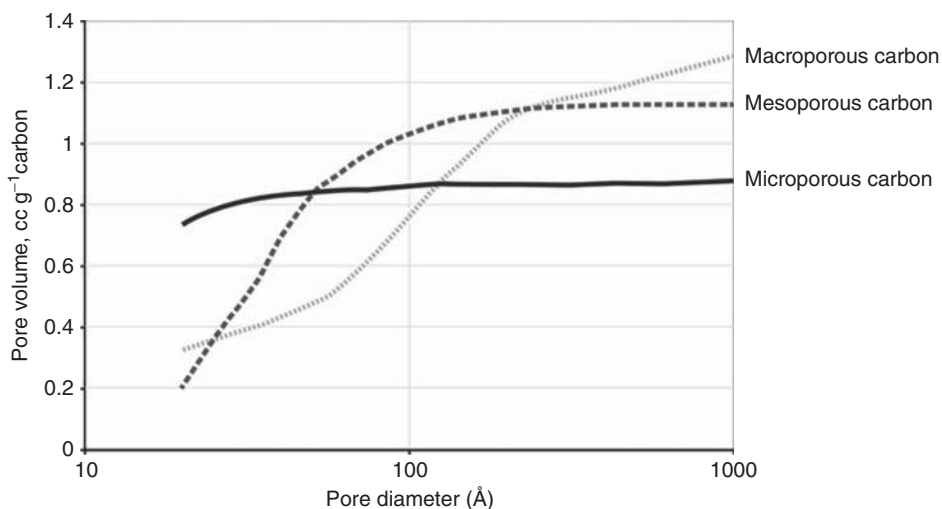
Activated Carbon Pores

The pores of an activated carbon are an intricate arrangement of “holes,” “passages,” and “caves,” providing a carbon with its adsorptive properties and the resultant ability to capture targeted mercury molecules in flue gas systems. The characterization of pore structure often includes microscopic analyses and molecular simulations of the morphological (pore shape and size) and topological (pore connectivity) character of carbons [16].

Carbon pores are defined by their shape and size. Pores have been represented in various geometries, ranging in shapes from tapered cylinders to elongated slits. It is commonly acknowledged that the elongated slits provide the best representation of pore shape and function [17–21]. Carbon pore sizes (width) are

Table 17.1 IUPAC classification of pore size.

Classification	Pore diameter (nm) (10^{-9} m)	Pore diameter, Å (10^{-10} m)
Micropore	<2	<20
Mesopore	2–50	20–500
Macropore	>50	>500

**Figure 17.9** Cumulative pore volume and pore size of activated carbons. (Reproduced with permission from MeadWestvaco Corporation.)

classified by the International Union of Pure and Applied Chemistry (IUPAC) as shown in Table 17.1 [22]. Pores with width <2 nm are designated as *micropores*. Pores between 2 and 50 nm are *mesopores*. Pores with width >50 nm are termed *macropores*.

Pore size distributions can be interpreted from gas porosimetry measurements using nitrogen or argon as the adsorbate. Figure 17.9 [23] shows a plot of cumulative pore volume in various pore size ranges for activated carbons possessing high degrees of micropores, mesopores, and macropores. For the microporous carbon, essentially all of the 0.8 cc g^{-1} pore volume is in pores <2 nm in diameter. The mesoporous carbon has minimal pore volume in micropores, and pore volume starts building progressively around 2 to about 30 nm. The macroporous carbon has the majority of its pore volume in pores >25 nm in diameter, building in macropore volume to 100 nm. What is apparent is that activated carbon is not one-size-fits-all, as the pore size distribution can be tuned to some extent to favor one size distribution over another.

Moreover, the molecular size of the target molecule in a particular end-use plays a key role in optimizing the pore size distribution of activated carbon. Because of

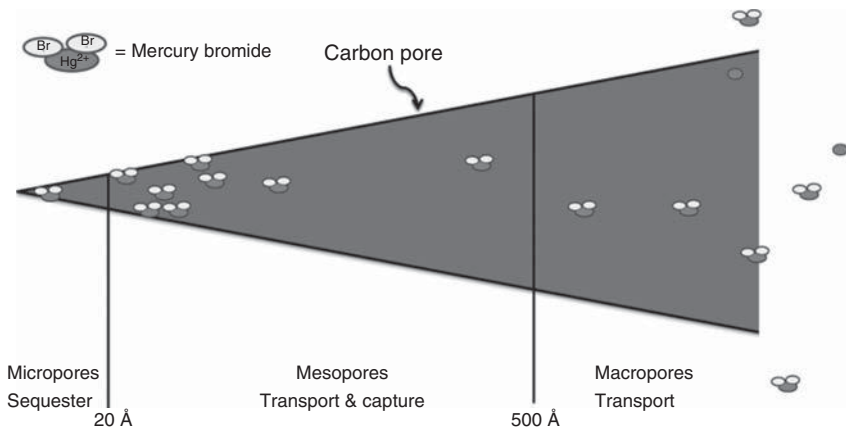



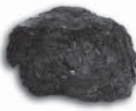

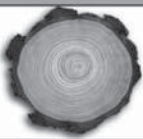
Figure 17.10 Activated carbon pore geometry and size range.

the prevalence of water treatment and food purification applications, traditional liquid- and gas-phase activated carbon pore size design is based on the adsorption performance of small iodine molecules (0.3–0.6 nm or 3–6 Å in molecular size) and large tannins, molasses, or methylene blue color bodies (>2 nm or 20 Å in molecular size). However, in the case of oxidized mercury, a mercury bromide molecule has a molecular size in between those two benchmarks on order of 1.0–1.3 nm (10–13 Å). From that simple analysis, it follows that using traditional activated carbon specifications based on adsorption of smaller molecules or larger color bodies would not be expected to result in the optimal mercury removal performance [24].

Figure 17.10 shows a graphical depiction of the role of each pore size required in capturing mercury. Starting from the right side of Figure 17.10 – in the high-temperature flue gas, highly energetic mercury species need to come in contact with the carbon particle and enter the larger macropores. Once in contact, the macropores transport the molecules into large mesopores. The molecules are eventually captured and sequestered in the small meso and micropores. Because this diffusion, transport, capture, and sequestration occur in a very short amount of time in the emission system, larger pores are required to increase the probability of capturing the gas-phase molecule and enhance pore diffusion/transport, while smaller micropores with high adsorptive energies are required to capture the mercury molecule and prevent diffusion back into the flue gas.

Commercial carbon manufacturers employ a variety of raw materials to produce activated carbon. Invariably, the starting raw material affects the porosity characteristics of the final activated product (Table 17.2). For example, raw coconut shells are hard and dense and produce activated carbons that are typically very high in micropores and have low amounts of mesopores and macropores. Cellulosic precursors, such as wood, are inherently low density and porous, leading to highly meso- and macroporous carbons. Bituminous coal-based carbons lean more toward micropores, while lignite coal carbons are highly mesoporous. It is

Table 17.2 Raw material impact on pore characteristics.

	Coconut activated carbon	Coal activated carbon	Lignite activated carbon	Wood activated carbon
Pore characteristics				
Micropores	High	High	Medium	Low
Mesopores	Low	Medium	High	High
Macropores	Low	Medium	Medium	High

recognized that these are typical porosity descriptions, and that enhanced activation conditions and/or additional processing steps can be added to shift the porosity characteristic from any raw material source. For example, Baker *et al.* [25] developed highly microporous carbons from wood by an intensive second-stage activation of a wood-based carbon with an alkali salt, such as potassium hydroxide.

17.5.3

Activated Carbon Particles

Another important feature of activated carbon is that it is a particle or form that transports key functional properties in and out of the emission system. Specifically, the carbon particle or carbon grain serves an important function as a carrier and disbursement mechanism for bromine or halogen as the mercury oxidant, minerals as oxidation catalyst, surface for other desired chemical functionalities, pores for mercury capture, and a medium to transport mercury out of the emission system through the electrostatic precipitator or filter fabric baghouse.

Knowing the operating conditions of the emission system is critical to maximizing the performance of the activated carbon particle. With such information, the properties of the activated carbon can be tuned to achieve the best performance in various operating configurations. For example, the activated carbon may need to function at high temperatures, such as in the case when injected “hot-side” before the air preheater (as opposed to “cold-side” after the air preheater or after the electrostatic precipitator) or may need to be compatible with other emission control devices (Figure 17.11).

In addition, activated carbon injected into the flue gas may have less than a second of time in order to capture the mercury before being removed from

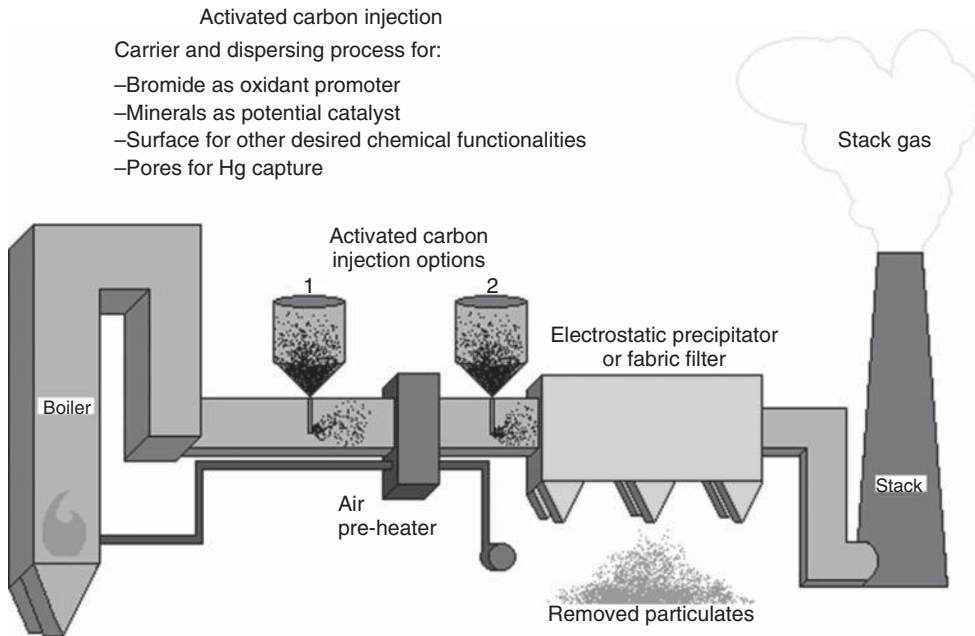


Figure 17.11 Activated carbon particles in emission systems.

the system. Consequently, its effectiveness is highly dependent on diffusional and kinetic considerations with the short residence time of contact between the carbon and the mercury. Much modeling has been conducted to discern drivers and rate-limiting mechanisms, including carbon pore diffusion and restrictions, as well as temperature effects [26].

In view of the kinetic considerations, the industry is trending toward the use of fine activated carbon particles with mean particle diameter $<25-30\ \mu\text{m}$. These smaller particles provide a higher propensity of surface for contacting the flue gas than larger carbon particles. However, the handling of these fine carbon particles in a power plant environment requires new particle handling protocols because of different flow characteristics in the injection equipment and removal dynamics in the emission train. Durham and Martin [27] developed a process for onsite size reduction of activated carbon particles to mitigate fine particulate handling issues, but this approach has not yet been adopted widely.

Another benefit of activated carbon particles is that once the mercury species is captured and sequestered on the carbon surfaces and pores, the particles can be readily removed from the emission train. Typical equipment used for this removal includes an electrostatic precipitator or filter fabric baghouse, whereby the spent activated carbon is removed along with the coal fly ash. This fly ash and PAC mixture can be safely land filled or used in producing cement.

17.6

Summary

Activated carbons are customizable adsorbent materials that are key enablers for controlling mercury emissions in power plant flue gas. Advances in understanding and tailoring activated carbon surface, pore, and particle features are providing insights and solutions to tackling the complex adsorptive, catalytic, and diffusional challenges faced in removing mercury in harsh, variable flue gas environments. These insights will help the coal-fired power energy industry move toward more pertinent carbon property specifications, much like the advances that have been made in defining activated carbon specifications for the well-established water treatment, sugar decolorization, and automotive gasoline emission control industries.

References

1. Marsh, H. and Rodriguez-Reinoso, F. (2006) *Activated Carbon*, Elsevier, London, p. 15.
2. Baker, F. S., Miller, C. E., Repik, A. J., and Tolles, E. D. (2003) *Kirk-Othmer Encyclopedia of Chemical Technology*, vol. 4, John Wiley & Sons, Inc., New York, p. 741.
3. Bansal, R. C. and Goyal, M. (2005) *Activated Carbon Adsorption*, Taylor & Francis Group, Boca Raton, FL.
4. ASTM D 2652-05a (2007) *Standard Terminology Relating to Activated Carbon*. Annual Book of ASTM Standards Volume: 1, ASTM.
5. Industry Market Group Publication (2011) *Activated Carbon Market Report*, April 2011, MCP-1825, Global Industry Analysts, Inc..
6. The Freedonia Group, Inc. (2010) *World Activated Carbon to 2014 – Demand and Sales Forecasts, Market Share, Market Size, Market Leaders*, June 2010, Study 2626.
7. Industry Market Group Publication (2008) *Industrial Minerals/The Economics of Activated Carbon*, 8th edn, Roskill.
8. Livengood, C. D., Mendelsohn, M. H., and Lani, B. W. (2004) *The chemistry of mercury oxidation*. Mercury Control Technology R&D Program Review, Pittsburgh, PA, July 14–15, 2004.
9. Granite, E. J. and Presto, A. A. (2008) Noble metal catalyst for mercury oxidation in utility flue gas. *Platinum Met. Rev.*, **52** (3), 144–154.
10. Miksche, S. J. and Ghorishi, S. B. (2007) Catalytic oxidation of elemental mercury at low temperatures. 32nd International Technical Conference on Coal Utilization and Fuel Systems, Clearwater, FL, June 10–15, 2007.
11. Rodriguez, S., Almquist, C., Lee, T. G., Furuuchi, M., Hedrick, E., and Biswas, P. (2004) A mechanistic model for mercury capture with in situ-generated titania particles: role of water vapor. *J. Air Waste Manage. Assoc.*, **54**, 149–156.
12. Bandosz, T. J. and Ania, C. O. (2006) in *Activated Carbon Surfaces in Environmental Remediation*, vol. 7 (ed T. J. Bandosz), Elsevier, Oxford, p. 159.
13. Cannon, F. S. and Nieto-Delgado, C. (2011) Conventional and tailored activated carbons for removing natural organic matter and targeted compounds from drinking water, in *Green Carbon Materials: Advances and Applications*, Pan Stanford Publishing (Preprint copy).
14. Huggins, F. E., Huffman, G. P., Dunham, G. E., and Senior, C. L. (1999) XAFS examination of mercury sorption on three activated carbons. *Energy Fuel*, **13** (1), 114–121.
15. Padak, B. and Wilcox, J. (2009) Understanding mercury binding on activated carbon. *Carbon*, **47**, 2855–2864.
16. Coasne, B., Alba-Simionesco, C., Audonnet, F., Dosseh, G., and Gubbins,

- K. E. (2011) Adsorption, structure and dynamics of benzene in ordered and disordered porous carbons. *Phys. Chem. Chem. Phys.*, **13**, 3748–3757.
17. Lastoskie, C., Gubbins, K. E., and Quirke, N. (1993) Pore size heterogeneity and the carbon slit pore: a density functional theory model. *Langmuir*, **9**, 2693–2702.
 18. Ravikovich, P. I., Jagiello, J., Tolles, D., and Neimark, A. V. (2001) Improved DFT methods for micropore size characterization of activated carbons: role of pore wall heterogeneity. Extended Abstracts Carbon '01, Lexington, KY.
 19. Olivier, J. P. (1998) Improving the models used for calculating the size distribution of micropore volume of activated carbons from adsorption data. *Carbon*, **36** (10), 1469–1472.
 20. Dombrowski, R. J., Hyduke, D. R., and Lastoskie, C. M. (2000) Pore size analysis of activated carbons from argon and nitrogen porosimetry using density functional theory. *Langmuir*, **16** (11), 5041–5050.
 21. McCusker, L. B., Liebau, F., and Engelhardt, G. (2001) Nomenclature of structural and compositional characteristics of ordered microporous and mesoporous materials with organic hosts. *Pure Appl. Chem.*, **73** (2), 381–394.
 22. Sing, K. S. W., Everett, D. H., Haul, R. A. W., Moscou, L., Pierotti, R. A., Pierotti, J., and Siemieniowska, T. (1985) Reporting physisorption data for gas/solid systems with special reference to the determination of surface area and porosity. *Pure Appl. Chem.*, **57** (4), 603–919.
 23. MWV Corporation (2011) Data and Graph Provided, October 2011.
 24. Huston, R., McNeill, J., Baldrey K., Sjostrom, S., and Siperstein J. (2011) On-site determination of the quality of commercial sorbents for the removal of mercury from combustion and process gas streams. Energy, Utility and Environment Conference (EUEC), Phoenix, AZ, January 31 – February 2, 2011.
 25. Baker, F.S., (1995) Production of Highly Microporous Activated Carbon Prooducts. US Patents 5,416,056, May 16, 1995; 5,626,637, (1997) Low Pressure Methane Storage with Highly Microporous Carbons. May 6, 1997; 5,710,092, (1998) Highly Microporous Carbon. Jan. 20, 1998, and 5,965,483, (1999) Highly Microporous Carbons and Process of Manufacture. Oct. 12, 1999; assigned to Westvaco Corporation.
 26. Flora, J. R. V., Hargis, R. A., O'Dowd, W. J., Pennline, H. W., and Vidic, R. D. (2003) Modeling sorbent injection for mercury control in baghouse filters: I-model development and sensitivity analysis. *J. Air Waste Manag. Assoc.*, **53**, 4.
 27. Durham, M. D. and Martin, C. E. (2011) Apparatus and process for preparing sorbents for mercury control at the point of use. US Patent 8034163, Oct. 11, 2011.

18

Activated Carbon Injection

Sharon M. Sjoström

18.1

Introduction

Activated carbon (AC) is effective in adsorbing mercury from the flue gas produced by many coal-combustion sources. AC can be installed as a fixed bed of carbon downstream of other pollution control equipment, or ground into a powder and injected upstream of a particulate collection device. This chapter provides information on activated carbon injection (ACI) into flue gas, factors limiting the effectiveness of ACI, and balance-of-plant considerations.

ACI is the most established commercial technology for reducing mercury emissions from coal-fired boiler flue gases. It has been proven through numerous full-scale demonstrations to be an effective, cost-efficient way to reduce mercury emissions from most plants that fire lower sulfur coals. Depending on the type of coal being burned and the type of air pollution control equipment installed on the plant, ACI can reduce mercury emissions by more than 90%, and can offer options for mercury trim at most plants. For plants firing low-halogen fuels, ACI can be used in conjunction with halogen-based coal additives to enhance performance.

ACI technology, which is shown in Figure 18.1, is relatively simple in comparison to typical emission control equipment. An ACI system is shown in Figure 18.1 to the right of an SO₂ scrubber and fabric filter (FF) in the photograph. An ACI system consists of a storage silo for the AC and a pneumatic conveying system that injects the AC at a controlled feed rate at the desired locations in the ductwork before the particulate control device. The mercury reacts with the AC sorbent and then is removed from the flue gas along with the fly ash by the plant's particle control device. Tests have shown that the mercury is not leachable from the sorbent [1] so that it can be disposed of in a landfill without concern for contamination of waterways. Because of their simplicity and small size, ACI systems can be retrofit on virtually any power plant with minimal engineering.



Figure 18.1 Perspective on ACI system in relation to other air pollution control equipment at a coal-fired power plant.

18.2

The Activated Carbon Injection System

Typical ACI system components include a silo to store the powdered activated carbon (PAC) before injection, process equipment to meter and convey the PAC to the injection location, and a distribution grid that includes manifolds and individual injection lances. Figure 18.2 shows a cutaway of a typical ACI system, including the storage module and process equipment, and a photograph of an ACI system installed at a coal-fired power plant. The ACI system shown has a storage silo with an enclosed process equipment room at grade level and a separate motor control building. Although the system appears relatively simple, there are critical aspects of the design that can result in poor control performance or poor reliability if attention is not paid to the details.

18.2.1

Powdered Activated Carbon Storage

The size of the PAC storage system is dependent on the unique needs of the plant. Factors include the projected PAC usage rate and the total days of storage that are required to assure continuous availability. PAC is usually delivered to the plant in a closed truck. The smallest silo for a commercial system typically holds more than a full delivery truck of PAC so that the truck can be unloaded without completely emptying the silo before unloading. This allows continuous availability of the material without demurrage or delays in availability of PAC.

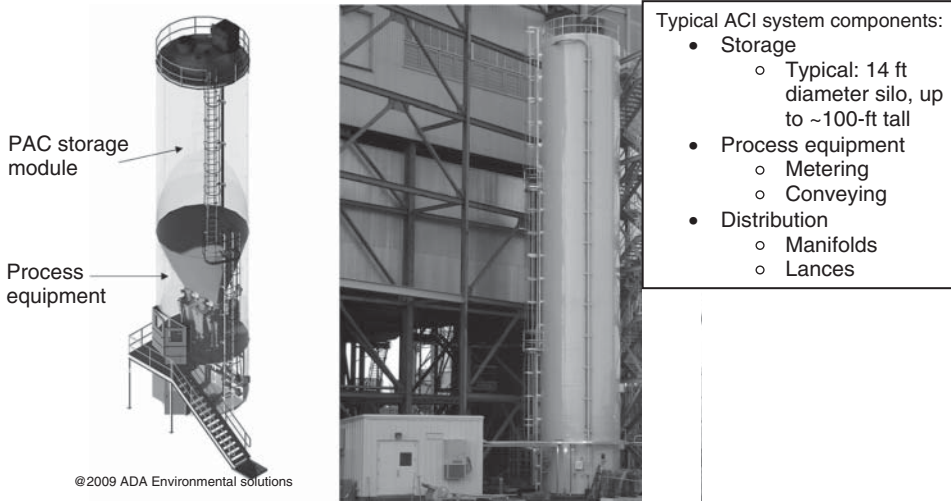


Figure 18.2 Cutaway and photograph of typical ACI system installed at a coal-fired power plant.

18.2.2

Process Equipment

18.2.2.1 Metering

The amount of PAC fed over time can be monitored in real time using either gravimetric or volumetric feeders. Gravimetric feeders are more accurate than volumetric feeders, but are two to three times the cost. One of the main disadvantages of volumetric feeders is that without use of a feedback control loop they may need to be recalibrated whenever a different sorbent with different properties is used. This can be a problem for sites that use multiple sorbents on a frequent basis. For plants that control the PAC feed rate to a set point, accurate calibrations are critical to cost control and to assuring sufficient PAC is being fed to meet mercury emission compliance. Plants that use feedback control from a mercury continuous emissions monitor can often benefit from a gravimetric feeder for inventory control.

18.2.2.2 Conveying

Both regenerative and positive displacement (PD) blowers are used in ACI systems for dilute phase conveying of PAC. The choice of blowers depends on how much PAC is being fed, conveying distance, number of elbows, and change in elevation. PD blowers are more expensive and have a larger footprint, but can provide higher flow and motive force, which is important for installations with long piping runs and many turns. The downstream components must be sized appropriately for the blower to minimize both sorbent fallout and pluggage from low velocities as well as component failures from abrasion due to the high velocities.

18.2.3

PAC Distribution

PAC is conveyed from the silo and feed system through main conveying lines. These are typically hard piped for permanently installed systems to minimize leaks associated with abrasion. The conveying lines terminate at a manifold that distributes the PAC into separate injection lances. These manifolds must be carefully designed to assure that the appropriate amount of PAC is delivered to each lance. There are typically several lances installed at the injection location to assure good distribution across the entire gas path. It is important to assure that all of the flue gas is being treated, especially for plants with electrostatic precipitators (ESPs) where most of the mercury adsorption takes place in-flight. Lance placement can be affected by several factors including access constraints that may limit the ability to install ports.

18.3

Factors Influencing the Effectiveness of Activated Carbon

Coal-combustion facilities that produce steam for electricity or heat fire a range of coals and are configured with a variety of pollution control devices. The effectiveness of ACI for mercury control at these facilities is contingent on several factors. Key factors can be categorized as

- 1) *Site specific*, including coal characteristics, flue gas temperature, SO₃ concentration in the flue gas, particulate control configuration,
- 2) *PAC specific*, including characteristics such as PAC quality, chemical treatment, and size distribution, and
- 3) *ACI system design specific*, including PAC injection location, grid design, and lance design.

18.3.1

Site-Specific Factors

Aside from the difference in heating value between bituminous and sub-bituminous coals, there are obvious differences in the sulfur and chlorine concentrations, as described in more detail in Chapter 2. In general, ACI is most effective for mercury control on flue gas derived from combustion of coals with lower sulfur contents, such as subbituminous coals, low-sulfur bituminous coals, and many lignite coals. In the United States, most subbituminous coal is mined in the Powder River Basin (PRB). PRB coal typically contains <1% sulfur and <50 µg g⁻¹ chlorine. Furthermore, ACI is more effective when used in conjunction with an FF, where flue gas must pass through a collected layer of sorbent, than in other particulate collectors, such as ESPs where in-flight capture is more critical. Some plants are installing FFs downstream of an existing ESP, a configuration developed by EPRI (Electric Power Research

Institute) called *TOXECON*[™] to provide higher efficiency mercury control and particulate trim.

18.3.1.1 Flue Gas Characteristics: Halogens and SO₃

URS Group, University of North Dakota Energy & Environmental Research Center (UNDEERC), and others have studied the effect of hydrogen chloride (HCl) and sulfur in the flue gas on the adsorption capacity of fly ash and AC for mercury in laboratory studies (see, for example, Refs [2, 3] as well as Chapter 25). In general, results from laboratory studies suggest that

- HCl and sulfuric acid (H₂SO₄) accumulate on the surface of carbon.
- HCl increases the mercury removal effectiveness of AC and fly ash for mercury, particularly as the flue gas HCl concentration increases from 1 to nominally 10 ppmv. The relative enhancement in mercury removal performance is not as great above 10 ppmv HCl. In the absence of HCl, the ability of carbon to remove elemental mercury is minimal. Other strong Brønsted acids such as the hydrogen halides HCl, HBr, or HI should have a similar effect. Halogens such as Cl₂ and Br₂ should also be effective in enhancing mercury removal effectiveness, but this may be a result of the halogens reacting directly with mercury rather than the halides promoting the effectiveness of the AC.
- Sulfur dioxide (SO₂) reduces the equilibrium capacity of AC and fly ash for mercury. AC catalyzes the oxidation of SO₂ on the surface of the carbon. Because the concentration of SO₂ is much higher than that of mercury in flue gas, the overall adsorption capacity is likely dependent on the SO₂ concentration in the gas as it forms H₂SO₄ on the surface of the carbon. Thus, the capacity of AC for mercury is higher in flue gas with lower concentrations of SO₂ in the flue gas.

When coal is combusted, mercury contained in the coal is volatilized. In the absence of halogens, the resulting vapor-phase mercury will be present primarily in the elemental form. If sufficient halogen is present in the coal, some of the mercury will react with the available halogen and form oxidized mercury. The fraction of oxidized mercury in the gas will be influenced by several factors including the presence of unburned carbon, whether the plant is configured with a selective catalytic reduction system (SCR) for NO_x control, the temperature of the gas where the mercury is measured, and the time–temperature history of the mercury.

Variations in the mercury control effectiveness of injected AC at different plants will be influenced by the speciation of the mercury and variations in the SO₂ and HCl in the flue gases. In 2001, AC-sorbent-based mercury control technology was first applied to full-scale plants burning PRB coals [4]. As noted, PRB fuel typically has very low-halogen content. With ACI, mercury removal for units configured with ESPs was generally limited to roughly 70%. This limitation likely represented the point where available HCl was removed from the gas stream by injected carbon. Excess carbon did not result in additional removal because insufficient HCl was available to promote oxidation and chemisorption of the remaining elemental mercury in the flue gas.

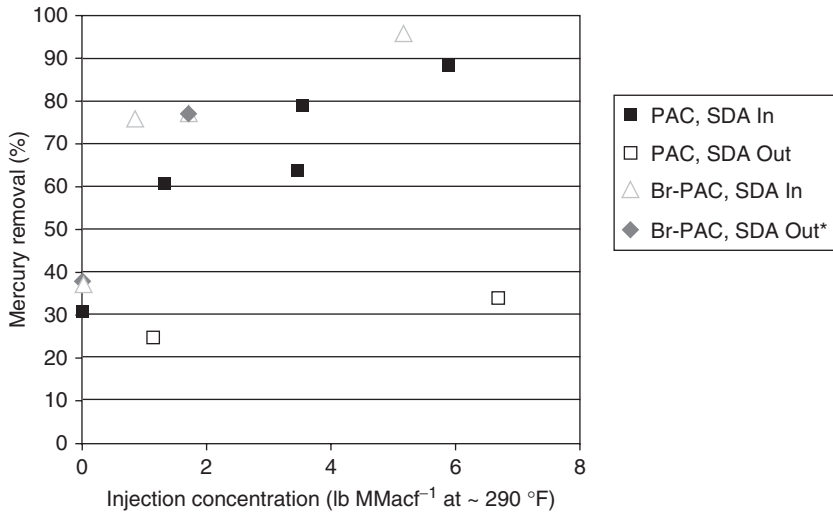


Figure 18.3 Results of injection location tests, Holcomb Station [5] (1 lb MMacf⁻¹ = 16 mg m⁻³).

Results from sites firing PRB and North Dakota lignite coals (low sulfur, low chlorine) configured with a spray dryer absorber (SDA) and an FF also indicate the importance of halogens for capturing elemental mercury using AC. In a typical SDA, slurry of lime is atomized to react with and control emissions of SO₂ and other acid gases. SDAs are very effective in removing HCl. In 2002, tests were conducted at Sunflower Electric's Holcomb Station [5]. The HCl measured at the inlet to the SDA was 0.13–0.61 ppmv. Results from ACI testing at Holcomb is shown in Figure 18.3. During the test, when PAC (DARCO[®]-Hg) was injected upstream of the Holcomb SDA, the mercury removal was much lower than would have been expected on a site without an SDA. An injection concentration of 91.2 g per actual cubic meter (5.7 lb MMacf⁻¹) was required to achieve 90% mercury removal. It is likely that the PAC did not fully react with the HCl between the PAC injection location and the SDA inlet before the remaining HCl was removed from the flue gas in the SDA. When PAC was injected downstream of the SDA, the mercury removal suffered further. The mercury removal was limited to <35% at injection concentrations up to 5.7 lb MMacf⁻¹, compared to 90% mercury removal at the inlet location. Most of the HCl was removed in the SDA and was not available to support mercury removal at the SDA outlet injection location [5–7].

On the basis of some of the studies conducted in the early 2000s, PAC vendors developed AC sorbents treated with halogens, typically bromine, to improve mercury control in low-halogen environments. Chapter 20 discusses brominated PAC in more detail. A PAC treated with bromine, DARCO Hg-LH (Norit Americas), was also tested at Holcomb. More than 90% mercury removal was achieved

1) 1 lb/10⁶ ft³ = 16 mg m⁻³; sorbent loading is typically measured per “actual” volume at the temperature of the particulate control device and is usually denoted as lb MMacf⁻¹.

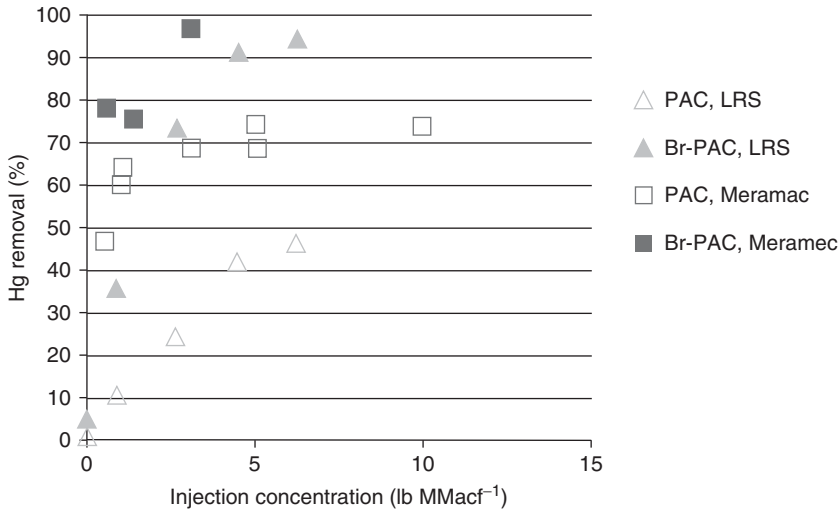


Figure 18.4 Comparison of PAC treated with bromine to nontreated PAC at two PRB-fired sites [8] ($1 \text{ lb MMacf}^{-1} = 16 \text{ mg m}^{-3}$).

at bromine-treated PAC concentrations $<2 \text{ lb MMacf}^{-1}$ and there was no difference in the performance of the bromine-treated PAC whether injected upstream or downstream of the SDA. These data are also included in Figure 18.3 [5].

Results from tests conducted with ACI at Ameren's Meramec Station and Basin Electric's Laramie River Station (LRS) are presented in Figure 18.4 [8]. Both Meramec and LRS were firing PRB coal during the testing period when both PAC treated with bromine-treated and nontreated PAC was tested. The results indicate that the mercury removal improved dramatically with the treated sorbent. At present, bromine-treated PAC is the standard sorbent for sites firing low-halogen coals. As an alternative, some sites treat the coal with halogens to improve the effectiveness of both unburned carbon and PAC.

Full-scale field tests indicate that standard AC is less efficient in high-sulfur environments. ACI tests were conducted at the University of Illinois' Abbott Power Plant in Champaign, IL in 2001 [9, 10]. This site fires high-sulfur (3.8%) bituminous coal with $2500 \mu\text{g g}^{-1}$ chlorine. Equilibrium adsorption capacity measurements were conducted on non-bromine-treated PAC samples at this site at temperatures of 191°C (375°F) and 163°C (325°F). The equilibrium adsorption capacity is measured by flowing flue gas through a fixed bed of PAC, typically mixed with sand to manage the pressure drop through the bed of powder, until the mercury at the inlet to the bed is equal to the outlet, or full breakthrough has been achieved. The equilibrium capacity is calculated as the mass of mercury in the bed to the mass of carbon. The value is often normalized to a mercury concentration in the gas of $50 \mu\text{g m}^{-3}$ by assuming a linear correlation between capacity and flue gas mercury concentration (i.e., the capacity at $50 \mu\text{g m}^{-3}$ is five times the capacity at $10 \mu\text{g m}^{-3}$). At 191°C (375°F), the equilibrium adsorption

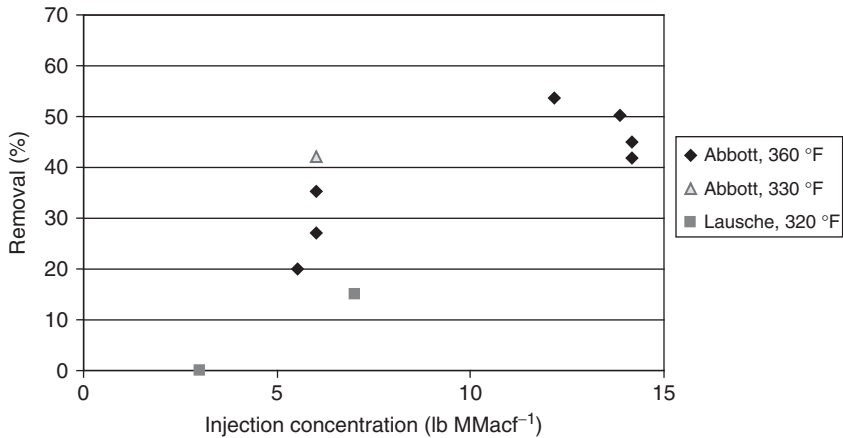


Figure 18.5 Injection test results from Abbott and Lausche Power Plants [9] (1 lb MMacf⁻¹ = 16 mg m⁻³).

capacity was 184 $\mu\text{g g}^{-1}$. At 163 °C (325 °F), the equilibrium adsorption capacity was 486 $\mu\text{g g}^{-1}$. Injection tests were conducted at Abbott at two flue gas temperatures: 182 °C (360 °F) and 166 °C (330 °F), and the results suggest a slight increase in the mercury removal performance of non-bromine-treated PAC at the lower temperature. Injection tests were also conducted at the Lausche plant of Ohio University (1000 ppmv SO₂ and 20 ppmv SO₃ in flue gas). Test results from both Abbott and Lausche, shown in Figure 18.5, indicate limited mercury removal performance of non-bromine-treated PAC.

Plants firing low-sulfur fuel may also face mercury control challenges from impacts related to sulfur compounds. For example, SO₃ is used to “condition” the flue gas to improve particulate capture in ESPs. This poses a unique problem because, across the United States, ~25 GW of power is produced by units that fire PRB and low-sulfur bituminous coals and that inject SO₃ to improve ESP performance. Many low-sulfur-fueled sites are also installing SCRs to control NO_x. The SCRs convert a portion of the flue gas SO₂ to SO₃. Low-conversion catalysts are available, but are typically more expensive and are often not considered necessary on low-sulfur applications unless mercury control is a consideration.

We Energies’ Pleasant Prairie Power Plant (P4) utilizes SO₃ for flue gas conditioning. Equilibrium adsorption capacity measurements were made at locations upstream and downstream of SO₃ injection [6]. These data indicate a significant impact on the mercury capacity of non-bromine-treated PAC due to both SO₃ and temperature. However, when the PAC was injected into the duct, no difference in performance was noted. In addition, decreasing the temperature at P4 using spray cooling from 149 °C (300 °F) to 121 °C (250 °F) did not improve the mercury removal measured across the ESP when injecting non-bromine-treated PAC for mercury control. This suggests that the threshold capacity, or the capacity at which a change in performance is expected during injection testing, was <425 $\mu\text{g g}^{-1}$ at P4, the equilibrium adsorption capacity measured at 149 °C (300 °F) in the

Table 18.1 Equilibrium adsorption capacities measured at two sites with SO₃ present in flue gas [6].

Site	SO ₃	Temperature (°C)	Equilibrium Adsorption Capacity (μg g ⁻¹) Normalized to 50 μg Nm ⁻³
P4	None	121	8823
P4	FGC	121	3355
P4 (PAC + lime ^a)	FGC	121	2091
P4	None	149	880
P4	FGC	149	425
P4 (PAC + lime ^a)	FGC	149	>1504
Abbott	Coal	191	148
Abbott	Coal	163	486

FGC, flue gas conditioner.

a) Lime to sorbent ratio was 60 : 1.

presence of SO₃. The equilibrium data also suggests that the capacity can be significantly improved at higher temperatures (149°C) in the presence of SO₃ if the sorbent is mixed with an alkali material such as lime. No improvement was noted at the lower temperature (121 °C). The P4 and Abbott results are presented in Table 18.1.

Full-scale injection testing conducted at Southern Company's Plant Daniel indicated that, unlike Pleasant Prairie, SO₃ used for flue gas conditioning had a negative impact on sorbent performance [11]. Daniel was firing a low sulfur western bituminous coal during the tests and is configured with an ESP for particulate control.

Results from testing conducted at Ameren's Labadie Power Plant [12] clearly show the impact of SO₃ on the mercury control effectiveness of AC. The mercury removal trends for brominated are summarized for 0, 5.4, and 10.7 ppmv SO₃ (0%, 30%, and 60% setting on SO₃ injection system) in Figure 18.6.

SO₃ levels may also be elevated if a selective catalytic reduction system (SCR) is in service to reduce NO_x and if the catalyst converts sufficient SO₂ to SO₃. Public Service of New Hampshire Merrimack Station is configured with an early-vintage SCR. Although the plant was not firing high-sulfur coal, the SO₂ to SO₃ conversion across the SCR was relatively high, resulting in SO₃ concentrations often above 10 ppmv. During long-term ACI testing [13], trona was injected for SO₃ control through four lances between the SCR and the air preheater (APH) at a rate of 550 lb h⁻¹ with Br-PAC for mercury control at a rate of 5 lb MMacf⁻¹. Under these conditions, 50–55% mercury removal was achieved but could not be sustained because of balance-of-plant impacts. While injecting trona at 550 lb h⁻¹, the APH differential pressure increased 1.2 in. H₂O during the 30 days of injection, indicating deposition of a sodium compound in the APH. These results are shown in Figure 18.7.

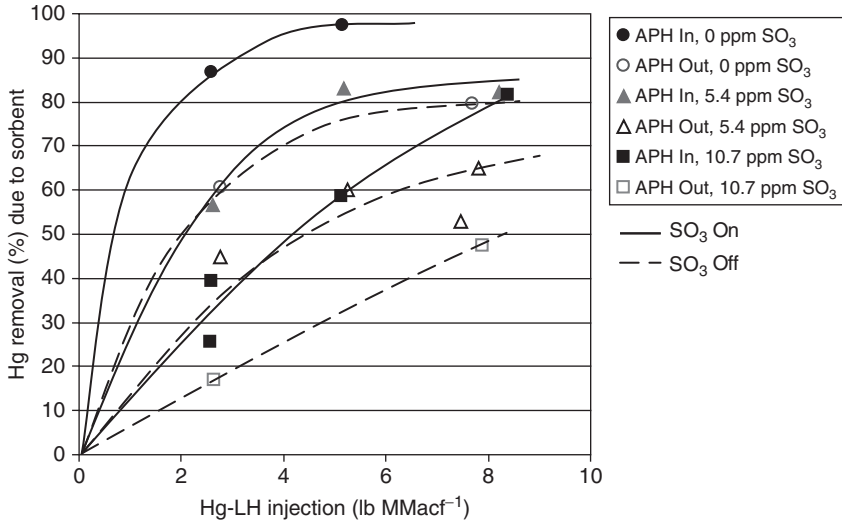


Figure 18.6 Comparison of APH inlet and outlet injection results for Br-PAC [12] (1 lb MMacf⁻¹ = 16 mg m⁻³).

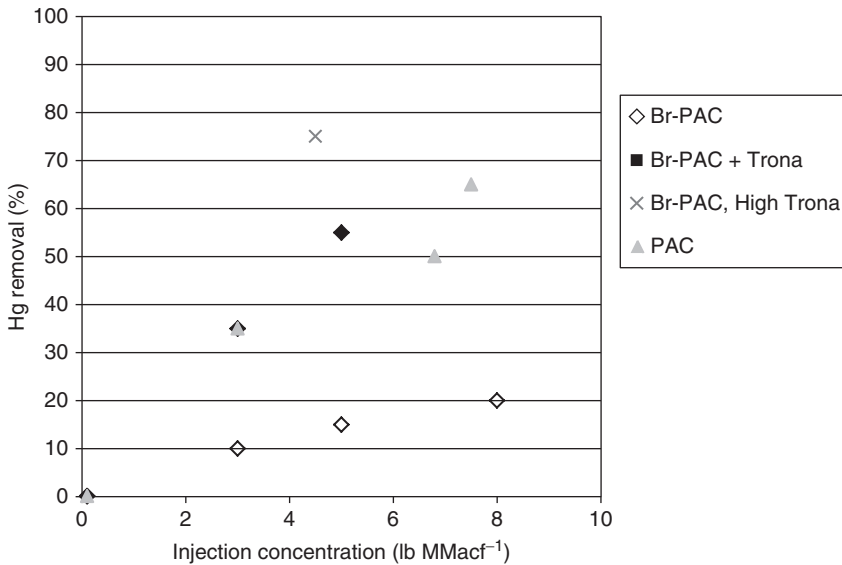


Figure 18.7 Merrimack test results [13] (1 lb MMacf⁻¹ = 16 mg m⁻³).

During a 3-day test, the trona injection rate was increased to 1000 lb h⁻¹ to assess the ability to improve mercury removal by lowering the SO₃ concentration. This resulted in an increase in mercury removal up to 75% at a Br-PAC injection concentration of 4.5 lb MMacf⁻¹. These short-term results show that optimizing the trona injection lances for better distribution could improve both SO₃ and

mercury removal, but the data are insufficient to determine long-term balance-of-plant impacts or sustainability.

Techniques to limit the impact of other pollution control devices on PAC effectiveness for mercury control are being developed. For example, chemicals to replace SO_3 for flue gas conditioning are under development and evaluation. For sites firing high-sulfur coal, or when SCR catalysts that convert sufficient SO_2 to SO_3 are in use, the most effective option evaluated to date is lowering the SO_3 concentration using techniques such as trona (sodium sesquicarbonate) or hydrated lime injection. As a result of decreased SO_3 levels, the mercury removal can be significantly increased. Unfortunately, the introduction of trona at some sites has also resulted in other balance-of-plant issues such as an increase in the pressure drop across the APH [13].

18.3.1.2 TOXECON™

The first commercial operation of a mercury-specific control system to the power industry was a TOXECON system installed at the We Energies' Presque Isle Power Plant in Marquette, Michigan [14]. This was as part of a DOE (Department of Energy) Clean Coal Program and significant tests were conducted to characterize performance. Typical of many first installations of emission control technology, some operating problems were encountered during startup. The Presque Isle system achieved 90% mercury control levels for more than a year of continuous operation during the testing program. The operating procedures developed are being implemented with all of the new TOXECON systems being installed.

18.3.2

PAC-Specific Factors

Although ACI is a viable commercial process, technology developers continue to evaluate options to reduce costs and increase removal levels. For example, results from modeling and full-scale ACI tests indicate that reducing the PAC particle size can result in significant improvements in PAC effectiveness. For example, reducing the PAC diameter by a factor of 2 will result in an increase in the particle density of 8 (2^3), and double the available surface area. In 1999, Meserole [15] developed a model for mercury removal with sorbent injection, and the beneficial impact of reduced particle size, given sufficient sorbent capacity, was reported.

PAC milled from a mean diameter of nominally 18–6 μm was evaluated at Ameren's Labadie Station. The milled PAC resulted in a reduction in PAC requirements of more than 50% at a constant mercury reduction percentage, as shown in Figure 18.8 [16].

Most PAC injection systems are designed to feed standard PAC, which typically has a mean diameter between 15 and 25 μm . Fine material has different handling characteristics and may result in ACI system reliability issues. Fine PAC may also reaggregate, especially if it is stored in the silo for prolonged periods.

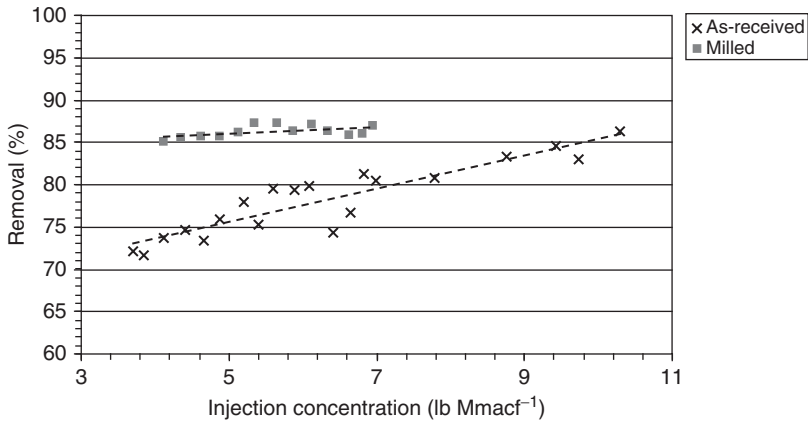


Figure 18.8 Improved mercury control using fine PAC [15] (1 lb MMacf⁻¹ = 16 mg m⁻³).

18.3.3

ACI System Design-Specific Factors

18.3.3.1 Injection Location

Injection location can make a significant difference in the residence time of the PAC in the gas stream, and improve the likelihood of good distribution. For some configurations, the biggest improvement in performance can be attained by moving the injection location from downstream of the APH, where the flue gas temperature is typically between 121 and 205 °C (250 and 400 °F), to upstream of the APH, where temperatures are typically 400–315 °C (750–600 °F). An example of improved mercury removal with PAC injection upstream of the APH is shown in Figure 18.9 [12]. In this case, higher mercury removal was achieved at half the injection rate when injected upstream of the APH. Note that although the *x*-axis presents the data as pound per million actual cubic feet, the actual flue gas volume for the calculation was at the APH downstream temperature in both cases. Although the effectiveness of a carbon for mercury degrades quickly as the temperature increases, injecting PAC upstream of the APH often results in overall improvements in PAC removal effectiveness. This effect is a result of several influences including increased residence time, which can promote both better distribution of the PAC in the duct, reactions between flue gas halogens and PAC, and increased time for reaction as the PAC moves through the APH.

18.3.3.2 Distribution

Either physical flow or computational fluid dynamics (CFD) modeling can be used to predict whether an injection grid is capable of getting PAC into all of the flue gas passages. Flue gas flow and temperature biases are often present. These can develop as a result of boiler design, duct structural members such as turning vanes, or for many plants that use rotary APHs, the rotation of the APH can

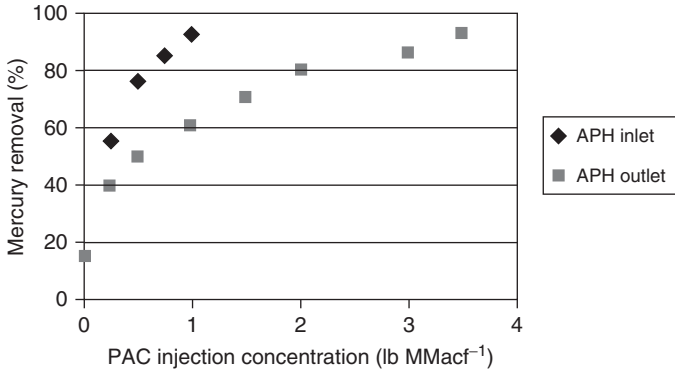


Figure 18.9 Mercury removal when AC was injected upstream and downstream of APH [11] ($1 \text{ lb MMacf}^{-1} = 16 \text{ mg m}^{-3}$).

cause temperature nonhomogeneity. CFD modeling can assist in determining whether additional lances are needed or if PAC injection should be biased into select lances to assure good distribution before the particulate collection device.

Caution should be exercised when designing PAC injection lances to assure that incremental improvements in short-term PAC distribution resulting from complex lance designs do not overshadow long-term maintenance and reliability concerns. Complicated lances, such as those with multiple injection nozzles, may provide enhanced distribution initially, but coal-combustion flue gas is not a forgiving environment. Nozzles can quickly become plugged, resulting in decreased overall distribution compared to simpler, more robust designs.

18.4

Balance-of-Plant Impacts

18.4.1

Coal Combustion By-Products

Fly ash has been used as a replacement for Portland cement in concrete since the 1920s when it was used in the construction of the Hoover Dam, then the largest concrete structure in the world. Air entrained in the concrete matrix improves the durability of the concrete over freeze–thaw cycles. In 2006, more than 72 million tons of fly ash were produced in the United States, 46% of which was used in concrete, concrete products, and grout, with another 6% used to make cement [17]. The remainder was placed in landfills or used in other applications. Fly ash landfilling costs are significant and can become one of the largest operating costs for plants after labor and fuel [18].

Air entrained in the concrete matrix improves the durability of the concrete over freeze/thaw cycles. Air-entraining agents are typically soaplike organic additives.

PAC in fly ash absorbs the organic air-entraining additives and can change the fly ash from a saleable product to a potential landfill liability.

Options to preserve ash sales while using ACI for mercury control include separating the PAC-laden ash from the bulk of the fly ash by using EPRI-patented techniques such as TOXECON, reducing the amount of PAC required through techniques such as using fine PAC, or use of a specialized ash-compatible AC. Chapter 21 discusses concrete-compatible carbons in more detail.

18.4.1.1 Autoignition of PAC in Ash Hoppers

There have been several reports of burning embers in baghouse and ESP ash hoppers collecting ash/PAC mixtures that have relatively high ratios of PAC to ash, such as TOXECON configurations where the majority of ash is removed before injecting PAC into the system [14, 19]. PAC is a relatively good insulator. If a hopper full of PAC is exposed to a localized heat source, such as a hopper heater or a welding spark, it can begin to smolder. PAC can also be oxidized via exothermic reactions in an air- or oxygen-rich environment. When the heat of oxidation increases faster than it can be liberated, temperatures increase, and can ignite the carbon.

Key factors contributing to autoignition are size of the bed or amount of ash/PAC in the hopper, temperature surrounding the bed from hopper heaters or high flue gas temperatures, concentration of carbon in the ash, and oxygen concentration.

Plants where autoignition has occurred have implemented maintenance procedures to prevent future occurrences of autoignition. Successful maintenance procedures include the following:

- Eliminate use of hopper heaters or lower the set point.
- Empty hoppers more frequently to minimize ash in the hopper.
- Ensure complete emptying of ash hoppers because AC becomes sticky when hot.
- Minimize fluidization.

Laboratory oven tests were conducted on different size square containers filled with PAC/ash mixtures collected in the hoppers of the TOXECON baghouse during PAC injection at Presque Isle. Thermocouples were placed in the oven and inserted into the bed of material at different levels to track temperature profiles over time. These tests confirmed that although the ignition temperature of the PAC was 850 °F, sufficient heat was internally generated at 430 °F for the PAC to increase the temperature of the mixture to ignition temperatures.

18.4.1.2 Impacts on Particulate Emissions

PAC is typically injected into flue gas at a rate that typically does not exceed 5% of the fly ash loading, and is often nearer to 1%, except for polishing applications such as TOXECON. There have been few reports of PAC injection negatively impacting particulate emissions [20], and some have reported that Br-PAC injection can improve the operation of the installed ESP [21].

18.4.1.3 Corrosion Issues

Injecting AC for mercury control is not expected to have adverse impacts on corrosion within the ductwork. However, when halogen-treated ACs are used, there is a possibility of inducing corrosion. Recent bench-scale corrosion tests have shown that bromine is capable of accelerating corrosion on metal surfaces [22]. Further investigations into long-term impacts of continuous halogen-treated ACI are under way.

18.5

Future Considerations

Advancements continue to be made in mercury control to assure compliance and minimize costs. PAC vendors are developing materials that are more effective, more tolerant to SO₃ and temperature, less corrosive, and concrete compatible. Equipment providers are required to provide equipment that can assure near-continuous reliability. Integrated solutions that incorporate multiple technologies such as coal additives to provide supplemental halogen, reagents to reduce the SO₃ concentration, catalysts to increase the fraction of oxidized mercury, and chemicals to improve the co-benefit mercury removal in SO₂ scrubbers are being refined. On the basis of its simplicity and cost, ACI will continue to be an important component of the installed mercury control technology base for the US coal-fired fleet.

References

1. Senior, C.L., Bustard, C.J., Durham, M.D., and Baldrey, K. (2004) Characterization of fly ash from full-scale demonstration of sorbent injection for mercury control on coal-fired power plants. *Fuel Process. Technol.*, **85**, 601–612.
2. Canadian Electricity Association (CEA) (2005) Mercury Information Clearinghouse, Quarter 5 –Mercury Fundamentals, January 2005.
3. Carey, T.C., Hargrove, O.W., Richardson, C.F., Chang, R., and Meserole, F.B. (1998) Factors affecting mercury control in utility flue gas using activated carbon. *J. Air Waste Manage. Assoc.*, **48**, 1166–1174.
4. Durham, M., Bustard, J., Starns, T., Martin, C., Schlager, R., Lindsey, C., Baldrey, K., and Afonso, R. (2002) Full-scale evaluations of sorbent injection for mercury control on power plants burning bituminous and subbituminous coals. Presented at Power-Gen 2002, Orlando, FL, December 10–12, 2002.
5. Sjostrom, S., Starns, T., Wilson, C., Amrhein, J., Durham, M., Bustard, J., Chang, R., and O'Palko, A. (2005) Full-scale evaluations of mercury control for units firing powder river basin coals. Proceedings of the Air Quality V Conference, Arlington, VA, September 19-21, 2005.
6. Bustard, J., Durham, M., Lindsey, C., Starns, T., Martin, C., Schlager, R., Sjostrom, S., Renninger, R., McMahon, T., Monroe, L., Goodman, J. M., and Miller, R. (2003) Results of activated carbon injection for mercury control upstream of a COHPAC fabric filter. Proceedings of DOE-EPRI-U.S. EPA -A&WMA Combined Power Plant Air Pollutant Control Symposium – The Mega Symposium, Washington, DC, May 19–22, 2003.

7. Machalek, T., Richardson, C., Dombrowski, K., Ley, T., Ebner, T., Fisher, K., Brickett, L., Chang, R., Strohfus, M., Smokey, S., and Sjostrom, S. (2004) Full-scale activated carbon injection for mercury control in flue gas derived from north dakota lignite. Proceedings of DOE-EPRI-U.S. EPA -A&WMA Combined Power Plant Air Pollutant Control Symposium – The Mega Symposium, Washington, DC, August 29 – September 2, 2004.
8. Sjostrom, S., Starns, T., Wilson, C., Amrhein, J., Durham, M., Bustard, J., O’Palko, A., and Chang, R. (2005) Full-scale evaluations of mercury control for units firing powder river basin coals. Proceedings of the Air Quality V Conference, Arlington, VA, September 19–21, 2005.
9. Sjostrom, S., Ebner, T., Ley, T., Slye, R., and Chang, R. (2002) Evaluation and comparison of novel, low-cost sorbents for mercury control. Proceedings of the Nineteenth Annual International Pittsburgh Coal Conference, Pittsburgh, PA, September 23–27, 2002.
10. Nelson, S., Landreth, R., Zhou, Q., and Miller, J. (2004) Accumulated power-plant mercury-removal experience with brominated PAC injection. Proceedings of DOE-EPRI-U.S. EPA -A&WMA Combined Power Plant Air Pollutant Control Symposium – The Mega Symposium, Washington, DC, August 29 – September 2, 2004.
11. Berry, M., Richardson, C., Dombrowski, K., Chapman, D., Chang, R., Monroe, L., Glessman, S., Campbell, T., and McBee, K. (2005) Full-scale evaluation of activated carbon injection. Proceedings of the Air Quality V Conference, Arlington, VA, September 19–21, 2005.
12. Sjostrom, S., Dillon, M., Donnelly, B., Bustard, J., Filippelli, G., Glesmann, R., Orscheln, T., Wahlert, S., Chang, R., and O’Palko, A. (2007) Influence of SO₃ on mercury removal with activated carbon: full-scale results. Proceedings of the Air Quality VI Conference, Arlington, VA, September 24–26, 2007.
13. Campbell, T., Sjostrom, S., Dillon, M., Brignac, P., O’Palko, A., Chang, R., Raichle, P., Auclair, A., and Keyes, H. (2008) Mercury control with activated carbon: results from plants with high SO₃. Proceedings of DOE-EPRI-U.S. EPA -A&WMA Combined Power Plant Air Pollutant Control Symposium – The Mega Symposium, Baltimore, MD, August 25–28, 2008.
14. Derenne, S., Sartorelli, P., Stewart, R., Bustard, J., Sjostrom, S., Johnson, P., McMillian, M., Sudhoff, F., and Chang, R. (2008) TOXECON™ demonstration for mercury and multi-pollutant control at we energies. In Proceedings of DOE-EPRI-U.S. EPA -A&WMA Combined Power Plant Air Pollutant Control Symposium – The Mega Symposium, Baltimore, MD, August 25–28, 2008.
15. Meserole, F., Chang, R., Carey, T., Machac, J., and Richardson, C. (1999) Modeling mercury removal by sorbent injection. *J. Air Waste Manage. Assoc.*, **49**, 694–704.
16. Sjostrom, S., Campbell, T., Dillon, M., Hantz, J., O’Palko, A., and Chang, R. (2008) TOXECON II™ and other options for preserving ash sales. Proceedings of DOE-EPRI-U.S. EPA -A&WMA Combined Power Plant Air Pollutant Control Symposium – The Mega Symposium, Baltimore, MD, August 25–28, 2008.
17. ACAA (2006) CCP Production and Use Survey, August 24, 2007, [http://www.acao-usa.org/associations/8003/files/2006_CCP_Survey\(Final-8-24-07\).pdf](http://www.acao-usa.org/associations/8003/files/2006_CCP_Survey(Final-8-24-07).pdf) (accessed July 2008).
18. Wen, H. (2008) High Carbon Fly Ash Finds Uses in Highway Construction. *Ash at Work*, Issue 2. Recycled Materials Resource Center, University of Wisconsin at Madison & Robert Patton, National Energy Technology Laboratory, Department of Energy.
19. Pavlish, J.H., Thompson, J.S., Martin, C.L., Musich, M.A., and Hamre, L.L. (2008) Field Testing of Activated Carbon Injection Options for Mercury Control at TXU’s Big Brown Station. Final Report, Cooperative Agreement No. DE-FC26-05NT42305, EERC for the National Energy Technology Laboratory, Department of Energy, April 2008.

20. Chang, R., Dombrowski, K., and Senior, C. (2008) Near and long term options for controlling mercury emissions from power plants. Proceedings of DOE-EPRI-U.S. EPA -A&WMA Combined Power Plant Air Pollutant Control Symposium – The Mega Symposium, Baltimore, MD, August 25-28, 2008.
21. Nelson, S., Jr., Landreth, R., Liu, X., Tang, Z., and Miller, J. (2007) brominated sorbents for small cold-side ESPs, hot-side ESPs, and fly ash use in concrete. Presented at DOE/NET's 2007 Mercury Control Technology Conference, Pittsburgh, PA, December 11-13, 2007.
22. Zhuang, Y., Chen, C., Timpe, R., and Pavlish, J. (2009) Investigations on bromine corrosion associated with mercury control technologies in coal flue gas. *Fuel*, **88** (9), 1692–1697.

19 Halogenated Carbon Sorbents

Robert Nebergall

19.1

Introduction

Activated carbon has been shown over the past several decades to be an effective adsorbent for the removal of mercury from flue gas. The technology was developed in Europe during the late 1980s where municipal waste combustion was a large contributor of anthropogenic (human produced) mercury emissions to the environment. In addition, hazardous waste and medical waste incinerators are also large contributors of mercury emissions to the environment [1]. Municipal, medical, and hazardous wastes typically contain sources of chlorine and hence form chlorine compounds in the flue gas. The chlorine compounds present in the flue gas provide an excellent oxidant in the gas stream for the conversion to oxidized mercury. Standard or untreated activated carbons only effectively remove oxidized mercury from the flue gas. The mercury concentration in the flue gas in these applications was typically relatively high. Owing to the prevalence of mercury in municipal waste and hazardous waste, concentrations of mercury $>200 \mu\text{g m}^{-3}$ of flue gas were not uncommon. Activated carbon treatment dosages of 3–6 pounds per million actual cubic feet (lb/MMacf)¹⁾ or $30\text{--}60 \text{ mg m}^{-3}$ of flue gas were also common [2].

19.2

Application of Activated Carbon for Mercury Control

When injecting activated carbon for mercury control, the mercury capture occurs in the particulate collection device. The two most common particulate collection devices installed at coal fired power plants are an electrostatic precipitator (ESP) and a fabric filter.

1) $1 \text{ lb}/10^6 \text{ ft}^3 = 16 \text{ mg m}^{-3}$; sorbent loading is typically measured per “actual” volume at the temperature of the particulate control device and is usually denoted as lb/MMacf.

ESPs electrically charge the ash and powdered activated carbon (PAC) particles in the flue gas to collect and remove them [3]. The unit comprises a series of parallel vertical plates through which the flue gas passes. Centered between the plates are charging electrodes that provide the electric field. The collecting plates are typically electrically grounded and are the positive electrode components. The discharge electrodes in the flue-gas stream are connected to a high-voltage power source (typically 55–75 kV DC) with a negative polarity. An electric field is established between the discharge electrodes and the collecting surface. As the flue gas passes through the electric field, the particulate takes on a negative charge, which, depending on particle size, is accomplished by field charging or diffusion.

Dust that has accumulated to a certain thickness on the collection electrode is removed by one of two processes, depending on the type of collection electrode. Collection electrodes in precipitators can be either plates or tubes, with plates being more common. Tubes are usually cleaned by water sprays, while plates can be cleaned either by water sprays or a process called *rapping*. Rapping is a process whereby deposited, dry particles are dislodged from the collection plates by sending mechanical impulses, or vibrations, to the plates. Precipitator plates are rapped periodically while maintaining the continuous flue-gas cleaning process. In other words, the plates are rapped while the ESP is online; the gas flow continues through the precipitator and the applied voltage remains constant. Plates are rapped when the accumulated dust layer is relatively thick (0.03–0.50 in.). This allows the dust layer to fall off the plates as large aggregate sheets and helps eliminate dust re-entrainment.

A fabric filter collects the dry particulate matter and PAC as the cooled gas passes through the filter material [4]. The fabric filter is comprised of a multiple-compartment enclosure, with each compartment containing up to several hundred long vertically supported, small-diameter fabric bags. The gas passes through the porous bag material, which separates the particulate and PAC from the flue gas.

With the typical coal-fired boiler, the PAC-laden flue gas enters the filter inlet plenum, which in turn distributes the gas to each of the compartments for cleaning. An outlet plenum collects the cleaned flue gas from each compartment and directs it toward the induced draft fan and stack. Each compartment has a hopper for particulate and PAC collection. The individual bags are closed at one end and connected to a tube sheet at the other end to permit the gas to pass through the bag assembly. The layer of dust and PAC accumulating on the bag is referred to as the *cake*. As the cake builds and the flue-gas pressure drop across the fabric filter increases, the bags must be cleaned. This occurs after a predetermined operating period or when the pressure drop hits a set point. Each compartment is sequentially cleaned to remove the excess cake and to reduce pressure drop. A residual cake coating is preferred to enhance further collection. Owing to the longer contact time when employing fabric filters, the dosage is up to 75% less than that needed for ESPs.

Table 19.1 Key coal properties [6].

Coal rank	Dry basis	Hg ($\mu\text{g g}^{-1}$)	Cl ($\mu\text{g g}^{-1}$)	S (wt%)	Ash (wt%)	Higher heating value, HHV (MJ kg^{-1})
Bituminous	Average	0.11	1033	1.69	11.10	31
	Range	0.04–0.28	48–2730	0.55–4.1	5.4–27.3	20.11–32.60
Subbituminous	Average	0.07	158	0.50	8.00	28
	Range	0.02–0.14	51–1143	0.22–1.16	4.7–26.7	20.02–20.63
Lignite	Average	>0.11	188	1.30	19.40	23
	Range	—	133–233	0.8–1.42	12.2–24.6	22.07–24.89

19.3

Development of Halogenated Activated Carbon

19.3.1

Motivation

In the United States, the federal Clean Air Mercury Rule (CAMR) was vacated by a Federal Court in February 2008, and a new federal standard for regulation of mercury emissions from power plants (the Mercury and Air Toxics Standards or MATS) has just been finalized. The MATS will not go into effect until 2015, at the earliest; however, as of 2011, 16 states had their own mercury emission regulations [5]. Before the vacatur of CAMR there was a need for the development of mercury control technologies from coal-derived flue-gas streams, and a new challenge for activated carbon. Low-rank coal fuels, including lignite and subbituminous fuels, typically have very low halogen content. As a result, mercury present in the flue gas from low-rank coal combustion is mostly elemental mercury, which provides a challenge for the standard activated carbons.

As discussed in Chapter 2, coal is ranked by age and key characteristics (calorific value, volatile matter, and carbon content). The three main coal ranks, lowest to highest, that power plants in the United States utilize as fuel are lignite, subbituminous, and bituminous. Each of these ranks contains subgroups that provide further differentiation of the key characteristics. Table 19.1 summarizes coal properties by rank relevant to mercury control in coal-fired boilers.

The relationship of coal rank to chlorine content is not easily explained and there are several factors involved over the lifetime of the formation of the coal. In the United States, bituminous coals have higher chlorine content by weight than lower rank coals,²⁾ with lignite having the least amount of chlorine content by weight.

2) The exception is that beginning with the higher ranked bituminous coals (low volatile and medium volatile), a decrease in chlorine content is seen because of the decreasing sorption capacity of the highly carbonized coal organic matter [17].

Leading up to the 2005 CAMR, much test work was completed in coal-fired power plants with support from the National Energy Technology Laboratory (NETL) division of the Department of Energy (DOE), as discussed in Chapter 10. It was demonstrated early in the plant testing programs that standard activated carbons had limited mercury removal capabilities in flue-gas streams from combustion of low-rank coal fuels. In all, the DOE NETL funded over 40 full-scale field tests for mercury removal with various APCDs (air pollution control devices) [7].

The DOE-sponsored testing program at Pleasant Prairie Power Plant in the early 2000s showed a distinct limitation of standard activated carbons for mercury emission control with Powder River Basin (PRB) subbituminous fuels [8]. Certain levels of mercury removal were possible, but reaching 80% or 90% removal was not achieved with standard PAC. Reduction curves demonstrating diminishing return on additional carbon dosage were developed from that work.

Similar results were achieved at Stanton Station in the same time period on lignite fuel [8, 9]. It was determined that the low halogen level in the low-rank coals was responsible for the low level of oxidized mercury in the flue gas, which prevented effective removal of mercury from the flue-gas stream with PAC.

In the Sunflower Electric testing of 2005 at Holcomb Station, this concept (elemental vs oxidized mercury) was tested at a facility that burned a PRB subbituminous coal and had a pollution control train including a spray dryer absorber and a fabric filter [10]. In this trial, 90% mercury removal efficiency was achieved at ~6 lb of untreated activated carbon injection per million actual cubic feet (MMacf) of gas flow. Correspondingly, 90% removal efficiency was achieved at just over 1 lb MMacf⁻¹ of an experimental halogenated activated carbon.

This step forward in technology was later duplicated at Meramec Station near St. Louis, Missouri, in a demonstration that also used a PRB coal fuel [10]. This site had an ESP and also an unusually high level of unburned carbon in the fly ash. Mercury removal levels of 90% were achieved at 3 lb MMacf⁻¹ activated carbon injection rate with a halogenated activated carbon. When standard activated carbon (not halogenated) was tested, mercury removal levels did not reach 80%, even at carbon injection rates as high as 15 lb MMacf⁻¹.

Since before the beginning of the DOE field test work, there was a great deal of speculation and research on the mechanism of mercury removal from flue gas when utilizing halogenated and nonhalogenated activated carbon. In general, activated carbon is a highly porous adsorption material with a complex structure composed primarily of carbon atoms (see Chapter 17). The structure consists of graphitic-like sheets of carbon atoms joined together by random cross-linkage. Unlike the orderly stacking of layers of carbon atoms in true graphite, an activate carbon has sheets or groups of atoms that are stacked unevenly and disorganized. This randomized bonding of the graphite sheets creates a highly porous structure with myriad nooks and crannies, cracks, and crevices between carbon layers. It is this molecular-size porosity and resulting enormous internal surface area that makes activated carbon such an effective material for adsorbing mercury. Activated carbon's pore surface is a defect structure with a cloud of unpaired electrons.

It contains an array of chemical functional groups containing oxygen that form active sites where adsorption occurs. It is not unreasonable to visualize an active carbon particle as one enormous carbon molecule. It is capable of reacting with, and bonding to, mercury as well as trapping it within its internal structure by electrostatic attraction.

19.3.2

Manufacture

Activated carbons are manufactured by one of two processes: high-temperature steam activation or chemical activation using a strong dehydrating agent. Steam activation is the most commonly used method for activated carbon production. It is performed in a furnace and consists of the following steps:

- 1) *Drying* – All of the raw materials currently in commercial use contain some residual moisture which must be removed before activation can take place.
- 2) *Devolatilization* – The lighter boiling organics are driven off the carbon raw material. These volatiles have some fuel value and may be used to reduce the overall energy requirements of the process.
- 3) *Charring* – The higher molecular weight organics are reduced to carbonaceous char residue. This char becomes the active carbon product during activation.
- 4) *Activation* – The activation step is generally conducted in a steam atmosphere at temperatures that vary depending on the type of carbon to be produced. Typically, half of the carbonaceous char material entering the activation step will be volatilized during activation to create the desired internal pore structure.

The International Union of Pure and Applied Chemistry IUPAC differentiates carbon pores by size; micropores have diameters <2 nm, mesopore has diameters between 2 and 50 nm, and macropore has diameters >50 nm. The iodine number, bromophenol blue number (BPB), moisture, bulk density, surface area, mesh size as well as bromine concentration are physical properties used to characterize halogenated activated carbon. The iodine number is a relative measure of microporosity. The BPB is a relative measure of range of mesoporosity. The moisture is the weight percent of moisture contained in the activated carbon. The bulk density is defined as the mass of many particles of the material divided by the total volume they occupy. The total volume includes particle volume, interparticle void volume, and internal pore volume. Surface area is the area contained in the particle including pores per gram of the material.

The size of an activated carbon is described by referring to a certain mesh size. By itself, this type of description is somewhat ambiguous. More precise specifications will indicate that a material will pass through some specific mesh (that is, have a maximum size; larger pieces will not fit through this mesh) but will be retained by some specific tighter mesh (that is, a minimum size; pieces smaller than this will have passed through the mesh). This type of description establishes

a range of particle sizes. Bromine percentage is the weight percent of bromine in the activated carbon.

The mechanism by which halogenated activated carbons adsorb elemental mercury is not completely understood at present, and it is a very complex question when considering the differences in activated carbons made from different raw materials and different processes. Chapters 23 and 25 discuss the underlying mechanisms in more detail.

Several different base raw materials including bituminous coal, subbituminous coal, lignite coal, peat, wood, and coconut shells may be used in the production of activated carbon for mercury removal from flue gas. All these raw materials will produce activated carbons with different pore structures, carbon lattices, ash compositions, and internal pore surface functional (oxygen) groups. Furthermore, any individual raw material will also create different surface groups when processed under different activation and cooling conditions.

19.3.3

Performance

It is well known in the industry that halogenation of the activated carbon increases the ability of the activated carbon to adsorb elemental mercury. Figures 19.1 and 19.2 show full-scale data on the removal of mercury across cold-side ESPs (Figure 19.1) and spray dryer plus fabric filter (Figure 19.2). In these figures, Darco Hg is a non-brominated carbon (Norit Americas). The brominated carbons are Darco Hg-LH (Cabot Norit Activated Carbon) and B-PAC (Albemarle).

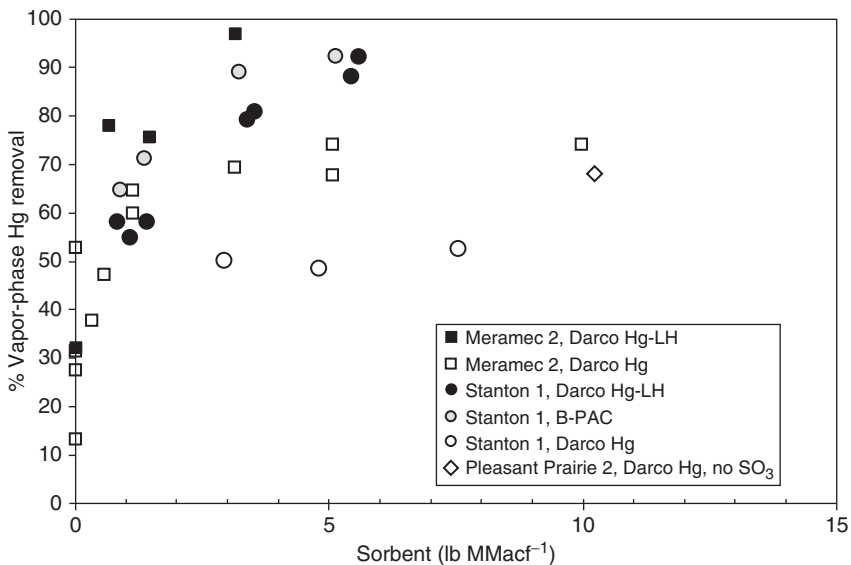


Figure 19.1 Mercury removal across cold-side ESPs at subbituminous-fired boilers; see text for discussion of carbon types [9, 10].

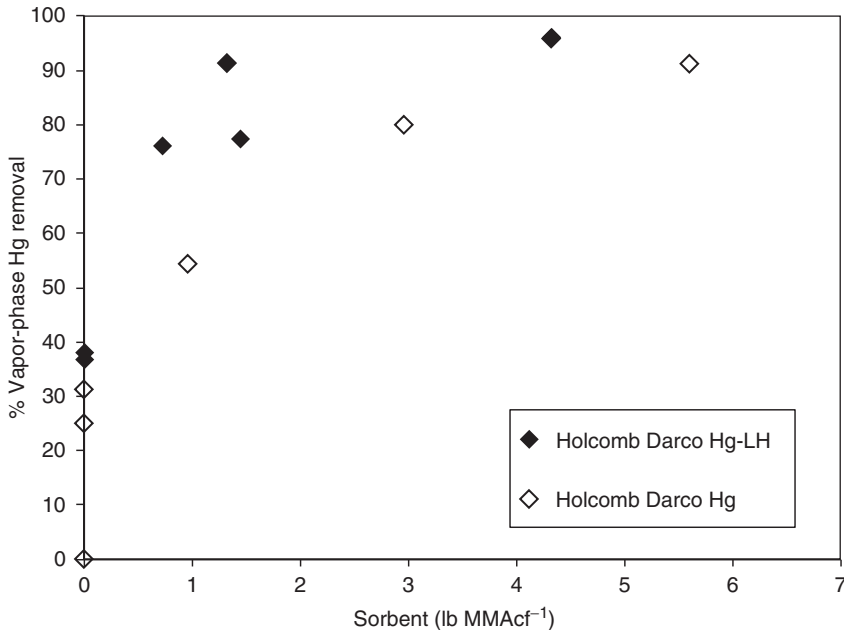


Figure 19.2 Mercury removal across spray dryer–fabric filter at subbituminous-fired boiler; see text for discussion of carbon types [10].

There are different theories as to the actual mechanism principally responsible for the adsorption. Elemental mercury is a highly polarizable atom because of its large number of electrons, which, by theory, should be subject to London dispersion forces [11]. In many activated carbon applications, it is generally believed that van der Waals forces of attraction are part of the mechanism of adsorption. Other theories have their basis in the idea that the surface of the activated carbon effectively acts similar to a Lewis acid through the formation of charge-transfer compounds on the surface of the carbon through halogenations [12].

Studies performed at Energy and Environmental Research Center have examined the effects of flue-gas acid species such as HCl, SO₂, NO, NO₂, on mercury capture as well as mercury binding and oxidation mechanism. In the model they propose, electrons must be accepted by a Lewis acid on activated carbon and then Hg²⁺, which is a Lewis acid that can bind to Lewis base sites on the surface competing with other acidic species. Chapter 25 provides more detail on this work.

To add to the difficulty of surely identifying the mechanism behind elemental mercury adsorption, one must first address what form the halogen has taken while being applied to the activated carbon. In terms of application, information in the public domain indicates two primary methods of application. Halogen salts (primarily chlorine, bromine, and iodine) have been identified as both fuel additives and treatments for activated carbon. Studies have indicated that the larger the atom added to the surface of the activated carbon, the more effective it would be in oxidizing elemental mercury on the surface of the activated carbon. A lesser used

but also effective method of application is gas-phase impregnation of the activated carbon with gaseous bromine compounds. It is unlikely that the halide salt addition is captured on the internal pore surfaces of the activated carbon in a manner identical to that of a gas-phase treatment. According to X-ray studies, it has been shown that adsorbed mercury is indeed bound on the carbon pore surface in an oxidized form [13]. In addition, adsorbed mercury bound on the activated carbon pore surface appears to be located at halogenated sites, according to the other X-ray studies [14].

As one considers the complexity of a power plant fuel mix, boiler configuration, and its APCDs, it becomes apparent that many variables affect the ability of activated carbon to remove mercury from flue gas. As an example, it is commonly known that relatively high concentrations of sulfur trioxide (SO_3) have a substantial and negative impact on the activated carbon's ability to effectively remove mercury.

The presence of high concentrations of sulfur trioxide in the flue gas can be attributed to two main applications. Intuitively, higher sulfur fuels (typically bituminous) create higher sulfur dioxide flue gases, and hence higher sulfur trioxide levels in the flue gas. In addition, if the APCDs include an SCR (selective catalytic reduction), sulfur trioxide levels will typically be higher, because the SCR catalyst oxidizes some fraction of SO_2 to SO_3 (Chapter 15). In some newer coal-fired power plants burning bituminous fuels, levels of 50 ppmv of sulfur trioxide are found in the flue gas [15]. More commonly, bituminous facilities will have sulfur trioxide levels in the range of 10–20 ppmv.

The other situation in which sulfur trioxide becomes an issue is in flue-gas conditioning for ESP performance improvement. Sulfur trioxide is injected into the flue gas to improve ESP particulate collection performance. Sulfur trioxide is injected into the flue gas to improve ESP particulate collection performance typically at a level of 4–10 ppmv of sulfur trioxide. The flue-gas conditioning treatment, as of this writing, is a very common challenge to the implementation of current mercury control programs using activated carbon injection.

The state of Illinois has implemented the most stringent mercury control regulations to date. Many units located in Illinois were designed for burning high-sulfur, Illinois-basin bituminous coal. These coals have high sulfur and moderate ash contents. Subbituminous coals, although lower in ash than eastern bituminous coals, have much less sulfur and the resistivity of the fly ash is higher.

Resistivity is a measure of the particle's ability to transfer charge. Fly ash resistivity is a function of the particle composition and also the conditions in the flue gas: temperature, moisture, and sulfur trioxide concentration. If the resistivity of fly ash is too high, the ESP will not be able to collect it efficiently. The resistivity of fly ash from a low-sulfur coal is generally higher than that from a high-sulfur coal. Switching from a high-sulfur coal to a low-sulfur coal, therefore, can degrade the efficiency of an ESP. Flue-gas conditioning involves injecting a chemical upstream of the ESP; the chemical lowers the resistivity of the fly ash and improves the collection efficiency of the ESP.

Most units are equipped with ESPs, and thus face the challenge of particulate capture efficiency. Many units need to apply flue-gas conditioning to improve their performance, and sulfur trioxide is a common technology used for this enhancement. Although the mechanism for adsorption of sulfur trioxide has not been well studied, as is the case in many gas-phase applications for activated carbon, capillary condensation is thought to be an important mechanism for the removal of condensable constituents from flue gas. As sulfur trioxide molecules accumulate in the pore structure of the activated carbon, the molecules become closer and closer in proximity and are effectively compressed and condense in the pore. This phenomenon has a higher probability of taking place in smaller diameter pores such as micropores. Correspondingly, it is less likely to take place in mesopores or macropores.

In commercial application, halogenated activated carbons show improved resistance to the mechanism contributing to decreased activated carbon efficiency. The mechanism for this improvement is not well understood.

Another flue-gas variable that affects removal efficiency of activated carbon in general is the temperature. As activated carbon adsorption processes are an equilibrium based on the concentration of the contaminant in the stream, higher temperatures tend to favor desorption rather than adsorption. This has been demonstrated in many of the DOE trial programs. Halogenated activated carbons have demonstrated better mercury capture at higher temperatures [16]. It is speculated that the improved resistance is due to imparting higher charge imbalance on the surface of the activated carbon and hence improving the kinetic equilibrium in favor of adsorption.

19.3.4

Balance-of-Plant Impacts

Mention was made earlier in the chapter about the potential halogens that may be used in this process. Chlorine, bromine, and iodine have all been evaluated through the development of halogenated carbons for mercury removal from flue gas and all are used commercially to at least some degree. Owing to both effectiveness (ability to oxidize mercury) and commercial considerations (price, availability, supply chain reliability), most commercial products have been formulated with the use of bromine or bromine compounds as the preferred halogen. Given the great diversity of flue-gas constituency and potential interactions of a strong oxidant within other compounds in the gas, at least some concern needs to be given to the potential reactions to avoid other undesirable side effects. As an example, ammonia slip in excess may react with sulfur trioxide and form ammonium sulfate precipitate on APCD equipment upon cooling. When SCR work first began, this was not an expected outcome, but had material impacts.

All halogens can have the potential of being corrosive if handled improperly or handled in inappropriately designed equipment. For the handling of halogenated activated carbons, the use of high-grade stainless steel is not uncommon,

particularly in the feeder portion of the systems, to ensure that the equipment is not degraded.

Halogenated activated carbons have been a major technological advance for the mercury removal from coal-derived flue gas. Advancements in the efficiency and method of application are ongoing and sure to be followed by step changes to come.

References

1. United Nations Environment Programme (UNEP) (2008) The Global Atmospheric Mercury Assessment: Sources, Emissions and Transport, UNEP, Chemicals Branch, Geneva, December, 2008, pp. 15–26.
2. U.S. EPA Air and Energy Engineering Research Laboratory (1993) Emission Test Report Field Test of Carbon Injection for Mercury control Camden County Municipal Waste Combustor, EPA-600/R-93-181, NTIS, Springfield, VA.
3. Stultz, S.C. and Kitto, J.B., (eds) (1992) *Steam its Generation and Use*, 40th edn, Babcock and Wilcox Company, Barberton, OH, pp. 33-4–33-5.
4. Stultz, S.C. and Kitto, J.B., (eds) (1992) *Steam its Generation and Use*, 40th edn, Babcock and Wilcox Company, Barberton, OH, pp. 33–37.
5. National Association of Clean Air Agencies (NCAA) (2011) State/Local Mercury/Toxics Programs for Utilities, February 8, 2011, <http://www.4cleanair.org/> (accessed 20 March 2014).
6. U.S. Environmental Protection Agency and Office of Research and Development (2005) Control of Mercury Emissions from Coal Fired Electric Utility Boilers: An Update, Research Triangle Park, NC, February 18, 2005, <http://www.epa.gov/ttn/atw/utility/hgwhitepaperfinal.pdf> (accessed 20 March 2014).
7. Feeley, T.J. and Jones, A.P. (2008) An Update on DOE/NETL's Mercury Control Technology Field Testing Program, July, 2008, <http://www.netl.doe.gov/technologies/coalpower/ewr/mercury/pubs/Updated%20netl%20Hg%20program%20white%20paper%20FINAL%20July2008.pdf> (accessed 20 March 2014).
8. Sjostrom, S., Bustard, J., Durham, M., and Chang, R. (2003) Analysis of key parameters impacting mercury control on coal-fired boilers. Proceedings of Air Quality IV Meeting, Arlington, VA, September 22–24, 2003.
9. Sjostrom, S., Ebner, T., Chang, R., and Slye, R. (2002) Full-scale evaluation of mercury control at Great River Energy's Stanton Generating Station using injected sorbents and a spray dryer/baghouse. Proceedings of Air Quality III Meeting, Arlington, VA, September 10–13, 2002.
10. Sjostrom, S., Starns, T., Wilson, C., Amrhein, J., Durham, M., Bustard, J., O'Palko, A., and Chang, R. (2005) Full-scale evaluation of mercury control for units firing powder river basin coals. Proceedings of Air Quality V Meeting, Arlington, VA, September 19-21, 2005.
11. Padak, B., Brunetti, M., Lewis, A., and Wilcox, J. (2006) Mercury binding on activated carbon. *Environ. Prog.*, **25** (4), 319–326.
12. Lui, S., Yan, N., Liu, Z., Qu, Z., Wang, H.P., Chang, S., and Miller, C. (2007) Using bromine gas to enhance mercury removal from flue gas of coal-fired power plants. *Environ. Sci. Technol.*, **41**, 1405–1412.
13. Huggins, F.E., Yap, N., Huffman, G.P., and Senior, C.L. (2003) XAFS characterization of mercury captured from combustion gases on sorbents at low temperatures. *Fuel Process. Technol.*, **82**, 167–196.
14. Hutson, N.D., Attwood, B.C., and Schechel, K.G. (2007) XAS and XPS characterization of mercury binding on

- brominated activated carbon. *Environ. Sci. Technol.*, **41**, 1747–1752.
15. Ritzenthaler, D.P. (2012) SO₃ formation and mitigation. Proceedings of 2012 NOx-Combustion Roundtable, Columbus, OH, February 13–14, 2012.
 16. Derenne, S., Sartorelli, P., Bustard, J., Stewart, R., Sjostrom, S., Johnson, P., McMillian, M., Sudhoff, F., and Chang, R. (2007) TOXECON clean coal demonstration for mercury and multi-pollutant control at the presque isle power plant. Proceedings of Air Quality VI, Arlington, VA, September 24, 27, 2007.
 17. Yudovich, Y.E. and Ketris, M.P. (2005) Mercury in coal: a review: part 2. Coal use and environmental problems. *Int. J. Coal Geol.*, **62**, 135–165.

20

Concrete-Compatible Activated Carbon

S. Behrooz Ghorishi

20.1

Introduction

The fly ash generated from coal combustion is virtually identical in its composition to volcanic ash and is ideal for concrete use. According to the American Coal Ash Association, the United States produced 65.6 million metric (MM) tons of fly ash in 2008. Replacing cement in concrete is the primary use of fly ash. About 11.5 MM tons of fly ash went to concrete market in 2008 [1]. This is the highest value use of coal combustion fly ash. Reuse of fly ash to partially substitute for cement in concrete is a major success in waste recycling in the US and has significant economic, environmental, and technical benefits. The economic benefits of using fly ash to replace a fraction of the cement in concrete include increased revenue from the sale of the ash, reduced costs for fly ash disposal, and savings from using the ash in place of the more costly cement. Concrete performance benefits include greater resistance to chemical attack, increased strength, and improved workability. Environmental benefits include reduced greenhouse gas emissions, reduced land disposal, and reduced virgin resource use.

Recently the U.S. EPA finalized new federal regulations on coal-fired power plant mercury emissions based on Maximum Achievable Control Technology (MACT). Twenty states have also started controlling the mercury emissions from utilities in their state by 70–90% [2]. For the majority of the coal-fired power plants, the leading technology to comply with the new mercury regulations is activated carbon injection (ACI) [3]. Power plants inject powdered activated carbon (PAC) based mercury sorbents into the flue gas to capture mercury. The carbon sorbent is injected upstream of the plant's existing particulate control device, usually either an electrostatic precipitator (ESP) or a fabric filter (FF) baghouse. Currently, 150 ACI systems have been installed by the coal-fired power plants across the country [4].

The main concern for power plants that sell their fly ash for cement replacement is that PAC-based sorbents make the fly ash incompatible with concrete, causing the fly ash to be landfilled. This is doubly negative, because not only must the fly ash be disposed of rather than beneficially used, but also the opportunity is missed

to physically and chemically sequester the mercury from release and interactions with the environment by encasing it in the concrete. Mercury that is sequestered in concrete is very stable. Golightly *et al.* [5] measured mercury release during curing of concrete that contained fly ash or fly ash/carbon that had mercury adsorbed on it. The mercury flux from the concrete samples resembled those from natural soils indicating no increase in baseline mercury emission from concrete that is made by inclusion of coal combustion fly ash/PAC. Because of the high surface area of typical PACs and their high adsorption capacity, if even the smallest amount gets mixed in with fly ash, the fly ash can no longer be used in concrete [6]. As shown by Senior *et al.* [6] in their field studies of class C fly ash mixed with activated carbon, the PAC adsorbs the air-entraining admixtures (AEAs) later added to the concrete slurry. These surfactants enable incorporation of the precise amount of air bubbles needed to create the air voids required for concrete workability and freeze-thaw capabilities.

Mercury emissions from cement kilns are also increasingly recognized as a problem. ACI offers the cement kilns a very cost-effective mercury control technology. PACs could similarly be injected into these exhaust gases and be collected in the particulate removal devices that separate the cement kiln dust (CKD) from the exhaust gases. However, because the collected CKD would then contain AEA-adsorbent PACs, it could no longer be sold as cement for air-entrained concretes.

To preserve the sale of fly ash and to continue the use of CKD, “concrete compatible” PAC needs to be developed. Concrete compatible activated-carbon-based mercury sorbent allows power plants to continue to sell their fly ash and cement kilns to continue the use of CKD while also having very good mercury capture performance. There are a number of concrete compatible activated carbon products, one of which is Albemarle Corporation’s Concrete-Friendly™, C-PAC™, which is now commercially available. Calgon Carbon Corporation and Norit Americas also offer concrete-compatible products referred to as *FLUEPAC®-CF PLUS* and *DARCO® Hg-CC*, respectively.

Topics covered in this chapter are as follows: new and innovative metrics to define the concrete-compatibility of mercury sorbent, production of concrete-compatible products including C-PAC™, C-PAC™ specifications, commercial application of C-PAC™ in various plants, and the results of concrete test with the resultant fly ash containing C-PAC™.

20.2

Concrete-Compatibility Metrics

Traditionally, the foam index method has been used to determine the concrete compatibility of different fly ashes. The foam index test is a relatively crude method used to predict the relative degree of adsorption of AEAs that a fly ash sample’s components, primarily carbon, will have in a concrete slurry. As described before, AEAs are surfactants that are added to concrete mixes to form fine, stable bubbles

that are needed for void volume so that concretes do not crack when interstitial water freezes. Foam index tests are usually done by titrating an AEA solution into a mixture of fly ash and water until a stable foam forms on the surface after agitation. The number of drops of AEA that it takes to saturate the fly ash components so that some is available to form a foam denotes the sample's foam index (FI). Dividing the FI by the amount of carbon in the sample provides a Specific Foam Index (SFI). Unfortunately, there is significant variability and, sometimes, a lack of repeatability in performing foam index measurements. These are the results of operator discretion, the use of different and variable reagents, varying laboratory equipments and "drop" sizes, non-standardized procedures, and the dynamic, nonequilibrium nature of the test. Also the foam index is specific to the AEA used in the particular measurement.

Pederson *et al.* [7] introduced a new method based on dynamic surface tension measurements (using a bubble pressure method) on filtrate from a fly ash and cement suspension. This method is claimed to have less variability as the foam index method. A pure surfactant is added to the suspension as a substitute for a commercial AEA. The surface tension method and the foam index test have been compared on fly ashes acquired from power plants in Denmark and the United States. The results revealed a good relationship between the two methods. This new method and the foam index technique are affected by changes in temperature. The authors stated that the surface tension method requires further work before a finished procedure is accomplished. Stencil *et al.* [8] introduced an automated foam index testing based on detecting acoustic waves emanating from a container in which cement-ash mixture is tested. AEA in water is dosed in the container and agitation is performed using precise computer control. The real-time nature of the acoustic emissions from the container provides dynamic assessment of foam stability. This method removes operator error in the foam index test, but it is still suffers from other drawbacks of this method as mentioned above.

In its development of a concrete-compatible mercury sorbent, Albemarle Corporation needed a standard, repeatable method to gauge the effect that different PACs would have on AEAs in a concrete mix. PACs are similar to the unburned carbon found in fly ash, but they have significantly higher surface area. The lack of reliability and precision encountered when trying to use foam index testing on PAC or PAC/fly ash blends proved unsatisfactory.

Consequently, a standardized and repeatable method for measuring the effect of fly ash carbon or mercury sorbent carbon on AEAs was developed to replace foam index test. This new method is a more accurate indicator of AEA interference than the traditional foam index test. It uses a standard reagent, tested at an equilibrium condition, and eliminates operator discretion in determining when a sample begins to "foam" by utilizing instrumental measurements. Based on this new method, Albemarle Corporation developed its Concrete-Friendly™ mercury sorbent known as *C-PAC*™.

20.2.1

The New and Innovative Concrete-Friendly™ Metrics; the Acid Blue Index

The new method is based on a standard reagent, acid blue 80 (AB80) (CAS 4474-24-2), rather than a non-standard AEA. Numerous dyes were evaluated for their correlations of adsorption with the foam indexes of various AEAs. AB80 provided the best results. Moreover, AB80 has a chemical structure and molecular size similar to some AEAs. Among the other tested dyes, one was methylene blue (CAS 7220-79-3; see Figure 20.1)

Methylene blue has been tried by other researchers for this role, however results indicates that the methylene blue adsorption of several commercially-available PACs does not correlate well with their foam index values, as indicated in Figure 20.2, while AB80 does.

AB80 is one of the anthraquinone type acid dyes (Figure 20.3).

The adsorption spectrum of an AB80 aqueous solution is shown in Figure 20.4. It has three peaks at 626, 581, and 282 nm, respectively. The appearance of several adsorption peaks for a given chromophore is common for a highly conjugated system.

The overall procedure of AB80 adsorption that was developed is very similar to ASTM D 3860-98 Standard Practice for Determination of Adsorptive Capacity of Activated Carbon by Aqueous Phase Isotherm technique. First, the PAC sample is oven-dried at 150 °C for 3 h prior to the test. Different dosages of dried carbon are then added to 50 ml of 100 mg l⁻¹ AB80 solution and well stirred. After

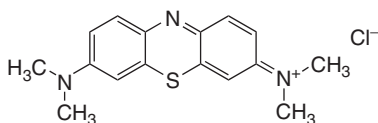


Figure 20.1 Structure of methylene blue.

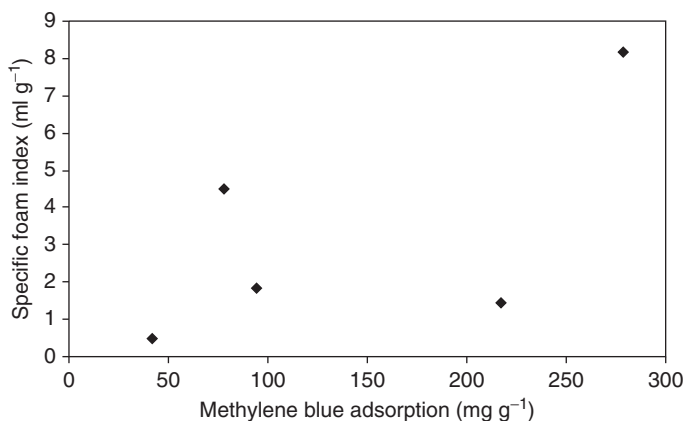


Figure 20.2 Correlation between specific foam index and methylene blue adsorption.

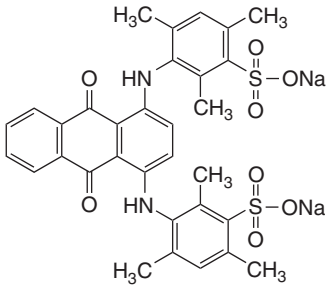


Figure 20.3 Structure of AB80.

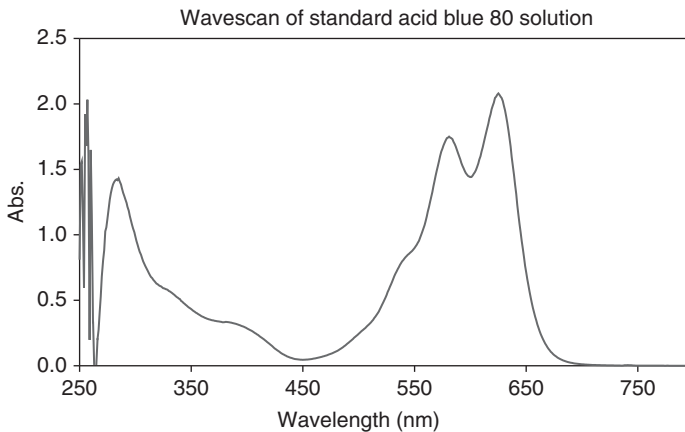


Figure 20.4 Adsorption spectra/wave scan of standard acid blue 80 solution.

the adsorption reaches an equilibrium, the carbon is separated from the AB80 solution by filtration. The concentration of the filtrate is determined, for example, by using Perkin Elmer Lambda EZ201 Spectrophotometer. The amount of AB80 removed by the activated carbon is determined by the relative change of AB80 solution prior to and after contact with activated carbon. The AB80 adsorption of the dosage carbon is then plotted with the equilibrium concentration of AB80 solution. The adsorptive capacity is calculated from a Freundlich isotherm plot at the original concentration of the AB80 solution, which is defined as Acid Blue Index (ABI) in the Albemarle-developed method.

During this method development, it was found that some chemically treated carbons interfere with AB80 adsorption. In order to eliminate this interference, such samples should be prewashed and extracted by deionized or distilled water until none of the impregnation chemicals is detected in the solution. For example, 5 g of B-PAC™ (an Albemarle Corporation's mercury sorbent; a non-concrete compatible brominated PAC) was washed with 250 ml of water, then filtered and rinsed with 1 l of water to properly prepare this brominated carbon for an ABI measurement. The sample weights of the activated carbons used in the

adsorption test may have to be adjusted depending on the adsorptive capacity of the activated carbon. A general guideline is that the concentration of the AB80 solution after contacting activated carbon should fit into the linear range of the AB80 working curve obtained based on the adsorption spectra at different concentrations (see Figure 20.5).

Based on the absorbance at 626 nm, the working curve for AB80 solutions was determined and is displayed in Figure 20.6. It can be used to calculate AB80 concentrations in solutions after adsorption by various activated carbons at various dosages.

The adsorption of AB80 by activated carbon fits well into a Freundlich Adsorption Isotherm, as shown in Figure 20.7. The AB80 adsorption of various activated carbons was determined based on Freundlich isotherms with the original AB80 solution concentration (100 mg l^{-1}) and the adsorption is defined as the ABI.

Depending on the different activation conditions, the pH of PACs can vary from very acidic to basic. Consequently, the effect of pH on the absorbance at 626 nm

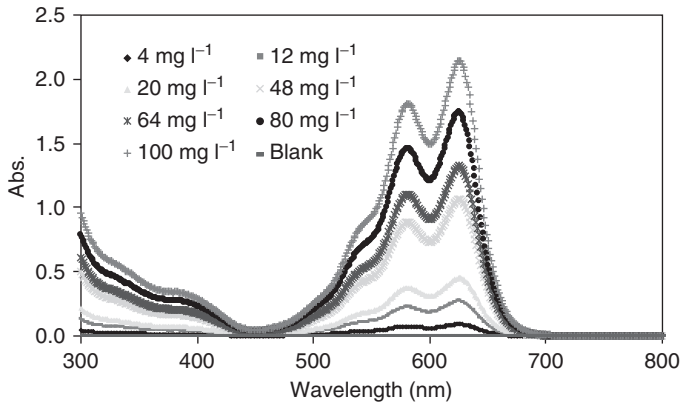


Figure 20.5 AB80 adsorption spectra at different concentrations.

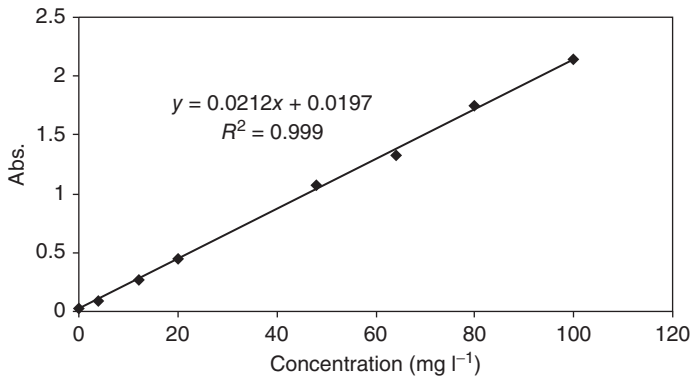


Figure 20.6 Working curve for AB80 solution.

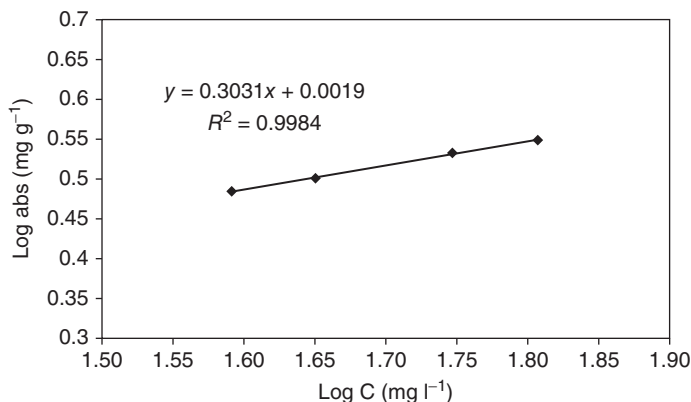


Figure 20.7 Freundlich isotherm for a tested activated carbon.

of AB80 solutions was investigated. The pH of the AB80 solutions was adjusted by H_2SO_4 or NaOH in order to obtain a series of AB80 solutions with different pHs. Within the test pH range of 2–12, the absorbance of the AB solutions vary about $\pm 2\%$, which suggests that the absorbance of AB80 solution is independent of the pH of solution. The time needed for the adsorption to reach equilibrium is another important parameter in this method. AB80 adsorption progresses relatively quickly, with the adsorption capacity reaching a plateau at about 30 min. This is the recommended time for carrying out the AB80 tests.

The Albemarle-developed ABI method has been extensively tested using a broad variety of carbon-containing materials. These include a series of laboratory-made activated carbons, a range of commercially-available activated carbons from different precursors, and different chemically treated activated carbons, including Albemarle Corporations' B-PAC™ and C-PAC™. A comparison of the ABIs and SFIs of some of these activated carbons using various commercially-available AEAs is shown in Figure 20.8. Use of different AEA compounds result in a wide range of SFI but a very narrow range of ABI, indicating that the ABI is the most appropriate method to determine concrete compatibility of a material. As evident from this figure C-PAC™ has ABI values below 10 mg g^{-1} and very low SFI. The data in this graph is used to set specification for concrete-compatibility of PAC/fly ash mixtures (see the next section).

20.3

Production of Concrete-Compatible Products Including C-PAC™

In C-PAC™ production, a one-step method is used. Before detailing this production technique, a review of a number of other techniques is presented. Fly ash that is mixed with carbon can be treated and passivated with ozone. Hurt *et al.* [9] in US Patent 6 136 089 teaches such method. Chen *et al.* [10] also discusses this technique in their paper. Ozone chemically passivates the surface of carbon in fly ash

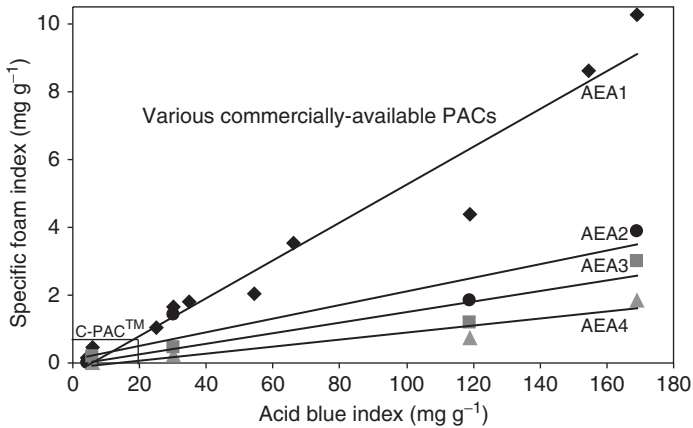


Figure 20.8 Comparison between ABIs and SFI of a number of activated carbons and C-PAC™.

and thus improves the air entrainment characteristic of fly ash. This process leaves the carbon in place, but adds surface oxygen complexes whose presence inhibits adsorption of the surfactant. This procedure requires treating large quantities of fly ash. Nelson [11] teaches a similar method that is only applied to the produced activated carbon before its injection into the flue gas and mixing with the fly ash. This method treats smaller volumes of solid material but still is an additional step in the production of activated carbon.

Jolicoeur *et al.* [12] discuss the use of “sacrificial agents or admixtures” to overcome the negative impact of carbon particles in adsorption of AEAs. The model sacrificial agent used in their study was ethyleneglycolphenylether (EGPE). They showed that addition of EGPE prevents the deleterious carbon effect on air entrainment by altering the surfactant adsorption and the surface energy (wetting behavior) of the carbon particles. They also observed that the addition of excessive dosages of EGPE has no detrimental consequences on air entrainment. However, this method still requires addition of another compound to the cement mixture. Another method to prevent the deleterious effect of carbon in fly ash is by carbon burnout [13]. In this method and before use in concrete mixture, the carbon in fly ash is simply burnt off in a fluidized-bed reactor with temperatures reaching 860 °F. Obviously, this process requires addition of external energy to accomplish carbon burn-off. This is a drawback of this technique.

A low-ABI carbon-based mercury sorbent can be produced by activating carbon using a one-step carbonaceous mercury sorbent precursor consisting of wood, lignite, coconut shell, or coal. The activation temperature and time period should be limited such that the ABI of the activated carbonaceous mercury sorbent does not exceed 15 mg g⁻¹ of sorbent (a specification discussed in the next section). This constitutes a one-step production process and no post-treatment processing of the activated carbon is required.

The keys to creating carbonaceous mercury sorbents that can be used together with fly ash in air-entrained concretes are: (i) a minimized PAC mesoporosity and/or (ii) a proper carbon surface chemistry. According to the International Union of Pure and Applied Chemistry's guidance on Reporting Physisorption Data for Gas/Solid Systems, activated carbon pores with widths less than 2 nm are considered micropores. Pores with widths between 2 and 50 nm are considered mesopores and pores with widths exceeding 50 nm are considered macropores. To create a concrete-compatible carbonaceous mercury sorbent, the carbon's mesoporosity must be minimized, while retaining adequate reactive microporosity. AEA compounds are relatively large molecules, on the order of 1–3 nm long. By minimizing the number of pores that the AEA molecules can fit into or be transported through, the amount of AEA that can be deleteriously adsorbed from the concrete slurry can also be minimized. The particular surface chemistry of the carbonaceous mercury sorbent is also very important in determining the degree of AEA adsorption on PACs. The presence of particular oxygen functional groups on the surface of the PAC and the net charge of the surface could promote or impede the attachment of AEAs. Oxygen-containing functional groups created during air activation should impart an acidic, hydrophilic character to the carbon surface, which can repel the hydrophilic heads of the AEA molecules. By increasing the hydrophilicity of the PACs the adsorption of AEAs may be retarded, with little deleterious effect on gas-phase mercury adsorption. Additional information regarding production of C-PAC™ can be found elsewhere [14, 15].

20.4 C-PAC™ Specification

Albemarle Corporation has developed a brominated activated-carbon-based mercury sorbent with a very low SFI value, called C-PAC™. The ABI of this material is less than 10 mg g⁻¹ (see Figure 20.8). ABI is the most important characteristic of this concrete-friendly™ material determining its use in concrete. Based on extensive testing, Albemarle has determined that ABI values of <15 mg g⁻¹ are acceptable. There are a number of other specifications that determine the effectiveness of C-PAC™ both for mercury removal and its concrete-friendliness. These values are listed in Table 20.1.

20.4.1 Commercial Application of C-PAC™

In this section, full-scale test results performed with C-PAC™ at a number of utilities and cement plants are presented and discussed. The focus is on the effectiveness of mercury removal using C-PAC™ and the effect of the sorbent on the concrete parameters of the resultant fly ash.

Table 20.1 C-PAC™ specifications.

Property	Value
Acid Blue 80 Index (mg g^{-1})	<15
Bromine (wt%)	7
Moisture (%)	8
Iodine number (mg g^{-1})	>500
Tapped bulk density (g cm^{-3})	0.56
Particle size less than 325 mesh (%)	>95
Ash content (wt%)	<12
Ignition temperature ($^{\circ}\text{C}$)	>400

20.4.2

Full-Scale C-PAC™ Trials at Midwest Generation's Crawford Station

The goal of the full-scale C-PAC™ injection for mercury control at the Crawford plant was to determine if greater than 70% reduction of mercury could be achieved while maintaining the quality of the fly ash for concrete sales. The Crawford Station Unit 7 fires PRB (Powder River Basin) coal and has an ESP with a specific collection area of 0.4 m^2 per actual cubic meters per minute (120 ft^2 per 1000 actual cubic foot per minute). Much of this plant's fly ash has historically been sold for concrete use. During the month-long continuous test, C-PAC™ was injected at an average rate of 74 mg/m^3 (4.6 pounds of sorbent per million actual cubic feet of flue gas or lb MMacf^{-1}). An average total mercury removal rate of over 80% was achieved, as indicated in Figure 20.9.

The sorbent injection rate varied over the course of the trial, as it might in commercial practice, putting varying amounts of the sorbent in the fly ash and

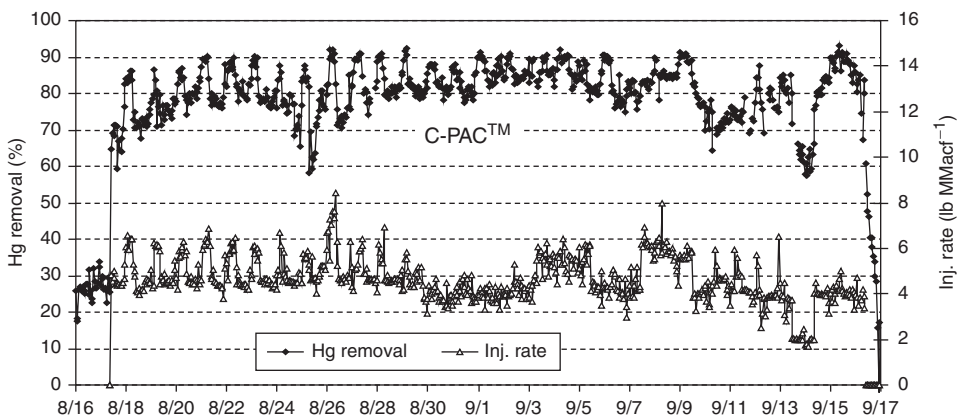


Figure 20.9 Crawford unit 7 mercury removal and injection rates over 30 days ($1 \text{ lb MMacf}^{-1} = 16 \text{ mg m}^{-3}$).

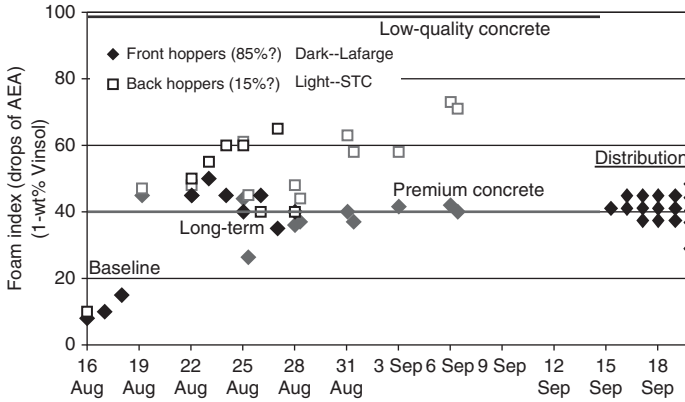


Figure 20.10 Foam index of Crawford fly ash during a 30-days C-PAC injection trial.

challenging the consistency of the fly ash for concrete use. Despite this, the resulting AEA adsorption of the ashes held to a tight band (see Figure 20.10). During the trial, the stack opacity improved, rather than degraded. It was observed that C-PAC™ injection had the co-benefit of improving the particulate collection performance of the ESP.

The resulting fly ash from this unit was usable in concrete. Moreover, fly ash from the front hoppers was usable in premium concrete (Figure 20.10). Using Vinsol® AEA, if the foam index is <40 drops, Crawford's fly ash is considered acceptable for cement replacement in premium concrete. At 99 drops or less, it can be used in standard concrete. The 40-drop cut off for premium concrete is a somewhat arbitrary value, based on the foam index of the unburned carbon and, particularly, on the variation observed in this value. The standard deviation of the C-PAC™-containing ash was only four drops, while that of the baseline control ash was even higher, at five drops.

20.4.3

Full-Scale C-PAC™ Trials the PPL Montana Corette Station

The purpose of the trial conducted at the Corette Steam Generating Station of PPL Montana was to determine whether the injection of C-PAC™ could reduce the mercury emissions by 80% while maintaining the ability to sell the fly ash for use in concrete. Two different continuous mercury monitors (PSA continuous emission monitor (CEM) and Ohio Lumex) and an Appendix K sorbent trap sampler were used for mercury measurements at this site. The injection trial was around the clock beginning at an injection rate of 3 lb MMacf⁻¹, based on an ESP inlet (cold-side) flow basis. In the first phase of the parametric testing, mercury removal rates of >80% were achieved at an injection rate of 3 lb MMacf⁻¹ and >90% at an injection rate of 5 lb MMacf⁻¹ (see Figure 20.11).

PPL Corette burns a PRB subbituminous coal. The coal samples contained about 30% moisture, <5% ash, and 0.3% sulfur. The coal heat content was slightly

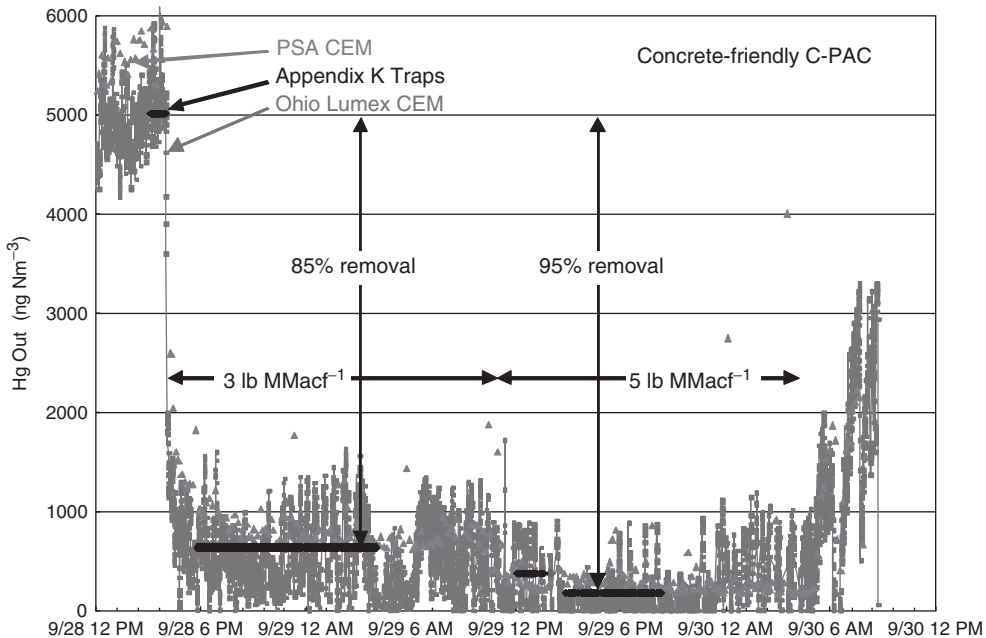


Figure 20.11 Mercury removal and C-PAC™ injection rate at Corette (1 lb MMacf⁻¹ = 16 mg m⁻³).

below 19.8 MJ kg⁻¹ (8500 Btu lb⁻¹). The average mercury content of the coal was approximately 0.080 μg g⁻¹ on a dry basis. Analysis of the fly ash samples collected during the test confirmed that the proper amount of mercury was being removed from the flue gas and collected in the fly ash. The foam index testing of the resulting fly ash indicated that the fly ash maintained its ability to be used in cement. All of the fly ash generated during the C-PAC™ injection period was transferred into PPL's storage silos and sold for concrete use.

20.4.4

Cement Kiln Mercury Emission Control Using C-PAC™

Portland cement kilns are another major mercury emission source, and the U.S. EPA promulgated in 2010 the final MACT standard for cement plants. One option for the cement plants to meet MACT Hg emission control requirement is to add a polishing baghouse to the kiln at a cost of millions of dollars. An alternative and cost-effective option is the injection of C-PAC™ at the existing baghouse, as illustrated in Figure 20.12.

In this technique, C-PAC™, which is both thermally stable and concrete-compatible, is injected as needed upstream of the primary existing particulate control device to reduce and maintain the mercury emission concentration to an acceptable level. Depending on the site, continuous C-PAC™ injection may

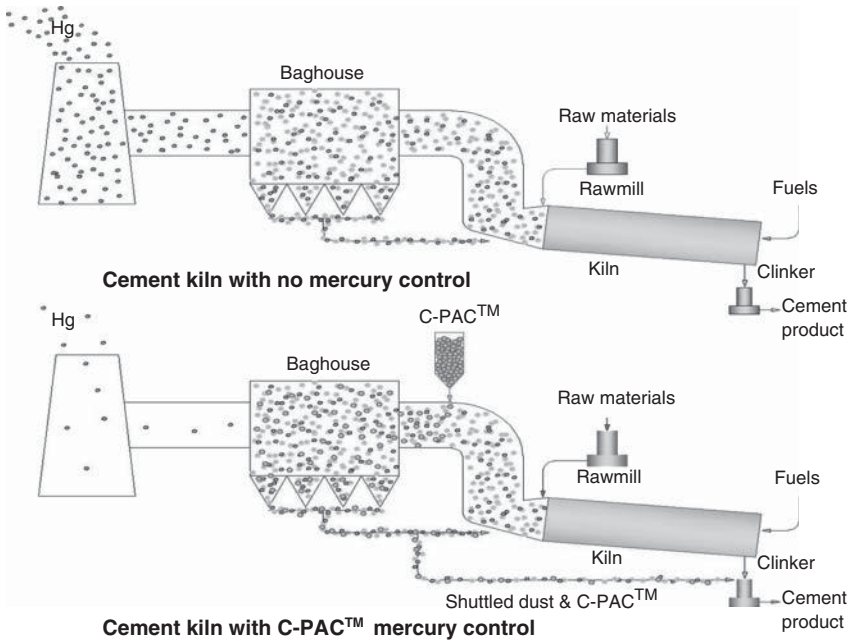


Figure 20.12 Illustration of C-PAC™ injection scheme at a cement plant.

be needed or C-PAC™ injection may only be required when the raw mill is off and Hg is at the highest level. (See Chapter 9 for a detailed discussion of mercury behavior in cement kilns.) Subsequently a percentage of the CKD containing mercury-laden sorbent is shuttled to the finished mill for use in the final cement product. In this way, no waste disposal or loss of the CKD occurs. Very good performance with C-PAC™ has been observed in several demonstrations, as well as commercial applications. The advantages of this in-process Hg control technique for the cement kilns include:

- 1) Requires only a sorbent injection system (low capital cost).
- 2) Sorbent is the main additional operating cost.
- 3) The timeframe for equipment design, procurement, and installation is short.

The sorbent requirements for this technique are that it must be temperature insensitive, concrete-compatible and have a high capability for Hg capture.

20.5

Concrete Compatibility Test – Field Fly Ash/C-PAC™ Mixture

In collaboration with two major fly ash marketers in the United States (Headwater Resources and Lafarge), Albemarle Corporation has examined in more detail the

concrete compatibility of the fly ash generated at Midwest Generation's Crawford Station. The results of these studies are summarized below.

20.5.1

Air Content of Fresh Concrete

The performance of C-PAC™/fly ash was compared with a non-sorbent control (fly ash only) and an alternative commercial PAC/fly ash. To make concrete with 6 vol% voids, about twice the amount of AEA additives was needed for C-PAC™/fly ash, while approximately 10 times the amount of AEA was needed for the alternative PAC/fly ash. Even though somewhat more AEA was required in the C-PAC™ concrete than in the non-sorbent control to achieve the same air content, the dosage still satisfied the contractor specifications. Furthermore, it was found that the properties of fly ash with C-PAC™ were very consistent, even more consistent than the baseline fly ash. The added cost of more AEA is negligible relative to the benefits of utilizing the fly ash in concrete production and eliminating the cost and environmental impact of the landfill.

20.5.2

Unconfined Compressive Strength (UCS)

Compressive strength is the capacity of the concrete to withstand axially directed compressive forces. Concretes produced with fly ash containing C-PAC™ met the target compressive strength of 4000 psi at 14 days (see Figure 20.13). In fact, it appears that the C-PAC™ also improves early strength relative to the control samples (no fly ash or base line fly ash) as shown in Figure 20.13.

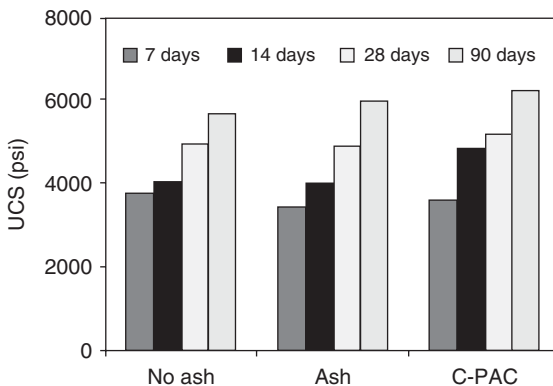


Figure 20.13 UCS of various concretes.

Table 20.2 Mercury leaching of the blank and ACI fly ashes.

Fly ash	Hg content (ng g ⁻¹)	Hg content in leachate (ng l ⁻¹)		
		DI water	Acetic acid	Sodium carbonate
Blank extraction solution		11	13	25
Baseline fly ash without mercury sorbent	39	15	9	34
Fly ash with C-PAC TM	2004	22	5	14

20.5.3

Stability of Mercury in Fly Ash and Concrete

To assess the effect of C-PAC on the stability of the mercury in fly ash and concrete, the EPA's Toxic Characteristic Leaching Procedure (TCLP) and Synthetic Groundwater Leaching Procedure (SGLP) was applied to a number of samples. The fly ash collected during the Crawford mercury emission control trial was tested and the results are summarized in Table 20.2.

The fly ash samples containing the mercury sorbent generally exhibited a lower rate of mercury release even though it contained as much as two orders of magnitude more mercury. In all cases except for distilled water, the mercury leachate concentration from the long-term fly ash samples was below that of the blank extraction solution. Senior *et al.* [6] also studied leachability of the captured mercury by activated carbon in fly ash and found minimal leaching under various leaching protocols. Liu *et al.* [16] also provides further evidence that the sequestered mercury in concrete is not leachable.

Other properties of concrete with C-PACTM-laden fly ash including air stability, air voids distribution, and setting time were also investigated and it was confirmed that C-PACTM mercury sorbents at appropriate dosage levels do not deleteriously affect any of the important properties of concrete.

Production of concrete-compatible, carbon-based mercury sorbents according to the procedures outlined in this chapter should result in continuous beneficial use of fly ash in concrete.

References

1. American Coal Ash Association (2008) Coal Combustion Product (CCP) Production and Use Survey Report, http://acaa.affiniscap.com/associations/8003/files/2008_ACAA_CCP_Survey_Report_FINAL_100509.pdf (accessed 5 October 2009).
2. National Association of Clean Air Agencies State/Local Mercury/Toxics Programs for Utilities, <http://www.4cleanair.org/Documents/StateTableupdatedApril2010.doc> (accessed 6 April 2010).

3. Feeley, T.J., III, and Jones, A.P. An Update on DOE/NETL's Mercury Control Technology Field Testing Program, <http://www.netl.doe.gov/technologies/coalpower/ewr/mercury/pubs/Updated%20netl%20Hg%20program%20white%20paper%20FINAL%20July2008.pdf> (accessed July 2008).
4. Institute of Clean Air Companies. Commercial Booking Lists, http://www.icac.com/files/members/Commercial_Hg_Bookings_060410.pdf (accessed June 2010).
5. Golightly, D.W., Cheng, C.-M., Sun, P., Weavers, L.K., Walker, H.W., Taerakul, P., and Wolfe, W.E. (2008) Gaseous mercury release during steam curing of aerated concretes that contain fly ash and activated carbon sorbent. *Energy Fuels*, **22**, 3089–3095.
6. Senior, C.L., Bustard, C.J., Durham, M.D., and Baldrey, K. (2004) Characterization of fly ash from full-scale demonstration of sorbent injection for mercury control on coal-fired power plants. *Fuel Process. Technol.*, **85**, 601–612.
7. Pedersen, K.H., Andersen, S.I., Jensen, A.D., and Dam-Johansen, K. (2007) Replacement of the foam index test with surface tension measurements. *Cem. Concr. Res.*, **37**, 996–1004.
8. Stencel, J.M., Ochsenein, M.P., and Cangialosi, F. (2009) Automated foam index testing: a quantitative approach to measure the capacity and dynamics during air entraining agent uptake. Proceedings of 2009 World of Coal Ash (WOCA) Conference, Lexington, KY, May 4–7, 2009.
9. Hurt, R., Suuberg, E., Gao, Y.-M., and Burnett, A. (2000) Apparatus and method for deactivating carbon in fly ash. US Patent # 6,136,089, Oct. 2000.
10. Chen, X., Farber, M., Gao, Y., Kulaots, I., Suuberg, E., and Hurt, R.H. (2003) Mechanisms of surfactant adsorption on non-polar, air-oxidized and ozone-treated carbon surfaces. *Carbon*, **41**, 1489–1500.
11. Nelson, S.G. (2003) Method and compositions to sequester combustion gas mercury in fly ash and concrete. US Patent 2003/0206843 A1, Nov. 2003.
12. Jolicoeur, C., To, T.C., Benoit, E., Hill, R., Zhang, Z., and Page, M. (2009) Ash-carbon effects on concrete air entrainment: fundamental studies on their origin and chemical mitigation. Proceedings of 2009 World of Coal Ash (WOCA) Conference, Lexington, KY, May 4–7, 2009.
13. PMI Ash Technologies Inc. <http://www.pmiash.com/docs/ACAA01paper.pdf> (accessed 20 March 2014).
14. Zhang, Y., Zhou, Q., and Nelson, S.G. (2010) Compositions and methods to sequester flue gas mercury in concrete. US Patent 2010/021550 A1, Aug. 26, 2010.
15. Landreth, R.R., Nelson, S.G., Zhang, Y., Zhou, Q., and Nalepa, C.J. (2011) Compositions and methods to sequester flue gas mercury in concrete. US Patent 2011/0197791 A1, Aug. 18, 2011.
16. Liu, R., Durham, S.A., and Rens, K.L. (2011) Effects of post-mercury-control fly ash on fresh and hardened concrete properties. *Constr. Build. Mater.*, **25**, 3283–3290.

21

Novel Capture Technologies: Non-carbon Sorbents and Photochemical Oxidations

Karen J. Uffalussy and Evan J. Granite

21.1

Introduction

This chapter focuses on removal of mercury by novel techniques. First, we begin with a brief overview of the pitfalls of current mercury removal strategies and materials that motivate the research, design, and demonstration of non-carbon sorbents. Next we review current non-carbon sorbent materials and photochemical technologies being developed for mercury and other trace contaminant removal from flue gas.

One of the current industrially validated technologies is the removal of oxidized mercury in scrubbers, and this is utilized in approximately 25% of US coal-fired power plants [1]. Elemental mercury is highly insoluble in water, and scrubbing systems are not always effective in removing this form of mercury [2]. Furthermore, the option of scrubber removal of mercury is not available or implemented at all coal-fired boilers, as is the case of western low-sulfur coal-derived flue gas, which does not necessitate further SO_x removal for compliance [3].

Another industrially validated and well-documented method is powdered activated carbon (PAC) injection, which is introduced into the ductwork upstream of either a cold-side electrostatic precipitator (ESP) or a fabric filter baghouse, in order to remove elemental and oxidized mercury by sorption at temperatures below approximately 400 °F (200 °C) [1, 4]. This retrofit technology is potentially applicable to 75% of coal-fired power plants that are not equipped with scrubbers in the United States [1]. The PAC has a short residence time within the ductwork, and the material must be well dispersed within the flue gas, typically at modest temperatures below 400 °F (200 °C), to achieve high mercury removal. Particle size and proper gas distribution and dispersion play important roles in achieving effective in-flight mercury capture for carbon-based sorbents [4, 5], and PAC injection must take place downstream of hot-side ESP because of the possibility that the carbon may ignite [6]. Carbon sorbents also can ignite in filter baghouses or hopper downstream, adding to a long list of challenges in designing and implementing effective carbon sorbent systems. Furthermore, an increase in flue gas SO₃ concentration results in decreased carbon sorbent effectiveness in removal of

mercury, and variations in coal type can be detrimental in achieving steady high mercury capture for multiple reasons [7]. The presence of activated carbon in fly ash is detrimental to the utilization of fly ash as a cement additive, and even the use of COHPAC and TOXECON systems (which supply the sorbent injection with its own dust capture system and separates the used sorbent from fly ash) does not sufficiently answer the problems with respect to SO_3 susceptibility or what to do with used PAC sorbent. As carbon sorbents can decrease the efficacy of fly ash as a cement additive, a replacement that is cement additive friendly is desired from both environmental and economic perspectives.

Carbon sorbents are typically used over a lower temperature range for mercury capture. The use of carbon sorbent at higher temperatures results in the volatilization of this captured mercury, with halogenated PAC materials extending this range to some extent. Finding a sorbent candidate that is effective at removing elemental mercury at high temperatures is beneficial as elemental mercury is most prevalent at higher process temperatures, and elemental mercury is the most difficult species to control because of its high volatility relative to other trace contaminants, low reactivity with conventionally used sorbents, and its low solubility in water [8–11]. Many inorganic compounds can react with mercury to facilitate its removal, including metal oxides, metal sulfides, and metal halides. Some of these materials can be utilized as sorbents, and may have advantages over activated carbons. These novel materials are discussed in detail in earlier work from the Department of Energy (DOE) [9, 11]. Sorbents that operate under varying conditions and circumstances are desirable, and here we present several such unique sorbents and their proposed processes.

Photochemical removal of mercury by application of ultraviolet (UV) light has several intriguing advantages over sorbent-based processes. The UV methods are potentially applicable in gases that poison carbon-based sorbents, and are also suitable as potential polishing techniques, ensuring near 100% removal of mercury.

21.2

Non-carbon Sorbents

21.2.1

Amended Silicates, Novinda

21.2.1.1 Background and Motivations

Amended Silicates are inexpensive, non-carbon substrates amended with mercury binding sites. The silicate-based substrate is chemically similar to fly ash; sites react with elemental and oxidized mercury species to bind the mercury to the sorbent. ADA (spun off later as Novinda) wanted to create a sorbent that would not affect fly ash quality for resale as a replacement for Portland cement [12], reduce or remove landfill burying costs associated with PAC and brominated PAC, and prevent the contamination of other high-value materials such as gypsum

[13]. Another major concern was that the use of the mineral sorbent should not interrupt or affect the overall process in any way. Their ideal sorbent would be nonleachable, inflammable, acid-gas resistant, and less corrosive than PAC, while also being overall economically and environmentally attractive. The company has developed several generations of sorbent materials made up of varying substrates and metal sulfides, which achieve these goals and are capable of capturing mercury at higher temperatures and pressures [14, 15]. Here, we discuss the sorbent's mercury capture mechanism and several of the material's sorbent demonstrations at various scales.

21.2.1.2 How Does the Amended Silicates Sorbent Work?

The Amended Silicates material is essentially made of an inexpensive phyllosilicate-type mineral substrate (montmorillonite, vermiculite, allophane) that has been "amended" by a metal sulfide functional group that acts as the active site for mercury capture [13, 16]. The flat sheetlike silicate structure is exposed to a solution of one or more polyvalent metal salts ($M = \text{Sn(II)}, \text{Sn(IV)}, \text{Fe(II)}, \text{Fe(III)}, \text{Ti}, \text{Mn}, \text{Zn}, \text{Mo}, \text{etc.}$), and an ion exchange reaction results in the initial form of the material. This material is then washed with water and subsequently exposed to either a gas or liquid sulfide (Thio-Red[®], Na_2S , CaS_x , CS_3^{2-}), and the insoluble metal sulfides precipitate to the surface of the silicate substrate lattice. The resulting material is spray dried, yielding the Amended Silicates material which is characterized by molecularly thin films of layered metal sulfide amendments (transition metal chalcogenides and/or polyvalent metal sulfides) [16]. This layered structure renders the sorbents unaffected by acidic flue gases, likely due to the polar acid gas molecules being unable to break through the interlayer sites (decorated with high-density sulfur atoms) where heavy metals are attracted. The exposure of these metals to the acid gas would otherwise degrade sorbent performance, as is the case for PAC- and zeolite-based sorbents. As the sorbent's active sites are concentrated at the surface, the most expensive part of the material (the metal sulfide) is more fully utilized compared to materials that undergo both internal and external capture mechanisms [16]. Therefore, the capture material is less likely to be limited by residence time requirements or internal diffusion limitations found with other materials.

Initial laboratory-scale packed bed tests reported in 2003 showed Amended Silicates to have a mercury capacity several times that of activated carbon [17], and further pilot testing demonstrated that significantly less Amended Silicates sorbent material is needed to keep mercury stack emissions below MATS limits (compared to PAC)[13]. This additional capacity is attributed to the material's chemisorption capture mechanism, and at elevated temperatures and pressures could be relatively high. Laboratory-scale investigations were performed at conditions as high as 770 °F and 200 psig [17]. At higher pressure, the mercury capacity actually increased by a factor of 5 compared to the sorbent capacity at atmospheric pressure (with sorbent mercury capacity in excess of 3% by weight). A large percentage of mercury remained on the sorbent even after the pressure was reduced

down to 20 psig, and it could only be removed by chemical digestion. Thus, it was determined that the Amended Silicates material is not suited for a regenerable sorbent material, but instead is better suited as a disposable sorbent bed material. This disposable material would be a great Portland cement additive candidate owing to the mercury-sorbent bond stability and could also be disposed of safely as a nonhazardous waste. On the basis of the high capacity at high pressures, it was suggested that 3.5 tons of sorbent in a fixed bed could be used to capture all of the mercury from 1 million tons of coal [17]. Several additional Amended Silicates formulations identified over the past 10 years are top-performing sorbents in varying coal flue gas compositions [14, 16–18]. One of the more recent formulations, AS-022, was found to be resistant to SO_3 poisoning, and retained 95% or greater mercury removal rates even over long periods of time (>20 min) and as much as 20 ppm of SO_3 at laboratory-scale testing [13].

21.2.1.3 Demonstrations

One of the earlier pilot tests performed by ADA was at the 275 MW Xcel Energy Comanche Station Unit 2 in Pueblo, Colorado, between November 2002 and March 2003. ADA designed and built the pilot plant for mercury sorbent testing of various particulate control configurations using a slipstream from the Powder River Basin (PRB) coal burning power plant. The low chloride content of PRB coal results in a larger percentage of elemental vapor-phase mercury, which is typically the more challenging species to remove from flue gas. The pilot plant was configured with a reverse gas baghouse particulate control module, and several injection and sampling ports. The injection rate varied (1.6–9 MMacf), along with the residence time, and injection temperature (200–325 F, with a target range between 280 and 300 °F). Mercury concentrations in the slipstream flue gas ranged from 4 to $8 \mu\text{g Nm}^{-3}$, with the fraction of particulate-bound mercury well under 20%. Impinger samples were taken and analyzed, and ADA found that their Amended Silicates resulted in 70–96% mercury capture using injection rates of 1.6–9 lb MMacf⁻¹, with 40% or more removed in the first 1 s of residence time. Increasing the injection rates resulted in increased mercury removal [17]. These slipstream tests agreed with another early pilot test where Amended Silicates exhibited rapid removal of vapor-phase mercury, suggesting that the material would perform considerably better than PAC in a plant equipped with an ESP [17]. More recent testing suggests that the Amended Silicates material lowers the bulk resistivity of PRB fly ash and thus can improve the performance of CS-ESPs [14].

Another major demonstration using Amended Silicates was performed at Duke Energy's North Bend, Ohio Miami Fort Unit 6 facility over a 6 week period in early 2006 (funded by DOE and EPA (Environmental Protection Agency)). This facility operates a 175 MW boiler with a cold-side ESP, and burns bituminous coal originating from KY, WV, OH, PA, and IL [12, 19]. Over 75 tons of the Amended Silicates material was made by BASF for this specific demonstration. A baseline was established at the beginning of the trial, where 0–10% of mercury was captured by native fly ash and 1/3 to 2/3 of the total mercury was found to be in

the elemental form [20]. After the baseline period, the Amended Silicates material was injected at various ratios in order to find optimum operating parameters, which was then followed by a 30 day trial at a target Amended Silicates injection ratio of 5–6 lb MMacf⁻¹. Afterwards, PAC (NORIT's DARCO HG) was injected for 5 days at several different ratios for comparison purposes. The results from the tests showed that Amended Silicates injection resulted in 40% mercury control, but that this was also achieved with the PAC sorbent, both at injection rates between 5 and 6 lb MMacf⁻¹. Increasing injection rates did not result in increased mercury capture for either material, which contradicts the findings from PRB coal slipstream studies. The ESP operating parameters and overall process were not affected by Amended Silicates sorbent injection [12]. Furthermore, tests performed by Boral and Separation Technologies found that Amended Silicates fly ash did not affect the sale of the material as a concrete additive, but that PAC fly ash was rendered unsuitable as a concrete additive material [12].

Changes to the Amended Silicates material were made, and new versions of the material were developed after the Miami Fort tests. The next major demonstration took place between February 2011 and November 2011 at the Gillette Energy Complex of Black Hill's Wygen Units 1, 2, and 3. These units burned PRB coal, utilized pulse jet baghouses for particulate and sorbent collection, selective catalytic reduction catalysts (SCR) for NO_x reduction, and a spray dryer absorber (SDA) for removal of SO₂ [14]. The sorbent trials were again run using varying Amended Silicates injection rates over short periods, constant Amended Silicates injection rates over longer periods, and PAC/Br-PAC injection for comparison purposes. Test results indicated that steady-state mercury removal was obtained after approximately 24 h of Amended Silicates injection, and that the mercury level was reduced by 70% in the first 90 min to 2 h after injection began. For higher injection rates of 3.3 lb MMacf⁻¹, the overall mercury removal was 90–95%, and for lower injection rates of 1.7 lb MMacf⁻¹, the overall mercury removal was over 85% [14]. After Amended Silicates injection was stopped, the filter bag cake dust continued to capture mercury, evidenced by the slow recovery of initial stack mercury levels up to 24 h, showing the additional mercury sorbent capture capacity. Not only was the Amended Silicates material capable of being used in the existing dry sorbent injection units (for PAC), but its use did not affect the plant's operation or equipment, nor did it affect fly ash viability for disposal or sale. A neighboring unit (Neil Simpson 2) employing a circulating dry scrubber (CDS) and a CS-ESP was used for testing a different particulate/SO₂ control system with Amended Silicates. The low mercury stack levels meant lower Amended Silicates injection rates were needed, and mercury stack levels well below the EPA/MATS (Mercury and Air Toxics Standard) were achieved. Furthermore, the injection of CaCl₂ to promote oxidation of volatile mercury compounds was studied, and it was found that for the baghouse/SDA configuration, a synergistic reduction in mercury was observed when using Amended Silicates. For the case of CS-ESP/CDS, there was no noticeable difference in stack emissions. While the Br-PAC and PAC injections did benefit from CaCl₂, neither cases outperformed the Amended Silicates material [14].

The most recent demonstration of ADA/Novinda's most recent Amended Silicates material (AS-022) was performed at the 315 MW Santee Cooper Winyah Station Unit 4, burning eastern bituminous coal and equipped with SCR/CS-ESP and a wet flue gas desulfurization unit (WFGD) [13, 18]. The host site uses their WFGD to generate gypsum that is then sold to wallboard manufacturers, so it was important that the use of Amended Silicates did not affect the salability of the gypsum product. While wanting to demonstrate the efficacy of the AS-022 material, they also wanted to observe the effect of varying the injection locations (temperature and air heater location) and simultaneous hydrated lime injection has on mercury stack emissions.

During pretrial characterization, it was found that a large percentage of SO_3 is removed via condensation at the air heater, so it was decided that AS-022 injection would be best after this point to reduce SO_3 interactions with the sorbent. Furthermore, the largest percentage of mercury removal already occurred at the WFGD, approximately ~90% of which was determined to be almost all Hg^{2+} , which is not surprising as eastern bituminous coal is high in chloride content and, along with SCR catalysts, will promote mercury oxidation. While the WFGD is capable of removing oxidized mercury, the challenge is in removing elemental mercury before it reaches the WFGD using sorbent injection. After AS-022 injection began, it took several days to establish mercury stack emission equilibrium, but this was determined to be a function of the WFGD volume and plant load. However, after that 3- to 4-day period, the majority of mercury was captured at the ESP with the Amended Silicates material, and the amount of dissolved mercury in the WFGD decreased substantially. The hydrated lime injection increased the amount of mercury removed at the ESP, but when the hydrated lime was shut off, the WFGD removed the balance to keep stack emissions under the EPA/MATS limits; any effect that SO_3 would have on the Amended Silicates material mercury capture was essentially controlled by the passive removal of mercury at the WFGD. In addition, the injection of AS-022 before the preheater was found to be optimal owing to increased flue gas and/or AS-022 contact time and more uniform distribution. As the hydrated lime injection was located below the SCR outlet and before the air heater, this was reducing the occurrence of SO_3 , which might have otherwise affected the AS-022 performance. Overall, the mercury stack emissions were measured at 0.5 lb TBtu^{-1} (below EPA/MATS 1.2 lb TBtu^{-1} limit), with the majority of mercury capture occurring at the ESP, which decreased the amount of mercury dissolved in WFGD fluid. Not only did the injection of Amended Silicates not affect the gypsum quality but a decrease in AS-022 flow rate kept the stack emissions below the EPA/MATS limit [13, 18].

21.2.1.4 Conclusions

The Amended Silicates material is reported to be a cost-competitive alternative to other sorbent materials, such as PAC and Br-PAC. This is a function of the inexpensive, large-scale manufacture of the material and the salability of the fly

ash as a Portland cement additive [13]. In addition, there is little impact to ongoing operation, as the injection of the material uses readily available and demonstrated injection equipment and Amended Silicates have continually been proved to not affect/damage any equipment nor affect any downstream processes [14, 17, 18]. The material's reliable mercury control performance was not affected by low-chlorine coals, moisture, or acid gas constituents. From an environmental perspective, disposal of used Amended Silicates material is much more attractive, as the mercury is tightly bound to the sorbent because of the chemical reaction converting bound mercury to a very stable and insoluble mercuric sulfide that occurs naturally in the Earth's crust, and TLCP fly ash leaching tests consistently report below detection for mercury [13].

21.2.2

MinPlus CDEM Group BV

21.2.2.1 Background and Motivations

MinPlus has been researching cost-effective and widely usable sorbent materials since 1995 for the capture of trace contaminants, as indicated by their wide range of patents for such materials [21–24]. The basis behind the MinPlus sorbent coupled with Mobotec's integrated process is the use of a highly reactive mineral sorbent combined with a highly effective delivery and dispersion system to achieve high-temperature removal of mercury from flue gas. Both MinPlus and Mobotec are interested in high-temperature removal of mercury directly from flue gas in the open radiant furnace itself. The MinPlus sorbent altogether eliminates the need for additional process equipment for mercury removal as it is directly injected into the boiler furnace.

MinPlus can be used upstream of hot-side ESPs because of its high-temperature operating range of 1650–2010 °F (900–1100 °C), removing mercury earlier in the process footprint, and the MinPlus sorbent will not ignite in hoppers or ESPs. MinPlus claims that their sorbent can easily handle variations in mercury concentration. The MinPlus material adds strength to cement as a fly ash additive, and is thus a unique candidate to use in place of carbon-based sorbents where increasing fly ash utilization is vital for cement manufacture. The conservation of the fly ash quality is due to the strong chemical binding of mercury to the MinPlus material and the unique mineral properties of the sorbent. More importantly, though, with respect to mercury capture, is that it takes an extended period of heating time at temperatures above 1700 °F (927 °C) for mercury to begin to be re-released, again supporting the material's stable nature and the chemisorption model [25].

21.2.2.2 How Does the MinPlus Sorbent Work?

The white fly ash like sorbent material is thermally produced from mixing $\text{Ca}(\text{OH})_2$, CaCO_3 , and $\text{Al}_2\text{O}_3\text{-}2\text{SiO}_2\text{-}2\text{H}_2\text{O}$, (kaolinite/calcite/lime) and is manufactured on the level of metric tons as a by-product from paper recycling residues [6, 26]. The material has a mean particle size of 10 μm based on Malvern particle size distribution analysis [26]. MinPlus is reactive over a wide range

of temperatures, undergoes rapid calcination and chemical transformations when injected into hot flue gas, and these transformations are what control its high-temperature mercury sorption behavior [6]. However, in order for mercury capture to occur in flue gas for this material, the gas mixture needs to contain at least 4000 ppm of oxygen, but the sorbent was reported to still effectively capture mercury in the presence of water [27].

Experimental work using a quartz tube reactor (47 mm I.D. \times 190 cm) through which varying feed rates of sorbent (1–6.9 g h⁻¹) and preheated flue gas mixture (2.2–4.7 L min⁻¹) were mixed with a steady supply of elemental mercury (\sim 25 μ g m⁻³) have shown that MinPlus mercury removal efficiency is sensitive to both sorbent feed rates and to furnace temperature, where increasing either sorbent feed rates or temperature increases mercury capture. This correlation suggests that the mechanism of mercury capture is chemisorption rather than physisorption based. Mercury is predominantly in its elemental form at higher temperatures, and it is this elemental mercury which MinPlus excels at capturing. In fact, between 83% and 90% removal efficiency was observed at temperatures between 1650 and 2010 °F (900–1100 °C) for laboratory-scale tests, yet negligible sorption below 1100 °F (600 °C) [6, 26].

Two types of capture mechanisms were observed, one of which is an “in-flight” capture mechanism with an average residence time of 8 s and optimal mercury capture temperature at approximately 1650 °F (900 °C). The in-flight mechanism involves sorbent initial activation by internal reactions, mercury sorption, and subsequent deactivation if temperatures are too high for too long a period because of a “catastrophic melt” that results in pore closure. Interestingly, analysis of the in-flight deactivated sorbent particles showed that spent solids contained calcium aluminosilicate (Gehlenite) and calcium silicate products, which are specifically formed during activation/calcination at higher temperatures and is likely part of the in-flight mercury capture mechanism and subsequent deactivation [6, 26]. The second type of capture mechanism is characterized by sorbent that formed “scales” on reactor walls and did not appear to undergo deactivation through some sort of wall-stabilization effect. In fact, over a period of time at 2010 °F (1100 °C), the wall-bound sorbent managed to continue capturing mercury without reaching a maximum even after sorbent flow was ceased.

Wendt *et al.* noted that there is an interesting effect that the sorbent interaction with the quartz wall reactor has on mercury capture and uptake, and that it is quite possible that the quartz wall reactor affected capture based on data inconsistencies [27]. Further tests showed that when compared to Inconel reactors, the quartz reactor improved mercury capture, and that adding some form of SiO₂ to the sorbent mixture also stimulates mercury capture [25]. This is postulated to be through the formation of some type of active species that is triggered through the presence of silica but limited by the type of silica content as well as contact time. Additional tests with different types of fly ash with differing types of silica content greatly affected the mercury uptake. This was most evident in full-scale tests that were performed with PRB fly ash, where low to no reactivity with the MinPlus sorbent was detected whatsoever [25].

21.2.2.3 Demonstrations of Sorbent

Successful fixed-bed tests at the University of Arizona and dispersed-phase testing in a 1.75 MW coal-fired pilot plant at the Southern Research Institute in Birmingham, Alabama, led MinPlus to full-scale tests to test the capabilities of their sorbent material. A collaboration with Mobotec's injection and mixing systems were part of this demonstration. These tests were performed at the Richmond Power and Light Whitewater Valley 65 MW Power Plant Unit 2 in Richmond, Indiana, and at a 154 MW power plant in North Carolina. Both plants were equipped with a rotating opposed fired air system (ROFA, supplied by Mobotec), which can generate a highly turbulent mixture of flue gas via asymmetric air nozzle flow. The Mobotec Rotamix system, designed for selective noncatalytic NO_x reduction (SNCR), coupled with ROFA results in effective direct in-furnace injection mixing and distribution of the MinPlus material that leads to greater utilization of the total furnace volume, optimal sorbent-flue gas contact time, and desirable sorbent temperature profiles [25].

The Richmond Power and Light Whitewater Valley power plant utilized in this demonstration burns bituminous high S Illinois coal, and is a tangentially fired Combustion Engineering pulverized coal-fired 12-boiler with a full load capacity of 65 MW at a steam pressure of 1450 psi and superheat temperature of 1005 °F (541 °C)[2, 7]. This system is equipped with an FSI system that was designed for the delivery of limestone for SO_x control, but the SNCR and SO_x control systems were not in service during the MinPlus demonstration. The mixing methodology is important with respect to the contact time and temperature at which the sorbent contacts the flue gas. Eight Rotomix/FSI injection ports, divided into two banks of four ports, were available, and typically either two or four of these ports were used. The MinPlus sorbent was injected pneumatically and fed through the injection ports at over 450 ft s⁻¹ directly into the furnace and flue gas (temperature at the injection ports between 2000 and 2200 °F (1093 and 1204 °C)). The demonstration lasted about a week (second week of November 2005), and the results show that the MinPlus sorbent yielded over 95% mercury capture, up to 98%, with mercury stack emission measurements decreasing from 4 μg Nm⁻³ (background; no mercury removal sorbent added) to 0.2 μg Nm⁻³ at 3% O₂ [2]. It is assumed that as elemental mercury is the predominant species at elevated temperatures, the MinPlus sorbent captures mercury in its elemental form. Therefore, any negative effect that plant load, equipment, and coal type have on a sorbent's ability to capture mercury is essentially eliminated with this sorbent material. In addition, mercury was found to be predominantly bound to mineral sorbent, and the wall-bound mercury sorbent capture mechanism appeared to be effective for a period of time after the injection was stopped [2]. There is also an enhanced capture observed over previous testing that occurred at the Southern Research Institute (1.75 MW) coal-fired pilot plant, which resulted in mercury capture rates of approximately 65% [28]. The authors attributed the higher Whitewater Valley mercury capture to a higher injection temperature and better injection/mixing system, where mixing

and distribution of the sorbent in the flue gas is critical [2]. The MinPlus injection did not affect any other aspect of the plant, including fly ash quality and ESP performance.

The next MinPlus sorbent demonstration was at the North Carolina 154 MW Power Plant, a 154 MW, 1956 Combustion Engineering corner-fired design with four levels of pulverized coal burners [7]. This plant also burns eastern bituminous coal, and the demonstration lasted 2 weeks in March 2006. In this plant, the MinPlus sorbent was fed through precalibrated feeding screws from a transportable silo and it was then pneumatically sent to the Rotamix air boxes, mixed into the Rotamix air, and then entered the boiler contacting flue gas at over 450 ft s^{-1} . Similar to the Whitewater test, eight ports were available, and variations of these eight were tested to find the optimal dispersion when using side ports while also using no more than four ports. The temperature of the flue gas it contacted was estimated to be between 1600 and 2670 °F (871 and 1466 °C) [7]. The results showed a 70–80% removal of mercury, where initial mercury measurements of $5 \mu\text{g Nm}^{-3}$ was reduced to $1 \mu\text{g Nm}^{-3}$, measured after ESP. This demonstration also found that use of the MinPlus sorbent did not affect any aspect of the plant, and leaching tests showed that there was complete binding of the mercury on the sorbent material [7].

MinPlus currently operates a full-scale demonstration plant located in Duiven, the Netherlands. This plant is operated as a joint venture between MinPlus-CDEM and a municipal and industrial waste incineration company with a focus on green pollution abatement technology in the paper recycling field.

21.2.2.4 Conclusions

The MinPlus sorbent is an inexpensive recycled material, and the used nonregenerable sorbent material is meant to be combined directly with fly ash. Ash quality measurements of the spent sorbent material mixtures found that the fly ash quality was not affected and could be used for resale as a Portland cement additive [2, 7]. The captured mercury and other trace contaminants do not revolatilize until approximately 1600 °F (871 °C), thus making this another stable mercury capture material that is a possible candidate for safe disposal [25]. The economic advantage of injecting directly into the boiler is that the majority of mercury is bound to sorbent and removed from the process before possible contamination of aluminum equipment downstream from the boiler. Furthermore, tax incentives might also be available for utilizing a process that recycles/reuses paper industry waste [29].

21.2.3

Pahlman Process – Enviroscrub

21.2.3.1 Background and Motivations

The Pahlman process is a closed-loop dry scrubbing process utilizing Pahlmanite™ sorbent, which is made up of low-density oxides of manganese (MnO , Mn_2O_3 , and MnO_2) black powder that can adsorb a large percentage of flue gas SO_x and NO_x (reported to be >97%) [30]. Upon regeneration, its

sorbent yields raw sulfates and nitrates that are used to manufacture marketable commercial byproducts such as sodium sulfate, ammonium nitrate, and potassium sulfate. The process can remove multiple pollutants by a single-, dual-, or multistage dry process, eliminates undesired waste streams, and ultimately is intended for the replacement of FGD (flue gas desulfurization), SCR, and activated carbon injection technology [31].

21.2.3.2 How Does the Process and Sorbent Work?

The dry sorbent is sprayed into contact with flue gas, mercury vapor is oxidized, and this oxidized via a proprietary mechanism. This oxidized mercury vapor is then adsorbed along with chlorides, SO_x , and NO_x . The sorbent has a high affinity for sulfur compounds and this reaction happens relatively quicker compared to mercury and NO_x adsorption. The temperature at which sulfates and nitrates of manganese decompose dictates the inlet process gas temperature range, and patent literature suggests that a typical temperature range would be 60 - 250 °F (16 - 121 °C), and the temperature should not exceed 350 °F (177 °C) [32–34]. A baghouse collects the sorbent and provides further residence time to contact the sorbent material with the flue gas [30]. Once the sorbent is removed from the baghouse, it is mixed with water and next regenerated via a persulfate oxidant and a base in a separate reactor. The insoluble manganese oxides are insoluble in water and separate out of solution with pollutant salts. A proprietary filter is used to separate trace contaminant metals such as mercury from the solution, which is reported to be a proprietary reaction forming a Mn–Hg complex. It is known that lattice oxygen from manganese oxides can react with elemental mercury to form mercury manganates. The pollutant salts can then be processed with potassium or ammonium to produce sulfate and nitrate salts of high value [30, 32–34].

21.2.3.3 Demonstrations

The first major demonstration of the Pahlman process was performed at the DTE Energy River Rouge Power Station Unit 3 located in Michigan in June 2003. The 290 MW pulverized coal wall-fired boiler plant was burning a PRB/eastern bituminous blend (40:60 to 60:40), and a 500–1000 SCFM slipstream was diverted to the mobile Enviroscrub pilot unit for processing [30]. The pilot unit used the slipstream to achieve its operating temperature, and subsequently the sorbent was loaded into the baghouse reaction chamber for testing. Inlet and outlet mercury measurements were conducted using the Ontario Hydro method and mercury semicontinuous emission monitors (SCEMs). Concentrations of O_2 , NO_x , SO_x , CO_2 , and CO were also measured during the test. Continuous emission monitoring system (CEMS) data gave an average steady state removal of SO_2 to be ~99.8%, NO_x removal of ~98.2%, and the Energy and Environmental Research Center from the University of North Dakota reported a mercury removal of ~97% (oxidized, 1.02–0.03 $\mu\text{g m}^{-3}$) [31].

The second major demonstration of the Pahlman process was performed on a slipstream at the 550 MW Unit 4 at Minnesota Power's Boswell Energy Center in Cohasset, Minnesota, between December 2003 and January 2004. A 500–1000

SCFM slipstream of flue gas was diverted from the coal-fired Combustion Engineering tangentially fired boiler utilizing PRB subbituminous coal to the same mobile Enviroscrub pilot unit that underwent identical processing procedures. CEMS data reported an average steady-state removal of SO_2 to be $\sim 99\%$, NO_x removal of $\sim 95.8\%$, and the Energy and Environmental Research Center from the University of ND reported a mercury removal of $\sim 94.3\%$ (84.4% oxidized, 99.2% elemental) [31].

21.2.3.4 Conclusions

Manganese oxide is inexpensive and abundant, and occurs in over 30 different forms, so acquiring this material easily is quite feasible. On the basis of Enviroscrub's design criteria, the plant runs at approximately 34.1% efficiency, requires about 3.3% of the power it generates in order to operate, and operating expense and capital costs both decrease as a function of plant capacity [31]. The capital cost savings for the Enviroscrub Pahlman process system is between 20% and 50% compared to conventional WFGD/SCR scrubbing technologies because of a decrease in operational equipment and space requirements. Furthermore, operating and maintenance costs decrease by 25–40% when considering the production of marketable byproducts and the removal of waste streams [30, 31]. However, progress still remains to be made on the front of optimization, simulations, and construction of a full-scale pilot plant for further testing and proof of concept at a larger scale than the current mobile unit set-up [35].

21.3

Photochemical Removal of Mercury from Flue Gas

The oxidation of mercury facilitates its capture. Although possessing numerous compounds, mercury is a semi-noble metal, and is exceedingly insoluble in water. Ultraviolet light can supply the needed activation energy to induce the reaction of mercury to more amenable compounds for removal. Compounds of mercury tend to condense upon surfaces such as fly ash, and can be captured in a wet scrubber. Photochemical reactions of mercury with various constituents of flue gas can be an attractive alternative or polishing step for sorbent- or scrubber-based processes for mercury capture. There are several potential routes for the photochemical removal of mercury. One method employs short-wave ultraviolet radiation to facilitate the oxidation and removal of mercury. A second technique uses long-wave ultraviolet light in combination with a photocatalyst to oxidize and capture mercury. These techniques are discussed here.

21.3.1

Sensitized Oxidation of Mercury: GP-254 Process

Elemental mercury will absorb or reemit (fluoresce) 253.7 nm ultraviolet light. This ability to absorb or reemit 254 nm light is the basis for detection through

atomic absorption, atomic emission, or atomic fluorescence detectors. In atomic absorption spectroscopy (AAS) detectors, elemental mercury absorbs a photon of 254 nm light and goes to the $6\ (^3P_1)$ excited state, denoted as Hg^* or $Hg\ 6\ (^3P_1)$, and shown here:



In atomic emission spectroscopy (AES) detectors for mercury, the atom of excited mercury emits a photon of 254 nm light, and goes back to the ground state.



In atomic fluorescence spectrometry (AFS) detection of mercury, steps (21.1) and (21.2) occur within an infinitesimal fraction of a second, and the intensity of the emitted light (fluorescence) is measured. These processes are the basis for continuous emissions monitors (CEMs) of mercury, and are discussed in Chapter 5.

Dickinson and Sherrill [36] discovered the photochemical formation of mercuric oxide in 1926 described by the reaction:



In the reaction mechanism, elemental mercury serves as a sensitizer for the formation of ozone, and ozone oxidizes mercury to form mercuric oxide. The term *sensitizer* means that elemental mercury in the $6\ (^3P_1)$ excited state induces chemical reactions to occur. When the mercury collides with another atom or molecule, it can transfer its energy from the excited state to this species, setting the stage for chemical reactions. Activation energy for chemical reactions are typically supplied by heat, but can also be supplied by light.

The eminent Canadian photochemist Harry Gunning discovered many reactions for which elemental mercury can serve as a sensitizer over five decades spanning the 1940s through 1980s. Some of these sensitized oxidation reactions discovered by Gunning and others [37–43] involve reactants such as moisture, nitrogen oxide, sulfur trioxide, hydrogen chloride, and carbon dioxide that are abundant in coal-derived flue gas, and are present at concentrations that are many orders of magnitude greater than the concentration of mercury (around 1 ppb). Some of these reactions include



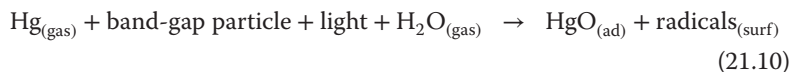
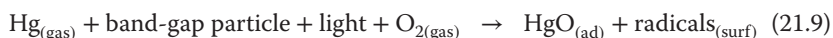
Granite and Pennline [44–47] employed reactions (21.3) through (21.8) to facilitate the removal of mercury from flue gases in the laboratory through pilot-scales.

The technology, dubbed GP-254 Process, is available for license through the DOE. The technology could serve as a small and inexpensive polishing step to guarantee near 100% removal of mercury from flue gas. It is noted that even 1 or 2 ppm of SO₃, commonly present within coal-derived flue gases, can severely poison the activated carbons used to capture mercury [48, 49]. Thus, the GP-254 UV Process could serve as a polishing step in these cases by reaction (21.7). It has also been recently suggested that NO₂ can hinder the performance of activated carbons for the capture of mercury [50], and this UV Process could again remove mercury in this case through reaction (21.6).

21.3.2

Photocatalytic Oxidation of Mercury

It is known that certain band-gap semiconductor oxides such as titanium oxide can serve as oxidation catalysts in the presence of long-wave ultraviolet light. Kaluza [51] discovered that titanium oxide and other oxides could photo-oxidize mercury to mercuric oxide in 1971. Biswas and coworkers [52–55] studied the capture of mercury in flue gas using titanium oxide particles and ultraviolet light. The ultraviolet light often emanated from the glowing discharge fields of the ESPs, present within many coal-fired power plants. The US DOE [56] studied the photo-catalytic oxidation of mercury to mercuric oxide using 365-nm long-wave ultraviolet light and both titanium oxide powders, as well as titanium oxide coated self-cleaning glasses. The reactions occurring on the titanium oxide surface can be crudely represented through (21.9) and (21.10) as [56]:



There are several band-gap semiconductor oxides such as titanium and zinc oxides present in air that can oxidize mercury under the influence of sunlight, potentially impacting the fate of mercury in the environment [56]. Additional research is merited on the use of photocatalysts for the oxidation and capture of mercury from flue gases.

Disclaimer

Neither the United States Government nor any agency thereof, nor any of their employees, makes any warranty, express or implied, or assumes any legal liability or responsibility for the accuracy, completeness, or usefulness of any information, apparatus, product, or process disclosed, or represents that its use would not infringe privately owned rights. Reference therein to any specific commercial product, process, or service by trade name, trademark, manufacturer, or otherwise does not necessarily constitute or imply its endorsement, recommendation,

or favoring by the United States Government or any agency thereof. The views and opinions of authors expressed herein do not necessarily state or reflect those of the United States Government or any agency thereof.

References

- Pavlish, J.H., Sondreal, E.A., Mann, M.D., Olson, E.S., Galbreath, K.C., Laudal, D.L., and Benson, S.A. (2003) *Fuel Process. Technol.*, **82**, 89.
- Biermann, J.J.P., Higgins, B., Wendt, J.O.L., Senior, C.L., and Wang, D. (2006) Mercury reduction in a coal fired power plant at over 2000 F using MinPlus sorbent through furnace sorbent injection. Electric Utilities Environmental Conference, Tuscon, AZ, 2006..
- Johnson, J. (2001) *Chem. Eng. News*, **79**, 18.
- Strivastava, R. (2010) Control of Mercury Emissions from Coal Fired Electric Utility Boilers. EPA/600/R-10/006, National Risk Management Research Laboratory, Air Pollution Prevention and Control Division, Research Triangle Park, NC.
- Madsen, J., O'Brien, T., Rogers, W., and Cugini, A. (2004) Computational modeling of mercury capture by activated carbon injection. DOE/NETL Mercury Control Technology R&D Program Review, Pittsburgh, PA.
- Wendt, J.O.L. and Lee, S.J. (2010) *Fuel*, **89**, 894.
- Biermann, J.J.P., Higgins, B., Hoeflich, P., and Ramme, B.W. (2006) Mercury reduction in coal fired power plants using MinPlus sorbent through furnace sorbent injection. Mega Symposium, Power Plant Air Pollutant Control Mega Symposium, Baltimore, MD, Vol. 1, p. 148.
- Granite, E.J., Myers, C.R., King, W.P., Stanko, D.C., and Pennline, H.W. (2006) *Ind. Eng. Chem. Res.*, **45**, 4844.
- Granite, E.J., Pennline, H.W., and Hargis, R.A. (1998) Sorbents for Mercury Removal from Flue Gas. US Department of Energy Topical Report DOE/FETC TR-98-01, Department of Energy.
- Granite, E.J., Pennline, H.W., and Hargis, R.A. (2000) *Ind. Eng. Chem. Res.*, **39**, 1020.
- Brown, T.D., Smith, D.N., O'Dowd, W.J., and Hargis, R.A. (2000) *Fuel Process. Technol.*, **65-66**, 311.
- Butz, J.R., Broderick, T.E., and Turchi, C.S. (2006) Amended Silicates™ for Mercury Control Project Final Report, DOE Award Number DE-FC26-04NT41988, Department of Energy.
- Novinda, B. Jr., (2013). Novinda's SO₃-tolerant Non-carbon Mercury Capture Reagent, <http://www.novinda.com/product-data/webinars/> (accessed 8 August 2013).
- Butz, J.R., Theis, G., and Moser, J. (2012) Full scale performance of mercury control with a non-carbon reagent, paper #123. *Proceedings Mega Symposium 2012*, CSC Publishing, Baltimore, MD.
- Gallup, J. and Hutson, N. (2004) Getting mercury out of coal combustion gases. *EPA Region 5 Science Forum*, EPA, Chicago, IL.
- Lovell, J.S., Turchi, C.S., and Broderick, T.E. (2007) Regenerable high capacity sorbent for removal of mercury from flue gas. Int. Cl. B01J 21/16, 27/02, 27/053, 23/08 ed., Office, U. S. P., Ed., ADA Technologies, Inc., United States.
- Butz, J.R., Lovell, J.S., Broderick, T.E., Sidwell, R.W., Turchi, C.S., and Kuhn, A.K. (2003) Evaluation of amended silicate sorbents for mercury control, paper 79. *Combined Power Plant Air Pollutant Control Mega Symposium*, Air & Waste Management Association, Washington, DC.
- Butz, J.R., Brown, C.H., Bernardo, B.N., and Henderson, T.N. (2012) Demonstrations of amended silicates for mercury control in coal fired generating units. PowerGen 2012, Orlando, FL, December 11–13, 2012..

19. Butz, J.R., Broderick, T.E., and Turchi, C.S. (2006) Trial of amended silicates for mercury control at miami fort station. Mercury Control Technology Conference DOE/NETL, December 11–13, 2006..
20. Laudal, D.L. (2006) Evaluation of an Amended Silicates, LLC, Mercury Sorbent Using Mercury Continuous Emission Monitors as Part of a Full-Scale Demonstration - Final Report, Energy & Environmental Research Center, November 2006.
21. Biermann, J., Bleijerveld, R., Voogt, N., and Hulscher, H.J. (2007) A method of preparing a puzzolanic material from paper residue and a method for the manufacture of cement from said material. Candian Intellectual Property Office, Int. Cl. C04B 18/10, B01J 6/00, C04B 2/06, C04B 7/12 ed., Office, C. I. P., Ed., MinPlus Holding B.V., Canada.
22. Voogt, N. and Biermann, J.J.P. (1999) Method of manufacturing a sorbent, a sorbent obtained by such a method, and method of cleaning a stream of hot gas. Canadian Intellectual Property Office, Int. Cl. B01J 20/16, B01D 53/02, B01D 53/50, B01D 53/64, B01D 53/70, B01J 20/30 ed., Office, C. I. P., Ed., CDEM Holland B.V., Canada.
23. Biermann, J.R. and Voogt, N. (2008) Method for the removal of mercury from a gas stream. United States Patent Application Publication, Int. Cl. B01D 53/64, B01D 53/02, B01J 20/04, B01J 20/12, B01J 20/16 ed., Office, U. S. P., Ed., MinPlus Holding B.V., United States.
24. Biermann, J.J.P. (2012) Method for the removal of mercury from a stream of flue gas obtained from the combustion of coal. US Patent 13/457,986, United States Patent Application Publication, Int. Cl. B01D 53/02 (2006.01) ed., Office, U. S. P., Ed., Biermann, Joseph J.P., United States, Vol. US 20120266751A1.
25. Biermann, J. and Wendt, J. (2010) SiO₂ and fly-ash effects on the efficacy of MinPlus sorbents for Hg capture. Electric Utilities Environmental Conference, Phoenix, AZ..
26. Lee, S.J., Wendt, J.O.L., and Biermann, J. (2009) *Asia-Pac. J. Chem. Eng.*, **5**, 259.
27. Wendt, J.O.L., Lee, S.J., and Blowers, P. (2009) Sorption Mechanism for Mercury Capture in Warm Post-Gasification Gas Clean-Up Systems - Experimental and Computational Studies, Final Report, Department of Energy, University of Arizona, <http://www.osti.gov/scitech/biblio/962689> (accessed 11 July 2014).
28. Biermann, J., Voogt, N., Sorooshian, A., Wendt, J., Merritt, R., and Gale, T. (2003) In-flight capture of elemental and oxidized mercury in coal combustion flue gases by a novel mineral sorbent between 320 and 1540 F (160 - 840 C). Mega Symposium..
29. MinPlus-CDEM (2013) <http://www.cdem.nl/node/27> (accessed June 2013).
30. Hammel, C. (2004) *Power*, **148**, 60.
31. Boren, R.M. (2004) Mercury removal results from two coal-fired utility boilers. NETL/DOE Mercury Control Technology R&D Program Review.
32. Pahlman, J.E., Carlton, S.C., Huff, R.V., Hammel, C.F., Boren, R.M., Kronbeck, K.P., Larson, J.E., Tuzinski, P.A., and Axen, S.G. (2003) Int. Cl. B01D 53/60 ed., Office, U. S. P., Ed., Enviro-Scrub Technologies Corporation, Vol. US006610263B2.
33. Hammel, C.F., Tuzinski, P.A., and Boren, R.M. (2006) Pretreatment and Regeneration of Oxides of Manganese. U. S. P. Office. United States, EnviroScrub Technologies Corporation, Bloomington, MN (US).
34. Pahlman, J.E., Pahlman, K., Carlton, S.C., Huff, R.V., Hammel, C.F., Boren, R.M., Kronbeck, K.P., Larson, J.E., Tuzinski, P.A., and Axen, S.G. (2005) System and process for removal of pollutants from a gas stream. US Patent 10,382,348, Int. Cl. B01D 53/43 ed., Office, U. S. P., Ed., Enviro-Scrub Technologies Corporation, United States.
35. Harris, L.E., Boren, R.M., and Hammel, C.F. (2005) NETL/DOE Mercury Control Technology R&D Program Review, NETL.
36. Dickinson, R.G. and Sherrill, M.S. (1926) *Proc. Natl. Acad. Sci. U.S.A.*, **12**, 175.
37. Gunning, H.E. (1958) *Can. J. Chem.*, **36**, 89.
38. Pertel, R. and Gunning, H.E. (1959) *Can. J. Chem.*, **37**, 35.

39. McDonald, C.C., McDowell, J.R., and Gunning, H.E. (1959) *Can. J. Chem.*, **37**, 930.
40. Moore, H.R. and Noyes, W.A. (1924) *J. Am. Chem. Soc.*, **46**, 1367.
41. Pierce, W.C. and Noyes, W.A. (1928) *J. Am. Chem. Soc.*, **50**, 2179.
42. Strausz, O.P. and Gunning, H.E. (1961) *Can. J. Chem.*, **39**, 2244.
43. Cline, J.E. and Forbes, G.S. (1941) *J. Am. Chem. Soc.*, **63**, 2152.
44. Granite, E.J., Pennline, H.W., and Hoffman, J.S. (1999) *Ind. Eng. Chem. Res.*, **38**, 5034.
45. Granite, E.J. and Pennline, H.W. (2002) *Ind. Eng. Chem. Res.*, **41**, 5470.
46. McLarnon, C.R., Granite, E.J., and Pennline, H.W. (2005) *Fuel Process. Technol.*, **87**, 85.
47. Granite, E.J. and Pennline, H.W. (2003) Method for removal of mercury from various gas streams. US Patent 6,576,092, United States Patent Application Publication. U. S. P. Office. United States, The United States of America as represented by the U.S. Department of Energy, Washington, DC (US).
48. Presto, A.A. and Granite, E.J. (2007) *Environ. Sci. Technol.*, **41**, 6579.
49. Presto, A.A., Granite, E.J., and Karash, A. (2007) *Ind. Eng. Chem. Res.*, **46**, 8273.
50. Senior, C. (2013) *Dry Sorbent Injection for SO₃ and MATS Application*, CSC Publishing, http://www.solvair.us/SiteCollectionDocuments/articles/20130201_AIR_Pollution_Control.pdf (accessed 11 July 2013).
51. Kaluza, U. and Boehm, H.P. (1971) *J. Catal.*, **22**, 347.
52. Biswas, P. and Wu, C.Y. (1998) *J. Air Waste Manage. Assoc.*, **48**, 113.
53. Lee, T.G. and Hyun, J.E. (2006) *Chemosphere*, **62**, 26.
54. Shi, L., Alam, M.K., and Bayless, D.J. (2002) Mercury removal using titania-coated membrane collectors in electrostatic precipitators. 19th International Pittsburgh Coal Conference, University of Pittsburgh, Pittsburgh, PA, Vol. 19.
55. Wu, C.Y., Lee, T.G., Tyree, G., Arar, E., and Biswas, P. (1998) *Environ. Eng. Sci.*, **15**, 137.
56. Granite, E.J., King, W.P., Stanko, D.C., and Pennline, H.W. (2008) *Main Group Chem.*, **7**, 227.

22

Sorbents for Gasification Processes

Henry W. Pennline and Evan J. Granite

22.1

Introduction

Gasification is a process whereby coal can be decomposed into simpler compounds by reacting it with steam and oxygen at elevated temperatures and pressures. The major product compounds include hydrogen (H_2) and carbon monoxide (CO), which can both be used as a fuel or as building blocks for chemicals (see Chapter 8 also). In chemical production, the $H_2 + CO$ mixture, called *synthesis gas* or *syngas*, can be sent to a catalyst assembly to fabricate various chemicals. Gasoline, diesel fuel, substitute natural gas, and other organic chemicals can be produced in such an operation. In power generation, the $H_2 + CO$ mixture, sometimes referred to as *fuel gas*, can be combusted and expanded in a gas turbine before recovering the heat of combustion in what is called an *integrated gasification combined cycle (IGCC)* operation. In either of the above-mentioned cases, the product gas from the gasification process is in a reducing atmosphere and the mercury that was in the coal is typically in the elemental form. With respect to sorbents, mercury removal in the gasification process can occur at either elevated temperatures (149–371 °C; 300–700 °F) or at lower temperatures (ambient to 100 °C). The temperature range is dependent on the final use of the gasification products. In IGCC, elevated temperature removal is desired so that a higher thermal efficiency of the power generation scheme can be maintained. This requirement may not apply to synfuels production. In addition, global warming and the impact that carbon capture and sequestration may have on mitigation of the greenhouse gas carbon dioxide could have a role in determining the process conditions for the removal of mercury. Sorbents for mercury removal can be characterized by the material type, such as activated carbons, stable metal oxides, and noble metals. The mercury removal capabilities with limitations for different families of materials are discussed.

22.2

Background

A major concern for power systems that use coal as an energy source is the air emissions from the plant. Although certain air emissions are currently regulated in the United States, the emergence of new regulations for other pollutants is on the near horizon. On the basis of a 1998 Report to Congress, the Environmental Protection Agency (EPA) in 2000 had announced its finding that regulation of mercury emissions from utility steam generating units was necessary and appropriate [1]. In addition, the Clear Skies Initiative was proposed in 2002 to dramatically limit the emissions of mercury from coal-utilizing facilities [2]. Emission standards were proposed in 2003 but promulgation did not occur until late 2011. The development of mercury emission regulations will have a direct impact on coal-using power-generation facilities, both conventional steam generating systems as well as IGCC systems.

Gasification is an important strategy for increasing the utilization of abundant domestic coal reserves. Owing to the increase in thermal efficiency for IGCC systems and the potential ability to effectively capture and sequester carbon dioxide emissions, the U.S. Department of Energy envisions increased use of gasification in the United States over the next 20 years [3]. A near-zero emissions goal will be strived for with respect to pollutants, including mercury.

For the gasification process and, in particular, for IGCC, the characterization of the location of mercury within the plant is critical with respect to the eventual capture of the mercury. A total characterization of an advanced gasification technology was conducted in 1995 with Dow Chemical's Louisiana Gasification Technology Inc. [4]. Gas, liquid, and solid streams around the plant were measured for mercury. Although the mercury material closure was poor for the comprehensive study and significant advances in mercury sampling techniques have been made since the study, several important findings were established. The mercury material closure around the plant was poor, possibly suggesting that some of the measurements were in error or that an accumulation of mercury within the plant occurred. Of the gas-phase mercury, over 70% left the plant in the turbine exhaust flue gas.

Later, as part of EPA's Information Collection Request, Tampa Electric's Polk Power Station and PSI Energy's Wabash River Generating Station – both IGCC units – were characterized with respect to mercury air emissions (a full characterization of all streams was not conducted) [4, 5]. In this exercise, the Ontario-Hydro sampling technique was used to speciate the mercury in the flue gas after the turbine combustor. The important conclusions from this data-gathering effort were that near 60% of the mercury in the coal exited in the turbine combustion flue gas and the vast majority of the mercury in this flue gas was in the elemental form. From the information on these units and pertaining to the final disposition of the mercury in the present IGCC systems, it is speculated that a majority of mercury migrates through the system as elemental mercury and that the remainder of the mercury is probably accumulated within one of the scrubbing systems needed to

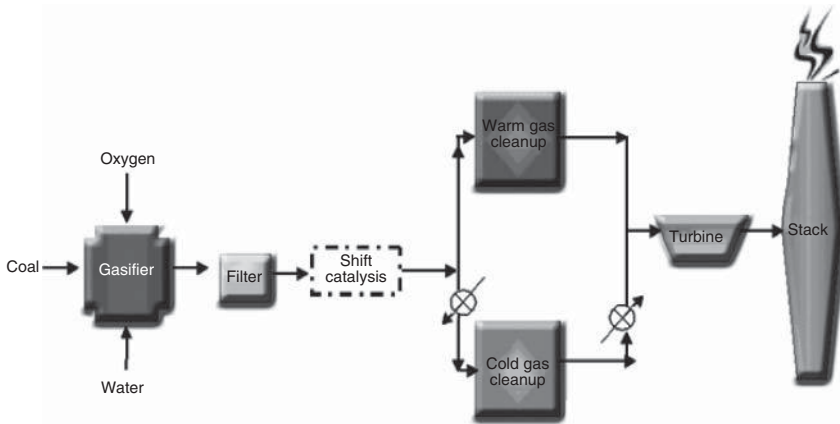


Figure 22.1 Simplistic flow schematic of an IGCC process.

clean the fuel gas before further processing it. In both these facilities, the fuel gas was cooled and then hydrogen sulfide was removed by a liquid solvent scrubbing technique before the gas was sent to the turbine combustor. Further evidence that the mercury in the fuel gas is mostly elemental can be found in gasification thermodynamic modeling or experimental studies [6–9].

Figure 22.1 is a rudimentary flow diagram of an IGCC installation with two options for gas cleanup. The lower path is similar to the one used at the Polk and Wabash Stations where a low temperature ($>38^{\circ}\text{C}$; 100°F) wet scrubbing technique, such as Selexol, is used to remove the hydrogen sulfide. The upper flow path in Figure 22.1 indicates the option where acid gas cleaning occurs within a warm gas cleanup (sometimes called *humid gas cleanup*) system rather than at the previously described cold (lower) temperatures. There are various reasons for opting for the warm gas mercury cleanup as compared to the cold gas cleanup. The main advantage in cleaning the gas in an IGCC application at higher temperature is that the thermal plant efficiency can be as much as 2–3% greater as compared to the lower temperature acid gas cleaning scenario. Provided the temperature is sufficient so that the dew point of the fuel gas is not approached, the moisture content in this warm/humid gas stream remains in the gas phase, as compared to the cold gas cleanup case, and can be used in the turbine expansion. Additional areas of efficiency improvements are that the transfer of heat and latent heat to the more efficient gas turbine cycle are maximized; the capital and operating costs are lowered by reducing the duty on any heat exchangers; and the need for waste water treatment facilities is eliminated [10, 11]. Note that a third option for mercury cleanup could be after the fuel is combusted in the gas turbine. However, the gas is expanded and thus a significantly greater volume of gas would need to be processed.

In addition to the improved IGCC plant thermal efficiency for warm gas cleanup, another reason is that the capability exists for removing a vast majority of the coal-inlet mercury at one location. As seen in the cold gas cleanup systems

at the Polk and Wabash Stations, a substantial amount of the inlet mercury within the feed coal was not accounted for. Although liquid streams were not monitored for mercury in the analysis, it is speculated that the lost mercury is probably within these streams. If mercury removal techniques could be implemented at the elevated warm gas temperature within the process at elevated pressure, then the potential issue of mercury appearing in condensate, wet scrubbing streams, and so on, is eliminated. The partial pressure and thereby the driving force of the gaseous mercury is also higher at the elevated pressure of the system. However, similar issues with potential mercury appearance in wet scrubbing streams occur if the mercury is collected after the combustion of the fuel gas in the turbine combustor exhaust stream. In addition, if Hg removal is left to after the fuel gas is combusted, a much higher volume of gas needs to be processed as compared to the precombustion pressurized case. Cost and equipment size considerations become important.

As in mercury mitigation from flue gas produced by the combustion of coal, the use of a sorbent is a feasible technique to remove mercury within a gasification process. The challenges are many. As mentioned, the temperature options may limit the type of sorbent. Activated carbons generally perform via adsorption of mercury and this is enhanced at a lower temperature as compared to the elevated warm gas temperature case. Conditions can be harsh depending on the location of the removal, as the sorbent could be exposed to various compounds at different concentrations, for example, hydrogen sulfide, moisture, hydrogen chloride, ammonia, and other trace components. Potential deactivation due to poisoning and sintering must be addressed. Although the challenges can be stringent, research in the sorbent area has progressed and thus the sorbents and operating information are addressed in the following sections.

22.3

Warm/Humid Gas Temperature Mercury Sorbent Capture Techniques

There is limited information available on the removal of mercury from high-temperature syngas streams, although there have been some contributions to the general knowledge since 2000. Results from a pilot-scale gasifier suggest that all of the mercury in the coal ends up in the fuel gas [7, 12]. The data from this pilot-scale gasifier suggest that activated carbon and other carbon sorbents will be unsuited for mercury capture from syngas at temperatures greater than 204 °C (400 °F) [7, 12]. Robust high-temperature sorbents, as well as other techniques, are needed for mercury capture from syngas for continued development and proliferation of gasification technology.

In the studies with the various warm gas sorbents, there are some commonalities with respect to the testing. Most of the sorbents tested are in the form of pellets or granular sized materials, although one group has used a monolith design. Sorbents are typically tested in a fixed bed. Elemental mercury permeation tubes are generally used to spike a known gas composition. In many cases, the

sorbent is envisioned as being a multipollutant absorber and besides the removal of mercury, other trace components within the synthesis/fuel gas are desired to be captured, that is, arsine, hydrogen selenide, and so on. Although there are online analyzers for mercury detection in flue gases produced by the combustion of coal, some modification needs to occur so that they can be used in fuel gas applications. Certain analytical techniques have been developed for some of the other trace compounds [13], but reliable continuous, standard, online analysis for mercury in reducing conditions needs to be established. In certain cases, analysis of solids for mercury after the sorbent testing has been used in the determination of the amount of mercury captured on the sorbent. Most studies would be considered laboratory- or bench-scale and have not progressed out of the laboratory setting. However, in certain investigations, the research was actually conducted with real synthesis gas produced from gasification facilities, such as the Power Systems Development Facility (PSDF) in Wilsonville, AL.

As to more mature development of a technology, TDA [14–16] has used their geode sorbent development for multicomponent control. In this novel sorbent design, pockets of active sorbent material are surrounded with a porous but hard, strong shell that provides a wear resistant pellet. This design is similar to a geode as it has a cavity with the desired crystals surrounded by a protective exterior. This structure is very strong because there is a continuous support phase; it effectively contains the sorbent inside small holes in the interior of the pellet, allows the sorbent to expand and contract freely without disrupting the pellet structure, and allows gases to diffuse quickly in and out of the pellet. Copper-based sorbent formulations have been used to remove trace contaminants from fuel gas streams, that is, arsenic [16]. Substrate materials included alumina, titania, or silica. The active material precursors and inert substrates were combined using the geode technology, enabling the incorporation of large quantities of active material into the final sorbent pellet, without plugging the pores of the substrate material and reducing its porosity.

Initial testing in a packed bed of pellets was conducted with simulated gas streams that were spiked with the trace contaminants. The mercury, arsenic, and selenium concentrations at the outlet of the reactor bed were continuously monitored with online analyzers. Breakthrough and saturation capacities of the sorbents were determined for temperatures between 160 and 260 °C and near 450 psig. Mercury capacities were high at the elevated temperatures, and the sorbent has a high capacity for arsenic even in the presence of high concentrations of sulfur. Experiments with multiple trace metals showed that the sorbent could simultaneously remove all these contaminants (mercury, arsenic, and selenium) from syngas in one step [14].

Demonstration tests using actual fuel gas from a gasifier were conducted at two locations: at the PSDF in Wilsonville, AL and at the University of North Dakota Energy and Environmental Research Center (EERC) where lignite and bituminous coals were the feed materials (see Figure 22.2). Overall, the test results indicated that the TDA sorbent was capable of removing multicontaminants in the coal-derived synthesis gas at high temperature. Mercury was successfully removed

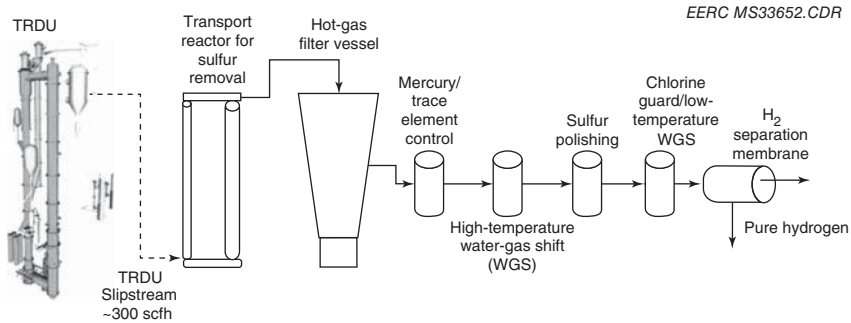


Figure 22.2 Schematic of demonstration unit at UNDEERC [15].

from the synthesis gas streams generated by different gasifiers using different coals at different sites and achieved greater than 95% Hg removal efficiency at 260 °C. This sorbent can be operated in a regenerable manner to remove Hg from the bed, while irreversibly removing all other trace metals including As, Se, and Cd with high capacity. From leaching tests, the fate of the mercury on the sorbent will remain on the sorbent once it is disposed [15].

The Gas Technology Institute (GTI) had developed the Ultra-Clean Process to control various pollutants from syngas, including mercury. The process injects fine sulfur and halide sorbent particles into two stages of barrier filter–reactors integrated in series, coupling efficient particle capture with an effective entrained and filter cake reaction environment. As can be seen in Figure 22.3, sulfur and halides are removed to extremely low levels by injection of various sorbents in the two stages, with the second stage temperature near 288 °C (550 °F). It is projected that for IGCC applications, the mercury removal could be a separate step or incorporated into the second stage of the process, and the mercury could be removed in the temperature range of 149–399 °C (300–750 °F), depending on the moisture content in the fuel gas [17].

Testing for mercury capture occurred in a packed bed reactor system using various simulated fuel gas mixtures and with a PSA Sir Galahad II analyzer. Materials that were tested were based on the oxides of copper, manganese, molybdenum, and zinc as well as mixed oxides and activated carbons. Some sorbents were purchased and others were made by GTI using a modified sol–gel technique or a wet impregnation method. The results with activated carbons were similar to other researchers in that elevated temperature hinders the adsorption of the mercury onto the carbon. With respect to the oxides, copper- and molybdenum-based sorbents, sulfidation of the sorbent is important in the mercury removal performance, possibly by altering the physical/chemical properties of the sorbent with a benefit for the higher loading of sulfur. In either case, the trend was that the effectiveness of the capture decreased as the temperature increased. In more recent work, nanocrystalline metal oxides/sulfides sorbents were evaluated in the temperature range of 150–260 °C, and again a temperature increase appears to have a negative impact on the mercury capacity of the sorbent [18].

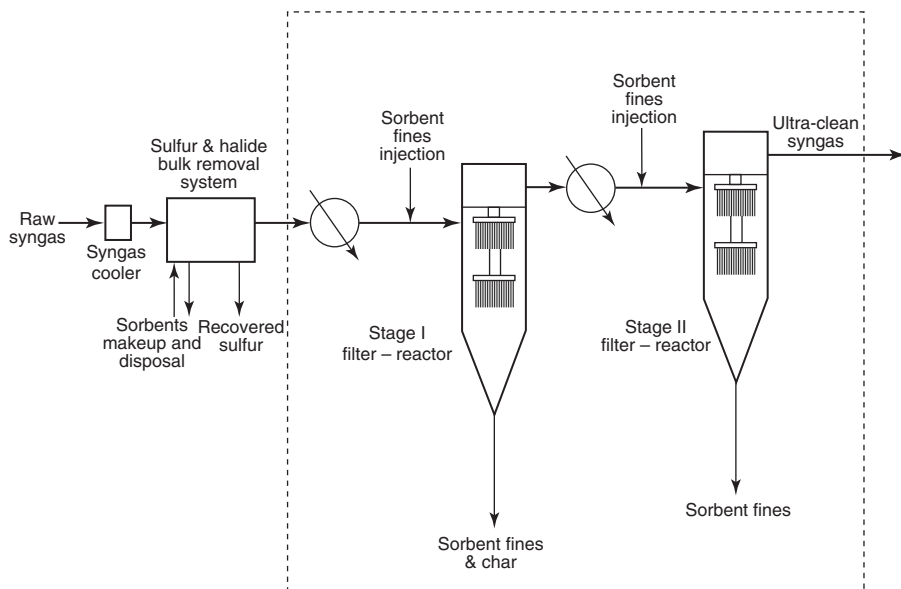


Figure 22.3 Ultra-Clean process flow diagram [17].

In a study conducted at the U.S. Department of Energy's National Energy Technology Laboratory (NETL), thermodynamic considerations followed by actual experimentation were used to screen candidates for mercury removal [19]. Interest was not only in mercury removal but also in the removal of selenium and arsenic. Samples were tested in a laboratory-scale reactor operating at ambient pressure, and capacities for mercury were calculated by flowing a known amount of mercury over the sorbent for a period of time (350 min) and having the spent sorbent solid chemically analyzed for mercury. Platinum and palladium were two candidates that had excellent capacities, even in the presence of simulated fuel gas with other components (hydrogen, carbon monoxide, carbon dioxide, hydrogen sulfide, and moisture). It was noted that the presence of these species impacts the adsorption of mercury as compared to testing under a spiked nitrogen flow. Mercury capacities remained appreciable in the 204–288 °C temperature range. As a noble metal is used, regeneration of the sorbent may be necessary and potential heat or chemical treatments are proposed to rejuvenate the spent sorbent [20].

In a collaboration between NETL and Johnson Matthey, further mercury capture studies with the palladium-alumina-supported sorbent were conducted with different metal loadings ranging from 2 to 9 wt% and over the temperature range of 204–388 °C [21]. The palladium-based sorbent performed better than the platinum-based one, and X-ray diffraction studies indicated a formation of solid solution of mercury within the palladium. Interestingly, a computational study that used *ab initio* methods based on density functional theory predicted material properties in which elemental mercury in the gaseous state would

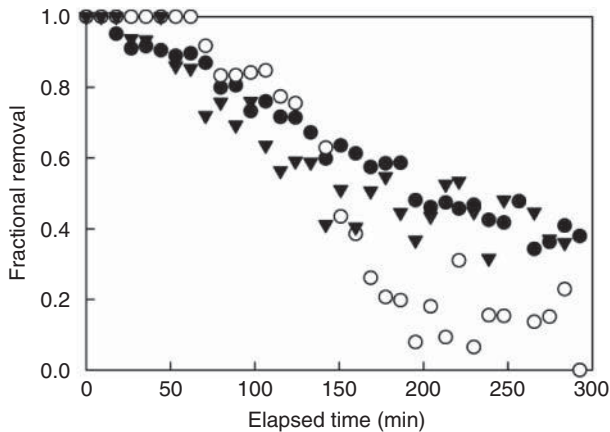


Figure 22.4 Fractional removal with time for 0.7 ppmv PH_3 , 2.5 ppmv AsH_3 , and 16.7 ppmv H_2Se removal on a 10 mg 5 wt% $\text{Pd}/\text{Al}_2\text{O}_3$ packed bed at 204 °C in the standard simulated fuel gas. Dark circle – AsH_3 ; open circle – H_2Se ; and triangle – PH_3 [23].

bind to a pure metal to form a binary amalgam [22]. The candidate materials for the highest amalgam formations were the noble metals, of which palladium was highlighted in the computational exercise. In later experimental studies, interest broadened for other contaminant materials to be removed in the fuel gas, including not only mercury but also arsenic, selenium, and phosphorus, which, in the reducing atmosphere, are in the forms of arsine, hydrogen selenide, and phosphine, respectively [23] see Figure 22.4). Tests were conducted using the same reactor system as before, but a gas chromatograph/ion trap mass spectrometer was used for detection of these other compounds [13]. Arsine, phosphine, and hydrogen selenide could be removed from the simulated fuel gas at warm gas cleanup temperatures with the palladium gamma-alumina sorbent.

For these laboratory-scale tests, exposure to the materials of removal interest is usually much larger than what the sorbent would see in an actual situation. This fact would make these sorbents even more amenable to removing trace pollutants as their capacities would most likely increase. Successful testing of the palladium sorbent at real conditions has occurred at the PSDF in Wilsonville, AL [24]. In the slipstream tests, a fixed packed bed of near 10 pounds of sorbent held at 260 °C removed nearly all of the selenium, arsenic, and mercury present within the fuel gas over several weeks. Additional tests with this sorbent in the PSDF have verified the removal capacities.

The University of North Dakota EERC has been investigating promoted monoliths in collaboration with Corning. The monolith is a honeycomb-shaped (parallel-channel) polymeric body with the major ingredient being phenolic resin, fabricated through extrusion, carbonization, and activation processes [25]. The polymer body is carbonized at an elevated temperature in an inert atmosphere, which converts the phenolic resin to graphitic carbon mixed with amorphous carbon domains. It is activated by the removal of the amorphous

carbon by reacting it with carbon dioxide at elevated temperature. Surface areas are typically around $500\text{-m}^2\text{ g}^{-1}$, and additives, such as sulfur, can be introduced before the extrusion step. In the testing rig, simulated fuel gas mixtures spiked with elemental mercury were flowed over the monolith at temperatures between 177 and 260°C and at elevated pressure. A modified PSA Sir Galahad was used to continuously monitor the mercury. Initial results with these monoliths and incorporating an undisclosed additive were successful in controlling mercury emissions, although with time online, some devolatilization of the mercury occurs but possibly due to the devolatilization of the additive.

Recent testing has also confirmed the ability of the monolith coated with an improved additive to remove mercury at a high level for an extended period of time (see Figure 22.2) [26]. Although the baseline testing occurs at 180°C , a test at 260°C (500°F) did show some decrease in the capacity of the sorbent for mercury removal. One Corning-treated monolith showed effective capture of mercury for over 150 h of testing at 180°C and was found to be very effective even at pressures up to 600 psig and temperatures up to 370°C . Additional testing of monoliths and sorbents with various additives revealed that these materials were able to remove other trace components in the fuel gas, that is, arsine and hydrogen selenide, at 204°C (400°F) [27].

RTI International is pursuing an approach to mercury removal that is analogous to the one used in their hot gas desulfurization from syngas, which is utilizing a chemically reactive sorbent. They realize that the thermodynamic efficiency of the IGCC cycle is improved if the thermal energy of the fuel gas can be preserved, and thus their sorbent-based desulfurization can be accomplished reliably at $260\text{--}316^\circ\text{C}$ ($500\text{--}600^\circ\text{F}$). Therefore, this temperature range is also targeted for their mercury removal [28].

The experimental approach taken was similar to that of King *et al.* [19]. Performance of the sorbent materials was based on the amount of mercury uptake as measured by offline analysis of the sorbent at the end of an exposure period. Initially, results with sorbents were reported by spiking a stream of nitrogen with elemental mercury. After a test protocol was established, candidate sorbents were typically exposed to the carrier gas/mercury vapor stream for 30-min at 572°F (300°C). Mixed metal oxide sorbents, both in sulfide and oxidized forms, were investigated along with commercially available materials. Some of the candidates performed quite well in removing the Hg from the gas stream, although a mechanism for capture was not discussed as the sorbents typically contained multiple components.

In a continuation of these studies [29], composite metal oxides were investigated along with proprietary sorbents and an impregnated activated carbon. The sorbents were selected on the basis of various factors, including surface area, predicted stability in the syngas matrix, expected material costs, and identification of materials that irreversibly bind with elemental mercury at the targeted temperature (typically near 300°C). The parameters of temperature and gas matrix were of interest with respect to mercury capacity. In general, screening results clearly favored lower temperatures as compared to the 300°C

baseline. At this temperature and exposed to Hg in nitrogen, the mixed metal oxide sorbents performed adequately. However, in a syngas with or without moisture and without hydrogen sulfide, these sorbents performed poorly. One potential explanation given was that the major syngas components chemically reduced the metal oxide components of the sorbents, thus decreasing the active oxide species responsible for the mercury retention. In addition, the presence of H₂S typically had a deleterious impact on the mercury capacity of the sorbents investigated.

The main thrust for the sorbents discussed was to remove mercury in the warm/humid gas range in an IGCC application. However, certain sorbents can be used in a more elevated temperature range beyond the warm/humid range. The University of Utah has worked with CDEM to demonstrate the MinPlus sorbent, which is an inorganic, mineral-based substance derived from a unique thermal process in which sludge from paper recycling is converted into the desired material [30]. The material serves as a special mineral additive to cement, and the primary constituents are limestone, meta-kaolinite, lime, inerts, and various trace components.

The sorbent was injected into a simulated gas flow in a dispersed-phase entrained bed reactor system. Overall mercury removal efficiency increased with increasing sorbent feed rate and with reaction temperature, suggesting an overall chemisorption mechanism. For the reactor configuration, an overall maximum Hg removal of about 83–90% was achievable at a temperature range of 900–1100 °C. The mercury removal was attributed to an in-flight mechanism as well as to one related to the deposition of the MinPlus sorbent on the reactor walls. It was shown that at 1100 °C, the sorbent ability to capture Hg was greatly diminished, possibly due to a change in composition and/or morphology of the initial material. The impact of the other components in fuel gas, especially hydrogen sulfide, was not discussed in the communication.

22.4

Cold Gas Cleanup of Mercury

From the previous discussion, mercury is most likely in the elemental form after the coal has been gasified. If not removed at elevated temperature in one location, the mercury can be impacted by various processes along the gas cleanup path as related to the final use of the fuel gas or syngas. It should be remembered that although there is a paucity of mercury information in actual commercial gasification systems, past information on actual IGCC units that use gas cleanup at cold temperatures indicate that not all the mercury is accounted for and leads to the speculation that some of the mercury may end up in some of the gas cleanup process streams. However, a substantial amount of mercury still remains in the fuel gas and would need to be removed. At low temperatures (<100 °C), it has been shown that activated carbon can remove the mercury. Other mercury sorbent

materials have also been investigated at these low temperatures. In addition, a wet scrubbing process has also been proposed.

22.4.1

Carbon-Based Materials

Eastman Chemical Company was the first company to operate a commercial coal gasification facility in the United States and has maintained greater than 98% availability for more than two decades [31]. Mercury removal has been commercially demonstrated in this gasification facility. Eastman has developed and successfully applied activated carbon-based mercury control technology at their facility located in Kingsport, TN. Eastman has been operating Chevron Texaco gasifiers at this facility since 1983 to provide syngas for the production of acetyl chemicals [4, 28]. Calgon's HGR-P sulfur-impregnated, pellet-activated carbon beds are utilized with the following performance characteristics:

- Operating conditions: Approximately 30 °C and 900 psi;
- Gas contact time in bed: Near 20 s based on total packed volume;
- Removal efficiency: 90–95%;
- Carbon lifetime: 12–18 months.

At the lower temperature of operation, this activated carbon technique can be considered proved and is the baseline technology for mercury removal. Various designs for gasification plants, more specifically IGCC, propose to use sulfur-promoted activated carbon beds for mercury control [32–34]. Once the efficiency price has been paid by cooling syngas to near 38 °C (100 °F), the incremental cost to remove other components is reduced because the gas cleaning occurs at essentially ambient temperature. Again, the challenge for fuel gas cleanup is to develop gas purification methods that do not require gas cooling that, in turn, lowers overall thermal plant efficiency.

Testing using activated carbons with actual fuel gas did occur at Tampa Electric's Polk Power Station [35]. A packed bed of sulfur impregnated activated carbon (Calgon HGR-P) was fed with a slip stream of syngas containing hydrogen sulfide. Mercury analyses of the gas and the solid followed. Although about half of the feed to the plant was petroleum coke rather than coal, over 90% of the mercury in the feed to the carbon bed was removed.

Various experimental studies with carbon-based materials have also been conducted and have resulted in similar findings. Reed *et al.* [7] obtained samples of fines that were collected in a hot gas filter following a gasifier. The composition of the material was primarily carbon with some sulfur, and the material was collected by a hot gas filter at 580 °C from a 2-MWt gasifier operated on a mixture of coal and sewage sludge. Although further work was needed, the sorbent was able to capture elemental mercury at temperatures below 200 °C, and significant mercury removal was observed at a temperature of 110 °C.

Spanish researchers [36] investigated the importance of sulfur promotion of an activated carbon. A Norit carbon (a peat-based, steam-activated carbon) was

the baseline, and this was impregnated with sulfur compounds to form a second sorbent candidate. Simulated syngas streams with a spike of elemental mercury were passed over beds of the materials. For the gasification case, a better retention of the mercury occurred with the sulfur-containing sorbent as compared to the baseline carbon sorbent, because it was speculated that chemisorptions and/or reaction between sulfur compounds and mercury may occur as compared to just physical adsorption. Surface chemistry was thought to be more important than porous texture in controlling mercury retention in activated carbons.

The impact of gaseous components within syngas was studied [37]. In this experimental study, an activated carbon made from coconut shell was investigated. A simulated syngas flowed over a packed bed of the material at atmospheric pressure and in the temperature range of 80–300 °C. The amount of HCl and H₂S in the gas stream could be varied along with the elemental mercury. It was found that the presence of HCl accelerated the mercury removal rate by the activated carbon. However, the presence of H₂S suppressed the mercury removal in the presence of HCl. The stabilities of the mercury species captured on the activated carbon depended on the presence of the acid gases HCl and H₂S. The effect of temperature was similar to the findings of others where, typically, an increase in temperature has a negative impact on the Hg adsorption capacity of the sorbent. In one of those studies, British researchers [38] investigated a commercial Norit Darco “Hg” activated carbon. Mercury spiked in nitrogen flowed over the packed bed of sorbent in the temperature range of 100–200 °C. As found previously, the capture efficiency is seen to decrease as the temperature is increased. It should be noted that this activated carbon had a high capacity for arsenic removal in the temperature range of 200–400 °C.

22.4.2

Other Materials

Various transition metal sulfides have been proposed as mercury sorbents for fuel gas. In one case, Japanese researchers [39] investigated iron-based sorbents where they envisioned the mercury removal unit to be located just before the wet desulfurization unit in the gas cleanup system. Experimentation was conducted in a thermogravimetric analyzer and packed bed where a simulated fuel gas was spiked with elemental mercury. Unsupported and supported iron oxides that were calcined to different temperatures were tested within the temperature range of 60–100 °C under atmospheric pressure. The effects of temperature and gas composition on the sulfidation of the iron oxides, mercury removal activity, and carbonyl sulfide (COS) formation were investigated. Results indicate that the fabrication of the sorbent, that is, calcination and support, plays an important role in its behavior. Sulfidation of the iron oxide decreased and COS formation decreased with increasing calcination temperature. With decreasing operating temperature, the mercury removal performance increased. For comparison, reagent grade FeS and FeS₂ were active for elemental mercury removal in the simulated fuel gas without forming any COS.

Copper-based mercury sorbents have also been proposed in a fuel gas application at 160 °C [40]. In addition, an effort to clean mercury using copper sulfide from a natural gas stream could have implications for synthesis/fuel gas cleanup. In this study [41], the concern was related to mercury in natural gas and its potential to cause corrosion of downstream aluminum heat exchangers as a result of amalgamation. The sorbent is a mixture of copper sulfide and other materials and was assumed to operate at ambient temperature. On the basis of experience with the material, various precautions were needed to get the sorbent bed up to standard operation, such as removal of oxygen from the inert purge gas during loading of the sorbent. Results indicate that the mercury reduction exceeded the expectations for this copper sulfide sorbent. These results are similar to a previous study [42] with CuS and its ability to remove elemental mercury below 90 °C, although that research effort was not conducted using an atmosphere of reducing gas that would be found in a fuel gas system.

A series of unpromoted and iodine-, bromide-, and/or sulfuric acid-modified chitosan/chitin sorbents were tested in a laboratory-scale fixed-bed reactor system [43]. Elemental mercury was spiked in nitrogen that contained moisture, and temperature of operation was varied from 40 to 135 °C. Although this mixture was to simulate a combustion flue gas, it could also be extrapolated as a simulated fuel gas. Promotion of the chitosan was deemed important with respect to mercury removal, and the presence of moisture can increase the modified chitosan sorbent capacity for mercury uptake. A better mercury uptake capacity and higher mercury removal efficiency occurred at 135 °C as compared to 40 °C and was thought to be associated with a chemisorption mechanism between mercury and the promoters within the sorbent.

Finally, the use of fly ash in mercury removal was investigated by Spanish researchers [44, 45]. In this particular case, fly ashes from different combustion sites were tested in a packed bed reactor by flowing a simulated fuel gas that contained elemental mercury at 120 °C. The mercury retention capacities on the fly ashes in the gasification atmosphere were similar to that found when just nitrogen was spiked with mercury. The nature of the fly ash is determinant in the control of mercury capture. In later studies [45], a temperature programmed decomposition was used to identify the species of mercury that were present on the spent sorbent. Mercury sulfides were determined to be present, and it would be expected in a gasification atmosphere that contained H₂S.

22.4.3

Wet Scrubbing Technique

Typical wet scrubbing processes for the removal of contaminants from fuel gas or syngas do not intentionally remove mercury, although there may be evidence that they unintentionally capture the mercury [28, 35]. One wet scrubbing process that was developed for multicontaminant removal in fuel gas was the University of California Sulfur Recovery Process at High Pressure or (UCSRP-HP) [46, 47]. Research at the University of California coupled with experimental work at

GTI led to the development of an integrated multicontaminant removal process, whereby syngas is sent to a reactor column at a temperature above the melting point and below the polymerization temperature of elemental sulfur at elevated pressure. Desulfurization occurs in the range of 285–300 °F and the process integrates the removal of trace contaminants and heavy metals. The countercurrent-flow reactor column is divided into two sections: a scrub section and the reactor section. In the reactor section, a stream of glycol ether, such as diethylene glycol methyl ether, is used to catalyze a reaction and form a liquid sulfur that can be separated from solvent. In the preceding scrub section, an aqueous glycol ether solvent, such as diethylene glycol, is used to remove hydrogen chloride and the heavy metals mercury, arsenic, and cadmium that will be absorbed to form their respective, very insoluble sulfides. Selenium will be absorbed to form highly soluble ammonium selenide under the conditions of operation. It was proposed that a small slipstream of the diethylene glycol stream be withdrawn for filtration and other treatment to remove the accumulated impurities, especially the mercury-containing one. Laboratory-scale tests indicated that 95% of the mercury could be removed with diethylene glycol as the solvent. Bench scale testing with coal-derived syngas has been proposed [47].

22.5

Summary

Gasification of coal for power generation and chemical production is projected to increase in the future. Many factors could impact this future market, such as the decreased consumption of domestic and foreign oil for chemical fabrication and the potential regulation of the greenhouse gas carbon dioxide. In any event, mercury emissions from gasification-based technologies in the United States will need to be controlled as mandated by law. Similar to post-combustion control of mercury, the use of sorbents is a necessity in the control of mercury. Along the gas cleanup pathway for gasification processes, it is beneficial to remove the mercury at one location and at elevated temperature. Various sorbent results have been discussed where this is applicable. In addition, sorbent investigations have been reported at lower temperatures. Because of the novelty of gasification-based processes and the more recent interest in mercury control, one sorbent-based process for mercury capture is not outstanding. Granted that activated carbon has been shown to be a valid technique at lower temperatures, one clear-cut sorbent technology does not stand out at the beneficial higher temperature of operation. More research and development in this fledgling area is needed.

Disclaimer

Neither the United States Government nor any agency thereof, nor any of their employees, makes any warranty, express or implied, or assumes any legal liability

or responsibility for the accuracy, completeness, or usefulness of any information, apparatus, product, or process disclosed, or represents that its use would not infringe privately owned rights. Reference therein to any specific commercial product, process, or service by trade name, trademark, manufacturer, or otherwise does not necessarily constitute or imply its endorsement, recommendation, or favoring by the United States Government or any agency thereof. The views and opinions of authors expressed herein do not necessarily state or reflect those of the United States Government or any agency thereof.

References

1. US EPA (2000) United States Environmental Protection Agency Mercury Web Site, www.epa.gov/mercury (accessed 20 March 2014).
2. US EPA (2002) United States Environmental Protection Agency Clear Skies Web Site, www.epa.gov/clearskies (accessed 20 March 2014).
3. DOE/NETL (2010) Carbon Dioxide Capture and Storage RD&D Roadmap, December 2010, <http://www.netl.doe.gov/sequestration> (accessed 20 March 2014).
4. Ratafia-Brown, J., Manfredo, L., Hoffman, J., and Ramezan, M. (2002) Major Environmental Aspects of Gasification-Based Power Generation Technologies. Final Report U.S. DOE Contract No. DE-AT26-99FT20101, US federal government, December 2002.
5. Kilgroe, J.D., Sedman, C.B., Srivastava, R.K., Ryan, J.V., Lee, C.W., and Thorneloe, S.A. (2002) *Control of Mercury Emissions From Coal-Fired Electric Utility Boilers: Interim Report Including Errata Dated 3-21-02*, EPA-600/R-01-109, NTIS, Springfield, VA.
6. Lu, D.Y., Granatstein, D.L., and Rose, D.J. (2004) Study of mercury from simulated coal gasification. *Ind. Eng. Chem. Res.*, **43**, 5400–5404.
7. Reed, G.P., Ergudenler, A., Grace, J.R., Watkinson, A.P., Herod, A.A., Dugwell, D., and Kandiyoti, R. (2001) Control of gasifier mercury emissions in a hot gas filter. *Fuel*, **80**, 623–634.
8. Galbreath, K.C. and Zygarrlicke, C.J. (1996) Mercury speciation in coal combustion and gasification flue gases. *Environ. Sci. Technol.*, **30**, 2421–2426.
9. Helble, J.J., Mojtahedi, W., Lyyranen, J., Jokiniemi, J., and Kauppinen, E. (1996) Trace element partitioning during coal gasification. *Fuel*, **75**, 931–939.
10. Pennline, H.W., Luebke, D.R., Jones, K.L., Myers, C.R., Morsi, B.I., Heintz, Y.J., and Ilconich, J.B. (2008) Progress in carbon dioxide capture and separation research for gasification-based power generation point sources. *Fuel Process. Technol.*, **89**, 897–907.
11. Gray, D., White, C., Plunkett, J., Salerno, S., and Tomlinson, G. (2006) Current and future IGCC technologies: bituminous coal to electric power. Proceedings of the 23rd Annual International Pittsburgh Coal Conference, Pittsburgh, PA.
12. Richaud, R., Lachas, H., Healy, A.E., Reed, G.P., Haines, J., Jarvis, K.E., Herod, A.A., Dugwell, D.R., and Kandiyoti, R. (2000) Trace element analysis of gasification plant samples by ICP-MS: validation by comparison of results from two laboratories. *Fuel*, **79**, 1077–1087.
13. Rupp, E.C., Granite, E.J., and Stanko, D.C. (2010) Method for detection of trace metal and metalloid contaminants in coal-generated fuel gas using gas chromatography/ion trap mass spectrometry. *Anal. Chem.*, **82**, 6315–6317.
14. Alptekin, G., Amalfitano, R., Dubovik, M., and Cesario, M. (2006) Sorbents for trace metal removal from coal-derived synthesis gas. Proceedings of the 23rd Annual International Pittsburgh Coal Conference, Pittsburgh, PA.
15. Alptekin, G.O. (2009) Novel Sorbent-Based Process for High Temperature Trace Metal Removal. Final Report,

- U.S. DOE Contract No. DE-FC26-05NT42460, US federal government, May 2009.
16. Alptekin, G.O. (2002) Removal of Catalyst Poisons from Coal Gasifier Effluents. Monthly Report, U.S. DOE Contract No. DE-FG03-01ER83308, US federal government, January 2002.
 17. Slimane, R.B., Jadhav, R., Pandya, K., Lau, F.S., Pratapas, J., Newby, R.A., and Jain, S.C. (2004) Sorbent-based syngas mercury removal in the ultra-clean process. Proceedings of the Natural Gas Technologies II Conference.
 18. Jadhav, R.A., Meyer, H.S., Winecki, S., and Breault, R.W. (2005) Evaluation of nanocrystalline sorbents for mercury removal from coal gasifier fuel gas. Proceedings of 2005 AIChE Annual Meeting, Cincinnati, OH, October 2005.
 19. King, W.P., Granite, E.J., and Pennline, H.W. (2003) A Review of Potential Sorbents for Mercury Removal from Fuel Gas. Topical Report DOE/NETL-2003/1192, US federal government, July 2003.
 20. Granite, E.J., Myers, C.R., King, W.P., Stanko, D.C., and Pennline, H.W. (2006) Sorbents for mercury capture from fuel gas with application to gasification systems. *Ind. Eng. Chem. Res.*, **45**, 4844–4848.
 21. Poulson, S., Granite, E.J., Pennline, H.W., Myers, C.R., Stanko, D.P., Hamilton, H., Rowsell, L., Smith, A.W.J., Ilkenhans, T., and Chu, W. (2007) Metal sorbents for high temperature mercury capture from fuel gas. *Fuel*, **86**, 2201–2203.
 22. Jain, A., Seyed-Reihani, S.A., Fischer, C.C., Couling, D.J., Ceder, G., and Green, W.H. (2010) Ab initio screening of metal sorbents for elemental mercury capture in syngas streams. *Chem. Eng. Sci.*, **65**, 3025–3033.
 23. Rupp, E.C., Granite, E.J., and Stanko, D.C. (2013) Laboratory scale studies of Pd/ γ -Al₂O₃ sorbents for the removal of trace contaminants from coal-derived fuel gas at elevated temperatures. *Fuel*, **108**, 131–136.
 24. Vimalchand, P., Morton, E.C., Datta, S., Lambrecht, R.C., Granite, E.J., Pennline, H.W., Stanko, D., Hamilton, H., Rowsell, L., Poulston, S., Smith, A., and Chu, W. (2009) Slipstream tests of palladium sorbents for high temperature capture of mercury, arsenic, selenium, and phosphorus from fuel gas. Presented at 2009 AIChE Spring National Meeting, Tampa, FL.
 25. Swanson, M., Dunham, G., Olson, E., Sharma, R., Musich, M., Shi, Y., Johnson, B., Hogue, L., and Tennant, J. (2006) Advanced mercury/trace metal control with monolith traps. Proceedings of the 23rd Annual International Pittsburgh Coal Conference, Pittsburgh, PA.
 26. Pavlish, J.H., Hamre, L.L., and Zhuang, Y. (2010) Mercury control technologies for coal combustion and gasification systems. *Fuel*, **89**, 838–847.
 27. Musich, M.A., Swanson, M.L., Dunham, G.E., and Stanislawski, J.J. (2010) Advanced Gasification Mercury/Trace Metal Control with Monolith Traps. Final Report, U.S. DOE/NETL Contract No. DE-FC26-05NT42461, US federal government, September 2010.
 28. Portzer, J.W., Albritton, J.R., Allen, C.C., and Gupta, R.P. (2004) Development of novel sorbents for mercury control at elevated temperatures in coal-derived syngas: results of initial screening of candidate materials. *Fuel Process. Technol.*, **85**, 621–630.
 29. Turk, B.S., Gupta, R.P., Gangwal, S., Toy, L.G., Albritton, R.R., Henningsen, G., Presler-Jur, P., and Trembly, J. (2008) Novel Technologies for Gaseous Contaminants Control. Final Report DOE/NETL Contract No. DE-AC26-99FT40675, US federal government, October 2008.
 30. Lee, S.J., Wendt, J.O.L., and Biermann, J. (2010) High-temperature sequestration of elemental mercury by noncarbon based sorbents. *Asia-Pac. J. Chem. Eng.*, **5**, 259–265.
 31. Blankinship, S. (2005) Mercury control now on the table. *Power Eng.*, **109** (5), 22–32.
 32. Provost, G.T., Erbes, M.R., Zitney, S.E., Phillips, J.N., McClintock, M., Stone, H.P., Turton, R., Quintrell, M., and Marasigan, J. (2008) Generic process design and control strategies used to develop a dynamic model and training software for an IGCC plant with CO₂

- sequestration. Proceedings of 2008 International Pittsburgh Coal Conference, Pittsburgh, PA, September 2008.
33. D'Ambrosi, F.D. and Jackson, R.G. (2006) Recent developments in modularized air-blown coal gasification systems for industrial applications. Proceedings of the 2006 International Pittsburgh Coal Conference, Pittsburgh, PA, September 2006.
 34. Casleton, K.H., Breault, R.W., and Richards, G.A. (2008) System issues and tradeoffs associated with syngas production and combustion. *Combust. Sci. Technol.*, **180**, 1013–1052.
 35. Steele, R.D., Ghani, J., and McDaniel, J. (2003) Monitoring and removal of mercury in a Texaco IGCC gasifier system. Presented at the Gasification Technologies Conference, San Francisco, CA, October 2003.
 36. Lopez-Anton, M.A., Tascon, J.M.D., and Martinez-Tarazona, M.R. (2002) Retention of mercury in activated carbons in coal combustion and gasification flue gases. *Fuel Process. Technol.*, **77-78**, 353–358.
 37. Uddin, M.A., Ozaki, M., Sasaoka, E., and Wu, S. (2009) Temperature-programmed decomposition desorption of mercury species over activated carbon sorbents for mercury removal from coal-derived fuel gas. *Energy Fuels*, **23**, 4710–4716.
 38. Charpentreau, C., Seneviratne, R., George, A., Millan, M., Dugwell, D.R., and Kandiyoti, R. (2007) Screening of low cost sorbents for arsenic and mercury capture in gasification systems. *Energy Fuels*, **21**, 2746–2750.
 39. Wu, S., Oya, N., Ozaki, M., Kawakami, J., Uddin, M.A., and Sasaoka, E. (2007) Development of iron oxide sorbents for Hg⁰ removal from coal derived fuel gas: sulfidation characteristics of iron oxide sorbents and activity for COS formation during Hg⁰ removal. *Fuel*, **86**, 2857–2863.
 40. Nunokawa, M., Kobayashi, M., Akiho, H., Yamaguchi, A., Tochiara, Y., Kawase, M., Ashizawa, M., and Ito, S. (2010) Development of dry gas cleaning system for biomass gasification power generation. *Trans. Jpn. Soc. Mech. Eng.*, **76**, 391–393.
 41. Baageel, O.M. (2010) Gas plant solves Hg problems with copper-sulfate absorbent. *Oil Gas J.*, **108**, 51–55.
 42. Martellaro, P.J., Moore, G.A., Peterson, E.S., Abbott, E.H., and Gorenbain, A.E. (2001) Environmental application of mineral sulfides for removal of gas-phase Hg⁰ and aqueous Hg²⁺. *Sep. Sci. Technol.*, **36**, 1183–1196.
 43. Zhang, A., Xiang, J., Sun, L., Hu, S., Li, P., Shi, J., Fu, P., and Su, S. (2009) Preparation, characterization, and application of modified chitosan sorbents for elemental mercury removal. *Ind. Eng. Chem. Res.*, **48**, 4980–4989.
 44. Lopez-Anton, M.A., Diaz-Somoano, M., and Martinez-Tarazona, M.R. (2007) Retention of elemental mercury in fly ashes in different atmospheres. *Energy Fuels*, **21**, 99–103.
 45. Lopez-Anton, M.A., Perry, R., Abad-Valle, P., Diaz-Somoano, M., Martinez-Tarazona, M.R., and Maroto-Valer, M.M. (2011) Speciation of mercury in fly ashes by temperature programmed decomposition. *Fuel Process. Technol.*, **92**, 707–711.
 46. Matonis, D., Meyer, H.S., and Leppin, D. (2006) Desulfurization of high-pressure gasified coal using the UC sulfur recovery process. Proceedings of the 23rd Annual International Pittsburgh Coal Conference, Pittsburgh, PA, September 2006.
 47. Meyer, H.S., Matonis, D., Tamale, T., Leppin, D., and Lynn, S. (2008) UCSRP-HP – an integrated multi-contaminant removal process for treating coal-derived syngas. Presentation at the International Pittsburgh Coal Conference, Pittsburgh, PA, October 2008.

Part VI
Modeling of Mercury Chemistry in Air Pollution
Control Devices

23

Mercury-Carbon Surface Chemistry

Edwin S. Olson

23.1

Nature of the Bonding of Mercury to the Carbon Surface

At low temperatures, elemental mercury is adsorbed to high-surface-area carbons by physisorption mechanisms. The term *physical adsorption* or *physisorption* implies a weak bond involving van der Waals or induced dipole forces between the mercury atom and the carbon surface. This means that the outer 6s electrons in the mercury atom, which are shielded from the nucleus by a lot of inner electrons, become polarized by dipole charges on the carbon surface so that they set up their own dipole moment, resulting in a dipole attraction to the carbon surface.

Although some early reports attributed mercury sorption at higher temperatures in air and flue gas to the physisorption mechanism [1], it is now understood that chemisorption is the primary mechanism in these conditions for mercury capture on carbon; elemental mercury becomes oxidized on the carbon and binds as a Hg(II) compound. Both spectroscopic and reactivity data provide compelling evidence for a chemisorption mechanism for mercury capture on carbons in flue gas at moderate temperatures. An early paper on mercury sorption on a nonimpregnated Saran carbon [2] showed an immediate and complete breakthrough of mercury at 150 °C in an air stream corresponding to a velocity/sorbent ratio of 2.5 l s⁻¹, indicating that physical adsorption cannot occur at this temperature. Later, using a stopped-flow reactor with activated carbons at temperatures in the range of 100–300 °C, Hall showed that the apparent reaction order for Hg⁰ sorption is half order in molecular oxygen [3]. Thus, the carbons are catalyzing the oxidation of mercury with oxygen as the primary oxidant. In a flow-through experiment with a nonimpregnated bituminous carbon at 140 °C in air at a slow flow rate (0.19 l s⁻¹), Krishnan *et al.* [4] observed an early breakthrough, but a gradual decrease in capacity. As there did not appear to be any effect of Hg⁰ concentration on the capture of Hg, the reaction was zero order with respect to Hg⁰ concentration. Thus, the limiting factor was the low number of active sites in the activated carbon. But why did Singha [2] not see any sorption? In more recent flow-through experiments at the EERC with granular carbon (Calgon

F400 or NORIT GAC1240) beds at 150 °C, we showed that at slow flow rates, the breakthrough time in nitrogen was instantaneous, but was significantly longer in air [5]. With F400 at fast flow rates, breakthrough was instantaneous for both gases; thus, there was clearly a space velocity factor in these experiments. Therefore, only at very slow flow rates can one see sorption occurring in air.

Further evidence for the formation of oxidized mercury on the carbon was obtained from desorption experiments. Heating the spent sorbent beds from a variety of experiments to temperatures over 200 °C resulted in release of mercury. Sometimes temperatures of 750 °C were needed to eliminate the mercury from the sorbent. Although the released mercury in these thermal experiments was mostly elemental, it is unlikely that any Hg^0 existed on the carbon, as Hg^0 volatilized easily at ambient temperatures in an air stream. When heated in a 10% hydrogen stream, the spent sorbents released mercury at 125 °C as Hg^0 . This is the reported temperature for reduction of Hg (II) compounds.

Some of the most conclusive evidence for chemisorption comes from an examination of the chemical form of mercury on the spent carbons using X-ray adsorption fine structure (XAFS) spectroscopy. XAFS is a powerful spectroscopic technique that can distinguish elemental and some of the oxidized mercury forms in a solid sample on the basis of the inflection point differences (IPDs) in the energy absorbance curve. Huggins *et al.* [6] showed that the mercury IPD of sorbents exposed to flue gas was not consistent with that of elemental mercury or with mercury bonded to oxygen. Rather, the IPD varied with gas composition and was consistent with a Hg(II) species bonded to a polarizable (soft) element such as chlorine, carbon, or reduced sulfur. This observation also rules out mercury compounds, such as HgO , HgSO_4 , or $\text{Hg}(\text{NO}_3)_2$, as well as bonds between Hg and surface oxygen groups, including phenoxide, lactone, or ketone groups that had been previously suggested as binding sites for mercury, and also most mineral surfaces, such as iron or other metal oxides, silicates, and carbonates. Organic and inorganic sulfides are rapidly oxidized to sulfonates and sulfates, respectively [7, 8] and these are also ruled out by the spectroscopic data [6], as they bind via the oxygen rather than the sulfur(VI). When a sorption experiment was carried out with moisture present, but no flue gas, the IPD data for the mercury line indicated that the mercury was bonded to at least one oxygen [9], so there is more than one possible structure resulting from chemisorption, depending on the oxidant, type of sorbent, or conditions, and this structure might include bonds to some combination of carbon, sulfur, oxygen, or halogen.

23.2

Effects of Acid Gases on Mercury Capacities on Carbon

As discussed, activated carbons have little affinity for elemental mercury in air, but the sorption properties of the same carbons change drastically in flue gas. The interactions of the acid gases with the carbon surface determine the reactivity of the carbon to the mercury, as well as the capacity of the carbon for mercury.

The description of this interaction has provided valuable clues to the detailed mechanism of Hg chemisorption and binding on carbon.

An early study on acid gas effects with mercury on a carbon surface was that conducted by Young and Musich, with carbons exposed to gas-phase Hg also containing HCl and SO₂ [10].

Enhanced Hg sorption was observed in gas containing HCl. Because HCl is the major form of halogen in flue gas (see Chapter 7), at least at temperatures at which Hg capture occurs, we need to understand its role in the capture mechanism. Because HCl is not an oxidant, and Hg is oxidized on carbon in the absence of HCl [5], it is clear that neither HCl nor Cl₂ derived from HCl are necessary or independently responsible for oxidation of Hg on the surface.

Two studies published in 1998 [1, 11] pointed out some important effects of flue gas components on mercury sorption; however, many of these effects were not understood until the interactions were later investigated. A large factorial series of tests [12] using powdered activated carbon (Norit Americas flue gas desulfurization (FGD) carbon) was conducted at the EERC in a bench-scale system consisting of a thin fixed-bed reactor in gas streams (100–150 °C) containing 11–15 μg m⁻³ of Hg⁰ in various simulated flue gas compositions consisting of acidic (SO₂, NO₂, and HCl) gases plus a base mixture of N₂, O₂, NO, CO₂, and H₂O. The results of these experiments (breakthrough curves) showed that NO₂ or the combination of HCl plus O₂ is required for effective Hg⁰ capture, so these represent the primary oxidants or electron acceptors for mercury oxidation. Some acid gases had negative effects on mercury sorption, especially in combination. In one series of tests conducted with constant NO₂ concentration [13], increasing the SO₂ concentration gave shorter mercury breakthrough times (Figure 23.1). When SO₂ was omitted, no breakthrough occurred. In another series of tests at a constant SO₂ concentration, increasing the NO₂ concentration gave shorter mercury breakthrough times (Figure 23.2). Not only was SO₂ retarding the mercury capture, the retarding effect became more important as the NO₂ concentration increased. Thus, understanding of a very important interaction between NO₂, SO₂, and the Hg sorption began to develop. This strong interaction indicated that the NO₂ was oxidizing the SO₂ as well as the mercury on the carbon surface, and the resulting sulfur(VI) was inhibiting the mercury capture and causing the breakthrough. This effect was consistent with previous studies on the carbon-catalyzed oxidation of SO₂ [14]. The water in the flue gas was also needed for breakthrough to occur, which could be attributed to a requirement for the formation of sulfur(VI) [12].

The EERC work [12] also established that the Hg emitted after breakthrough (i.e., when there is no more net Hg sorption on the carbon) was mostly oxidized and can exceed inlet Hg concentration immediately following breakthrough. Olson showed that Hg emitted after breakthrough in the absence of HCl was Hg(NO₃)₂ [15], although in the presence of high HCl (50 ppm) concentrations, the emitted oxidized form is undoubtedly HgCl₂. This does not mean, however, that either of these two compounds has collected in the carbon before breakthrough. In fact, both forms easily desorb from an inert solid surface at 150 °C [16, 17], and so are not likely to be present on the carbon before breakthrough.

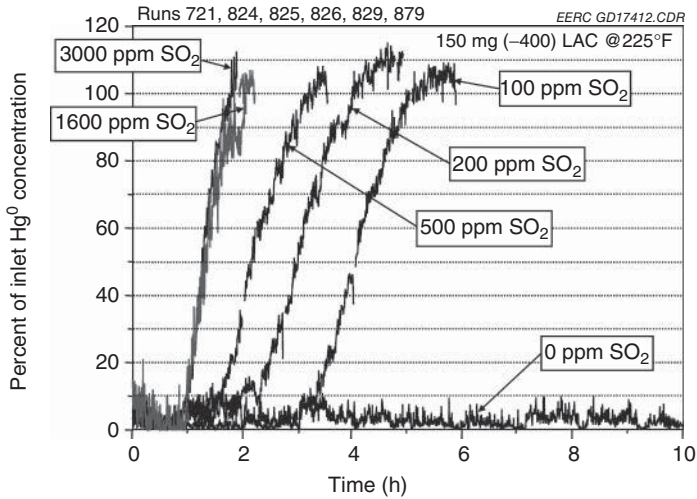


Figure 23.1 Mercury breakthrough curves for set of SO_2 concentrations with $15 \mu\text{g m}^{-3}$ Hg^0 , 50 ppm HCl, 300 ppm NO, 20 ppm NO_2 , and other baseline gases [13]. (Used with permission of the Energy and Environmental Center.)

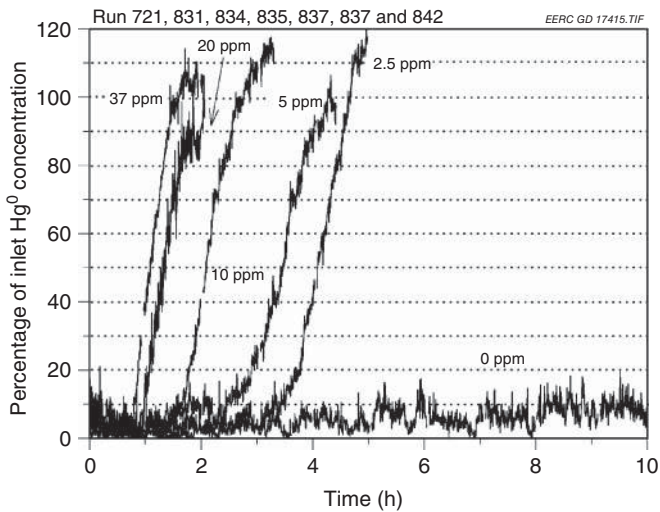


Figure 23.2 Mercury breakthrough curves for set of NO_2 concentrations with $15 \mu\text{g m}^{-3}$ Hg^0 , 50 ppm HCl, 300 ppm NO, 1600 ppm SO_2 , and other baseline gases [13]. (Used with permission of the Energy and Environmental Center.)

On the basis of these parametric studies and recognition that mercury is still converted to Hg(II) after breakthrough, an initial mechanism for chemisorption [18] that described the chemisorption mechanism as oxidation and competitive binding of the oxidized mercury with a catalytic carbon site or sites was presented. Oxidation of Hg^0 to form a bound Hg(II) species occurs with the electrons donated

to an electron-accepting (i.e., Lewis acid) site on the carbon. The electrons may be lost to NO_2 or O_2 the primary oxidants. Thus, the carbon plays a catalytic role, but the resulting oxidized mercury is bonded to the carbon structure. A donated electron pair results in formation of a carbon–mercury covalent bond, but this structure is labile, as the parametric tests revealed. An explanation for the SO_2 , NO_2 , H_2O inhibition of mercury capture is that the breakthrough behavior in the parametric tests was dominated by the competition for binding sites between the $\text{Hg}(\text{II})$ and acid components, mainly H_2SO_4 generated from the oxidation of SO_2 on the carbon, which continue to build up on the carbon surface during exposure to flue gas. When the binding sites are completely occupied by acidic species derived from the flue gas, $\text{Hg}(\text{II})$ salts are displaced from the binding sites. The equilibrium is shifted toward Hg salt release because of the high concentration and lower volatility of H_2SO_4 .

But mercury oxidation still occurs even after complete breakthrough. That is, oxidation occurs in the presence of the bound sulfuric acid, although not always at the same rate as the initial rate. The loss of capacity must not be the result of pore plugging by species resulting from acid gases, as this would stop both oxidation and binding. But pore plugging could slow the oxidation rate.

The competitive inhibition of Hg binding by S(VI) was further demonstrated by Presto and Granite [19]. Halogenated and nonhalogenated carbon samples exposed to SO_3 or impregnated with H_2SO_4 (10 wt%) showed significantly decreased mercury capacity. The effect of water and NO_2 in converting SO_2 on the carbon to sulfuric acid was also confirmed.

Carey *et al.* [1] showed that increasing the inlet Hg concentration resulted in increasing the capacity of the carbon. What is now understood is that the capacity is determined largely by the sulfur(VI) formation and this occurs at the same rate no matter what the mercury concentration is. As the number of active sites for oxidation is very large, the more inlet mercury there is, the more is captured until the binding sites are filled with sulfur VI. Fundamentally, the breakthrough sorption curves that were being drawn did not provide the equilibrium capacity of the sorbent for mercury; instead, they gave an indication of how fast the sorbent was being poisoned by sulfuric acid.

The extensive mineral matter (35%) of the Norit Americas FGD sorbent could contribute basic sites for Hg binding, but a sequential removal of the inorganic matter from the FGD sorbent did not significantly affect the breakthrough behavior [20]. Basic mineral groups, such as CaO present in the FGD sorbent, therefore played no role in the mercury–flue gas interactions that determine the breakthrough capacity. Actually, several activated carbons prepared from pure carbon precursors were perfectly good sorbents. This suggests that the bound Hg is actually an organometallic complex. However, sorption of HgCl_2 from a flue gas may not exhibit this exclusivity, because an oxidation site is not needed and any basic site on the sorbent may bind $\text{Hg}(\text{II})$.

Further evidence for a competitive binding mechanism for $\text{Hg}(\text{II})$ and flue-gas-derived components at a carbon site was provided in a series of studies carried out at the EERC, in which carbons were exposed to various combinations of flue

gases representative of high Cl coals for different times and the spent carbons were analyzed by X-ray photoelectron spectroscopy (XPS) [7, 8]. These studies verified that sulfur(VI) (sulfate, bisulfate, sulfonate, or sulfuric acid) was the major sulfur species on all the exposed sorbent samples, and the longer the exposure to SO_2 , the more sulfate was found in the sample. When NO_2 or H_2O was omitted from the flue gas, less sulfate accumulated. Thus, adsorbed SO_2 was clearly oxidized on the sorbent surface to sulfur(VI) species in a process facilitated by NO_2 and H_2O . Additional XPS work [8] with flue gas streams containing low concentrations of HCl typical of western coals, showed that organochlorine intermediates build up on the carbon surface and then disappear along with the bound mercury as the concentration of sulfuric acid increases. The XPS data also indicate that two types of chlorine are present: ionic and covalent, and that both chlorine forms disappeared from the sample at breakthrough. That chlorine is present as both chloride ion and covalent (organic) chlorine indicates that the HCl in the flue gas can donate a hydrogen ion to a basic site, as well as add both hydrogen and chlorine to a basic site to form the organochlorine product. The accumulation of chlorine in the absence of SO_2 as well as the disappearance of chlorine after continued exposure in SO_2 is explained by competition of HCl with bisulfate or sulfuric acid. As more H_2SO_4 is generated from SO_2 at the carbon surface, it displaces the more volatile HCl. Because disappearance of chlorine is coincident with mercury breakthrough, it is clear that Hg(II) is also in competition at the same site. Because of the interference caused by silicon, XPS data could not be obtained for the mercury species present in the exposed sorbents.

23.3

Kinetic HCl Effect

Although the early experiments revealed the nature of the competitive effects of flue gas components on mercury capacity, determining their role in the oxidative portion of the capture mechanism required further analysis. This information would be essential to designing sorbents with faster oxidation. The key to understanding the role of HCl in the oxidation mechanism was provided by testing of carbon sorbents in atmospheres containing low amounts of HCl. In parametric bench-scale tests conducted in very low HCl concentrations, such as those obtained when low-Cl coals (1 ppmv in the flue gas) are burned, the capture efficiency at the start of the run was low (about 50% of inlet concentration), followed by an increase in capture efficiency to the 90–95% capture rate [12]. This effect was also seen in breakthrough curves for a number of sorbents prepared from low-rank coals [21]. This behavior contrasts with the capture of mercury in relatively high HCl concentrations (50 ppm), where capture at the start was always very high (more than 95% of inlet concentration). The higher HCl concentration thus eliminated this induction period during which poor capture is obtained, and, therefore,

a promotional effect of the accumulating HCl on the activity of the carbon in catalyzing the oxidation of mercury was indicated. Ghorishi *et al.* [22] reported an increase in sorbent capacity as a result of pretreating the sorbent with aqueous HCl. Thus, consideration of the effects of HCl on Hg sorption curves led to a concept for understanding how the HCl promotes the mercury oxidation. This promotion was not because the HCl was directly involved in the oxidation, as it is in fact a highly reduced form of chlorine, and it is therefore not thermodynamically feasible to oxidize Hg with HCl.

The possible role of atomic chlorine in surface reactions was briefly examined. For HCl-promoted activated carbon (AC), Hg oxidation was not impeded by the presence of free radical scavengers, indicating that an alternative mechanism involving Cl atoms was not likely [23]. Furthermore, the addition of olefins (cyclohexene and styrene) to an HCl-treated carbon gave no substitution products, which would have resulted from abstraction of hydrogen by any Cl atoms present [24]. In contrast, the addition of HCl to the styrene occurred exclusively via the Markownikoff regioselectivity, indicating a cation mechanism. Thus, all four experiments indicated the absence of a radical or halogen atom pathway.

Several features of the oxidation site were inferred from the HCl promotion and bonding effects that led to development of a detailed chemical mechanism of mercury capture on the carbon surface [23–26]. This mechanism assumes a single carbon site for oxidation and binding but in two different forms and thus offers more detail on the nature of the bonding site and its interaction with flue gases and Hg. The mechanism, shown in Figure 23.3, used the concept proposed by Radovic and Bockrath [27] that zigzag carbene edge structures represent active sites for carbon reactivity. The mechanism for the catalytic role of acids, such as HCl, in the mercury oxidation step proposed addition of HCl and other acids to the carbene edge carbons to form carbenium chloride ion pairs (Lewis acid) that represent an oxidation site [26]. Reactions of the edge carbon with molecular halogens generate similar highly reactive carbenium structures. The

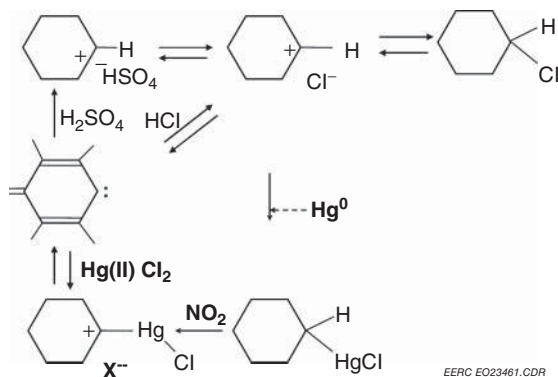


Figure 23.3 Oxidation mechanism – carbenium ion oxidant.

mechanism proceeds with Hg^0 oxidation by the carbenium halide ion pair to form an organomercury intermediate. This intermediate can be subsequently oxidized by NO_2 to a bound Hg^{2+} species. After breakthrough, HgCl_2 is continuously released as sulfuric acid competes for the site.

The oxidation of activated carbon is promoted not only by the addition of HCl , but any other acid, including small amounts of sulfuric acid [5, 24]. Comparative testing of a large number of acid-promoted ACs showed that they exhibit a specific acid catalysis, not a general acid catalysis. That is, those acids with polarizable counterions ($\text{HI} > \text{HBr} > \text{HCl}$) show faster initial rates compared with strong and weak oxyacids and fluoroacids [24]. This finding is consistent with a mechanism where the halide ion proximate to the cation actually can assist in the oxidation mechanism by stabilizing the incipient mercurinium ion forming in the transition state.

Later, the mechanism was somewhat modified to include the role of NO_2 in helping to promote the oxidation site [28]. The combination of HCl and NO_2 in the gas was a very effective promoter of mercury oxidation. The current thought is that multiple charges in the aromatic system may concentrate more of the positive charge and, thus, the oxidation potential at the protonated edge site [29, 30].

The number of active sites on a carbon-based sorbent can be estimated by determining the amount of accumulated sulfate at the time of Hg breakthrough, when essentially all of the binding sites are occupied by sulfate and unavailable for binding Hg . The amount of bound sulfate was calculated from the measured rate of SO_2 oxidation on Norit Americas Darco FGD [31] and the breakthrough time in a fixed-bed bench-scale test. This calculation gave 3.4 mol of potential sites per kilogram of carbon. The question in actual use of the carbon is how fast these sites are promoted to active status.

Early research [1] determined that mercury capacity was inversely related to temperature, and was incorrectly attributed to physisorption. A better explanation for the lower capacity in flue gas at higher temperature is that the rate of oxidation of SO_2 to sulfuric acid increases with temperature, so that the buildup of poisoning H_2SO_4 on the sorbent occurs at a faster rate. It may also be true in general that the rate of loss of HgCl_2 from the active sites is faster at high temperature than the rate of oxidation. This is not a true equilibrium as elemental mercury is going on the carbon and oxidized mercury is coming off. The question of temperature dependence of the oxidation was only recently answered. Comparisons of the initial capture efficiency (where kinetic rather than capacity effects predominate) in low- Cl gas at high and low temperature showed that Hg^0 was captured more effectively at the higher temperature. As the rate increases with temperature, the oxidation step is rate controlling and the physisorption reverse reaction is not of importance in controlling the rate. The implications of this finding for control technology are that when contact time is very short and reactivity is important, then higher temperatures will give faster oxidation rates for both mercury and SO_2 , but the effect of faster SO_2 reaction to sulfate is not important because binding sites are still abundant in the short time period. For sorbents

collected on a filter bag and in contact with the flue gas for a long time, the capacity will be greater at a lower temperature, because sulfate builds up more slowly at the lower temperature.

Halogenated carbons typically exhibit very high initial rates of mercury oxidation, with no induction period. So they are very effective in mercury capture in utilities where the contact time of the sorbent carbon and the gas phase in the duct is short. However, the capacity of the halogenated carbons may actually be less than that of the nonhalogenated carbons. Presto and Granite demonstrated that in a packed bed reactor with good gas–solid contact, bromination of the carbon does not increase the capacity [19].

Current work involves decoupling the oxidation from the binding steps so that effects of gas components on the oxidation step can be determined, and rate constants derived. These experiments utilize a sorbent bed that has broken through so that most of the inlet Hg^0 is oxidized by the bed in the flue gas, but no mercury is captured [31]. Then, by measuring the Hg^0 and total Hg in the effluent gas simultaneously for a matrix of experiments in which one, two, three, and four components are deleted or reduced, rates of oxidation, and changes in binding chemistry can be determined for each condition. Thus, removal of NO_2 resulted in a significant decrease in oxidation rate, but oxidation was still able to occur (pseudo first order $k = 1.41 \text{ s g}^{-1} \text{ sorbent}$) with O_2 and NO present. Removal of HCl from the gas composition decreased the oxidation rate, consistent with the specific acid catalysis mechanism, but, because oxidation still occurred, the oxidation can evidently occur via the sulfate-bound carbenium ion.

23.4

Summary

Several factors that determine the amount and rate of Hg capture on carbons have been described. Most important are (i) the competitive interactions of the flue gas components with each other and oxidized mercury on the carbon surface sites in determining mercury capacity on carbon and (ii) the interactions of the acid gases with the carbon surface in determining the reactivity of the carbon for oxidation of mercury. The description and understanding of these interactions has provided valuable clues to the mechanism of Hg chemisorption and binding on carbon. The key to understanding the role of HCl was the finding that sorption experiments conducted in low amounts of or no HCl experienced an induction effect, an initial period of time where the reactivity to Hg oxidation develops [5]. This finding led to the concept of acid promotion of a carbon site to form a carbenium ion that is highly reactive for oxidation, resulting in formation of an organomercury intermediate. The direction in sorbent research recently has been guided by the insight that more reactive or more selective oxidation sites can be generated by varying the carbenium ion structures that are formed.

References

- Carey, T.R., Hargrove, O.W., Richardson, C.F., Chang, R., and Meserole, F.R. (1998) *J. Air Waste Manage. Assoc.*, **48**, 1166.
- Singha, R.K. and Walker, P.L. (1972) *Carbon*, **10**, 754.
- Hall, B., Schager, P., and Weesmaa, J. (1995) *Chemosphere*, **30** (4), 611–627.
- Krishnan, S.V., Gullett, B.K., and Jozewicz, W. (1994) *Environ. Sci. Technol.*, **28**, 1506–1512.
- Olson, E.S., Miller, S.J., Sharma, R.K., Dunham, G.E., and Benson, S.A. (2000) *J. Hazard. Mater.*, **74**, 61–79.
- Huggins, R.E., Yap, N., Huffman, G.P., and Senior, C.L. (2003) *Fuel Process. Technol.*, **82**, 167.
- Laumb, J.D., Benson, S.A., and Olson, E.S. (2004) *Fuel Process. Technol.*, **85** (6–7), 577–585.
- Olson, E.S., Crocker, C.R., Benson, S.A., Pavlish, J.H., and Holmes, M.J. (2005) *J. Air Waste Manage.*, **55** (6), 747–754.
- Li, Y.H., Lee, C.W., and Gullett, B.K. (2002) *Carbon*, **40**, 65.
- Young, B.C. and Musich, M.A. (1995) *Prep. Fuel Div. Am. Chem. Soc.*, **40** (4), 833–837.
- Miller, S.J., Olson, E.S., Dunham, G. E., and Sharma, R.K. (1998) Air and waste manage. Association 91st Annual Management, San Diego, California, June 14–18, 1998, Paper 98-RA79B.07.
- Miller, S.J., Dunham, G.E., Olson, E.S., and Brown, T.D. (2000) *Fuel Process. Technol.*, **65–66**, 343–363.
- Dunham, G.E., Olson, E.S., and Miller, S.J. (2000) Task 2.1 – Value-Added Sorbent Development, Final Report for U.S. Department of Energy National Energy Technology Laboratory Cooperative Agreement No. DE-FC26-98FT40320, EERC Publication 00-EERC-07-05, Energy & Environmental Research Center, Grand Forks, ND, July 2000, <http://osti.gov/scitech/biblio/824975> (accessed 10, July 2014).
- Cofer, W.R., Schryer, D.R., and Rogowski, R.S. (1980) *Atmos. Environ.*, **14** (5), 571–575.
- Olson, E.S., Sharma, R.K., and Pavlish, J.H. (2002) *Anal. Bioanal. Chem.*, **6**, 1045.
- Olson, E.S. (2002) Annual Report, Center for Air Toxic Metals, Energy and Environmental Research Center, pp. 39–43.
- Rallo, M., Lopez-Anton, M.A., Perry, R., and Maroto-Valer, M.M. (2010) *Fuel*, **89**, 2157–2159.
- Olson, E.S., Laumb, J.D., Benson, S.A., Dunham, G.E., Sharma, R.K., Miller, S.J., and Pavlish, J.H. (2002) *Prepr. Pap. - Am. Chem. Soc., Div. Fuel Chem.*, **47** (24), 481.
- Presto, A.A. and Granite, E.J. (2007) *Environ. Sci. Technol.*, **41**, 6579–6584.
- Dunham, G.E., Olson, E.S., and Miller, S.J. (2000) Proceedings of the Air Quality II: Mercury, Trace Elements, and Particulate Matter Conference, McLean, VA, September 19–21, 2000, Paper A4-3.
- Pavlish, J.H., Holmes, M.J., Benson, S.A., Crocker, C.R., and Galbreath, K.C. (2002) Proceedings of Air Quality III, Mercury, Trace Elements, and Particulate Matter Conference, September 9–12, 2002.
- Ghorishi, S.B., Keeney, R.M., Serre, S.D., Gullett, B.K., and Jozewicz, W.S. (2002) *Environ. Sci. Technol.*, **36**, 4454–4459.
- Olson, E.S., Laumb, J.D., Benson, S.A., Dunham, G.E., Sharma, R.K., Mibeck, B.A., Crocker, C.R., Miller, S.J., Holmes, M.J., and Pavlish, J.H. (2003) Proceedings of the Air Quality IV: Mercury, Trace Elements, and Particulate Matter Conference, Arlington, VA, Sept 22–24, 2003.
- Olson, E.S., Mibeck, B.A., Benson, S.A., Laumb, J.D., Crocker, C.R., Dunham, G.E., Sharma, R.K., Miller, S.J., and Pavlish, J.H. (2004) *Prepr. Pap. - Am. Chem. Soc., Div. Fuel Chem.*, **49**, 6.
- Olson, E.S., Laumb, J.D., Benson, S.A., Dunham, G.E., Sharma, R.K., Mibeck, B.A., Miller, S.J., Holmes, M.J., and Pavlish, J.H. (2003) *J. Phys. IV France*, **107**, 979–982.
- Olson, E.S., Laumb, J.D., Benson, S.A., Dunham, G.E., Sharma, R.K., Miller,

- S.J., and Pavlish, J.H. (2003) *Prepr. Pap. - Am. Chem. Soc., Div. Fuel Chem.*, **48** (1), 30–31.
27. Radovic, L.R. and Bockrath, B. (2002) *Fuel Chem. Div. Prepr.*, **47** (2), 428.
28. Olson, E.S., Mibeck, B.A., Dunham, G.E., Miller, S.J., and Pavlish, J.H. (2009) *Prepr. Pap. - Am. Chem. Soc., Div. Fuel Chem.*, **54** (1), 236–238.
29. Azenkeng, A., Laumb, J.D., Jensen, R.R., Olson, E.S., Benson, S.A., and Hoffmann, M.R. (2008) *J. Phys. Chem. A*, **112**, 5269–5277.
30. Olson, E.S., Azenkeng, A., Laumb, J.D., Jensen, R.R., Benson, S.A., and Hoffmann, M.R. (2009) *Fuel Process. Technol.*, **90** (11), 1360–1363.
31. Olson, E.S. and Mibeck, B.A. (2005) *Prepr. Pap. - Am. Chem. Soc., Div. Fuel Chem.*, **50** (1), 68–70.

24 Atomistic-Level Models

Jennifer Wilcox

24.1

Introduction

Understanding the speciation of mercury throughout the coal-combustion process is crucial to the design of efficient and effective mercury removal technologies. Mercury oxidation takes place through combined homogeneous (i.e., strictly in the gas phase) and heterogeneous (i.e., gas–surface interactions) pathways. Both bench-scale combustion experiments [1] and quantum-chemistry-based theoretical model efforts [2, 3] indicate that homogeneous mercury oxidation is responsible for, at most, 10% of the overall oxidation in a typical coal-fired flue gas with chlorine levels at 500 ppmv (e.g., HCl equivalent). These studies have been additionally confirmed by recent work that compares model predictions to bench-scale experiments, with the simulation predictions dependent on previous kinetic submodels developed specifically for Hg oxidation [4, 5]. Mercury speciation in coal-fired flue gases are extremely complex and depend on many factors, some of which include the mineralogy and chemistry of the coal, combustion conditions, power plant configuration, flue-gas composition, and temperature-time history from the boiler to the stack.

The extent to which particulate-bound mercury (Hg_p), gaseous oxidized mercury (Hg^{2+}), and gaseous elemental mercury (Hg^0) are emitted from the stack is also dependent on the existing pollution controls in a given power plant. The effective removal of Hg through existing flue-gas control technologies acts as a co-benefit (as discussed elsewhere in this book). For instance, electrostatic precipitators (ESPs), in particular cold-side ESPs and hot-side ESPs, capture, on average, 27% and 4% of Hg, while fabric filters (FFs) are more effective with approximately 58% Hg removal [6]. In general, Hg_p or Hg^{2+} is easier to capture using one of these control technologies. In addition, oxidized Hg may also be captured in existing flue-gas desulfurization (FGD) units as the oxidized form is water-soluble. Activated carbon injection (ACI) is a direct method used for Hg capture, in which powdered activated carbon (PAC) is injected into the plant's flue-gas stream where it adsorbs gaseous Hg and is collected in downstream particulate control devices, such as FFs or ESPs. Heterogeneous investigations include both adsorption and

oxidation mechanisms associated with natural surfaces present in the flue gas such as fly ash, but also include surfaces associated with existing control technologies, such as selective catalytic reduction (SCR) catalysts or specific Hg-control technologies such as activated carbon (AC) or precious-metal sorbents and catalysts. The fundamental model investigations carried out to date may be classified into three major categories: homogeneous Hg oxidation kinetics, chemisorption on AC, and adsorption and amalgamation of Hg with precious metals.

24.2

Homogeneous Mercury Oxidation Kinetics

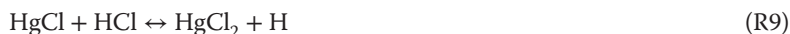
24.2.1

Mercury–Chlorine Chemistry

Gas-phase oxidation occurs primarily via chlorine species originally present in the coal as the gases cool down through the air preheater and air pollution control devices. Thermodynamic calculations predict that Hg oxidation occurs at temperatures below approximately 700 °C and that Hg will be completely oxidized at or below 450 °C [7]. Regardless of the thermodynamic equilibrium model predictions, experimental evidence has found that not all of the Hg is oxidized in the flue gas, regardless of the chlorine content of the coal. These experimental findings have led the Hg control community to determine that Hg oxidation is kinetically, rather than thermodynamically, limited [7]. For this reason, there has been significant investigation of determining accurate Hg oxidation kinetics from quantum-mechanical-based estimates because of the difficulty of the flue-gas measurements.

Some of the first studies to include quantum chemistry into the examination of the oxidation kinetics of Hg for flue-gas applications are those of Sliger *et al.* [8, 9], in which a homogeneous kinetic model for Hg oxidation via chlorine was determined and coupled with bench-scale combustion experiments. On the basis of these experiments, it was found that oxidation increases with increasing HCl concentration, which is consistent with previous experiments carried out by Hall *et al.* [10, 11] Adding to these initial investigations, the work of Wilcox *et al.* [12–14] and Krishnakumar and Helble [15] provide a fairly complete set of Hg oxidation kinetics via Cl-containing compounds for the following set of reactions:





Reactions 1, 2, 4, and 7 are all unimolecular decomposition reactions in the reverse direction and are often written in terms of a collision partner “M” on either side of the reaction. The collision partner is omitted here and as such the rate constants reported herein are in units of $\text{cm}^3 \text{ mol}^{-1} \text{ s}^{-1}$ for the forward directions and s^{-1} for the reverse directions. If the concentration of the collision partner is taken into account, the forward direction of the recombination reactions would have units of $\text{cm}^6 \text{ mol}^2 \text{ s}^{-1}$. The remaining reactions are classified as bimolecular with reported units of $\text{cm}^3 \text{ mol}^{-1} \text{ s}^{-1}$. A variety of quantum-mechanical-based approaches have been carried out to accurately predict the rate constants of R1–R10. As there are limited experimental data available for these reactions, especially at high temperature, the levels of theory employed have been benchmarked against available experimental structural and thermochemical data. A comparison of predicted to measured vibrational frequency and bond distance data is presented in Tables 24.1 and 24.2, respectively. The levels of theory considered in Tables 24.1 and 24.2 are based on previous high-level kinetics predictions that have relied on these combined methods and basis set choices. The methods that have resulted in the most accurate predictions include B3LYP, MP2, MP4, QCISD, QCISD(T), and CCSD(T), and have been used alongside a variety of basis sets. Owing to the large number of electrons in Hg [16], basis sets incorporating relativistic effects for the inner-core electrons are required. The work of Wilcox *et al.* on Hg oxidation via Cl-containing compounds has relied primarily upon two basis sets, that is, the “60VDZ” basis set of the Stevens *et al.* [17] group and the “60MDF” basis set of the Stuttgart [18] group. Both of these basis sets replace 60 of Hg’s atomic core electrons with a relativistic effective core potential. The work of Krishnakumar and Helble [15] has relied upon the “SDD” basis set for Hg, which uses Stuttgart [18] pseudopotentials, in addition to the “CEP-121G” basis set, which uses pseudopotentials developed from the Stevens [17] group. For the non-Hg species, either the D95++(3df,3pd) or the Pople 6-311++G(3pd,3df) basis set was used. Both of these basis sets include diffused and polarization functions on the O, Cl, Br, and H atoms. For the prediction of Hg oxidation via Br-containing compounds, Wilcox and Okano [19] used the augmented correlation-consistent basis set developed by Peterson *et al.* [20, 21], termed AVTZ.

Table 24.1 Comparison between experimental and theoretical vibrational frequencies (cm^{-1}) for various mercury-containing compounds.

Molecular species	Vibrational frequency (cm^{-1})		Level of theory ^{a)}
	Experiment	Prediction	
HgCl	292.61 [22]; 298.97 [23]	244.4	B3LYP/60VDZ
		280.6	QCISD(T)/SDD
		285.5	MP4/SDD
		290.3	QCISD/CEP-121G
		290.6	QCISD/60VDZ
		303.0	MP2/CEP-121G
HgBr	188.3 [24]	153.8	CCSD(T)/AVTZ
		162.7	B3LYP/60MDF
HgO	NA	390	QCISD(T)/60VDZ
HgCl₂ (symmetric stretch)	313–366 [25, 26]	318	B3LYP/60VDZ
		340	QCISD/60VDZ
(Bend)	100 [27]	92	B3LYP/60VDZ
		97	QCISD/60VDZ
(Asymmetric stretch)	376–413 [28]	374	B3LYP/60VDZ
		394	QCISD/60VDZ
HgBr₂ (symmetric stretch)	218–229 [29–32]	201	B3LYP/60MDF
		218	CCSD(T)/AVTZ
(Bend)	68 [27]	60	B3LYP/60MDF
		67	CCSD(T)/AVTZ
(Asymmetric stretch)	293 [33]	271	B3LYP/60MDF
		289	CCSD(T)/AVTZ

a) All predictions from Wilcox *et al.* [12–14, 19] with the exception of SDD and CEP-121G basis sets, which were sourced from Krishnakumar and Helble [15].

The predicted vibrational frequencies of the ground states of HgCl, HgBr, HgO, HgCl₂, and HgBr₂, have all been compared to experimental data, except in the case of HgO, in which experimental data was unavailable. There have been two experimental reports of the single vibrational mode of HgCl reported in the literature, that is, 292.61 [22] and 298.97 cm^{-1} [23] and a number of experimental investigations [25–28] on the vibrational modes of HgCl₂. From Table 24.1 it can be seen that the QCISD (CEP-121G, 60VDZ) and MP2/CEP-121G levels of theory agree best with experiment. In addition, the QCISD/60VDZ level of theory was also able to accurately predict the vibrational frequencies of HgCl₂. A number of experimental measurements [24, 27, 29–31, 33] have also been made on HgBr and HgBr₂, and a comparison of experiment to prediction shown in Table 24.1 indicates that the CCSD(T)/AVTZ level of theory is the most accurate.

Table 24.1 also includes a comparison of the predicted equilibrium bond distances to available measured data. Experimental measurements [34–36] of HgCl bond distances range from 2.23 to 2.50 Å. All of the levels of theory investigated predict bond distances within this range. The experimental bond distances [34, 38, 39] for HgCl₂ range from 2.25 to 2.44, and again, both levels of theory considered

Table 24.2 Comparison between experimental and theoretical bond lengths (Å) for various mercury-containing compounds.

Molecular species	Bond length (Å)		Level of theory ^{a)}
	Experiment	Prediction	
HgCl	2.23–2.50 [34–36]	2.40	MP4/SDD
		2.41	QCISD (CEP-121G; 60VDZ)
		2.48	QCISD(T)/SDD
		2.49	B3LYP/60VDZ
HgBr	2.62 [24]	2.62	MP2/CEP-121G
		2.64	B3LYP/60VDZ
		2.64	B3LYP/60MDF
		2.70	CCSD(T)/AVTZ
HgO	2.03 [37]	2.07	QCISD(T)/60VDZ
HgCl₂	2.25–2.44 [34, 38, 39]	2.30	QCISD/60VDZ
		2.32	B3LYP/60VDZ
HgBr₂	2.378 [40]	2.40	CCSD(T)/AVTZ
		2.46	B3LYP (60MDF; 60VDZ)

a) All predictions from Wilcox *et al.* [12–14, 19] with the exception of SDD and CEP-121G basis sets, which were sourced from Krishnakumar and Helble [15].

provide accurate predictions. The QCISD(T)/60VDZ level of theory predicts a bond distance of 2.07 Å for HgO, which agrees reasonably well with the experimental value [37] of 2.03 Å from X-ray diffraction measurements. The HgBr bond distance was measured by Tellinghuisen and Ashmore [24] using emissions spectra photography, with an estimated bond distance of 2.62 Å, which matches exactly with the predicted value from B3LYP/60VDZ. Experimental results of Deyanov *et al.* [40] yield an Hg–Br bond distance within the HgBr₂ molecule of 2.378 Å. In general, the CCSD(T)/AVTZ level of theory predicts both the HgBr and HgBr₂ geometries reasonably accurately, deviating from experiment by 0.08 and 0.03 Å, respectively.

In addition to the spectroscopic and structure comparison, the enthalpy changes of the reactions of interest have also been predicted and directly compared to available experimental data. Table 24.3 shows both thermochemical and kinetic parameter predictions along with available experimental estimates for reaction enthalpies. In particular, Reaction 1 has received a lot of attention because of the discrepancies reported in the literature and it has been established as the rate-determining step for homogeneous Hg oxidation. The rate constant has been measured experimentally by Donohoue *et al.* [41] using laser-induced fluorescence and by Horne *et al.* [42] using flash photolysis. An effective second-order rate constant of $4.57 \times 10^{11} \text{ cm}^3 \text{ mol s}^{-1}$ was calculated by Donohoue *et al.* from their reported Arrhenius expression at 260 K and 1 atm. Similarly, the second-order rate constant reported by Horne *et al.* at 393 K and 1 atm is $1.95 \times 10^{13} \text{ cm}^3 \text{ mol s}^{-1}$. There has been one quantum-based theoretic prediction for the rate constant of the forward recombination pathway of Reaction 1 by

Table 24.3 Comparison between thermochemical (reaction enthalpy) and kinetic (rate constant) parameters of mercury oxidation via chlorine-containing compounds over various levels of theory.

Reaction	Thermochemistry		Kinetics		Level of theory
	ΔH_{rxn} (kcal mol ⁻¹) Experiment [38]	Prediction	A (cm ³ mol s ⁻¹) Prediction	E_a (kcal mol ⁻¹)	
R1. Hg + Cl ↔ HgCl	-24.91	-25.41	2.34 ^a [11]	2.12	MP2/CEP-121G [15]
Reverse R1: HgCl ↔ Hg + Cl	24.91	25.27	2.42 ^b [8]	15.7	QCISD/60VDZ [14]
R2. Hg + O ↔ HgO	-4.00[43]; -8.92[44]; -13.97[39]; -64.22	-10.58	5.62 ^c [5]	3.03	QCISD(T)/60VDZ [13]
R3. Hg + Cl ₂ ↔ HgCl + Cl	33.07	31.79	6.15 [13]	43.3	B3LYP/60VDZ [12]
R4. Hg + Cl ₂ ↔ HgCl ₂	-51.63	33.00	4.52 [13]	35.9	QCISD/CEP-121G [15]
R5. Hg + HCl ↔ HgCl + H	78.24	-55.03	1.77 [5]	8.64	B3LYP/60MDF [13]
R6. Hg + HOCl ↔ HgCl + OH	31.21	79.00	1.93 [13]	93.3	B3LYP/60VDZ [12]
R7. HgCl + Cl ↔ HgCl ₂	-82.70	79.99	2.76 [15]	79.7	QCISD(T)/SDD [15]
R8. HgCl + Cl ₂ ↔ HgCl ₂ + Cl	-24.72	29.65	3.06 [13]	36.6	B3LYP/60VDZ [12]
R9. HgCl + HCl ↔ HgCl ₂ + H	20.46	30.69	2.69 [14]	31.8	QCISD(T)/SDD [15]
R10. HgCl + HOCl ↔ HgCl ₂ + OH	-26.60	-79.44	7.00 ^c [11]	8.567	B3LYP/60MDF [13]
		-83.79	2.02 ^d [10]	1.20	MP4/SDD [15]
		-24.32	1.43 [9] to 2.47 [10]	0	B3LYP/60MDF
		-24.33	5.18 ^e [4]	-3.40	B3LYP/MDF60 [15]
	20.46	20.50	1.95 [9]	24.9	QCISD/60MDF [14]
		20.50	2.49 [13]	24.9	B3LYP/MHF60 [15]
		-26.47	1.74 [9] to 3.48 [10]	0.5	B3LYP/60MDF
		-26.45	3.28 ^e [5]	0.3	B3LYP/MDF60 [15]

a) Temperature-dependent rate expression is $k = AT e^{-E_a/RT}$.

b) Units of A are in per second.

c) Temperature-dependent rate expression is $k = A \left(\frac{T}{298} \right)^{-n}$, with n listed in the E_a column.

d) Temperature-dependent rate expression is $k = AT e^{-E_a/RT}$.

e) Temperature-dependent rate expression is $k = AT^{2.4} e^{-E_a/RT}$.

Numbers in parentheses represent powers of 10.

Krishnakumar and Helble [15] at the MP2/CEP-121G level of theory, which is 3.77×10^9 and $1.52 \times 10^{10} \text{ cm}^3 \text{ mol}^{-1} \text{ s}^{-1}$ at 260 and 939 K, respectively. The reverse rate constant of Reaction 1 may be estimated on the basis of available experimental equilibrium constant as the equilibrium constant is equal to the ratio of the forward and reverse rate constants. The reverse unimolecular decomposition of HgCl was investigated by Wilcox *et al.* [14] at the QCISD/60DVZ level of theory with a prediction of $1.45 \times 10^4 \text{ s}^{-1}$, compared to the experimentally calculated estimate of $4.31 \times 10^3 \text{ s}^{-1}$, derived from the measurement of Horne *et al.* at 393 K and 1 atm. Both MP2/CEP-121G and QCISD/60VDZ levels of theory predict the heat of reaction for HgCl decomposition accurately to within 1 kcal mol^{-1} , as shown in Table 24.3.

For the HgO formation reaction (R2), both the forward and reverse rate constants have been predicted by Wilcox [13] at 1 atm and over a temperature range of 298–2000 K, with the kinetic parameters of the forward recombination reaction presented in Table 24.3. It is noted that the thermal decomposition temperature of mercuric oxide is 773 K. There are no experimental rate constant data to compare to, but the heat of reaction has been compared against previously reported theoretical and experimental estimates. Estimating the enthalpy of formation of HgO has received a great deal of attention in the literature, and this formation enthalpy is required for accurate estimation of the reaction enthalpy. Theoretical calculations [39, 43, 44] have reported enthalpies of formation ranging between 60.2 and 81.2 kcal mol^{-1} , with an experimental estimate [38] of 10 kcal mol^{-1} . The reaction enthalpy estimates are listed in Table 24.3 and range from -4.00 to $-13.97 \text{ kcal mol}^{-1}$ based on theory to $-64.22 \text{ kcal mol}^{-1}$ based on experiment. The QCISD(T)/60VDZ level of theory predicts an enthalpy of reaction of -10.58 , which agrees well with previous estimates and was used to determine the temperature-dependent rate constant parameters at 1 atm. Both thermochemical and kinetic parameters are available in Table 24.3 for Reactions 3–10, with the details of comparison and calculation available in the original work of these previous studies. The goal of these fundamental gas-phase sub-models is to provide kinetic data to global reaction models that would otherwise be deficient owing to the limited experimental data available over the flue-gas temperature range of interest.

Bench-scale simulated flue-gas experiments have been carried out by Fry *et al.* [45] and Cauch *et al.* [1] to accurately measure Hg oxidation as a function of quench rate. Fry *et al.* [45] carried out experiments to evaluate the effects of quench rate and quartz surface area on Hg oxidation and performed a detailed kinetic modeling analysis of homogeneous Hg oxidation reactions. In their system, Hg and Cl_2 are injected into a natural gas-fired premixed burner to produce a radical pool representative of real combustion systems and passed through a quenching section following the hot temperature region in the furnace as the quench rate of the flue gas can influence the extent of Hg oxidation. Two different temperature profiles were employed, producing quench rates of -210 and -440 K s^{-1} . The Hg concentration in the reactor was $25 \mu\text{g m}^{-3}$, while Cl_2 concentrations ranged from 100 to 600 ppmv (equivalent HCl concentration).

At Cl_2 concentrations of 200 ppmv, the larger quench rate resulted in a 52% increase in Hg oxidation compared to the lower quench rate. On the basis of kinetic modeling of the post-flame chlorine species, it was assumed that the Cl_2 molecules are converted to Cl radical species as they pass through the flame and then are subsequently converted predominantly to HCl. When investigating the effect of surface area of the quartz reactor, a threefold increase in surface area resulted in a 19% decrease in Hg oxidation, which is explained by the chlorine radical termination at the surface. It was concluded that quartz surfaces do not catalyze Hg oxidation reactions, but inhibit them, and that these surface interactions are negligible.

Recent experimental results of Cauch *et al.* [1] have shown that previously reported homogeneous Hg oxidation in the presence of chlorine may be exaggerated because of bias when using wet-chemistry measurement techniques. Linak *et al.* [46] have shown that Cl_2 , in a simulated flue gas in the absence of SO_2 , creates a bias in the Ontario Hydro method and overpredicts the concentrations of oxidized Hg. It has been shown that as little as 1 ppmv Cl_2 is enough to create a bias of 10–20% in the amount of oxidized Hg captured in the KCl solution. Within this study, the bias was eliminated by adding SO_2 to the flue gas or adding sodium thiosulfate ($\text{Na}_2\text{S}_2\text{O}_3$) to the KCl impinger. Similarly, Ryan and Keeney [47], in an actual flue-gas environment, have demonstrated that 10 ppmv Cl_2 added to the flue gas without SO_2 results in 91.5% oxidized Hg, with a decrease to 39% when the KCl impingers are spiked with sodium thiosulfate. A simulation study has been carried out by Gharebaghi *et al.* [4, 5] using the results from the experiments of Cauch *et al.* [1] with the corrected conditioning system to test the performance of the fundamental homogeneous Hg oxidation kinetics. Simulation of Hg speciation was carried out using the PREMIX module of the CHEMKIN II software package [48]. The Arrhenius parameters for the model predictions were taken from a combination of sources, with Reactions 1, 3, 5–10 included in the model in particular. The experimental rate constant determined by Donohoue *et al.* [41] was used for Reaction 1, model predictions from Niksa *et al.* [49] were used for Reactions 3 and 7, and quantum-level theoretical predictions were provided from Wilcox *et al.* [12, 14] for Reactions 5, 6, 8–10. Additional supporting mechanisms include chlorine chemistry from Roesler *et al.* [50], C/H/O mechanism by Dreyer *et al.* [51], and the Leeds SO_x and NO_x mechanism [52], resulting in a global combustion model of 80 species and 361 reactions. Figure 24.1 shows the results of the simulation predictions and their comparison to the bench-scale experiments of Cauch *et al.* [1]. The model provides reasonable agreement with the experimental data at the 440 K s^{-1} quench rate, but underpredicts the data at 210 K s^{-1} .

The experimentally derived activation energies and rate constants can have significant errors due to wall effects as well as uncertainties in the determination of mercury and its compounds down to parts per billion and lower levels in flue gas. Noting these potentially large experimental uncertainties introduced by heterogeneous chemistry occurring on the reactor walls, and the measurement uncertainties, the models appear to reasonably reflect the experimental data.

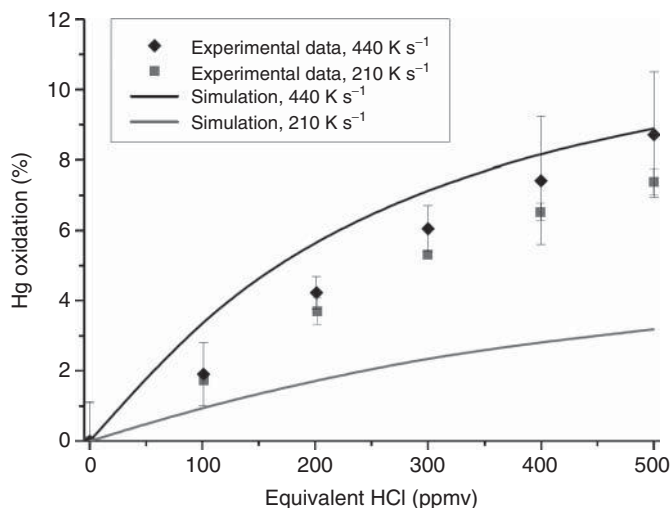


Figure 24.1 Error bars represent the standard deviation from analysis of multiple experiments.

24.2.2

Mercury–Bromine Chemistry

Significant attention has been paid to Hg oxidation via bromine, in addition to chlorine, because of the enhanced Hg oxidation kinetics of Br-containing compounds. Previous investigations report that bromine reacts faster than chlorine toward the production of HgBr_2 . Similar to the Hg oxidation reactions involving Cl-containing species, Gharebaghi *et al.* [4] have also simulated Hg oxidation based on the following reactions:



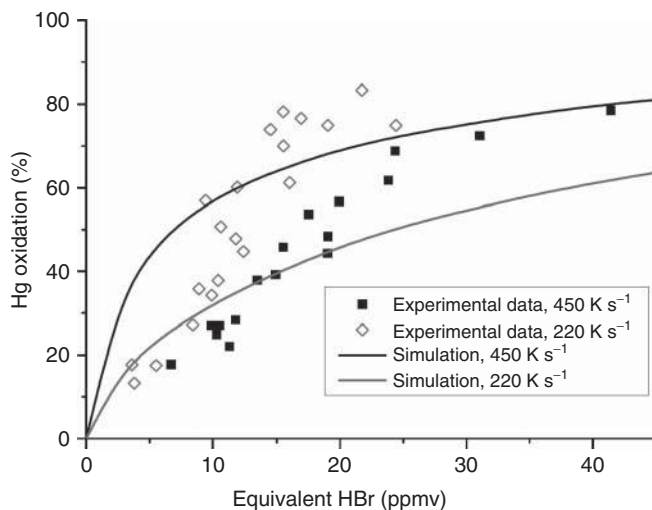


Figure 24.2 Comparison of measured and predicted Hg oxidation with HBr addition at two different reactor temperature quench rates [4].

Similar to the methodology previously discussed, Gharebaghi *et al.* [4] have used a variety of fundamentally derived rate parameters to simulate the global oxidation behavior of these reactions and have directly compared to experimental predictions of Cauch *et al.* [1], as shown in Figure 24.2. The rate parameters of Reaction 11 were taken from the experiments of Donohoue *et al.* [53] using laser-induced fluorescence, while the rate parameters of Reactions 14, 16, and 18 were taken from work carried out by Niksa *et al.* [54]. The rate parameters for Reaction 15 was calculated from first principles by Goodsite *et al.* [55], while the parameters for Reactions 12, 13, and 17 were provided by Wilcox and Okano [19] and are based on first-principle quantum mechanical calculations. Table 24.4 provides a fairly complete list of thermochemical and kinetic parameters associated with 8 of the 10 Hg–Br reactions of interest. In previous work, Wilcox and Okano [19] compared their predicted rate data of Reactions 11, 12, and 15 to available experimental [53, 56] and theoretical [55–60] data in the literature. In particular, the theoretical rate constant prediction of $3.84 \times 10^{11} \text{ cm}^3 \text{ mol}^{-1} \text{ s}^{-1}$ at the CCSD(T)/AVTZ level of theory for the forward direction of Reaction 11 agrees well with other theoretical [56–59] (ranging between 1.80×10^{11} and $1.92 \times 10^{12} \text{ cm}^3 \text{ mol}^{-1} \text{ s}^{-1}$) and experimental [53] (ranging between 1.08×10^{11} and $3.25 \times 10^{11} \text{ cm}^3 \text{ mol}^{-1} \text{ s}^{-1}$) estimates at 298 K and 1 atm. In addition, for Reaction 12, the theoretical rate constant prediction of $9.9 \times 10^{-8} \text{ cm}^3 \text{ mol}^{-1} \text{ s}^{-1}$ at the B3LYP/60VDZ level of theory for the forward direction agrees well with a slight underprediction compared to other theoretical calculations [60], which range between 1.96×10^{-7} and $3.25 \times 10^{-7} \text{ cm}^3 \text{ mol}^{-1} \text{ s}^{-1}$ at 298 K and 1 atm. Additional details are available in the manuscript of Wilcox and Okano [19].

Table 24.4 Comparison between thermochemical (reaction enthalpy) and kinetic (rate constant) parameters of mercury oxidation via bromine-containing compounds over various levels of theory.

Reaction	Thermochemistry		Kinetics		Level of theory [19]
	ΔH_{rxn} (kcal mol ⁻¹)		A (cm ³ mol s ⁻¹)	E_a (kcal mol ⁻¹)	
	Experiment [38]	Prediction	Prediction		
R11. Hg + Br \leftrightarrow HgBr	-16.51	-16.72	2.00 ^a [12]	1.91	B3LYP/60VDZ
R12. Hg + Br ₂ \leftrightarrow HgBr + Br	29.56	-15.74	4.00 ^a [11]	0.85	CCSD(T)/AVTZ
		31.59	1.15 [15]	30.08	B3LYP/60VDZ
R13. Hg + HBr \leftrightarrow HgBr + H	70.95	67.69	1.86 [13]	71.58	CCSD(T)/AVTZ
R15. HgBr + Br \leftrightarrow HgBr ₂	-72.02	-71.94	2.00 ^a [12]	9.18	B3LYP/60VDZ
		-70.13	8.00 ^a [10]	7.644	CCSD(T)/AVTZ
R16. HgBr + Br ₂ \leftrightarrow HgBr ₂ + Br	-25.95	-24.61	4.02 [11]	0.87	B3LYP/60MDF
R17. HgBr + HBr \leftrightarrow HgBr ₂ + H	15.44	14.28	9.41 [12]	18.68	CCSD(T)/AVTZ

a) Temperature-dependent rate expression is $k = A \left(\frac{T}{298} \right)^{-n}$ with n listed in the E_a column. Numbers in parentheses represent powers of 10.

The concentration of equivalent HBr was varied between 0 and 45 ppmv compared to a range of 0–500 ppmv of equivalent HCl as HBr dissociates more readily than HCl, resulting in a greater quantity of Br radicals for Hg oxidation. The homogeneous Hg oxidation model via bromine predicts that oxidation begins at a higher temperature than in the case of chlorine, at approximately 1100 K compared to 800 K (chlorine). The simulated results are in reasonable agreement with experiment for the 450 K s⁻¹ quench rate above 25 ppmv equivalent HBr, but overestimate oxidation at lower concentrations. On the other hand, for the 220 K s⁻¹ quench rate, the simulations underpredict oxidation at high temperature and show reasonable agreement at concentrations less than 10 ppmv equivalent HBr. Owing to the disagreement between the simulation predictions and experiments, it is clear that additional work is still required in this area. It is also noted that there is substantial uncertainty in the experimentally derived kinetic parameters.

From these previous combined modeling-experimental studies it is clear that homogeneous Hg oxidation is only one aspect of the complete mechanism in the complex flue-gas environment. In reality, surfaces are present in the form of unburned carbon, which may serve to both adsorb and oxidize Hg. Oxidized Hg may be captured in existing downstream wet FGD units and Hg^p may be captured via ESPs or FFs. Therefore, understanding the mechanism of Hg reactivity across carbon surfaces is imperative to its effective control.

24.3

Heterogeneous Chemistry

24.3.1

Mercury Adsorption on Activated Carbon

AC has been extensively tested in laboratory- and full-scale systems and has shown the capacity to capture both elemental and oxidized Hg in coal combustion flue gas. A relatively large amount of AC injection is required for the control of Hg from subbituminous-coal- or lignite-combustion flue gas. Depending on the system conditions, an AC-to-mercury mass ratio of at least 3000–20 000 (C/Hg) may be necessary to achieve 90% Hg removal [61–63]. Currently, the design of more effective Hg capture technology is limited by incomplete understanding of the mechanism(s) of Hg oxidation and adsorption on carbon surfaces [64].

The development of accurate fundamental models for Hg–AC reactivity requires careful characterization experiments on materials exposed to well-controlled reaction conditions. Therefore, an overview of such experiments will be discussed before the theoretical model efforts. It is generally accepted that acidic sites on the surface are responsible for elemental Hg capture on AC [65, 66]. In its atomic state, Hg acts as a base in that it has the propensity to oxidize (i.e., donates electrons to a surface or another gas-phase molecule); therefore, Hg will readily interact with acidic sites on the carbon surface. However, once oxidized, and thus acidic in nature, Hg species are thought to compete with acidic gases for the basic sites available on the carbon surface.

The presence of halogens (i.e., bromine, chlorine, and iodine) promotes Hg oxidation on carbon surfaces [66, 67]. Subsequently, AC demonstrates higher Hg removal performance in the flue gas of coals with greater chlorine content, as the combustion of such coal results in a higher concentration of HCl in the flue gas. Hutson *et al.* [68] exposed brominated and chlorinated AC to Hg-laden simulated flue gas and characterized the sorbents using X-ray absorption spectroscopy (XAS) and X-ray photoelectron spectroscopy (XPS). Within this work no evidence was found for homogeneous oxidation of Hg, and no Hg was found present on the AC surface; however, oxidized Hg was found on the surface, present as a chlorinated or brominated species. It is important to note that owing to the low coverage of Hg on the carbon, the speciation of Hg was not determined. Given the results, the authors proposed Hg capture on chlorinated and brominated carbons occurs via surface oxidation of Hg with subsequent adsorption on the carbon surface. Similar to its role in homogeneous Hg oxidation, bromine is thought to have a stronger promotional effect on Hg oxidation/adsorption, but the reason for the difference between bromine and chlorine is not well understood. Recently, the Hg oxidation was demonstrated on a wood-derived Cl-promoted AC in both N₂ and flue gas [69]. The adsorption of Hg on AC was shown to be a chemisorption process, where all Hg was oxidized to Hg²⁺ on the surface as a result of chlorine promotion. While chlorine was consumed, Hg²⁺ was still noted as being present in the outlet gas, indicating that the AC was also capable of catalyzing Hg oxidation.

Huggins *et al.* [70] characterized AC samples after testing in Hg-laden simulated flue-gas conditions using X-ray absorption fine structure (XAFS) spectroscopy. The XAFS results revealed that chlorine and sulfur are adsorbed on the AC surface after exposure to HCl and SO₂, and Hg-anion chemical bonds are formed in the sorbent materials. They suggest that the acidic flue-gas species (e.g., HCl, HNO₃, H₂SO₄) promote the creation of active sites for Hg chemisorption on the carbon surface, and that an oxidation process, either in the gas phase or simultaneously as the Hg atom interacts with the sorbents, is involved in the capture of Hg. Olson *et al.* [66] performed fixed-bed tests with various gas conditions for Hg and HgCl₂ adsorption on AC and found that the presence of both HCl and NO₂ reduced the induction period of Hg oxidation, and that in general acid flue-gas components significantly impacted the adsorption of oxidized Hg species. The formation and presence of the oxidized form, Hg(NO₃)₂, was observed in the effluent gas in the presence of NO₂, but in the absence of HCl. Laumb *et al.* [71] carried out surface analyses using XPS on ACs exposed to Hg-laden simulated flue gas (e.g., SO₂, NO₂, HCl, H₂O), but were unable to determine the oxidative state of surface-bound Hg due to interference with silicon (Si), which is present at comparable levels to Hg within the carbon matrix. Wilcox *et al.* [72] investigated the binding mechanism of Hg on brominated AC sorbents with a combination of XPS and theoretical modeling. It was found that Hg exists in the oxidized forms on brominated carbon surfaces, as shown in Figure 24.3.

Ab initio electronic structure investigations based on density functional theory (DFT) have been conducted to elucidate the interaction of Hg with AC, using simplified carbon models to represent AC. There have been a limited number of theoretical investigations, and, to the authors' knowledge, the effect of acid flue-gas species on Hg-AC interactions has not been investigated. AC is very difficult to model given its highly inhomogeneous structure. Several initial theoretical investigations have been conducted using cluster models to represent graphene, ranging from single benzene rings [73] to multiple fused rings [74] with embedded halogens as shown in Figure 24.4.

Carbon with Cl-containing functional groups exhibits enhanced Hg adsorption capacity. Furthermore, the most stable Hg surface species was HgCl, while Hg and HgCl₂ were found to be thermodynamically unstable on these simplified surfaces of AC [74]. Theoretical calculations by Olson *et al.* [76] supported the role of acidic sites on the AC in Hg capture. They hypothesized that HCl is energetically stable at the cationic zigzag edge sites of AC and proposed three possible models of Hg oxidation:

- 1) Hg charge transfer complex forms on the cationic center of HCl on AC and is subsequently attacked by Cl⁻,
- 2) elemental Hg interacts simultaneously with the cationic HCl-AC site and Cl⁻,
or
- 3) oxidation by the dictation site formed by HCl and NO₂ on AC.

Olsen *et al.* [76] suggested that Hg has the propensity to be oxidized by donating its electrons to a surface or another gas-phase molecule; therefore, in its elemental

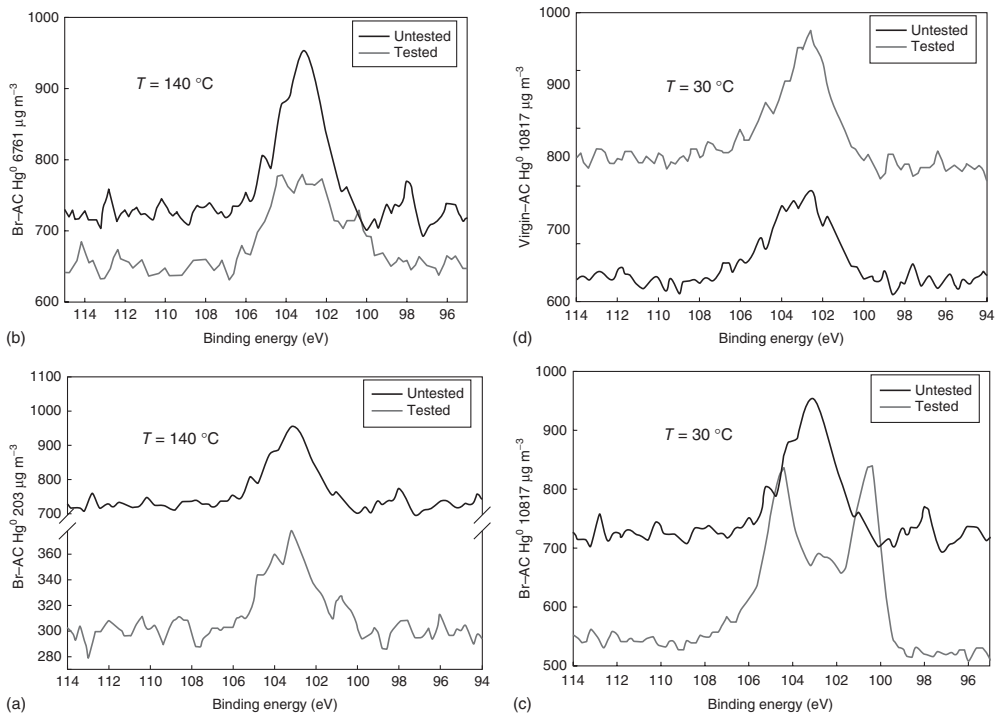


Figure 24.3 Hg 4f core level XPS spectra for activated carbon sorbents at various indicated conditions; (a–c) brominated AC sorbents and (d) virgin AC sorbent [72]. (Reprinted with permission from (Wilcox et al., *J Air & Waste Manag. Assoc.*, 61(4), 418, 2011). Copyright (2011) Taylor & Francis.)

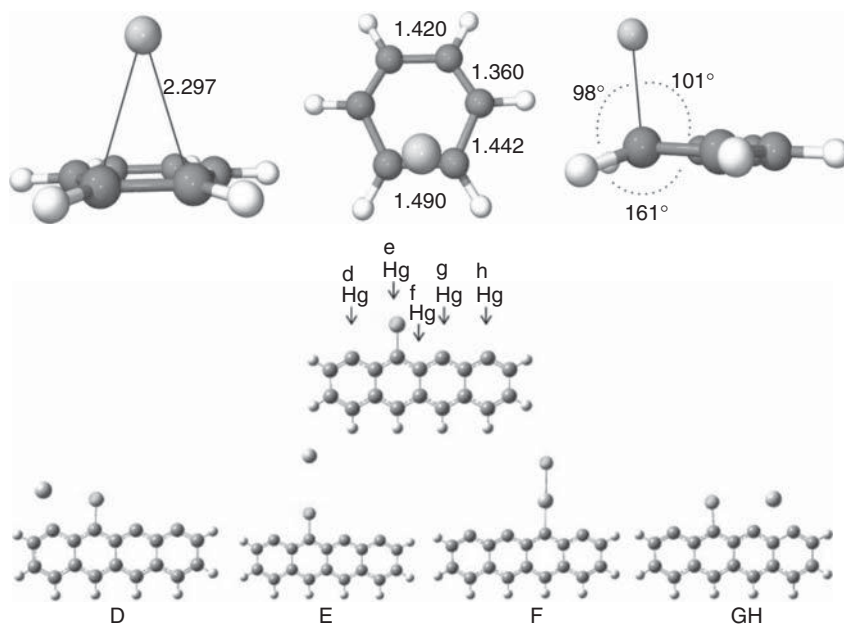


Figure 24.4 Hg–benzene complex investigated at the MP2/AVDZ level of theory (top) [73] (reprinted with permission from (Steckel, *Chem. Phys. Lett.*, 409, 322, 2005). Copyright (2005) Elsevier.) and Hg-halogenated fused

rings calculated at the B3LYP/LANL2DZ level of theory (bottom) [75]. (reprinted with permission from (Padak et al., *Carbon*, 47(12), 2855, 2009). Copyright (2009) Elsevier.)

state, Hg acts as a Lewis base with the desire to interact with an acidic site, thereby forming a strong C–Hg covalent bond on the carbon surface.

More recent investigations have used plane-wave DFT to model AC, which allows for the use of periodic systems such as a graphene. Graphene ribbons with exposed edge sites have been used for investigations of the reactivity of carbonaceous surfaces to various gas species [77]. Several investigations support the zigzag carbene structure model, where the zigzag edge site acts as a Lewis base and reacts with acid gas components thereby serving as a potential adsorption site for oxidized Hg [77, 78]. A recent DFT study [79] on the effect of chemical functional groups on Hg adsorption on carbon surfaces supports this suggestion. The study indicates that an embedded halogen atom promotes chemisorption on the neighboring site, which is consistent with experimental results, and indicative of Hg oxidation. Results also indicate a varying effect of organic groups on Hg adsorption, with lactone, carbonyl, and semiquinone groups promoting Hg chemisorption while phenol and carboxyl functional groups promote physisorption and reduce overall Hg capture. A mechanistic study of Hg oxidation due to halides on carbon materials proposes that the interactions of microcrystalline graphitic structures with halide ions result in the withdrawal of electrons from the graphitic structure, producing a strong Lewis

acid site [80], with Hg adsorption combined with the electron-transfer results in Hg oxidation.

To date, little work has been conducted on the effect of Br on Hg-AC interactions. Wilcox *et al.* [72] investigated the binding mechanism of Hg on brominated AC sorbents with a combination of experimental work, as discussed previously, and quantum-mechanical modeling using a nine-benzene-rings-wide graphene ribbon. Consistent with Padak and Wilcox's [75] results for Hg adsorption in the presence of chlorine, it was found that HgBr species are more stable on the carbon surface than HgBr₂ species. Furthermore, DFT and density of states (DOSs) calculations indicate that Hg is more stable when it is bound to the edge C atom interacting with a single Br atom bound atop of Hg. However, while the form of Hg adsorbed on the AC surface may be oxidized, the exact speciation of the adsorbed Hg remains in question. Furthermore, the Hg adsorption mechanism on the carbon surface and the effects of the flue-gas components are not well understood. Additional work, including closely coupled experimental and theoretical investigations, is required to determine the binding mechanism of Hg on AC sorbents in various flue-gas environments and to further elucidate the adsorption mechanism of Hg on AC.

24.3.2

Mercury Adsorption on Precious Metals

In general, precious metal adsorption of Hg has been applied to Hg capture from fuel gases of coal gasification processes as these metals, in contrast to carbon-based sorbents, may withstand the high temperatures of gasification processes. For gasification applications, the product is termed a *fuel gas*, and consists primarily of H₂, CO₂, and CO, while in the case of traditional coal combustion, the exhaust gas is termed a *flue gas* and is comprised primarily of N₂ and CO₂.

Precious metals, including palladium (Pd), platinum (Pt), gold (Au), iridium (Ir), and rhodium (Rh), have traditionally been used as modifiers for graphite-tube atomic absorption or emission analysis of solid and liquid samples. Among them, Pd has been identified as the best modifier for the adsorption of Hg [16]. In a study carried out by Steckel [81], DFT is used to carry out electronic structure calculations on slab models representing the (001) and (111) surfaces of silver (Ag), Au, copper (Cu), nickel (Ni), Pd, and Pt. Relatively strong binding for all of the metals was noted, with binding energies of ~1 eV for Pt and Pd. However, the DFT method used appears to underestimate the adsorption energy when compared directly to experimental results. Mercury has been predicted to have a stronger bond with the (001) surface, where fourfold hollow sites exist, in contrast to the threefold hollow sites on (111) surfaces. Aboud *et al.* [82] performed a DFT study of Pd alloyed with small amounts Au, Ag, and Cu and found that doping of the Pd surface increased the overall binding energy of Hg, which is beneficial for a sorption process. Furthermore, the binding energy increased the most when the dopants remained subsurface. In a continuation of the work, Sasmaz *et al.* [83] showed that Pd is primarily responsible for interacting with Hg in both alloys and

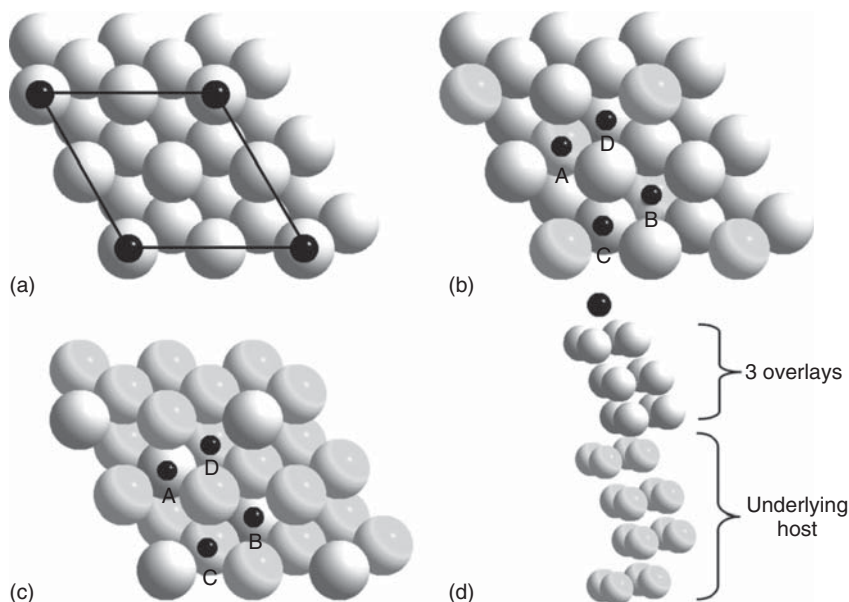


Figure 24.5 (a) Scheme of a supercell of (111) surfaces. (b) Threefold adsorption sites of Pd_3M binary alloys: (A) pure-hexagonal close packed (hcp) site, (B) pure-face-centered cubic (fcc) site, (C) mixed-hcp site, and (D) mixed-fcc site. (c) Threefold adsorption sites of PdM_3 binary alloys: (A)

pure-hcp site, (B) pure-fcc site, (C) mixed-hcp site, and (D) mixed-fcc site. (d) Side view of $3\text{Pd}/\text{M}(111)$ structure [83]. (Reprinted with permission from (Sasmaz, et al., *J. Phys. Chem. C*, 113, 7813, 2009). Copyright (2009) American Chemical Society.)

overlays and that the interaction is a result of overlap between the s- and p-states of Pd and the d-state of Hg. Figure 24.5 shows various adsorption sites of Hg on binary alloys and overlays of Pd with other metals, M, such that M represents either gold, silver, or copper.

Jain *et al.* [84] theoretically screened potential high-temperature metal sorbents for Hg capture in syngas streams. Using DFT predictions, the enthalpy of amalgamation and oxidation for metals was evaluated to predict the capability of Hg sorption and oxidation in the gas stream, demonstrating that Pd has the highest amalgamation enthalpy of all metals. Figure 24.6 shows the Hg amalgam formation enthalpy versus the binary oxide formation enthalpy to clarify the tendency of various metals for amalgamation and oxidation. Metals above the O_2 gas chemical potential line (i.e., dashed horizontal line) are estimated to form oxides and metals to the right of the Hg gas chemical potential (i.e., dashed vertical line) are estimated to form amalgams in the syngas stream. Metals satisfying both criteria (i.e., Section (II) in Figure 24.6) were found to form oxides rather than amalgams according to the grand canonical potential predictions. An ideal metal, which amalgamates without oxidizing, is located in Section (IV) of Figure 24.6. No metals are available in the most desirable area, but Pd is the closest to the area, indicating that Pd is the most promising metal for Hg capture.

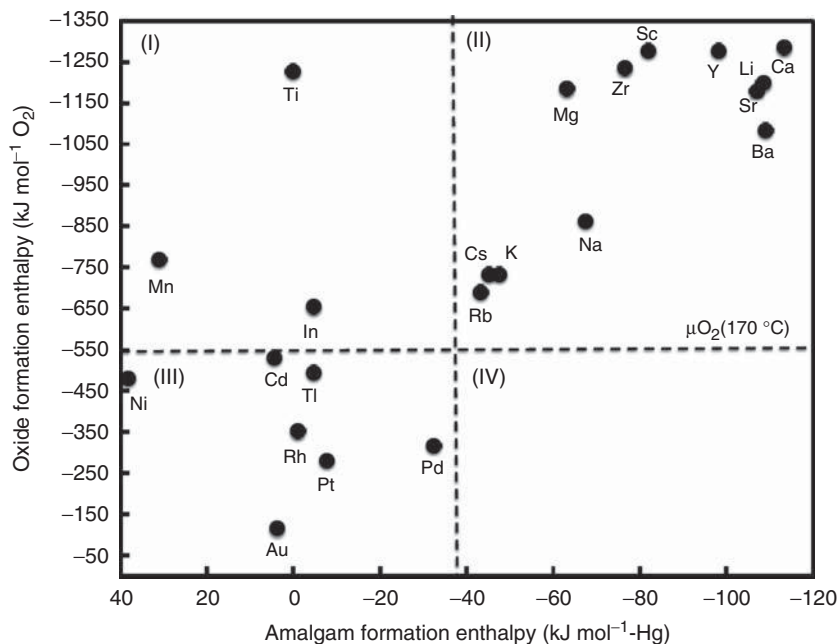


Figure 24.6 Estimated amalgam formation enthalpies of binary Hg amalgam versus binary oxide, normalized per mol of Hg and per mol of O_2 , respectively. Dashed horizontal and vertical lines represent the O_2 gas and Hg gas chemical potentials, respectively [84]. (Reprinted with permission from (Jain et al., Chem. Eng. Sci., 65, 3025,2010). Copyright (2010) Elsevier.)

Earlier experiments have validated the mechanisms of reactivity proposed by theory. For example, Baltrus *et al.* [85, 86] showed some evidence of Hg amalgamation on Pd/ Al_2O_3 . Maximum Hg adsorption on Pd/ Al_2O_3 occurs at 204 °C and at low loadings of Pd (<8.5 wt% Pd). An interesting finding is that Hg adsorption is suppressed by an excess of As; however, H_2S in fuel gas can improve this imbalance by moderately inhibiting the As adsorption while enhancing the Hg adsorption [86]. Poulston *et al.* [87] compared the Hg removal capacities of Pd and Pt sorbents supported on alumina and found that Pd is superior to Pt sorbents for Hg removal. This trend is supported by Figure 24.5, which indicates that Pt is located farther from the Section (IV) than Pd. The Hg removal capacity of both Pd and Pt sorbents increase with metal loading but decreases with sorbent temperature. Although most metal sorbent candidates exhibit poor capacities for Hg at temperatures greater than 204 °C, Pd proves to be an attractive sorbent for the Hg removal at elevated temperatures [16]. Fuel-gas substances that may affect the Hg adsorption on metal sorbents may include moisture, H_2S , CO, and H_2 [16]. Baldeck *et al.* [88] presented data on the use of Au traps for the quantitative fuel-gas separation of Hg in the form of an amalgam of Au_2Hg_3 . It was suggested that Hg removal on Au is not affected by corrosive substances such as SO_2 , H_2S , and organic compounds that may be present in flue gas.

24.4

Conclusions and Future Work

Atomistic modeling efforts have resulted in important insight into the homogeneous and heterogeneous mercury chemistry in power plant flue gases. Future work may focus upon the heterogeneous chemistry of mercury on common fly ash metal oxides, the ductwork walls within the power plants, and the SCR catalysts employed for reduction of NO_x. Recent and past works [62, 89, 90] hint at a possible important role for iodine and its compounds for promoting the oxidation of mercury in flue gas. It is suggested that further work is merited on the halogens, including both the heterogeneous chemistry on carbon, as well as the gas phase chemistry involving chlorine, bromine, and iodine species.

References

1. Cauch, B., Silcox, G.D., Lighty, J.A.S., Wendt, J.O.L., Fry, A., and Senior, C.L. (2008) Confounding effects of aqueous-phase impinger chemistry on apparent oxidation of mercury in flue gases. *Environ. Sci. Technol.*, **42** (7), 2594–2599.
2. Wilcox, J. (2004) On the path to elucidating the speciation of mercury in the flue gases of coal combustion. PhD Thesis, The University of Arizona.
3. Padak, B. (2011) Mercury reaction chemistry in combustion flue gases from experiments and theory. PhD Thesis, Stanford University, Stanford, CA.
4. Gharebaghi, M., Gibson, J., Hughes, K.J., Irons, R., Porter, R.T.J., Pourkashanian, M., and Williams, A. (2010) A modeling study of mercury transformation in coal-fired power plants. Proceedings of the American Flame Research Committee 2010 Pacific Rim Combustion Symposium, Maui, HI, 2010.
5. Gharebaghi, M., Hughes, K., Porter, R., Pourkashanian, M., and Williams, A. (2011) Mercury speciation in air-coal and oxy-coal combustion: a modelling approach. *Proc. Combust. Inst.*, **33** (2), 1779–1786.
6. Wang, Y., Duan, Y., Yang, L., Zhao, C., and Xu, Y. (2010) Mercury speciation and emission from the coal-fired power plant filled with flue gas desulfurization equipment. *Can. J. Chem. Eng.*, **88** (5), 867–873.
7. Senior, C.L., Sarofim, A.F., Zeng, T., Helble, J.J., and Mamani-Paco, R. (2000) Gas-phase transformations of mercury in coal-fired power plants. *Fuel Process. Technol.*, **63** (2-3), 197–213.
8. Sliger, R., Going, D.J., and Kramlich, J. C. (1998) Kinetic Investigation of the High-Temperature Oxidation of Mercury by Chlorine Species.
9. Sliger, R.N., Kramlich, J.C., and Marinov, N.M. (2000) Towards the development of a chemical kinetic model for the homogeneous oxidation of mercury by chlorine species. *Fuel Process. Technol.*, **65**, 423–438.
10. Hall, B., Schager, P., and Lindqvist, O. (1991) Chemical reactions of mercury in combustion flue gases. *Water Air Soil Pollut.*, **56** (1), 3–14.
11. Widmer, N., Cole, J., Seeker, W.R., and Gaspar, J. (1998) Practical limitation of mercury speciation in simulated municipal waste incinerator flue gas. *Combust. Sci. Technol.*, **134** (1-6), 315–326.
12. Wilcox, J. (2009) A kinetic investigation of high-temperature mercury oxidation by chlorine. *J. Phys. Chem. A*, **113** (24), 6633–6639.
13. Wilcox, J. (2011) A kinetic investigation of unimolecular reactions involving trace metals at post-combustion flue gas conditions. *Environ. Chem.*, **8** (2), 207–212.
14. Wilcox, J., Robles, J., Marsden, D.C.J., and Blowers, P. (2003) Theoretically predicted rate constants for mercury oxidation by hydrogen chloride in coal

- combustion flue gases. *Environ. Sci. Technol.*, **37** (18), 4199–4204.
15. Krishnakumar, B. and Helble, J.J. (2012) Determination of transition state theory rate constants to describe mercury oxidation in combustion systems mediated by Cl, Cl₂, HCl and HOCl. *Fuel Process. Technol.*, **94** (1), 1–9.
 16. Granite, E.J., Myers, C.R., King, W.P., Stanko, D.C., and Pennline, H.W. (2006) Sorbents for mercury capture from fuel gas with application to gasification systems. *Indust. Eng. Chem. Res.*, **45** (13), 4844–4848.
 17. Stevens, W.J., Krauss, M., Basch, H., and Jasien, P.G. (1992) Relativistic compact effective potentials and efficient, shared-exponent basis sets for the third-, fourth-, and fifth-row atoms. *Can. J. Chem.*, **70** (2), 612–630.
 18. Figgen, D., Rauhut, G., Dolg, M., and Stoll, H. (2005) Energy-consistent pseudopotentials for group 11 and 12 atoms: adjustment to multi-configuration Dirac-Hartree-Fock data. *Chem. Phys.*, **311** (1-2), 227–244.
 19. Wilcox, J. and Okano, T. (2011) Ab initio-based mercury oxidation kinetics via bromine at postcombustion flue gas conditions. *Energy Fuel*, **25** (4), 1348–1356.
 20. Peterson, K.A., Figgen, D., Goll, E., Stoll, H., and Dolg, M. (2003) Systematically convergent basis sets with relativistic pseudopotentials. II. Small-core pseudopotentials and correlation consistent basis sets for the post-d group 16, 18 elements. *J. Chem. Phys.*, **119**, 11113.
 21. Peterson, K.A. and Puzzarini, C. (2005) Systematically convergent basis sets for transition metals. II. Pseudopotential-based correlation consistent basis sets for the group 11 (Cu, Ag, Au) and 12 (Zn, Cd, Hg) elements. *Theor. Chem. Acc.: Theory Comput. Model. (Theor. Chim. Acta)*, **114** (4), 283–296.
 22. Chase, M.W. Jr. (1998) *NIST-JANAF Thermochemical Tables*, Journal of Physical and Chemical Reference Data (Monograph), 4th edn, vol. 9, American Chemical Society, Washington, DC; American Institute of Physics for the National Institute of Standards and Technology, Woodbury, NY.
 23. Tellinghuisen, J., Tellinghuisen, P.C., Davies, S.A., Berwanger, P., and Viswanathan, K. (1982) B → X transitions in HgCl and Hgl. *Appl. Phys. Lett.*, **41** (9), 789–791.
 24. Tellinghuisen, J. and Ashmore, J.G. (1982) The B → X transition in 200Hg 79Br. *Appl. Phys. Lett.*, **40** (10), 867–869.
 25. Aylett, B. (1973) *Group IIB*, vol. 3, Pergamon Press, Elmsford, NY, pp. 187–328.
 26. Bell, S., McKenzie, R., and Coon, J. (1966) The spectrum of HgCl₂ in the vacuum ultraviolet. *J. Mol. Spectrosc.*, **20** (3), 217–225.
 27. Malt'sev, A.A., Selivanov, G.K., Yampolsky, V.I., and Zavalishin, N.I. (1971) *Nat. Phys. Sci.*, **231**, 157.
 28. Adams, D.M. and Hills, D.J. (1978) Single-crystal infrared study and assignment for mercury (II) chloride and bromide. *J. Chem. Soc., Dalton Trans.*, (7), 776–782.
 29. Braune, H. and Engelbrecht, G. (1932) On the Raman-effect of some inorganic halogenides in the liquid and gaseous state. *Z. Phys. Chem. Abt. B*, **19**, 303.
 30. Sponer, H. and Teller, E. (1941) Electronic spectra of polyatomic molecules. *Rev. Mod. Phys.*, **13** (2), 75.
 31. Clark, R.J.H. and Rippon, D.M. (1973) Vapour phase Raman spectra of mercury (II) chloride, mercury (II) bromide and mercury (II) iodide. v1 (Σ + g) band contours and the mercury-halogen bond polarisability derivatives. *J. Chem. Soc., Faraday Trans. 2*, **69**, 1496–1501.
 32. Beattie, I.R. and Horder, J.R. (1970) Gas-phase Raman spectra of some dihalides of zinc and mercury, of “GaCl₂” and of GaCl₂Br and GaBr₂Cl. *J. Chem. Soc. A*, 2433–2435.
 33. Klemperer, W. and Lindeman, L. (1956) Infrared spectrum of mercuric chloride and bromide. *J. Chem. Phys.*, **25**, 397.
 34. Kaupp, M. and von Schnering, H.G. (1994) Origin of the unique stability of condensed-phase Hg₂²⁺. An ab initio investigation of MI and MII species (M = Zn, Cd, Hg). *Inorg. Chem.*, **33** (18), 4179–4185.
 35. Strömberg, D., Strömberg, A., and Wahlgren, U. (1991) Relativistic quantum calculations on some mercury sulfide

- molecules. *Water Air Soil Pollut.*, **56** (1), 681–695.
36. Cundari, T.R. and Yoshikawa, A. (1998) Computational study of methane activation by mercury (II) complexes. *J. Comput. Chem.*, **19** (8), 902–911.
 37. Ščavničar, S. (1955) The crystal structure of trimercuric oxychloride, $\text{HgCl}_2 \cdot 2\text{HgO}$. *Acta Crystallogr.*, **8** (7), 379–383.
 38. Chase, M.W. Jr., Davies, C.A., Downey, J.R., Frurip, D.J., McDonald, R.A., and Syverud, A.N. (1985) *JANAF Thermochemical Tables, Part 1 Al-Co*, Journal of Physical and Chemical Reference Data, vol. 14 (Suppl. 1), 3rd edn, American Institute of Physics, p. 1.
 39. Strömberg, D., Gropen, O., and Wahlgren, U. (1989) Non-relativistic and relativistic calculations on some Zn, Cd and Hg complexes. *Chem. Phys.*, **133** (2), 207–219.
 40. Deyanov, R., Petrov, K., Ugarov, V., Shchedrin, B., and Rambidi, N. (1985) Automatic background subtraction in gas electron diffraction: the covariance matrix in least-squares structure-parameter analysis. *J. Struct. Chem.*, **26** (5), 698–703.
 41. Donohoue, D.L., Bauer, D., and Hynes, A.J. (2005) Temperature and pressure dependent rate coefficients for the reaction of Hg with Cl and the reaction of Cl with Cl: A pulsed laser photolysis-pulsed laser induced fluorescence study. *J. Phys. Chem. A*, **109** (34), 7732–7741.
 42. Horne, D., Gosavi, R., and Strausz, O. (1968) Reactions of metal atoms. I. The combination of mercury and chlorine atoms and the dimerization of HgCl . *J. Chem. Phys.*, **48**, 4758.
 43. Shepler, B.C. and Peterson, K.A. (2003) Mercury monoxide: a systematic investigation of its ground electronic state. *J. Phys. Chem. A*, **107** (11), 1783–1787.
 44. Dewar, M.J.S. and Jie, C. (1989) AM1 calculations for compounds containing mercury. *Organometallics*, **8** (6), 1547–1549.
 45. Fry, A., Cauch, B., Silcox, G.D., Lighty, J.A.S., and Senior, C.L. (2007) Experimental evaluation of the effects of quench rate and quartz surface area on homogeneous mercury oxidation. *Proc. Combust. Inst.*, **31** (2), 2855–2861.
 46. Linak, W.P., Ryan, J.V., Ghorishi, B.S., and Wendt, J.O.L. (2001) Issues related to solution chemistry in mercury sampling impingers. *J. Air Waste Manage. Assoc.*, **51** (5), 688–698.
 47. Ryan, J.V. and Keeney, R.M. (2004) Symposium on Air Quality Measurement Methods and Technology, Research Triangle Park, NC, 2004.
 48. Kee, R.J., Rupley, F.M., and Miller, J.A. (1993) CHEMKIN-2: A Fortran Chemical Kinetics Package for the Analysis of Gas-Phase Chemical Kinetics. Sandia Laboratories Report: 589-8009B. Sandia Laboratory.
 49. Niksa, S., Helble, J.J., and Fujiwara, N. (2001) Kinetic modeling of homogeneous mercury oxidation: the importance of NO and H_2O in predicting oxidation in coal-derived systems. *Environ. Sci. Technol.*, **35** (18), 3701–3706.
 50. Roesler, J.F., Yetter, R.A., and Dryer, F.L. (1995) Kinetic interactions of CO, NO_x, and HCl emissions in postcombustion gases. *Combust. Flame*, **100** (3), 495–504.
 51. Li, J., Zhao, Z., Kazakov, A., Chaos, M., Dryer, F.L., and Scire, J.J. Jr., (2007) A comprehensive kinetic mechanism for CO, CH_2O , and CH_3OH combustion. *Int. J. Chem. Kinet.*, **39** (3), 109–136.
 52. University of Leeds <http://www.chem.leeds.ac.uk/Combustion?Combustion.html> (accessed 19 March 2014).
 53. Donohoue, D.L., Bauer, D., Cossairt, B., and Hynes, A.J. (2006) Temperature and pressure dependent rate coefficients for the reaction of Hg with Br and the reaction of Br with Br: a pulsed laser photolysis-pulsed laser induced fluorescence study. *J. Phys. Chem. A*, **110** (21), 6623–6632.
 54. Niksa, S., Naik, C.V., Berry, M.S., and Monroe, L. (2009) Interpreting enhanced Hg oxidation with Br addition at Plant Miller. *Fuel Process. Technol.*, **90** (11), 1372–1377.
 55. Goodsite, M.E., Plane, J., and Skov, H. (2004) A theoretical study of the oxidation of Hg^0 to HgBr_2 in the troposphere. *Environ. Sci. Technol.*, **38** (6), 1772–1776.
 56. Ariya, P.A., Khalizov, A., and Gidas, A. (2002) Reactions of gaseous mercury

- with atomic and molecular halogens: kinetics, product studies, and atmospheric implications. *J. Phys. Chem. A*, **106** (32), 7310–7320.
57. Shepler, B.C., Balabanov, N.B., and Peterson, K.A. (2007) Hg + Br → HgBr recombination and collision-induced dissociation dynamics. *J. Chem. Phys.*, **127**, 164304.
 58. Khalizov, A.F., Viswanathan, B., Larregaray, P., and Ariya, P.A. (2003) A theoretical study on the reactions of Hg with halogens: Atmospheric implications. *J. Phys. Chem. A*, **107** (33), 6360–6365.
 59. Spicer, C., Satola, J., Abby, A., Plastridge, R., and Cowen, K. (2002) Kinetics of Gas-Phase Elemental Mercury Reactions with Halogen Species, Ozone, and Nitrate Radical Under Atmospheric Conditions, Battelle Columbus. Final Report to Florida Department of Environmental Protection under Contract AQ174 2002. DEP.
 60. Balabanov, N.B., Shepler, B.C., and Peterson, K.A. (2005) Accurate global potential energy surface and reaction dynamics for the ground state of HgBr₂. *J. Phys. Chem. A*, **109** (39), 8765–8773.
 61. Matsumura, Y. (1967) Adsorption of mercury vapor on the surface of activated carbons modified by oxidation or iodization. *Atmos. Environ.*, **8** (12), 1321–1327.
 62. Granite, E.J., Pennline, H.W., and Hargis, R.A. (2000) Novel sorbents for mercury removal from flue gas. *Ind. Eng. Chem. Res.*, **39** (4), 1020–1029.
 63. Krishnan, S., Gullett, B.K., and Jozewicz, W. (1994) Sorption of elemental mercury by activated carbons. *Environ. Sci. Technol.*, **28** (8), 1506–1512.
 64. Hower, J.C., Senior, C.L., Suuberg, E.M., Hurt, R.H., Wilcox, J.L., and Olson, E.S. (2010) Mercury capture by native fly ash carbons in coal-fired power plants. *Prog. Energy Combust. Sci.*, **36** (4), 510–529.
 65. Mibeck, B.A.F., Olson, E.S., and Miller, S.J. (2009) HgCl₂ sorption on lignite activated carbon: analysis of fixed-bed results. *Fuel Process. Technol.*, **90** (11), 1364–1371.
 66. Olson, E., Mibeck, B., Benson, S., Laumb, J., Crocker, C., Dunham, G., Sharma, R., Miller, S., and Pavlish, J. (2004) The mechanistic model for flue gas-mercury interactions on activated carbons: the oxidation site. *Prepr. Pap. - Am. Chem. Soc., Div. Fuel Chem.*, **49** (1), 279.
 67. Ghorishi, B. and Gullett, B.K. (1998) Sorption of mercury species by activated carbons and calcium-based sorbents: effect of temperature, mercury concentration and acid gases. *Waste Manag. Res.*, **16** (6), 582.
 68. Hutson, N.D., Attwood, B.C., and Scheckel, K.G. (2007) XAS and XPS characterization of mercury binding on brominated activated carbon. *Environ. Sci. Technol.*, **41** (5), 1747–1752.
 69. Hu, C., Zhou, J., Luo, Z., and Cen, K. (2010) Oxidative adsorption of elemental mercury by activated carbon in simulated coal-fired flue gas. *Energy Fuel*, **25** (1), 154–158.
 70. Huggins, F.E., Yap, N., Huffman, G.P., and Senior, C.L. (2003) XAFS characterization of mercury captured from combustion gases on sorbents at low temperatures. *Fuel Process. Technol.*, **82** (2-3), 167–196.
 71. Laumb, J.D., Benson, S.A., and Olson, E.A. (2004) X-ray photoelectron spectroscopy analysis of mercury sorbent surface chemistry. *Fuel Process. Technol.*, **85** (6-7), 577–585.
 72. Wilcox, J., Sasmaz, E., Kirchofer, A., and Lee, S. (1995) Heterogeneous mercury reaction chemistry on activated carbon. *J. Air Waste Manage. Assoc.*, **61** (4), 418.
 73. Steckel, J. (2005) Ab initio modelling of neutral and cationic Hg-benzene complexes. *Chem. Phys. Lett.*, **409** (4-6), 322–330.
 74. Padak, B., Brunetti, M., Lewis, A., and Wilcox, J. (2006) Mercury binding on activated carbon. *Environ. Progr.*, **25** (4), 319–326.
 75. Padak, B. and Wilcox, J. (2009) Understanding mercury binding on activated carbon. *Carbon*, **47** (12), 2855–2864.
 76. Olson, E.S., Azenkeng, A., Laumb, J.D., Jensen, R.R., Benson, S.A., and Hoffmann, M.R. (2009) New developments in the theory and modeling of

- mercury oxidation and binding on activated carbons in flue gas. *Fuel Proc. Technol.*, **90** (11), 1360–1363.
77. Radovic, L.R. and Bockrath, B. (2005) On the chemical nature of graphene edges: origin of stability and potential for magnetism in carbon materials. *J. Am. Chem. Soc.*, **127** (16), 5917–5927.
 78. Huggins, F.E., Huffman, G.P., Dunham, G.E., and Senior, C.L. (1999) XAFS examination of mercury sorption on three activated carbons. *Energy Fuel*, **13** (1), 114–121.
 79. Liu, J., Cheney, M.A., Wu, F., and Li, M. (2011) Effects of chemical functional groups on elemental mercury adsorption on carbonaceous surfaces. *J. Hazard. Mater.*, **186** (1), 108–113.
 80. Qu, Z., Chang, J.J., Hsiung, T.L., Yan, N., Wang, H.P., Dod, R., Chang, S.G., and Miller, C. (2010) Halides on carbonaceous materials for enhanced capture of Hg^0 : Mechanistic study. *Energy Fuel*, **24** (6), 3534–3539.
 81. Steckel, J.A. (2008) Density functional theory study of mercury adsorption on metal surfaces. *Phys. Rev. B*, **77** (11), 115412.
 82. Aboud, S., Sasmaz, E., and Wilcox, J. (2008) Mercury adsorption on PdAu, PdAg and PdCu alloys. *Main Group Chem.*, **7** (3), 205–215.
 83. Sasmaz, E., Aboud, S., and Wilcox, J. (2009) Hg binding on Pd binary alloys and overlays. *J. Phys. Chem. C*, **113** (18), 7813–7820.
 84. Jain, A., Seyed-Reihani, S.A., Fischer, C.C., Couling, D.J., Ceder, G., and Green, W.H. (2010) Ab initio screening of metal sorbents for elemental mercury capture in syngas streams. *Chem. Eng. Sci.*, **65** (10), 3025–3033.
 85. Baltrus, J.P., Granite, E.J., Stanko, D.C., and Pennline, H.W. (2008) Surface characterization of Pd/ Al_2O_3 sorbents for mercury capture from fuel gas. *Main Group Chem.*, **7** (3), 217–225.
 86. Baltrus, J.P., Granite, E.J., Pennline, H.W., Stanko, D., Hamilton, H., Rowsell, L., Poulston, S., Smith, A., and Chu, W. (2010) Surface characterization of palladium-alumina sorbents for high-temperature capture of mercury and arsenic from fuel gas. *Fuel*, **89** (6), 1323–1325.
 87. Poulston, S., Granite, E.J., Pennline, H.W., Myers, C.R., Stanko, D.P., Hamilton, H., Rowsell, L., Smith, A.W.J., Ilkenhans, T., and Chu, W. (2007) Metal sorbents for high temperature mercury capture from fuel gas. *Fuel*, **86** (14), 2201–2203.
 88. Baldeck, C.M., Kalb, G.W., and Crist, H.L. (1974) Determination of elemental mercury in an emission source having a high sulfur dioxide concentration by amalgamation with gold and ultraviolet spectrophotometry. *Anal. Chem.*, **46** (11), 1500–1505.
 89. Granite, E.J., Pennline, H.W., and Hargis, R.A. (1998) Sorbents for Mercury Removal from Flue Gas 1998, DOE Topical Report TR-98-01. DOE.
 90. Durham, M.D., Sjostrom, S., and Baldrey, K.E. (2013) Method and system for controlling mercury emissions from coal-fired thermal processes. US Patent 8,496,894, Jul. 30, 2013.

25

Predicting Hg Emissions Rates with Device-Level Models and Reaction Mechanisms

Stephen Niksa and Balaji Krishnakumar

25.1

Introduction and Scope

At the turn of the past century, the American utility industry needed to demonstrate which Hg control technologies could be immediately deployed to comply with impending regulations on Hg emissions from coal-fired power plants. This imperative was confounded by the large number of factors that affected Hg emissions, because even Environmental Protection Agency's (EPAs) first Information Collection Request (ICR) testing program had shown that fuel quality, the configuration of units in the gas cleaning system, and numerous gas cleaning conditions affected Hg speciation; hence, the prospects for controlling Hg emissions.

While the bulk of the R&D community was compiling a database of field test measurements that covered the most common fuels, unit configurations, cleaning conditions, and external Hg controls, a small group set out to develop reaction mechanisms and models that could, first, quantitatively interpret the field test database and, ultimately, predict Hg emissions for a particular gas cleaning system as accurately as the Hg speciation could be monitored. Statistical approaches based on regressions of various types of test data never achieved the accuracy needed for strategic compliance planning [1–4]. But some of the approaches based on reaction mechanisms did, and are now being used by both utility companies and original equipment manufacturers to forecast Hg emissions at individual plants and across regional fleets of power stations.

Our collection of reaction mechanisms, called *Mercurator*[™] in its commercial implementation, is the basis for this survey of reaction mechanisms that can accurately predict Hg emissions across the entire domain of commercial gas cleaning conditions. Over two dozen previously published articles [5] have evaluated the quantitative accuracy of the model predictions for an assortment of gas cleaning situations, to demonstrate the predictive capabilities. In total, more than 200 field test datasets have been quantitatively interpreted, usually within measurement uncertainties. Here we simply acknowledge that

Mercurator™ predicts Hg emissions within the measurement uncertainties for any coal in any cleaning configuration across the commercial domain of gas cleaning conditions and, on the basis of that performance, use the mechanisms to assess the most important factors in the practice of Hg emissions control.

25.2

The Reaction System

Our scope covers the properties, compositions, quantities, and operating conditions needed to predict Hg speciation and removals along full-scale flue gas cleaning systems. Pilot-scale gas cleaning systems are also relevant, although the primary reaction systems of interest are commercial. The most important consideration is the distribution of Hg species at all points along the cleaning system; the so-called Hg speciation. Hg vapors are grouped into two forms, elemental (Hg^0) and oxidized (Hg^{2+}), while a single species, particulate Hg (Hg_p), is bound to the unburned carbon (UBC) in fly ash or to injected carbon sorbents. Speciation is crucial to Hg emissions control because Hg^{2+} is completely soluble in flue gas desulfurization (FGD) scrubber solutions (neglecting any reemission of Hg^0 from the FGD solution), whereas Hg^0 is completely insoluble, and Hg_p is removed in any particle collection device (PCD) in proportion to the collection efficiency for UBC, which usually approaches 100%. Consequently, in cleaning systems that effectively capture Hg^{2+} in wet flue gas desulfurization (WFGD) and Hg_p in an electrostatic precipitator (ESP) or fabric (or baghouse) filter (FF), nearly all the Hg leaving the stack will be Hg^0 . But in systems without an FGD, the Hg stack emissions will be a mixture of Hg^0 and Hg^{2+} species. Contributions to the stack emissions from Hg_p are almost always negligible for plants with PCDs.

The power plant is first subdivided into a furnace and a gas cleaning system, which are connected at the furnace exit plane upstream of the economizer (ECN). The gas cleaning system is a continuous series of heat exchangers and air pollution control devices (APCDs). Most systems move the flue gas through an ECN into a selective catalytic reduction (SCR) unit, if present; through an air preheater (APH) into a PCD, which is usually a cold-side electrostatic precipitator (ESPC) or FF or mechanical or venturi particle scrubber; and on through a WFGD, if present, and into the stack. One popular variation uses lime injected into a spray drier absorber (SDA) to remove SO_x followed by a FF to recover particulates. Another variation locates the ESP immediately downstream of the ECN (hot-side electrostatic precipitator (ESPh)), and may or may not have a FF downstream of the APH. The gas cleaning configuration is the sequence of units in the cleaning system. Ductwork that connects these units is apportioned to the adjacent units.

The two forms of Hg control are inherent and external. Inherent controls rely on the Hg transformations (and capture) within APCDs primarily devoted to controlling other pollutants, such as an SCR for deNO_x and WFGD and SDA for deSO_x . External Hg controls are technologies added to a power plant

specifically to control Hg emissions. The most popular examples are (i) activated carbon injection (ACI) with conventional or brominated carbon sorbents; (ii) addition of halogenation agents to supplement the concentrations of either Cl or Br species in the flue gas; and (iii) additives to WFGDs to ensure that dissolved Hg(II) species are not reemitted into the flue gas as Hg⁰. Numerous other control strategies are being developed, including dedicated Hg oxidation units upstream of WFGDs when no SCR is present and various non-carbon sorbents. These are beyond the scope of this article because they are not yet commercially important. Fuel preprocessing to reduce the Hg content, either with froth flotation or density classification schemes or with thermal treatments, are also beyond our scope on the assumption that the Hg content and composition of the fuel fed into a furnace must always be known in advance to forecast the Hg stack emissions.

We assume that flow through the ductwork and heat exchangers in a cleaning system is fully developed and turbulent, so that the concentrations of all flue gas species may be analyzed in a single spatial dimension or in the transit time. Mixing is more important wherever sorbents or halogenation agents are injected into the flow, although the applications community generally appreciates the importance of uniform dispersion of Hg control agents over the flow duct area (notwithstanding several early injector design issues). In contrast, the flows through the channels in an SCR monolith are laminar, by design, as are the flows through the plate spacings within ESPs.

Early analytical work established that the Hg speciation at equilibrium should become dominated by sulfates in the condensed phase at PCD operating temperatures, but these species have never been detected. Instead, measured Hg speciation spans the full gamut from negligible to predominant Hg_p at the PCD, along with negligible to predominant levels of Hg⁰ or Hg²⁺, depending on numerous parametric factors. So equilibrium compositions are irrelevant to Hg emissions prediction. Consequently, our analytical framework will be a time-dependent analysis governed by the chemical reaction kinetics. Such an analysis can only be implemented if supported by an assortment of operating conditions, each specified as a function of the transit time. The most important is the thermal history, which is the mean flue gas temperature as a function of transit time. As seen subsequently, it consists of a series of quench stages for each heat exchanger interrupted by isothermal stages for the SCR, PCD, and WFGD. To incorporate realistic chemical reaction mechanisms, the flue gas composition based on all major species (O₂, H₂O, CO₂, N₂) must be specified, along with several key minor species concentrations (NO, SO₂, SO₃, HCl, total Br, and total Hg). The fly ash loading and its variation in transit time (due to the variable gas density along the quench cycle) must be specified. The UBC level in fly ash is estimated from a measured loss-on-ignition (LOI) level. The UBC specific surface area, in square meters per gram, is also required. Note that the total surface area (and activation) of UBC varies in transit time because the fly ash loading changes, even while LOI and the specific surface area stay the same as the fly ash moves through the cleaning system. Despite many claims to the

contrary in older literature, the participation of any of the mineral phases in fly ash in Hg transformations has never been demonstrated, so we regard UBC as the only reaction substrate in the fly ash. Many other pertinent APCD-specific operating conditions are introduced later, when the Hg transformations through each unit are described.

25.3

Hg Transformations

The following four distinct stages of Hg transformations must be characterized: in-furnace, in-flight, along SCR catalysts, and within WFGDs and SDAs. The in-furnace transformations are rudimentary for Hg, but also cover several much more subtle connections among the ways that pulverized fuels (p.f.s) are injected into furnaces and subsequent Hg conversion throughout gas cleaning systems. In-flight Hg transformations are determined by chemistry in the flue gas stream as it moves through the heat exchangers, ductwork, and PCDs in a cleaning system. The governing chemistry comes in two forms: heterogeneous Hg chemistry occurs via the interaction of select flue gas species and reaction sites on the suspended UBC and sorbent particles in the flow, and on UBC and sorbent deposits on the walls of heat exchangers and, perhaps, ESPs. Homogeneous Hg chemistry involves only gaseous species in the flue gas, with no participation whatsoever by UBC, minerals, or deposits. Transformations along SCR catalysts are restricted to the oxidation of Hg^0 into Hg^{2+} on sites on the promoted V_2O_5 catalysts. However, this Hg^0 oxidation can only be described as an element of a more comprehensive analysis that also describes simultaneous NO reduction, due to essential aspects of a competitive adsorption among NH_3 and the species associated with Hg^0 oxidation. The transformations within WFGDs determine whether any of the aqueous Hg(II) species can be reemitted as Hg^0 into the flue gas and thereby diminish the Hg removal across these units. Each form of the Hg transformations is characterized in turn in succeeding sections.

25.3.1

In-Furnace Transformations

Here we restrict our attention to large utility furnaces fed with whole coals or coal blends in the p.f. size grade. Stoker furnaces, fluidized bed combustors (FBCs), and circulating fluidized bed combustors (CFBCs) are beyond our scope. No chemistry needs to be described in detail within the furnace, because essentially all the Hg and halogens in the fuel are released into the flue gas as vapors, and none of the vapors are scavenged by molten minerals upstream of the furnace exit. Even when pyrite – the densest mineral, by far, which is usually present as extraneous particles – is recovered as bottom ash, it is first heated sufficiently to release its Hg into the flue gas. Similarly, all the Cl and Br in the fuel are released into the flue gas at hundreds of degrees below the

maximum flame temperatures. Chlorine may be incorporated into CaCl_2 within molten mineral mixtures with certain low-rank coals and with certain subbituminous/bituminous blends. But, even so, this is always a relatively minor phase that usually sequesters only a small portion of the available Cl, except with some low-rank fuels that have very little inherent Cl to begin with as well as favorable mineral compositions.

On the basis of these observations, the initial condition for the kinetic analysis is the equilibrium flue gas composition at the furnace exit gas temperature (of approximately 1050 °C). To evaluate the equilibrium composition, a furnace stoichiometry is first assigned to match a specified O_2 level in the flue gas at the ECN or, more directly, from specified flow rates for fuel and all the air streams. Such an equilibrium composition cannot accurately estimate the levels of NO, CO, or SO_3 in the flue gas, because the NO and CO concentrations are determined by extremely complex chemistry in the furnace. To circumvent an ambiguous analysis, we stipulate the NO concentration at the ECN as an input parameter. The SO_3 concentration could also be specified as an input parameter but, because it is usually unknown, we use a detailed reaction mechanism in 134 steps that also accounts for heterogeneous production on the Fe-oxides in fly ash and across SCR catalysts [6]. At the furnace exit, all coal-Hg will be present as Hg^0 . This equivalence determines the total Hg inventory, which is the Hg concentration that all measured speciation components must sum to, accounting for any Hg removed in downstream APCDs. In practice, there are often very large discrepancies among the estimates based on coal-Hg and summed measured speciation components, because it is always difficult to recover fuel samples that actually represent the fuel properties being converted while the Hg speciation data were recorded. The Cl-species at the furnace exit are completely dominated by HCl, as the concentration of Cl-atoms is on the order of tens of parts per billion and that of Cl_2 is even smaller. But when Br is added to the fuel as an aqueous spray, the concentration of Br-atoms often exceeds that of HBr at the furnace exit, and a detailed homogeneous reaction mechanism is used to describe the Br speciation and its evolution in transit time, as explained subsequently.

Despite the complete vaporization of Hg and halogens in the furnace, it is a mistake to suppose that furnace firing configuration is irrelevant to Hg emissions control, because firing configuration strongly affects the amounts and properties of UBC suspended in the fly ash. Cyclone firing gives the greatest LOI but this LOI is based on the minimum fly ash loadings, owing to the rejection of most coal ash as bottom ash, and its UBC has the minimum specific surface areas [7]. Low- NO_x burners in wall-fired units and low- NO_x controls in T-fired furnaces give more LOI than high-efficiency firing practices [8]. Coal quality is another independent influence on both LOI levels and the specific surface areas of UBC. LOI with low-rank fuels is usually well below 1 wt% of the fly ash, but becomes markedly greater with bituminous coals and, especially, with low-volatility coals. The specific surface area of the LOI from low-rank fuels is several times greater than that with bituminous coals [9], because only bituminous coals melt during

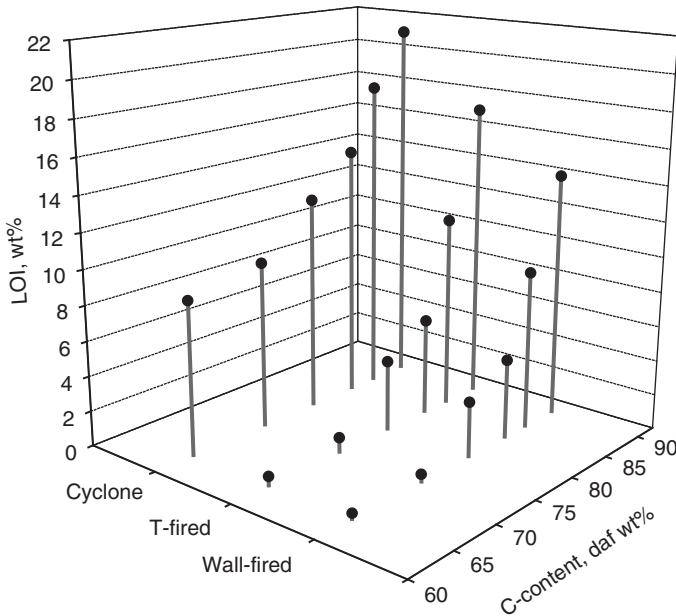


Figure 25.1 Visualization of LOI as a function of the fuel C-content and firing configuration.

the initial stages of combustion and thereby lose most of their internal surface areas.

This rather complicated situation is visualized in 3D in Figure 25.1, which plots LOI for high-efficiency firing practices versus both the C-content of the fuel and the firing configuration. For T- and wall-fired furnaces, the coal quality impact dominates and LOI levels are markedly greater with low-volatility coals than bituminous, and with bituminous than with low-rank coals. The coal quality impact weakens for cyclone firing, although the absolute LOI levels are much greater with this firing configuration than with the other two across the entire range of coal quality. An analogous surface for low- NO_x firing practices would have much greater LOI levels with bituminous and low-volatility coals for T- and wall firing, but similar levels with low-rank coals in all firing configurations and with cyclone firing throughout the range of coal quality. Therefore, the entire surface would be similar except that the LOI with high-rank coals for T- and wall firing would be greater. However, to gauge the impact of these variations on Hg transformations, we must also account for the variations in the specific surface areas. The adjustment between LOI and total UBC surface area for coal quality is about a factor of 7, so that 1 wt% LOI from a subbituminous has a comparable activity to about 7 wt% LOI from a bituminous coal. Of course, LOI is referenced to the total fly ash loading and low-rank coals generally have less mineral matter than high-rank fuels and, therefore, generate less fly ash. But on the basis of equal levels of UBC suspended in flue gas, the UBC from low-rank coals is several times more

active than that from high-rank coals due, in part, to its much greater specific surface area. These observations have great relevance for combustion-modification techniques for enhancing the capture of mercury. We also suspect that the finely dispersed alkali and alkaline earth cations on the UBC from low-rank coals also enhance its chemical activity toward Hg, but this aspect has not yet been characterized in the laboratory.

The impact of coal quality on halogen levels is much simpler. Chlorine is the only significant halogen in the fuel, except in infrequent instances where the Cl-contents in a handful of lignites were so small that the normally negligible levels of coal-Br became relatively significant. In general, low-rank coals generate HCl concentrations in flue gas from single-digit parts per million levels to 20 ppm; high-rank coals generate 25–150 ppm; while bituminous coals from the Illinois Basin and from the United Kingdom generate substantially greater concentrations. Aqueous solutions of calcium chlorides and bromides are sometimes sprayed on the fuel to compensate for any natural halogen deficiencies. Perhaps the most important aspect of coal-Cl is its inordinate variability. The testing literature contains instances where coal-Cl varied by as much as a factor of 5 while all other coal properties remained the same during a month-long testing campaign. These variations are completely independent of the primary fuel properties, and can only be accounted for by monitoring coal-Cl on every day of testing, and by running test-specific simulations.

The impact of coal quality and the inherent variability of coal-Hg are much weaker. But the overriding consideration with coal-Hg is that total Hg concentrations in flue gas, at 1–10 ppb, are always much too low to affect the concentrations of any other species; in other words, even complete conversion of total Hg leaves the concentrations of all other species unchanged. Of course, coal-Hg and the total Hg concentration in flue gas are scales for the emissions rates and stack Hg concentrations, which are obviously important. But Hg's impact on the process chemistry is severely restricted by its very low absolute concentration. The important implication is that all surface coverages associated with Hg species must be miniscule in the steady state; otherwise, the relaxation times to reach steady states will be incompatible with the reported rapid response times to step changes in the gas cleaning conditions, such as Cl concentrations.

25.3.2

In-Flight Transformations

At the furnace exit, the whole flue gas composition has been specified, including the levels of Hg⁰, HCl, HBr, and Br-atoms. The loading and total surface area of UBC in suspension have also been specified. Nearly all the most reactive sites on the UBC have been oxidized but are otherwise accessible. We are now ready to progress forward into the cleaning system, first, to complete the specification of the cleaning conditions and, second, to describe the in-flight Hg transformations.

Regardless of the APCDs in any gas cleaning system, one primary imperative is to extract as much heat as possible from the flue gas before it reaches the stack.

From the furnace exit to the ECN inlet, superheaters reduce the temperature from 1050 to 750 °C in about 1 s, and the ECN cools it to 375 °C in 0.5 s. SCRs operate near-isothermally at 340–390 °C with residence times from 1 to 3 s. The APH then quenches the stream to PCD operating temperatures which, for ESPs, vary from 140 to 180 °C with residence times to 15 s and, for FFs, from 120 to 140 °C with times to several seconds. SDAs operate at ESP temperatures, whereas WFGDs operate from 40 to 60 °C. Stack temperatures are usually around 80 °C. A typical thermal history for a cleaning system with only ESPc appears in Figure 25.2. This history is consistent with measured temperatures along several full-scale cleaning systems, although thermal histories for many systems often exhibit large and usually uncharacterized deviations from any baseline thermal history because of differences in the lengths of ductwork and unit sizes. One way to account for these variations is to include detailed specifications on the ductwork in the input requirements. A much less cumbersome way is to adjust the thermal history to match predicted Hg speciation to measured values recorded for baseline operating

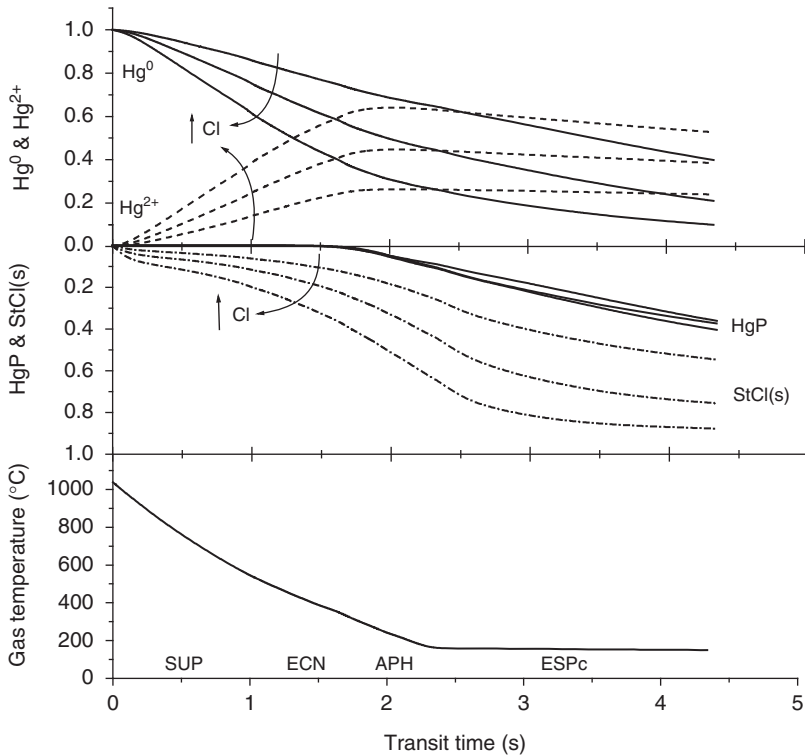


Figure 25.2 Mercurator™ predictions for Hg speciation and (middle panel) the fractional coverage of chlorinated sites on UBC (labeled as StCl(s)) for 7% LOI from a

bituminous coal that released 17, 34, and 64 ppm HCl in an ESPc-only cleaning system. The lower panel shows a typical thermal history for commercial gas cleaning systems.

conditions; that is, use the intermediate temperatures in the thermal history to calibrate the analysis to a subject cleaning system. Thermal histories also need to be adjusted as the furnace load is regulated, to account for the longer transit times and cooler operating temperatures under reduced load operation.

These aspects of the thermal history along a cleaning system are important, but the paramount implication from the thermal history in Figure 25.2 reflects the extents of the changes in both temperature and transit time. No process in nature could possibly sustain the same rate-limiting step over such a broad range of temperature; therefore, any proposed reaction mechanism for in-flight Hg transformations must depict several dramatic shifts among the main conversion channels, and these shifts must occur on time scales of only a few seconds. Failure to recognize this essential characteristic of all gas cleaning systems is the main reason that the bulk of testing at laboratory scale is irrelevant to the Hg transformations in commercial cleaning systems. Isothermal laboratory-scale tests can only, at best, be relevant for an instant in the time-temperature pathway of a coal-fired power plant.

Our mechanism for in-flight transformations with only Cl-species has three broad stages, two of which are illustrated in Figure 25.2, and several shifts in the rate-limiting process. In the first stage, the reaction sites on UBC are chlorinated, thereby generating the sites for subsequent Hg chemistry. Such chlorination has never been monitored on coal-derived UBC, but carbon from other sources is known to readily absorb Cl from the gas phase, especially at superheater and ECN operating temperatures [10]. As seen in Table 25.1, we represent this stage as an adsorption equilibrium that balances HCl adsorption, heterogeneous Cl atom recombination, and a hydration reaction. Such a simple adsorption scheme omits the competitive adsorption by S- and N-species, not because they are truly negligible. Rather, these competitions are omitted because the UBC in cleaning systems will always be heavily sulfated and nitrated, so explicitly resolving this competition would add adjustable parameters without improving the fidelity of the surface coverage of the chlorinated sites, which is crucial.

Table 25.1 Heterogeneous Hg conversion mechanism for Cl species on carbon.

Chlorination ^{a)}	
$\text{StSA(s)} + \text{HCl} \rightarrow \text{StCl(s)} + \text{H}$	Chlorination
$\text{StCl(s)} + \text{Cl} \rightarrow \text{Cl}_2 + \text{StSA(s)}$	Heterogeneous Cl-atom recombination
$\text{StCl(s)} + \text{H}_2\text{O} \rightarrow \text{HCl} + \text{OH} + \text{StSA(s)}$	Hydration
Hg conversion	
$\text{StCl(s)} + \text{Hg}^0 \rightarrow \text{StHgCl(s)}$	Hg^0 adsorption
$\text{StHgCl(s)} + \text{HCl} \rightarrow \text{StSA(s)} + \text{HgCl}_2 + \text{H}$	Oxidation with desorption
$\text{StHgCl(s)} \rightarrow \text{StSA(s)} + \text{HgCl}$	Desorption
$\text{StCl(s)} + \text{HgCl}_2 \rightarrow \text{StHgCl(s)} + \text{Cl}_2$	Back adsorption

a) Converts open sites (StSA(s)) into chlorinated sites (StCl(s)).

The second stage describes the Hg transformations on the chlorinated sites. Hg adsorption is restricted to the chlorinated sites, because X-ray photoemission spectroscopy (XPS) analysis indicates the presence of Hg–Cl–C bonds on UBC sampled from flue gas [11]. The surface intermediate $\text{StHgCl}(s)$ is either chlorinated further and released as HgCl_2 or released as HgCl to be fully oxidized in the gas phase. While these two steps are global processes in our mechanism, this stage has been resolved in detail by Olsen and coworkers, as described elsewhere in this volume. Hg^{2+} can also back adsorb onto a chlorinated site on UBC.

The shifts in rate-limiting steps are evident in Figure 25.2 as shifts in the Hg speciation. UBC chlorination dominates through the superheaters and into the ECN. As the appearance of Hg^{2+} without any Hg_p signals the first Hg transformations, the conversion rate is initially adsorption controlled, as expected at high temperatures. Further along the quench cycle, Hg_p appears as evidence of a more balanced conversion under chemical reaction control. Within the APH and into the ESPc, Hg_p continues to accumulate while both vapor species diminish, which signals desorption control. Further into the ESPc, essentially all chlorinated surface area on UBC is removed from the flue gas (although only the maximum accumulation of Hg_p is shown in Figure 25.2) which, along with the low temperature, terminates the Hg transformation chemistry. The time to remove sufficient chlorinated carbon surface from the flue gas to quench Hg chemistry is a small fraction of the total transit time through an ESPc, because most fly ash is recovered in the first and second upstream fields.

The tendency for progressively greater Cl concentrations is also shown in Figure 25.2. Greater Cl levels shift the Cl adsorption equilibrium toward larger populations of chlorinated sites on UBC, which promotes faster Hg^0 oxidation at high temperature but the same accumulation of Hg_p at low temperature, due to the slower adsorption of Hg^{2+} compared to Hg^0 . Consequently, the same Hg is removed in the ESPc, and there is substantially less Hg^0 in the stack emissions. The tendency for progressively greater LOI levels would be completely analogous for the vapor species, and more LOI would also enhance Hg_p provided that the flue gas contained sufficient Cl to actually expand the population of chlorinated sites.

This same reaction mechanism describes the markedly enhanced Hg removals for ACI with untreated and brominated carbons with three important differences, two of which are seen in Figure 25.3. The first is that carbon sorbents have surface areas from 500 to 1200 $\text{m}^2 \text{g}^{-1}$, which are 2–40 times greater than UBC specific surface areas. The second difference is that the chlorination stage is shifted to much cooler temperatures because ACI is usually positioned immediately downstream or, less frequently, immediately upstream of the APH. As this location is hundreds of degrees cooler than where inherent UBC is chlorinated, we were surprised to see that our chlorination mechanism remained accurate in ACI applications after only very small adjustments to the rate constants. If the sorbent is halogenated before injection, then the chlorination step is simply omitted altogether. The third difference is that progressively greater ACI concentrations generate much more Hg_p at the expense of both Hg^0 and Hg^{2+} . In general, the back

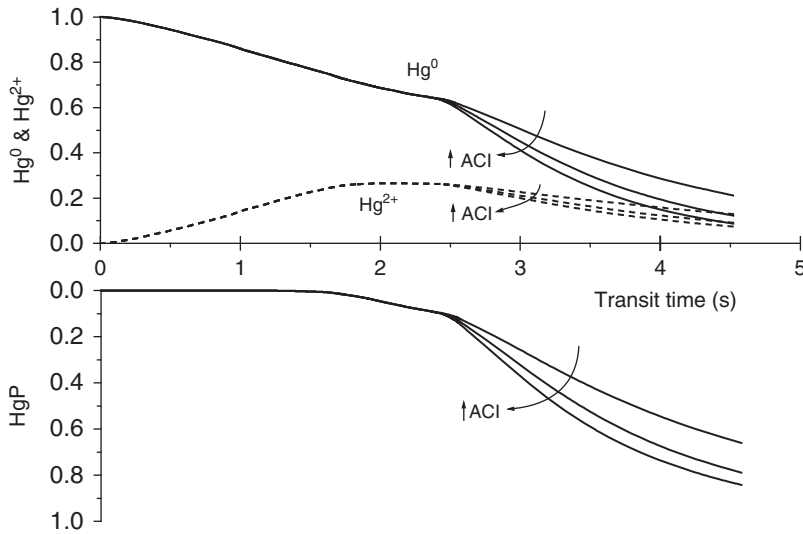


Figure 25.3 Mercurator™ Hg speciation for untreated ACI at 3, 6, and 9 lb/MMacf for 7% LOI from a bituminous coal that released 17 ppm HCl in an ESPc-only cleaning system.

adsorption of Hg^{2+} onto vacant sites tends to be much more important with sorbent than with inherent UBC, simply because the vacant site population is almost always much greater in ACI applications. For this same reason, Cl availability often limits the asymptotic, ultimate removal for even the largest ACI concentrations when applied with low-rank fuels. The asymptotic removals with high-Cl, high-rank fuels tend to approach 95%, where the difference with complete removal is thought to reflect imperfect particle dispersion (mixing of the sorbent) in turbulent flow fields. But asymptotic removals are often no greater than 65–75% with low-rank fuels, because Cl availability limits the size of the population of chlorinated sites. Under these circumstances, further increases in the ACI concentration simply redistributes the same population of chlorinated sites among a larger number of sorbent particles, without increasing the population size.

Another potentially critical limitation of ACI performance is described by the third stage of our in-flight mechanism, inhibition by SO_3 . During gas quenching, whenever the local flue gas temperature cools below the SO_3 dew point, sufficient H_2SO_4 – the product of SO_3 hydration – condenses onto any accessible surface to equalize the dew point to the local temperature. According to our analysis [6], the surface area of all fly ash, not just UBC, participates in the condensation. The portion that condenses onto sites on both UBC and carbon sorbents inhibits heterogeneous Hg conversion chemistry. The loss of activity is determined by the condensation of H_2SO_4 onto the population of sites that can potentially be chlorinated on the basis of the total surface area. Once covered by H_2SO_4 , these sites no longer participate in any Hg conversion chemistry. SO_3 condensation first diminishes the population of chlorinated sites (just as a lower ACI concentration would) which, in turn, is responsible for less Hg_p ; hence, lower Hg removals, as seen in

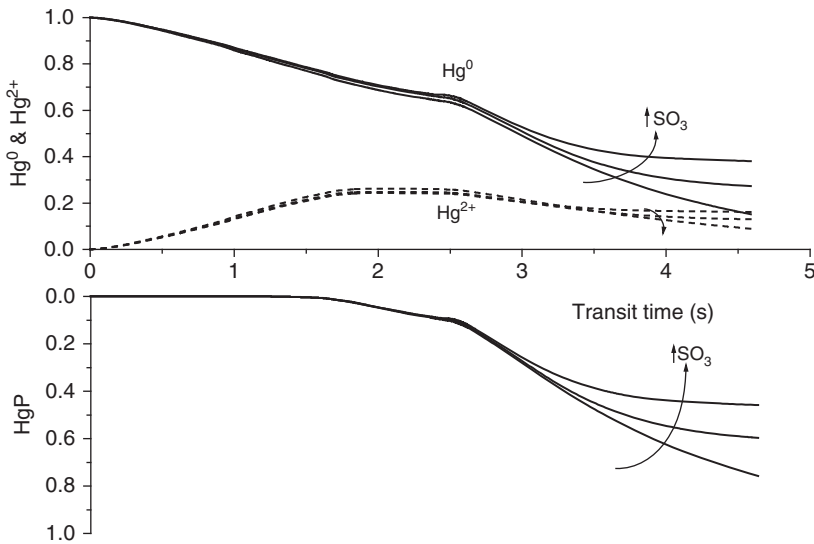


Figure 25.4 Mercurator™ Hg speciation for untreated ACI at 6 lb/MMacf for 7% LOI from a bituminous coal that released 17 ppm HCl in an ESPc-only cleaning system that generated 9.5, 27, and 32 ppm SO_3 .

Figure 25.4. Temperatures from the back-end of the APH into the PCD are critical, because Hg removals can be cut in half by this form of inhibition. Accordingly, either ACI is not recommended with high-S fuels, or high sulfur trioxide levels are mitigated possibly through alkaline sorbents or additives.

When a cleaning system uses ESPh instead of ESPc, Hg removals will be markedly lower because an ESPh operates at temperatures well above the onset of Hg_p production; that is, before the mechanism starts shifting toward desorption control. If it uses FF instead of an ESPc, then all Hg transformations upstream of the FF remain the same, but the behavior within the FF is dramatically different, as seen in Figure 25.5. Very little chemistry occurs during the several seconds needed to transport the flue gas into the filtercake on the filter bags. But immediately after the flue gas contacts the filtercake, there are step changes in the levels of Hg_p and Hg^{2+} , with complete elimination of Hg^0 (via enhanced gas-solid contact between flue gas and the sorbent due to formation of a packed bed-type configuration). The exorbitant surface area of the filtercake is responsible for the near-critical behavior because, on a volumetric basis, the surface area of UBC in a filtercake is five orders of magnitude greater than the surface area of suspended UBC in flue gas for a case with 5 wt% LOI from a coal with 10% ash. Preliminary analysis showed that the Hg conversion chemistry is confined to a relatively thin outer layer of the filtercake, across which the Hg speciation relaxed to the composition for an adsorption equilibrium. Because the layer is relatively thin, it is not necessary to resolve the extent of Hg conversion through the filtercake; we simply evaluate the Hg speciation for adsorption equilibrium. The equilibrium

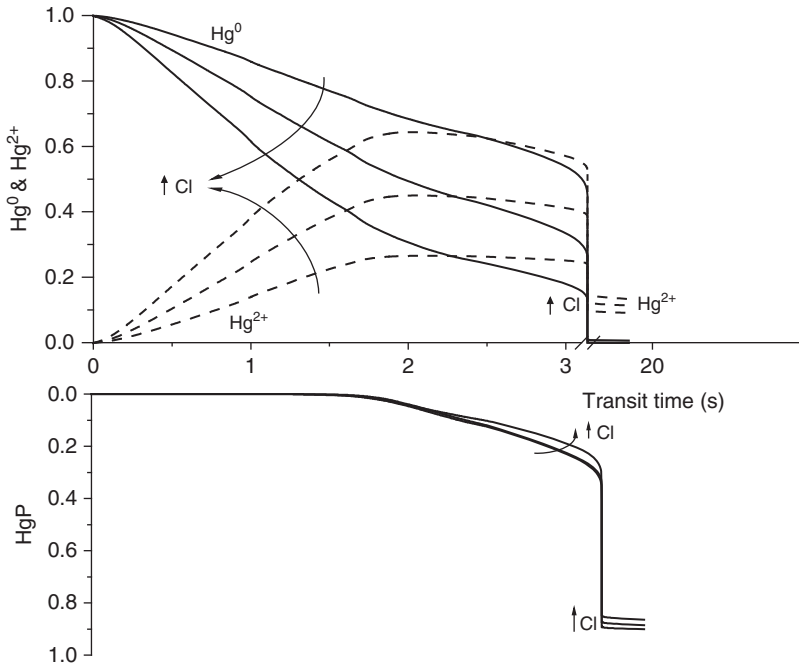


Figure 25.5 Mercurator™ Hg speciation for 7% LOI from a bituminous coal that released 17, 34, and 64 ppm HCl in a FF-only cleaning system.

speciation is not necessarily dominated by Hg_p , because the levels of Cl and carbon surface area determine the proportions of Hg^0 , Hg^{2+} , and Hg_p . As seen in Figure 25.5, progressively more Cl shifts the equilibrium speciation toward Hg^{2+} at the expense of Hg_p , while Hg^0 is always miniscule.

According to our interpretation, in-flight Hg transformations with Cl species are determined by only the heterogeneous reaction mechanism. This is because the extremely low concentrations of Cl atoms and Cl_2 under commercial gas cleaning conditions cannot drive the two-step, autocatalytic cycle whereby Cl-atoms partially oxidize Hg^0 into $HgCl$ which, in turn, is fully oxidized into $HgCl_2$ by Cl_2 to restore the original Cl atom [12]. Even in homogeneous Hg oxidation mechanisms with somewhat different primary conversion channels, the extent of homogeneous Hg oxidation is negligible compared with measured values under commercial cleaning conditions.

However, in-flight Hg transformations with Br species must be attributed to both homogeneous and heterogeneous reaction mechanisms. As seen in Figure 25.6, simulations with only a homogeneous Hg/Br reaction mechanism [13] demonstrate one of the most distinctive features of Hg oxidation by Br species. For a typical thermal history along a gas cleaning system and with 9.4 ppm Br in flue gas, the predicted extent of Hg oxidation approaches 70%. In contrast, the comparable performance with 20 ppm HCl is no Hg oxidation

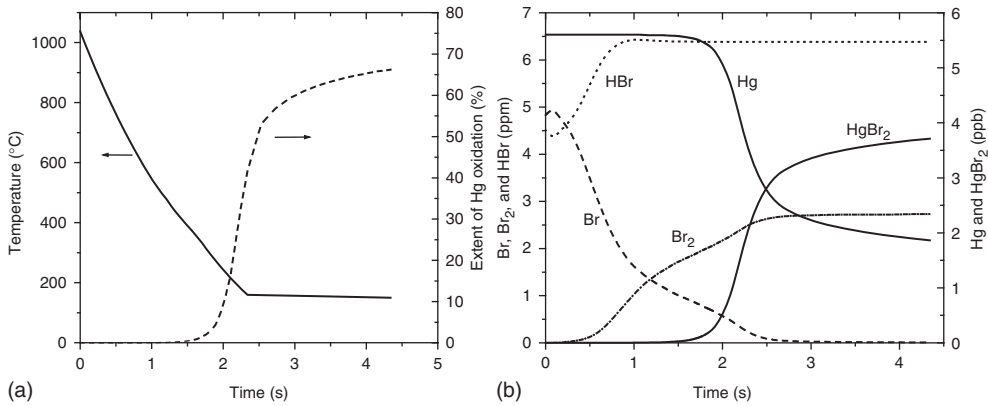


Figure 25.6 (a) Solid curve: typical thermal history for a gas cleaning system whose only APCD is an ESPc and (dashed curve) predicted extent of homogeneous

Hg oxidation with 9.4 ppm Br in flue gas. (b) Solid curves: Hg vapor speciation and (dashed curves) Br speciation for the same conditions.

whatsoever. Homogeneous Hg oxidation by Br begins to produce HgBr₂ as the flue gas cools below 500 °C and accelerates sharply when the temperature cools below 300 °C. At higher temperatures, the instability of an HgBr intermediate fails to sustain HgBr₂ production.

At the furnace exit, Br atoms are present in concentrations that are comparable to HBr levels, in marked contrast to the much lower concentrations of Cl atoms at these conditions. The primary reason that Br is a much more effective Hg oxidizer than Cl is that HBr dissociates into the most reactive atomic species much more extensively than HCl at typical post-flame conditions. As flue gas moves further into the gas cleaning system, Br atoms rapidly recombine through the back-end heat exchangers, first, into HBr, then, into Br₂, so that the HBr concentration plateaus at 600 °C and the Br₂ concentration plateaus at 160 °C. As the flue gas cools in the APH and further downstream, the HgBr₂ concentration surges. HgCl₂ is not produced because homogeneous Hg oxidation by Cl species is too slow under these conditions. All these species approach ultimate steady concentrations in the ESPc because of the low temperatures.

To account for the impact of variations in UBC levels on Hg transformations by Br species, we supplement the homogeneous reaction mechanism with a heterogeneous mechanism that is completely analogous to the heterogeneous mechanism for Cl species in Table 25.1 [13]. The key difference between the contributions from the in-flight mechanisms on UBC for Br and Cl species is that the much higher concentration of Br atoms promotes heterogeneous recombination into Br₂. This process maintains much smaller populations of brominated sites on the UBC than the chlorinated sites. Consequently, the contribution of heterogeneous in-flight chemistry with Br species is smaller, and much lower levels of Hg_p form at the lowest temperatures of interest. This prediction is consistent with several field test results in which Br addition strongly

enhanced Hg^{2+} levels but left Hg_p levels unchanged. Unfortunately, contradictory findings have also been reported, which are compounded by as-yet unresolved interferences in semi-continuous emissions monitor (SCEM) detectors by Br species. We currently expect Br addition to promote substantial homogeneous Hg^0 oxidation through the ECN and upstream of an SCR with little effect on Hg_p levels, because of the heterogeneous recombination of Br atoms into Br_2 . However, such observations must remain tentative until the measurement issues are rectified.

In a similar manner, brominated carbon sorbents are analyzed with the analogous heterogeneous mechanism for Br species, without any bromination stage, and with minimal contributions from homogeneous Hg/Br chemistry, because of the low gas temperatures at ACI locations.

25.3.3

Hg⁰ Oxidation across SCR Catalysts

The oxidation of Hg^0 across the promoted V_2O_5 catalysts on SCR monoliths is completely independent of its in-flight oxidation on UBC. In fact, the catalytic oxidation channel often provides the fastest means to oxidize Hg^0 , especially in the presence of Br species, which may seem surprising because no SCR has yet been designed or optimized to oxidize Hg^0 . Extents of Hg^0 oxidation of 90% or more are routinely recorded in full-scale field tests [14], provided that the flue gas contains abundant Cl- or Br-species and that the SCR provides sufficient reactivity, favorable mass transport rates, and ample residence time for the chemistry to proceed to near completion. When these conditions are satisfied, SCR/ESP/FGD combinations are the technology of choice for Hg control because they require no special operating procedures or reagents to lower Hg emissions, except when Br- and Cl-species are injected to counteract the inherent halogen deficiencies in low-rank coals.

Our first reaction mechanism for catalytic oxidation described simultaneous NO reduction and Hg^0 oxidation in terms of lumped catalyst reactivities that resolved film transport of reactants onto the external catalyst channel wall from an overall chemical reactivity [15]. The key features were a competition between NH_3 and HCl for surface sites, and an Hg^0 oxidation reaction on chlorinated catalyst sites. This competitive adsorption subdivides the catalyst into two stages. An entry stage sustains NO reduction with high concentrations of adsorbed NH_3 , but the population of chlorinated sites remains very small as long as the HCl concentration is much lower than the NH_3 concentration. This small population oxidizes small proportions of the Hg^0 . Once the NH_3 has been consumed, a trailing stage is chlorinated much more extensively and thereby able to rapidly oxidize Hg^0 . This mechanism interpreted extents of Hg^0 oxidation by Cl species in laboratory-, pilot-, and full-scale SCR units for the complete domain of utility gas cleaning conditions, and was recently expanded for oxidation by Br-species [16]. The strong coupling between NO reduction and Hg^0 oxidation via competitive adsorption of

NH₃ and HCl was also independently validated with an extensive series of laboratory tests [17].

Additional modeling work expanded the original lumped analysis in two ways into a legitimate multipollutant analysis [18]. First, simultaneous SO₂ oxidation was incorporated and, second, the analysis resolves internal pore diffusion across the catalyst wall thickness from the intrinsic reactivity of adsorbed species on the catalyst surface with a conventional Thiele analysis, to directly relate catalyst morphology and composition to the multipollutant performance of the SCR reactor. Consequently, the analysis directly relates factors that can be manipulated in the design of SCRs – the size and shape of monolith channels, the composition, and pore size characteristics of the catalyst layer, and the temperature – to the multipollutant performance for specified ranges of flue gas composition and flow rate. It is especially well suited to predicting the performance of a particular SCR across broad domains of flue gas conditions for current and foreseen specifications on fuel quality and furnace firing conditions, and also to optimize SCR design parameters to meet specifications on Hg⁰ oxidation with new and replacement SCR catalysts. The goal is to enable plant operators to take better advantage of fuel switching opportunities by calling for additives or operational adjustments that will enhance Hg removals while maintaining high NO_x removals and acceptable SO₃ levels.

The NO reduction mechanism was developed and fully validated for commercial SCR catalysts by Tronconi and coworkers [19], based on submechanisms for film transport, an Ely-Rideal (ER) reaction mechanism with NH₃ chemisorption (gas phase NO reacting with adsorbed NH₃), and pore diffusion. Similarly, the SO₂ oxidation mechanism was also adapted from Tronconi's work [20], albeit with no mediation by any transport phenomena. Our original mechanism for catalytic Hg⁰ oxidation has been incorporated into this validated framework to account for the mediation of competitive HCl and NH₃ adsorption by pore diffusion. A simple premise connects NO and SO₂ conversion to the Hg⁰ oxidation behavior on SCRs: That HCl, HBr, and Br₂ compete for surface sites with NH₃, and that Hg⁰ contacts these halogenated sites either from the gas phase or as a weakly adsorbed species. On the assumption that the competitive adsorption coverages are independent, the rate expression for adsorbed Hg oxidation is given by

$$r_{\text{Hg}} = {}^{\text{Cl}}k_{\text{Hg}} C_{\text{Hg}}^{\text{S}} \Theta_{\text{Cl}} + {}^{\text{Br}}k_{\text{Hg}} C_{\text{Hg}}^{\text{S}} \Theta_{\text{Br}} = \left[\frac{{}^{\text{Cl}}k_{\text{Hg}} K'_{\text{HCl}} + {}^{\text{Br}}k_{\text{Hg}} K'_{\text{HBr}}}{1 + H K'_{\text{NH}_3} C_{\text{NH}_3}^{\text{S}}} \right] C_{\text{Hg}}^{\text{S}}$$

As the surface coverages of the halide species are independent, the net rate is the sum of independent contributions from Cl and Br, and the original mathematical form of the analysis of only Cl species can be retained. The effective rate constants on the right contain the concentrations of HCl, HBr, and Br₂, which are uniform across the SCR in the steady state.

The common characteristics among the reactivities for NO reduction, SO₂ oxidation, and Hg⁰ oxidation are that (i) NH₃ strongly inhibits all three processes and (ii) all rates are directly proportional to the concentrations of the primary reactant.

Otherwise, SO_2 oxidation is weakly promoted by NO and O_2 , and weakly inhibited by moisture, whereas Hg^0 oxidizes in proportion to the surface coverages of halide species supplied via adsorption of the halogen vapors. These coverages vary along the catalyst length even while the concentrations of halogen vapors remain uniform because they are not consumed in any chemical process other than Hg^0 oxidation, and the Hg^0 concentration is orders of magnitude smaller than all other reactant concentrations. Several analytical solutions were integrated into the analysis to avoid a computationally expensive 2D simulation along and into the catalyst wall, as elaborated elsewhere [18].

According to both of our analyses, the various SCR design specifications and operating conditions can be understood in terms of how they affect the lengths of the two stages for NO reduction and for the oxidation of Hg^0 and SO_2 . Factors that accelerate the transport rates of reactants onto the catalyst walls, such as smaller channel pitches and converting from square to circular channels, shorten the length of the NO reduction stage and thereby promote Hg^0 oxidation. Factors that enhance surface halogenation, such as higher inlet halogen concentrations and lower NH_3/NO ratios, also promote Hg^0 oxidation. Br species dramatically accelerate Hg^0 oxidation rates on some catalysts by as much as a factor of 40 compared to the rates for Cl species [16]. The design analysis also showed that shifting the pore size distribution toward macropores in a final catalyst layer appears to be an effective means to directly enhance Hg^0 oxidation. According to our calculations, this strategy will not increase NH_3 slip, because it raises the effectiveness factor for NO reduction, nor will it increase the extent of SO_2 oxidation by a significant amount, because transport effects are negligible in SO_2 oxidation. But it does have the potential to significantly enhance extents of Hg^0 oxidation, all other SCR operating conditions being the same. Most of these benefits were realized in the increase in macroporosity from 5% to only about 15%, which makes this strategy potentially easier to implement. Increases in the micropore size also enhance Hg^0 oxidation, presumably due to the associated increases in the effective diffusivity of Hg, but the impact is not nearly as large as that for increases in macroporosity.

Perhaps the most important result is that SCR design specifications and operating conditions are at least as important as the halogen concentrations, simply because the domain of these specifications across the industry is enormous. Our database on Hg^0 oxidation across full-scale SCRs covers temperatures from 335 to 395 °C; gas hourly space velocity (GHSV) from 1800 to 4700 h^{-1} ; HCl concentrations from 1 to 130 ppm; Br concentrations from 0 to 50 ppm; inlet NO concentrations from 280 to 900 ppm; and NO reduction efficiencies (or NH_3/NO ratios) from 0 (for out-of-service SCRs) to 0.95. SCRs from four catalyst vendors represent plate-monoliths with pitches to 11 mm and honeycomb monoliths with square and triangular channels of pitches to 10 mm. As seen in Figure 25.7, the predictions from the lumped analysis are generally within 10% of the measured values for all cases except EES8U13, even though the measured extents of Hg^0 oxidation vary from 20% to more than 90%. Such performance could not possibly

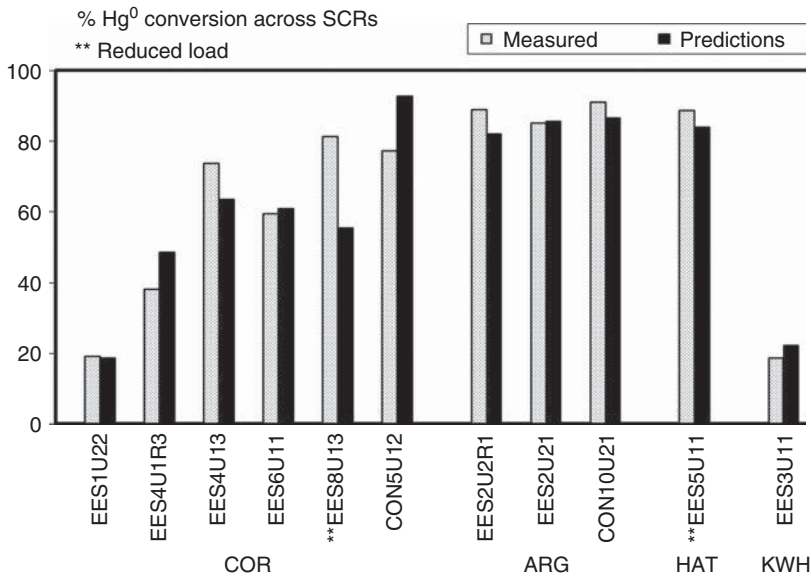


Figure 25.7 Evaluation of extents of Hg⁰ oxidation across various full-scale SCR from Mercurator™ (solid) with measured values representing four catalyst vendors (gray).

be achieved unless the impact of the operating conditions and design specifications was accurately described, in conjunction with the appropriate dependencies on the halogen concentrations.

25.3.4

Hg Transformations within WFGDs

The Hg field-testing literature shows that WFGDs usually capture at least 90% of the Hg²⁺ in flue gas, but virtually none of the Hg⁰, because Hg⁰ is insoluble in aqueous solutions. However, several full- and bench-scale tests have documented Hg reemission whereby the Hg⁰ concentration at the FGD exit is greater than that at the inlet, suggesting that some of the Hg(II) in the scrubber solution must be reduced and reemitted as Hg⁰ vapor. Hg reemissions have also been observed in natural waters and atmospheric cloud and rain-water cycles [21–23], where S(IV) species promote the reduction of Hg²⁺. Bench-scale studies under well-controlled scrubbing conditions showed that Cl⁻ and O₂ suppress reemission, whereas Ca²⁺ and Mg²⁺ species promote it.

We recently developed a quantitative analysis that identifies and rank-orders the factors involved in Hg reemission during wet FGD scrubbing, to support efforts to mitigate Hg reemission from full-scale, commercial wet FGDs. To simulate Hg transformations WFGD scrubbers, one must first model SO₂ absorption to describe the major solution species (S, Ca, Cl) and their variations with FGD operating conditions (L/G, droplet diameter, T). The conventional simulation strategy

builds numerous equilibrium constraints into a mass transport analysis of the exchange of species from the flue gas into the spray droplets along an absorber tower, with simultaneous limestone dissolution and sulfite oxidation within slurry droplets. Given the absorber temperature and the inlet compositions of flue gas and slurry, the conventional FGD analysis predicts the correct pH and reasonable SO₂ absorption rates along the absorber. It also depicts realistic tendencies for variations in the inlet SO₂ level, and identifies distinctive conditions where elevated HCl levels will reduce SO₂ removal efficiencies by 5–10%, and greater SO₂ removal for smaller slurry droplets, all else the same.

While the conventional FGD analysis relates gross FGD operating conditions to SO₂ absorption efficiencies, it is unsuitable for trace metal transformations, especially for Hg reemission. The reason is that conventional formulations implicitly assume that all oxygen is consumed in sulfite oxidation at the liquid interface on a slurry droplet, and evaluate the rate of sulfite oxidation as an average based on bulk liquid concentrations. The requisite analysis for Hg²⁺ chemistry and, presumably, other trace metal transformations must automatically shift the redox potential of bulk liquid in the spray from oxidizing to reducing through a balance among the finite-rate reagent fluxes that participate in sulfite oxidation. Our SO₂ capture analysis allows oxygen to penetrate through the liquid film and accumulate in the bulk liquid if its concentration exceeds the stoichiometric requirement for bisulfate oxidation. We also propose a finite-rate reaction for Hg(II) reduction that depends on temperature, pH, and S(IV) species which, in the absence of sufficient oxygen, promote Hg(II) reduction to Hg⁰ vapor.

The computerized implementation covers the process chemistry occurring in both a counterflow absorber and slurry holding tank [24]. The tank analysis determines the required limestone feed rate for a given tank residence time distribution (RTD) and the solids size distribution into the spray nozzles within the absorber. It also determines how much liquid must be extracted to maintain a target Cl concentration in the tank. The absorber analysis determines the SO₂ capture and the compositions of liquid and solids that return into the holding tank. Given the absorber temperature and the inlet compositions of flue gas and slurry, the analysis predicts the SO₂ capture efficiency, complete slurry composition and flue gas composition, slurry pH, the quantitative enhancement of mass transfer by acid dissociations in the slurry, and the relative contributions of liquid and gas resistances to the overall mass transfer rate. All quantities are resolved as functions of distance along the absorber axis.

For the operating conditions and bulk species concentrations reported for a full-scale limestone WFGD, the analysis correctly predicts that SO₂ was continuously removed along the length of the absorber, whereas most of the Hg was removed in the lower section at a much greater efficiency than SO₂ removal, owing to the high aqueous solubility of HgCl₂. For the baseline case with 20% Hg⁰, the predicted reemission gradually increased to 20%, and the total Hg removal reached only 65%.

According to the analysis, aqueous Hg species segregate into two groups, Hg–Cl species and Hg–S(IV) species. How variations in the scrubber operating conditions shift the proportions of these two groups is critical, because only the

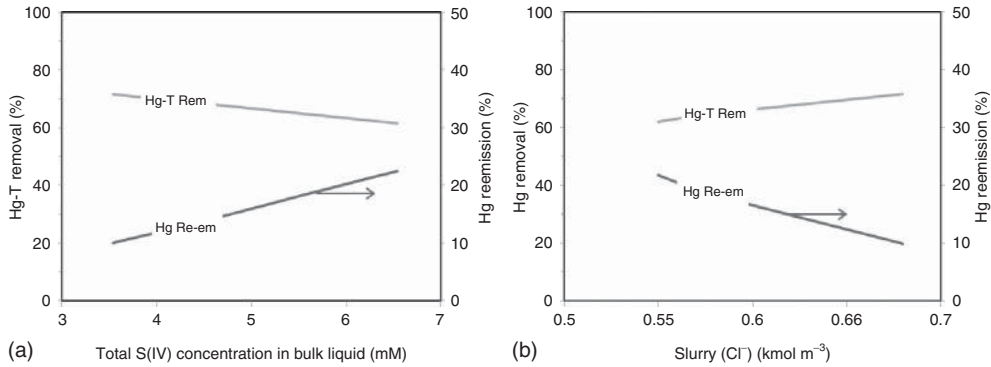


Figure 25.8 Effect of bulk liquid (a) S(IV) and (b) slurry Cl⁻ concentrations on total Hg removal (left y-axis) and percentage Hg reemission (right y-axis).

Hg-S(IV) species can be reduced and subsequently reemitted as Hg⁰ back into the flue gas. The two most important factors are shown in Figure 25.8, which shows the total Hg removals and extents of Hg⁰ reemission for concentration ranges of S(IV) and Cl⁻ species. As the S(IV) concentration was increased from approximately 3.5 to 6.5 mM, the Hg removal decreased from 72 to 62% with an increase in Hg reemission by a similar percentage. For a twofold increase in S(IV) concentrations, the Hg-S(IV) fraction in the solution at the absorber exit increased from 14 to 36% with a corresponding decrease in Hg-Cl levels. The predicted Hg reemission therefore linearly tracks the Hg-S(IV) levels. Conversely, for progressively greater Cl⁻ in solution, the Hg(II) species preferentially partition into Hg-Cl complexes that reduce reemission, which is consistent with the observations in bench- and pilot-scale experiments. As the Cl⁻ concentration was increased from 0.5 to 0.68 kmol m⁻³, the Hg-Cl ions increased from 66 to 84% with a corresponding decrease in Hg-S(IV) complexes. The change in Cl⁻ did not affect Hg²⁺ absorption as it was in excess of 99% in all cases. The increased partitioning of Hg(II) into Hg-Cl complexes decreased reemission by 11% and increased the Hg removal from 62 to 72%.

Most additives to control Hg reemission from scrubbers, such as Na₂S₄, TMT-15™, and NaHS, release S(II) ions in the slurry and precipitate Hg as HgS(s). We examined the addition of small amounts of S(II) into the base case scrubber solution and simulated Hg capture. Even at 1 μM concentrations of the additive, all the Hg(II) precipitated as HgS(s), which establishes the maximum Hg²⁺ concentration in the solution as only 10⁻³³. According to our simulations with 80% HgCl₂ in the flue gas, essentially all Hg(II) was retained in the solid phase. These predictions are consistent with the B&W tests at Endicott station [25], where the addition of NaHS almost completely suppressed Hg reemission and the extent of reemission did not bear any relation to the additive feed rate. We also simulated the addition of S(II) under oxidizing conditions where the pH was increased to 6.5 and the S(IV) concentration was reduced to the point where oxygen was in excess, to characterize lime-based WFGDs. Under such conditions, equilibrium shifts the added S(II)

species to their oxidized forms, which prevents any precipitation of HgS solids. This is consistent with B&W tests at the Mg/lime WFGD at Zimmer station [25], where adding NaHS did not improve the baseline Hg-T capture efficiency even at high additive feed rates.

At this point in its development, our FGD scrubbing analysis predicts reasonable extents of Hg removals and Hg reemission under realistic FGD operating conditions, without any parameter adjustments. Most Hg²⁺ in flue gas is captured near the flue gas inlet at the bottom of the absorber, but Hg reemission can occur along the entire absorber at a rate that accelerates slightly along the upper elevations. Predicted Hg removals are insensitive to droplet diameter, whereas smaller slurry droplets reemit more Hg because they sustain faster absorption of all the reagent gases involved in Hg(II) reduction. The total S(IV) species concentration in the slurry promotes reemission; conversely, the analysis correctly predicts less reemission for greater Cl⁻ concentrations in the slurry, in accord with a well-established tendency. Simulations with added S(II) species, as released from commercial additives to suppress Hg reemission, correctly gave complete precipitation of Hg(II) as HgS(s). These predictions are consistent with full-scale field tests where the addition of NaHS almost completely suppressed Hg reemission and the extent of reemission did not bear any relation to the additive feed rate.

25.4

Summary

Collectively, the reaction mechanisms described in this chapter cover all the most common fuels, firing configurations, and gas cleaning configurations, and enable accurate estimates for Hg emissions rates from virtually any commercial power plant. Such estimates are the most expedient and economical means to evaluate potential Hg control technologies, both inherent and external. The fact is that even many individual power plants and, certainly, regional utility operations use so many fuel types that testing all of them becomes a practical impossibility. And such variations will only expand in the foreseeable future as operators develop strategies to comply with new regulations and new fuel sources open up.

Beyond the predictive capabilities resting upon these mechanisms, this level of analysis has clearly exposed the determining factors for Hg emissions. In-flight Hg transformations are determined by halogen concentrations, the halogenated surface area on UBC and carbon sorbents, the type of PCD, and, in ACI applications, the ACI concentration. Unless halogens are added to compensate for low inherent coal-Cl, the enormous inherent variability of coal-Cl levels is a primary consideration, and this variability can only be established by measurements because it is completely independent of all other coal properties. Chlorinated surface areas on UBC reflect the furnace firing configuration, fly ash LOI, and, especially, the coal rank. These influences tend to counteract each other insofar as low-rank coals give UBC with very high specific surface areas but generate very low LOI levels. Conversely, high-rank coals give UBC with low surface areas but generate much

higher LOI levels. Even so, it is impossible to accurately depict in-flight Hg transformations without an accurate account of all three influences on the chlorinated surface area. ACI with untreated carbon sorbents mitigates the inherent variations in chlorinated surface area, but does not necessarily eliminate the halogen dependence. This limitation is clearly seen in the much-lower-than expected asymptotic Hg removals for ACI with many low-rank coals. ACI with brominated carbon is the only current means to completely circumvent these limitations. Unfortunately, even this “universal” solution may be diminished by SO₃ inhibition. Whenever flue gas SO₃ levels are high enough to drive the SO₃ dew point below the local gas temperature in the APH and further downstream, condensed H₂SO₄ will deactivate halogenated sites on UBC and carbon sorbents, whether or not they have been brominated. As this inhibition can cut Hg removals in half, ACI is not recommended with high-S fuels, unless sorbent additives or sulfur trioxide mitigation are implemented.

In cleaning systems that exclusively rely on in-flight Hg transformations to control Hg emissions, relatively very high LOI levels are needed to generate sufficient UBC to produce appreciable Hg_p levels that can be removed in the PCD, even with high-Cl coals. Therefore, impending Hg emission regulations can only be met with ACI. Whether or not the sorbent is brominated, Hg removals for ACI upstream of a FF are significantly greater than ESPc removals, and this scheme requires much lower ACI concentrations to achieve a targeted Hg removal. This is because the enormous volumetric surface area in an FF filtercake brings the Hg speciation to adsorption equilibrium, while ESPs rapidly eliminate all the chlorinated carbon surface area from the flue gas and shut down the Hg conversion chemistry. Our analysis indicates that the only PCD-only cleaning configuration that can match the Hg removal performance of an SCR + ESPc + WFGD configuration is when ACI is positioned between an ESPc and a FF (Toxecon™-I).

The Hg⁰ oxidation performance of SCRs is no less variable than the in-flight transformations, because SCR design specifications and operating conditions are at least as important as the halogen concentrations. This variability reflects the fact that none of the SCRs in service were designed, let alone optimized, to oxidize Hg⁰. The essential feature is that NH₃ adsorption inhibits the adsorption of the species involved with Hg⁰ oxidation, which subdivides the catalyst into two stages. An entry stage sustains NO reduction with high concentrations of adsorbed NH₃ but too few chlorinated sites to sustain Hg⁰ oxidation. Once the NH₃ has been consumed, a trailing stage is chlorinated much more extensively and thereby able to rapidly oxidize Hg⁰. The various SCR design specifications and operating conditions can be understood in terms of how they affect the lengths of these two stages. Factors that enhance surface halogenation, such as higher inlet halogen concentrations and lower NH₃/NO ratios, also promote Hg⁰ oxidation. Br species dramatically accelerate Hg⁰ oxidation rates on some catalysts by as much as a factor of 40 compared to the rates for Cl species. The analysis also shows that shifting the pore size distribution toward macropores in a final catalyst layer appears to be an effective means to directly enhance Hg⁰ oxidation.

The WFGD analysis predicts Hg reemission along the entire absorber, but not in the slurry holding tank for a limestone, forced oxidation system. The total S(IV) species concentration in the slurry promotes reemission; conversely, the analysis correctly predicts less reemission for greater Cl^- concentrations. Simulations with added S(II) species, as released from commercial additives to suppress Hg reemission, correctly gave complete precipitation of Hg(II) as HgS(s). These predictions are consistent with full-scale field tests where the addition of NaHS almost completely suppressed Hg reemission and the extent of reemission did not bear any relation to the additive feed rate. But this analysis needs additional validation with data from full-scale WFGDs before it can deliver accurate quantitative interpretations.

References

1. Chu, P., Behrens, G., and Laudal, D. (2001) Estimating total and speciated mercury emissions from US coal-fired power plants. Proceedings of the Air and Waste Management Association Specialty Conference on Mercury Emissions: Fate, Effects, and Control, Chicago, IL, August 21–23, 2001.
2. Afonso, R. and Senior, C. (2001) Assessment of mercury emissions from full scale power plants. Proceedings of the Air and Waste Management Association Specialty Conference on Mercury Emissions: Fate, Effects, and Control, Chicago, IL, August 21–23, 2001.
3. Rubin, E.S., Berkenpas, M.B., Farrell, A., Gibbon, G.A., and Smith, D.N. (2001) Multi-pollutant emission control of electric power plants. Proceedings of the Air and Waste Management Association Specialty Conference on Mercury Emissions: Fate, Effects, and Control, Chicago, IL, August 21–23, 2001.
4. Weilert, C.V. and Randall, D.W. (2001) Analysis of the ICR data for mercury removal from wet and dry FGD. Proceedings of the Air and Waste Management Association Specialty Conference on Mercury Emissions: Fate, Effects, and Control, Chicago, IL, August 21–23, 2001.
5. Naik, C.V., Krishnakumar, B., and Niksa, S. (2010) Predicting Hg emissions from utility gas cleaning systems. *Fuel*, **89**, 859–867.
6. Krishnakumar, B. and Niksa, S. (2011) Predicting the impact of SO_3 on mercury removal by carbon sorbents. *Proc. Combust. Inst.*, **33** (2), 2779–2785.
7. Lu, Y., Rostam-Abadi, R., Chang, R., Richardson, C., and Paradis, J. (2007) Characteristics of fly ashes from full-scale coal-fired power plants and their relationship to mercury adsorption. *Energy Fuels*, **21**, 2112–2120.
8. Hurt, R.H. and Gibbins, J.R. (1995) Residual carbon from pulverized coal fired boilers: 1. Size distribution and combustion reactivity. *Fuel*, **74** (4), 471–480.
9. Kulaots, I., Hurt, R.H., and Suuberg, E.M. (2004) Size distribution of unburned carbon in coal fly ash and its implications. *Fuel*, **83**, 223–230.
10. Puri, B.R. (1970) Surface complexes on carbons, in *Chemistry and Physics of Carbon*, vol. 6 (ed. P.L. Walker Jr.), Marcel Dekker, New York.
11. Huggins, F.E. and Huffman, G.P. (1999) XAFS examination of mercury sorption on three activated carbons. *Energy Fuels*, **13** (1), 114.
12. Niksa, S., Helble, J.J., and Fujiwara, N. (2001) Kinetic modeling of homogeneous mercury oxidation: the importance of NO and H_2O in predicting oxidation in coal-derived systems. *Environ. Sci. Technol.*, **35**, 3701–3706.
13. Niksa, S., Padak, B., Krishnakumar, B., and Naik, C.V. (2010) Process chemistry of Br addition to utility flue gas for Hg

- emissions control. *Energy Fuels*, **24** (2), 1020–1029.
14. Chu, P., Laudal, D., Brickett, L., and Lee, C.W. (2003) Power plant evaluation of the effect of SCR technology on mercury. Proceedings of DOE-EPRI-U.S. EPA -A&WMA Combined Power Plant Air Pollutant Control Symposium – The Mega Symposium, Washington, DC, May 19–22, 2003.
 15. Niksa, S. and Fujiwara, N. (2005) A predictive mechanism for mercury oxidation on SCR catalysts under coal-derived flue gas. *J. Air Waste Manage. Assoc.*, **56**, 1866–1875.
 16. Niksa, S., Naik, C.V., Berry, M.S., and Monroe, L. (2007) Interpreting enhanced Hg oxidation with Br addition at Plant Miller. Proceedings of Air Quality VI, Arlington, VA, September 24–26, 2007.
 17. Kamata, H., Ueno, S.-I., Naito, T., and Yukimura, A. (2008) Mercury oxidation over the $V_2O_5(WO_3)/TiO_2$ SCR catalyst. *Ind. Eng. Chem. Res.*, **47**, 8136–8141.
 18. Niksa, S. and Freeman Sibley, A. (2010) Relating catalyst properties to the multipollutant performance of full-scale SCR systems. *Ind. Eng. Chem. Res.*, **49**, 6332–6341.
 19. Tronconi, E., Forzatti, P., Gomez Martin, J.P., and Malloggi, S. (1992) Selective catalytic removal of NO_x : a mathematical model for design of catalyst and reactor. *Chem. Eng. Sci.*, **47** (9–11), 2401–2406.
 20. Svachula, J., Alemany, L.J., Ferlazzo, N., Forzatti, P., and Tronconi, E. (1993) Oxidation of SO_2 to SO_3 over honeycomb $DeNO_x$ ing catalysts. *Ind. Eng. Chem. Res.*, **32**, 826–834.
 21. Brosset, C. (1987) The behavior of mercury in the physical environment. *Water Air Soil Pollut.*, **34**, 145–166.
 22. Munthe, J., Xiao, Z.F., and Lindqvist, O. (1991) The aqueous reduction of divalent mercury by sulfite. *Water Air Soil Pollut.*, **56**, 621–630.
 23. Van-Loon, L., Mader, E., and Scott, S.L. (2000) Reduction of the aqueous mercuric ion by sulfite: UV spectrum of $HgSO_3$ and its intramolecular redox reaction. *J. Phys. Chem. A*, **104**, 1621–1626.
 24. Krishnakumar, B. and Niksa, S. (2011) Interpreting the re-emission of elemental mercury during wet FGD scrubbing. Proceedings of Air Quality VIII, Crystal City, VA, October 23–27, 2011.
 25. Amrhein, G.T., Bailey, R.T., Downs, W., Holmes, M.J., Kudlac, G.A., and Madden, D.A. (1999) Advanced Emissions Control Development Program- Phase III. Final Report to U.S. Department of Energy Under Contract# DE-FC22-94PC94251, Babcock and Wilcox Power Generation Group, Inc, Barberton, OH, July, 1999.

Index

a

activated carbon 277–280. *See also* carbon sorbents for pollution control

- application 282–283
- for mercury control 311–312
- B-PAC™ 327, 329
- C-PAC™ 329–331
- properties in emission systems 283–285
- particles 289–290
- pores 286–289
- surface 285–286

activated carbon injection 156–157, 171, 293–294

- balance-of-plant impacts
- coal combustion by-products 305–307
- chemically treated PAC 173–175
- conventional PAC with chemical additives 175–176
- economic analyses 181
- effectiveness and influencing factors 296
- distribution 304–305
- flue gas characteristics 297–303
- injection location 304
- PAC-specific factors 303–304
- site-specific factors 296–297
- TOXECON™ 305
- system 294
- conveying 295
- distribution 296
- metering 295
- powdered activated carbon storage 294
- untreated PAC 171–172
- upstream of hot-side ESP 176

air-entraining agents (AEAs) 211, 324–325

air pollution control devices on utility and industrial boilers 117–118

- boiler populations in United States 120–121

- NO_x control 119
- PM control 118
- SO₂ control 119

air preheater (APH) 112

amended silicates 344–345

- background and motivations 340–341
- demonstrations 342–344
- working 341–342

ash-to-carbon ratio 212

ASTM Method D6784-02. *See* Ontario Hydro method

atomic fluorescence spectrometry (AFS) 351

atomistic-level models 389–390

- heterogeneous chemistry
- mercury adsorption on activated carbon 400–404
- mercury adsorption on precious metals 404–406
- homogeneous mercury oxidation kinetics
- mercury–bromine chemistry 397–399
- mercury–chlorine chemistry 390–397

b

baghouse 339, 342, 349. *See also* fabric filter

batch methods for mercury monitoring 91

- dry batch methods
- method overview 97
- relative accuracy and quality assurance/quality control 100–105
- sampling protocol procedure and apparatus 99–100
- sorbent trap method history 95–96
- speciation measurements 98–99
- total Hg measurements 97–98
- trap analysis 100
- recommendations 105

- – expected mercury concentration in flue gas 105
- – installation and operation complexity 106
- – particulate matter 105
- – real-time data need 106
- – total versus speciated mercury 105
- wet chemistry batch methods
 - – early EPA total Hg methods 91–93
 - – method application and data quality considerations 94–95
 - – methods to speciate Hg 93–94
- best available technique or technology/best environmental practice (BAT/BEP) 51, 54
- biogeochemical cycle 5, 8–9
- boiler chemical addition 213–214
 - challenges and responses 215–218
 - combined technologies 214–215
- bromide leaching from fly ash 217–218
- bromine (Br) 32–35
- bromine-salt mercury oxidation 242
- bromophenol blue number (BPB) 315
- bubble pressure method 325
- bulk density 315
- burning zone 145

- c**
- cake 312
- calciner 146
- calcium
 - and carbon synergism to conditions 234, 236
 - as enhancer of mercury retention on carbon 233–234
- capture efficiency 165, 169, 181
- carbon burnout method 330
- carbonization 280
- carbon monoxide (CO) 357
- carbon sorbents for pollution control
 - activated carbon 277–280
 - – applications 282–283
 - – properties in emission systems 283–290
 - carbon materials 277
 - carbon particle shapes and forms 280, 282
 - – granular activated carbon (GAC) 281
 - – powdered activated carbon (PAC) 280–281
 - – shaped activated carbon 282
- catalysts, for mercury oxidation 253
 - affecting parameters 254–255
 - – heterogeneous oxidation 256–257
 - – Hg^0 oxidation and SO_2/SO_2 conversion 259–261
 - – homogeneous oxidation 255
 - – reaction mechanism 255
 - – SCR operation- Hg^0 reaction effects 257–259
- future research 260
- process overview 253–254
- cement kiln dust (CKD) 143, 324
- cement kiln system 147–153
- cement manufacturing industry and mercury emission control 141
 - cement kiln system 147–153
 - mercury emissions control solutions in cement industry 153–155
 - – activated carbon injection (ACI) 156–157
 - – selective catalytic reduction and wet scrubbing 158–159
 - – wet scrubbing 157–158
 - process description 141–144
 - – dry process kiln 145–147
 - – wet process kiln 144–145
- chemical additives 170. *See also* boiler chemical addition
- chemisorption 194, 195
- chlorine (Cl) 30–32, 397
 - speciation in coal-fired power plants 227–228
- circulating fluidized bed combustors (CFBCs) 416
- clarifiers 265
- Clean Air Act (CAA) (1970) 45, 48–49
- Clean Air Act Amendments (CAAA) 45
- Clean Air Mercury Rule (CAMR) 47, 95, 122
- clinker 143–145
- coal blending 236–237
- coal combustion by-products 305–307
 - corrosion issues 307
 - impacts on particulate emissions 306
 - PAC autoignition in ash hoppers 306
- coal combustion residues and by-products 201
- coal combustion systems and mercury behavior 111
 - air pollution control devices on utility and industrial boilers 117–118
 - – boiler populations in United States 120–121
 - – NO_x control 119
 - – PM control 118
 - – SO_2 control 119
 - coal combustion boilers 112

- in coal-fired boilers
 - – data sources 121–123
 - – mercury behavior in APCDs 123, 125–129
 - mercury chemistry in combustion systems 113–117
 - COALQUAL database 16–19
 - coal utilization byproducts (CUB) R&D program 182–183
 - cold-side electrostatic precipitators (C-ESPs) 118
 - cold vapor atomic absorption spectrometry (CVAAS) 15, 73–74, 93
 - cold vapor atomic fluorescence spectrometry (CVAFS) 15, 74–75
 - combustion modification and mercury control 227
 - chlorine speciation in coal-fired power plants 228
 - effects on mercury oxidation across SCR catalysts 238
 - – mercury oxidation inhibition 238
 - mercury speciation governing mechanisms 228–229
 - potential strategies to mitigate mercury emissions 236–238
 - unburned carbon in mercury oxidation and adsorption 229–231
 - – carbon type nature 231–232
 - – concentration needed to oxidize and remove mercury from flue gas 232–233
 - – synergistic relationship with calcium in fly ash 233–234
 - concrete-compatible activated carbon 323–324. *See also* activated carbon
 - – cement kiln mercury emission control 334–335
 - – commercial application 331
 - – full-scale trials 332–334
 - field fly ash/C-PAC™ mixture 335–336
 - – air content of fresh concrete 336
 - – mercury stability in fly ash and concrete 337
 - – unconfined compressive strength (UCS) 336–337
 - metrics 324–325
 - – Concrete-Friendly™ and acid blue index 326–329
 - Concrete-Friendly™ 325
 - continuous emission monitoring (CEM) 58
 - continuous mercury monitors (CMMs) 71–73
 - components 73
 - – calibration system 79–82
 - – mercury analyzer 73–75
 - – pretreatment/conversion systems and probe 75–79
 - installation and verification requirements 82
 - – CMM verification 82–84
 - – installation 82
 - tests 84–87
 - vendors 87
 - Cooper Environmental 75
 - C-PAC™ 329–331
 - and field fly ash mixture 335–336
 - – air content of fresh concrete 336
 - – mercury stability in fly ash and concrete 337
 - – unconfined compressive strength (UCS) 336–337
 - full-scale trials 332–334
 - Cross-State Air Pollution Rule (CSAPR) 220
 - crystalline materials 277–279
- d**
- density functional theory (DFT) 401, 403–405
 - Department of Energy (DOE)'s mercury control technology research, development, and demonstration program 165
 - background 165–166
 - – activated carbon injection (ACI) 171–176
 - – catalysts 170–171
 - – chemical additives 170
 - – coal utilization byproducts (CUB) R&D program 182–183
 - – field testing program results 169
 - – fly ash impacts 176–178
 - – mercury control cost estimates 180–182
 - – mercury control technologies 168–169
 - – mercury control technology commercial demonstrations 180
 - – mercury fate determination in FGD byproducts 183–184
 - – mercury fate determination in fly ash 184–185
 - – mercury speciation 167–168
 - – National Energy Technology Laboratory (NETL)'s mercury control technology R&D 166–167
 - – NETL in-house development of novel control technologies 179
 - – oxidation enhancements 169
 - – sulfur trioxide interference 178–179

- devolatilization 232, 279
 - direct mercury analysis (DMA) 15
 - dry batch methods
 - method overview 97
 - relative accuracy and quality assurance /quality control 100–105
 - sampling protocol procedure and apparatus 99–100
 - sorbent trap method history 95–96
 - speciation measurements 98–99
 - total Hg measurements 97–98
 - trap analysis 100
 - dry process kiln 145–147
 - dry sorbent injection (DSI) 220
 - dual-path method 73
 - dust shuttling 155
- e**
- Eastman Chemical Company 367
 - economizer (ECN) 414, 417, 420
 - electric generating units (EGUs) 46–47
 - Electric Power Research Institute (EPRI) 95, 205
 - boiler chemical addition 213–214
 - challenges and responses 215–218
 - combined technologies 214–215
 - controls integration for mercury with controls for air pollutants 220–222
 - installed controls co-benefits 205
 - selective catalytic reduction/flue gas desulfurization 205–206
 - unburned carbon 206–207
 - mercury control novel concepts 218
 - Gore[®] carbon polymer composite modules 218–219
 - Sorbent Activation Process[®] 219–220
 - TOXECON II[®] 218
 - sorbent injection 207
 - challenges and responses 211–212
 - electrostatic precipitator units 208–209
 - fabric filter units and TOXECON[™] 209, 210
 - electrostatic precipitators (ESPs) 296, 297, 300, 306, 311, 312, 316, 318–319
 - eastern bituminous coals and high-sulfur flue gases 208–209
 - performance optimization 211–212
 - western coals 208
 - Eley–Rideal mechanism 256
 - emission limit values (ELVs) 54
 - emissions 45
 - endothermic reactions 112, 134
 - Energy & Environmental Research Center (EERC) 85–86, 137, 361, 364
 - Center for Air Toxic Metals[®] 86
 - Envimetrics 75
 - Environmental Protection Agency (US EPA) 45–46, 95
 - Office of Enforcement and Compliance Assurance (OECA) 49
 - research program 191
 - coal combustion residues and by-products 201
 - congressionally mandated studies 191–193
 - control technology from work on municipal waste combustors (MWCs) 193–194
 - EPA SBIR program 202
 - halogenated activated carbon sorbents 196–197
 - mercury chemistry, adsorption, and sorbent development 194–195
 - mercury control in wet-FGD scrubber 198–199
 - non-carbonaceous sorbents 197–198
 - SCR effect on mercury oxidation/capture 199–201
 - EPRI PISCES program 96
 - ethyleneglycolphenylether (EGPE) 330
 - exothermic reactions 134
- f**
- fabric filter (FF) 209–210, 293, 296, 298, 311–312, 317
 - flue gas adsorption for mercury speciation (FAMS) method 96
 - flue gas desulfurization (FGD) 54, 119, 128–129
 - mercury fate determination in byproducts 183–184
 - wet FGD enhancement economic analyses 181–182
 - flue gas mercury oxidation technologies effects on FGD capture 272–274
 - flue gas mercury sorbent speciation (FMSS) 96
 - flue gas temperature influence 212
 - fluidized bed combustors (FBCs) 416
 - fluorine (F) 35–36
 - fly ash
 - bromide leaching 217–218
 - impacts 176–178
 - mercury fate determination 184–185
 - sales preservation 211, 217
 - foam index 325

Frontier Geosciences 96
 fuel additive injection equipment
 242–243
 fuel and flue-gas additives 241–242. *See also* boiler chemical addition
 – bromine-salt mercury oxidation 242
 – case study results 243–250
 – fuel additive injection equipment
 242–243
 fuel gas 404
 furnace intrusion modifications 237–238

g

gaseous elemental mercury (GEM) 7–8
 gasification process sorbents 357
 – background 358–360
 – cold gas cleanup of mercury 366–369
 – – carbon-based materials 367–368
 – – wet scrubbing technique 369–370
 – warm/humid gas temperature mercury
 sorbent capture techniques 360–366
 gasification systems
 – applications and downstream gas cleanup
 and processing 135
 – coal gasification principles 133–134
 – mercury and MATS rule for gasifiers
 139
 – mercury control technologies for
 gasification 138–139
 – mercury measurement in reducing
 environment 137–138
 – mercury transformations and fate 135,
 137
 – technologies and gasifier descriptions
 134–135
 Gas Technology Institute (GTI) 362
 gold amalgamation 73–74
 Gore[®] carbon polymer composite modules
 218–219
 grasshopper effect 9

h

halogen 3, 207–208, 213, 255–256, 285
 halogenated carbon sorbents 196–197,
 311. *See also* activated carbon
 – balance-of-plant impacts 319–320
 – manufacture 315–316
 – motivation 313–315
 – performance 316–319
 halogens in coal 29
 – bromine (Br) 32–35
 – chlorine (Cl) 30–32
 – fluorine (F) 35–36
 – iodine (I) 35

hazardous air pollutants (HAPs) 45–47
 hopper fibers 212
 hot-side electrostatic precipitators (H-ESPs)
 118
 HovaCal[®] gravimetric approach 81, 82
 humid gas cleanup 359
 hydrocyclones 265–266
 hydrogen 357

i

Industrial Emissions Directive (IED)
 56
 inertial separation probe (ISP) 76–77
 inflection point differences (IPDs) 378
 “in-flight” capture mechanism 348
in situ analyzer 75
 instrumental neutron activation analysis
 (INAA) 15
 integrated gasification combined cycle
 (IGCC) 138–139, 179, 357
 – flow schematic 359
 Integrated Pollution Prevention and Control
 (IPPC) Directive 53
 international legislations and trends
 51–53
 – Asia 60, 63–64
 – – China 60–62
 – – Japan 62–63
 – Australia 64–65
 – Canada 65
 – Europe 59
 – – Germany 59
 – – Netherlands 59–60
 – European Union (EU) 53–58
 – Russia 65
 – South Africa 65
 – UNEP instrument on mercury (Minamata
 Convention) 53
 International Union of Pure and Applied
 Chemistry (IUPAC) 315, 331
 iodine (I) 35

k

KEMA TRACE MODEL[®] 60

l

Langmuir–Hinshelwood mechanism
 256
 Large Combustion Plant Directive (LCPD)
 54
 leaching 184–185
 limestone 261, 262
 loss-on-ignition (LOI) level 415

m

- macropores 287
 - Mars–Maessen/Mars–van Krevelen mechanism 256
 - maximum achievable control technology (MACT) 45, 47, 85, 86, 95, 166, 323
 - measurement error 83
 - MerCal™ 81
 - MerControl® 130, 242, 244–249
 - Mercurator™ 413, 414, 420, 423, 424, 425
 - mercury, in environment 3–4
 - as chemical element 4–6
 - – associations with minerals and fuels 6
 - – atmospheric reactions and lifetime 7–8
 - – atmospheric transport and deposition 7
 - – biogeochemical cycling 8–9
 - – direct uses 6–7
 - – physical and chemical properties of forms 6
 - mercury adsorption
 - on activated carbon 400–404
 - on precious metals 404–406
 - mercury analyzer 72–73
 - analytical methods 75
 - cold-vapor atomic absorption spectrometry (CVAAS) 73–74
 - cold-vapor atomic fluorescence spectrometry (CVAFS) 74–75
 - Mercury and Air Toxics Standards (MATS) 19, 30, 95, 139, 313
 - existing sources 47–49
 - new sources 49–50
 - mercury–bromine chemistry 397–399
 - mercury capture in wet flue gas desulfurization systems 261–263
 - flue gas mercury oxidation technologies effects on FGD capture 272–274
 - – mercury in FGD by-product streams 264–267
 - – phase partitioning 263–264
 - reemissions from wFGDs
 - – additives 271–272
 - – chemistry 269–271
 - – definition and reporting conventions 267–269
 - mercury–carbon-surface chemistry
 - acid gases effects on mercury capacities on carbon 378–382
 - – kinetic HCl effect 382–385
 - mercury bonding nature to carbon surfaces 377–378
 - mercury–chlorine chemistry 390–397
 - mercury emission rates prediction 413–414
 - mercury transformations 416
 - – Hg⁰ oxidation across SCR catalysts 427–428
 - – Hg transformations within WFGDs 430–433
 - – in-flight transformations 419–427
 - – in-furnace transformations 416–419
 - reaction system 414–416
 - Mercury Experiment to Assess Atmospheric Loading in Canada and the United States (METAALICUS) experiment 8–9
 - mercury in coal
 - in international coals
 - – Australia 26
 - – China 23–24
 - – India 24, 26
 - – Indonesia 29
 - – review in largest coal producers 22–23
 - – Russian Federation 27–29
 - – South Africa 26–27
 - mode of occurrence in coal 13–14
 - – mercury determination methods 15–16
 - – pre-combustion mercury removal effectiveness 14–15
 - in U.S. coals
 - – coal databases 16–22
 - mercury speciation adsorption (MESA) method 95–96
 - Mercury Study 46, 192
 - mesopores 287
 - method 30B 98
 - micropores 287
 - Minamata Convention 51, 53
 - MinPlus CDEM group BV 348
 - background and motivations 345
 - demonstrations 346, 348
 - working 345–346
 - Mobotec Rotamix system 347
 - modern: preindustrial ratios 4
 - multicollector inductively coupled plasma mass spectrometry (ICP-MS) 15
 - municipal waste combustors (MWCs) 193–194
- n**
- National Academy of Sciences (NAS) 46, 192
 - National Action Plan 56
 - National Emission Reduction Plan (NERP) 54, 56
 - National Emission Standards for Hazardous Air Pollutants (NESHAP) program 45, 80

- National Energy Technology Laboratory (NETL) 165, 314, 363
- in-house development of novel control technologies 179
 - mercury control technology R&D 166–167
- National Environmental Protection Measures (NEPM) (Australia) 64
- National Health and Medical Research Council (NHMRC) 64
- National Institute of Environmental Health Sciences (NIEHS) 46, 192
- National Institute of Standards and Technology (NIST) 80–81, 98
- net mercury removed by wet FGD systems
- mercury in FGD by-product streams 264–267
 - phase partitioning 263–264
- non-carbonaceous sorbents 197–198
- non-carbon sorbents
- amended silicates 344–345
 - – background and motivations 340
 - – demonstrations 342–344
 - – working 341–342
 - MinPlus CDEM group BV 348
 - – background and motivations 345
 - – demonstrations 347–348
 - – working 345–346
 - Pahlman process 349–350
 - – background and motivations 348
 - – demonstrations 349
 - – working 349
- NO_x control 119
- o**
- Ontario Hydro method 93–94, 96, 105
- Opsis 75
- oxidation 149, 152, 199–201, 229–236, 238, 242, 272–274. *See also* atomistic-level models; catalysts, for mercury oxidation; mercury emission rates prediction
- enhancements 169
 - photocatalytic 352
- oxidation-reduction potential (ORP) 264
- oxygen 378
- p**
- Pahlmanite™ sorbent 350
- Pahlman process 349–350
- background and motivations 348
 - demonstrations 349
 - working 349
- particulate matter (PM) 117
- control 118
- Perkin Elmer Lambda EZ201 Spectrophotometer 327
- photochemical removal of mercury, from flue gas 350
- GP-254 process 350–351
 - photocatalytic oxidation 352
- physisorption 194, 377
- plasma emission spectroscopy (PES) 75
- Portland cement. *See*: cement manufacturing industry and mercury emission control
- positive displacement (PD) 295
- powdered activated carbon (PAC) 294, 303–304, 323–325, 331
- autoignition in ash hoppers 306
 - conveying 295
 - distribution 296
 - metering 295
- pre-combustion mercury removal effectiveness 14–15
- pretreatment/conversion systems and probe 75–76
- pretreatment and mercury conversion 77–79
 - sampling probe 76–77
- PS-12B 97–98
- pyroprocessing 141, 143, 144
- q**
- quench rate 113, 115, 125
- QuickSEM 95
- r**
- rapping 312
- raw mill on and raw mill off conditions 143
- reactive gaseous mercury (RGM) 8
- reburning 237
- reduced combustion efficiency 237
- reemissions 262
- additives 271–272
 - chemistry 269–271
 - definition and reporting conventions 267–269
- reference dose (RfD) 46, 192
- regulations
- background 45–46
 - electric generating units (EGUs) 46–47
 - Mercury and Air Toxics Standards (MATS)
 - – existing sources 47–49
 - – new sources 49–50
- relative accuracy test audit (RATA) 83–84, 96
- resistivity 318
- retrofit 60, 62

- s**
- sacrificial agent model 330
 - scales capture mechanism 346
 - selective catalytic reduction (SCR) 54, 58, 63, 238, 245–247, 249, 427–430
 - effect on mercury oxidation/capture 199–201
 - and flue gas desulfurization 205
 - – wet scrubbing 158–159
 - selective non-catalytic reduction (SNCR) 54, 58, 119
 - semi-continuous emissions monitor (SCEM) detectors 427
 - sequential chemical extraction (SCE) 201
 - seven-day calibration drift 83
 - slurry 261, 263–264
 - SO₂ control 119
 - sorbent 138–139
 - Sorbent Activation Process® 219–220
 - sorbent enhancement additives (SEA) 175–176. *See also* boiler chemical addition
 - sorbent injection 207
 - challenges and responses 211–212
 - electrostatic precipitator units 208–209
 - fabric filter units and TOXECON™ 209
 - sorbent trap methods 91, 95–98
 - speciation 141, 150
 - spike mercury 8–9
 - standard hydrogen electrode (SHE) 264
 - sulfur trioxide interference 178–179
 - syngas 135, 357, 360, 366, 368
- t**
- Tekran CMM availability (2009) 87
 - temperature programmed desorption (TPD) 169
 - Thermo Scientific elemental calibrator 80
 - Thermo Scientific probe 78–79
 - Thief Process 238
 - TOXECON II® 218
 - TOXECON™
 - and fabric filter units 209–210
 - performance and fabric filter optimization 212–213
- u**
- U.S. coal databases 16
 - comparison 20–22
 - EPA ICR
 - – 1999 19
 - – 2010 19–20
 - USGS COALQUAL database 16–19
 - U.S. Geological Survey (USGS) 15
 - ultra-clean process 362–363
 - unburned carbon (UBC) 206–207, 247–248, 414–415
 - in mercury oxidation and adsorption 229–231
 - – carbon type nature 231–232
 - – concentration needed to oxidize and remove mercury from flue gas 233
 - – synergistic relationship with calcium in fly ash 234–236
 - unconfined compressive strength (UCS) 336–337
 - United Nations Environment Programme (UNEP) 51
 - instrument on mercury (Minamata Convention) 53
 - US Department of Energy research program. *See* Environmental Protection Agency (US EPA)
 - Utility Mercury Reduction Rule 95
 - Utility Study 46
- v**
- volatilization 148, 151
- w**
- Waste Incineration Directive (WID) 54, 56
 - wet chemistry batch methods
 - early EPA total Hg methods 91–93
 - method application and data quality considerations 94–95
 - methods to speciate Hg 93–94
 - wet flue gas desulfurization (wFGD) 430. *See also* mercury capture in wet flue gas desulfurization systems
 - chemistry and mercury partitioning 216
 - enhancement economic analyses 181–182
 - net mercury removal by wet FGD systems
 - scrubber 198–199
 - systems
 - – corrosion 216–217
 - – selenium partitioning 217
 - wet process kiln 144–145
 - wet scrubbing 157–158
 - World Coal Quality Inventory (WoCQI) 15, 22, 23, 26
- x**
- X-ray absorption fine structure (XAFS) 15, 32, 34, 195, 378, 401

- X-ray absorption near edge structure (XANES) 32
 - X-ray absorption spectroscopy (XAS) 196, 201, 400
 - X-ray fluorescence spectroscopy (XRF) 75, 201
 - X-ray photoelectron spectroscopy (XPS) 196, 382, 400, 401
- Z**
- Zeeman effect 74

Disclaimer

This report was prepared as an account of work sponsored by an agency of the United States Government. Neither the United States Government nor any agency thereof, nor any of their employees, makes any warranty, express or implied, or assumes any legal liability or responsibility for the accuracy, completeness, or usefulness of any information, apparatus, product, or process disclosed, or represents that its use would not infringe privately owned rights. Reference herein to any specific commercial product, process, or service by trade name, trademark, manufacturer, or otherwise does not necessarily constitute or imply its endorsement, recommendation, or favoring by the United States Government or any agency thereof. The views and opinions of authors expressed herein do not necessarily state or reflect those of the United States Government or any agency thereof.

WILEY END USER LICENSE AGREEMENT

Go to www.wiley.com/go/eula to access Wiley's ebook EULA.